Pif1- and Exo1-dependent nucleases coordinate resection at uncapped telomeres

James Michael Dewar

Doctor of Philosophy

Institute for Ageing and Health

March/2011

Abstract

Telomeres are present at the ends of most eukaryotic chromosomes and are bound by specialized telomere 'capping' proteins, preventing them from initiating a DNA Damage Response and cell cycle arrest analogous to that triggered by DNA Double Strand Breaks (DSBs). Resection of 'uncapped' telomeres and DSBs to generate extensive single-stranded DNA (ssDNA) is one of the most upstream events in this DDR, but while the nuclease activities that resect DSBs are well-defined, only a single nuclease, Exo1, is known to function at uncapped telomeres.

This work establishes that the helicase Pif1, is required for a nuclease activity that resects uncapped telomeres in a parallel pathway to one defined by Exo1, Rad27 (Flap Endonuclease 1) and Rad24 (the 9-1-1 clamp loader). Following inactivation of the essential telomere capping protein Cdc13, Pif1 is shown to resect telomeres independently of Exo1 close to the chromosome end, but to play a less-crucial role in extensive resection. Furthermore, elimination of both Pif1 and Exo1 prevents the accumulation of ssDNA, thus eliminating the DDR at uncapped telomeres. Although Pif1 has no role in the resection of DSBs and has primarily been studied as a negative regulator of telomerase, it is shown to contribute to the DDR at uncapped telomeres in cells lacking telomerase and also to be crucial for telomere maintenance in telomerase-deficient cells.

Cdc13 inhibits the DDR at uncapped telomeres and is believed to be required for telomerase recruitment. Astonishingly, elimination of Pif1 and Exo1 permits the viability of cells lacking Cdc13 and *cdc13*Δ *exo1*Δ *pif1*Δ mutants maintain and lengthen their telomeres over time, in a manner dependent on Ku, Rad52 and telomerase. Thus, Cdc13 is not a requirement for telomerase recruitment and elimination of the nuclease activities that function at uncapped telomeres can by pass the requirement for otherwise-essential telomere capping proteins.

Dedication

I dedicate my thesis to my Grandmother, Janet Roberts. Her unconditional and unreserved support and encouragement over the past few years have been invaluable. I feel thoroughly privileged to have such a person in my life and her continued advice that I “keep on smilin’!” may be the best I have ever received.

Acknowledgements

I would like to thank all members of the Lydall laboratory for providing a nurturing and supportive lab environment throughout the duration of this work. I owe a great debt to Steve Addinall, Amanda Greenall, Stephanie Merchan, Alan Leake, Peter Banks, Greg Ngo, Kaye Chapman, Hsin-Yu Chang, Eva Holstein and Elizabeth Andrew for this. In particular, Stephanie Merchan and Amanda Greenall have both provided emotional support when it was needed the most and words cannot thank them enough for this.

An acknowledgement section does not do justice to the invaluable assistance that Alan Leake has provided over the course of this work. The majority of the media used, in addition to many of the stock solutions were prepared by him. He is accommodating and enthusiastic and has always found a way to assist me, no matter how obscure my requests might be. I would not have progressed as quickly, nor would many of my data have been so robust, if it were not for the high quality and consistency of his work.

Similarly, I thank Conor Lawless for providing me with the services of Colonyzer prior to its publication and aiding me in all manner of queries regarding image processing. His advice has helped me learn how to present aesthetically pleasing images that neither obscure nor distort the underlying data and this can be seen throughout the work here.

I would also like to thank my internal assessors Brian Morgan and Thomas von Zglinicki for providing constructive criticism and advice at each annual assessment. Likewise I extend thanks to my co-supervisor Jan Quinn, to whom I am very thankful for providing sufficient freedom in her mentoring to allow me to pursue my different projects.

The *PIF1* Synthetic Genetic Array (SGA) was carried out in collaboration with Alain Nicolas' lab at Institut Curie, Paris. He envisaged the experiment and members of his lab confirmed or refuted the hits that the screen highlighted. Steve Addinall taught me the robotic procedures associated with the screen and provided valuable counsel on how to perform the screen.

Finally, I thank my supervisor David Lydall. He has given me an unparalleled amount of freedom in my work and his mentoring and patience have been above-and-beyond

the call of duty. He constitutes the most significant single influence on my scientific career to date and any measure of success I achieve will bear his influence. Though his advice can be unconventional and his caustic sense of humour has occasionally left me baffled, he has consistently provided both encouragement and opportunity for me to achieve well beyond what I expected to be capable of. When I was an undergraduate investigating PhD opportunities, he was my first choice in the UK for a supervisor and even with hindsight I am convinced that I was correct.

Table of Contents

Table of Figures

Table of Tables

List of Abbreviations

BIR	Break-Induced Replication
BP	Base Pair
DDR	DNA Damage Response
DC	*Dyskeratosis congenita*
dNTPs	Deoxyribonucleotide triphosphate
DNA	Deoxyribonucleic acid
DSB	DNA Double Strand Break
DSBR	Double Strand Break Resection
dsDNA	double-stranded DNA
GC Content	Percentage Guanine and Cytosine content of DNA
HR	Homologous Recombination
KB	Kilobase
kDa	Kilodalton
mtDNA	Mitochondrial DNA
MQ Water	Milli-Q Water (Dispensed from a Millipore Water Purification System)
NHEJ	Non-Homologous End Joining
PBS(T)	Phosphate Buffered Saline (Tween)
PCR	Polymerase Chain Reaction
rDNA	Ribosomal DNA
RFLP	Restriction Fragment Length Polymorphism
RPM	Revolutions Per Minute
SDS	Sodium Dodecyl Sulphate
ssDNA	single-stranded DNA
SSC	Saline Sodium Citrate
TAE	Tris-Acetic Acid-EDTA
TBE	Tris-Boric Acid-EDTA
TCA	Trichloroacetic Acid
TE	Tris-EDTA
T_m	Melting Temperature (of DNA)

Budding yeast genetic nomenclature

CDC13 is a gene, encoding the protein Cdc13 (or Cdc13p). *cdc13-1* is a mutant allele of *CDC13* encoding the mutant protein Cdc13-1 (Garvik et al., 1995). It is possible to delete *CDC13* from the yeast genome, resulting in the null mutation *cdc13*Δ and preventing Cdc13 being produced (Larrivee and Wellinger, 2006, Petreaca et al., 2006, Zubko and Lydall, 2006).

TLC1 encodes the RNA subunit of telomerase TLC1, which is not transcribed to produce a protein (Singer and Gottschling, 1994).

The protein Pif1 exists as mitochondrial and nuclear isoforms produced by transcription of the gene *PIF1* from beginning at either the first methionine (m1) or second methionine (m2), respectively (Schulz and Zakian, 1994). *pif1-m2* is mutated at the second methionine in the *PIF1* open reading frame and produces only the mitochondrial form of Pif1, while *pif1-m1* is mutated at the first methionine in the *PIF1* open reading frame and produces only nuclear Pif1. *pif1-m1* encodes the protein Pif1-m1 (the nuclear form) while *pif1-m2* encodes the protein Pif1-m2 (the mitochondrial form) (Boule et al., 2005).

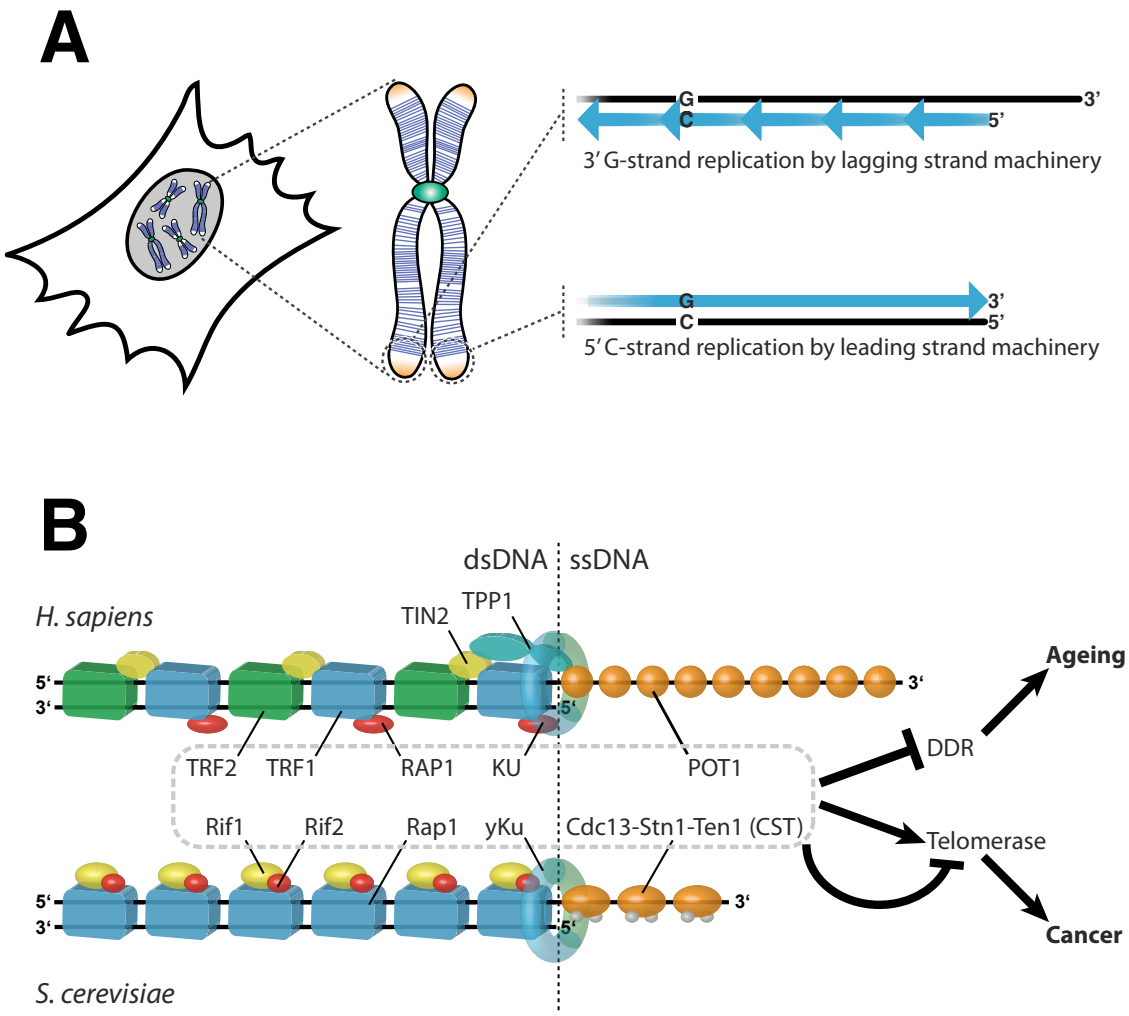
A
G
C
3'
5'
3' G-strand replication by lagging strand machinery
G
C
3'
5'
5' C-strand replication by leading strand machinery
B
dsDNA
ssDNA
H. sapiens
TIN2
TPP1
5'
3'
TRF2
TRF1
RAP1
KU
POT1
3'
5'
DDR
Ageing
Telomerase
Cancer
Rif1
Rif2
Rap1
yKu
Cdc13-Stn1-Ten1 (CST)
5'
3'
3'
5'
S. cerevisiae

Figure 1: Telomeres permit maintenance of terminal chromosomal sequences

A. The DNA at chromosome ends is replicated unidirectionally and the lagging strand is not able to replicate all the way to the chromosome end, resulting in sequence loss following each mitosis. Illustrated are the replication products (blue arrows) of a single leading and lagging strand telomere, of a single chromosome from a single cell.

B. Telomeres are nucleoprotein caps present at the ends of most eukaryotic chromosomes, consisting of dsDNA with a ssDNA overhang, bound by dsDNA- and ssDNA-binding proteins. Collectively, the telomere binding proteins 'cap' the telomere and serve to regulate telomerase activity and inhibit the DDR, posing a barrier to cancer and cellular ageing, respectively. In budding yeast the telomeric dsDNA is bound by Rap1, which recruits the accessory factors Rif1 and Rif2. In humans the telomeric dsDNA is bound by TRF1 and TRF2 (held together by TIN2) and TRF2 recruits RAP1 to telomeres. In budding yeast, Cdc13 binds the telomeric ssDNA and recruits Stn1 and Ten1 to form the CST complex, while in humans the telomeric ssDNA is bound by POT1. In human beings, POT1 and TRF1-TRF2-TIN2 are linked together by TPP1, which may permit the adoption of higher-order structures. In both budding yeast and humans, the Ku complex, a DDR component that binds to both telomeres and DSBs, also binds and plays a protective role. Model based on data discussed in Section **1.3**.

1 Introduction

"Humans are a good model organism for studying yeast"

- *Steve Elledge*

1.1 The end replication problem

Eukaryotes possess linear chromosomes and replicate their DNA bidirectionally, from internal origins. Thus, synthesis from the terminal origin of replication to the end of the chromosome will result in unreplicated DNA at the end of the lagging strand as the replication machinery will, at the very least, be unable to replicate the region of the template strand occupied by the terminal Okazaki fragment primer (approximately 8-12 bases) (Waga and Stillman, 1998). This is termed 'the end replication problem' and has the consequence that ends of chromosomes will lose terminal sequences with each cell division, ultimately guaranteeing that loss of viability will occur when the sequence loss reaches an essential gene (Olovnikov, 1971, Watson, 1972). Thus, a special mechanism of DNA replication is required at the chromosomal terminus in order for chromosomes to be maintained (Figure 1A).

The shortening caused by the end replication problem is likely to be much greater than the theoretical minimum for two reasons. First, on the lagging strand, approximately 30 bases of RNA-DNA synthesized by Polymerase α are actually required to prime Okazaki fragment synthesis, and loss of even this theoretical minimum will only occur if the terminal Okazaki fragment can be primed from the very end of the chromosome (Waga and Stillman, 1998). If the distance between the sub-terminal Okazaki fragment and the chromosome end is too great to facilitate priming at very end of the chromosome, then the terminal Okazaki fragment will need to be primed away from the chromosome end, in principle leading to sequence loss of up to one Okazaki fragment in size (up to approximately 200 bases) (Waga and Stillman, 1998). Second, although leading strand replication is usually assumed to proceed to the very end of the chromosome, the replication machinery is unlikely to be able to replicate the region of the template strand occupied by the replisome itself (approximately 20-40 bases in metazoans) (Raschle et al., 2008). Furthermore, both these considerations also fail to take into account the nucleolytic processing that might be required of the chromosome ends (Dionne and Wellinger, 1996). Thus, a specialized mechanism for the replication of chromosome ends is of paramount importance.

1.1.1 Telomeres and Telomerase

Telomeres are specialized nucleoprotein structures that exist at the ends of most eukaryotic chromosomes, usually consisting of double-stranded DNA (dsDNA) with a 3' single-stranded DNA overhang (ssDNA) (Figure 1A-B) (Blackburn et al., 2006, de Lange, 2009, Lydall, 2009). Telomeres contain specific, simple GC-rich repeat sequences that are G rich on the 3' strand (the TG strand) and C-rich on the 5' strand (the AC strand) (Figure 1B). Telomeric repeat sequences function to recruit specialized proteins to the telomere that mediate its function and telomeric repeat sequences can also be added *de novo* to the chromosome end by the enzyme telomerase in order to counteract telomere shortening caused by the end replication problem. Both the general structure and function of telomere structure are conserved, from human beings down to the budding yeast *Saccharomyces cerevisiae* and thus model organisms has been highly informative in the study of telomere biology (Figure 1B) (Blackburn et al., 2006).

Telomerase is a specialized reverse transcriptase, consisting of a catalytic core of a RNA template (TERC in mammals, TLC1 in budding yeast) and a catalytic subunit (TERT in mammals, Est2 in budding yeast), which is sufficient for telomerase activity *in vitro* (Bianchi and Shore, 2008, Blackburn et al., 2006, de Lange, 2009). *In vivo* in budding yeast, the accessory factors Est1 and Est3 are also required for telomerase recruitment to the telomeres (Lendvay et al., 1996, Lingner et al., 1997).

In budding yeast, it appears that two pathways recruit telomerase to the telomeres. In G1, the Ku complex (a DDR component that binds to both telomeres and DSBs) recruits the Est2-TLC1 catalytic core to the telomeres in a pathway that promotes telomerase activity at telomeres and supports telomere maintenance but is insufficient for telomere maintenance (Fisher et al., 2004, Lendvay et al., 1996, Peterson et al., 2001, Porter et al., 1996). In G2, Cdc13 (a specialized telomere-binding protein that binds to telomeric ssDNA) interacts with Est1 to recruit the Est2-TLC1 catalytic core in a second pathway that is both necessary and sufficient for telomere maintenance by telomerase (Chan et al., 2008, Nugent et al., 1996). The role of Est3 in telomerase recruitment is poorly defined, although it likely plays a role in the G2 pathway of telomerase recruitment (given that it is required for telomere maintenance) and this may occur through interactions with Est1 or Est2 (Friedman et al., 2003, Hughes et al., 2000, Lendvay et al., 1996, Osterhage et al., 2006). Though the regulation of telomerase in

mammalian cells is much less well understood, the telomere-binding protein POT1 may have similar roles to Cdc13 in regulating telomerase (Churikov and Price, 2008).

1.2 The 'end protection problem'

The ends of linear chromosomes resemble one half of a DNA Double Strand Break (DSB) and have the potential to be recognized and processed as a DSB (Sandell and Zakian, 1993). DSBs initiate a robust cell cycle arrest and are either processed by nucleases for repair by homologous recombination (HR) or repaired by Non-Homologous End Joining (NHEJ) (Harrison and Haber, 2006). Therefore, chromosome ends are at risk of preventing cell cycle progression, being degraded or undergoing chromosome-chromosome fusion events. This has been termed 'the end protection problem' in analogy to the 'end replication problem' (de Lange, 2009).

1.2.1 The cellular response to DSBs

In budding yeast, following the induction of a DSB, DNA ends are either rapidly directed towards HR or, where HR is impaired or cannot function, repaired by NHEJ (Usui et al., 2001). The initial step in this process is resection to generate ssDNA, the presence of which can be considered the stimulus for HR and the absence of which (impaired resection) can be considered the stimulus for NHEJ (Usui et al., 2001). The presence or absence of an ssDNA intermediate leads to the recruitment of sensor kinases (Mec1, Tel1) to the DSB, and the activation of kinase cascades, ultimately leading to checkpoint activation, cell cycle arrest and repair of the damage (Usui et al., 2001, Zou and Elledge, 2003).

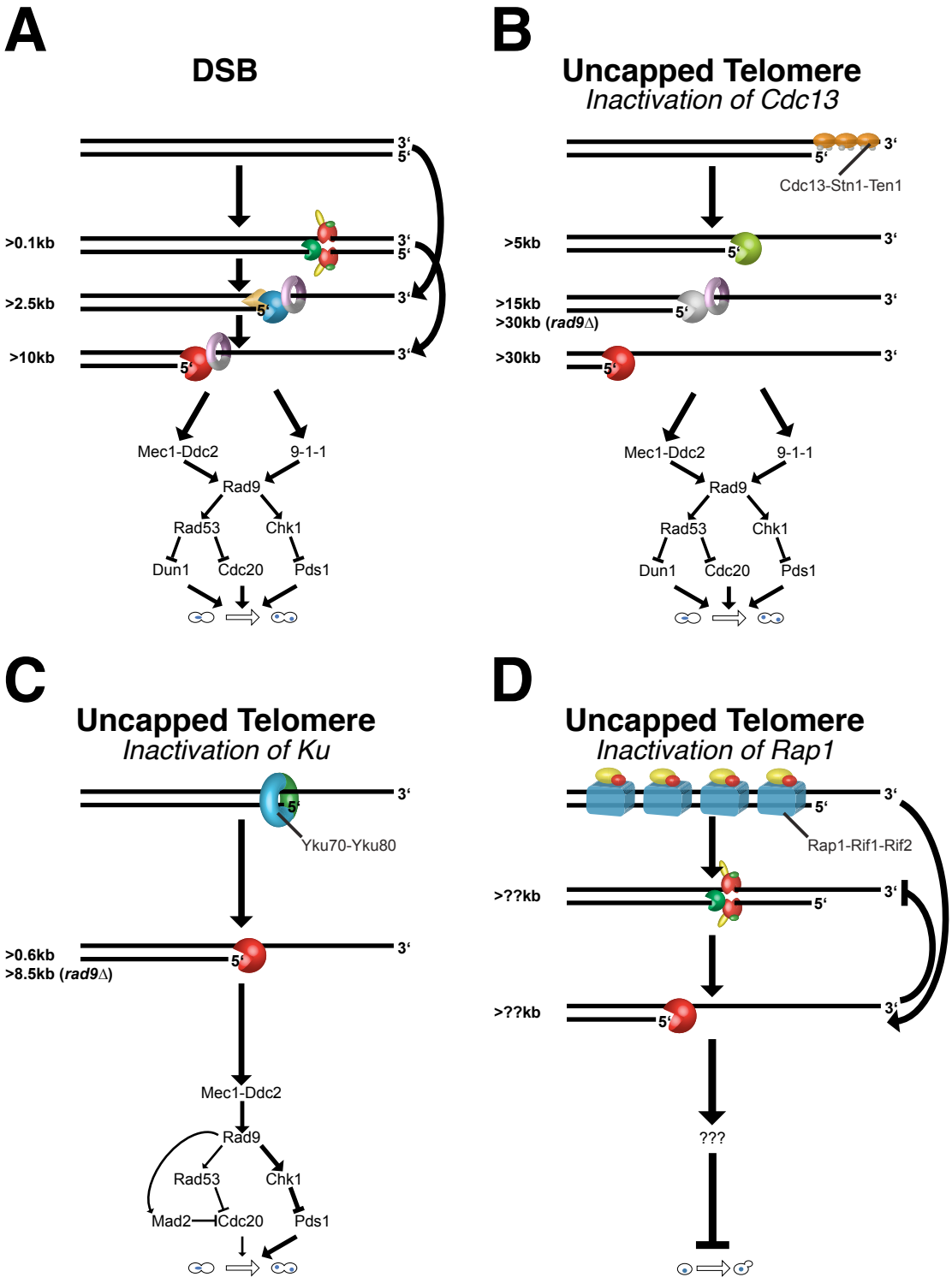
A
DSB
>0.1kb
>2.5kb
>10kb
Mec1-Ddc2
9-1-1
Rad9
Rad53
Chk1
Dun1
Cdc20
Pds1
B
Uncapped Telomere
Inactivation of Cdc13
Cdc13-Stn1-Ten1
>5kb
>15kb
>30kb (rad9Δ)
>30kb
C
Uncapped Telomere
Inactivation of Ku
Yku70-Yku80
>0.6kb
>8.5kb (rad9Δ)
Mad2
D
Uncapped Telomere
Inactivation of Rap1
Rap1-Rif1-Rif2
>??kb
???
Sae2
MRX
Sgs1
Dna2
9-1-1
Exo1
ExoY
ExoX

Figure 2: The DDR at DSBs and uncapped telomeres

A. At DSBs, resection of blunt ends is initiated by the MRX complex (Mre11-Rad50-Xrs2) in combination with the nuclease Sae2 to generate the initial overhang and extensive resection is carried out by Exo1. A nuclease activity dependent upon the helicase Sgs1 and the nuclease Dna2 has partially-overlapping function with both MRX/Sae2 and Exo1 and has roles in both generation of the initial overhang and in extensive resection. The 9-1-1 complex contributes to resection and is presumed to tether either Sgs1/Dna2 or Exo1 or both to the DNA but could possibly promote resection by an unidentified nuclease. 3' ssDNA exposed by resection then stimulates checkpoint activation and metaphase arrest dependent upon both the 9-1-1 complex and Mec1-Ddc2. (See Section **1.2.2** for detailed discussion).

B. At telomeres, inactivation of the ssDNA-binding protein Cdc13 leads to resection by at least three distinct nuclease activities. Exo1 carries out extensive resection >30kb from the chromosome end. ExoX is a hypothetical 9-1-1-dependent nuclease activity involved in resection >15kb from the chromosome end and which is inhibited by Rad9 and causes extensive (>30kb) resection of uncapped telomeres when Rad9 is eliminated. ExoY is a hypothetical nuclease believed to function independently of Exo1 and ExoX >5kb from the chromosome end. Exposed telomeric ssDNA then stimulates checkpoint activation and metaphase arrest dependent upon both the 9-1-1 complex and Mec1-Ddc2. (See Section **1.3.1** for detailed discussion).

C. At telomeres, inactivation of the Ku complex leads to resection >0.6kb from the chromosome end by Exo1. Elimination of Rad9 causes resection >8.5kb from the chromosome end and thus Rad9 is believed to inhibit Exo1. Exposed telomeric ssDNA triggers checkpoint activation and metaphase arrest dependent upon Mec1-Ddc2 but not the 9-1-1 complex. Thicker arrows represent pathways more important for arrest. Checkpoint activation is primarily dependent upon Chk1, though the kinases Rad53 and Mad2 also function. (See Section **1.3.2** for detailed discussion).

D. At telomeres, inactivation of Rap1 leads to resection primarily by Exo1. In the absence of Exo1, resection is carried out by another nuclease that appears to be inhibited by Exo1 and is likely to be dependent upon MRX. Cells accumulate in G1

following inactivation of Rap1 but the stimulus and transduction pathway behind this cell cycle defect are unknown. (See Section **1.3.3** for detailed discussion).

1.2.2 Resection

The initial nuclease activity that functions at DSBs is dependent upon the MRX complex (Mre11-Xrs2-Rad50) and the nuclease Sae2 (Ivanov et al., 1994, Lee et al., 1998b, Mimitou and Symington, 2008). Sae2 appears to create small, step-wise cuts on the 5' strand to generate 50-100 nucleotide overhangs of 3' ssDNA (Mimitou and Symington, 2008). Short ssDNA overhangs generated by Sae2/MRX appear to be processed by a second nuclease activity dependent upon Exo1 to generate many kilobases of 3' ssDNA (Tsubouchi and Ogawa, 2000). A third nuclease activity dependent upon the helicase Sgs1 and the multifunctional helicase-nuclease Dna2 also appears to be involved in both the generation of the initial overhang and extensive resection (Bonetti et al., 2009, Gravel et al., 2008, Mimitou and Symington, 2008, Zhu et al., 2008). The cooperation between these three nuclease activities has been exquisitely demonstrated by showing that elimination of Sae2, Sgs1 and Exo1 completely eliminates the formation of detectable ssDNA following the induction of a DSB (Mimitou and Symington, 2008). The best explanation for these data is that MRX/Sae2 cooperates with Sgs1/Dna2 in the initial overhang generation and then Sgs1/Dna2 cooperates with Exo1 in extensive resection (Figure 2A). Such a model explains how elimination of Sgs1 and Exo1 or Sae2 and Sgs1 essentially eliminates resection, while elimination of Sae2 and Exo1 does not (Bonetti et al., 2009, Mimitou and Symington, 2008, Zhu et al., 2008). Consistent with this model, end resection can be reconstituted *in vitro* either by the combined activities of MRX (but not Sae2) and Sgs1-Dna2 (Cejka et al., 2010, Niu et al., 2010) or by the combined activity of MRX/Sae2 and Exo1 (Nicolette et al., 2010). However, this model does not explain how elimination of Mre11 and Exo1 or Sgs1 essentially eliminates repair (Gravel et al., 2008), though there are conflicting reports about this (Tsubouchi and Ogawa, 2000).

The 9-1-1 complex is named after the mammalian orthologues Rad9-Hus1-Rad1 and is composed of the yeast proteins Rad17-Mec3-Ddc1 (Ellison and Stillman, 2003, Majka and Burgers, 2003). This specialized PCNA analogue has dual roles contributions to resection and checkpoint activation and is referred to as the 'checkpoint clamp' due to its homology to the 'DNA clamp' PCNA (Venclovas and Thelen, 2000). Just as PCNA is loaded onto DNA by the 'clamp loader' RFC (Rfc1-6), the 9-1-1 complex is loaded onto DNA by the 'checkpoint clamp loader', an alternate RFC in which Rfc1 is replaced

by Rad24 (Venclovas and Thelen, 2000). Likewise, just as PCNA tethers Polymerase δ to DNA, the 9-1-1 complex is presumed to tether a nuclease to the DNA (Lydall and Weinert, 1995, Zubko et al., 2004). The 9-1-1 complex probably functions downstream of MRX/Sae2, as it requires ssDNA to be loaded, but does not seem to be affected by the level of extensive ssDNA (Figure 2A) (Lisby et al., 2004, Nakada et al., 2004). If the 50-100 nucleotide overhangs generated by MRX/Sae2 (following elimination of Exo1 and Sgs1/Dna2) are sufficient for the 9-1-1 complex to be loaded, this would suggest that the 9-1-1 complex tethers either Exo1 or Sgs1/Dna2 or both (Figure 2A) (Mimitou and Symington, 2008). It is most likely that the 9-1-1 complex contributes to the tethering of both Exo1 and Sgs1/Dna2 at DSBs, as elimination of Rad24 confers a severe defect in resection, while elimination of either Exo1 or Sgs1/Dna2 confers only a minimal resection defect (Mimitou and Symington, 2008, Aylon and Kupiec, 2003). However, this remains to be tested and it is possible that the 9-1-1 complex is responsible for loading an unknown nuclease (ExoX) whose role at DSBs has not yet been elucidated (Figure 2A) (Zubko et al., 2004).

Following resection, the 3' ssDNA that is generated becomes coated in RPA and serves as the stimulus for checkpoint activation by the sensor kinase Mec1 in cooperation with the 9-1-1 complex (Lisby et al., 2004, Zou et al., 2003) (Figure 2A). Resection by Sae2 appears to stimulate Mre11 nuclease activity, which is believed to cleave the DSB and liberate the MRX complex (Lisby et al., 2004). In the absence of resection, MRX remains stably associated with the break and serves as the stimulus for checkpoint activation by the kinase Tel1, via its Xrs2 subunit (Nakada et al., 2003, Usui et al., 2001).

1.2.3 Checkpoint activation

RPA-coated ssDNA is recognized and bound by a heterodimer of Mec1 and Ddc2 and this is absolutely required for checkpoint activation (Lisby et al., 2004, Sanchez et al., 1999). In parallel, the 9-1-1 complex is loaded onto RPA-coated ssDNA and plays a critical role in checkpoint activation, but is not required for it (Lisby et al., 2004). Initiation of signaling by Mec1-Ddc2 and the 9-1-1 complex appears to require extensive (>100 nucleotides) ssDNA, as elimination of Sgs1 and Exo1 prevents activation of the downstream checkpoint kinase cascade (Gravel et al., 2008). Subsequently Mec1-phosphorylated histone H2A and methylated histone H3 accumulate at the site of DNA damage, to which Rad9 binds (Hammet et al., 2007,

Wysocki et al., 2005, Downs et al., 2004). Rad9 then functions as an adaptor to permit Mec1 to activate the effecter kinases Rad53 and Chk1, thus activating the checkpoint (Sanchez et al., 1999, Sun et al., 1998). Strikingly, the recruitment of Rad9 appears to negatively regulate resection by the 9-1-1 complex (Lazzaro et al., 2008, Lydall and Weinert, 1995).

Mec1 phosphorylates a series of conserved Serine/Threonine motifs in Rad9 which promote oligomerization of Rad9 (Usui et al., 2009). Rad53 is then recruited and also oligomerizes by binding to the phosphorylated Serine/Threonine motifs on Rad9, via its FHA domains (Schwartz et al., 2002). Rad53 then stimulates its own autophosphorylation, leading to the production of hyperphosphorylated, active Rad53 (Sweeney et al., 2005). Chk1 appears to bind to the N-terminus of Rad9, stimulating its phosphorylation and activation (Blankley and Lydall, 2004). Activated Chk1 and Rad53 function in parallel to prevent sister chromatid separation, thus inhibiting anaphase and sustaining cell cycle arrest at metaphase (Sanchez et al., 1999). To do this, Chk1 hyperphosphorylates Pds1 ('Securin', which functions to maintain sister chromatid cohesion), preventing its ubiquitinylation and degradation by the Anaphase Promoting Complex (APC), while Rad53 inhibits Cdc20, which is required for the APC to recognize Pds1 (Agarwal et al., 2003, Ciosk et al., 1998, Sanchez et al., 1999). Activated Rad53 also inhibits mitotic exit by phosphorylating and activating the downstream checkpoint kinase Dun1 (Chen et al., 2007, Hu et al., 2001, Lee et al., 2003, Sanchez et al., 1999). In addition to inhibition of mitotic exit, Dun1 also has other roles, such as regulating ribonucleotide biosynthesis (Zhao and Rothstein, 2002).

Although ssDNA is an important DDR stimulus for activation of this Mec1-dependent kinase cascade and thus is required for repair of damage, ssDNA is generated by the resection of the 5' strand to generate 3' ssDNA (Figure 2) and does itself constitute damage. Thus, it is unsurprising that negative feedback loops exist to limit the extent of the damage incurred. Indeed, Rad53 phosphorylates Exo1 following initiation of the DDR to limit resection (Jia et al., 2004, Morin et al., 2008, Segurado and Diffley, 2008). Furthermore, even without activation of Rad53, the binding of Rad9 to chromatin appears to inhibit resection (Lazzaro et al., 2008, Lydall and Weinert, 1995, Jia et al., 2004). Thus, negative feedback exists by multiple molecular mechanisms to prevent inappropriately high levels of ssDNA being generated at the site of damage.

In the absence of ssDNA generation, it appears that MRX remains stably associated with the break site and is able to recruit the sensor kinase Tel1 (Lisby et al., 2004). Tel1 then functions analogously to Mec1 to recruit the adaptor Rad9 and initiate the downstream checkpoint kinase cascade, activating the checkpoint (Usui et al., 2001). However, it should be noted that the full role of Tel1 is likely far more complex than this simple model, as Tel1 appears to have a second role in promoting resection at DSBs which cannot currently be well-explained (Mantiero et al., 2007).

1.2.4 Differences in metazoan and yeast responses to DSBs

In metazoans, the Mre11-Rad50-Nbs1 (MRN) complex and the nuclease CtIP initiate DSB processing in an analogous manner to the function of MRX and Sae2 (Sartori et al., 2007). Overhangs generated by MRN/CtIP are then processed further two nuclease activities dependent upon the helicase BLM and the metazoan EXO1, analogously to the nuclease activities dependent on Sgs1/Dna2 and Exo1 in budding yeast, to generate RPA-coated ssDNA that can by recognized by sensor kinases (Gravel et al., 2008). Additionally, the 9-1-1 complex also operates to generate ssDNA in mammalian cells, composed of its namesakes Rad9, Hus1 and Rad1 (Ellison and Stillman, 2003).

Metazoan cells possess a similar checkpoint machinery to yeast. The sensor kinase ATR binds to its interacting partner ATRIP to form an ATR-ATRIP complex that recognizes RPA-coated ssDNA in a manner analogous to Mec1-Ddc2 (Zou and Elledge, 2003). The sensor kinase ATM also functions similarly to Tel1 (Falck et al., 2005). However, metazoans also possess a third kinase, DNA-PK, which specifically regulates NHEJ at DSBs but does not appear to activate downstream effector kinases (Ciccia and Elledge, 2010). Additionally, ATM appears to cooperate to promote ATR activation at DSBs, in contrast to the situation in yeast where Tel1 does not contribute to Mec1 activation (Jazayeri et al., 2006). Still, these sensor kinases function via the mediators 53BP1, MDC1 and BRCA1 (all similar to Rad9) to activate the downstream effector kinases CHK1 (Chk1) and CHK2 (Rad53), so the general scheme is conserved (Harrison and Haber, 2006). Roles for the mediators in restraining nuclease activities are also conserved, as it appears that 53BP1 also inhibits resection, just like Rad9 (Bunting et

al., 2010, Lazzaro et al., 2008). Interestingly, metazoans primarily rely upon NHEJ for the repair of DSBs, which may account for some of the differences in checkpoint signaling, including utilization of an additional kinase (DNA-PK) specifically to regulate NHEJ (Lansdorp, 2009).

1.2.5 Telomeres confer 'end protection'

The processes described above ensure that a rapid DNA damage response is mounted against a DSB, leading to checkpoint activation and ultimately activating processes involved in repair of the damage. However, in budding yeast, 64 telomeres exist following the completion of S phase, each resembling a DSB and yet, under conditions of homeostasis, the cell cycle progresses relatively unhindered (Lydall, 2009). Thus, telomeres function as specialized structures to render DNA ends inert from DNA damage responses such as NHEJ (which would lead to chromosome-chromosome fusions) and HR (which would lead to resection and generation of ssDNA) (Figure 1B).

1.3 Telomeres are nucleoprotein caps

Telomeres do not initiate a DDR or activate the checkpoint and thus are said to 'cap' chromosome ends. This requires the tethering of telomere-specific 'capping' proteins to the chromosome ends by their recognition of the telomeric DNA sequence (Figure 1B). Paradoxically, though the DDR is attenuated at telomeres it appears that DDR components are present at telomeres but instead of promoting the DDR are co-opted to inhibit activation of downstream DDR components and this scheme occurs at both yeast and mammalian telomeres (de Lange, 2009, Lydall, 2009).

1.3.1 Cdc13 and the CST complex

The telomeric ssDNA-binding protein Cdc13 has essential roles at the telomeres of budding yeast in both chromosome end protection and in telomerase regulation, which can be eliminated by the *cdc13-1* and *cdc13-2* alleles, respectively (Garvik et al., 1995, Nugent et al., 1996). These separate roles appear to be due to the ability of Cdc13 to nucleate the formation of either the protective CST complex (with Stn1 and Ten1) or a telomerase-binding complex (Gao et al., 2007, Li et al., 2009).

The Cdc13-Stn1-Ten1 (CST) complex is an evolutionarily conserved RPA-like complex, that binds to the ssDNA overhang at the telomeres of budding yeast and prevents telomeres being recognized as DSBs, presumably at least in part by out-competing RPA for binding to the telomeric ssDNA (Figure 1B) (Gao et al., 2007,

Garvik et al., 1995, Miyake et al., 2009, Surovtseva et al., 2009). Using the temperature-sensitive allele *cdc13-1*, telomere end protection by the CST complex can be eliminated and telomeres become 'uncapped' (Garvik et al., 1995). Inactivation of Cdc13 leads to resection of the telomeric DNA by nucleases to generate extensive (≥30 kilobase) tracts of ssDNA, causing loss of viability and stimulating Mec1-dependent checkpoint, which culminates in a robust cell cycle arrest, as occurs in response to DSBs (Figure 2B) (Jia et al., 2004, Lydall and Weinert, 1995). However, the nuclease activities that function at 'uncapped' telomeres and DSBs are different, despite the similar schemes of ssDNA generation and Mec1-dependent checkpoint activation.

At DSBs, resection is initiated by MRX/Sae2 and extensive resection occurs due to the activity of Exo1 and Dna2/Sgs1-dependent nucleases. However, at uncapped telomeres in *cdc13-1* mutants, MRX plays an important role in inhibiting resection and inactivation of MRX causes increased levels of ssDNA (Foster et al., 2006). MRX binds specifically to leading strand telomeres and is required for the binding of Cdc13 to leading strand telomeres so MRX could generate overhangs for Cdc13 or other protective telomeric proteins to bind to, potentially inhibiting resection (Faure et al., 2010). One candidate for this is telomerase itself, which appears to inhibit the resection of uncapped telomeres (Vega et al., 2007). Alternatively, as suggested, the nuclease activity of MRX may somehow be rendered inert at the telomere and MRX might inhibit resection by physically occluding other nucleases (Foster et al., 2006).

Exo1 is involved in the resection of DSBs but elimination of Exo1 alone has relatively little effect on the efficiency and extent of resection (Mimitou and Symington, 2009, Tsubouchi and Ogawa, 2000). In contrast, Exo1 appears to be the major nuclease that functions at uncapped telomeres in *cdc13-1* mutants, as the extent of ssDNA is reduced from ≥30 kilobases from the chromosome end to ≤5 kilobases, and the quantity of ssDNA generated ≤5 kilobases of the chromosome end is severely diminished (Figure 2B) (Maringele and Lydall, 2002, Zubko et al., 2004). One possible explanation for this difference that 3' ssDNA overhangs occur natively at telomeres, while at DSBs processing by MRX/Sae2 is required to generate them. Indeed, *in vitro* MRX/Sae2 appears to promote Exo1 activity by generating overhangs for Exo1 (Nicolette et al., 2010). Thus, the function of Exo1 at uncapped telomeres in *cdc13-1* mutants might be equivalent to the combined activity of Exo1 and MRX/Sae2 at DSBs (Mimitou and Symington, 2008). Indeed, elimination of Exo1 and MRX/Sae2 appears to severely

diminish resection at a DSB (Tsubouchi and Ogawa, 2000). However, if Exo1 plays a more prominent role in resection at telomeres due to its ability to process the native telomeric overhangs, it would probably only be involved in resection of the lagging strand because, as mentioned above, MRX appears to be required for overhang generation at leading strand telomeres (Faure et al., 2010). This is certainly feasible, as significantly less than 50% of telomeric loci in cells with uncapped telomeres are single-stranded (Zubko et al., 2004).

Sgs1/Dna2 are also involved in the resection of DSBs (Mimitou and Symington, 2008, Zhu et al., 2008). Sgs1 also plays an important role in the resection of uncapped telomeres in *cdc13-1* mutants, though the role of Dna2 has not yet been examined (Ngo and Lydall, 2010). At DSBs, elimination of Sgs1 and Exo1 appears to cause a synergistic decrease in ssDNA at DSBs, limiting ssDNA generation to <100 bases (Mimitou and Symington, 2008). However, at uncapped telomeres, elimination of Sgs1 and Exo1 appears to have no more effect than elimination of Exo1 alone and $\geq$ 5,000 bases of ssDNA are still generated (Figure 2B) (Ngo and Lydall, 2010). Thus, in contrast to the situation at DSBs, Sgs1 appears to support Exo1 in resection at uncapped telomeres and an Exo1- and Sgs1-independent nuclease termed 'ExoY' appears to play a significant role in residual resection at uncapped telomeres (Mimitou and Symington, 2008, Ngo and Lydall, 2010).

Perhaps the greatest similarity between the resection at DSBs and uncapped telomeres is the critical requirement for the 9-1-1 complex. At DSBs, elimination of Rad24 and thus loading of the 9-1-1 complex imparts a severe resection defect and appears to prevent the formation of ssDNA approximately $\geq$1,000 bases from the break site (Aylon and Kupiec, 2003). Similarly at uncapped telomeres in *cdc13-1* mutants, it appears that loading of the 9-1-1 complex by Rad24 contributes to resection $\geq$15,000 bases from the chromosome end (Figure 2B) (Zubko et al., 2004). Even more striking is that at both DSBs and uncapped telomeres, Rad9 appears to specifically inhibit nuclease activity that is dependent on the 9-1-1 complex (Lazzaro et al., 2008, Lydall and Weinert, 1995). It appears this is due to the ability of Rad9 to bind to chromatin following a DDR (Lazzaro et al., 2008). Additionally, Sgs1 appears to be required for the Rad9-inhibited resection that occurs at uncapped telomeres and high levels of Dna2 disrupt telomeric chromatin structure, suggesting that a Sgs1/Dna2-dependent nuclease activity at uncapped telomeres might be opposed by Rad9 and chromatin (Figure 2B) (Ngo and

Lydall, 2010, Singer et al., 1998). Thus, it has been suggested that Sgs1 is a component of 'ExoX', which is a hypothetical Rad24-dependent nuclease activity that generates high levels of extensive (≥30,000 bases) ssDNA in the absence of Rad9 (Ngo and Lydall, 2010, Zubko et al., 2004).

The 'end protection' function of Cdc13 is essential and elimination of Cdc13 causes robust arrest within a cell cycle, while elimination of the telomerase-recruitment function of Cdc13 does not immediately cause loss of viability (Lydall and Weinert, 1995, Nugent et al., 1996). At low rates, cells can be generated that are viable in the absence of Cdc13, either by elimination of checkpoint components and nucleases (rate of approximately $4\text{-}6\text{x}10^{-5}$) or selective overexpression of Stn1 and Ten 1 (rate of approximately $1.6\text{x}10^{-1}$) (Petreaca et al., 2006, Zubko et al., 2004). Fusion of the DNA-binding domain of Cdc13 to Stn1 also eliminates the lethality associated with loss of Cdc13 (Pennock et al., 2001). Collectively, these observations indicate that the essential role of Cdc13 is to recruit Stn1 and Ten1 to telomeres to prevent inappropriate activation of the DNA damage response. Thus, it would appear that Cdc13 functions as a platform for end protection by Stn1 and Ten1. Indeed, specific inactivation of Ten1 also causes telomere uncapping and induces resection, despite Cdc13 remaining associated with the telomeres (Xu et al., 2009).

Though nonessential for viability, the role of Cdc13 in telomerase regulation is very important. Inactivation of this function in *cdc13-2* mutants leads to continued telomere shortening with passage and loss of proliferative capacity (i.e. senescence, as seen in cells lacking telomerase) (Nugent et al., 1996). To recruit telomerase to telomeres, Cdc13 binds to Est1, which in turns binds to the TLC1 subunit of the catalytic core of telomerase (Chan et al., 2008, Nugent et al., 1996). This recruitment appears to be stimulated by phosphorylation of Cdc13 by the cyclin-dependent kinase Cdk1, causing Cdc13 to exchange Stn1-Ten1 for Est1-telomerase (Li et al., 2009). As the CST complex forms an RPA-like structure, it is tempting to speculate that Cdc13-Est1-telomerase also forms an alternative RPA-like structure (Gao et al., 2007). In addition to being required for the recruitment of telomerase, Cdc13 also functions as a negative regulator of telomerase and inhibits extension of the telomeres by telomerase (Chandra et al., 2001). Interestingly the negative regulation of telomerase by Cdc13 appears dependent upon Stn1, suggesting that following binding of Est1-telomerase to Cdc13, Stn1-Ten compete for binding to Cdc13 with Est1-telomerase, ultimately causing the

dissociation of telomerase and reforming the CST complex (Chandra et al., 2001). However, it is also possible that Cdc13 regulates telomerase by some other mechanism, which is more sensitive to Cdc13 levels than the CST complex formation, as the net effect of decreased cellular Cdc13 levels is increased telomere length (Ungar et al., 2009).

1.3.2 The Ku Complex

Similarly to how MRX plays a role in mounting the DDR at DSBs, but plays a role in inhibiting the DDR at uncapped telomeres, so does the Ku complex function to 'cap' telomeres. The Ku complex in yeast is a heterodimer of Yku70-Yku80 that binds to all DNA ends, including telomeres and DSBs. At DSBs, the Ku complex cooperates with DNA Ligase IV (Dnl4) to coordinate non-homologous end joining (Wilson et al., 1997). Additionally, the Ku complex is required for the recruitment of telomerase to telomeres in G1 by binding specifically to a 48 nucleotide stem-loop on TLC1 to recruit the catalytic core of telomerase (Chan et al., 2008, Peterson et al., 2001). The telomerase recruitment role of the Ku complex is critcally important, as cells lacking Ku have short telomeres (Porter et al., 1996).

The Ku complex also has a role in end protection, partially distinct from its role in telomerase recruitment. Elimination of Ku increases the length of the telomeric ssDNA overhangs and causes them to persist throughout the cell cycle (Gravel et al., 1998, Polotnianka et al., 1998). Yeast cells lacking Ku also display a temperature-sensitive growth defect, which can be partially suppressed by overexpression of telomerase subunits, suggesting that at high temperatures a telomere-specific defect occurs (Feldmann and Winnacker, 1993, Teo and Jackson, 2001). Accordingly, at high temperatures cells, telomeres in cells lacking Ku become 'uncapped' and undergo resection specifically at the telomeres, resulting in ssDNA accumulation, cell cycle arrest and loss of viability (Maringele and Lydall, 2002). Checkpoint activation at telomeres lacking Ku occurs similarly to at DSBs, in that both Rad53 and Chk1 activation occur (Figure 2A,C). However in contrast to DSBs, Chk1 is primarily responsible for arrest at uncapped telomeres lacking Ku, Rad53 is only weakly activated and Dun1 has no role in arrest (Maringele and Lydall, 2002, Teo and Jackson, 2001). Additionally it appears that the spindle checkpoint kinase Mad2, which also inhibits the APC, contributes to checkpoint activation at uncapped telomeres lacking Ku (Maringele and Lydall, 2002). It is unclear how Mad2 is activated in response to uncapped

telomeres lacking Ku, but likely that it occurs through Mec1 and (presumably) Rad9 (Kim and Burke, 2008).

Resection at uncapped telomeres in *yku70*Δ mutants occurs less rapidly than in *cdc13-1* mutants, and multiple cell cycles in the presence of uncapped telomeres are required for ssDNA to accumulate (Figure 2C) (Lydall and Weinert, 1995, Maringele and Lydall, 2002). Indeed, *yku70*Δ mutants accumulate less ssDNA than *cdc13-1* mutants and the extent of resection is reduced from ≥30,000 bases in *cdc13-1* mutants compared to <8,500 bases in *yku70*Δ mutants (Maringele and Lydall, 2002, Zubko et al., 2004). Furthermore, although both *yku70*Δ mutants and *cdc13-1* mutants undergo a Mec1-dependent checkpoint activation following telomere uncapping, the 9-1-1 complex appears to play no role in checkpoint activation following telomere uncapping in *yku70*Δ mutants (Maringele and Lydall, 2002). Thus, the inability of the 9-1-1 complex to support checkpoint activation at uncapped telomeres in *yku70*Δ mutants may account for the relatively weak arrest and Rad53 activation compared to that seen at DSBs and following telomere uncapping in *cdc13-1* mutants. Given these collective observations, it is unsurprising that the regulation of nuclease activities at uncapped telomeres in *cdc13-1* mutants and *yku70*Δ mutants is quite different.

At uncapped telomeres in *yku70*Δ mutants, resection is essentially entirely dependent upon Exo1 (Figure 2C) (Maringele and Lydall, 2002). In fact, elimination of Exo1 prevents accumulation of detectable ssDNA at the telomeres of *yku70*Δ mutants and permits the growth of *yku70*Δ mutants at high temperature (Maringele and Lydall, 2002). Perhaps most strikingly, the 9-1-1 complex appears to have no role in the resection of uncapped telomeres in *yku70*Δ mutants, in contrast to its prominent role in *cdc13-1* mutants (Lydall and Weinert, 1995, Maringele and Lydall, 2002). This is consistent with the inability of the 9-1-1 complex to contribute to checkpoint activation at uncapped telomeres in *yku70*Δ mutants.

However, two salient similarities do exist between the resection of uncapped telomeres in *yku70*Δ and *cdc13-1* mutants. The MRX complex inhibits resection at uncapped telomeres of both *cdc13-1* and *yku70*Δ mutants, and elevated levels of ssDNA accumulate in the absence of MRX (Foster et al., 2006, Maringele and Lydall, 2002). This increased ssDNA generated in *yku70*Δ *mre11*Δ mutants is dependent on Exo1, suggesting that the same may be true for uncapped telomeres in *cdc13-1* mutants.

Second, Rad9 also inhibits resection at uncapped telomeres of *yku70*Δ mutants (Maringele and Lydall, 2002). The nuclease that Rad9 inhibits at uncapped telomeres in *yku70*Δ mutants has not formally been identified, but is likely to be Exo1, which appears to be the only nuclease activity that functions at uncapped telomeres of *yku70*Δ mutants. However, in principle ExoX could be required for the Rad9-inhibited nuclease at uncapped telomeres in *yku70*Δ mutants (Lydall and Weinert, 1995). This could only be the case if ExoX was able to recognize uncapped telomeres independently of the 9-1-1 complex at uncapped telomeres in *yku70*Δ mutants as the 9-1-1 complex appears to have no effect in *yku70*Δ *rad9*Δ mutants with uncapped telomeres (Maringele and Lydall, 2002).

1.3.3 Rap1-Rif1-Rif2

Rap1 binds to telomeric dsDNA and other sites within the budding yeast genome and also provides a platform for the binding of Rif1 and Rif2 via its C-terminus (Shore and Nasmyth, 1987, Wotton and Shore, 1997). Like the CST and Ku complexes, the Rap1-Rif1-Rif2 complex appears to have roles in both telomerase regulation and end protection, but these are much less well defined. Rif1 and Rif2 appear to function in a generalized manner by inhibiting the binding of Tel1 at both telomeres and DSBs, presumably with the telomeric consequence of inhibiting the phosphorylation of Cdc13 by Tel1 that is required for telomerase recruitment to the telomere (Hirano et al., 2009, Mishra and Shore, 1999). Rif1 and Rif2 appear to display a high level of redundancy because elimination of either causes modest telomere lengthening, while elimination of both or of the C-terminus of Rap1 leads to massive telomere lengthening (Wotton and Shore, 1997).

Inactivation of Rap1 leads to telomere 'uncapping' and resection that is primarily dependent upon Exo1, but – surprisingly – without the consequence of Mec1-dependent checkpoint activation, and instead leading to accumulation of cells in G1 (Figure 2D) (Vodenicharov et al., 2010). Intriguingly, low levels of Exo1-independent resection occur following inactivation of Rap1 and this Exo1-independent resection persists, and may even be inhibited by Exo1, in stationary phase cells (Vodenicharov et al., 2010). *RAP1* is an essential gene, but cells are viable with a C-terminal deletion, which leads to telomere lengthening due to the inability to recruit Rif1-Rif2 (Wotton and Shore, 1997). Interestingly, elimination of the C-terminal domain leads to accumulation of MRX-dependent telomeric ssDNA (Bonetti et al., 2010). Thus it appears that the essential

function of Rap1 is to cap telomeres and inhibit Exo1, but it also has non-essential roles to inhbit resection by MRX and regulation telomere length via Rif1-Rif2 (Figure 2D). Paradoxically, the central domain of Rap1 has also been shown to inhibit NHEJ at telomeres, independently of Rif1-Rif2 (Marcand et al., 2008, Pardo and Marcand, 2005). This is surprising because ssDNA should inhibit NHEJ, yet elimination of Rap1 renders telomeres vulnerable to both NHEJ and resection (Vodenicharov et al., 2010). Clearly further work is required to elicidate the complex role of Rap1 at telomeres.

1.3.4 Mammalian and Fission Yeast telomeres

In broad terms, the telomeres of mammalian and fission yeast cells are similar to those of budding yeast in that they contain specialized dsDNA- and ssDNA-binding proteins (Figure 1B) (de Lange, 2005, Lydall, 2009). However, the specific complexes involved are different, perhaps as a reflection of the slightly different threats posed by the DDRs of mammalian and fission yeast cells.

In mammalian cells, the telomeric dsDNA is bound by TRF1 and TRF2, while the ssDNA overhang is bound by POT1 (Figure 1B) (Baumann and Cech, 2001, Bilaud et al., 1997, Broccoli et al., 1997, Zhong et al., 1992). Humans possess a RAP1 orthologue which is recruited to telomeres by TRF2 (Figure 1B) (Li et al., 2000). In contrast to the situation in budding yeast, where separate complexes bind the telomeric ssDNA and the dsDNA, in mammalian cells POT1 and TRF1/TRF2/RAP1 are linked together by TIN2/TPP1 to form a single complex referred to as ‘shelterin’ (de Lange, 2005, Houghtaling et al., 2004, Kim et al., 1999, Liu et al., 2004, Ye et al., 2004). This linkage of the ssDNA- and dsDNA- binding components of shelterin has been proposed to function in promoting higher-order DNA structures at mammalian telomeres that might function to occlude telomerase and components of the DDR (de Lange, 2005, Griffith et al., 1999, Stansel et al., 2001).

In the fission yeast *Schizosaccharomyces pombe*, a partially-analagous partially-orthologous shelterin-like complex exists. In *S. pombe*, the telomeric dsDNA is bound by Taz1 (like TRF1-TRF2), while the ssDNA overhang is bound by Pot1 (Baumann and Cech, 2001, Cooper et al., 1997, Cooper et al., 1998). Fission yeast Rap1 is recruited to telomeres by its interaction with Taz1, analogously to the recruitment of Rap1 to mammalian telomeres by Trf2 (Chikashige and Hiraoka, 2001, Kanoh and Ishikawa, 2001). Pot1 and Taz1 are linked together by Tpz1, analogously to the linkage between

POT1 and TRF1-TRF2 by TIN2/TPP1 (Miyoshi et al., 2008). Of all the components of the fission yeast shelterin-like complex, Pot1 has the greatest level of conservation with the mammalian shelterin complex and has been highly informative as to POT1 function in mammalian cells (Baumann and Cech, 2001).

Broadly speaking, POT1 appears to fulfill similar roles to the Cdc13 in budding yeast. Inactivation of Pot1 in either fission yeast or POT1 in mammalian cells leads to rapid loss of telomeric DNA, involving resection of telomeres (presumably by nucleases, though none have yet been identified) and checkpoint activation (Baumann and Cech, 2001, Palm et al., 2009, Pitt and Cooper, 2010, Wu et al., 2006). Much like Cdc13 requires Stn1/Ten1 to protect telomeres from the DDR, POT1 does not appear to function in isolation, as Tpz1/TPP1 is required for protection of the telomeric DNA by Pot1/POT1 (Hockemeyer et al., 2007, Miyoshi et al., 2008). Furthermore just as Cdc13 negatively regulates telomerase, POT1 also appear to, though unlike Cdc13, no roles in telomerase recruitment have yet been identified for POT1 (Churikov and Price, 2008, Kelleher et al., 2005).

Recently, orthologues of the CST complex were discovered in both mammalian and plant cells, making the comparison of Cdc13 to POT1 somewhat contentious (Miyake et al., 2009, Surovtseva et al., 2009). Just as inactivation of the budding yeast CST complex leads to rapid degradation of telomeric DNA and ssDNA generation, so does inactivation of the mammalian and plant CST complexes (Miyake et al., 2009, Surovtseva et al., 2009). However, mammalian CST does not have specific affinity for telomeric repeats and localizes both telomeric and non-telomeric chromosomal regions, leading to the suggestion that the CST complex is involved in DNA replication in a manner that is frequently required by the telomeres, but also by other loci (Miyake et al., 2009). More work is clearly required to understand the role of the CST complex in higher organisms, and how this more generalized complex in mammalian cells can fulfill such a specialized telomeric role in budding yeast.

RAP1 appears to inhibit NHEJ at human telomeres, similarly to the ability of Rap1 to inhibit NHEJ in budding yeast (Bae and Baumann, 2007, Bombarde et al., 2010). Strikingly, inactivation of RAP1 can also lead to HR occurring between mammalian telomeres, without activation of ATR checkpoint kinase (Sfeir et al., 2010). This is potentially similar to the resection that occurs following inactivation of Rap1 at budding

yeast telomeres, which does not lead to activation of the Mec1 checkpoint kinase (Vodenicharov et al., 2010).

Though the binding of TRF1 and TRF2 to mammalian telomeric dsDNA is comparable to the binding of Rap1 to yeast telomeric dsDNA, the similarities between mammalian RAP1 and yeast Rap1 leave TRF1/TRF2 without yeast analogues. It appears that TRF2 functions primarily to repress NHEJ and prevent activation of the ATM checkpoint kinase but also has roles in ensuring proper telomere replication (Bombarde et al., 2010, Celli and de Lange, 2005, Karlseder et al., 1999, Ye et al., 2010). TRF1 on the other hand appears to regulate telomere length via POT1 in addition to having roles in ensuring proper telomere replication (Loayza and De Lange, 2003, Ohki and Ishikawa, 2004, Sfeir et al., 2009, van Steensel and de Lange, 1997). It has been speculated that the increased time spent at G1/interphase in mammalian cells might necessitate more stringent mechanisms of repressing NHEJ/ATM than budding yeast might require for the repression of NHEJ/Tel1, which would explain the lack of a TRF2 analogue in budding yeast (de Lange, 2009). Likewise, as human telomeres are much longer (approximately 15,000 bases) than those of budding yeast (approximately 350 bases), it is interesting to speculate that replication of much longer tract of telomeric repeats requires a special aid to replication in human cells, explaining the lack of TRF1/TRF2 analogues in yeast (Allshire et al., 1989, de Lange et al., 1990, Shampay and Blackburn, 1988).

In budding yeast, the Ku complex is present at the telomeres and has dual roles in telomerase recruitment and end protection (Maringele and Lydall, 2002, Peterson et al., 2001). Similarly, mammalian Ku is also present at the telomeres and may be able to recruit telomerase (Ting et al., 2005). Interestingly, although Ku is able to bind telomeric DNA with high affinity *in vitro* it appears to be localized to telomeres indirectly, via an interaction with TRF1, *in vivo* (Bianchi and de Lange, 1999, Hsu et al., 1999, Hsu et al., 2000). Surprisingly, though elimination of Ku in yeast appears to cause resection of the telomeric DNA and ssDNA generation, elimination of Ku in mammalian cells leads to telomere fusions via NHEJ, suggesting that although Ku does inhibit a DDR at telomeres, it does not guard against resection (Samper et al., 2000). However, elimination of Ku at human telomeres also leads to telomeric deletions and formation of extrachromosomal circles of telomeric DNA, which is compatible with Ku inhibiting HR and thus resection (Wang et al., 2009). Inhibition of both NHEJ and,

potentially, HR at mammalian telomeres by Ku would be surprising as resection required for HR would be expected to inhibit NHEJ. Clearly it will be important to understand these potentially contradictory roles of Ku at mammalian telomeres. As discussed earlier (Section **1.3.3**) Rap1 in budding yeast also has roles in both inhibition of resection and inhibition of NHEJ and thus might provide insight into these roles of Ku at mammalian telomeres.

1.3.5 Drosophila and Caenorhabditis telomeres

Though the telomeres of budding yeast and humans serve as valuable models for understanding telomere telomere biology, organisms with different telomere structures do exist. *Drosophila* are a striking example as they lack TG-rich repeat sequences or any telomere-specific repeat at all (George et al., 2006). Instead, *Drosophila* telomeres are maintained by transposable elements and chromosome ends are protected from the DDR by maintaining high levels of heterochromatinisation (Rong, 2008). This mechanism of telomere maintenance may be less atypical than it appears, as there is conjecture that in fission yeast elimination of telomerase can in rare cases lead to the generation of rare mutants that use heterochromatin to cap their telomeres (Jain et al., 2010).

Though telomeres are usually composed of telomeric dsDNA with a 3' ssDNA overhang, *Caenorhabditis* telomeres are maintained by telomerase yet possess persistent 3' and 5' overhangs (Raices et al., 2008). 5' overhangs have been reported in mammalian cells, but it is thought these are transient intermediates stemming from impaired leading strand regulation (Cimino-Reale et al., 2003). Remarkably, *Caenorhabditis* utilize telomerase for telomere maintenance, so although complexes such as the CST complex function in budding yeast to maintain 3' overhangs as a substrate for telomerase, other organisms are remarkably flexible in the DNA structure at the ends of chromosomes (Raices et al., 2008).

1.3.6 Shortened telomeres

Shortened telomeres are presumed to be 'uncapped' if there is insufficient telomeric DNA for capping proteins to bind and short telomeres are preferentially recognized by telomerase for elongation (Bianchi and Shore, 2007). Consistent with this, induction of a short telomere leads to recruitment of DDR components such as RPA, in addition to recruitment of Cdc13 and telomerase (Bianchi et al., 2004, Khadaroo et al., 2009).

However, this response is clearly distinct from that caused specifically by elimination or inactivation of telomere cap components, as resection at DSB-induced short telomeres is dependent upon Sae2/MRX, Sgs1/Dna2 and Exo1 in essentially the exact same manner that DSBs are resected and this resection readily leads to elongation by telomerase (Bonetti et al., 2009).

The most popular tool for inducing a shortened telomere is an inducible DSB with an adjacent tract of telomeric TG repeats (Bianchi et al., 2004, Bonetti et al., 2009). Thus, one interpretation of this data (particularly that the coordination of nucleases at shortened telomeres is identical to that at DSBs) is that these so-called 'shortened telomeres' are more reflective of DSBs. However, modulation of the nuclease activities that function to generate overhangs at inducible shortened telomeres can have a significant effect on telomere length homeostasis – for example, elimination of Sgs1 and Sae2 eliminates overhang generation at DSB-induced short telomeres and causes drastic telomere shortening (Bonetti et al., 2009). This suggests the lessons learned from DSB-induced short telomeres are generally applicable to telomere biology.

Interestingly, it appears that Cdc13 potently inhibits ssDNA generation at DSB-induced short telomeres, but has essentially no effect at control telomeres 'induced' to wild type length (Negrini et al., 2007). Furthermore, DSB-induced short telomeres have been used to further dissect the roles of the Ku complex and Rap1-Rif1-Rif2 in resection – while both complexes inhibit resection, Ku appears to primarily inhibit the initiation of resection at the end of the telomere, while Rap1-Rif1-Rif2 appear to primarily limit the extent of any resection that does occur (Bonetti et al., 2010). When considering the differential regulation of nucleases at DSB-induced short telomeres compared to uncapped telomeres, it is important to recognize that DSB-induced short telomeres do not constitute telomere dysfunction, as they are readily elongated by telomerase and restored to homeostasis (Bianchi et al., 2004, Bonetti et al., 2009). This is in stark contrast to the sustained degradation and checkpoint activation that occurs following inactivation of specific telomere capping components (Maringele and Lydall, 2002, Vodenicharov et al., 2010, Zubko et al., 2004). Thus, uncapped telomeres are considered to be dysfunctional while shortened telomeres are not, and there is differential coordination of nuclease activities at uncapped compared to shortened telomeres. The key question remaining is whether nuclease activities at uncapped telomeres cause telomere dysfunction or whether the differential coordination of

nuclease activities is a consequence of some upstream molecular even that marks a telomere as dysfunctional or not.

1.3.7 Telomerase-deficient telomeres

Inactivation of telomerase in cultures of budding yeast prevents cells from solving the end replication problem (Cohn and Blackburn, 1995, Singer and Gottschling, 1994). Consequentially, telomeres shorten following each S phase and the growth of the culture becomes limited by telomere length, causing a loss in proliferative capacity termed 'senescence' (Lundblad and Blackburn, 1993). Usually within the senescent culture, rare clones arise that utilize telomerase-independent, HR-dependent (specifically BIR-dependent) mechanisms of telomere maintenance to maintain and lengthen their telomeres, though telomerase-and-recombination-independent mechanisms can also occur (Lydeard et al., 2007, Maringele and Lydall, 2004b, Teng and Zakian, 1999). As these 'survivors' overtake the culture, it regains its proliferative capacity.

When telomerase-deficient telomeres become critically short, there is an increase in recruitment of HR proteins in addition to Cdc13 and Tel1, presumably in a failed attempt to elongate telomeres by telomerase (Khadaroo et al., 2009). Additionally, critically-short telomeres become coated in RPA and recognized by Mec1, triggering a DDR similar to that at DSBs and preventing further growth (Abdallah et al., 2009). It has been speculated that exposed ssDNA from non-telomeric sequences is ultimately what activates the senescence-inducing DDR and consistent with this, elimination of Exo1 or Tel1 (which both contribute to resection at DSBs) inhibits the rate of senescence and telomere shortening that occur following senescence (Abdallah et al., 2009, Maringele and Lydall, 2004a, Ritchie et al., 1999). However, the response to telomerase-deficient shortened telomeres is clearly more complex as the helicase Sgs1 contributes to resection at DSBs but inhibits entry into senescence in telomerase deficient cells (Cohen and Sinclair, 2001).

1.4 Telomeres and disease states

The study of telomere biology began in the 1980's using basic model organisms to ask fundamental questions about how cells maintain chromosome ends. By the 1990's the number of papers published that dealt with telomere biology was increasing exponentially, primarily due to the profound implications that the field has for human

health (Blackburn et al., 2006). This was further acknowledged when the Nobel Prize for Physiology or Medicine 2009 was awarded to Elizabeth Blackburn, Carol Greider and Jack Szostack for "the discovery of how chromosomes are protected by telomeres and the enzyme telomerase" (Blackburn et al., 2009).

1.4.1 Senescence

The growth of cells in culture is limited by a phenomenon known as 'replicative senescence' (Blasco, 2007, Hayflick, 1965). At the whole organism level, 'senescence' is defined as the irreversible loss of proliferative capacity and leads to ageing and ultimately mortality. As telomeres shorten with each cell division and are of paramount importance for cell survival, telomere shortening is a prime candidate for a causal agent in mammalian ageing.

Telomerase activity is not detectable in most human somatic (differentiated) tissues, thus a progressive loss of telomere length is inevitable (Kim et al., 1994). Accordingly, just as telomerase-deficient budding yeast undergo telomere shortening and an eventual loss of proliferative capacity over passage, so do human fibroblasts in culture (Harley et al., 1990). A causal role for telomere shortening in cellular ageing was established by the demonstration that re-introduction of telomerase into human cells increased telomere length and life span (Bodnar et al., 1998). At the whole organism level it has been shown that late-generation telomerase knock-out mice display premature ageing phenotypes (Blasco et al., 1997, Lee et al., 1998a). Crucially, the demonstration that late, rather than early generation telomerase knock-out mice show premature ageing phenotypes provides a robust demonstration that the premature ageing seen is a consequence of short, dysfunctional telomeres rather than some toxic effect caused by lack of telomerase. Finally, and most astonishingly, reactivation of telomerase in late generation telomerase knock-out mice prevents further telomere shortening and alleviates the progression of premature ageing phenotypes (Jaskelioff et al., 2010). This result stops short of reversing telomere dysfunction-driven senescence, but does indicate that restoring telomere homeostasis at any stage of telomere dysfunction is likely to inhibit the progression of further pathologies.

Though ethical and technical considerations limit the strong establishment of such a strong causal effect in human beings, it has been shown that replicatively senescent human cells (i.e. aged, non-dividing) are kept locked in senescent by a persistent DDR,

to which shortened telomeres contribute (d'Adda di Fagagna et al., 2003). Furthermore, inactivation of components of the telomere cap in human cells can mimick such a DDR and trigger senescence (Takai et al., 2003). Collectively, these data argue that at both the cellular and whole organism level in humans and mice, telomere shortening increases with age, until telomeres become so short that telomeres become 'uncapped' and a DDR is initiated, triggering senescence.

1.4.2 Cancer

Cancer usually stems from uncontrolled proliferation of an organism's own cells (though transmissible cancer has been reported between canines) (Murgia et al., 2006). As telomeres shorten with each division and telomere shortening ultimately results in senescence, they provide a potent barrier to cancer. In fact, telomere shortening can be viewed as a double-edged sword; on the one hand it contributes to the mortality of the organism by promoting senescence; on the other hand promotes the vitality of the organism by limiting the number of divisions any given cell can go through and thus preventing the continued proliferation required for oncogenesis (Blasco, 2007).

Therefore, a necessary step in the establishment of any immortal cancer is the establishment of a mechanism of indefinite telomere maintenance (Cesare and Reddel, 2010). In the majority (approximately 85%) of cancers this occurs simply through up-regulation of telomerase components while in a minority this occurs without telomerase up-regulation through 'ALT' mechanisms (Bryan et al., 1997, Kim et al., 1994). ALT mechanisms are believed to be similar to the recombination-based mechanisms used by budding yeast for the generation of telomerase-independent 'survivors' and indeed, recombination within the telomeric DNA has been shown to be prevalent in human ALT cells but not wild type cells (Dunham et al., 2000). Furthermore, progression of cancers appears to be associated with increased chromosome fusion events and telomere dysfunction, likely indicating that telomere dysfunction drives genomic instability and thus promotes the accumulation mutations that facilitate cancer (Lin et al., 2010).

1.4.3 Dyskeratosis congenita

Dyskeratosis congenita (DC) is a rare, inherited syndrome in humans leading to bone marrow failure and cancer predisposition (Bessler et al., 2010). DC can be caused by mutations in genes encoding either the catalytic core components of telomerase (*TERT* or *TERC*) or *DKT1*, which was discovered due to its causal role in some forms of

Dyskeratosis congenita and encodes Dyskeratin, a protein important for stabilizing TERC RNA (Heiss et al., 1998, Mitchell et al., 1999, Vulliamy et al., 2001, Yamaguchi et al., 2005).

DC patients have short telomeres, which effect the two major pathologies of DC (Bessler et al., 2010). First, shorter telomeres reduce the number of divisions a cell can go through, so in DC patients the somatic tissues need to be more frequently replenished by hematopoietic stem cells, leading to their depletion. Second, short telomeres are believed to readily become dysfunctional, inducing genome instability and predisposing patients to cancer. Thus, defective telomerase does not directly cause DC, but instead DC is caused by the telomere dysfunction, which is a consequence of defective telomerase in DC patients. This is highlighted by 'anticipation' seen in DC patients – as telomere length decreases in later generations of families affected by DC, the onset of disease occurs more severely and at an earlier age (Vulliamy et al., 2004). This is similar to disease states that are specifically seen in late generation telomerase knock-out mice, which occur due to telomere shortening rather than the absence of telomerase *per se*, highlighting how informative model organisms can be in understanding human diseases (Blasco et al., 1997, Lee et al., 1998a).

1.4.4 Diabetes

Telomere dysfunction has been linked to both diabetes and obesity (Fuster and Andres, 2006). Insulin resistance is a hallmark of obesity and recently it has been exquisitely shown that late-generation telomerase knock-out mice are more prone to developing insulin-resistance in the liver (Minamino et al., 2009). Remarkably, it has been shown that transplanting dysfunctional adipose tissue from late generation telomerase knock-out mice into wild type mice led to the induction of insulin resistance and this appeared to be dependent upon a DDR occurring in the adipose tissue (Minamino et al., 2009). Though it is premature to try and generalize based on a single study, it will be interesting to know whether there is a specific link between diabetes and telomere dysfunction, or whether this is a sign that telomere homeostasis is necessary to safeguard against a wide range of diseases that can be induced by tissue dysfunction.

1.4.5 Uncapped telomeres in budding yeast as a model for senescence

As discussed above, studies in budding yeast over the last two decades have been informative into the nature of DNA damage responses and particularly how telomere

dysfunction can initiate a DDR. Additionally, understanding the regulation of telomerase at telomeres may provide valuable insight into how to combat cancer, given that the majority of cancers depend upon telomerase for survival. Perhaps the most clinically-relevant information provided thus far by the study of telomere biology, has been that working knowledge of how ALT cancers maintain their telomeres has been primarily derived from studies of the rare events that lead to recombination-dependent telomerase-independent telomere maintenance in budding yeast (Cesare and Reddel, 2010).

Work originating in budding yeast demonstrated that the exonuclease Exo1 had a particularly pivotal role in the initiation of the DDR at uncapped telomeres (Maringele and Lydall, 2002, Zubko et al., 2004). It was subsequently shown that elimination of murine EXO1 extended the life span of telomerase knock-out mice by alleviating the DDR at dysfunctional telomeres (Schaetzlein et al., 2007). Remarkably, the lifespan extension obtained in telomerase knock-out mice occurred without the consequence of increased cancer susceptibility, demonstrating that a genuine lifespan extension had occurred (Schaetzlein et al., 2007). Interestingly, EXO1-knock out mice do show premature mortality compared to Wild Type mice due to cancer susceptibility, indicating that simply eliminating EXO1 is unlikely to extend lifespan except in organisms where telomeres are highly dysfunctional (Wei et al., 2003). However, these data suggest the possibility that careful modulation of EXO1 activity in whole organisms may be sufficient to extend the lifespan of a wild type organism, or combat the pathologies seen in diseases of telomere dysfunction, such as Dyskeratosis congenita. Considering this, determining the identity of other nuclease activities that function to resect uncapped telomeres in budding yeast (ExoX and ExoY) may have profound implications for human health (Zubko et al., 2004).

Finally, EXO1 appears to degrade both telomerase-deficient and ‘uncapped’ telomeres, both of which are able to initiate a DDR (Garvik et al., 1995, Khadaroo et al., 2009, Maringele and Lydall, 2002, Maringele and Lydall, 2004a). It will be important to understand which of these two sets of dysfunctional telomeres more closely resembles the situation seen in senescent mammalian and human cells and this will be facilitated by the identification of nuclease activities involved in the resection of either telomerase-deficient or uncapped telomeres but not both.

1.5 Aims and Objectives

Telomere dysfunction plays a causal role in ageing and can play causal roles in diseases such as cancer and DC (Bessler et al., 2010, Lin et al., 2010, Blasco et al., 1997, Lee et al., 1998a). The exonuclease Exo1 has been shown to play a pivotal role in driving telomere dysfunction at both 'uncapped' telomeres in budding yeast and at dysfunctional telomeres in telomerase knock-out mice (Maringele and Lydall, 2002, Schaetzlein et al., 2007). Thus, Exo1 is likely to be a determinant of cellular ageing and may promote disease states such as cancer and DC. At uncapped telomeres in budding yeast, additional nucleases that function independently of Exo1 (such as ExoX and ExoY) are known to exist but have not yet been identified (Zubko et al., 2004). These unidentified nucleases, like Exo1, might also play critical roles at dysfunctional telomeres in higher organisms. Thus, the purpose of this work was; to identify novel determinants of Exo1-independent nuclease activities that function at uncapped telomeres in budding yeast; to assess the contribution of Exo1-independent nuclease activities to resection of uncapped telomeres in *cdc13-1* mutants and subsequent checkpoint activation; to gain mechanistic insight into the roles of Exo1-independent nuclease activities at uncapped telomeres.

2 Methods

2.1 Yeast Strains and Growth

2.1.1 Yeast Strains

All strains used in this study were in the W303 background and were *ade2-1 trp1-1 can1-100 leu2-3,112 his3-11,15 ura3 GAL+ psi+ ssd1-d2 RAD5*$^{+}$. Gene deletions were all constructed using PCR-based cassettes and confirmed by PCR to check the presence of the TEF promoter (Goldstein and McCusker, 1999, Longtine et al., 1998).

Point mutations were confirmed by restriction digest of PCR products to confirm the presence of an RFLP carried by the mutant allele. M1877 and M1878 were used to amplify a 500bp fragment of Pif1 that contained an ApaI site in *pif1-m1* strains or a XhoI site in *pif1-m2* strains (Schulz and Zakian, 1994). M1879 and M1880 were used to amplify a 350bp fragment of Pif1 that contained a MboI site in *pif1-hd* mutants (Ribeyre et al., 2009).

For all *cdc13*Δ mutants and *cdc13-1* mutants able to grow at 36°C, the presence of a null mutation in *CDC13* was confirmed by mating to a *cdc13-1* mutant of the opposite mating type to confirm that the diploid was thermosensitive at 36°C.

BAR1^{+}*/bar1*Δ mutants were typed by PCR with either primers M1114 and M1156 to amplify a fragment of *BAR1* or M1157 and M1158 to amplify the hisG sequence, which replaced *BAR1*$^{+}$.

Presence of the *cdc15-2* mutation was confirmed by mating to a *cdc15-2* mutant of the opposite mating type (DLY349/DLY350) to see whether the diploid was thermosensitive at 36°C (homozygous for *cdc15-2*).

Strain Number	Genotype	Source
DLY349	*MATa cdc15-2*	Kim Nasmyth Lab.
DLY350	*MATα cdc15-2*	Kim Nasmyth Lab.
DLY640	*MATa*	Rodney Rothstein
DLY657	*MATa rad9Δ::HIS3*	(Zubko et al., 2004)
DLY658	*MATα rad9Δ::HIS3*	(Zubko et al., 2004)
DLY1108	*MATa cdc13-1*	(Zubko et al., 2004)
DLY1195	*MATα cdc13-1*	(Zubko et al., 2004)
DLY1255	*MATa cdc13-1 rad9Δ::HIS3*	(Zubko et al., 2004)
DLY1256	*MATα cdc13-1 rad9Δ::HIS3*	(Zubko et al., 2004)
DLY1256	*MATα cdc13-1 rad9Δ::HIS3*	(Zubko et al., 2004)
DLY1257	*MATa cdc13-1 rad24Δ::TRP1*	(Zubko et al., 2004)
DLY1258	*MATα cdc13-1 rad24Δ::TRP1*	(Zubko et al., 2004)
DLY1259	*MATa cdc13-1 rad24Δ::TRP1 rad9Δ::HIS3*	(Zubko et al., 2004)
DLY1272	*MATα exo1Δ::LEU2*	(Zubko et al., 2004)
DLY1273	*MATα exo1Δ::LEU2*	(Zubko et al., 2004)
DLY1296	*MATa cdc13-1 exo1Δ::LEU2*	(Zubko et al., 2004)
DLY1297	*MATα cdc13-1 exo1Δ::LEU2*	(Zubko et al., 2004)
DLY1358	*MATα cdc13-1 rad24Δ::TRP1 rad9Δ::HIS3*	(Zubko et al., 2004)
DLY1377	*MATa rad27Δ::TRP1*	LSY702 2A. Generous gift from Alain Nicolas.
DLY1408	*MATa exo1Δ::LEU2 yku70::HIS3*	(Maringele and Lydall, 2002)
DLY1412	*MATa yku70Δ::HIS3*	(Maringele and Lydall, 2002)
DLY1434	*MATa bar1Δ::hisG cdc15-2 cdc13-1 exo1Δ::LEU2 rad24Δ::TRP1*	(Zubko et al., 2004)
DLY1470	*MATa bar1Δ::hisG cdc15-2 cdc13-1 rad9Δ::HIS3*	(Zubko et al., 2004)
DLY1569	*MATα rad52Δ::TRP1*	(Maringele and Lydall, 2004a)
DLY1628	*MATα tlc1Δ::HIS3 yCP::TLC1::URA3*	(Maringele and Lydall, 2004a)
DLY1692	*MATa cdc13-1 rad9Δ::HIS3 exo1Δ::LEU2*	(Zubko et al., 2004)
DLY1693	*MATα cdc13-1 rad9Δ::HIS3 exo1Δ::LEU2*	(Zubko et al., 2004)
DLY1694	*MATα cdc13-1 rad24Δ::TRP1 rad9Δ::HIS3 exo1Δ::LEU2*	(Zubko et al., 2004)
DLY1695	*MATa cdc13-1 rad24Δ::TRP1 rad9Δ::HIS3 exo1Δ::LEU2*	(Zubko et al., 2004)

DLY1696	*MATα cdc13-1 exo1Δ::LEU2 rad24Δ::TRP1*	(Zubko et al., 2004)
DLY1696	*MATα cdc13-1 rad24Δ::TRP1 exo1Δ::LEU2*	(Zubko et al., 2004)
DLY1697	*MATα cdc13-1 rad24Δ::TRP1 exo1Δ::LEU2*	(Zubko et al., 2004)
DLY1701	*MATα exo1Δ::LEU2 rad24Δ::TRP1*	(Zubko et al., 2004)
DLY2384	*MATa cdc13-1 pif1Δ::KANMX*	(Downey et al., 2006)
DLY3001	*MATα*	Rodney Rothstein
DLY3799	*MATα can1Δ ::STE2pr-Sp_his5 lyp1Δ::STE3pr-LEU2 his3Δ1 leu2Δ0 ura3Δ0*	Y8205
DLY4681	*MATa cdc13-1 pif1Δ::KANMX ogg1Δ::NATMX*	2384 transformed with *ogg1Δ::NATMX*
DLY4718	*MATα cdc13-1 sgs1Δ::KANMX*	(Ngo and Lydall, 2010)
DLY4719	*MATa cdc13-1 sgs1Δ::KANMX*	(Ngo and Lydall, 2010)
DLY4721	*MATa sgs1Δ::KANMX*	(Ngo and Lydall, 2010)
DLY4722	*MATa sgs1Δ::KANMX*	(Ngo and Lydall, 2010)
DLY4863	*MATa pif1-m1*	DLY640 transformed with pDL1213 and popped-out
DLY4866	*MATa pif1-m2*	DLY640 transformed with pDL1215 and popped-out
DLY4872	*MATa cdc13-1 pif1Δ::NATMX*	DDY244
DLY4872	*MATa pif1Δ::NATMX*	DDY244
DLY4872	*MATa pif1Δ::NATMX*	DDY244
DLY4873	*MATα cdc13-1 pif1Δ::NATMX*	DDY244
DLY4873	*MATα pif1Δ::NATMX*	DDY244
DLY4873	*MATα pif1Δ::NATMX*	DDY244
DLY4874	*MATa cdc13-1 pif1Δ::NATMX*	DDY244
DLY4875	*MATα cdc13-1 pif1Δ::NATMX*	DDY244
DLY4876	*MATa pif1Δ::NATMX rad9Δ::HIS3*	DDY244
DLY4877	*MATα pif1Δ::NATMX rad9Δ::HIS3*	DDY244
DLY4878	*MATa cdc13-1 rad9Δ::HIS3 pif1Δ::NATMX*	DDY244
DLY4879	*MATα cdc13-1 rad9Δ::HIS3 pif1Δ::NATMX*	DDY244
DLY4880	*MATa ogg1Δ::NATMX*	DDY241
DLY4881	*MATα ogg1Δ::NATMX*	DDY241
DLY4882	*MATa cdc13-1 ogg1Δ::NATMX*	DDY241
DLY4883	*MATα cdc13-1 ogg1Δ::NATMX*	DDY241
DLY4884	*MATa ogg1Δ::NATMX rad9Δ::HIS3*	DDY241
DLY4885	*MATα ogg1Δ::NATMX rad9Δ::HIS3*	DDY241

DLY4886	*MATa cdc13-1 ogg1Δ::NATMX*	DDY241
DLY4887	*MATα cdc13-1 ogg1Δ::NATMX*	DDY241
DLY4940	*MATα ogg1Δ::NATMX pif1Δ::KANMX*	4681 x 658
DLY4941	*MATα ogg1Δ::NATMX pif1Δ::KANMX*	4681 x 658
DLY4942	*MATα cdc13-1 pif1Δ::KANMX ogg1Δ::NATMX*	4861 x 658
DLY4943	*MATα cdc13-1 pif1Δ::KANMX ogg1Δ::NATMX*	4861 x 658
DLY4944	*MATa pif1Δ::KANMX ogg1Δ::NATMX rad9Δ::HIS3*	4681 x 658
DLY4945	*MATα pif1Δ::KANMX ogg1Δ::NATMX rad9Δ::HIS3*	4681 x 658
DLY4946	*MATa cdc13-1 ogg1Δ::NATMX pif1Δ::KANMX rad9Δ::HIS3*	4861 x 658
DLY4947	*MATα cdc13-1 ogg1Δ::NATMX pif1Δ::KANMX rad9Δ::HIS3*	4861 x 658
DLY5110	*MATα can1Δ::STE2pr-Sp_his5 lyp1Δ::STE3pr-LEU2 his3Δ1 leu2Δ0 ura3Δ0 pif1Δ::NATMX*	Marker Swap of DLY5318 with pDL1155
DLY5205	*MATα bar1Δ::hisG cdc15-2 cdc13-1 pif1Δ::NATMX*	1470 x 4873
DLY5318	*MATα pif1Δ::KANMX*	*pif1*Δ from Lydall Lab deletion library v1.
DLY5323	*MATa cdc13-1 exo1Δ::LEU2 pif1Δ::NATMX*	4874 x 1696
DLY5324	*MATα cdc13-1 exo1Δ::LEU2 pif1Δ::NATMX*	4874 x 1696
DLY5325	*MATa cdc13-1 rad24Δ::TRP1 pif1Δ::NATMX*	4874 x 1696
DLY5326	*MATα cdc13-1 rad24Δ::TRP1 pif1Δ::NATMX*	4874 x 1696
DLY5327	*MATa cdc13-1 rad24Δ::TRP1 exo1Δ::LEU2 pif1Δ::NATMX*	4874 x 1696
DLY5328	*MATα exo1Δ::LEU2 rad24Δ::TRP1 pif1Δ::NATMX cdc13-1*	4874 x 1696
DLY5328	*MATα cdc13-1 rad24Δ::TRP1 exo1Δ::LEU2 pif1Δ::NATMX*	4874 x 1696
DLY5331	*MATa cdc13-1 exo1Δ::LEU2 rad9Δ::HIS3 pif1Δ::NATMX*	4878 x 1694
DLY5332	*MATα cdc13-1 exo1Δ::LEU2 rad9Δ::HIS3 pif1Δ::NATMX*	4878 x 1694
DLY5333	*MAT cdc13-1 rad24Δ::TRP1 rad9Δ::HIS3 pif1Δ::NATMX*	4878 x 1694
DLY5334	*MAT cdc13-1 rad24Δ::TRP1 rad9Δ::HIS3 pif1Δ::NATMX*	4878 x 1694
DLY5335	*MATa cdc13-1 rad24Δ::TRP1 rad9Δ::HIS3 exo1Δ::LEU2 pif1Δ::NATMX*	4878 x 1694
DLY5336	*MATα cdc13-1 rad24Δ::TRP1 rad9Δ::HIS3 exo1Δ::LEU2 pif1Δ::NATMX*	4878 x 1694
DLY5337	*MATα rad27Δ::TRP1*	1377 x 4879
DLY5338	*MATa rad27Δ::TRP1 pif1Δ::NATMX*	1377 x 4879
DLY5339	*MATα rad27Δ::TRP1 pif1Δ::NATMX*	1377 x 4879
DLY5340	*MATa cdc13-1 rad27Δ::TRP1*	1377 x 4879
DLY5341	*MATα cdc13-1 rad27Δ::TRP1*	1377 x 4879
DLY5342	*MATa cdc13-1 rad27Δ::TRP1 pif1Δ::NATMX*	1377 x 4879

DLY5343	*MATα cdc13-1 rad27Δ::TRP1 pif1Δ::NATMX*	1377 x 4879
DLY5353	*MATa cdc13-1 pif1-m2*	4866 x 1256
DLY5358	*MATa bar1Δ::hisG cdc15-2 cdc13-1*	1434 x 5205
DLY5359	*MATa bar1Δ::hisG cdc15-2 cdc13-1 pif1Δ::NATMX*	1434 x 5205
DLY5360	*MATa bar1Δ::hisG cdc15-2 cdc13-1 exo1Δ::LEU2*	1434 x 5205
DLY5361	*MATa bar1Δ::hisG cdc15-2 cdc13-1 exo1Δ::LEU2 pif1Δ::NATMX*	1434 x 5205
DLY5395	*MATa exo1Δ::LEU2 pif1Δ::NATMX*	4872 x 1701
DLY5396	*MATα exo1Δ::LEU2 pif1Δ::NATMX*	4872 x 1701
DLY5460	*MATa cdc13-1 exo1Δ::LEU2 pif1-m2*	5353 x 1696
DLY5461	*MATα cdc13-1 exo1Δ::LEU2 pif1-m2*	5353 x 1696
DLY5506	*MATa yku70::HIS3*	1408 x 4873
DLY5507	*MATα yku70Δ::HIS3*	1408 x 4872
DLY5508	*MATa yku70Δ::HIS3 pif1Δ::NATMX*	1408 x 4872
DLY5509	*MATα yku70Δ::HIS3 pif1Δ::NATMX*	1408 x 4872
DLY5510	*MATa yku70Δ::HIS3 exo1Δ::LEU2*	1408 x 4872
DLY5511	*MATα yku70Δ::HIS3 exo1Δ::LEU2*	1408 x 4872
DLY5512	*MATa yku70Δ::HIS3 exo1Δ::LEU2 pif1Δ::NATMX*	1408 x 4872
DLY5513	*MATα yku70Δ::HIS3 exo1Δ::LEU2 pif1Δ::NATMX*	1408 x 4872
DLY5532	*MATa cdc13-1 pif1-m1*	4863 x 1256
DLY5678	*MATa pif1-hd*	DLY640 transformed with pDL1293 and popped-out
DLY5682	*MATa cdc13-1 exo1Δ::LEU2 pif1-m1*	5532 x 1696
DLY5683	*MATα cdc13-1 exo1Δ::LEU2 pif1-m1*	5532 x 1696
DLY5702	*MATα pol32Δ::KANMX*	DDY335
DLY5703	*MATa pol32Δ::KANMX*	DDY335
DLY5704	*MATα pol32Δ::KANMX*	DDY335
DLY5715	*MATa cdc13-1 sgs1Δ::KANMX pif1Δ::NATMX*	4719 x 5324
DLY5716	*MATα cdc13-1 sgs1Δ::KANMX pif1Δ::NATMX*	4719 x 5324
DLY5717	*MATa cdc13-1 pol32Δ::KANMX*	DDY335
DLY5718	*MATa cdc13-1 pol32Δ::KANMX*	DDY335
DLY5723	*MATa cdc13-1 pif1-hd*	5678 x 1256
DLY5742	*MATa pif1Δ::NATMX dna2Δ::HPHMX*	DDY352
DLY5743	*MATα pif1Δ::NATMX dna2Δ::HPHMX*	DDY352

DLY5744	*MATa cdc13-1 pif1Δ::NATMX dna2Δ::HPHMX*	DDY352
DLY5745	*MATalpha cdc13-1 pif1Δ::NATMX dna2Δ::HPHMX*	DDY352
DLY5771	*MATa sgs1Δ::KANMX pif1Δ::NATMX*	4721 x 5396
DLY5772	*MATα sgs1Δ::KANMX pif1Δ::NATMX*	4721 x 5396
DLY5781	*MATa cdc13-1 exo1Δ::LEU2 pif1-hd*	5723 x 1696
DLY5782	*MATα cdc13-1 exo1Δ::LEU2 pif1-hd*	5723 x 1696
DLY5860	*MATα pif1Δ::NATMX exo1Δ::LEU2 cdc13Δ::HPHMX*	DDY341, passage 1 (23°C)
DLY5861	*MATα pif1Δ::NATMX exo1Δ::LEU2 cdc13Δ::HPHMX*	DDY341, passage 1 (23°C)
DLY5862	*MATα pif1Δ::NATMX exo1Δ::LEU2 cdc13Δ::HPHMX*	DDY341, passage 1 (23°C)
DLY5863	*MATα pif1Δ::NATMX exo1Δ::LEU2 cdc13Δ::HPHMX*	DDY341, passage 1 (23°C)
DLY5864	*MATa pif1Δ::NATMX exo1Δ::LEU2 cdc13Δ::HPHMX*	DDY341, passage 1 (23°C)
DLY5909	*MATα pif1Δ::NATMX exo1Δ::LEU2 cdc13Δ::HPHMX*	DDY341, passage 11 (23°C)
DLY5910	*MATα pif1Δ::NATMX exo1Δ::LEU2 cdc13Δ::HPHMX*	DDY341, passage 11 (23°C)
DLY5911	*MATα pif1Δ::NATMX exo1Δ::LEU2 cdc13Δ::HPHMX*	DDY341, passage 11 (23°C)
DLY5912	*MATα pif1Δ::NATMX exo1Δ::LEU2 cdc13Δ::HPHMX*	DDY341, passage 11 (23°C)
DLY5913	*MATa tlc1Δ::HIS3*	5395 x 1628, passage 1 (23°C)
DLY5914	*MATα tlc1Δ::HIS3*	5395 x 1628, passage 1 (23°C)
DLY5915	*MATa exo1Δ::LEU2 pif1Δ::NATMX*	5395 x 1628, passage 1 (23°C)
DLY5916	*MATα exo1Δ::LEU2 pif1Δ::NATMX*	5395 x 1628, passage 1 (23°C)
DLY5917	*MATa tlc1Δ::HIS3 exo1Δ::LEU2 pif1Δ::NATMX*	5395 x 1628, passage 1 (23°C)
DLY5918	*MATα tlc1Δ::HIS3 exo1Δ::LEU2 pif1Δ::NATMX*	5395 x 1628, passage 1 (23°C)
DLY5919	*MATa tlc1Δ::HIS3*	5395 x 1628, passage 11 (23°C)
DLY5920	*MATα tlc1Δ::HIS3*	5395 x 1628, passage 11 (23°C)
DLY5921	*MATa exo1Δ::LEU2 pif1Δ::NATMX*	5395 x 1628, passage 11 (23°C)
DLY5922	*MATα exo1Δ::LEU2 pif1Δ::NATMX*	5395 x 1628, passage 11 (23°C)
DLY5923	*MATa tlc1Δ::HIS3 exo1Δ::LEU2 pif1Δ::NATMX*	5395 x 1628, passage 11 (23°C)
DLY5924	*MATα tlc1Δ::HIS3 exo1Δ::LEU2 pif1Δ::NATMX*	5395 x 1628, passage 11 (23°C)
DLY5925	*MATa*	5395 x 1628, passage 1 (30°C)
DLY5926	*MATa pif1Δ::NATMX*	5395 x 1628, passage 1 (30°C)
DLY5927	*MATa exo1Δ::LEU2*	5395 x 1628, passage 1 (30°C)
DLY5928	*MATa exo1Δ::LEU2 pif1Δ::NATMX*	5395 x 1628, passage 1 (30°C)
DLY5929	*MATa tlc1Δ::HIS3*	5395 x 1628, passage 1 (30°C)

DLY5930	*MATα tlc1Δ::HIS3*	5395 x 1628, passage 1 (30°C)
DLY5931	*MATa tlc1Δ::HIS3 pif1Δ::NATMX*	5395 x 1628, passage 1 (30°C)
DLY5932	*MATα tlc1Δ::HIS3 pif1Δ::NATMX*	5395 x 1628, passage 1 (30°C)
DLY5933	*MATa tlc1Δ::HIS3 exo1Δ::LEU2*	5395 x 1628, passage 1 (30°C)
DLY5934	*MATα tlc1Δ::HIS3 exo1Δ::LEU2*	5395 x 1628, passage 1 (30°C)
DLY5935	*MATa tlc1Δ::HIS3 exo1Δ::LEU2 pif1Δ::NATMX*	5395 x 1628, passage 1 (30°C)
DLY5936	*MATα tlc1Δ::HIS3 exo1Δ::LEU2 pif1Δ::NATMX*	5395 x 1628, passage 1 (30°C)
DLY5937	*MATa*	5395 x 1628, passage 15 (30°C)
DLY5938	*MATa pif1Δ::NATMX*	5395 x 1628, passage 15 (30°C)
DLY5939	*MATa exo1Δ::LEU2*	5395 x 1628, passage 15 (30°C)
DLY5940	*MATa exo1Δ::LEU2 pif1Δ::NATMX*	5395 x 1628, passage 15 (30°C)
DLY5941	*MATa tlc1Δ::HIS3*	5395 x 1628, passage 15 (30°C)
DLY5942	*MATα tlc1Δ::HIS3*	5395 x 1628, passage 15 (30°C)
DLY5943	*MATa tlc1Δ::HIS3 pif1Δ::NATMX*	5395 x 1628, passage 15 (30°C)
DLY5944	*MATα tlc1Δ::HIS3 pif1Δ::NATMX*	5395 x 1628, passage 15 (30°C)
DLY5945	*MATa tlc1Δ::HIS3 exo1Δ::LEU2*	5395 x 1628, passage 15 (30°C)
DLY5946	*MATα tlc1Δ::HIS3 exo1Δ::LEU2*	5395 x 1628, passage 15 (30°C)
DLY5947	*MATa tlc1Δ::HIS3 exo1Δ::LEU2 pif1Δ::NATMX*	5395 x 1628, passage 15 (30°C)
DLY5948	*MATα tlc1Δ::HIS3 exo1Δ::LEU2 pif1Δ::NATMX*	5395 x 1628, passage 15 (30°C)
DLY5989	*MATα pif1Δ::NATMX exo1::LEU2 cdc13::HPHMX yEP::URA3::CDC13*	5860 transformed with pDL1012
DLY5991	*MATa pif1Δ::NATMX exo1::LEU2 cdc13::HPHMX yEP::URA3::CDC13*	5864 transformed with pDL1012
DLY6093	*MATα yEP::URA3::CDC13*	DDY419 (30°C)
DLY6094	*MATα tlc1Δ::HIS3 yEP::URA3::CDC13*	DDY419 (30°C)
DLY6095	*MATa exo1Δ::LEU2 pif1Δ::NATMX yEP::URA3::CDC13*	DDY419 (30°C)
DLY6096	*MATα tlc1Δ::HIS3 exo1Δ::LEU2 pif1Δ::NATMX yEP::URA3::CDC13*	DDY419 (30°C)
DLY6097	*MATa cdc13Δ::HPHMX yEP::URA3::CDC13*	DDY419 (30°C)
DLY6098	*MATα cdc13Δ::HPHMX tlc1Δ::HIS3 yEP::URA3::CDC13*	DDY419 (30°C)
DLY6099	*MATα cdc13Δ::HPHMX exo1Δ::LEU2 pif1Δ::NATMX yEP::URA3::CDC13*	DDY419 (30°C)
DLY6100	*MATα cdc13Δ::HPHMX tlc1Δ::HIS3 exo1Δ::LEU2 pif1Δ::NATMX yEP::URA3::CDC13*	DDY419 (30°C)
DLY6331	*MATα ade2::NATMX est2::KANMX yCP::URA3::EST2*	YAB618. Generous Gift from Alessandro Bianchi.
DLY6369	*MATα est2::KANMX yCP::URA3::EST2*	640 x 6331

DLY6440	*MATα yEP::URA3::CDC13*	5991 x 1628
DLY6441	*MATα yEP::URA3::CDC13*	5991 x 1628
DLY6442	*MATa yEP::URA3::CDC13 pif1Δ::NATMX exo1Δ::LEU2*	5991 x 1628
DLY6443	*MATa yEP::URA3::CDC13 pif1Δ::NATMX exo1Δ::LEU2*	5991 x 1628
DLY6444	*MATa yEP::URA3::CDC13 tlc1Δ::HIS3*	5991 x 1628
DLY6445	*MATa yEP::URA3::CDC13 tlc1Δ::HIS3*	5991 x 1628
DLY6446	*MATa yEP::URA3::CDC13 pif1Δ::NATMX exo1Δ::LEU2 tlc1Δ::HIS3*	5991 x 1628
DLY6447	*MATα yEP::URA3::CDC13 pif1Δ::NATMX exo1Δ::LEU2 tlc1Δ::HIS3*	5991 x 1628
DLY6448	*MATa yEP::URA3::CDC13 cdc13Δ::HPHMX*	5991 x 1628
DLY6449	*MATa yEP::URA3::CDC13 cdc13Δ::HPHMX*	5991 x 1628
DLY6450	*MATa yEP::URA3::CDC13 pif1Δ::NATMX exo1Δ::LEU2 cdc13Δ::HPHMX*	5991 x 1628
DLY6451	*MATα yEP::URA3::CDC13 pif1Δ::NATMX exo1Δ::LEU2 cdc13Δ::HPHMX*	5991 x 1628
DLY6452	*MATα yEP::URA3::CDC13 tlc1Δ::HIS3 cdc13Δ::HPHMX*	5991 x 1628
DLY6453	*MATα yEP::URA3::CDC13 tlc1Δ::HIS3 cdc13Δ::HPHMX*	5991 x 1628
DLY6454	*MATα yEP::URA3::CDC13 pif1Δ::NATMX exo1Δ::LEU2 tlc1Δ::HIS3 cdc13Δ::HPHMX*	5991 x 1628
DLY6455	*MATa yEP::URA3::CDC13 pif1Δ::NATMX exo1Δ::LEU2 tlc1Δ::HIS3 cdc13Δ::HPHMX*	5991 x 1628
DLY6456	*MATa yEP::URA3::CDC13*	5991 x 5702
DLY6457	*MATα yEP::URA3::CDC13*	5991 x 5702
DLY6458	*MATα yEP::URA3::CDC13 pif1Δ::NATMX exo1Δ::LEU2*	5991 x 5702
DLY6459	*MATα yEP::URA3::CDC13 pif1Δ::NATMX exo1Δ::LEU2*	5991 x 5702
DLY6460	*MATa yEP::URA3::CDC13 pol32Δ::KANMX*	5991 x 5702
DLY6461	*MATα yEP::URA3::CDC13 pol32Δ::KANMX*	5991 x 5702
DLY6462	*MATa yEP::URA3::CDC13 pif1Δ::NATMX exo1Δ::LEU2 pol32Δ::KANMX*	5991 x 5702
DLY6463	*MATα yEP::URA3::CDC13 pif1Δ::NATMX exo1Δ::LEU2 pol32Δ::KANMX*	5991 x 5702
DLY6464	*MATa yEP::URA3::CDC13 cdc13Δ::HPHMX*	5991 x 5702
DLY6465	*MATa yEP::URA3::CDC13 cdc13Δ::HPHMX*	5991 x 5702
DLY6466	*MATa yEP::URA3::CDC13 pif1Δ::NATMX exo1Δ::LEU2 cdc13Δ::HPHMX*	5991 x 5702
DLY6467	*MATα yEP::URA3::CDC13 pif1Δ::NATMX exo1Δ::LEU2 cdc13Δ::HPHMX*	5991 x 5702
DLY6468	*MATα yEP::URA3::CDC13 pol32Δ::KANMX cdc13Δ::HPHMX*	5991 x 5702
DLY6469	*MATa yEP::URA3::CDC13 pol32Δ::KANMX cdc13Δ::HPHMX*	5991 x 5702
DLY6470	*MATa yEP::URA3::CDC13 pif1Δ::NATMX exo1Δ::LEU2 pol32Δ::KANMX cdc13Δ::HPHMX*	5991 x 5702

DLY6471	*MATα yEP::URA3::CDC13 pif1Δ::NATMX exo1Δ::LEU2 pol32Δ::KANMX cdc13Δ::HPHMX*	5991 x 5702
DLY6520	*MATa yEP::URA3::CDC13*	5506 x 5989
DLY6521	*MATα yEP::URA3::CDC13*	5506 x 5989
DLY6522	*MATα yEP::URA3::CDC13 pif1Δ::NATMX exo1Δ::LEU2*	5506 x 5989
DLY6523	*MATa yEP::URA3::CDC13 pif1Δ::NATMX exo1Δ::LEU2*	5506 x 5989
DLY6524	*MATa yEP::URA3::CDC13 yku70Δ::HIS3*	5506 x 5989
DLY6525	*MATα yEP::URA3::CDC13 yku70Δ::HIS3*	5506 x 5989
DLY6526	*MATα yEP::URA3::CDC13 pif1Δ::NATMX exo1Δ::LEU2 yku70Δ::HIS3*	5506 x 5989
DLY6527	*MATα yEP::URA3::CDC13 pif1Δ::NATMX exo1Δ::LEU2 yku70Δ::HIS3*	5506 x 5989
DLY6528	*MATa yEP::URA3::CDC13 cdc13Δ::HPHMX*	5506 x 5989
DLY6529	*MATα yEP::URA3::CDC13 cdc13Δ::HPHMX*	5506 x 5989
DLY6530	*MATα yEP::URA3::CDC13 pif1Δ::NATMX exo1Δ::LEU2 cdc13Δ::HPHMX*	5506 x 5989
DLY6531	*MATa yEP::URA3::CDC13 pif1Δ::NATMX exo1Δ::LEU2 cdc13Δ::HPHMX*	5506 x 5989
DLY6532	*MATa yEP::URA3::CDC13 yku70Δ::HIS3 cdc13Δ::HPHMX*	5506 x 5989
DLY6533	*MATa yEP::URA3::CDC13 yku70Δ::HIS3 cdc13Δ::HPHMX*	5506 x 5989
DLY6534	*MATa yEP::URA3::CDC13 pif1Δ::NATMX exo1Δ::LEU2 yku70Δ::HIS3 cdc13Δ::HPHMX*	5506 x 5989
DLY6535	*MATα yEP::URA3::CDC13 pif1Δ::NATMX exo1Δ::LEU2 yku70Δ::HIS3 cdc13Δ::HPHMX*	5506 x 5989
DLY6552	*MATa yEP::URA3::CDC13*	5991 x 1569
DLY6553	*MATα yEP::URA3::CDC13*	5991 x 1569
DLY6554	*MATa yEP::URA3::CDC13 pif1Δ::NATMX exo1Δ::LEU2*	5991 x 1569
DLY6555	*MATα yEP::URA3::CDC13 pif1Δ::NATMX exo1Δ::LEU2*	5991 x 1569
DLY6556	*MATa yEP::URA3::CDC13 rad52Δ::TRP1*	5991 x 1569
DLY6557	*MATα yEP::URA3::CDC13 rad52Δ::TRP1*	5991 x 1569
DLY6558	*MATa yEP::URA3::CDC13 pif1Δ::NATMX exo1Δ::LEU2 rad52Δ::TRP1*	5991 x 1569
DLY6559	*MATa yEP::URA3::CDC13 pif1Δ::NATMX exo1Δ::LEU2 rad52Δ::TRP1*	5991 x 1569
DLY6560	*MATa yEP::URA3::CDC13 cdc13Δ::HPHMX*	5991 x 1569
DLY6561	*MATa yEP::URA3::CDC13 cdc13Δ::HPHMX*	5991 x 1569
DLY6562	*MATα yEP::URA3::CDC13 pif1Δ::NATMX exo1Δ::LEU2 cdc13Δ::HPHMX*	5991 x 1569
DLY6563	*MATa yEP::URA3::CDC13 pif1Δ::NATMX exo1Δ::LEU2 cdc13Δ::HPHMX*	5991 x 1569
DLY6564	*MATα yEP::URA3::CDC13 rad52Δ::TRP1 cdc13Δ::HPHMX*	5991 x 1569
DLY6565	*MATα yEP::URA3::CDC13 rad52Δ::TRP1 cdc13Δ::HPHMX*	5991 x 1569

DLY6566	*MATa yEP::URA3::CDC13 pif1Δ::NATMX exo1Δ::LEU2 rad52Δ::TRP1 cdc13Δ::HPHMX*	5991 x 1569
DLY6567	*MATα yEP::URA3::CDC13 pif1Δ::NATMX exo1Δ::LEU2 rad52Δ::TRP1 cdc13Δ::HPHMX*	5991 x 1569
DDY179	*cdc13-1/CDC13^{+} rad9Δ::HIS3/RAD9^{+}*	DLY640 x DLY1256
DDY241	*cdc13-1/CDC13^{+} rad9Δ::HIS3/RAD9^{+} ogg1Δ::NATMX/OGG1^{+}*	Transformation of DDY179 with *ogg1Δ::NATMX*
DDY244	*cdc13-1/CDC13^{+} rad9Δ::HIS3/RAD9^{+} pif1Δ::NATMX/PIF1^{+}*	Transformation of DDY179 with *pif1Δ::NATMX*
DDY335	*cdc13-1/CDC13^{+} rad9Δ::HIS3/RAD9^{+} pol32Δ::KANMX/POL32^{+}*	Transformation of DDY179 with *pol32Δ::KANMX*
DDY340	*cdc13Δ::HPHMX/CDC13^{+} pif1Δ::NATMX/PIF1^{+} exo1Δ::LEU2/EXO1^{+}*	Transformation of DLY4872 x DLY1273 with *cdc13Δ::HPHMX*
DDY341	*cdc13Δ::HPHMX/CDC13^{+} pif1Δ::NATMX/PIF1^{+} exo1Δ::LEU2/EXO1^{+}*	Transformation of DLY4872 x DLY1273 with *cdc13Δ::HPHMX*
DDY351	*cdc13Δ::HPHMX/CDC13^{+} tlc1Δ::HIS3/TLC1^{+} pif1Δ::NATMX/PIF1^{+} exo1Δ::LEU2/EXO1^{+}*	Transformation of DLY5395 x DLY1628 with *cdc13Δ::HPHMX*
DDY352	*cdc13-1/CDC13^{+} rad9Δ::HIS3/RAD9^{+} pif1Δ::NATMX/PIF1^{+} dna2Δ::NATMX/DNA2^{+}*	Transformation of DLY1256 x DLY4872 with *dna2Δ::HPHMX*
DDY419	*cdc13Δ::HPHMX/CDC13^{+} tlc1Δ::HIS3/TLC1^{+} pif1Δ::NATMX/PIF1^{+} exo1Δ::LEU2/EXO1^{+}yEP::URA3::CDC13*	Transformation of DDY351 with pDL1012

Table 1: yeast strains used in this study

2.1.2 Conditional mutants used in this study

The *cdc13-1* mutation in the essential gene *CDC13* causes a temperature-sensitive capping defect, permitting growth at 23°C (permissive temperature), eliminating growth at 36°C (non-permissive) and inhibiting growth at 25°C-30°C (semi-permissive) (Garvik et al., 1995).

The *cdc15-2* mutation in the essential gene *CDC15* causes a temperature-sensitive defect in mitotic exit. At the non-permissive temperature, mitotic exit is inhibited and cells remain arrested without loss of viability (Lydall and Weinert, 1995).

The *yku70*Δ mutation eliminates the Yku70 subunit of the Ku complex and causes a temperature-sensitive telomere capping defect, with a permissive temperature of 30°C, a non-permissive temperature of 37.5°C and a semi-permissive temperature of 34°C-37°C (Feldmann and Winnacker, 1993, Teo and Jackson, 2001).

The *pif1*Δ mutation eliminates the Pif1 helicase and causes a temperature-sensitive defect in mtDNA maintenance, with a permissive temperature on a non-fermentable carbon source (e.g. YEPG) of 23°C and a semi-permissive temperature range of 30°C-36°C, while being permissive at all temperatures on a fermentable carbon source (Van Dyck et al., 1992).

2.1.3 Strains with passage-dependent phenotypes

Strains lacking telomerase components (TLC1, Est2) or Cdc13 displayed passage-dependent phenotypes so, unless otherwise stated, all experimental strains and controls were germinated in parallel and (where possible) from the same diploid.

2.1.4 Standard Growth Conditions

Yeast strains were grown on agar plates by streaking for colonies and allowing growth to occur at 23°C for 3 days. To identify genetic markers, single colonies were patched onto YEPD plates and grown overnight, then replicated to selective plates and allowed to grow for 1-2 days. To make liquid cultures, 3-5 single colonies were pooled, and a small amount was innoculated into 2 ml YEPD and then grown at 23°C overnight (for overnight cultures) or for 2 days (for saturated cultures) in lidded glass tubes with aeration. Exponentially-dividing cultures were prepared by diluting a saturated culture 1:500-1:1500 and allowing to grow for approximately 16 hours at 23°C with shaking at

180 RPM. Exponentially-dividing cultures were kept at 0.5-2.0x10^7 cells/ml with shaking at 180 RPM at the appropriate experimental temperature.

2.1.5 Recipes for yeast media

All reagents were from Sigma or Formedium, unless otherwise stated.

Yeast Extract, Peptone, Dextrose (YEPD)

1% yeast extract, 2% peptone, 2% dextrose, 75 mg/L adenine.

For 1L of media: 10 g of yeast extract and 20 g peptone were made up to 935 ml with MQ water, shaken to mix, autoclaved then cooled to 60°C, before 50 ml of 40% (w/v) dextrose and 15 ml of 0.5% (w/v) adenine were added.

For solid media, 20 g agar was added prior to autoclaving.

YEPD + G418/ClonNAT/Hygromycin B

Same as for YEPD except 1ml of 200 mg/ml G418, 1 ml 100 mg/ml ClonNAT or 1 ml 300 mg/ml Hygromycin B was added following autoclaving.

Camptothecin Media (CPT)

Same as for YEPD except 10 mM Camptothecin in DMSO was added following autoclaving to a final concentration of 4-500 μM.

Yeast extract, Peptone, Glycerol (YEPG)

1% yeast extract, 2% peptone, 3% glycerol, 75 mg/L adenine.

Same as for YEPD except 30 ml glycerol was added prior to autoclaving and dextrose was substituted with MQ water.

Synthetic Media

0.13% amino acids, 0.17% yeast nitrogen base, 0.5% ammonium sulphate

For 1 L of media: 1.3 g of amino acid drop out powder (2.5 g adenine, 1.2 g argenine, 6.0 g aspartic acid, 6.0 g glutamic acid, 1.2 g histidine, 3.6 g leucine, 1.8 g lysine, 1.2 g methionine, 3.0 g phenylalanine. 22.5 g serine, 12.0 g threonine, 2.4 g tryptophan, 1.8 g tyrosine, 9.0 g valine, 1.2 g uracil), 1.7 g of yeast nitrogen base and 5 g of ammonium sulphate were made up to 500 ml with MQ water, shaken to mix, autoclaved, mixed

with 500 ml of autoclaved MQ water (or 500 ml autoclaved MQ water containing 20 g agar, for solid media), then cooled to 60°C.

-Histidine/-Uracil/-Leucine/-Tryptophan Media

Same as synthetic media, except with exclusion of the appropriate amino acid(s) from the drop out powder.

TMPyP4 Media (TMPyP4)

Same as synthetic media, except TMPyP4 (50 mg/ml stock in water) was added to a final concentration of 100 μM following autoclaving.

5-Fluoroorotic Acid Media (FOA)

0.13% amino acids, 0.67% yeast nitrogen base, 0.005% uracil, 0.1% FOA

For 1L of media: 1.3g of -Ura amino acid drop out powder (same as for synthetic media, but lacking uracil), 6.7g of yeast nitrogen base, 50mg Uracil and 1g of 5-fluoroorotic acid were made up to 500ml with MQ water, shaken to mix, autoclaved, mixed with 500ml of autoclaved MQ water (or 500ml autoclaved MQ water containing 20g agar, for solid media), then cooled to 60°C.

2.2 Bacterial strains and growth

2.2.1 Bacterial strains

Bacteria used were all transformants of XL1-Blue competent *Escherichia coli* (*recA1 endA1 gyrA96 thi-1 hsdR17 supE44 relA1 lac [F′ proAB lacI^{q}ZΔM15 Tn10 (Tet^{r})]*) from Stratagene.

2.2.2 Standard growth conditions

Bacteria were grown on agar plates by streaking for colonies and allowing to grow at 36°C for 16 hours. To make overnight cultures, single colonies were innoculated into 2ml LB and then grown at 36°C for 16 hours in a lidded glass tubes with aeration.

2.2.3 Recipes for bacterial media

Lysogeny Broth (LB)

0.5% yeast extract, 1% peptone, 1% NaCL

For 1 L of media: 5 g of yeast extract, 10 g of peptone and 10 g of NaCl were made up to 1 L with MQ water, shaken to mix, autoclaved then cooled to 60°C.

For solid media, 20 g agar was added prior to autoclaving

LB + Ampicillin (LB + Amp)

0.5% yeast extract, 1% peptone, 1% NaCL, 50μg/ml Ampicillin

Same as LB but 1 ml of 50 mg/ml Ampicillin was added after cooling.

Super Optimal broth with Catabolite repression (SOC)

0.5% yeast extract, 2% tryptone, 9.7 mM NaCl, 2.2 mM KCl, 0.36% glucose, 10 mM $MgCl_2$, 10 mM $MgSO_4$

For 1 L of media: 5 g of yeast extract, 20 g of tryptone, 0.585 g NaCL, 0.166 g KCl, 3.6 g Glucose, 10 ml $MgCl_2$ (1 M) and 10 ml $MgSO_4$ (1 M) was made up to 1 L with MQ water, shaken to mix, autoclaved then cooled to 60°C.

2.2.4 Bacterial transformation

XL1-Blue cells (Stratagene) were transformed with 1 μL of plasmid DNA as per the manufacturer's instructions, then plated onto LB + Amp and grown 16 hours at 36°C.

2.2.5 Plasmid minipreps

Overnight cultures in LB + Amp were spun in a bench-top centrifuge at 13,000 RPM to pellet cells, the supernatant was aspirated and then minipreps were performed using QIAprep Spin Miniprep Kits (Qiagen) using a microcentrifuge, as per the manufacturer's instructions.

2.2.6 Plasmids used in this study

Plasmids used in this study are listed below and are stored at -20°C in 1X TE under standard conditions.

Plasmid Number	Details	Source
pDL698	Plasmid for amplification of hphMX4 gene deletion cassette by PCR.	pAG32 (Goldstein and McCusker, 1999). Generous gift from Vincent Geli.
pDL987	Carries a ~1000bp fragment of a yeast chromosomal end that contains 120-base pair telomere repeats and part of the Y' repeat, which can be released by digestion with BamHI and XhoI.	pHT128 (Tsubouchi and Ogawa, 2000). Generous gift of Hideo Tsubouchi.
pDL1012	*yEP::URA3::CDC13* yeast 2μ plasmid carrying *CDC13* on a 4.5kbp ApaI fragment, marked with *URA3*	yep24::CDC13-1-4 (Garvik et al., 1995)
pDL1042	Plasmid for amplification of kanMX6 gene deletion cassette by PCR	pFA6a-kanMX6 (Longtine et al., 1998)
pDL1155	Plasmid for switching deletion cassettes to *NATMX*. Cut with EcoRI and transform in to swap markers.	pCRII-TOPO[TA::MX4-natR] (Tong and Boone, 2006)
pDL1213	Plasmid for integrating *pif1-m1* point mutation into the genome by pop-in-pop-out. Cut with HindIII to transform and pop-in.	pVS30 (Schulz and Zakian, 1994). Generous gift from Virginia Zakian.
pDL1215	Plasmid for integrating *pif1-m2* point mutation into the genome by pop-in-pop-out. Cut with HindIII to transform and pop-in.	pVS31 (Schulz and Zakian, 1994). Generous gift from Virginia Zakian.
pDL1221	Plasmid for amplification of natMX4 gene deletion cassette by PCR.	pAG25 (Goldstein and McCusker, 1999). Generous gift from Vincent Geli.
pDL1223	Centromeric plasmid expressing both *URA3* and the *NATMX* resistance cassette.	pAG36 (Goldstein and McCusker, 1999). Generous gift from Vincent Geli.
pDL1293	Plasmid for integrating *pif1-hd* (K264R) point mutation into the genome by pop-in-pop-out. Cut with Bsu36I to transform and pop-in.	pJL71 (Ribeyre et al., 2009). Generous gift from Alain Nicolas.

Table 2: plasmids used in this study

2.3 Yeast Genetics and Cell Biology

2.3.1 Determination of mating type

Patches of individual colonies were replicated onto lawns of *MATa* and *MATα* cells, grown overnight to permit mating and then replicated onto media that would only permit the growth of diploid cells. DLY26 (*MATa*) and DLY2440 (*MATα*) were *HIS⁻ LEU⁻ URA⁻ TRP⁻* but would complement deficiencies in those biosynthetic pathways to form a *HIS⁺ LEU⁺ URA⁺ TRP⁺* diploid when mated to a W303 strain and thus could conveniently be used to score mating type.

2.3.2 Mating, sporulation and tetrad analysis

Two parental strains of opposite mating type were picked up by toothpick, mixed on a YEPD plate and incubated overnight at 23°C to mate. Diploids were either struck onto selective plates (that selected for markers present in both parents) and allowed to form colonies or obtained by streaking for single colonies, patching onto YEPD plates and replica plating to identify non-mating strains.

Individual diploid colonies were inoculated into 2ml YEPD and grown overnight with aeration. 0.5 ml of overnight culture was washed twice by spinning for 3 minutes at 1,000 RPM and washing with with 4 ml sterile water. Diploid cells were re-suspended in 2 ml 1% KOAc and cultured for 2-3 days at 23°C with aeration. After 3 days sporulation, the culture was examined by phase contrast microscopy to check for the presence of spores. If spores were present, the culture was transferred to an eppendorf tube and the cells were pelleted by spinning at 13,000 RPM for 10 seconds. The cell pellet was washed twice in sterile water and re-suspended in a final volume of 1 ml sterile water then stored at 4°C. 40 µl of spores were transferred to a sterile eppendorf and mixed with 2.4 µl glusulase enzyme and incubated at 30°C for 10-13 min (usually 12.5 min) until the sack around the tetrads was removed. The digested spores were then transferred to ice and 0.8 ml sterile water was added. 100 µl of digested spores were pipetted from the bottom of the tube and spread onto a YEPD plate along a marked line. Individual spores from ≤11 tetrads per plate were micromanipulated apart using a Microtec tetrad microscope then allowed to germinate and form colonies at 23°C for 3-5 days or 30°C for 2-3 days.

Germinated spores were patched to another YEPD plate and grown overnight at 23°C. The YEPD plate was then replica plated onto appropriate selection plates for genotype identification.

2.3.3 Gene deletion using antibiotic resistance constructs

Gene deletion constructs were designed and amplified using plasmids constructs, as previously described (Goldstein and McCusker, 1999, Longtine et al., 1998) using PCR to amplify and tag antibiotic resistance cassettes with approximately 20 base pairs of sequence immediately flanking the relevant ORF. Constructs were designed to replace only the ORF and no flanking sequence, except when the flanking sequence contained repeat- or low GC-sequences that precluded primer design.

Gene deletion constructs were amplified by PCR, run on an agarose, gel extracted and then transformed into diploid strains by high efficiency transformation of yeast (see Section **2.3.4**).

Presence of the deletion cassette was confirmed by PCR of yeast colonies, using inward-facing primers upstream and downstream of the ORF in combination with outward facing primers specific for the TEF promoter (m1942) and TEF terminator (m1941) which were present in the deletion cassettes.

2.3.4 High efficiency transformation of yeast

Exponentially-dividing cultures were allowed to reach $2x10^7$ cells/ml. Cells were harvested at 3000 rpm for 3 min, the medium was poured off. Cells were washed once in 25 ml sterile water and then resuspended in 1 ml 0.1 M (1X) LiAc. Cells were transferred to an eppendorf tube and spun down at 13,000 RPM for 30 sec. LiAc was removed by aspiration. Cells were resuspended in a final volume of 0.5 ml by adding 0.4 ml of 0.1M LiAc (2×10^9 cells/ml). Samples were vortexed and 50 µl of cell suspension was alliquoted out for each transformation. Cells were then kept on ice until ready for transformation. For each strain to be transformed, both positive and negative controls were carried out. Negative controls utilized water instead of transforming DNA was carried out to confirm selection for the transforming marker was successful. Positive controls utilized pDL1223 (a centromeric plasmid expressing both *URA3* and *NATMX*) as transforming DNA and were selected for on -URA or ClonNAT plates, to confirm that the experiment supported successful transformation of auxotrophy or

antibiotic resistance markers (as appropriate). To transform, cell suspensions were pelleted at 13,000 rpm for 30 seconds, LiAc removed by aspiration and then the following reagents were then added in the following order:

240 µl PEG 4000 (50% w/v)
36 µl 1M (10X) LiAc
50 µl Salmon Sperm DNA (10 mg/ml)
50 µl Transforming DNA in Water (0.1 – 10 µg)

Samples were vortexed vigorously to ensure cell pellet was completely mixed, then incubated at 30°C for 30 min before being heat shocked at 42°C for 20 min. Cells were pelleted at 13 000 RPM for 30 sec and transformation mix removed by aspiration. Cells were resuspended in 200 µl sterile water then either plated onto selection plate to select for auxotrophy markers, or plated onto YEPD, incubated at 23°C overnight and then replica plated the next day onto plates containing antibiotics. Transformants were allowed to grow at 23°C for 4-5 days. Single colonies were then picked and struck out onto selective media to colony purify and prevent false positives.

Salmon Sperm DNA (10 mg/ml)

10 mg of DNA-sodium salt from Salmon testes (Sigma) per ml of water by was dissolved by sonicating for 10-20 second pulses. Prior to use, DNA was denatured by boiling for 5 minutes at 95°C and cooled rapidly on ice for 5 minutes.

2.3.5 Quick transformation of yeast

100 µl of stationary phase culture was spun down in a microcentrofuge for 1 minute at 13,000 RPM then resuspended in 100 µl of one-step buffer, pipetting gently to mix. Transforming DNA (1 µl of plasmid miniprep, see Section **2.2.5**, or 15 µl of high efficiency preparation of DNA, see Section **2.4.6**) and 5.3 µl salmon sperm DNA (10 mg/ml, see Section **2.3.4**) were added then the transformation mix was vortexed and incubated at 45°C for 30 minutes. Transformation mix was then plated directly onto selective media and incubated at 23°C for 3-7 days.

One-step buffer

0.2 M LiAC, 40% PEG, 100 mM DTT. For 5 ml:

1 ml 2 M Lithium acetate

4 ml 50% (V/V) PEG

75 mg DTT

2.3.6 Introduction of point mutations into yeast strains

URA3-marked integrating plasmids were cut by restriction digest using the appropriate restriction enzyme, purified by high efficiency preparation of DNA and then transformed into haploid yeast by high efficiency transformation.

Single colonies from the transformation plates were restruck onto -URA plates to ensure purity. Single colonies were then restruck across half a YEPD plate, allowed to grow overnight, replica plated to FOA and allowed to grow overnight once more, then replica plated to FOA a final time and allowed to grow for 5-7 days so strains that had lost the insert could form colonies.

Presence or absence of the point mutation was confirmed by colony PCR and restriction digest to test for the presence/absence of a restriction site introduced by the point mutation.

2.3.7 Growth assays

A 5-fold dilution series of stationary phase culture was prepared in a 96 well plate by adding 40 µl of the culture to 160 µl of fresh media then performing a serial dilution across the plate. 3-5 µl of each dilution was then spotted onto agar plates using a sterilized 48-prong replica plating device (Sigma).

2.3.8 Passage experiments

*tlc1*Δ strains and all controls were germinated for 3 days at 30°C, then restreaked for single colonies (passage 1 and onwards). *cdc13*Δ strains and all controls were germinated for 7 days at 23°C then patched onto a fresh YEPD plate (passage 1) before being restreaked for single colonies (passage 2 and onwards). For each passage, multiple single colonies were pooled and restreaked and each passage was stored at 4°C for the duration of the experiment.

To generate stationary phase cultures for growth assays or DNA preps, plates corresponding to the appropriate strain and passage number were retrieved from 4°C and multiple single colonies were inoculated into 2 ml YEPD and grown to saturation for 2 days with aeration. To quantify growth at each passage, growth assays were performed on YEPD plates at 23°C for 4 days for *cdc13*Δ strains or 30°C for 3 days for

*tlc1*Δ strains, plates were photographed using a spImager (S&P Robotics) and the sum of the pixel intensity of the growth corresponding to each yeast strain was quantified using Colonyzer (Lawless et al., 2010).

2.3.9 CDC13 Plasmid loss assay

To test whether *CDC13* was an essential gene, strains containing *pURA3[CDC13]* were generated by tetrad dissection, passaged on -URA plates for 3 days at 30°C to ensure retention of the plasmid, then multiple colonies were inoculated into YEPD, grown to stationary phase, and growth assays were performed on YEPD for 2 days, -URA for 3 days and FOA for 5 days. For strains grown on FOA plates, either single colonies or the highest density spot were struck for single colonies onto YEPD, which were then patched and replica plated to determine genotype of any FOA-resistant colonies.

2.3.10 Isolation of DNA from yeast (Yale DNA Preps)

Yeast cells were grown to saturation in 2 ml YEPD. Cultures were transferred to an eppendorf tube and spun at 13,000 RPM (1 min) and the supernatant was removed by aspiration. Cells were resuspended in 250 µl 0.1M EDTA (pH 7.5), 1:1000 dilution β-mercaptoethanol containing 2.5 mg/ml zymolase 20T. Cells were incubated at 37°C for approximately 1 hour until spheroplasted (monitored by microscopy), then shaken briefly after 15 minutes and vortexed at the end. 50 µl of miniprep mix (0.25 M EDTA pH 8.5, 0.5 M Tris base, 2.5% SDS) was then added to each of the tubes. Samples were mixed by inversion and incubated at 65°C for 30 min, mixing by inversion after 15 minutes. Samples were vortexed before 68 µl of 5 M KAc was added, then vortexed again. Samples were then incubated on ice for 30 min until a viscous precipitate had formed, then spun at 13,000 RPM for 20 min before transferring supernatants to a new tube containing 720 µl of 100% ethanol. A visible DNA precipitate formed upon mixing by inversion. The samples were spun at 13,000 RPM for 10 min. 130 µl of TE containing 1 mg/ml RNAase A was added to the undried pellet and samples were resuspended by incubating at 37°C for 35 min with occasional vortexing. DNA was reprecipitated with 130 µl of isopropanol. Samples were mixed by inversion and spun for 20 minutes at 13,000 RPM. Tubes were then drained and 100 µl of 70% ethanol (vol/vol) was added to wash DNA and remove salts. Tubes were then spun again at 13,000 RPM for 5 minutes before ethanol was aspirated. The pellets were then air dried for 30 minutes and resuspended in 40 µl TE with incubation at 37°C for 30 minutes, vortexing vigorously. Samples obtained contained approximately 10 µg of genomic

DNA and were stored at -20°C.

2.3.11 Telomere uncapping in asynchronous cultures

Asynchronously dividing ($1x10^7$ cells/ml) *cdc13-1* mutants at 23°C were shifted to 36°C. Every hour, cell density was counted by hemocytometry and, when necessary, diluted back down to $1x10^7$ using media warmed to 36°C.

2.3.12 Telomere uncapping and DSB induction in synchronous cultures

Synchronous culture experiments were performed similarly to those described (Zubko et al., 2006). Exponentially-dividing *bar1*Δ *cdc13-1* mutants, growing in culture flasks at 23°C were diluted down to 250 ml of $1.5x10^7$ buds/ml (approximately $7.5x10^6$ cells/ml). α factor was added to 20nM (10 μl of 500 μM stock) and cells were grown for a further 2.5 hours at 23°C. Cells were counted again by hemocytometry and culture was removed from the highest density cultures so that each flask contained the same number of cells.

Cultures were transferred to 250 ml tubes, 23°C YEPD was added up to 250 ml where necessary, then cells were spun down at 1,000 RPM for 4 minutes before discarding the supernatant. (This time point was noted as -40 minutes). The pellet was resuspended twice, each time resuspending in 50 ml YEPD and respinning in 50 ml Falcon tubes for 3 min at 2,000 RPM. The final pellet was resuspended in 150ml of YEPD at 23°C in a 500 ml flask and the culture was left at room temperature (23°C) until time 0.

To induce telomere uncapping, 125 ml of YEPD at 51°C was added and then cultures were incubated at 36°C. To induce DSBs, 125 ml of YEPD at 23°C was added in addition to bleomycin to a final concentration of 50 μg/ml

<u>α factor (500 μM stock)</u>

0.842 mg dissolved per ml in water (25,000X for *bar1*Δ strains)

2.3.13 Determination of cell number

500 μl samples were taken from cultures and sonicated for 6 seconds at 5 microns (Sanyo Soniprep 150 sonicator) to separate clumps of cells. 10 μl of culture was then applied to a hemocytometer and >100 cells were counted to measure the number of cells in 100 nl, which was multiplied by 10,000 to obtained the number of cells per ml.

2.3.14 Determination of viability

500 µl of culture was removed, vortexed thoroughly and 20 µl was removed and added to 980 µl of sterile water, before vortexting thoroughly to mix (1:50 dilution). 10 µl was then removed and added to 990 µl of sterile water (1:100 dilution) before vortexing to mix. 50 µl of the final 1:5,000 dilution was spread onto half an agar plate with a glass pipette, then another 50 µl spread onto the other half of the plate. Plates were incubated for 3 days at 23°C and viable cell number was determined as the mean number of colonies formed on each half of the plate.

2.3.15 Scoring of cell cycle position

2 ml of cell culture was fixed in Ethanol by spinning down at 13,000 rpm in a microcentrifuge for 10 seconds, aspirating the supernatant and then resuspending the pellet in 1 ml 70% Ethanol (V/V). Samples could then be stored at 4°C for up to a year. Ethanol was then washed out by spinning down again and resuspending in 500 µl sterile water, twice. Cells were then spun down once more, water aspirated and resuspended in 200 µl – 500 µl of 0.2 µg/ml DAPI (4,6-diamidino-2-phenylindole). Samples were stored at 4°C in the dark.

Samples were sonicated (Sanyo Soniprep 150 sonicator) for 1-10 seconds at 5 microns to separate clumps of cells, then 1-3 µl was applied to a cover slip and photographed under a fluorescence microscope (Nikon eclipse 50i) ensuring that the cells were not moving and to prevent preferential counting of larger cells. Photographs were then analyzed using the cell counter plugin for ImageJ (Abramoff et al., 2004), scoring cells as either G1 (no bud), S phase (single nucleus, bud less than or equal to half the diameter of the mother cell), metaphase (single nucleus, bud greater than half the diameter of the mother cell), anaphase (two nuclei) or other (none of the previous) as described (Zubko et al., 2006).

2.3.16 Synthetic Genetic Array

Synthetic genetic array was performed as described (Tong and Boone, 2006). The Lydall Lab deletion mutant library v2 was used as a deletion mutant array. The query strain for the *pif1*Δ SGA was *pif1*Δ *MAT*α (DLY5110). To make DLY5110, *MATa* DLY5318 (*pif1*Δ*::KANMX* from Lydall Lab deletion mutant library v1) was mated to the *MAT*α switcher strain (DLY3799), then the diploid transformed with cut pDL1155 (pCRII-TOPO[TA::MX4-natR]) to swap *pif1*Δ*::KANMX* to *pif1*Δ*::NATMX* then which was then sporulated and tetrad dissected to produce DLY5110.

2.4 Molecular Biology

2.4.1 Oligonucleotides

Oligonucleotides listed below were stored at 20°C in 1X TE at 200 μM under standard conditions. The exception to this was CY5-labelled oligos, which were stored in Sigma H_2O.

Oligo Number	Sequence	Function
M933	TGCAGGAATTTGGATCACACACTACAC	Forward primer that binds upstream of TG repeats in pDL987. With m934 amplifies a ~180bp fragment which can be labeled to detect telomeric TG repeats on Southern Blots.
M934	GCCGGGTAAGGAGTGACAGCG	Reverse primer that binds downstream of TG repeats in pDL987. With m933 amplifies a ~180bp fragment which can be labeled to detect telomeric TG repeats on Southern Blots.
M935	AGCCCTACAACACTTCTACATAGCCCTAAA	Forward primer that binds upstream of Y' sequence in pDL987. With m936 amplifies a ~820bp fragment which can be labeled to detect Y' sequences on Southern Blots.
M936	TGTAATACGACTCACTATAGGGCGAATTGG	Reverse primer that binds downstream of Y' sequence in pDL987. With m935 amplifies a ~820bp fragment which can be labeled to detect Y' sequences on Southern Blots.
M1012	AGCAAAGCAATAGTTCCCGTG	Forward primer that binds within *CDC13*. With m1013 amplifies a ~1500bp product which contains an EcoRI site in *cdc13-1* mutants.(Zubko and Lydall, 2006)
M1013	TTGTGCGAGACGGATCGA	Reverse primer that binds within *CDC13*. With m1011 amplifies a ~1500bp product which contains an EcoRI site in *cdc13-1* mutants.(Zubko and Lydall, 2006)
M1045	CTGCATTTGGCTCCATTTT	Forward primer that binds within *CDC15*. With m1046 amplifies a ~1800bp fragment which can be labeled to detect a single band from XhoI-digested DNA to serve as a loading control for telomere southern blots.(Foster et al., 2006)
M1046	TGTTGTAATGGGGACGGAAA	Reverse primer that binds within *CDC15*. With m1045 amplifies a ~1800bp fragment which can be labeled to detect a single band from XhoI-digested DNA to serve as a loading control for telomere southern blots.(Foster et al., 2006)
M1114	AGCGTCGACTATTGTGGGATA	Reverse primer for amplifying *BAR1*. Binds within *BAR1* and produces a 150bp product with M1156 in *BAR1*$^{+}$ strains.
M1156	AATAATCGATGTGGTCGCGTA	Forward primer for amplifying *BAR1*. Binds within *BAR1* and produces a 150bp product with M1114 in *BAR1*$^{+}$ strains.
M1157	CATATCCGCACCTCCTCAA	Forward primer for amplifying *hisG*. Binds within *hisG* and produces a 225bp product with *M1158* in strains carrying a *hisG* locus.
M1158	CTCTGTGCCATCTCACCGT	Reverse primer for amplifying *hisG*. Binds within *hisG* and produces a 225bp product with *M1157* in strains

		carrying a *hisG* locus.
M1362	CGCACTTAACTTCGCATCTGGGC	Reverse primer that recognizes the TEF terminator used in PCR based deletion modules. Used for confirming deletions.
M1417	CGTGCGATACGTTTTTGAGT	Forward primer which binds ~500bp upstream of *OGG1*. Used with m1362 to confirm gene deletion.
M1475	TTGCTGGCCTATCTTCATTG	Forward primer which binds ~500bp upstream of *PIF1*. Used with m1362 to confirm gene deletion.
M1579	tttgtgcaagcaaacactgacaattgaagagatcgtcagg CACATACGATTTAGGTGACAC	Forward primer for gene deletion of *DNA2* using PCR based deletion modules (Goldstein and McCusker, 1999)
M1580	tagctttcctgttatggagaagctcttcttattccccctg AATACGACTCACTATAGGGAG	Reverse primer for gene deletion of *DNA2* using PCR based deletion modules (Goldstein and McCusker, 1999)
M1581	agcgtcctgattcataattgcgattttatttatcaaccag CACATACGATTTAGGTGACAC	Forward primer for gene deletion of *OGG1* using PCR based deletion modules (Goldstein and McCusker, 1999)
M1582	tcgcgtgcttttatcgtggtatttactatgacttttaag AATACGACTCACTATAGGGAG	Reverse primer for gene deletion of *OGG1* using PCR based deletion modules (Goldstein and McCusker, 1999)
M1583	tccattgagcgattagcttacttgtatcaatcaattttac CACATACGATTTAGGTGACAC	Forward primer for gene deletion of *PIF1* using PCR based deletion modules (Goldstein and McCusker, 1999)
M1584	gcagtttgtattctatataactatgtgtattaatatgtac AATACGACTCACTATAGGGAG	Reverse primer for gene deletion of *PIF1* using PCR based deletion modules (Goldstein and McCusker, 1999)
M1736	acaaccagaaataggctttagttaactcaatcggtaatta CGGATCCCCGGGTTAATTAA	Forward primer for gene deletion of *POL32* using PCR based deletion modules (Longtine et al., 1998)
M1737	tttgtattatacattacatcacaattagtaatggaaagtg GAATTCGAGCTCGTTTAAAC	Forward primer for gene deletion of *POL32* using PCR based deletion modules (Longtine et al., 1998)
M1743	CAGCTCAGTGTGCAAGTTGTT	Forward primer which binds ~500bp upstream of *POL32*. Used with m1362 to confirm gene deletion
M1828	ctctttggatacgaatgaccgtggaaactatcgcctaaaa CACATACGATTTAGGTGACAC	Forward primer for gene deletion of *CDC13* using PCR based deletion modules(Goldstein and McCusker, 1999)
M1829	gcaatttggcaccgccgcgttgggctgcgcggatcatgtc AATACGACTCACTATAGGGAG	Reverse primer for gene deletion of *CDC13* using PCR based deletion modules(Goldstein and McCusker, 1999)
M1877	GGCGCGTCTTAATTTTCTTC	Forward primer which binds upstream of *PIF1*. With m1878 amplifies a ~500bp product which contains an ApaI site in *pif1-m1* mutants, a XhoI site in *pif1-m2* mutants and neither site in $PIF1^{+}$ strains.
M1878	TCGTTCCAGGATAAAGGACTG	Reverse primer that binds within *PIF1*. With m1877 amplifies a ~500bp product which contains an ApaI site in *pif1-m1* mutants, a XhoI site in *pif1-m2* mutants and neither site in $PIF1^{+}$ strains.
M1897	TCTCCGCCATAGAATCATCA	Forward primer which binds ~500bp upstream of *CDC13*. Used with

		m1362 to confirm gene deletion.
M1970	ATCGTTCGGACAGAAAATGG	Forward primer which binds ~500bp upstream of *DNA2*. Used with m1362 to confirm gene deletion.
M2188	[CY5] CCCACCACACACACCCACACCC	Fluorescent oligo labeled with Cy5 at the 5' end for detection of telomeric ssDNA by in-gel assay
M1879	CGCAAAGACCTAGCTTCACTG	Forward primer which binds within *PIF1*. With m1880 amplifies a ~350bp product which contains a MboI site in *pif1-hd* mutants.
M1880	TTATCCGCATCACCTTTTCC	Reverse primer which binds within *PIF1*. With m1879 amplifies a ~350bp product which contains a MboI site in *pif1-hd* mutants.

Table 3: Oligonucleotides used in this study

2.4.2 Restriction digests

Restriction digests were performed using restriction enzymes, buffers (10X) and BSA (100X) from New England Biolabs (NEB). A master mix was prepared and added to DNA samples to give final reaction conditions of 4-10% enzyme, 1X NEB buffer and 1X BSA. Buffers were used as per the manufacturer's recommendation and where multiple buffers were suitable, NEB Buffer 4 was preferentially used.

2.4.3 Primer Design

Primers for PCR reactions were designed to be 18-24 bp in length with a GC content of approximately 50% and a T_m of 55-59°C. For genomic DNA primers, Primer3 [http://fokker.wi.mit.edu/primer3/] (Rozen and Skaletsky, 2000) was used to pick the most appropriate primers for a target sequence and primers were searched against the yeast genome by BLASTN search to check they had ≤70% homology to any non-target sequence and hence ensure specificity.

2.4.4 Polymerase Chain Reaction (PCR)

Reactions were set up with to final concentration of 0.3 µM Forward primer, 0.3 µM Reverse primer, 0.24 mM dNTPs, 0.05 U/µl Ex Taq (TaKaRa Bio), 1X Ex Taq Buffer (TaKaRa Bio). 20 µl reactions were prepared:

1 µl	template DNA
0.2 µl	Forward primer (30 µM stock in TE)
0.2 µl	Reverse primer (30 µM stock in TE)
1.92µl	dNTP mix (2.5 mM each of dATP, dTTP, dGTP, dCTP)
0.2 µl	Ex Taq (5 U/µl stock)
2 µl	Ex Taq Buffer (10X)
14.48 µl	Sigma water

Reactions were prepared by making up a master mix to 1.1X the required volume (to account for pipetting errors) and aliquoting out 19 µl of master mix to each tube, before adding template.

Template was either a 1:100-1:1000 dilution of plasmid miniprep, 1 µl of 1:25 dilution of yeast genomic DNA prep or 1 µl of colony lysate for colony PCR (single colony picked into 20 µl of TE, vortexted and lysed at 95°C for 10 minutes prior to use as template).

Standard reaction conditions were as follows:

95°C	X	5’	
94°C	X	30s	} 35 Cycles
55°C	X	30s	
72°C	X	1’	
4°C	X	∞	

For most sequences an extension time of 1’/kb of product size was sufficient. However, for amplification of PCR-based deletion cassettes a 5’ extension time was always used.

2 µl of PCR product was then run out on an agarose gel to visualize reaction products.

2.4.5 Gel extraction of DNA

Samples were run out on an agarose gel then gel extracted using QIAquick Gel Extraction Kit (Qiagen) according to the manufacturer’s conditions.

2.4.6 High efficiency preparation of DNA for transformation

15µl of plasmid miniprep was restriction digested with appropriate enzyme(s) in a 40 µl reaction. 0.8 µl 0.5 M EDTA, 4 µl NaAc pH 5.2 and 120 µl isopropanol were added then DNA was precipitated at -20°C for 10 minutes. DNA was pelleted by spinning in a microcentrifuge at 13,000 RPM for 5 minutes. DNA was washed by addition of 250 µl 70% ethanol (V/V), re-spinning at 13,000 RPM for 5 minutes, aspirating the ethanol and allowing the pellet to air dry in a fume hood. Pellet was resuspended in 40 µl TE and 1 µl run out on an agarose gel to check recovery. 10 µl was used per transformation.

2.4.7 Agarose gel electrophoresis

1% agarose gels containing 1X SYBR Safe or 1 µg/ml EtBr were made up by adding 1 g agarose to 100 ml buffer TBE (0.5X) or buffer TAE (1X) and dissolving in a microwave before cooling to 50°C and then adding 10 µl of SYBR SAFE (10,000X) or

10 µl EtBr (10 mg/ml). Molten agarose was poured into a casting tray, using combs with 3mm, wells to produce gels of the desired thickness and allowed to set. Samples were run until separated at ≤5 V/cm. All components were from the Mini-Sub Cell GT and Wide Mini-Sub Cell GT systems from Bio-Rad.

Loading buffer (6X, blue or orange) was added to DNA samples to a final concentration of 1X prior to loading and DNA samples were run alongside 0.1 µg of 1KB DNA Ladder (Invitrogen) per mm of lane width. (E.g. 5 µl of 1 KB DNA Ladder at 0.1 µg/µl into lanes 5 mm wide).

Blue Loading Buffer (6X)

0.25% bromophenol blue, 0.25% xylene cyanol, 15% ficoll, 120 mM EDTA pH 8.0. For 50 ml:

0.125 g	bromophenol blue
0.125 g	xylene cyanol
7.5 g	Ficoll (Type 400, Pharmacia)
12 ml	0.5 M EDTA (pH 8.0)
to 50 ml	Water

Orange Loading Buffer (6X)

0.25% Orange G, 15% ficoll, 120 mM EDTA pH 8.0. For 50 ml:

0.125 g	Orange G
7.5 g	Ficoll (Type 400, Pharmacia)
12 ml	0.5 M EDTA (pH 8.0)
to 50 ml	Water

Note: in both loading buffers, 30% glycerol can be used as an alternative to 15% Ficoll by substitution of Ficoll for 15 ml glycerol.

2.4.8 TCA Extraction of Proteins

TCA extractions were performed as desrcribed (Foiani et al., 1994).

10^8 cells in liquid culture were spun down (1,000 RPM, 3 minutes), resuspended in 10 ml sterile ice-cold water then spun down again and the supernatent poured off. Cells

were resuspended in 1 ml TCA (20%), transferred to a 2 ml tube and pelleted at 13,000 RPM for 1' in a microcentrifuge. Supernatent was aspirated with a pipette and the pellet was resuspended in 100 µl of TCA (20%) and frozen at -20°C.

Suspension was thawed at room temperature, an equal volume of glass beads (acid-washed, 425 µm – 600 µm, Stratch) was added (using a 0.2 ml tube) and samples were vortexed for 4 minutes.

Extract was transferred to a fresh tube, then beads were washed twice with 100 µl of TCA (5%), each time transferring the extract to the new tube, to give 300 µl of extract in 10% TCA. Proteins were pelleted by centrifugation at 3,000 RPM for 10 minutes in a microcentrifuge and supernatent was aspirated with a pipette. Sample was resuspended in 100 µl Laemmli loading buffer and neutralized by adding 50 µl of 2 M Tris.

Sample was boiled for 3' then centrifuged at 3,000 RPM for 10 minutes in a microcentrifuge and the pellet was discarded, to yield crude denatured protein extracts.

Laemmli loading buffer

50 µl of β-mercaptoethanol was added to 950 µl of Laemmli loading buffer (Bio-Rad).

2.4.9 Western Blots

5 µl of TCA protein extract was run on a 7.5% Tris-glycine gel (7.5% Ready gel, 15 well, Bio-Rad) at 100 V alongside prestained protein markers (precision plus dual color standards, Bio-Rad) until the 50 kDa band was close to the bottom of the gel.

Before the gel had finished running, a piece of nitrocellulose membrane (Hybond-ECL, GE Healthcare) and 2-4 sheets of Whatman paper (3MM, Scientific Laboratory Supplies) were cut slightly larger than the gel and soaked in transfer buffer. Fibre pads were also soaked in transfer buffer and an ice-pack containing frozen transfer buffer was inserted into the tank before the tank was filled with pre-cooled transfer buffer.

When the gel had finished running, the wells were cut off and the remaining gel was placed in transfer buffer. While submerged in transfer buffer, the gel was then sandwiched against the membrane, with 1-2 pieces of Whatman paper either side, between two fibre pads. The fibre pads/whatman paper/membrane/gel composite was then inserted into the transfer cassette, air bubbles rolled out using a glass test tube, the cassette closed and inserted into the transfer tank, with the membrane between the gel

and the positive electrode. Transfer was performed for 2 hours at 100 V in a cold room (4-10°C).

When the transfer was complete, the cassette was disassembled and the membrane removed from the Whatman paper and gel. (Note: if the gel stuck to the membrane, it was removed at this stage by gently stroking the membrane with a blank piece of membrane). The membrane was rinsed briefly in water, then stained for protein by incubating with 2-3 drops of Ponceau S on a rocker for 5 minutes, to confirm transfer. (Note: the Ponceau S stained any remaining pieces of gel stuck to the membrane, making it easy to identify and remove them by wiping with a blank piece of membrane soaked in Ponceau S). After confirming that the proteins had transferred, the membrane was rinsed with tap water to allow the salts in the water to destain it.

The membrane was blocked in 5% milk for 1 hour, then incubated with 10 ml of primary antibody solution (1% milk containing primary antibody) overnight at 4°C. (Note: could be shortened to 2 hours at room temperature for convenience). The primary antibody was poured off (which could be saved at 4°C and re-used) and blot was rinsed briefly with sterile water. The membrane was washed with 80 ml of 5% milk for 1 hour. (Note: could be eliminated to save time). Milk was tipped off and the membrane was washed with 80 ml of PBST for 1 hour. (Note this could also be eliminated to save time). Membrane was washed 3 more times with 80 ml of PBST for 10 minutes each wash.

PBST was removed and the membrane was incubated with 10 ml of secondary antibody solution (1% milk containing secondary antibody). The secondary antibody was poured off (which could also be saved at 4°C and re-used) and the blot was rinsed briefly with sterile water. Membrane was washed 5 times with 80 ml of PBST for 10 minutes each wash. (Note: this could be shortened to 3 washes to save time).

After the last wash, the membrane was incubated with a 1:1 ratio of peroxide and luminol solutions (SuperSignal West Pico Chemiluminescent substrate) for 5 minutes with rocking. Membrane was then placed face-up on a clear glass plate and covered with a piece of parafilm then immediately imaged with a chemiluminescent imager (Fuji LAS 4000) for 3 minutes at 15 second increments to detect bands.

Membrane was incubated with 10 ml stripping solution for 30 minutes at room temperature, then washed twice with 80ml PBST, for 15 minutes each. Membrane could then be blocked again and probed with a second set of antibodies.

Running Buffer

For 1 L:

100 ml	10X tris/glycine/SDS buffer (Bio-Rad)
900 ml	MQ Water

Transfer Buffer

For 1 L:

100 ml	10X tris/glycine buffer (Bio-Rad)
200 ml	methanol
700 ml	MQ water

Ponceau S

For 500 ml:

2.5 g	Ponceau S
to 495 ml	MQ Water
5 ml	acetic acid

Filter before use.

PBST

For 1 L:

999 ml	MQ Water
5	PBS Tablets (Sigma)
1 ml	tween 20

1%/5% milk

PBST containing 1%/5% (W/V) powdered milk (Marvel)

Primary antibodies

Goat polyclonal anti-Rad53	(Santa Cruz Biotech)	Dilute 1:1,000
Mouse monoclonal anti-tubulin	(DLAb42)	Dilute 1:1,000

Secondary antibodies

Donkey polyclonal anti-goat-HRP	(Santa Cruz Biotech)	Dilute 1:5,000
Goat polyclonal anti-mouse-HRP	(DLAb6)	Dilute 1:5,000

Stripping Solution

For 10.07 ml:

2ml 10% SDS

8ml PBST

70µl β-mercaptoethanol

2.4.10 Normalization of DNA preps by densitometry

20-fold dilutions of DNA preps were made (2 µl plus 38 µl of TE) along with a 4-fold dilution of a good quality DNA prep of Wild Type yeast (5 µl of DNA plus 16 µl TE). 6 tubes of a 2-fold dilution series of the Wild-Type DNA was prepared (10 µl of the 4-fold dilution plus 10 µl of TE). 6X loading buffer was added to each dilution and 2.4 µl was run on a thinly poured 1X TAE gel for 20-30 minutes at 70V.

The gel was imaged and visualized in ImageJ. A rectangular selection was moved across the gel and the area measured to quantify the mean pixel intensity in each well and in blank wells. The mean pixel intensity of the blank wells was then subtracted from all other wells to measure signal. The signal intensity of the 2-fold dilution series was plotted against the dilution factor to determine the linear range of measurement and the points corresponding to this range had a trend line fit to them. The equation of the trend line was then used to calculate the relative quantities of each DNA prep.

Sufficient 1X loading buffer was added to each diluted DNA prep to normalize them to the same concentration. 2.4 µl of each was diluted DNA prep was then re-run on a gel

alongside the 2-fold dilution series. (Note: if diluting the DNA preps was expected to bring the quantity of the preps outside of or towards the lower end of the linear range of the dilution series, the volume was increased). All lanes were then re-quantified and the final measurement was multiplied by the total dilution to determine the relative quantity of each DNA prep.

2.4.11 PCR synthesis of Digoxigenin-labelled probes

To synthesize Digoxigenin-labelled probes, PCR was performed as described above, substituting 2.5 mM dNTPs for 2mM DIG-11-dUTP-containing dNTP mix (Roche Applied Science) to the same final concentration. Successful labelling of the PCR product with DIG-dUTP by decreased mobility on an agarose gel compared to an unlabelled control.

TG probe was ~180 bp of TG repeats synthesized from pDL987 using oligos M933 and M934. Y' probe was ~180 bp of Y' sequence amplified from pDL987 using oligos M935 and M936. *CDC15* probe was ~1.8 kb of *CDC15* sequence amplified from yeast genomic DNA by oligos M1045 and M1046.

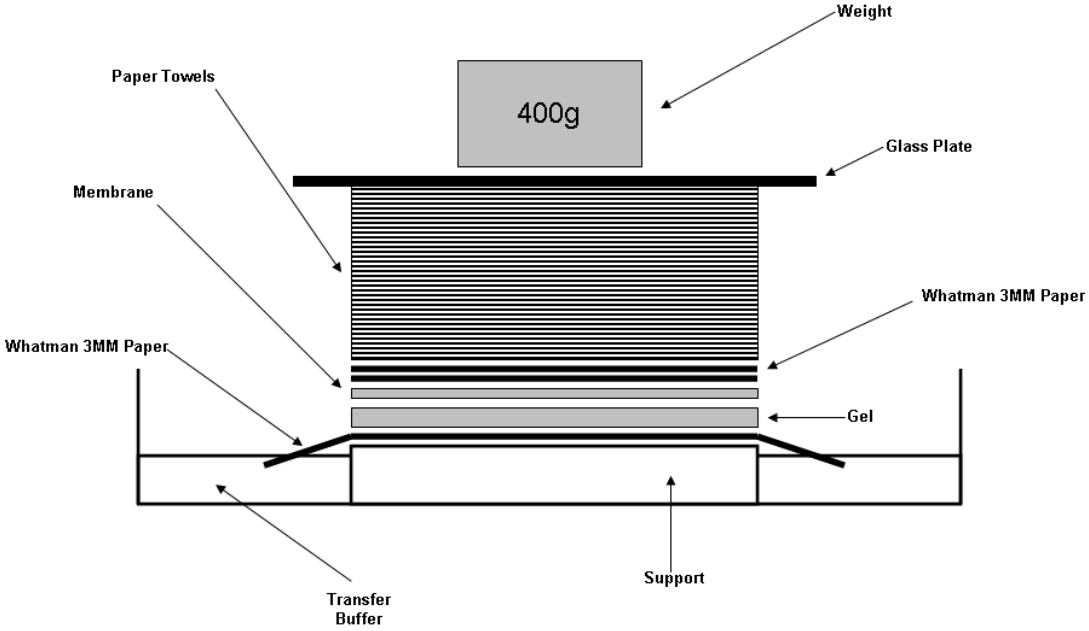
Weight
400g
Paper Towels
Glass Plate
Membrane
Whatman 3MM Paper
Whatman 3MM Paper
Gel
Support
Transfer
Buffer

Figure 3: Transfer of DNA from an agarose gel to a membrane for a Southern Blot
Diagram showing how to set up transfer apparatus for a Southern Blot. A support was assembled in a container of transfer buffer and a strip of Whatman paper laid across the support, making contact with the transfer buffer at each end. The agarose gel was placed face-down on the Whatman paper with a sheet of nylon membrane on top and two wet pieces of Whatman paper on top of that. Gel was surrounded with parafilm then a stack of paper towels were placed on top, along with a glass plate and a 400 g weight.

As an alternative to the support and reservoir shown, a glass backing plate could be placed atop of a large plastic container as a support/reservoir and a long piece of whatman placed over the glass plate, dipping into the transfer buffer at each side.

2.4.12 Telomere Southern Blots

Genomic DNA equivalent to 3 µl of a Wild Type prep from a 2ml stationary phase culture was cut with XhoI in a 25 µl digest (4% final concentration of enzyme) for 8 hours at 37°C then chilled on ice, before adding 5 µl of loading buffer.

A 120ml agarose gel in TBE was poured with 2 mm wide lanes and loaded with half of each digest (the remaining half was saved at -20°C in case the gel needed to be re-run) alongside 5 µl of DIG-labelled DNA ladder (DNA molecular weight marker III, DIG labeled, Roche Applied Science) and 2 µl of unlabelled DNA ladder (1 kb DNA ladder, invitrogen). Gel was run overnight at 1 - 1.5 V/cm. To detect strains that might have short telomeres or be undergoing senescence, gel was run until the 0.5 kb band was off the gel, while for all other situations the gel was run until the 1 kb band was off the gel. Gel was then trimmed with a scalpel to remove the wells and edges.

Gel was soaked in 10 volumes of denaturation solution with gentle agitation for 45 minutes. (Note: for this and subsequent wash steps the gel floated towards the surface, preventing thorough soaking. To keep the gel submerged, partially-filled 50 ml falcon tubes were added to the container). Denaturation solution was poured off and gel was washed in 10 volumes of neutralization solution for 30 minutes then washed with another 10 volumes of neutralization solution for 15 minutes.

(Note: prior to denaturation, the gel could be soaked soaking in several volumes of 0.2N HCl is recommended until the bromophenol blue/xylene canol turned yellow, then washed in several volumes of water, to improve the transfer of >15kb fragments. However, no fragments of this size are detected when probing for telomere length).

During the final wash step, positively charged nylon membrane (Roche Applied Science) and two sheets of Whatman paper (Scientific Laboratory Supplies) were cut to the same size as the gel. Membrane was soaked for 5 minutes in MQ water, then the membrane and Whatman sheets were soaked in transfer buffer for at least 5 minutes.

While the Whatman and membrane soaked in transfer buffer, a support and reservoir were assembled as in Figure 3 with a piece of 3MM Whatman paper cut to the same width as the shortest dimension of the gel (length or width) and a length long enough

for both ends to be submerged in the reservoir. The Whatman paper was then wetted by pipetting transfer buffer along its length.

When the final wash had finished, the gel was placed faced down on the support, on top of the Whatman paper (Figure 3) and air bubbles were forced out using gloved hands, before the gel was surrounded with parafilm. The wet membrane was placed carefully onto the gel, ensuring no air bubbles were trapped, then the two wet sheets of Whatman paper were placed on top (Figure 3) and air bubbles were rolled out using a 15 ml Falcon tube pre-wetted in transfer buffer. A 5-8 cm stack of paper towels was then placed on top, followed by a glass plate and a 400 g weight (Figure 3). Wet paper towels were removed after 1 hour and replaced with dry paper towels, then transfer was allowed to proceed for 12-72 hours.

When the transfer was complete, the membrane and two sheets of Whatman were soaked in 6X SSC for 5 minutes. The membrane was then placed face-up on the wet Whatman paper and crosslinked in a UV Stratalinker 2400 (Stratagene) for 0.15 J/cm^2 at 254 nm.

To hybridize, the membrane was first transferred to a glass hybrization tube and incubated with pre-warmed prehybridization solution (10 ml per 100 cm^2 of membrane or a minimum of 20 ml) in a hybridization oven at the hybridization temperature (appropriate to the probe being used) with constant agitation, for at least 30 minutes. Hybridization temperature (T_{opt}) was calculated as follows:

$$T_m = 49.82 + 0.41\ (\%\ GC) - (600/l)$$

%GC = GC Content of the sequence (%)

l = length of the sequence in bases

$$T_{opt} = T_m - 20 \text{ to } 25\ °C$$

For TG Probe a hybridization temperature of 44°C was used while for Y' and *CDC15* probes a hybridization temperature of 42°C was used (see Section **2.4.11** for probe synthesis details).

Hybridization solution was poured off and saved, then hybridization solution was added (3.5 ml per 100 cm^2 of membrane or a minimum of 6 ml) and hybridization was allowed to proceed overnight with constant agitation.

The next morning, hybridization solution was poured off and saved. The membrane was washed twice at room temperature for 5 minutes with 25 ml of low stringency wash buffer while rocking, before being washed twice at 68°C (in the hybridization oven) with 25ml of high stringency wash buffer with constant agitation.

All subsequent steps were performed with thorough rocking at room temperature and each time solutions were changed, the membrane was transferred to a fresh container that had been washed thoroughly and wiped down with 70% ethanol. Membrane was washed for 5 minutes with washing buffer (100 ml per 100 cm^2 of membrane), blocked with blocking solution (100 ml per 100 cm^2 of membrane) for 30 minutes, incubated with antibody solution for 30 minutes (20 ml per 100 cm^2 of membrane), then washed twice for 15 minutes each with washing solution (100 ml per 100 cm^2 of membrane). Finally, the membrane was incubated for 2-5 minutes in detection buffer (20 ml per 100 cm^2 of membrane).

The membrane was placed face-up on a clean glass plate and CSPD, ready to use (Roche Applied Science) was applied along the length of the membrane, then spread evenly by applying a piece of parafilm over the membrane. The membrane was incubated for 5 minutes at room temperature, before using a PCR plate sealer (Applied Biosystems) to stroke the surface of the parafilm and squeeze out all bubbles and excess CSPD. The membrane was then imaged within 24 hours.

The membrane was then detected in a chemiluminescent imager (Fuji LAS 4000) with an increment of 5-10 minutes, typically for less than an hour. When detecting telomeres, it was optimal to choose an exposure at which the Y' bands were strong but did not merge.

To strip the membrane, it was added to a container of 1 L of boiling 0.1% SDS (microwaved 15-20 minutes), which was then sealed and allowed to cool to room temperature with gentle agitation for several hours (or overnight). The membrane was then rinsed for 5 minutes at room temperature with 2X SSC and was then ready to be prehybridized again and hybridized with another probe.

<u>Denaturation solution</u>

1.5 M NaCl 0.5 M NaOH. For 1 L:

87.67 g NaCl

20 g	NaOH
to 1 L	MQ Water

Note: dissolving the NaCl first speeds up dissolving of the NaOH

Neutralization solution

1 M Tris (pH 7.5) 1.5M NaCl. For 1 L:

87.67g	NaCl
to 1 L	1M Tris (pH7.5)

Transfer buffer

10X SSC. For 1 L:

500 ml	20X SSC
500 ml	Water

Prehybridization Solution

DIG Easy Hyb was made up by adding 32 ml of water to DIG Easy Hyb granules (Roche Applied Science), stirring at 37°C for 5 minutes, then adding another 32 ml of water and stirring at 37°C until dissolved. DIG Easy Hyb was then preheated to the hybridization temperature.

Following hybridization the prehybridization solution could be saved and used a further 3-4 times.

Hybridization solution

DIG-labelled probe was denatured by heating at 95°C for 10' in a PCR machine then rapidly cooling to 4°C. Denatured probe was then added to DIG easy hyb (preheated to the hybridization temperature) to a final concentration of 25 ng/ml.

Low stringency wash buffer

2X SSC 0.1% SDS. For 50 ml:

5 ml	SSC (20X)

44.5 ml MQ Water

0.5 ml SDS (10%)

High stringency wash buffer

0.5X SSC 0.1% SDS. For 50 ml:

1.25 ml SSC (20X)

48.25 ml MQ Water

0.5 ml SDS (10%)

Washing buffer

0.1 M Maleic acid, 0.15 M NaCl; pH 7.5, 0.3% (v/v) Tween 20. For 100 ml:

10 ml Washing Buffer (10X, Roche Applied Science)

90 ml MQ Water

Shake vigorously before use.

Maleic Acid Buffer

0.1 M Maleic acid, 0.15 M NaCl; pH 7.5. For 100 ml:

10 ml Maleic Acid Buffer (10X, Roche Applied Science)

90 ml MQ Water

Blocking Buffer

10X blocking buffer (Roche Applied Science) was diluted in maleic acid buffer to 1X final concentration.

Antibody Solution

Anti-Digoxigenin-AP conjugate (Roche Applied Science) was spun for 5 minutes at 10,000 RPM in a microcentrifuge, then pipetted from the surface and diluted 1:10,000 (75 U/ml) in blocking buffer.

Detection Buffer

0.1 M Tris-HCl, 0.1 M NaCl, pH 9.5. For 20 ml:

2 ml	Detection buffer (10X, Roche Applied Science)
18 ml	MQ Water

2.4.13 Quantitative Amplification of ssDNA (QAOS)

Quantitative Amplification of ssDNA was performed essentially as described (Zubko et al., 2006). The only exceptions being that all samples and PCR mixes were aliquotted out by manual pipetting (rather than using multichannel pipettes or repeating pipettes) to improve accuracy and prior to real time PCR, template DNA was aliquoted fresh from stocks thawed in Eppendorf tubes at 4°C (rather than template DNA being pre-aliquotted into 96-well plates and stored at -20°C) to prevent loss of volume during freezing/thawing.

2.4.14 In-gel assay

50 ml of exponentially-dividing or G1-arrested cells, or 30 ml of G2/M arrested cells were chilled on ice water then spun down at 2,000 RPM for 5 minutes in a centrifuge chilled to 4°C and the supernatant was discarded. Pellets were resuspended in 1 ml ice cold sterile water, transferred to pre-chilled 1.5 ml Eppendorf tubes, pelleted at 13,000 RPM for 5 minutes in a microcentrifuge chilled to 4°C. Supernatent was poured off, tubes were spun for a further 1 minute, then the remaining liquid was aspirated with a pipette before the pellets were frozen at -80°C.

Cell pellets were thawed on ice, then resuspended in 200 µl lysis buffer by pipetting before transferring to a 2 ml screw cap tube with skirt (Sarstedt) containing 0.3 g of glass beads (acid-washed, 425µm-600µm, Stratch). 200 µl of phenol:chloroform:isoamyl alcohol (25:24:1, saturated with 10 mM Tris pH 8.0, 1 mM EDTA, Sigma) was added to each tube, lids were capped tightly and cells were lysed at 5.5 power for 60 s using a Precellys 24 automated homogeniser. Tubes were spun for <5 seconds in a microcentrifuge to remove traces of phenol from the lids, then 200 µl of TE was added to each sample before vortexing briefly to mix.

Tubes were spun at 13,000 RPM for 5 minutes in a microcentrifuge chilled to 4°C, ensuring that the tube label was positioned to one side (not the top or bottom) and would not obstruct view of the interface between the aqueous and organic phases. The aqueous phase was transferred to a fresh 1.5 ml tube by aspirating 175µl of aqueous

phase twice with a P200 pipette. (Note: to ensure a clean interface for each sample, it was best to remove 3-4 tubes from the microcentrifuge at once and keep the rest spinning so that tubes were not sat around for more than a couple of minutes before aspiration of the aqueous phase). Screw cap tubes were discarded.

350 µl of chloroform:isoamyl alcohol (24:1, saturated with 10 mM Tris pH 8.0, 1 mM EDTA, Sigma) was added to each 1.5 ml tube and samples were mixed by inverting in a rack every 15 seconds for 2 minutes. The aqueous phase was aspirated incrementally with a P200 into a new tube, angling the tube slightly, pipetting from the side of the tube at which the aqueous phase was deepest and ceasing when the aqueous phase no longer occupied the entire diameter of the tube. Tubes containing the vitreous phase were discarded.

1 ml of 100% ethanol was added to each aqueous phase, tubes were inverted gently and left to precipitate at room temperature for 5 minutes. Tubes were spun in a microcentrifuge at 13,000 RPM for 3 minutes, the supernatant was poured off, then tubes were re-spun for 1 minute and the remaining supernatant aspirated with a pipette. Tubes were dried in a fume hood for 5 minutes.

400 µl TE and 3 µl RNase A (10 mg/ml, Sigma) was added to each tube. Tubes were incubated in a 37°C water bath for 30 minutes, vortexing thoroughly after 5, 15 and 30 minutes. 13 µl of NaAc (3M, pH 5.2) and 1 ml of 100% ethanol were added to each tube. Tubes were inverted gently and left to precipitate at room temperature for 15 minutes.

Tubes were spun in a microcentrifuge for 3 minutes at 13,000 RPM. Supernatant was poured off, tubes were re-spun for 1 minute and the remaining supernatant aspirated with a pipette. Tubes were dried in the fume hood for 30 minutes.

25 µl of TE was added to each DNA pellet and samples were resuspended by incubation in a 37°C water bath, vortexing thoroughly at 5, 15 and 30 minutes, then allowing to equilibrate on ice for 30 minutes.

DNA samples were quantified by densitometry. DNA equivalent to 5-8 µl of the lowest-yield DNA prep (equivalent to approximately 3-5 µl of a good quality DNA prep from a G1 arrested or asynchronously dividing culture) was cut in a 20 µl digest with XhoI (10% final concentration). Digests were heat-inactivated at 65°C for 20 minutes, then 1

µl of Cy5-labelled AC probe (oligo m2188, 500 nM in Sigma Water) was added to each tube. Tubes were mixed by flicking, spun down briefly, incubated at 37°C for 10 minutes to anneal the probe then chilled on ice for 30 minutes.

5 µl Orange G loading buffer (6X) was added to each tube. Tubes were mixed by flicking, then spun briefly and kept on ice. Blanks were prepared containing TE, NEB buffer, BSA, probe (but not enzyme) to the same final concentration.

A 1% TBE agarose gel, 120 ml in volume, containing no EtBr or SYBR Safe was prepared. (Note: it was important that all measuring and casting apparatus were free of EtBr and SYBR Safe contamination, best accomplished by thorough cleaning prior to use and reserving a conical flask specifically for melting agarose for non-SYBR Safe/EtBr gels). Samples were loaded onto the gel, all lanes were blanked with an equivalent volume and DNA ladder was loaded into one of the edge wells using orange loading buffer. Gel was run at 5 V/cm for 90 minutes, then detected on a Typhoon Trio Imager (GE Healthcare) at maximum resolution and sensitivity, with the appropriate settings for detection of Cy5.

Following detection for Cy5, gel was post-stained (1X SYBR Safe in a large enough volume of TBE to cover the gel) for 1 hour with constant agitation, then visualized to detect total DNA. To detect loading and confirm complete digestion, the gel was then used for a Southern Blot to detect *CDC15*.

To quantify ssDNA the images corresponding to Cy5 and SYBR Safe detection were scaled to the same size using the background visibility of the gel. The DNA ladder on the SYBR Safe image was used to determine sizes on the Cy5 image. The mean pixel intensity of each lane between 0.8kb and 12kb was quantified in ImageJ by moving a rectangular selection across the gel and quantifying each lane. Background was quantified as the mean pixel intensity of the signal between the lanes within the 0.8kb and 12kb range. Signal-noise was determined as the pixel intensity of each lane, minus the mean pixel intensity of the background either side. Background was quantified in the same way for the *CDC15* southern blot, and ssDNA signal was normalized for *CDC15* signal.

Lysis buffer

2% Triton X-100, 1% SDS, 100 mM NaCl, 10 mM Tris (pH 8.0), 1 mM EDTA (pH 8.0),

For 5 ml:

100 µl	Triton X-100
500 µl	SDS (10%)
500 µl	NaCl (1M)
100 µl	Tris (0.5M, pH8.0)
10 µl	EDTA (0.5M, pH8.0)
3.79 ml	MQ Water

2.5 Bioinformatics

Genetic interactions from Biogrid v2.0.53 (Stark et al., 2006) were parsed into Cytoscape (Cline et al., 2007) to create a genetic interaction network using ORF names as unique identifiers. Gene names were annotated using Saccharomyces Genome Database (Costanzo et al., 2009). Genes that affect telomere uncapping were annotated according to published work (Addinall et al., 2008, Downey et al., 2006, Foster et al., 2006, Tsolou and Lydall, 2007, Zubko et al., 2004). Genes that increase or decrease telomere length were annotated if they appeared in any published high throughput screen for telomere length (Askree et al., 2004, Gatbonton et al., 2006, Ungar et al., 2009).

Genes that shared genetic interactions with *EXO1* were identified based on how many of the first neighbors of *EXO1* they had a genetic interaction with. This involved identifying the number of genetic interactions each first neighbor had with the other first neighbors and separately identifying how many of the first neighbors genes outside the first neighbors had a genetic interaction with. These two sets of genes were then merged and edges linking them to *EXO1* were created, weighted by the number of shared genetic interactions. Genes connected by the top 10% most heavily weighted edges to *EXO1* were isolated.

3 The search for the determinants of nuclease activities at uncapped telomeres

"If you want to have good ideas you must have many ideas. Most of them will be wrong, and what you have to learn is which ones to throw away."

- Francis Crick

3.1 Introduction

3.1.1 Exo1 and other unknown nucleases resect uncapped telomeres

Uncapped telomeres and DSBs both initiate a potent DDR, leading to resection by nucleases, which generate vast tracts of ssDNA to stimulate checkpoint activation (Lydall, 2009). At DSBs, this resection is dependent upon three nucleases activities dependent upon Exo1, Sgs1/Dna2 and Sae2/MRX (Gravel et al., 2008, Mimitou and Symington, 2008, Zhu et al., 2008). A most striking validation of this model is the demonstration that if Sae2 is conditionally inactivated in a cell lacking Exo1 and Sgs1, no detectable resection (<50bp) of a HO-induced DSB can be seen (Mimitou and Symington, 2008). In contrast, comparatively little is known about the resection of uncapped telomeres (Maringele and Lydall, 2002, Ngo and Lydall, 2010, Zubko et al., 2004).

At uncapped telomeres in *cdc13-1* mutants nuclease activities dependent upon Exo1 or Rad24 (which loads the 9-1-1 complex) are active, but in cells lacking either Exo1 or Rad24, or both, ≥5,000bp of ssDNA is still generated following telomere uncapping in *cdc13-1* mutants (Maringele and Lydall, 2002, Zubko et al., 2004). It is unlikely that a Sae2/MRX-dependent nuclease activity also resects uncapped telomeres because MRX plays a protective role in cells with uncapped telomeres and inactivation of Rad50 leads to increased ssDNA generation at uncapped telomeres (Foster et al., 2006). Additionally, although Sgs1 and Exo1 function in different pathways to carry out extensive resection at DSBs, Sgs1 appears to function in the same pathway as Exo1 at uncapped telomeres in *cdc13-1* mutants (Ngo and Lydall, 2010).

Exo1 inhibits the growth of *cdc13-1* mutants with uncapped telomeres, due to its role in the resection of uncapped telomeres, which leads to loss of viability and stimulates checkpoint activation (Maringele and Lydall, 2002, Zubko et al., 2004) (Figure 2B). Genome-wide screens have been performed to identify genes that, like Exo1, inhibit the

growth of *cdc13-1* mutants (Addinall et al., 2008, Downey et al., 2006). >200 genes have now been identified that inhibit the growth of *cdc13-1* mutants but none of them are obvious candidates for nuclease activities (Addinall et al., 2008). Thus, the nuclease activities at uncapped telomeres are poorly defined and no striking candidates for residual nuclease activities exist.

There are multiple reasons why a nuclease that functions at uncapped telomeres might not have been discovered by genetic screening for genes that inhibit the growth of *cdc13-1* mutants. First, genes responsible for nuclease activities that function at uncapped telomeres may have been highlighted by genetic screening (Addinall et al., 2008, Downey et al., 2006) but may encode a protein that is not an obvious nuclease. Secondly, genes encoding a nuclease activity may not have been tested or identified in the genetic screens carried out.

The genetic screens performed by Addinall *et al.* and Downey *et al.* were based upon the SGA methodology (Tong and Boone, 2006) whereby a library of deletion mutants are each individually combined with a query mutation. There are many genes absent from the library due to poor growth or inviability of the null mutation (Addinall et al., 2008). Thus, there are potential nuclease genes that have not been tested. Additionally, the screens performed by Addinall *et al.* and Downey *et al.* relied upon the temperature-sensitive growth of *cdc13-1* mutants to inactivate Cdc13. Thus, any candidate nuclease genes that also displayed temperature-sensitive growth may have been assayed but scored as false negative results, for technical reasons.

To identify the determinants of nuclease activities apart from Exo1 that function at uncapped telomeres, this work focused on identifying and testing candidate genes by two different criteria. 1.) Bioinformatic analysis of candidate genes highlighted by Downey *et al.* and Addinall *et al.* to identify candidate nuclease genes that might not be obvious nucleases. 2.) Testing of genes required for known nuclease activities that were either essential for growth or conferred temperature-sensitive growth.

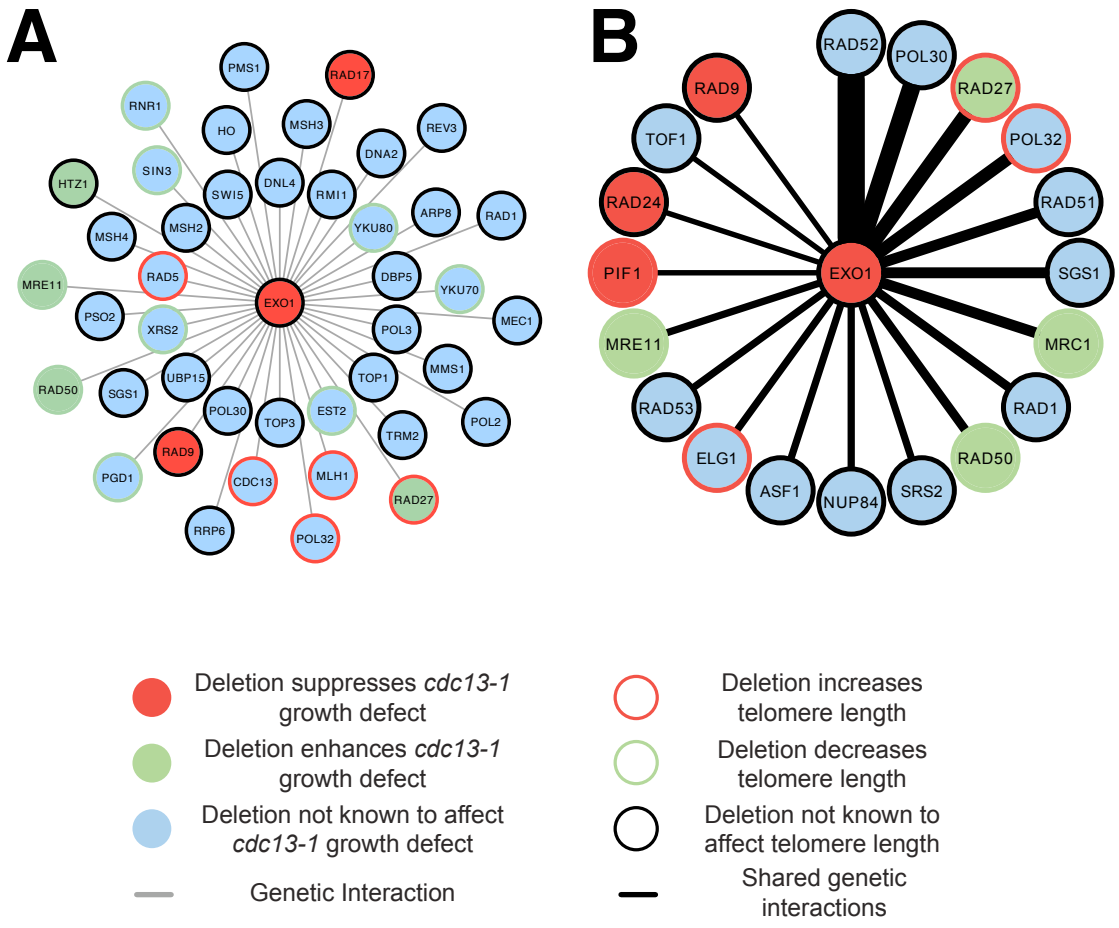
A
PMS1
RAD17
RNR1
HO
MSH3
REV3
DNA2
SIN3
HTZ1
SWI5
DNL4
RMI1
ARP8
RAD1
MSH2
YKU80
MSH4
RAD5
DBP5
MRE11
YKU70
EXO1
PSO2
XRS2
POL3
MEC1
MMS1
RAD50
SGS1
UBP15
TOP1
POL30
TOP3
EST2
POL2
TRM2
RAD9
PGD1
CDC13
MLH1
RAD27
RRP6
POL32
B
RAD52
POL30
RAD9
RAD27
TOF1
POL32
RAD24
RAD51
PIF1
EXO1
SGS1
MRE11
MRC1
RAD53
RAD1
ELG1
RAD50
ASF1
NUP84
SRS2
Deletion suppresses cdc13-1 growth defect
Deletion enhances cdc13-1 growth defect
Deletion not known to affect cdc13-1 growth defect
Genetic Interaction
Deletion increases telomere length
Deletion decreases telomere length
Deletion not known to affect telomere length
Shared genetic interactions

Figure 4: *PIF1* shares genetic interactions with *EXO1*

A. Genes that have a genetic interaction with *EXO1* as obtained from BioGRID (Stark et al., 2006). **B.** A ranked list of genes that share a genetic interaction with *EXO1* (i.e. have a genetic interaction with those genes shown in A.)

Genes are colored according to their effect on *cdc13-1* mutants with uncapped telomeres and circled according to their effect on telomere length (Addinall et al., 2008, Askree et al., 2004, Downey et al., 2006, Foster et al., 2006, Gatbonton et al., 2006, Shachar et al., 2008, Tsolou and Lydall, 2007, Ungar et al., 2009).

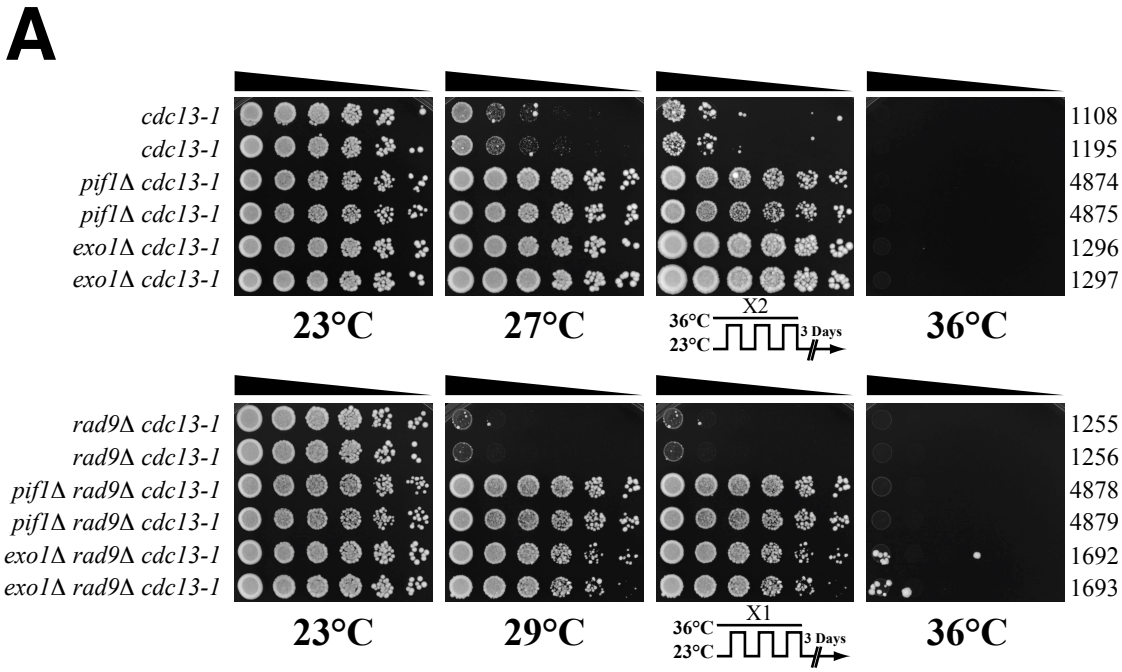
A
cdc13-1
cdc13-1
pif1Δ cdc13-1
pif1Δ cdc13-1
exo1Δ cdc13-1
exo1Δ cdc13-1
1108
1195
4874
4875
1296
1297
23°C
27°C
X2
36°C
23°C
3 Days
36°C
rad9Δ cdc13-1
rad9Δ cdc13-1
pif1Δ rad9Δ cdc13-1
pif1Δ rad9Δ cdc13-1
exo1Δ rad9Δ cdc13-1
exo1Δ rad9Δ cdc13-1
1255
1256
4878
4879
1692
1693
23°C
29°C
X1
36°C
23°C
3 Days
36°C

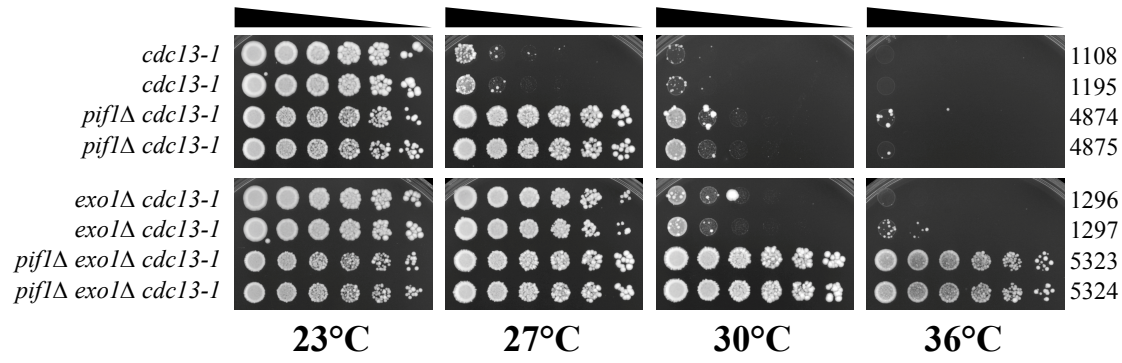
B
cdc13-1
cdc13-1
pif1Δ cdc13-1
pif1Δ cdc13-1
exo1Δ cdc13-1
exo1Δ cdc13-1
pif1Δ exo1Δ cdc13-1
pif1Δ exo1Δ cdc13-1
1108
1195
4874
4875
1296
1297
5323
5324
23°C
27°C
30°C
36°C

Figure 5: Pif1 and Exo1 inhibit growth of *cdc13-1* and *cdc13-1 rad9*Δ mutants and function in parallel pathways

A. and **B.** Saturated cultures of the indicated genotypes were serially diluted across agar plates and grown on YEPD plates either at the temperature indicated for 3 days or cycled from 23°C for 4 hours to 36°C for 4 hours for the number of times indicated then then allowed to form colonies on YEPD plates at 23°C for 3 days. For this figure and all onward, strain numbers (DLYs) are given as numbers adjacent to the strain in the figure.

3.2 Results

3.2.1 PIF1 has similar genetic interactions to EXO1

A bioinformatics-based search was applied to identify candidate genes for nuclease activities at uncapped telomeres amongst those that had already been identified by genetic screening (Addinall et al., 2008, Downey et al., 2006). It was hypothesized that any gene product responsible for a nuclease activity at uncapped telomeres would behave like Exo1 and thus its encoding gene would have similar genetic interactions to *EXO1*, in addition to inhibiting the growth of *cdc13-1* mutants, like *EXO1*.

To identify such genes, total genetic interactions from the BioGRID database were downloaded to permit the identification of all genes which had a genetic interaction with *EXO1* (Figure 4A) (Stark et al., 2006). These 39 genes were also annotated using data from high throughput screens for genes that affect the growth of *cdc13-1* mutants (Addinall et al., 2008, Downey et al., 2006) and for genes that affect telomere length (Askree et al., 2004, Gatbonton et al., 2006, Ungar et al., 2009). The BioGRID database was then used to identify genes that also interacted with any of the 39 genes that had a genetic interaction with *EXO1* (and thus behaved like *EXO1*) and this list was ranked according to the number of genetic interactions they had with these 39 genes. The top 10% of this list was then taken and displayed as a ranked graph (Figure 4B). The final ranked list of genes that had similar genetic interactions to *EXO1* contained 19 '*EXO1*-like' genes.

If there was validity to the bioinformatic search that had been applied, then the 19 most '*EXO1*-like' genes should include known nucleases, including those that cooperate with Exo1 in resection. To test this hypothesis, we examined the 19 most '*EXO1*-like' genes to look for nuclease activities (Figure 4B). Components of 4 different nucleases that did not inhibit the growth of *cdc13-1* mutants were identified; *RAD27* (encoding Flap Endonuclease 1) (Reagan et al., 1995); *SGS1* (encoding a component of the Sgs1/Dna2 nuclease) (Gangloff et al., 1994); *RAD1* (a ssDNA endonuclease involved in NER) (Tomkinson et al., 1993); *MRE11* and *RAD50* (encoding components of the MRX complex) (Ivanov et al., 1994). Rad27 cooperates with Exo1 during Okazaki fragment processing, while the Sgs1/Dna2 and MRX dependent nucleases play roles in DSBR along with Exo1 (Gravel et al., 2008, Mimitou and Symington, 2008, Stith et al., 2008,

Zhu et al., 2008). It was concluded that the bioinformatic search that had been applied was a valid method for identifying Exo1-like nuclease activities.

Any *EXO1*-like nuclease with roles in the resection of uncapped telomeres might be expected to also resect telomeres under conditions of homeostasis. Though elimination of *EXO1* itself does not affect telomere length (Tsubouchi and Ogawa, 2000), it was hypothesized that an *EXO1*-like nuclease could potentially be more potent and degrade telomeres transiently during each cell cycle, for example, following temporary displacement of telomere capping proteins due to DNA replication (Lydall, 2009). If this were the case, then a null mutation in the gene encoding such a nuclease activity might increase telomere length.

To test this hypothesis, data from high throughput screens was used to examine the effect on telomere length of null mutations in the nuclease activities identified amongst the most '*EXO1*-like' genes (Figure 4B). Null mutations in *SGS1* and *RAD1* did not affect telomere length or growth of *cdc13-1* mutants; null mutations in *RAD27* increased telomere length but inhibited growth of *cdc13-1* mutants; null mutations in *MRE11* and *RAD50* decreased telomere length and inhibited growth of *cdc13-1* mutants (Figure 4B) (Addinall et al., 2008, Downey et al., 2006). It was concluded that there was no correlation between *EXO1*-like nucleases, their effect on the growth of *cdc13-1* mutants and their effect on telomere length that could be used to help identify unknown nuclease activities that function at telomeres.

It was hypothesized that the most likely candidates for unidentified nuclease activities at uncapped telomeres would inhibit the growth of *cdc13-1* mutants, like Exo1. To test this hypothesis, the 19 most '*EXO1*-like' genes were examined for genes encoding products that inhibit the growth of *cdc13-1* mutants (Figure 4B). It was found that 3 of the '*EXO1*-like' genes encoded proteins that, like Exo1, inhibited the growth of *cdc13-1* mutants; *RAD9* encodes a mediator protein, required for checkpoint activation in response to telomere uncapping and also plays a pivotal roles in inhibiting ssDNA generation at uncapped telomeres (Lydall and Weinert, 1995); *RAD24* encodes a component of the clamp loader and is responsible for loading the 9-1-1 complex, which is required for checkpoint activation following telomere uncapping and is also required for a nuclease activity at uncapped telomeres (Zubko et al., 2004); *PIF1* encodes a helicase that is believed to negatively regulate telomerase at telomeres, in addition to

having roles in unwinding G quadruplexes, disassembling stalled replication forks and generating ssDNA to be cleaved by nucleases during Okazaki fragment processing (Boule et al., 2005, Chang et al., 2009, Pike et al., 2009, Ribeyre et al., 2009, Rossi et al., 2008). Both Rad9 and Rad24 had well-characterized roles in the resection of uncapped telomeres, while Pif1 did not (Lydall and Weinert, 1995, Zubko et al., 2004). In conclusion, Pif1 is the most likely candidate for an unknown nuclease activity at uncapped telomeres.

To test the hypothesis that Pif1 functions like Exo1 at uncapped telomeres, the effect of null mutations in *PIF1* and *EXO1* on the growth of *cdc13-1* mutants was examined. At low temperatures, such as 23°C, Cdc13-1 is completely active and all cells containing the *cdc13-1* allele are able to grow (Figure 5A) while at high temperatures, such as 36°C, Cdc13-1 is completely inactive and no cells containing the *cdc13-1* allele are able to grow (Figure 5A) (Maringele and Lydall, 2002). At intermediate temperatures, such as 27°C, low levels of Cdc13-1 activity persist and *cdc13-1* mutants are unable to grow unless proteins that inhibit the growth of *cdc13-1* mutants, such as Exo1, are eliminated (Zubko et al., 2004). Figure 5A shows that at 27°C, *cdc13-1* mutants are unable to grow, while *cdc13-1 pif1*Δ and *cdc13-1 exo1*Δ mutants are. In conclusion, Pif1, like Exo1, inhibits the growth of *cdc13-1* mutants at uncapped telomeres.

At intermediate temperatures, such as 27°C, growth of *cdc13-1* mutants is inhibited by checkpoint proteins (which cell cycle arrest) and by nuclease activities (which cause resection and loss of viability). It was hypothesized that Pif1 would function like Exo1 at uncapped telomeres and inhibit the growth of *cdc13-1* mutants independently of the checkpoint. To test this hypothesis, the effect of Pif1 and Exo1 on the growth of *cdc13-1* mutants repeatedly cultured at 36°C was examined. Checkpoint-proficient *cdc13-1* mutants will undergo rapid cell cycle arrest at 36°C and undergo very little loss in viability for up to 4 hours, while checkpoint-defective *cdc13-1* mutants, continue to divide at 36°C and rapidly lose viability (Zubko et al., 2004). Checkpoint-proficient *cdc13-1* mutants do eventually lose viability after repeated rounds of growth at 36°C, unless nuclease activities that function at uncapped telomeres (such as Exo1) are eliminated (Zubko et al., 2004). Figure 5A shows that after 6 cycles of growth at 36°C for 4 hours, *cdc13-1* mutants had almost completely lost viability while *cdc13-1 pif1*Δ and *cdc13-1 exo1*Δ mutants still grew well. In conclusion, Pif1, like Exo1, inhibits the viability of *cdc13-1* mutants even when grown at 36°C.

Pif1, like Exo1, inhibits the growth of *cdc13-1* mutants at 27°C and contributes to the loss of viability of *cdc13-1* mutants at 36°C, suggesting that Pif1, like Exo1, is required for a nuclease activity at uncapped telomeres (Figure 4A). In *cdc13-1 rad9*Δ mutants, the absence of Rad9 prevents checkpoint activation and only the level of resection at uncapped telomeres limits growth. Thus, to test the hypothesis that Pif1 is required for a nuclease activity at uncapped telomeres, the effect of Pif1 and Exo1 on the growth of *cdc13-1 rad9*Δ mutants was examined. At 29°C, *cdc13-1 rad9*Δ *pif1*Δ and *cdc13-1 rad9*Δ *exo1*Δ mutants are able to grow, while *cdc13-1 rad9*Δ mutants were not (Figure 5A). After 3 cycles of growth at 36°C for 4 hours, *cdc13-1 rad9*Δ *pif1*Δ and *cdc13-1 rad9*Δ *exo1*Δ mutants grew well, while *cdc13-1 rad9*Δ mutants had completely lost viability (Figure 5A). In conclusion, Pif1 is most likely required for a nuclease activity at uncapped telomeres, like Exo1.

Pif1 appeared to be required for a nuclease activity at uncapped telomeres. To test whether Pif1 functioned in the same pathway as Exo1 or in a different pathway, the effect of Pif1 on the growth of *cdc13-1 exo1*Δ mutants was examined. At 27°C *cdc13-1 exo1*Δ mutants grew well, but grew very poorly at 30°C and not at all at 36°C (Figure 5B). However, *cdc13-1 exo1*Δ *pif1*Δ mutants grew well at 27°C and 30°C and even at 36°C when *cdc13-1* was completely inactivated (Figure 5B). In conclusion, Pif1 and Exo1 inhibit the growth of *cdc13-1* mutants through different pathways and elimination of Pif1 and Exo1 might eliminate the requirement for Cdc13.

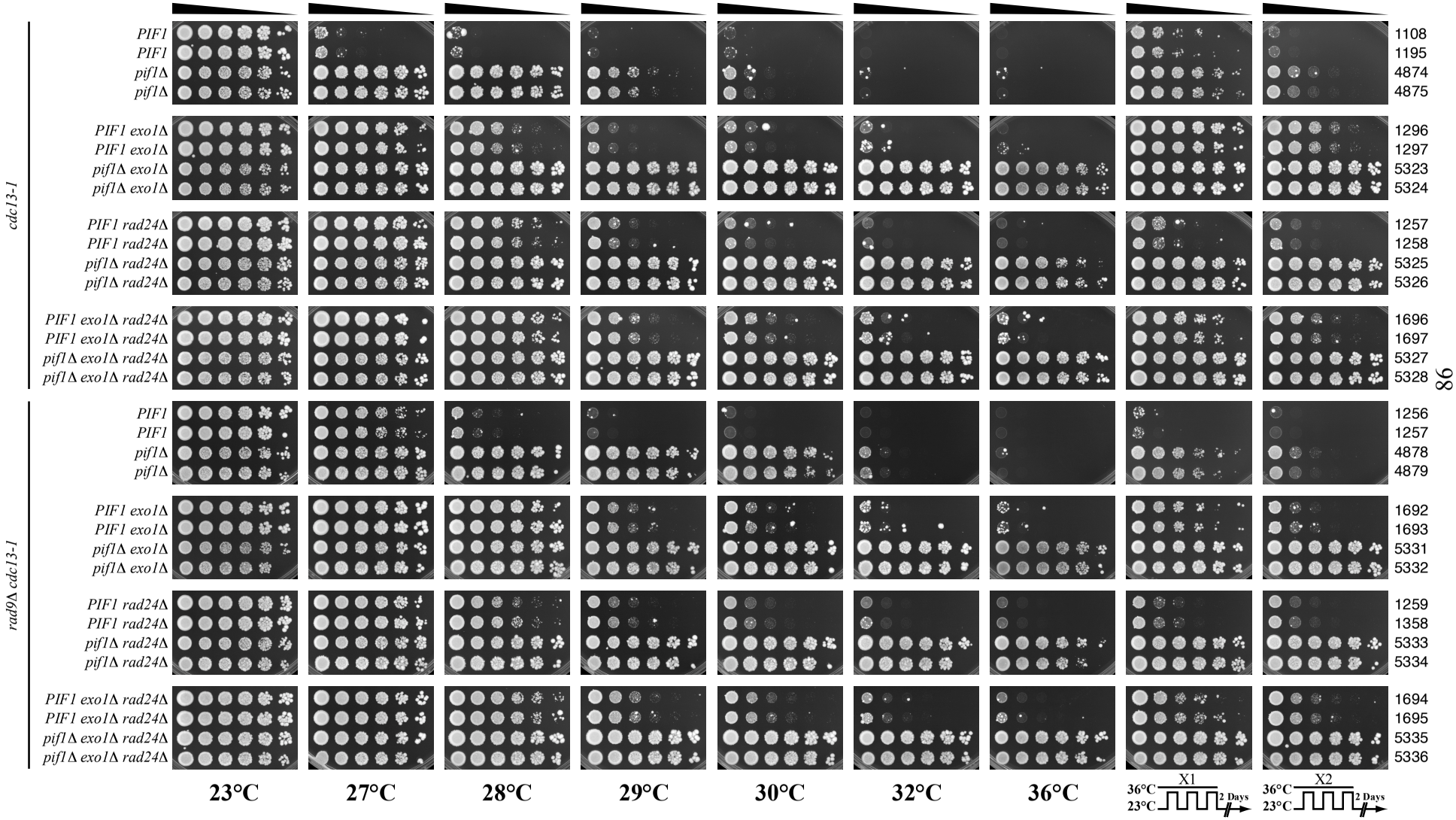
cdc13-1
rad9Δ cdc13-1
PIF1
PIF1
pif1Δ
pif1Δ
PIF1 exo1Δ
PIF1 exo1Δ
pif1Δ exo1Δ
pif1Δ exo1Δ
PIF1 rad24Δ
PIF1 rad24Δ
pif1Δ rad24Δ
pif1Δ rad24Δ
PIF1 exo1Δ rad24Δ
PIF1 exo1Δ rad24Δ
pif1Δ exo1Δ rad24Δ
pif1Δ exo1Δ rad24Δ
1108
1195
4874
4875
1296
1297
5323
5324
1257
1258
5325
5326
1696
1697
5327
5328
1256
1257
4878
4879
1692
1693
5331
5332
1259
1358
5333
5334
1694
1695
5335
5336
23°C
27°C
28°C
29°C
30°C
32°C
36°C
36°C
23°C
X1
2 Days
36°C
23°C
X2
2 Days

Figure 6: Pif1 inhibits the growth of *cdc13-1* mutants in a parallel pathway to Exo1 and Rad24

Saturated cultures of the indicated genotypes were serially diluted across agar plates and grown on YEPD plates either at the temperature indicated for 3 days or cycled from 23°C for 4 hours to 36°C for 4 hours for the number of times indicated and then allowed to form colonies at 23°C for 2 days.

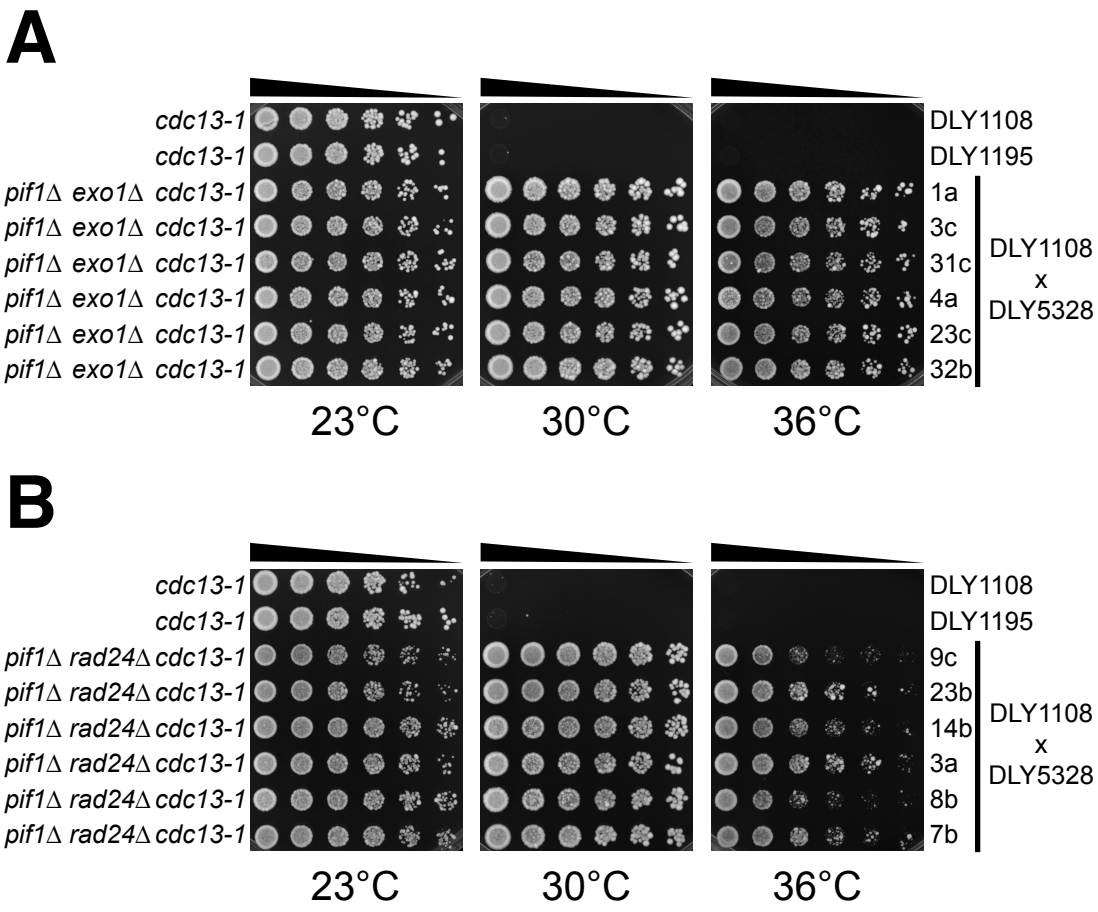
A
cdc13-1
cdc13-1
pif1Δ exo1Δ cdc13-1
pif1Δ exo1Δ cdc13-1
pif1Δ exo1Δ cdc13-1
pif1Δ exo1Δ cdc13-1
pif1Δ exo1Δ cdc13-1
pif1Δ exo1Δ cdc13-1
DLY1108
DLY1195
1a
3c
31c
4a
23c
32b
DLY1108
x
DLY5328
23°C
30°C
36°C
B
cdc13-1
cdc13-1
pif1Δ rad24Δ cdc13-1
pif1Δ rad24Δ cdc13-1
pif1Δ rad24Δ cdc13-1
pif1Δ rad24Δ cdc13-1
pif1Δ rad24Δ cdc13-1
pif1Δ rad24Δ cdc13-1
DLY1108
DLY1195
9c
23b
14b
3a
8b
7b
DLY1108
x
DLY5328
23°C
30°C
36°C

Figure 7: Growth of *cdc13-1 exo1*Δ *pif1*Δ and *cdc13-1 exo1*Δ *rad24*Δ mutants at 36°C is not due to a second site suppressor

*cdc13-1 exo1*Δ *pif1*Δ and *cdc13-1 rad24*Δ *pif1*Δ meiotic progeny from the crosses indicated in **A.** and **B.** were randomly selected and saturated cultures of the indicated genotypes were serially diluted across agar plates and grown at the temperature indicated for 3 days.

3.2.2 Pif1 inhibits the growth of cdc13-1 mutants in a parallel pathway to Exo1 and Rad24

Pif1 inhibits the growth of *cdc13-1* mutants most likely by controlling a nuclease activity that is independent of the nuclease Exo1 (Figure 5B). Rad24 loads the 9-1-1 complex in response to DNA damage and has also been shown to control a nuclease activity at uncapped telomeres, so it was hypothesized that Rad24 might contribute to Pif1-dependent nuclease activity and thus inhibit the growth of *cdc13-1* mutants in a Pif1-dependent manner. To test this hypothesis, the effect of Rad24 on the growth of *cdc13-1 pif1*Δ mutants was examined. As previously reported, *cdc13-1 rad24*Δ mutants were able to grow at 27°C while *cdc13-1* mutants were not (Figure 6), thus Rad24 inhibits the growth of *cdc13-1* mutants (Figure 6). *cdc13-1 pif1*Δ mutants grew well at 23°C-28°C, poorly from 29°C-30°C and not at all from 32°C-36°C while, surprisingly, *cdc13-1 pif1*Δ *rad24*Δ mutants grew well from 23°C-32°C and showed only a very slight growth defect at 36°C (Figure 6). In conclusion, Rad24 inhibits the growth of *cdc13-1* mutants through a different pathway to Pif1 and *cdc13-1 pif1*Δ *rad24*Δ mutants, like *cdc13-1 pif1*Δ *exo1*Δ mutants, are able to grow at 36°C, even with *cdc13-1* completely inactivated.

Elimination of Pif1 and Exo1 permitted growth of *cdc13-1* (*pif1*Δ *exo1*Δ) mutants at 36°C without any noticeable loss in viability (Figure 5B) while elimination of Pif1 and Rad24 permitted growth of *cdc13-1* (*pif1*Δ *rad24*Δ) mutants at 36°C, but with a very slight loss in viability (Figure 6). It was hypothesized that the slight loss in viability seen in *cdc13-1 pif1*Δ *rad24*Δ mutants at 36°C might be due to Exo1. To test this hypothesis, the effect of Exo1 on the growth of *cdc13-1 pif1*Δ *rad24*Δ mutants was examined. At 36°C, *cdc13-1 pif1*Δ *rad24*Δ mutants displayed a very slight growth defect (compared to the viability of *cdc13-1 pif1*Δ *rad24*Δ mutants at 23°C) while *cdc13-1 pif1*Δ *rad24*Δ *exo1*Δ mutants did not (Figure 6). In conclusion, the slight loss in viability seen in *cdc13-1 pif1*Δ *rad24*Δ mutants at 36°C is dependent upon Exo1.

A possible explanation for the ability of *cdc13-1 pif1*Δ *exo1*Δ and *cdc13-1 pif1*Δ *rad24*Δ mutants to grow at 36°C and for the Exo1-dependent decrease in viability of *cdc13-1 pif1*Δ *rad24*Δ mutants at 36°C was that Pif1 functioned to inhibit the growth of *cdc13-1* mutants in a parallel pathway to Exo1 and Rad24, in which Rad24 was critical-

but-not-essential-for Exo1 activity. To test this hypothesis, the effect of Rad24 on the growth of *cdc13-1 exo1*Δ mutants was examined. At 28°C, *cdc13-1 exo1*Δ *rad24*Δ mutants grew better than *cdc13-1 exo1*Δ mutants, indicating that Rad24 inhibited the growth of *cdc13-1* mutants independently of Exo1 (Figure 6). However, Rad24 is required for checkpoint activation following telomere uncapping and thus could have been inhibiting the growth of *cdc13-1 exo1*Δ mutants by promoting checkpoint activation. To test this hypothesis, the effect of Rad24 on the growth of *cdc13-1 rad9*Δ *exo1*Δ mutants (in which checkpoint activation has been eliminated) was examined. At 28°C-30°C no improvement in growth could be seen in *cdc13-1 rad9*Δ *exo1*Δ *rad24*Δ mutants compared to *cdc13-1 rad9*Δ *exo1*Δ mutants (Figure 6), as seen previously (Zubko et al., 2004). In conclusion, Rad24 inhibits the growth of *cdc13-1* mutants in a manner dependent upon the checkpoint and Exo1.

In addition to contributing to checkpoint activation, Rad9 also limits resection at uncapped telomeres and this Rad9-inhibited resection (ExoX activity) is dependent upon Rad24 (Lydall and Weinert, 1995). It was hypothesized that ExoX activity might function independently of Pif1 and Exo1 at uncapped telomeres. To test this hypothesis, it was examined whether there was a Rad24-dependent loss of viability in *cdc13-1 rad9*Δ *exo1*Δ *pif1*Δ mutants. Surprisingly, *cdc13-1 rad9*Δ *exo1*Δ *pif1*Δ mutants showed no obvious loss in viability at 36°C compared to 23°C and this was the same for *cdc13-1 rad9*Δ *exo1*Δ *pif1*Δ *rad24*Δ mutants (Figure 6). Furthermore, *cdc13-1 rad9*Δ *rad24*Δ *pif1*Δ mutants still showed only a very slight growth defect at 36°C, while *cdc13-1 rad9*Δ *rad24*Δ *pif1*Δ *exo1*Δ mutants did not, demonstrating that the slight growth defect of *cdc13-1 rad9*Δ *rad24*Δ *pif1*Δ mutants at 36°C was due to Exo1 (Figure 6). In conclusion, it is likely that no ExoX activity occurs in *cdc13-1 pif1*Δ *exo1*Δ mutants and it is possible that all nuclease activities identified to date at uncapped telomeres are dependent upon Pif1 or Exo1, or both.

Finally, the ability of *cdc13-1 exo1*Δ *pif1*Δ and *cdc13-1 rad24*Δ *pif1*Δ strains to grow at 36°C (even with *cdc13-1* completely inactive) was remarkable. However, it was possible that this could have been due to a second site suppressor arising in one of the parental strains used. To test this hypothesis, a *cdc13-1 exo1*Δ *rad24*Δ *pif1*Δ strain able to grow at 36°C was back-crossed to a *cdc13-1* strain unable to grow at 36°C. Progeny from the cross were assayed for growth, and all *cdc13-1 exo1*Δ *pif1*Δ (Figure 7A) and *cdc13-1 rad24*Δ *pif1*Δ (Figure 7B) progeny were able to grow at 36°C. In conclusion,

the striking genetic interactions between *PIF1* and *EXO1/RAD24* in *cdc13-1* mutants are legitimate and not a consequence of background mutations.

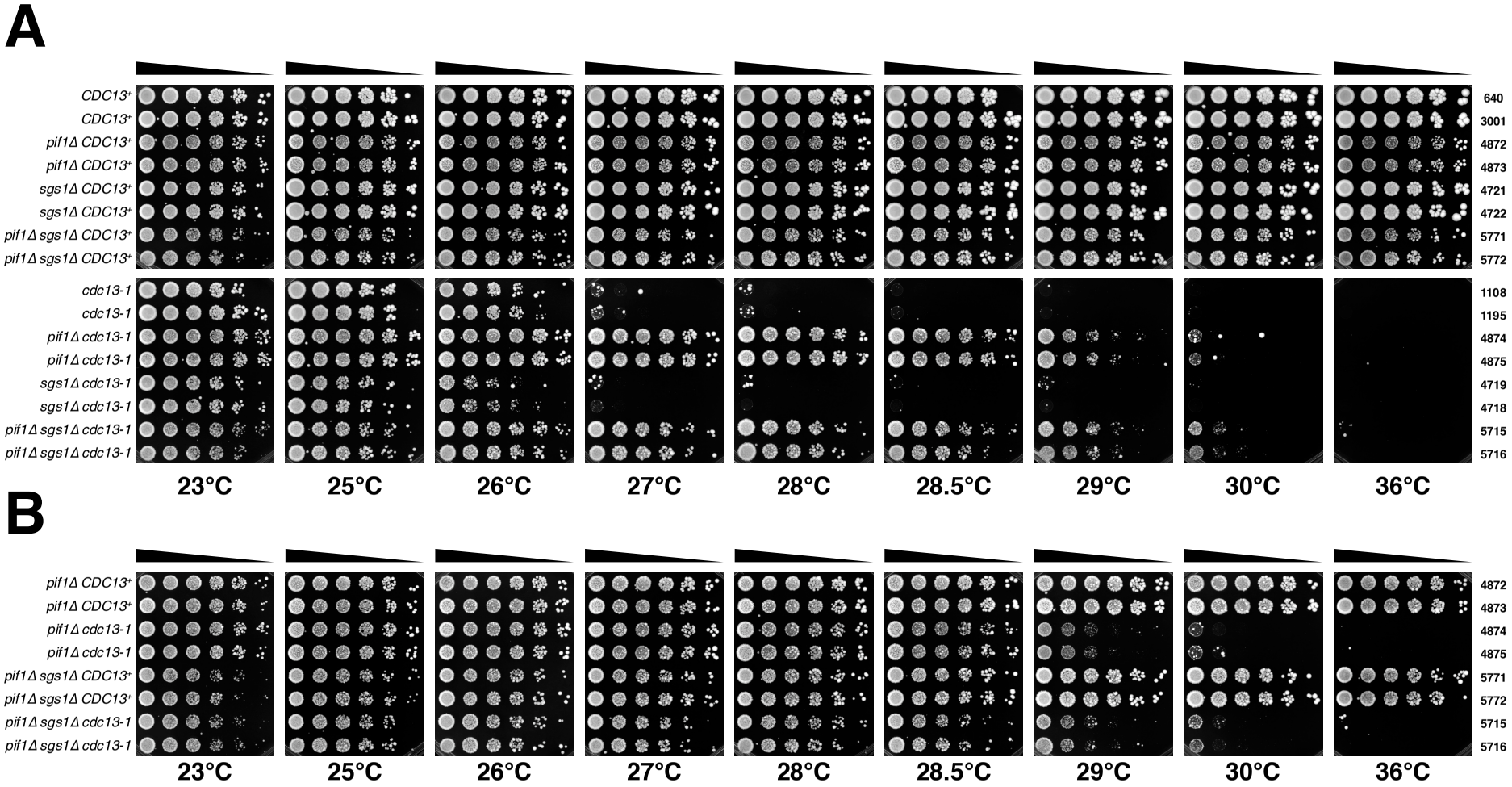
A
CDC13+
CDC13+
pif1Δ CDC13+
pif1Δ CDC13+
sgs1Δ CDC13+
sgs1Δ CDC13+
pif1Δ sgs1Δ CDC13+
pif1Δ sgs1Δ CDC13+
cdc13-1
cdc13-1
pif1Δ cdc13-1
pif1Δ cdc13-1
sgs1Δ cdc13-1
sgs1Δ cdc13-1
pif1Δ sgs1Δ cdc13-1
pif1Δ sgs1Δ cdc13-1
640
3001
4872
4873
4721
4722
5771
5772
1108
1195
4874
4875
4719
4718
5715
5716
23°C
25°C
26°C
27°C
28°C
28.5°C
29°C
30°C
36°C
B
pif1Δ CDC13+
pif1Δ CDC13+
pif1Δ cdc13-1
pif1Δ cdc13-1
pif1Δ sgs1Δ CDC13+
pif1Δ sgs1Δ CDC13+
pif1Δ sgs1Δ cdc13-1
pif1Δ sgs1Δ cdc13-1
4872
4873
4874
4875
5771
5772
5715
5716
23°C
25°C
26°C
27°C
28°C
28.5°C
29°C
30°C
36°C

Figure 8: Sgs1 promotes the vitality of *cdc13-1* mutants in a different pathway to Pif1

A. and **B.** saturated cultures of the indicated genotypes were serially diluted across agar plates and grown at the temperatures indicated for 3 days.

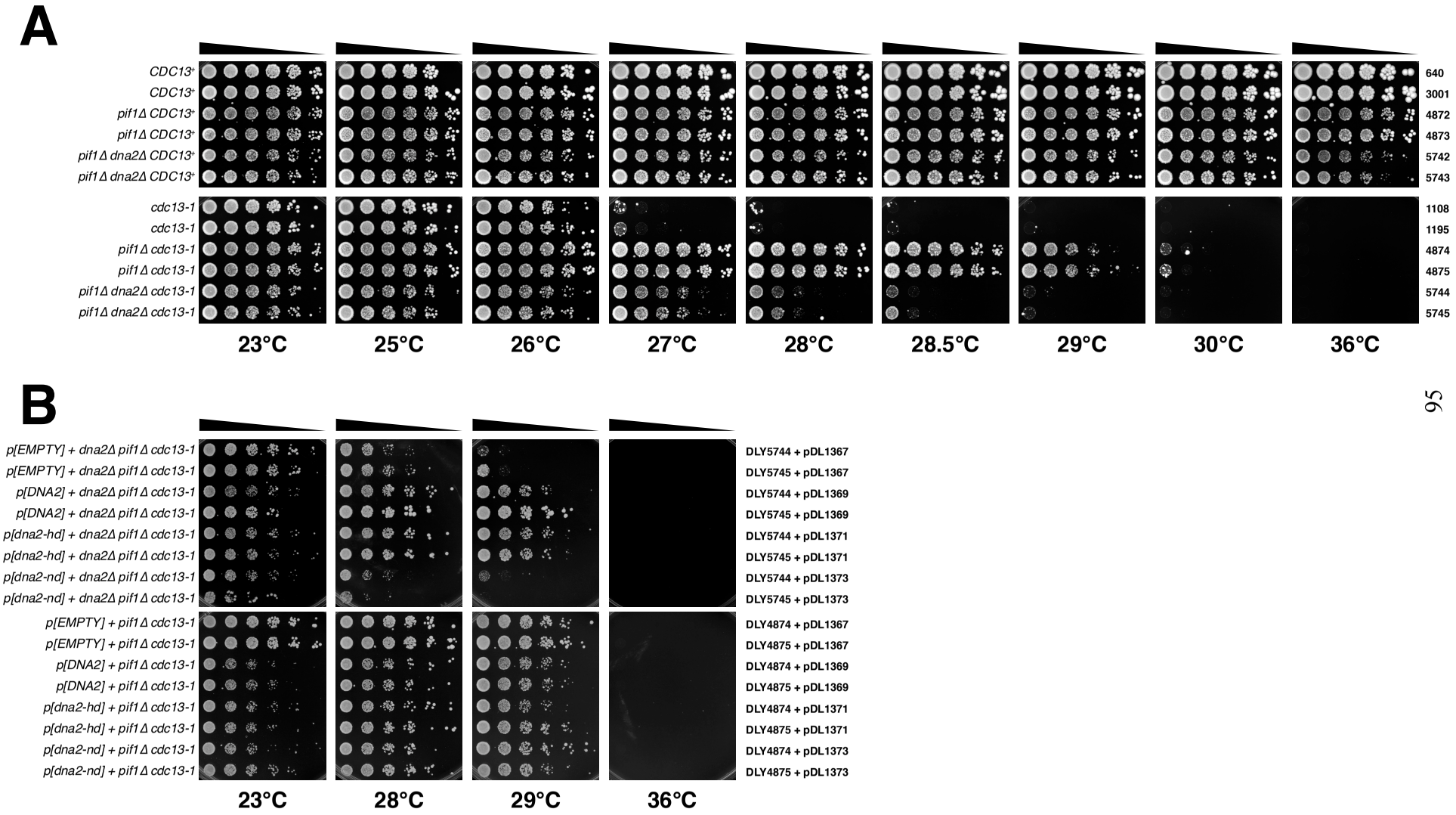
A
CDC13+
CDC13+
pif1Δ CDC13+
pif1Δ CDC13+
pif1Δ dna2Δ CDC13+
pif1Δ dna2Δ CDC13+
cdc13-1
cdc13-1
pif1Δ cdc13-1
pif1Δ cdc13-1
pif1Δ dna2Δ cdc13-1
pif1Δ dna2Δ cdc13-1
640
3001
4872
4873
5742
5743
1108
1195
4874
4875
5744
5745
23°C
25°C
26°C
27°C
28°C
28.5°C
29°C
30°C
36°C
B
p[EMPTY] + dna2Δ pif1Δ cdc13-1
p[EMPTY] + dna2Δ pif1Δ cdc13-1
p[DNA2] + dna2Δ pif1Δ cdc13-1
p[DNA2] + dna2Δ pif1Δ cdc13-1
p[dna2-hd] + dna2Δ pif1Δ cdc13-1
p[dna2-hd] + dna2Δ pif1Δ cdc13-1
p[dna2-nd] + dna2Δ pif1Δ cdc13-1
p[dna2-nd] + dna2Δ pif1Δ cdc13-1
p[EMPTY] + pif1Δ cdc13-1
p[EMPTY] + pif1Δ cdc13-1
p[DNA2] + pif1Δ cdc13-1
p[DNA2] + pif1Δ cdc13-1
p[dna2-hd] + pif1Δ cdc13-1
p[dna2-hd] + pif1Δ cdc13-1
p[dna2-nd] + pif1Δ cdc13-1
p[dna2-nd] + pif1Δ cdc13-1
DLY5744 + pDL1367
DLY5745 + pDL1367
DLY5744 + pDL1369
DLY5745 + pDL1369
DLY5744 + pDL1371
DLY5745 + pDL1371
DLY5744 + pDL1373
DLY5745 + pDL1373
DLY4874 + pDL1367
DLY4875 + pDL1367
DLY4874 + pDL1369
DLY4875 + pDL1369
DLY4874 + pDL1371
DLY4875 + pDL1371
DLY4874 + pDL1373
DLY4875 + pDL1373
23°C
28°C
29°C
36°C

Figure 9: Dna2 nuclease activity promotes the vitality of *cdc13-1 pif1*Δ mutants
Saturated cultures of the indicated genotypes were serially diluted across agar plates and grown at the temperatures indicated on either **A.** YEPD for 3 days or **B.** –URA for 4 days.

3.2.3 Sgs1 and Dna2 have protective roles at uncapped telomeres

Two distinct nuclease activities dependent upon Exo1 and Sgs1/Dna2 resect DNA double-strand breaks (Gravel et al., 2008, Mimitou and Symington, 2008, Zhu et al., 2008). Despite this, Sgs1 and Dna2 were unlikely candidates for nuclease activities at uncapped telomeres because neither gene was highlighted by high throughput screening as inhibiting the growth of *cdc13-1* mutants (Addinall et al., 2008, Downey et al., 2006). However, Sgs1 has been identified as contributing to nuclease activity at uncapped telomeres (Ngo and Lydall, 2010) and Dna2 is an essential gene, so could not have been screened for (Budd et al., 2006). Thus, it was decided to test whether Sgs1 and Dna2 might also function as nuclease activities at uncapped telomeres and whether they might do so in the same pathway as Pif1.

To test whether Sgs1 might function as a nuclease activity at uncapped telomeres and whether it functioned in the same pathway or a different pathway to Pif1, the effect of Sgs1 on the growth of *cdc13-1* and *cdc13-1 pif1*Δ mutants was examined. At 26°C, *cdc13-1* mutants showed a slight growth defect, while *cdc13-1 sgs1*Δ mutants showed a more severe growth defect (Figure 8A), consistent with other work (Ngo and Lydall, 2010). At 27°C-28.5°C, *cdc13-1 pif1*Δ mutants grew well, while *cdc13-1 pif1*Δ *sgs1*Δ mutants showed a slight growth defect (Figure 8A). In conclusion, Sgs1 promotes growth of *cdc13-1* mutants independently of Pif1.

It was noted, *cdc13-1 pif1*Δ *sgs1*Δ mutants also grew poorly at 23°C, when *cdc13-1* should have been completely active. Thus, it was hypothesized that the growth defect in *cdc13-1 pif1*Δ *sgs1*Δ mutants at 27°C-28.5°C was due to the poor growth of *pif1*Δ *sgs1*Δ mutants and that Sgs1 might actually function in a Pif1-dependent manner. To test this hypothesis, the growth of $CDC13^{+}$*pif1*Δ and *cdc13-1 pif1*Δ mutants was compared to the growth of $CDC13^{+}$ *pif1*Δ *sgs1*Δ and *cdc13-1 pif1*Δ *sgs1*Δ mutants. At 27°C-28.5°C there was no noticeable growth defect in *cdc13-1 pif1*Δ mutants compared to $CDC13^{+}$ *pif1*Δ mutants (Figure 8B). At 23°C, *cdc13-1 pif1*Δ *sgs1*Δ mutants and $CDC13^{+}$ *pif1*Δ *sgs1*Δ mutants grew equally and both grew worse than *cdc13-1 pif1*Δ mutants (Figure 8B). However, at 27°C-28.5°C, *cdc13-1 pif1*Δ *sgs1*Δ mutants grew worse than $CDC13^{+}$ *pif1*Δ *sgs1*Δ mutants. In conclusion, *pif1*Δ *sgs1*Δ mutants grow poorly, but this does not account for the growth defect seen in *cdc13-1 pif1*Δ *sgs1*Δ

mutants at 27-28.5°C, and thus Sgs1 does indeed promote the growth of *cdc13-1* mutants independently of Pif1.

Dna2 is an essential gene, but the lethality of a *dna2*Δ mutant can be suppressed in a *pif1*Δ background (Budd et al., 2006). To test whether Dna2 had any Pif1-independent functions at uncapped telomeres, the effect of Dna2 on the growth of *cdc13-1 pif1*Δ mutants was examined. At 27°C-28.5°C, *cdc13-1 pif1*Δ mutants grew well while *cdc13-1 pif1*Δ *dna2*Δ mutants grew extremely poorly (Figure 9A). In conclusion, Dna2 promotes the growth of *cdc13-1* mutants independently of Pif1. Interestingly, *cdc13-1 pif1*Δ *dna2*Δ mutants are unable to grow at 28.5°C (Figure 9A) while *cdc13-1 pif1*Δ *sgs1*Δ mutants are (Figure 8A), suggesting that Dna2 is more important than Sgs1 in protecting uncapped telomeres and, possibly, that Sgs1 and Dna2 have different roles at uncapped telomeres.

Dna2 is both a helicase and a nuclease. Dna2 nuclease, but not helicase, activity is required for DSBR (Zhu et al., 2008). Dna2 helicase activity at telomeres is believed to be important to unwind G-quadruplex structures (Sfeir et al., 2009) and Dna2 has been shown to be important for processing of G-quadruplex structures during replication (Lopes et al., 2002). It was hypothesized that Dna2 nuclease activity might inhibit the growth of *cdc13-1* mutants with uncapped telomeres by playing a role in resection, while Dna2 helicase activity might play a protective role by unwinding G-quadruplex structures. If the loss of protective helicase activity were more detrimental to the cell than the harmful nuclease activity, then deletion of *DNA2* would cause a net decrease in growth and *cdc13-1 pif1*Δ *dna2*Δ mutants would be expected to grow worse than *cdc13-1 pif1*Δ mutants, as observed (Figure 9A).

To test whether the helicase and nuclease activities of Dna2 might have opposing roles at uncapped telomeres, *cdc13-1 pif1*Δ and *cdc13-1 pif1*Δ *dna2*Δ mutants were transformed with over-expression plasmids containing either no insert, wild type *DNA2* or helicase- or nuclease-defective *DNA2* (Zhu et al., 2008). *cdc13-1 pif1*Δ *dna2*Δ mutants containing an empty over-expression plasmid grew much worse than *cdc13-1 pif1*Δ mutants containing an empty over-expression plasmid at 28°C and 29°C (Figure 9B), as expected (Figure 9A). At 28°C and 29°C *cdc13-1 pif1*Δ *dna2*Δ mutants over-expressing wild type *DNA2* or helicase-defective *DNA2* (*dna2-hd*) grew as well as *cdc13-1 pif1*Δ mutants over-expressing wild type *DNA2* or helicase-defective *DNA2*

(Figure 9B), demonstrating that over-expression of Dna2 nuclease activity could restore growth. At 28°C and 29°C *cdc13-1 pif1*Δ *dna2*Δ mutants over-expressing nuclease-defective *DNA2* (*dna2-nd*) grew worse than *cdc13-1 pif1*Δ mutants over-expressing nuclease-defective *DNA2* (Figure 9B), demonstrating that over-expression of Dna2 helicase activity could not restore growth. It was concluded that that, as expected, the helicase and nuclease activities of Dna2 had different roles at uncapped telomeres, but unexpectedly Dna2 nuclease activity appeared to have a protective role.

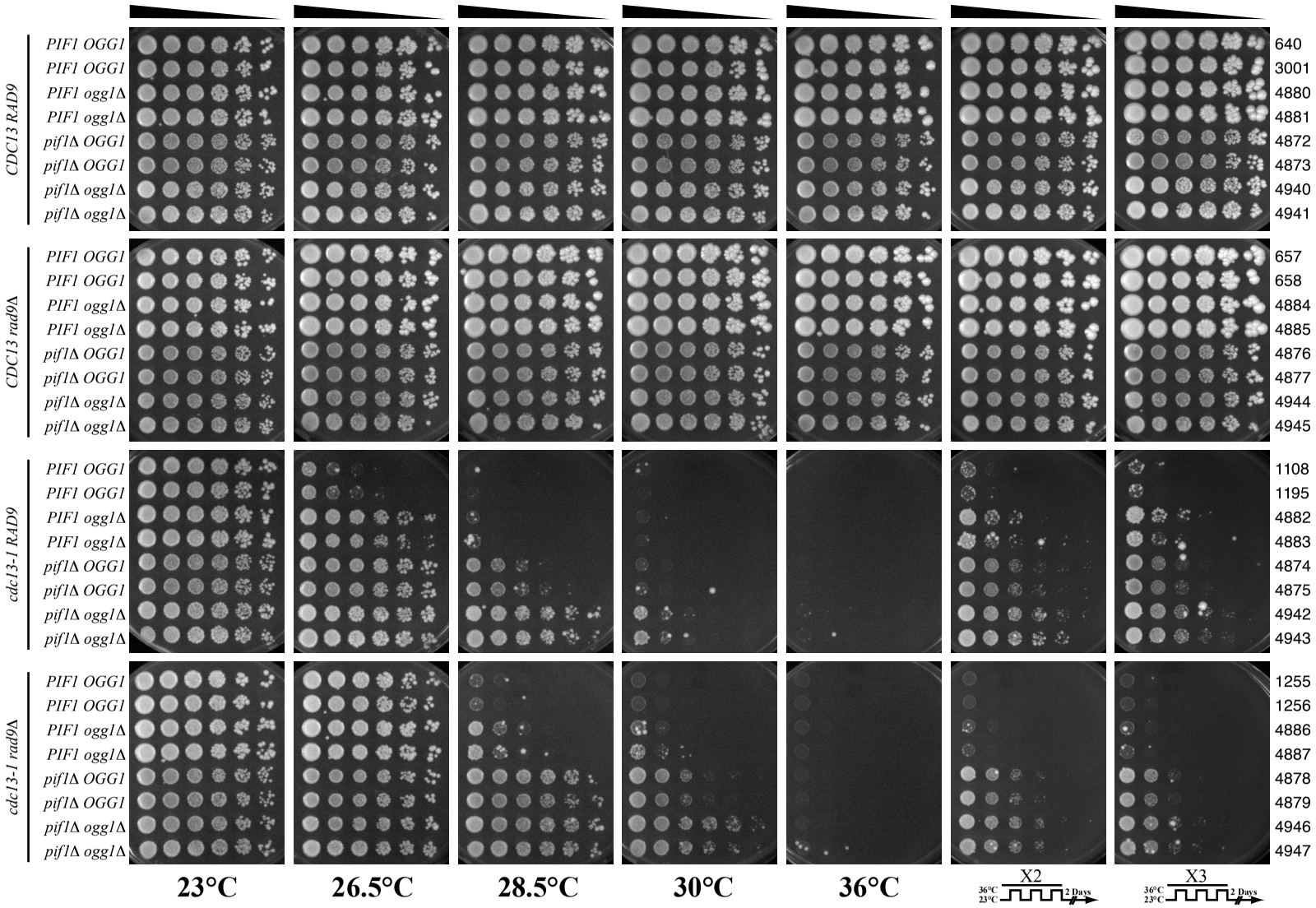
CDC13 RAD9
PIF1 OGG1
PIF1 OGG1
PIF1 ogg1Δ
PIF1 ogg1Δ
pif1Δ OGG1
pif1Δ OGG1
pif1Δ ogg1Δ
pif1Δ ogg1Δ
640
3001
4880
4881
4872
4873
4940
4941
CDC13 rad9Δ
PIF1 OGG1
PIF1 OGG1
PIF1 ogg1Δ
PIF1 ogg1Δ
pif1Δ OGG1
pif1Δ OGG1
pif1Δ ogg1Δ
pif1Δ ogg1Δ
657
658
4884
4885
4876
4877
4944
4945
cdc13-1 RAD9
PIF1 OGG1
PIF1 OGG1
PIF1 ogg1Δ
PIF1 ogg1Δ
pif1Δ OGG1
pif1Δ OGG1
pif1Δ ogg1Δ
pif1Δ ogg1Δ
1108
1195
4882
4883
4874
4875
4942
4943
cdc13-1 rad9Δ
PIF1 OGG1
PIF1 OGG1
PIF1 ogg1Δ
PIF1 ogg1Δ
pif1Δ OGG1
pif1Δ OGG1
pif1Δ ogg1Δ
pif1Δ ogg1Δ
1255
1256
4886
4887
4878
4879
4946
4947
23°C
26.5°C
28.5°C
30°C
36°C
X2
36°C
23°C
2 Days
X3
36°C
23°C
2 Days

Figure 10: Pif1 and Ogg1 inhibit the growth of *cdc13-1* mutants through different pathways

Saturated cultures of the indicated genotypes were serially diluted across agar plates and grown on YEPD plates either at the temperature indicated for 3 days or cycled from 23°C for 4 hours to 36°C for 4 hours for the number of times indicated and then allowed to form colonies on YEPD plates at 23°C for 2 days.

3.2.4 Ogg1 and Pif1 function in different pathways at uncapped telomeres

Ogg1 is a glycosylase/lyase responsible for recognizing and directing oxidized guanines to the BER and NER pathways. Ogg1 recognizes and excises oxidized guanines, before creating a single-strand break adjacent to the apurinic site, which is then a substrate for BER or NER (Boiteux and Guillet, 2004). Ogg1 was also identified as inhibiting the growth of *cdc13-1* mutants (Addinall et al., 2008). As Ogg1 creates single-strand breaks at oxidized guanines and telomeres are guanine rich, it was possible that Ogg1 could be creating single-strand breaks that were then processed by other nuclease activities at uncapped telomeres. However, *OGG1* is adjacent to and shares a promoter with *PIF1*, so it was possible that Ogg1 did not affect telomere uncapping directly and the *ogg1*Δ mutation interfered with *PIF1* gene expression (Cherry et al., 1997).

To test the hypothesis that Ogg1 inhibited the growth of *cdc13-1* mutants independently of Pif1, the effect of Ogg1 on the growth of *cdc13-1* and *cdc13-1 pif1*Δ mutants was examined. At 26.5°C, *cdc13-1 ogg1*Δ mutants grew well, while *cdc13-1* mutants did not (Figure 10) and at 28.5°C, *cdc13-1 pif1*Δ *ogg1*Δ mutants grew well, while *cdc13-1 pif1*Δ mutants did not (Figure 10). It was concluded that Ogg1 inhibits the growth of *cdc13-1* mutants independently of Pif1. This suggests that deletion of *OGG1* does not significantly decrease *PIF1* function, consistent with other reports that *ogg1*Δ mutants do not display altered *PIF1* expression compared to $OGG1^{+}$ mutants (Lu and Liu, 2009).

Ogg1 appeared to have a Pif1-independent role following telomere uncapping. It was hypothesized that Ogg1 might create single-strand breaks to permit nucleases access to uncapped telomeres and thus that the role of Ogg1 would not be checkpoint-dependent. To test this hypothesis, the effect of Ogg1 on the growth of *cdc13-1 rad9*Δ and *cdc13-1 rad9*Δ *pif1*Δ mutants was examined. At 28.5°C, *cdc13-1 rad9*Δ *ogg1*Δ mutants could grow poorly, while *cdc13-1 rad9*Δ mutants did not grow at all (Figure 10) and at 30°C, *cdc13-1 rad9*Δ *pif1*Δ *ogg1*Δ mutants grew better than *cdc13-1 rad9*Δ *pif1*Δ mutants. In conclusion, Ogg1 inhibits the growth of *cdc13-1* mutants independently of the checkpoint and independently of Pif1.

If Ogg1 did indeed contribute to nuclease activity at uncapped telomeres, then it was hypothesized that Ogg1 should inhibit the growth of *cdc13-1* and *cdc13-1 rad9*Δ

mutants at 36°C, like Exo1 and Pif1 (Figure 5A). To test this hypothesis, the effect of Ogg1 on the growth of *cdc13-1* and *cdc13-1 rad9*Δ mutants was examined. After 6 or 9 cycles of growth at 36°C, *cdc13-1 ogg1*Δ mutants grew better than *cdc13-1* mutants and *cdc13-1 pif1*Δ *ogg1*Δ mutants grew better than *cdc13-1 pif1*Δ mutants (Figure 10). However, after 6 or 9 cycles of growth at 36°C neither *cdc13-1 rad9*Δ *n*or *cdc13-1 rad9*Δ *ogg1*Δ mutants were able to grow and *cdc13-1 rad9*Δ *pif1*Δ *ogg1*Δ mutants grew no better than *cdc13-1 rad9*Δ *pif1*Δ mutants (Figure 10). It was concluded that Ogg1 probably does not contribute to a nuclease activity at uncapped telomeres, but does inhbit the growth of *cdc13-1* mutants independently of the checkpoint and independently of Pif1.

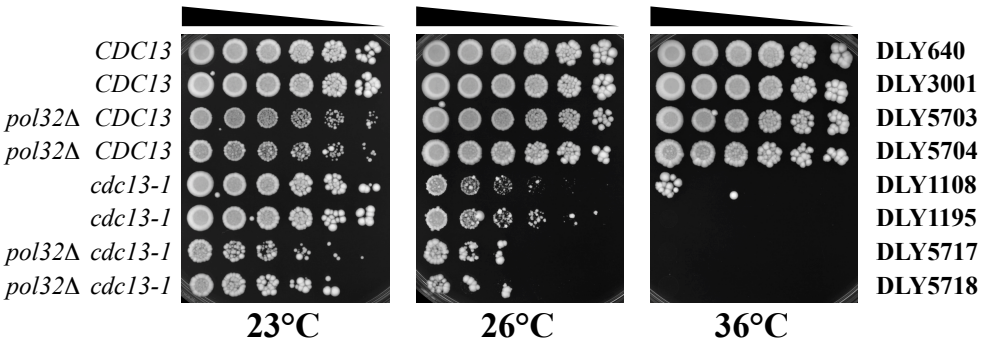
CDC13
CDC13
pol32Δ CDC13
pol32Δ CDC13
cdc13-1
cdc13-1
pol32Δ cdc13-1
pol32Δ cdc13-1
DLY640
DLY3001
DLY5703
DLY5704
DLY1108
DLY1195
DLY5717
DLY5718
23°C
26°C
36°C
4 days growth

Figure 11: Pol32 promotes the vitality of *cdc13-1* mutants

Saturated cultures of the indicated genotypes were serially diluted across agar plates and grown on YEPD plates at the temperatures indicated for 4 days.

3.2.5 Pol32 plays a protective role at uncapped telomeres

DNA Polymerase δ possesses intrinsic nuclease activity that can substitute during Okazaki fragment processing for other nucleases, such as Rad27 (Jin et al., 2001). Yeast *POL32*, encoding the Pol32 subunit of Polymerase δ genetically interacts with *PIF1* and grows poorly at low temperatures (Budd et al., 2006). In previous screens for genes that inhibit the growth of *cdc13-1* mutants, strains were constructed in a high throughput manner at 23°C (Addinall et al., 2008). Any *pol32*Δ strains constructed in this manner would have grown poorly and could have accumulated suppressor mutations, preventing a valid assessment of whether Pol32 promoted or inhibited the growth of *cdc13-1* mutants. Thus, Pol32 could inhibit the growth of *cdc13-1* mutants but this may have been masked by the poor growth of *pol32*Δ mutants at 23°C.

To test the hypothesis that Pol32 contributes to a nuclease activity at uncapped telomeres but this had not previously been detected due to the poor growth of *pol32*Δ mutants at 23°C, the effect of Pol32 on the growth of *cdc13-1* mutants was examined by generating *cdc13-1 pol32*Δ and *CDC13*$^+$ *pol32*Δ mutants with minimal passage at 23°C. In order to do this, *CDC13*$^+$ *pol32*Δ mutants first were germinated from spores of a *POL32*$^+$*/pol32*Δ *CDC13*$^+$*/cdc13-1* diploid (DDY335) and allowed to form colonies at 30°C. *CDC13*$^+$ *pol32*Δ colonies were then restreaked at 23°C and allowed to form single colonies while, simultaneously, *cdc13-1 pol32*Δ mutants were germinated from spores of the same *POL32*$^+$*/pol32*Δ *CDC13*$^+$*/cdc13-1* diploid (DDY335) and allowed to form colonies at 23°C. Single colonies of *CDC13*$^+$ *pol32*Δ and *cdc13-1 pol32*Δ mutants were then restreaked at 23°C, and then grown to stationary phase in YEPD at 23°C (along with *CDC13*$^+$ *POL32*$^+$ and *cdc13-1 POL32*$^+$ strains), serially-diluted across agar plates and grown at a range of temperatures alongside *CDC13*$^+$ *POL32*$^+$ and *cdc13-1 POL32*$^+$ mutants (Figure 11). This allowed the growth of *CDC13*$^+$ *POL32*$^+$ and *cdc13-1 POL32*$^+$ mutants to be compared to the growth of *cdc13-1 pol32*Δ and *CDC13*$^+$ *pol32*Δ that had undergone minimal passage at 23°C.

Even at 23°C, *cdc13-1 pol32*Δ mutants were very sick and grew much worse than *cdc13-1 POL32*$^+$ mutants (Figure 11). It was possible that the poor growth of *cdc13-1 pol32*Δ mutants at 23°C was due to the cold sensitivity conferred by the *pol32*Δ mutation. To test this hypothesis, the growth of *CDC13*$^+$ *pol32*Δ mutants was compared to that of *CDC13*$^+$ *POL32*$^+$ mutants. At 23°C, *CDC13*$^+$ *pol32*Δ mutants grew only

slightly worse than *CDC13*$^{+}$ *POL32*$^{+}$ mutants (Figure 11) so the cold-sensitivity of *pol32*Δ mutants could only slightly account for the poor growth of *cdc13-1 pol32*Δ mutants at 23°C. In conclusion, Pol32 is unlikely to function as a nuclease that resects uncapped telomeres, but instead has an important protective role and strongly promotes the vitality of *cdc13-1* mutants.

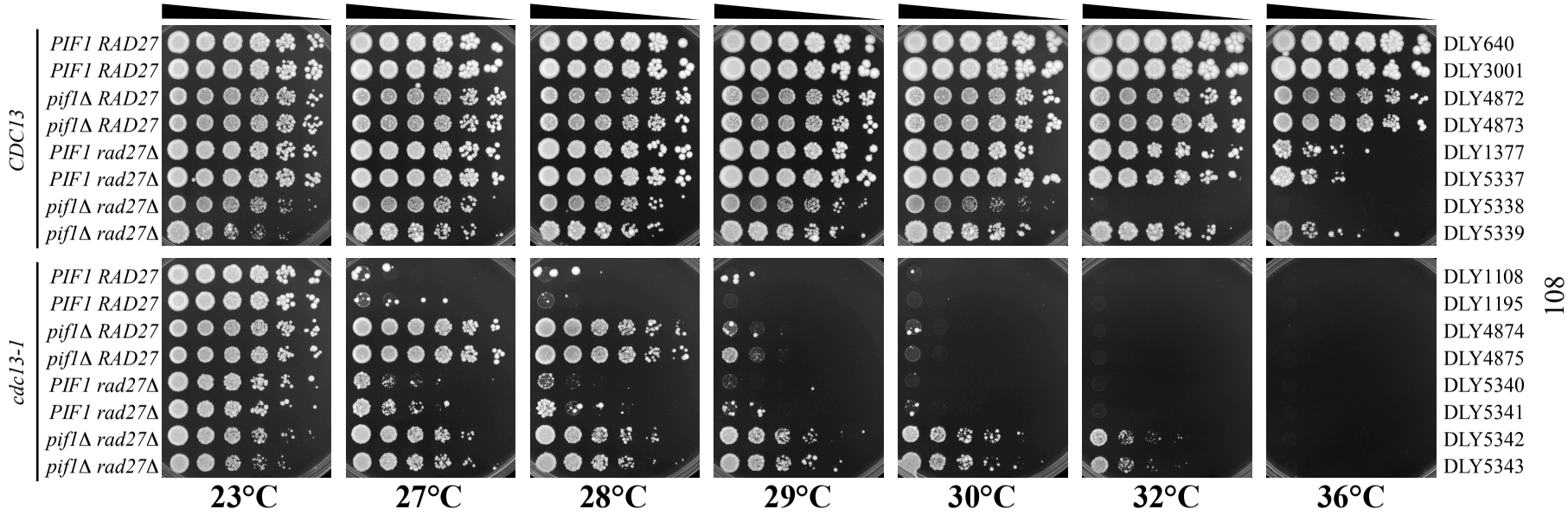
CDC13
PIF1 RAD27
PIF1 RAD27
pif1Δ RAD27
pif1Δ RAD27
PIF1 rad27Δ
PIF1 rad27Δ
pif1Δ rad27Δ
pif1Δ rad27Δ
DLY640
DLY3001
DLY4872
DLY4873
DLY1377
DLY5337
DLY5338
DLY5339
cdc13-1
PIF1 RAD27
PIF1 RAD27
pif1Δ RAD27
pif1Δ RAD27
PIF1 rad27Δ
PIF1 rad27Δ
pif1Δ rad27Δ
pif1Δ rad27Δ
DLY1108
DLY1195
DLY4874
DLY4875
DLY5340
DLY5341
DLY5342
DLY5343
23°C
27°C
28°C
29°C
30°C
32°C
36°C

Figure 12: Rad27 inhibits the growth of *cdc13-1* mutants in a parallel pathway to Pif1

Saturated cultures of the indicated genotypes were serially diluted across agar plates and grown on YEPD plates at the temperature indicated for 3 days.

3.2.6 Rad27 inhibits the growth of cdc13-1 mutants in a parallel pathway to Pif1

Rad27 and Exo1 have homologous nuclease domains and have functional overlap during Okazaki Fragment processing (Tran et al., 2002). Thus, it was hypothesized that Rad27, like Exo1, might be involved in the resection of uncapped telomeres in parallel to Pif1. To test this hypothesis, the effect of Rad27 on the growth of *cdc13-1* and *cdc13-1 pif1*Δ mutants was examined. At 27°C *cdc13-1 rad27*Δ mutants displayed a very slight increase in growth compared to *cdc13-1* mutants, while at 29°C-32°C, *cdc13-1 pif1*Δ *rad27*Δ mutants grew much better than *cdc13-1 pif1*Δ mutants (Figure 12). It was concluded that Rad27 inhibits the growth of *cdc13-1* mutants in a parallel pathway to Pif1.

*cdc13-1 pif1*Δ *rad27*Δ mutants could not grow at 36°C. However, *rad27*Δ mutants are themselves temperature sensitive (Reagan et al., 1995) so it was possible that *CDC13*$^{+}$ *pif1*Δ *rad27*Δ mutants might also be unable to grow at 36°C and thus that *cdc13-1 pif1*Δ *rad27*Δ mutants were not affected by inactivation of *cdc13-1*. To test this hypothesis, we compared the growth of *CDC13*$^{+}$*pif1*Δ *rad27*Δ mutants to that of *cdc13-1 pif1*Δ *rad27*Δ mutants. At 30°C, *CDC13*$^{+}$*pif1*Δ *rad27*Δ and *cdc13-1 pif1*Δ *rad27*Δ mutants were able to grow, however at 36°C neither *cdc13-1 pif1*Δ *rad27*Δ strain could grow, but only one *CDC13*$^{+}$ *pif1*Δ *rad27*Δ strain could grow (Figure 12). Thus, it is possible that telomere uncapping causes no growth defect in *cdc13-1 pif1*Δ *rad27*Δ but without consistent *CDC13*$^{+}$ *pif1*Δ *rad27*Δ strains to compare to, no definitive conclusions can be made. Furthermore, the striking differences in growth at 36°C of the two genetically-identical *CDC13*$^{+}$*pif1*Δ *rad27*Δ is perhaps an indicator that strains of this genotype are very sick and will be difficult to obtain reproducible results from.

3.3 Discussion

It has been shown here that Pif1, Exo1 and Rad24 strongly inhibit the growth of *cdc13-1* mutants and elimination of Pif1 and Exo1, or Pif1 and Rad24, but not Exo1 and Rad24, permits the growth of *cdc13-1* mutants at 36°C (Figure 6). As *cdc13-1* is believed to be completely inactive at 36°C, it suggests that the defect associated with inactivation of *cdc13-1* is dependent upon the presence of Pif1 and either Rad24 or Exo1. This suggests the existence of two pathways that inhibit the growth of *cdc13-1* mutants, one dependent upon Pif1 and one dependent upon either Exo1 or Rad24. While Exo1 and Rad24 have previously been proposed to have different roles at

uncapped telomeres, this is based largely upon molecular observations occurring in *cdc13-1 rad9*Δ mutants at 36°C held within a single cell cycle at 36°C for several hours (Zubko et al., 2004). While such an experimental system is useful, it must be noted that *cdc13-1 rad9*Δ mutants generate elevated levels of extensive ssDNA and a budding yeast cell cycle takes less than two hours at 36°C (Lydall and Weinert, 1995). Thus, while inferring pathways from growth assays alone might seem speculative, the ability of *cdc13-1 pif1*Δ *exo1*Δ and *cdc13-1 pif1*Δ *rad24*Δ mutants to grow at 36°C provides a complementary approach by providing an opportunity to delineate the pathways that prevent growth of *cdc13-1* mutants allowed to proliferate following telomere uncapping.

If Rad24 and Exo1 function in the same pathway to inhibit the growth of *cdc13-1* mutants, this would suggest that the 9-1-1 complex (which Rad24 loads onto ssDNA) tethers Exo1 to the DNA. The suggestion that Exo1 and Rad24 function in the same pathway is bolstered by the observation that Rad24 does not inhibit the growth of *cdc13-1 rad9*Δ *exo1*Δ mutants (Figure 6). As Pif1, Exo1 and Rad24 inhibit the growth of checkpoint-defective *cdc13-1* mutants (*cdc13-1 rad9*Δ mutants, Figure 6) it suggests these three proteins inhibit the growth of *cdc13-1* mutants by resecting uncapped telomeres to generate ssDNA, which is the stimulus for checkpoint activation and the root cause of the loss of viability that occurs following telomere uncapping. Three nuclease activities have been proposed to function at uncapped telomeres in *cdc13-1* mutants (Zubko et al., 2004) – Exo1, ExoX (the Rad24-dependent nuclease tethered by the 9-1-1 complex) and ExoY (a Rad24- and Exo1-independent nuclease activity). Thus, it is proposed that Pif1 constitutes ExoY (Figure 2B).

Previous work proposed that Exo1 and Rad24 control independently-functioning nucleases (Zubko et al., 2004) and a model in which Exo1 and Rad24 function in the same pathway to inhibit the growth of *cdc13-1* mutants is in clear conflict with this. However, the evidence that Exo1 and Rad24 function in different pathways is primarily based on the observation that in *cdc13-1 rad9*Δ mutants (which accumulate ssDNA more rapidly and extensively than *cdc13-1* mutants) Rad24 is required for extensive (>30kb) ssDNA generation while Exo1 is not (Zubko et al., 2004) and thus Rad24 has been interpreted to be more important than Exo1 for ssDNA generation in *cdc13-1 rad9*Δ mutants. Additionally, Exo1 contributes to residual ssDNA generation in *cdc13-1 rad9*Δ *rad24*Δ mutants (Zubko et al., 2004), so Exo1 and Rad24 have been interpreted

to act independently. However, Exo1 is required for extensive (>5kb) ssDNA generation in *cdc13-1 RAD9*$^{+}$ mutants while Rad24 is not (Zubko et al., 2004) and Rad24 does not appear to contribute to ssDNA generation in *cdc13-1 exo1*Δ mutants (Zubko et al., 2004) so Rad24 could also be interpreted to be dependent upon Exo1 for ssDNA generation. Taken together, these observations indicate that Rad24 functions dependent upon Exo1 in *cdc13-1* mutants but independently of Exo1 in *cdc13-1 rad9*Δ mutants.

Two simple modifications to the existing model for nuclease regulation at uncapped telomeres (Zubko et al., 2004) can be proposed to reconcile these data. First, it is proposed that two pathways exist in *cdc13-1* mutants – one dependent upon Pif1 (now termed the Pif1-dependent pathway) and one dependent upon Exo1 and ExoX (now termed the Exo1-dependent pathway). It is proposed that Rad24 promotes the activity of Exo1 and ExoX at uncapped telomeres by loading the 9-1-1 complex which then tethers Exo1 and ExoX to ssDNA at uncapped telomeres. Alternatively, it is possible that the 9-1-1 complex functions to stabilize a DNA substrate that is recognized and degraded by Exo1-ExoX. Second, it is proposed that in *cdc13-1* mutants, ExoX either has no effect on ssDNA generation or supports Exo1 activity, while in *cdc13-1 rad9*Δ mutants ExoX is able to generate ssDNA independently of Exo1. ExoX may have functions independent of Exo1 in *cdc13-1 rad9*Δ mutants because ExoX is either specifically inhibited by Rad9 or because extensive ssDNA generation (>30kb) occurs in *cdc13-1 rad9*Δ mutants and ExoX is required for generation of long tracts of ssDNA.

This model is useful for explaining multiple experimental observations related to telomere uncapping. According to this model, Pif1, Exo1 and Rad24 inhbit the growth of *cdc13-1* mutants and *cdc13-1 exo1*Δ *pif1*Δ and *cdc13-1 rad24*Δ *pif1*Δ mutants are able to grow at 36°C (Figure 6) because both the Pif1-dependent and Exo1-dependent pathways have been essentially eliminated, while *cdc13-1 exo1*Δ *rad24*Δ mutants are unable to grow at 36°C (Figure 6) because only the Exo1-dependent pathway has been eliminated. This model also stipulates that *cdc13-1 exo1*Δ *pif1*Δ mutants are able to grow at 36°C because Pif1 and Exo1 are responsible for resection in *cdc13-1* mutants and have been eliminated. *cdc13-1 rad24*Δ *pif1*Δ mutants show a slight growth defect at 36°C because Rad24 promotes Exo1 activity but is not absolutely essential for it, so some residual Exo1 activity occurs (hence why *cdc13-1 exo1*Δ *rad24*Δ *pif1*Δ mutants show no growth defect at 36°C.) Finally, in *cdc13-1 exo1*Δ mutants, Rad24 does not

contribute to resection because ExoX is not involved in resection or requires Exo1 to function, while in *cdc13-1 rad9*Δ *exo1*Δ mutants Rad24 does contribute to resection because ExoX can function independently of Exo1 resection (Zubko et al., 2004).

Finally, recent work indicates that Sgs1 contributes to a nuclease activity that functions in the same pathway as Exo1 to generate ssDNA in *cdc13-1* mutants, but independently of Exo1 to generate extensive ssDNA in *cdc13-1 rad9*Δ mutants (Ngo and Lydall, 2010). Interestingly, even in *cdc13-1 rad9*Δ mutants, Sgs1 appears to contribute to Exo1-dependent ssDNA generation at the very end of the chromosome (<5kb) but independently of Exo1 beyond this point, consistent with a model where Sgs1 is important for supporting Exo1 in extensive ssDNA generation (Ngo and Lydall, 2010). Thus, it is proposed that Sgs1 is ExoX.

The flap endonuclease Rad27 appears to strongly inhibit the growth of *cdc13-1 pif1*Δ mutants and the improved growth in *cdc13-1 pif1*Δ *rad27*Δ mutants is quite remarkable (Figure 12), especially considering the temperature-sensitive nature of *rad27*Δ mutants. However, these data are difficult to interpret, due to the observed variability in growth of *CDC13*$^{+}$ *pif1*Δ *rad27*Δ mutants (Figure 12). Still, it seems reasonable to assume that Rad27 plays an important role in the Exo1-dependent pathway at uncapped telomeres. Even taking into account the temperature-sensitivity of the *rad27*Δ mutation, Rad27 appears to inhibit the growth of *cdc13-1 pif1*Δ mutants less than Exo1 or Rad24 (Figure 6, Figure 12). This suggests that Rad27 either functions upstream of Exo1 to promote Exo1 activity at substrates which accumulate at uncapped telomeres or that Rad27 functions downstream of Exo1 to process a sub-set of substrates generated by Exo1.

Dna2 and Sgs1 are both involved in the resection of DSBs and shortened telomeres, and resection of uncapped telomeres is believed to be due to inappropriate activation of DSB-like DDRs (Lydall, 2009, Zhu et al., 2008, Mimitou and Symington, 2008). In this context, the protective roles of Dna2 and Sgs1, in a different pathway to Pif1, are surprising (Figures 8-9). However, even though Sgs1 promotes the vitality of *cdc13-1* mutants (Figure 8) it has been shown to be involved in Exo1-dependent ssDNA generation in *cdc13-1* mutants (Ngo and Lydall, 2010). As Sgs1 and Dna2 are believed to function as a single nuclease activity in resection, it is likely that Sgs1 and Dna2 both contribute to Exo1-dependent ssDNA generation at uncapped telomeres and that their contribution to resection somehow plays a protective role. Consistent with this

hypothesis, Dna2 nuclease activity (required for the role of Dna2 in the resection of DSBs) was shown to play a protective role at uncapped telomeres (Figure 9B).

If Sgs1/Dna2 do function in the same pathway as Exo1 at uncapped telomeres (Figures 8-9) but function in parallel to Exo1 to cause extensive resection at DSBs then it suggests that in *cdc13-1* mutants the Exo1-dependent pathway is DSB-like while the Pif1-dependent pathway is distinct. Consistent with this hypothesis, Pif1 plays no role in the resection of DSBs (Zhu et al., 2008) while the Pif1-dependent pathway at uncapped telomeres is likely to be involved in resection (Figure 6). Hence, it is unlikely that uncapped telomeres in *cdc13-1* mutants are simply recognized as DSBs but instead are recognized and processed in a DSB-like pathway (Exo1-dependent) and a DSB-distinct pathway (Pif1-dependent).

Finally, the endonuclease Ogg1 (Figure 10) and the exonucleolytic Pol32 subunit of polymerase δ (Figure 11) have been assessed as potential nucleases functioning at uncapped telomeres. Though Ogg1 clearly inhibits the growth of *cdc13-1* and *cdc13-1 rad9*Δ mutants, the interaction was not striking enough to follow up (Figure 10). However, it has since been reported that oxidized guanines accumulate at the telomeres in *ogg1*Δ and inhibit the binding of Rap1 to telomeres (Lu and Liu, 2009). As Rap1-binding inhibits resection of telomeres by Mre11 (which has a protective role at uncapped telomeres in *cdc13-1* mutants), it is possible that Ogg1 inhibits the growth of *cdc13-1* mutants by indirectly promoting Rap1 binding and thus inhibiting Mre11 activity (Foster et al., 2006, Bonetti et al., 2009). Pol32 was discounted as a possible nuclease activity as it clearly has a strong protective role in *cdc13-1* mutants (Figure 11). However, given that Sgs1 has a strong protective role in *cdc13-1* mutants (Figure 8) but also functions in resection, Pol32 cannot be discounted as having a role as a nuclease activity at uncapped telomeres.

3.4 Further Work

3.4.1 Pif1, Exo1 and Rad24

The primary question arising from this work is how Pif1, Exo1 and Rad24 interact with each other in the resection of uncapped telomeres. As Pif1 inhibits the growth of *cdc13-1* mutants in a different pathway to Exo1 and Rad24, it will be important to determine the contribution of Pif1 to checkpoint activation and ssDNA generation in *cdc13-1* mutants. As *cdc13-1 exo1*Δ *pif1*Δ mutants grow robustly at 36°C (Figure 6) while

*cdc13-1 rad24*Δ *pif1*Δ mutants show a clear growth defect (Figure 6) it will also be important to determine whether any ssDNA is generated at uncapped telomeres in *cdc13-1 exo1*Δ *pif1*Δ mutants and whether this is slightly increased in *cdc13-1 rad24*Δ *pif1*Δ mutants. Finally, to conclusively determine whether Exo1 and Rad24 function in the same or different pathways to resect uncapped telomeres, it will be important to directly compare ssDNA generated at uncapped telomeres in *cdc13-1*, *cdc13-1 exo1*Δ, *cdc13-1 rad24*Δ and *cdc13-1 exo1*Δ *rad24*Δ mutants.

Perhaps most importantly, it will be interesting to carry out screens similar to those described (Addinall et al., 2008, Downey et al., 2006) to identify genes that inhibit the growth of *cdc13-1 exo1*Δ and *cdc13-1 rad24*Δ mutants and *cdc13-1 pif1*Δ mutants. This should identify genes involved in the same pathways as *PIF1* (those which inhibit the growth of *cdc13-1 exo1*Δ and *cdc13-1 rad24*Δ mutants) and *EXO1* (those which inhibit the growth of *cdc13-1 pif1*Δ mutants) and, if so, it will be interesting to see whether any novel combinations of mutations permit the growth of *cdc13-1* mutants at 36°C.

3.4.2 Sgs1/Dna2

Sgs1 and Dna2 both inhibit the growth of *cdc13-1 pif1*Δ mutants (Figures 8-9) suggesting they both contribute to the vitality of *cdc13-1* mutants, and thus do not resect uncapped telomeres. However, recent work has shown that Sgs1 contributes to resection at uncapped telomeres in *cdc13-1* mutants and inhibits the growth of *cdc13-1 rad9*Δ *exo1*Δ mutants. Thus it is possible both Dna2 and Sgs1 contribute to resection at uncapped telomeres and this should be tested. If both Dna2 and Sgs1 contribute to resection at uncapped telomeres, it will be important to understand why these two proteins contribute to the vitality of *cdc13-1* mutants when the other proteins that contribute to well-defined resection activities at uncapped telomeres (Exo1 and Rad24) contribute to the lethality seen in *cdc13-1* mutants.

It is believed that uncapped telomeres are recognized and resected in a manner analogous to unrepaired DSBs, at which Sgs1 and Dna2 appear to cooperate and form a single functional unit involved in resection (Cejka et al., 2010, Niu et al., 2010). However, *cdc13-1 pif1*Δ *sgs1*Δ mutants grow much better than *cdc13-1 pif1*Δ *dna2*Δ mutants (Figures 8-9). This suggests that Dna2 has a much more important role than Sgs1 in promoting the vitality of *cdc13-1* mutants and thus, in contrast to the situation at DSBs, Dna2 and Sgs1 have different roles at uncapped telomeres. It will be important to

assess the contribution of Sgs1 and Dna2 to resection and checkpoint activation in *cdc13-1* mutants, as it may provide valuable insight as to how uncapped telomeres differ from DSBs and how the functions of Dna2 and Sgs1 are coordinated.

3.4.3 Rad27

The growth of *cdc13-1 pif1*Δ *rad27*Δ mutants at 32°C (Figure 12) is remarkable, given that *CDC13*$^{+}$ *pif1*Δ *rad27*Δ mutants grow poorly above 30°C. However, there is clear variability in the growth of *CDC13*$^{+}$ *pif1*Δ *rad27*Δ mutants (Figure 12). It will be important to generate consistently-growing *rad27*Δ mutants of all relevant genotypes to assess whether there is a growth defect in *cdc13-1 pif1*Δ *rad27*Δ mutants compared to *CDC13*$^{+}$*pif1*Δ *rad27*Δ mutants. It will then be important to establish whether Rad27 contributes to resection at uncapped telomeres and to formally demonstrate that Rad27 functions in the same pathway as Pif1 or Exo1. However, this will be challenging as *rad27*Δ mutants are inviable at 36°C (the temperature usually used to induce telomere uncapping in culture experiments) and the *rad27*Δ mutation is lethal with many checkpoint proteins (such as Rad24) and nucleases (such as Exo1).

4 Pif1 is a component of the DDR at uncapped telomeres

"Molecular Biology is, essentially, the practise of biochemistry without a license."

- Erwin Chargaff

4.1 Introduction

Of the multiple proteins that had been assessed for their potential as nuclease activities at uncapped telomeres (Pif1, Sgs1, Dna2, Ogg1, Pol32, Rad27, Figures 4-12) Pif1 was the most promising. Most strikingly, *cdc13-1 pif1*Δ *exo1*Δ and *cdc13-1 pif1*Δ *rad24*Δ mutants were both able to grow at 36°C (Figure 6) a temperature at which Cdc13-1 is believed to be completely active. As these strains were viable at 36°C, it suggested that the DDR and subsequent checkpoint activation following telomere uncapping was severely diminished or possibly eliminated.

To date, only two mechanisms have been identified through which cells with uncapped telomeres can avoid checkpoint activation and metaphase arrest in response to telomere uncapping. First, elimination of essential components of the G2/M checkpoint (such as Rad9, Mec1 or Rad53) prevents checkpoint activation and metaphase arrest and permits *cdc13-1* mutants continue to divide at 36°C, but causes a rapid loss in viability due to resection at uncapped telomeres (Jia et al., 2004, Zubko et al., 2004). Second, elimination of Exo1, which is critically important for the resection of uncapped telomeres, reduces resection at uncapped telomeres and leads to a diminished checkpoint response, allowing a fraction of *cdc13-1 exo1*Δ mutants at 36°C to escape arrest while undergoing only a very moderate loss of viability (Zubko et al., 2004). Pif1 was unlikely to function simply as a component of the checkpoint because 1.) *cdc13-1 rad24*Δ *pif1*Δ mutants can grow at 36°C but *cdc13-1 rad24*Δ mutants do not undergo checkpoint activation and rapidly lose viability at 36°C and 2.) *cdc13-1 exo1*Δ *pif1*Δ mutants can grow at 36°C but elimination of the checkpoint in *cdc13-1 exo1*Δ mutants (e.g. in *cdc13-1 sml1*Δ *mec1*Δ *exo1*Δ mutants) does not permit growth at 36°C (Jia et al., 2004, Zubko et al., 2004). Instead, Pif1 was likely to function as a DDR component, responsible for loss of viability in *cdc13-1 rad24*Δ mutants and residual checkpoint activation in *cdc13-1 exo1*Δ mutants.

This purpose of this work was to define the role of Pif1 in the response to telomere uncapping, to gain insight into the DDR and checkpoint activation both at uncapped telomeres and in response to other stimuli, focusing on the interaction between Pif1 and Exo1 as neither of which were essential components of the G2/M checkpoint response to telomere uncapping in *cdc13-1* mutants.

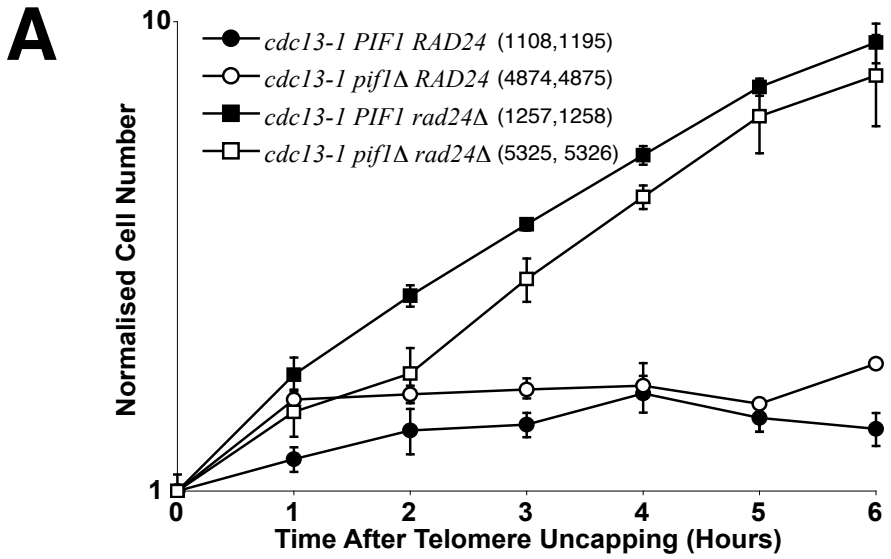
A
cdc13-1 PIF1 RAD24 (1108,1195)
cdc13-1 pif1Δ RAD24 (4874,4875)
cdc13-1 PIF1 rad24Δ (1257,1258)
cdc13-1 pif1Δ rad24Δ (5325, 5326)
Normalised Cell Number
10
1
0
1
2
3
4
5
6
Time After Telomere Uncapping (Hours)

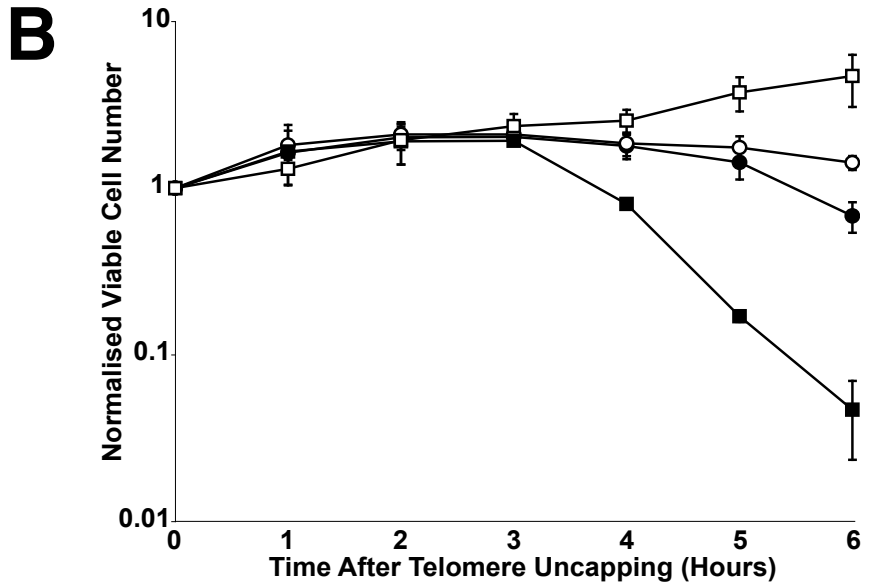
B
Normalised Viable Cell Number
10
1
0.1
0.01
0
1
2
3
4
5
6
Time After Telomere Uncapping (Hours)

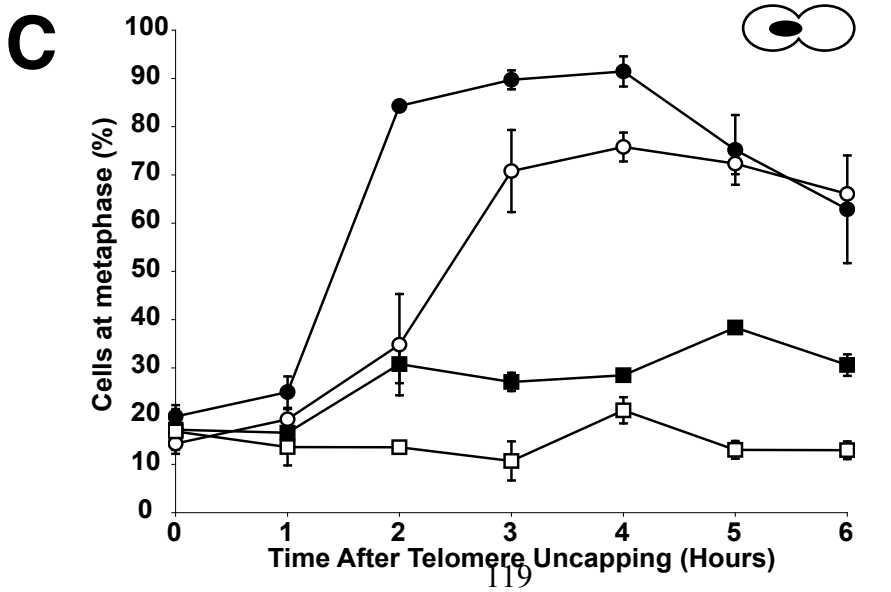
C
Cells at metaphase (%)
100
90
80
70
60
50
40
30
20
10
0
0
1
2
3
4
5
6
Time After Telomere Uncapping (Hours)

Figure 13: Pif1 is responsible for the loss of viability and residual checkpoint activation seen in *cdc13-1 rad24*Δ mutants

Exponentially-dividing cultures of the genotypes indicated were shifted from 23°C to 36°C to induce telomere uncapping for 6 hours. Every hour, samples were taken to measure **A.** total cell number **B.** viable cell number and **C.** percentage of cells at metaphase. Error bars represent the standard error of the mean for 3 independent biological replicates, the strain numbers for 2 of which are listed in the key.

4.2 Results

4.2.1 Pif1 is responsible for the loss of viability seen in cdc13-1 rad24Δ mutants

*cdc13-1 rad24*Δ mutants do not undergo checkpoint activation at 36°C but cannot form colonies, while *cdc13-1 rad24*Δ *pif1*Δ mutants were able to form colonies at 36°C (Figure 6). This suggested that Pif1 was responsible for the loss of viability seen in *cdc13-1 rad24*Δ mutants and possibly contributed to loss of viability in *cdc13-1* mutants. To test this hypothesis exponentially dividing *cdc13-1*, *cdc13-1 pif1*Δ, *cdc13-1 rad24*Δ and *cdc13-1 rad24*Δ *pif1*Δ mutants were shifted from 23°C to 36°C to induce telomere uncapping and cell number and viability were followed over time. *cdc13-1 rad24*Δ mutants continued to divide and increase in cell number following telomere uncapping (Figure 13A) but this corresponded to a marked loss in the number of viable cells (Figure 13B), as expected. In contrast, *cdc13-1 rad24*Δ *pif1*Δ mutants continued to increase in both cell number (Figure 13A) and viable cell number (Figure 13B) over time, following telomere uncapping. Both *cdc13-1* and *cdc13-1 pif1*Δ mutants underwent a very limited increase in cell number following telomere uncapping (Figure 13A) and after 6 hours at 36°C, *cdc13-1* mutants had began to lose viability, but *cdc13-1 pif1*Δ mutants had retained viability (Figure 13B). It was concluded that Pif1 is responsible for the loss of viability seen in *cdc13-1 rad24*Δ mutants with uncapped telomeres and Pif1 also contributes to loss of viability in *cdc13-1* mutants at 36°C.

Exo1 contributes to loss of viability in *cdc13-1* mutants and also contributes to cell cycle arrest following telomere uncapping. It was hypothesized that Pif1 might behave in the same manner. To test this hypothesis, exponentially dividing *cdc13-1* and *cdc13-1 pif1*Δ mutants were shifted from 23°C to 36°C to induce telomere uncapping and the fraction of cells at metaphase was measured (Figure 13C). After 2 hours at 36°C, >80% of *cdc13-1* mutants had accumulated at metaphase and this persisted up to 4 hours, after which the fraction of cells at metaphase began to decrease as the cells began to adapt to the checkpoint (Figure 13C). *cdc13-1 pif1*Δ mutants did not accumulate at metaphase until 3 hours after telomere uncapping and only >70% of cells accumulated at metaphase, where they remained up until 6 hours (Figure 13C). It was concluded that Pif1 contributes to cell cycle arrest of *cdc13-1* mutants following telomere uncapping.

It has been consistently reported that *cdc13-1 rad24*Δ mutants display a slight metaphase accumulation following telomere uncapping (Jia et al., 2004, Zubko et al., 2004). This could potentially represent a very low level of checkpoint activation, to which Pif1 could contribute in the same manner as it contributes to cell cycle arrest in *cdc13-1* mutants. To test this hypothesis, exponentially dividing *cdc13-1 rad24*Δ and *cdc13-1 rad24*Δ *pif1*Δ mutants were shifted from 23°C to 36°C to induce telomere uncapping and the fraction of cells at metaphase was measured (Figure 13C). As expected, there was a slight accumulation at metaphase of *cdc13-1 rad24*Δ mutants following telomere uncapping – at 23°C, approximately 15% of *cdc13-1 rad24*Δ mutants were at metaphase, but after shift to 36°C there was an increase to approximately 30% of *cdc13-1 rad24*Δ mutants at metaphase (Figure 13C). Strikingly, *cdc13-1 rad24*Δ *pif1*Δ mutants showed no significant accumulation at metaphase following shift to 36°C. It was concluded that Pif1 was responsible for the slight metaphase accumulation seen in *cdc13-1 rad24*Δ mutants at 36°C and that this may constitute a very low level of Pif1-dependent checkpoint activation.

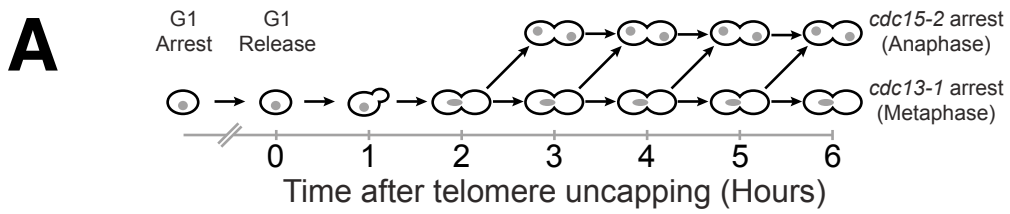

5358 *cdc15-2 cdc13-1*
5359 *cdc15-2 cdc13-1 pif1Δ*
5360 *cdc15-2 cdc13-1 exo1Δ*
5361 *cdc15-2 cdc13-1 exo1Δ pif1Δ*

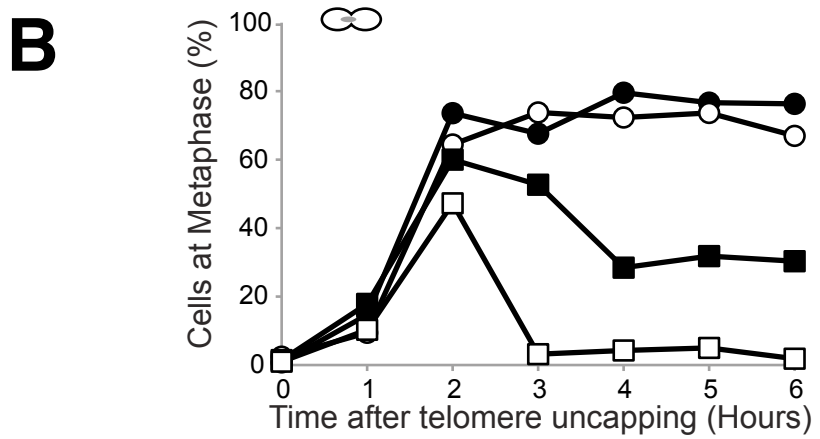

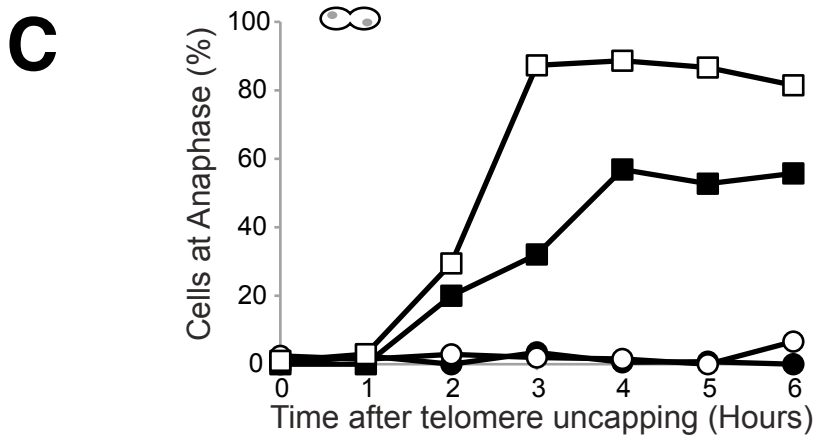

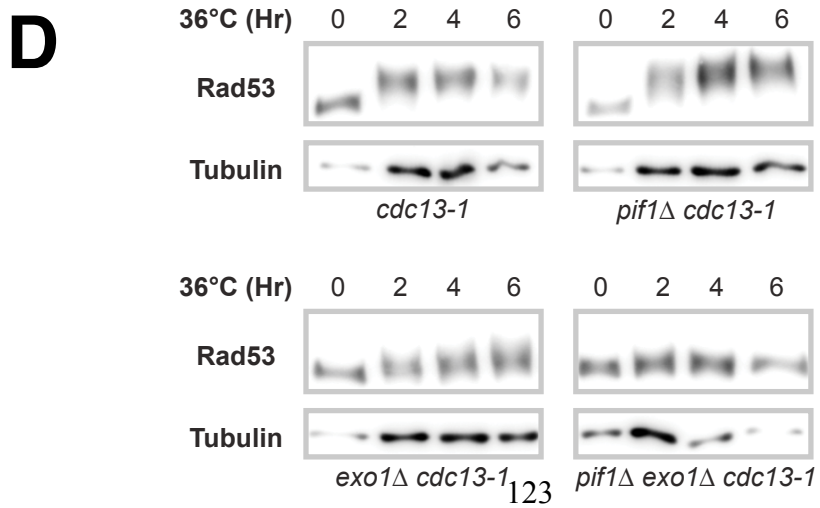

Figure 14: Pif1 and Exo1 coordinate checkpoint activation following telomere uncapping in *cdc13-1* mutants

A. Synchronous cultures were subjected to telomere uncapping according to the diagram shown. Exponentially-dividing *bar1*Δ cells were arrested at 23°C in G1 using α factor then released from arrest and shifted to 36°C to uncap telomeres. Cells that arrested due to telomere uncapping (*cdc13-1*) would accumulate at metaphase, while cells which did not arrest due to telomere uncapping or escaped arrest would accumulate at anaphase (*cdc15-2*).

Synchronous cultures of the genotypes indicated were subjected to telomere uncapping as in **A.** and samples taken every hour for 6 hours to measure **B.** fraction of cells at metaphase **C.** fraction of cells at anaphase and **D.** Rad53 phosphorylation by Western Blot.

5358 *cdc15-2 cdc13-1*
5359 *cdc15-2 cdc13-1 pif1Δ*
5360 *cdc15-2 cdc13-1 exo1Δ*
5361 *cdc15-2 cdc13-1 exo1Δ pif1Δ*

A

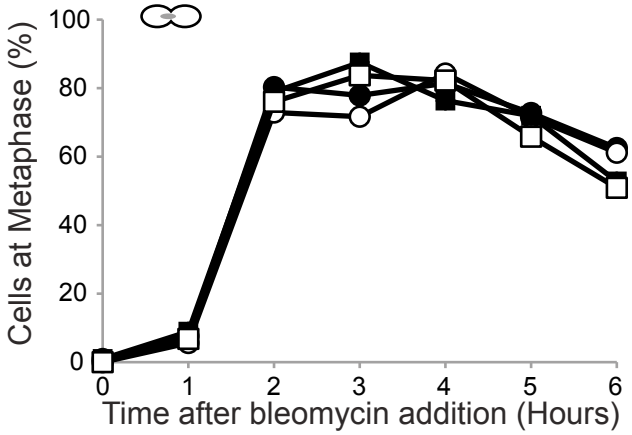

B

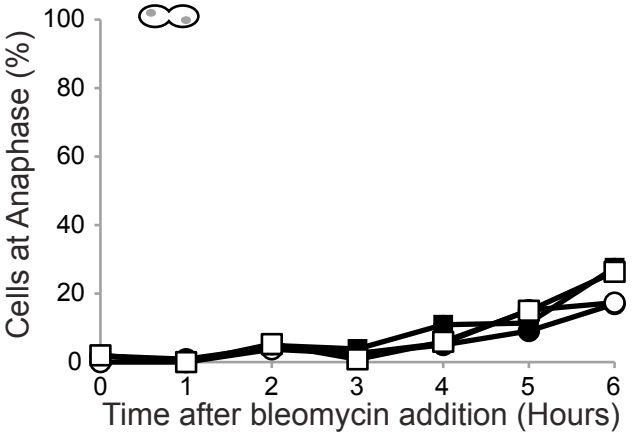

C

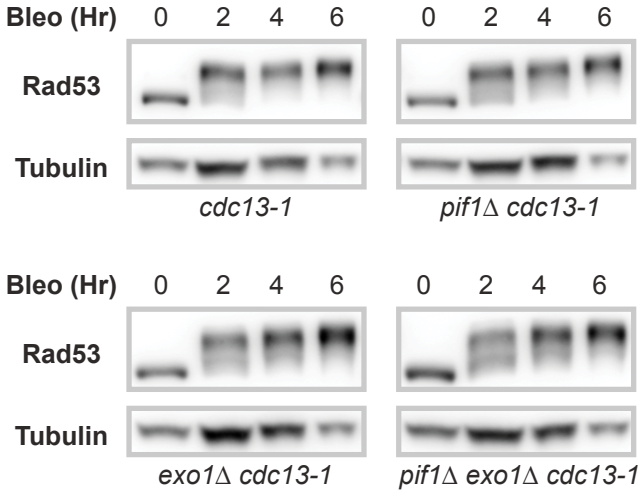

Figure 15: Pif1 and Exo1 do not coordinate checkpoint activation following DSB induction

Synchronous cultures were performed as in Figure 14A but instead of shifting the cultures to 36°C to uncap telomeres, DSBs were induced by addition of bleomycin. Following bleomycin treatment in synchronous cultures of the genotypes indicated, samples were taken every hour for 6 hours to measure **A.** fraction of cells at metaphase **B.** fraction of cells at anaphase and **C.** Rad53 phosphorylation by Western Blot.

4.2.2 Pif1 and Exo1 are responsible for checkpoint activation specifically in response to telomere uncapping

Pif1 appeared to contribute to checkpoint activation in *cdc13-1* mutants (Figure 13C), Exo1 is also known to contribute to checkpoint activation in *cdc13-1* mutants (Zubko et al., 2004) and *cdc13-1 exo1*Δ *pif1*Δ mutants were able to form colonies at 36°C (Figure 6). It was hypothesized that Pif1 and Exo1 might function in parallel to initiate checkpoint activation following telomere uncapping.

To investigate the roles of Pif1 and Exo1 in telomere uncapping, a synchronous culture system was used to enable the checkpoint response of a single population of cells to be measured (Figure 14A) (Lydall and Weinert, 1995). Briefly, cells containing the *cdc13-1* allele were arrested in G1 with α factor, then released from arrest and shifted to 36°C to induce telomere uncapping. All cells also carried the *cdc15-2* allele, which at 36°C prevented exit from anaphase, ensuring that any cells escaping from *cdc13-1*-induced metaphase arrest would not be able to enter another cell cycle.

cdc13-1 mutants accumulated at metaphase (Figure 14B) but not at anaphase (Figure 14C). Unexpectedly, *cdc13-1 pif1*Δ mutants also accumulated at metaphase and did not pass through to anaphase (Figure 14B,C). *cdc13-1 exo1*Δ mutants accumulated transiently at metaphase, but a subpopulation of cells leaked through to anaphase , as previously described (Figure 14B,C) (Jia et al., 2004, Zubko et al., 2004). *cdc13-1 exo1*Δ *pif1*Δ mutants showed a peak at metaphase at 2 hours (Figure 14B) but then essentially all accumulated at metaphase. It was concluded that when cells passed through a single cell cycle with uncapped telomeres, Pif1 was not necessary for full metaphase arrest of *cdc13-1* mutants but Pif1 was responsible for the arrest of a subpopulation of *cdc13-1 exo1*Δ mutants following telomere uncapping. Furthermore, elimination of Pif1 and Exo1 eliminated metaphase arrest in response to telomere uncapping (Figure 14B,C).

It was surprising that Pif1 did not appear to contribute to the arrest of *cdc13-1* mutants subjected to telomere uncapping in a synchronous culture system (Figure 14B,C), as asynchronously dividing *cdc13-1 pif1*Δ mutants shifted to 36°C showed a defect in metaphase arrest (Figure 13C). The likely explanation for this difference is due to the experimental system – using a synchronous culture system, all cells must pass from G1

to metaphase with uncapped telomeres, while using an asynchronous culture system means that cells are distributed throughout the cell cycle and significant fraction will only pass from S phase or G2 to metaphase with uncapped telomeres. Thus, it was concluded that Pif1 is important for checkpoint activation following telomere uncapping (Figure 13C) but was not necessary for full metaphase arrest in cells that passed from G1 to metaphase with uncapped telomeres (Figure 14B,C).

One of the most upstream events in checkpoint activation in response to telomere uncapping, is hyperphosphorylation and activation of Rad53, leading to phosphorylation of downstream effector kinases and ensuing cell cycle arrest (Morin et al., 2008, Sweeney et al., 2005). To investigate how Pif1 and Exo1 affected activation of Rad53 following telomere uncapping, synchronous cultures of *cdc13-1* mutants were subjected to telomere uncapping and then Western Blots were performed to detect Rad53. Following telomere uncapping, there was a marked decrease in mobility of Rad53 in *cdc13-1* mutants, indicating hyperphosphorylation and activation and this was not altered in *cdc13-1 pif1*Δ mutants (Figure 14D) corresponding to the full metaphase arrest seen in *cdc13-1* and *cdc13-1 pif1*Δ mutants following telomere uncapping (Figure 14B). *cdc13-1 exo1*Δ mutants showed a slight decrease in mobility of Rad53 phosphorylation, but it was severely reduced compared to *cdc13-1* mutants (Figure 14D) corresponding to the reduced metaphase arrest seen in *cdc13-1 exo1*Δ mutants compared to *cdc13-1* mutants (Figure 14B). In *cdc13-1 exo1*Δ *pif1*Δ mutants, no discernable increase in Rad53 mobility was seen. It was concluded that Pif1 was not necessary for Rad53 activation of *cdc13-1* mutants but Pif1 was responsible for the residual Rad53 activation seen in *cdc13-1 exo1*Δ mutants following telomere uncapping (Figure 14D).

DSBs and uncapped telomeres in *cdc13-1* mutants undergo checkpoint activation in a similar manner, involving resection to generate ssDNA and subsequent Mec1-dependent checkpoint activation (Lydall, 2009). To determine whether Pif1 and Exo1 were affecting checkpoint activation specifically in response to uncapped telomeres or in a more generalized manner, the checkpoint response to DSBs was assessed in the same strains used in Figure 14B. Briefly, cultures were synchronized at 23°C using α factor, released from G1, treated with bleomycin to induce DSBs and then assessed for cell cycle arrest and Rad53 phosphorylation. *cdc13-1*, *cdc13-1 pif1*Δ, *cdc13-1 exo1*Δ and *cdc13-1 exo1*Δ *pif1*Δ mutants all accumulated at metaphase with similar kinetics

(Figure 15A) before gradually leaking out to anaphase from 4 hours onwards (Figure 15B) and all strains were able to fully phosphorylate Rad53 in response to bleomycin (Figure 15C). It was concluded that *cdc13-1 exo1*Δ and *cdc13-1 exo1*Δ *pif1*Δ mutants were specifically defective in metaphase arrest and Rad53 activation in response to telomere uncapping (Figure 14B-D) and this was not due to a general checkpoint defect.

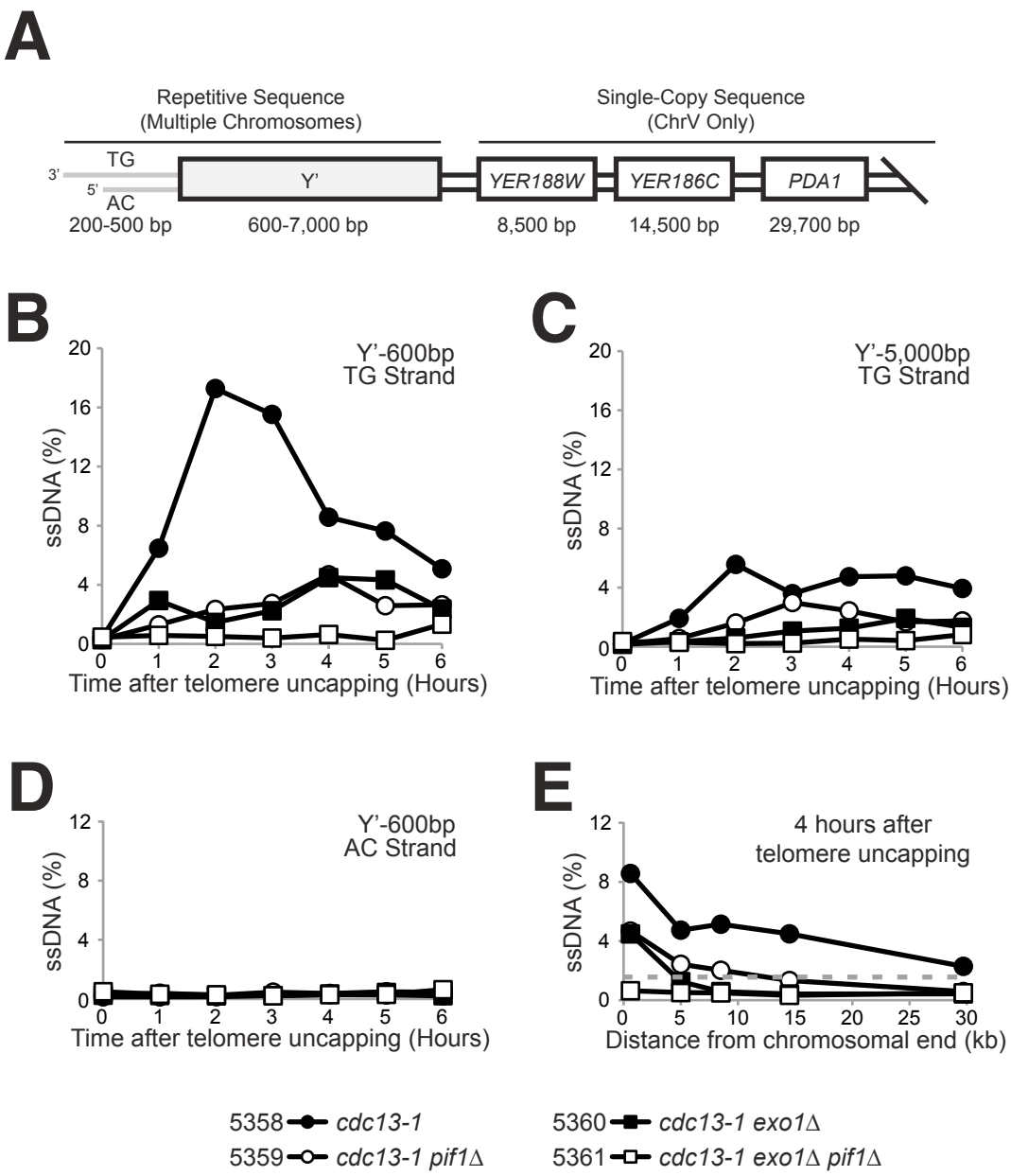
A
Repetitive Sequence
(Multiple Chromosomes)
Single-Copy Sequence
(ChrV Only)
TG
AC
3'
5'
Y'
YER188W
YER186C
PDA1
200-500 bp
600-7,000 bp
8,500 bp
14,500 bp
29,700 bp
B
Y'-600bp
TG Strand
ssDNA (%)
Time after telomere uncapping (Hours)
C
Y'-5,000bp
TG Strand
ssDNA (%)
Time after telomere uncapping (Hours)
D
Y'-600bp
AC Strand
ssDNA (%)
Time after telomere uncapping (Hours)
E
4 hours after
telomere uncapping
ssDNA (%)
Distance from chromosomal end (kb)
5358 cdc13-1
5359 cdc13-1 pif1Δ
5360 cdc13-1 exo1Δ
5361 cdc13-1 exo1Δ pif1Δ

Figure 16: Pif1 and Exo1 coordinate ssDNA generation following telomere uncapping

Synchronous cultures of *cdc13-1* mutants (Figure 14A) were shifted to 36°C to induce telomere uncapping and samples were taken every hour to measure ssDNA at the loci indicated in **A.** Percentage ssDNA is shown **B.** on the TG strand at the Y'600 locus **C.** on the TG at the Y'5,000 locus **D.** on the AC strand at the Y'600 locus **E.** at various loci, 4 hours after telomere uncapping.

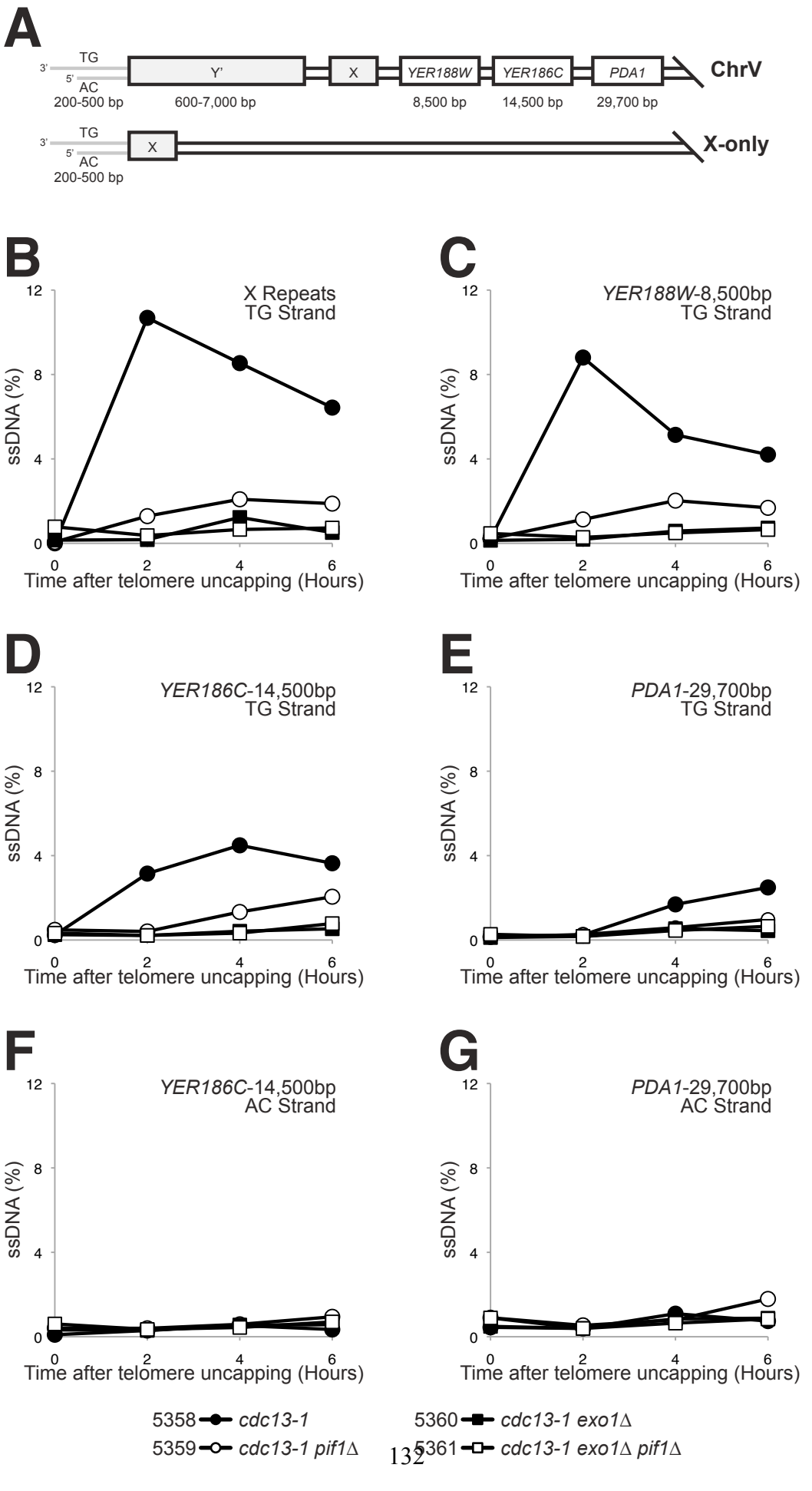
A
TG
AC
3'
5'
200-500 bp
Y'
600-7,000 bp
X
YER188W
8,500 bp
YER186C
14,500 bp
PDA1
29,700 bp
ChrV
X-only
B
X Repeats
TG Strand
C
YER188W-8,500bp
TG Strand
D
YER186C-14,500bp
TG Strand
E
PDA1-29,700bp
TG Strand
F
YER186C-14,500bp
AC Strand
G
PDA1-29,700bp
AC Strand
ssDNA (%)
Time after telomere uncapping (Hours)
5358 cdc13-1
5359 cdc13-1 pif1Δ
5360 cdc13-1 exo1Δ
5361 cdc13-1 exo1Δ pif1Δ

Figure 17: Exo1 is more important than Pif1 for ssDNA generation at loci further from the chromosome end

Synchronous cultures of *cdc13-1* mutants (Figure 14A) were shifted to 36°C to induce telomere uncapping and samples were taken every hour to measure ssDNA at the loci indicated in **A.** Percentage ssDNA is shown **B.** on the TG strand in the X repeats **C.** on the TG strand at the *YER188W* locus **D.** on the TG strand at the *YER186C* locus **E.** on the TG strand at the *PDA1* locus **F.** on the AC strand at the *YER186C* locus **G.** on the AC strand at the *PDA1* locus.

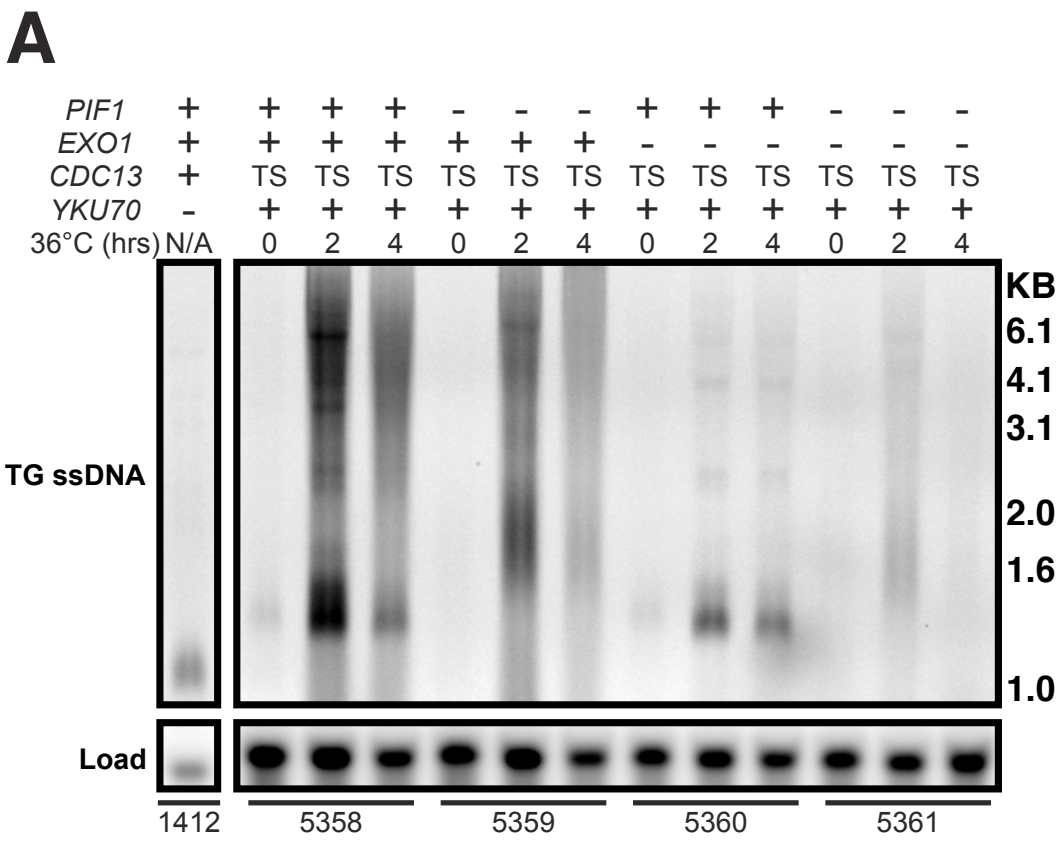
A
PIF1 + + + + - - - + + + - - -
EXO1 + + + + + + + - - - - - -
CDC13 + TS TS TS TS TS TS TS TS TS TS TS TS
YKU70 - + + + + + + + + + + + +
36°C (hrs) N/A 0 2 4 0 2 4 0 2 4 0 2 4
KB
6.1
4.1
3.1
2.0
1.6
1.0
TG ssDNA
Load
1412
5358
5359
5360
5361

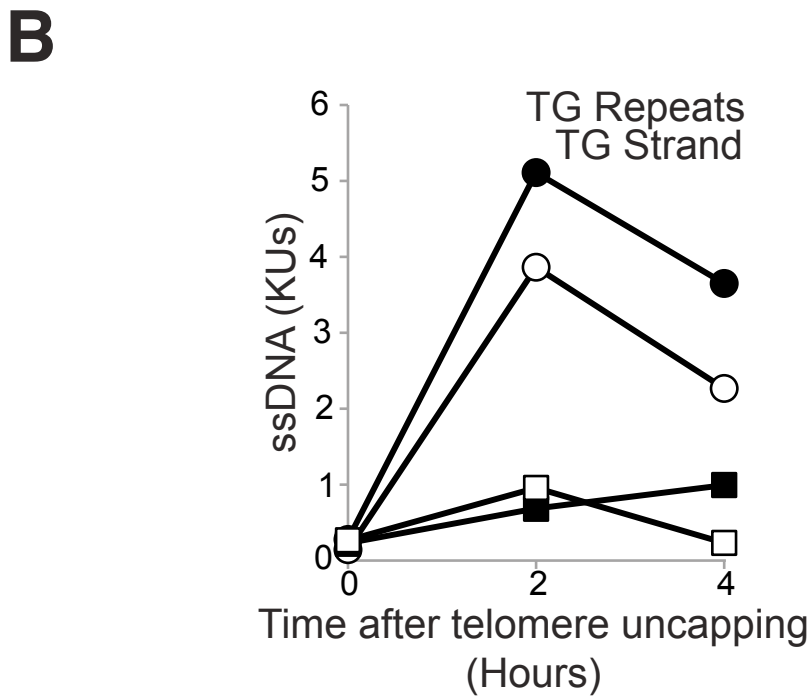
B
TG Repeats
TG Strand
ssDNA (KUs)
0
1
2
3
4
5
6
0
2
4
Time after telomere uncapping
(Hours)

Figure 18: Exo1 is more important than Pif1 for ssDNA generation in the TG repeats

A. Synchronous cultures of *cdc13-1* mutants (Figure 14A) were shifted to 36°C to induce telomere uncapping and samples were taken every hour to measure ssDNA in the TG repeats by in-gel assay, then performing a Southern Blot to probe for *CDC15* as a loading control. **B.** Quantification of the data shown in **A.**, normalized for load using the *CDC15* signal. ssDNA is expressed in Ku Units (KUs). A KU is defined as the amount of ssDNA detectable in the TG repeats of an exponentially-dividing *yku70*Δ mutant at 23°C.

4.2.3 Pif1 and Exo1 are the determinants of ssDNA generation at uncapped telomeres in cdc13-1 mutants

*cdc13-1 exo1*Δ *pif1*Δ mutants did not undergo cell cycle arrest or checkpoint activation, specifically in response to telomere uncapping. A possible explanation was that resection at uncapped telomeres (which is the stimulus for cell cycle arrest and checkpoint activation in response to telomere uncapping) had been eliminated.

It was hypothesized that Pif1 and Exo1 both contributed to ssDNA generation at uncapped telomeres and elimination of both Pif1 and Exo1 prevented ssDNA generation at uncapped telomeres, thus preventing checkpoint activation. To test this hypothesis, synchronous cultures of *cdc13-1* mutants were subjected to telomere uncapping (Figure 14A) and then ssDNA at various loci were measured (Figure 16A) using Quantitative Amplification of Single-Stranded DNA (QAOS) (Booth et al., 2001, Zubko et al., 2006). In Y' elements (which are components of most telomeres in budding yeast) *cdc13-1* mutants generated ssDNA at loci approximately 600bp (Y'600) and 5,000bp (Y'5,000) from the chromosome end and this was reduced in *cdc13-1 pif1*Δ and *cdc13-1 exo1*Δ mutants (Figure 16B,C). Strikingly, in *cdc13-1 exo1*Δ *pif1*Δ mutants, no detectable ssDNA was measured in the Y' sequences 600bp or 5,000bp from the chromosome end (Figure 16B,C). It was confirmed that ssDNA generation in *cdc13-1*, *cdc13-1 pif1*Δ and *cdc13-1 exo1*Δ mutants was specifically on the TG strand and not due to generalized unwinding of telomeric duplex DNA as no ssDNA could be detected on the AC strand in the Y' elements (Figure 16D). In conclusion, Pif1 and Exo1 are both required for resection of uncapped telomeres and elimination of Pif1 and Exo1 prevents ssDNA generation at uncapped telomeres, thus preventing checkpoint activation.

Elimination of Pif1 or Exo1 reduced ssDNA generation in the Y'600 elements following telomere uncapping to a similar extent. However, elimination of Pif1 had very little effect on checkpoint activation and cell cycle arrest following telomere uncapping, while elimination of Exo1 conferred a severe defect in checkpoint activation and cell cycle arrest (Figure 14B). This constituted a paradox, as ssDNA is believed to be the stimulus for checkpoint activation following telomere uncapping. It was hypothesized that the extensiveness of ssDNA generation at uncapped telomeres, rather

than the quantity of ssDNA at the chromosome end, might be more important for determining checkpoint activation. To test this hypothesis, ssDNA was measured at various single-copy loci on Chromosome V (Figure 16A) 4 hours after telomere uncapping, which was the time point at which no further alterations in the fraction of *cdc13-1 exo1*Δ cells at metaphase were seen. Following telomere uncapping, *cdc13-1* mutants generated detectable ssDNA at all loci examined, ≤30kb from the chromosome end, with the level of ssDNA decreasing further from the chromosome end (Figure 16E). In contrast, *cdc13-1 pif1*Δ mutants generated ssDNA ≤15kb from the chromosome end, while *cdc13-1 exo1*Δ mutants generated ssDNA ≤5kb from the chromosome end (i.e. only in the Y' elements) and *cdc13-1 exo1*Δ *pif1*Δ mutants had no detectable ssDNA at any locus examined (Figure 16E). In conclusion, the more extensive ssDNA generated in *cdc13-1 pif1*Δ mutants compared to *cdc13-1 exo1*Δ mutants following telomere uncapping (Figure 16E) most likely accounts for the sustained checkpoint activation in *cdc13-1 pif1*Δ mutants compared to the attenuated checkpoint activation seen in *cdc13-1 exo1*Δ mutants (Figure 14D). Interestingly, just as *cdc13-1 exo1*Δ mutants generate ssDNA ≤5kb from the chromosome end, *exo1*Δ mutants with an irreparable DSB generate ssDNA ≤5kb away from the break on each side (Mimitou and Symington, 2008).

There are 64 G2 telomeres in budding yeast, so 1.6% (1/64) ssDNA would be expected to correspond to one single-stranded locus per cell. Essentially full metaphase arrest is seen in *cdc13-1 pif1*Δ mutants (Figure 14D) and >1.6% ssDNA is generated ≥9 kb but <15 kb from the chromosome end in *cdc13-1 pif1*Δ mutants (Figure 16E). Assuming one single-stranded telomere per cell is sufficient to cause sustained metaphase arrest (in an analogous manner to how one DSB per cell can cause sustained metaphase arrest), this suggests that one telomere with 9-15 kb of ssDNA is sufficient to cause sustained metaphase arrest. Consistent with this, elimination of Exo1 and Sgs1 limits resection to approximately 1.5-3.0kb either side of an irreparable DSB (3.0-6.0kb of ssDNA in total) and causes a severe checkpoint defect (Gravel et al., 2008, Mimitou and Symington, 2008, Zhu et al., 2008).

The conclusion that the extensiveness of ssDNA generated at uncapped telomeres explained the difference in metaphase arrest seen in *cdc13-1* mutants was drawn from a single time point (Figure 16E). To test whether this result was robust, ssDNA at other loci was measured 0, 2, 4 and 6 hours after telomere uncapping. X repeats are telomeric

sequences present on all chromosomes in *S. cerevisiae*, either present behind the Y' elements on Y'-containing telomeres, such as Chromosome V (and thus far from the chromosome end, Figure 17A) or present close to the chromosome end on telomeres that do not contain Y' elements (X-only telomeres, Figure 17A). Following telomere uncapping, *cdc13-1* mutants generated ssDNA in the X repeats, *cdc13-1 pif1*Δ mutants generated less ssDNA and no detectable ssDNA could be measured in *cdc13-1 exo1*Δ or *cdc13-1 exo1*Δ *pif1*Δ mutants (Figure 17B). At the *YER188W* and *YER186C* loci, which are 6,500bp and 14,500bp respectively from the end of Chromosome V, the same trend was present – *cdc13-1* mutants generated ssDNA, while *cdc13-1 pif1*Δ mutants generated less ssDNA and no detectable ssDNA was measured in *cdc13-1 exo1*Δ or *cdc13-1 exo1*Δ *pif1*Δ mutants (Figure 17C,D). However, at the *PDA1* locus, which is 29,700bp from the end of Chromosome V, *cdc13-1* mutants generated ssDNA but no detectable ssDNA was measured in *cdc13-1 pif1*Δ, *cdc13-1 exo1*Δ or *cdc13-1 exo1*Δ *pif1*Δ mutants (Figure 17E). It was confirmed that ssDNA was generated specifically on the TG strand at the more internal loci, as no detectable ssDNA was measure on the AC strand at *YER186C* or *PDA1* (Figure 17F,G). In conclusion, the result presented in Figure 17E is robust – *cdc13-1 pif1*Δ mutants generate more extensive ssDNA than *cdc13-1 exo1*Δ mutants and this ssDNA occurs specifically on the TG strand.

Pif1 negatively regulates telomere length and *pif1*Δ mutants have long telomeres, <500 bases longer than those seen in wild type cells (Schulz and Zakian, 1994). Thus it was necessary to consider the possibility that in *cdc13-1 pif1*Δ mutants the reduced ssDNA measured in comparison to *cdc13-1* mutants was simply due to resection initiating further from the loci measured. To test this hypothesis, ssDNA measured in *cdc13-1 pif1*Δ mutants was compared ssDNA measured further from the chromosome end in *cdc13-1 PIF1*$^{+}$ mutants. At the Y'600 locus, approximately 600 bases from the chromosome end, the ssDNA generated in *cdc13-1 pif1*Δ mutants was a maximum of 4% (Figure 16B), which was comparable to the maximum ssDNA generated in *cdc13-1 PIF1*$^{+}$ mutants at *YER186C* (Figure 17C), approximately 14,500 bases from the chromosome end (and thus approximately 14,000 bases away from the Y'600 locus). Additionally, *cdc13-1 pif1*Δ mutants generated much less ssDNA at *YER188W* than *cdc13-1 PIF1*$^{+}$ mutants did at *YER186C*, despite the loci being approximately 6,000 bases apart (Figure 17 C,D). It was concluded that reduction in ssDNA measured in *cdc13-1 pif1*Δ mutants in comparison to *cdc13-1 PIF1*$^{+}$ mutants following telomere

uncapping corresponded to a defect in resection of many kilobases (approximately 6,000 to 14,000) and could not simply be attributed to an increase in telomere length corresponding to a few hundred bases (<500) and thus that Pif1 actively played a role in the resection of uncapped telomeres in *cdc13-1* mutants.

No ssDNA could be detected in *cdc13-1 exo1*Δ *pif1*Δ mutants with uncapped telomeres and no checkpoint activation or cell cycle arrest could be seen (Figure16, Figure14). However, *yku70*Δ mutants at 23°C do not undergo checkpoint activation or cell cycle arrest, but have detectable ssDNA in the telomeric TG repeats, at the very end of the chromosome. It was hypothesized that the same might be true of *cdc13-1 pif1*Δ *exo1*Δ mutants. To test this hypothesis, synchronous cultures of *cdc13-1* mutants were subjected to telomere uncapping (Figure 14A) and then ssDNA in the telomeric TG repeats was measured by in-gel assay. *cdc13-1* mutants generated 4-5 times the level of ssDNA of a *yku70*Δ mutants in the TG repeats following telomere uncapping and this was slightly reduced in *cdc13-1 pif1*Δ mutants (Figure 18A,B). *cdc13-1 exo1*Δ mutants generated slightly less ssDNA than a *yku70*Δ mutant in the TG repeats following telomere uncapping (Figure 18A,B). In contrast, *cdc13-1 exo1*Δ *pif1*Δ mutants transiently generated a similar level of ssDNA to a *yku70*Δ mutant 2 hours after telomere uncapping, but by 4 hours no ssDNA was detectable (Figure 18B). In conclusion, *cdc13-1 exo1*Δ *pif1*Δ mutants do generate ssDNA following telomere uncapping, but it is transient and not sustained.

Interestingly, *cdc13-1 pif1*Δ mutants generated only slightly less ssDNA than *cdc13-1* mutants in the TG repeats (Figure 18A,B) yet *cdc13-1 pif1*Δ mutants generated much less ssDNA in the Y' elements than *cdc13-1* mutants (Figure 16B). This was in contrast to *cdc13-1 exo1*Δ mutants which generated very little ssDNA in the telomeric TG repeats (Figure 18A,B), but similar levels of ssDNA in the Y' elements to Pif1 (Figure 16B). These data indicate that the importance of Pif1 in ssDNA generation peaks in the Y' elements while the importance of Exo1 peaks in the TG repeats. These data therefore suggest that Exo1 recognizes a substrate at the very end of the chromosome in the TG repeats, while Pif1 recognizes a substrate away from the chromosome end, towards the Y' elements.

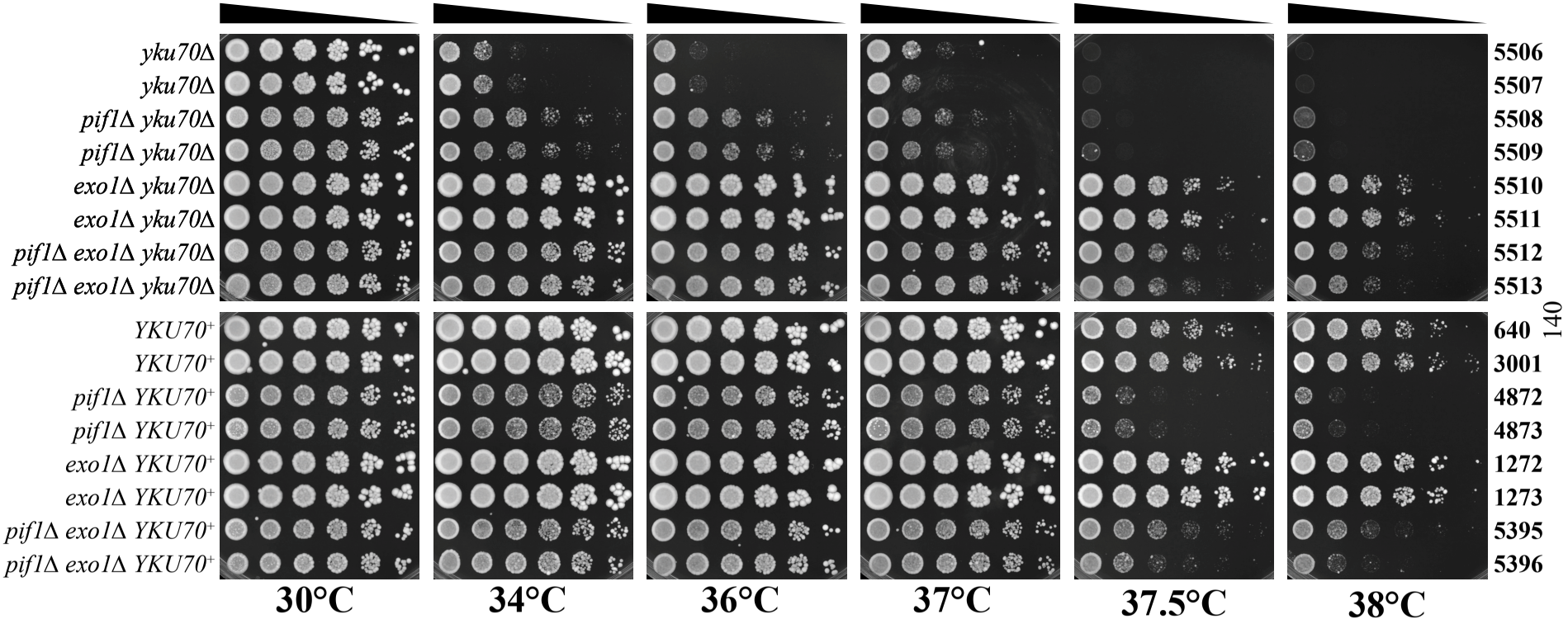
yku70Δ
yku70Δ
pif1Δ yku70Δ
pif1Δ yku70Δ
exo1Δ yku70Δ
exo1Δ yku70Δ
pif1Δ exo1Δ yku70Δ
pif1Δ exo1Δ yku70Δ
YKU70+
YKU70+
pif1Δ YKU70+
pif1Δ YKU70+
exo1Δ YKU70+
exo1Δ YKU70+
pif1Δ exo1Δ YKU70+
pif1Δ exo1Δ YKU70+
5506
5507
5508
5509
5510
5511
5512
5513
640
3001
4872
4873
1272
1273
5395
5396
140
30°C
34°C
36°C
37°C
37.5°C
38°C

Figure 19: Pif1 and Exo1 inhibit the growth of *yku70*Δ mutants through parallel pathways

Saturated cultures of the indicated genotypes were serially diluted across agar plates and grown on YEPD plates at the temperatures indicated for 2 days.

4.2.4 Pif1 inhibits the growth of yku70Δ mutants in a parallel pathway to Exo1

Thus far in this study, uncapped telomeres caused by inactivation of *cdc13-1* have been used as a paradigm for telomere uncapping. However, telomere capping and ensuing metaphase arrest can be stimulated by multiple means (Figure 2B-D). Perhaps the most significant of these is the thermosensitive telomere capping defect conferred by *yku70*Δ mutants. Like *cdc13-1* mutants, when *yku70*Δ mutants are exposed to semi- and non-permissive temperatures they accumulate ssDNA and undergo metaphase arrest (Maringele and Lydall, 2002). Unlike ssDNA generation at uncapped telomeres in *cdc13-1* mutants, which depends upon two parallel pathways dependent upon Pif1 and Exo1 (Figures 16-18), ssDNA generation at uncapped telomeres in *yku70*Δ mutants has been reported to be entirely dependent upon Exo1 (Maringele and Lydall, 2002). However, Pif1 does inhibit the growth of *yku70*Δ mutants with uncapped telomeres (Vega et al., 2007). This suggested that Pif1 might generate ssDNA in the same pathway as Exo1 at uncapped telomeres in *yku70*Δ mutants. Growth of *yku70*Δ mutants at non-permissive temperatures is inhibited by accumulation of telomeric ssDNA, which stimulates cell cycle arrest and causes loss of viability (Maringele and Lydall, 2002). Thus, it was hypothesized that if Pif1 generated ssDNA in the same pathway as Exo1 at uncapped telomeres in *yku70*Δ mutants, it would also inhibit the growth of *yku70*Δ mutants at non-permissive temperatures in the same pathway as Exo1.

To test this hypothesis, the effect of Pif1 on the growth of *yku70*Δ and *yku70*Δ *exo1*Δ mutants at non-permissive temperatures was examined. At 34°C-36°C, *yku70*Δ *pif1*Δ mutants grew noticeably better than *yku70*Δ mutants, confirming that Pif1 inhibited the growth of *yku70*Δ mutants, as previously described (Figure 19) (Vega et al., 2007, Smith et al., 2008). At 34°C-37°C, *yku70*Δ *exo1*Δ mutants grew noticeably better than *yku70*Δ mutants, confirming that Exo1 also inhibited the growth of *yku70*Δ mutants, as previously described (Figure 19) (Maringele and Lydall, 2002). However, at 37.5°C-38°C, *yku70*Δ *exo1*Δ mutants grew noticeably worse than $YKU70^{+}$ *exo1*Δ mutants, indicating that there was a residual defect caused by telomere uncapping (Figure 19). *yku70*Δ *exo1*Δ *pif1*Δ mutants grew poorly at 37.5°C-38°C but there was no noticeable growth defect compared to $YKU70^{+}$ *exo1*Δ *pif1*Δ mutants, indicating that there was no residual defect caused by telomere uncapping (Figure 19). In conclusion, Pif1 inhibits the growth of *yku70*Δ mutants in a different pathway to Exo1, but does not inhibit the

growth of *yku70*Δ mutants as potently as Exo1. This suggests that Pif1 and Exo1 might function in parallel pathways to generate ssDNA at uncapped telomeres in *yku70*Δ mutants, just like in *cdc13-1* mutants (Figures 16-18).

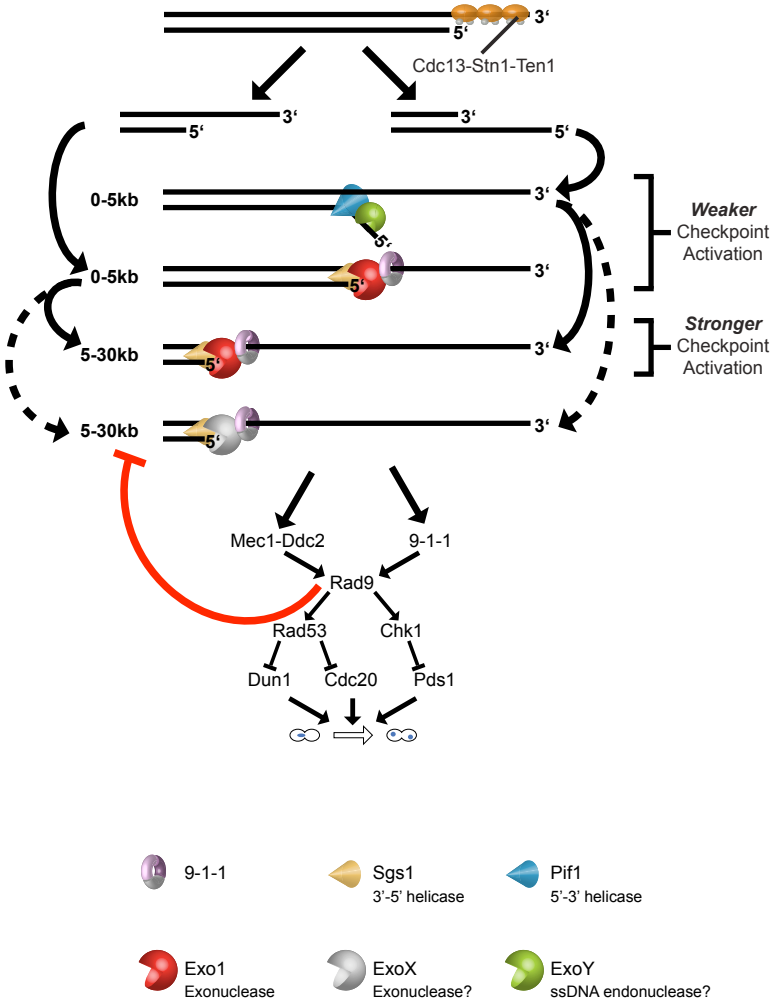
3‘
5‘
Cdc13-Stn1-Ten1
0-5kb
0-5kb
5-30kb
5-30kb
Weaker
Checkpoint
Activation
Stronger
Checkpoint
Activation
Mec1-Ddc2
9-1-1
Rad9
Rad53
Chk1
Dun1
Cdc20
Pds1
9-1-1
Sgs1
3’-5’ helicase
Pif1
5’-3’ helicase
Exo1
Exonuclease
ExoX
Exonuclease?
ExoY
ssDNA endonuclease?

Figure 20: a model for the DDR at uncapped telomeres in *cdc13-1* mutants
Following telomere uncapping by inactivation of Cdc13, both 3' and 5' overhangs occur and are substrates for resection and generation of 3' tracts of ssDNA by Exo1 and Pif1, respectively. Pif1 in combination with an unidentified ssDNA endonuclease (ExoY) generates ssDNA from 5' overhangs 0-5kb from the chromosome end while Exo1 in combination with Sgs1 and the 9-1-1 complex generates ssDNA from 3' overhangs 0-5kb from the chromosome end. This processing $\leq$5kb from the chromosome end causes weak checkpoint activation, sufficient to cause robust arrest in a subpopulation of cells. >5kb from the chromosome end 3' ssDNA is extended by Exo1 to cause robust checkpoint activation in essentially all cells. In the absence of Rad9, a third nuclease activity (ExoX) also supported by Sgs1 and Rad24 is able to resect uncapped telomeres 5-30kb from the chromosome end generating high levels of extensive ssDNA.

4.3 Discussion

Here it has been shown that Pif1 contributes to the DDR at uncapped telomeres, playing an important role in both resection (Figures 16-18) and checkpoint activation (Figure 14). Furthermore, elimination of Pif1 and Exo1 eliminates resection at uncapped telomeres along with the ensuing cell cycle arrest and checkpoint activation (Figures 14,16). This permits a model for checkpoint activation at uncapped telomeres to be proposed (Figure 20).

Figure 20 shows that following telomere uncapping, both Pif1 and Exo1 independently resect uncapped telomeres within 5kb of the chromosome end, causing weak checkpoint activation sufficient to arrest a subpopulation of cells in metaphase (Figure 14). Following this weak, initial checkpoint activation, Exo1 then extensively processes both Pif1- and Exo1- generated substrates to up to 30KB from the chromosome end, causing stronger, more robust checkpoint activation (Figure 20). According to this model, *cdc13-1 pif1*Δ mutants still undergo full checkpoint activation (Figure 14), despite the reduction in resection (Figures 16-17) seen in these cells because extensive resection and robust checkpoint activation by Exo1 still occur. This model also indicates, as previously suggested (Zubko et al., 2004), that a fraction of *cdc13-1 exo1*Δ mutants are able to escape from arrest (Figure 14) because extensive resection and robust checkpoint activation by Exo1 does not occur, but less extensive and weak checkpoint activation by Pif1 does occur. Finally, no checkpoint activation is seen in *cdc13-1 exo1*Δ *pif1*Δ mutants because resection is eliminated (Figure 14). Notably, this model indicates that Pif1 is required for ExoY activity, the previously-hypothetical nuclease activity proposed to function in parallel to Exo1 to generate ssDNA ≤5kb from the chromosome end (Zubko et al., 2004). Based on the data from earlier (Figure 6) as well as other published data (Ngo and Lydall, 2010, Zubko et al., 2004) the model assumes that Sgs1 and the 9-1-1 complex support resection by Exo1 in *RAD9*$^{+}$ and *rad9*Δ cells, while the 9-1-1 complex and Sgs1 can carry out Exo1-independent resection with ExoX in *rad9*Δ cells.

The model proposed in Figure 20 assumes that, like at DSBs, it is the extent of the ssDNA generated that determines checkpoint activation. However, it should be noted that the 0-5kb range in which Pif1 has been demonstrated to carry out Exo1-

independent resection (Figure 16) is within the Y' elements. Thus, it is possible that it is the location of the ssDNA that determines checkpoint activation, not the length of the ssDNA tract i.e. resection beyond the Y' elements might cause checkpoint activation, regardless of the extent of the ssDNA tract, as previously proposed (Zubko et al., 2004). However, without testing this hypothesis in strains of yeast lacking Y' elements, no clear conclusions can be drawn.

*cdc13-1 exo1*Δ *pif1*Δ mutants can grow at 36°C and do not undergo checkpoint activation or generate detectable ssDNA at their telomeres. Other recent work demonstrates that *cdc13-1 exo1*Δ *sgs1*Δ mutants cannot grow at 36°C, do undergo checkpoint activation and generate detectable ssDNA ≤5kb from the chromosome end (in the Y' elements) (Ngo and Lydall, 2010). However, *cdc13-1 rad9*Δ *sgs1*Δ *exo1*Δ mutants are able to grow at 36°C due to inactivation of the checkpoint despite still generating ssDNA ≤5kb from the chromosome end, which is presumably due to Pif1 activity (Ngo and Lydall, 2010). One possible explanation for the ability of *cdc13-1 rad9*Δ *sgs1*Δ *exo1*Δ mutants but not *cdc13-1 sgs1*Δ *exo1*Δ mutants to grow at 36°C is that the ssDNA generated <5kb from the chromosome end in *cdc13-1 exo1*Δ *sgs1*Δ mutants is sufficient to cause checkpoint activation but not to cause loss of viability. Thus, removal of Rad9 eliminates the checkpoint and as Sgs1 is responsible for the increased ssDNA generated in *cdc13-1 rad9*Δ mutants (i.e. Sgs1 is required for ExoX as proposed in Figure 20), no net increase in ssDNA is seen in *cdc13-1 rad9*Δ *exo1*Δ *sgs1*Δ mutants and so the checkpoint is eliminated without compromising viability.

The above hypothesis suggests that the ssDNA generated by Pif1 can cause checkpoint activation but not loss of viability. However, *cdc13-1 rad24*Δ *exo1*Δ mutants, which do not activate the checkpoint and should only generate Pif1-dependent ssDNA, are unable to grow at 36°C. Furthermore, an Exo1-dependent increase in ssDNA generation is seen in *cdc13-1 mec1*Δ mutants compared to *cdc13-1* mutants and Mec1 is required for checkpoint activation in *cdc13-1 exo1*Δ mutants, yet *cdc13-1 mec1*Δ *exo1*Δ mutants (which, again, do not activate the checkpoint and should only generate Pif1-dependent ssDNA) are unable to grow at 36°C. These two observations suggest that Pif1-dependent ssDNA in *cdc13-1 rad24*Δ *exo1*Δ strains and *cdc13-1 mec1*Δ *exo1*Δ strains is sufficient to cause loss of viability.

An alternative explanation for the growth of *cdc13-1 rad9*Δ *exo1*Δ *sgs1*Δ mutants but not *cdc13-1 RAD9*$^{+}$ *exo1*Δ *sgs1*Δ mutants at 36°C is that perhaps in cells lacking Rad9, Sgs1 generates ssDNA from substrates that are usually processed by Pif1. This would suggest that in the absence of certain checkpoint components, a re-wiring of ssDNA generation pathways occurs and thus *cdc13-1 rad9*Δ *exo1*Δ *sgs1*Δ mutants are viable at 36°C because Pif1 has less of a role in ssDNA generation in *cdc13-1 rad9*Δ mutants than in *cdc13-1 RAD9*$^{+}$ mutants or alternatively that Pif1 has to cooperate with Sgs1 for ssDNA generation in *cdc13-1 rad9*Δ mutants. It will be tremendously important to investigate the interplay between Pif1, Sgs1 and Rad9 in the resection of uncapped telomeres.

Figure 20 proposes that Pif1 functions to generate ssDNA to be cleaved by an unidentified ssDNA endonuclease, analogously to its proposed roles in Okazaki fragment processing and disassembly of replication forks (Pike et al., 2009, Rossi et al., 2008, Chang et al., 2009). According to this model, Pif1 acts upon 5' (AC) ssDNA as Pif1 is a 5'-3' helicase and would need to act upon exposed 5' ssDNA in order to generate ssDNA in a telomere-to-centromere direction (Figure 16E) (Lahaye et al., 1991). However, Pif1 is primarily thought of as a negative regulator of telomerase at telomeres and has been proposed to inhibit the growth of *cdc13-1* mutants by removing telomerase from the telomere, thus promoting access of nucleases to the telomeric DNA (Zhou et al., 2000, Boule et al., 2005, Vega et al., 2007). Work presented here clearly shows that Pif1 has a very strong contribution to ssDNA generation in the Y' elements (Figure 16) but only a slight contribution in the TG repeats (Figures 16,18). This is inconsistent with a model in which Pif1 removes telomerase from the telomere, as the effect would be expected to be greatest in the TG repeats, where telomere-bound telomerase should be present. Thus, any model of how Pif1 contributes to resection at uncapped telomeres must explain why Pif1 has such a strong effect in the Y' regions, but a relatively subtle effect at the chromosome end. A model in which Pif1 supports nuclease activity at a substrate arising away from the very end of the chromosome and towards the Y' elements (such as a stalled replication fork) explains this (Chang et al., 2009). Additionally, the 5' (AC) ssDNA that Pif1 is proposed to act upon at uncapped telomeres could, in principle occur on the leading strand of a stalled replication fork.

Pif1 is not required for full cell cycle arrest if cells progress from G1 to metaphase with uncapped telomeres (Figure 14B-C). However, when asynchronously-dividing

populations of *cdc13-1* mutants are subjected to telomere uncapping, Pif1 is required for rapid cell cycle arrest (Figure 13C). This suggests that while resection by Exo1 can effect full cell cycle arrest at metaphase when cells pass from G1 to metaphase with uncapped telomeres, if telomere uncapping occurs mid cell cycle (as would be the case for many cells in an asynchronously dividing population) then Pif1 is necessary to cooperate with Exo1 to cause full checkpoint activation and robust arrest. This may have important physiological consequences cells, as telomere dysfunction is unlikely to occur spontaneously at G1. Alternatively, it might suggest that the resection by Pif1 and Exo1 is cell cycle coordinated. This alternative is particularly interesting when considering that the slight reduction in TG repeat ssDNA caused by elimination of Pif1 (Figure 18) correlates with the low level of ssDNA that has been reported to occur at uncapped telomeres in *cdc13-1* mutants in the TG repeats during S phase (Vodenicharov and Wellinger, 2006). It is also interesting to consider that the large reduction in TG repeat ssDNA caused by elimination of Exo1 (Figure 18) correlates with the high level of ssDNA that has been reported to occur at uncapped telomeres in *cdc13-1* mutants in the TG repeats during metaphase (Vodenicharov and Wellinger, 2006).

Interestingly, slight accumulation at metaphase is seen in *cdc13-1 rad24*Δ mutants and this Pif1-dependent (Figure 13C), suggesting a very low level of checkpoint activation. Thus, loading of the 9-1-1 complex is unlikely to be absolutely required for checkpoint activation but instead promotes checkpoint activation. This is highly analogous to the role proposed here (section 3.3) for Rad24 in promoting resection by loading the 9-1-1 complex, but not being absolutely required for it (presumably because the nucleases have natural affinity for telomeric DNA). Thus, the 9-1-1 complex might promote nuclease activity at uncapped telomeres and promote checkpoint activation, but be non-essential for either. It is interesting to speculate that limited resection by ExoX might be the stimulus for checkpoint activation and telomere homeostasis might rely on the ability of Rad9 to inhibit ExoX, limiting its function to checkpoint activation and preventing extensive resection.

Finally, Pif1 inhibits the growth of *yku70*Δ mutants and is responsible for the residual growth defect in *yku70*Δ *exo1*Δ mutants (Figure 19). This demonstrates that Pif1 and Exo1 constitute parallel pathways that inhibit the growth of uncapped telomeres in *cdc13-1* and *yku70*Δ mutants (Figure 4, Figure 19). Thus, the Pif1- and Exo1-

dependent nucleases are likely to be general feature of dysfunctional telomeres. Unfortunately, at the temperatures at which *yku70*Δ *exo1*Δ mutants show a growth defect (37.5°C-38.0°C) even *YKU70*$^{+}$ mutants show a defect, and *YKU70*$^{+}$ *pif1*Δ mutants grow poorly, so it will be difficult to assess the contribution of Pif1 to Exo1-independent ssDNA generation in *yku70*Δ mutants.

4.4 Further Work

Pif1 and Exo1 resect uncapped telomeres in *cdc13-1* mutants and *cdc13-1 exo1*Δ *pif1*Δ mutants do not generate any detectable ssDNA >600bp from the chromosome end (Y' elements, Figure 16B) and generate only transient ssDNA at the very end of the chromosome (the TG repeats, Figure 18). Rad9 inhibits resection at uncapped telomeres and *cdc13-1 rad9*Δ mutants generate elevated levels of ssDNA compared to *cdc13-1* mutants, dependent upon Sgs1 and Rad24 (Lydall and Weinert, 1995, Ngo and Lydall, 2010, Zubko et al., 2004). It will be interesting to know whether any detectable ssDNA can be seen in the Y' elements of *cdc13-1 rad9*Δ *exo1*Δ *pif1*Δ mutants and if so, whether this ssDNA is dependent upon Rad24 or Sgs1, or both. Furthermore, *cdc13-1 rad9*Δ *sgs1*Δ *exo1*Δ mutants are viable for several generations at 36°C despite residual ssDNA generation still occurring in the Y' elements (Ngo and Lydall, 2010). This residual ssDNA is, presumably, dependent upon Pif1 and it will be important to formally show this.

If the residual ssDNA generated in *cdc13-1 rad9*Δ *exo1*Δ *sgs1*Δ mutants is dependent upon Pif1, then it will suggest that Pif1-dependent ssDNA can prevent growth at 36°C by stimulating checkpoint activation but the loss of viability incurred by Pif1 activity is negligible for short term growth at 36°C. Alternatively, in *cdc13-1 rad9*Δ mutants, substrates usually processed by Pif1 might be processed by Sgs1 and thus there might be less Pif1-dependent ssDNA generated in *cdc13-1 rad9*Δ mutants than *cdc13-1* mutants. It will be important to see what the contribution of Pif1 to ssDNA generation in *cdc13-1 rad9*Δ mutants is.

Pif1 appears to contribute to the very slight loss in viability in *yku70*Δ *exo1*Δ mutants at high temperatures (Figure 19). Thus, it will be important to investigate whether Pif1 also functions in parallel to Exo1 in *yku70*Δ mutants to generate ssDNA. As essentially no ssDNA is generated in *yku70*Δ *exo1*Δ mutants, even $\geq$600bp from the chromosome ends, this could likely only be assessed by in-gel assay. Alternatively, it may be

possible to carry out the experiments at a higher temperature, with the caveat that *pif1*Δ mutants are very sick at this temperature (Figure 19).

Finally, it will be important to investigate the role of Rad24 in checkpoint activation and ssDNA generation following telomere uncapping, especially as strong evidence has been presented here that some Rad24-independent Pif1-dependent checkpoint activation does occur in *cdc13-1* mutants following telomere uncapping (Figure 13C). It also will be of particular interest to investigate how the roles of Rad24 and Exo1 overlap, as elimination of either permits the growth of *cdc13-1 pif1*Δ (Figure 6) or *cdc13-1 rad9*Δ *sgs1*Δ mutants (Greg Ngo, Personal Communication) at 36°C.

5 What is Pif1 doing at Uncapped telomeres?

"There is no adequate defence, except stupidity, against the impact of a new idea."

- Percy Williams Bridgman

5.1 Introduction

The primary role of Pif1 in yeast is believed to be negative regulation of telomerase at DSBs and telomeres, which Pif1 is believed to effect by unwinding the telomerase RNA subunit (TLC1, in yeast) from the telomeric DNA (Boule et al., 2005, Makovets and Blackburn, 2009, Schulz and Zakian, 1994, Zhou et al., 2000). Data presented in Chapter 4 shows that Pif1 appears to control a nuclease activity, which functions at uncapped telomeres in parallel to Exo1 (Figures 16-18). It has been suggested that in the absence of Pif1, increased levels of telomerase at the telomeres can inhibit nuclease activities in *cdc13-1* mutants (Vega et al., 2007). However, telomerase binds to the very ends of chromosomes, in the telomeric TG repeats, so this model is inconsistent with data presented in Section **4**, showing that Pif1 has only a moderate effect in the TG repeats (Figure 18) and functions primarily away from the TG repeats, towards the Y' elements (Figure 16).

Data presented in Section **4** is consistent with other models for Pif1 function, suggesting that Pif1 is involved in unwinding G-quadruplex structures (Ribeyre et al., 2009) or in destabilizing stalled replication forks (Chang et al., 2009). Additionally, Pif1 is believed to play a role in generating long flaps during Okazaki fragment processing (Budd et al., 2006) and has been shown to be capable *in vitro* of unwinding dsDNA to generate ssDNA to be cleaved by nucleases involved in Okazaki fragment processing (Pike et al., 2009). Finally, Pif1 also has roles in mitochondrial DNA maintenance (Van Dyck et al., 1992), which are unlikely to account for the role of Pif1 at uncapped telomeres in the nucleus.

The purpose of this work was to gain insight into whether Pif1 function could be attributed to telomerase-dependent or telomerase-independent roles in the nucleus or mitochondria.

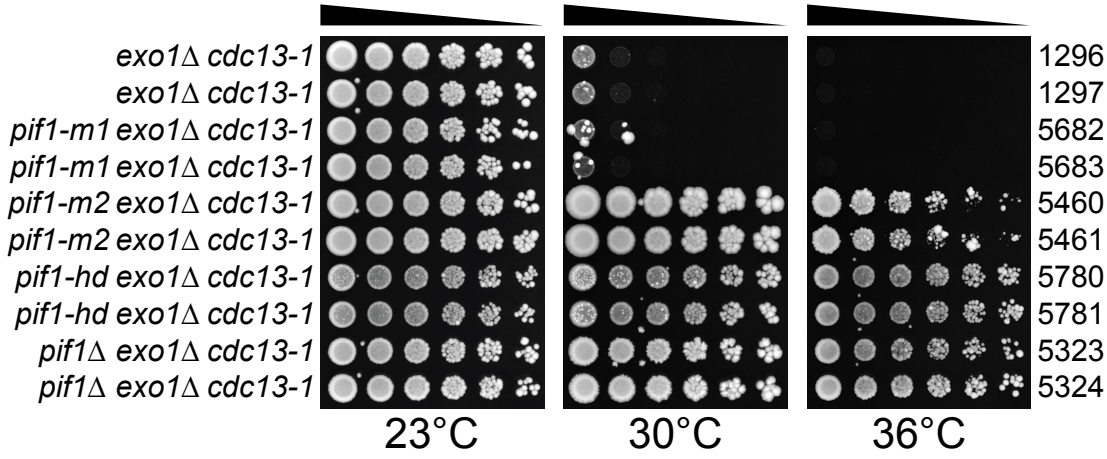
exo1Δ cdc13-1 1296
exo1Δ cdc13-1 1297
pif1-m1 exo1Δ cdc13-1 5682
pif1-m1 exo1Δ cdc13-1 5683
pif1-m2 exo1Δ cdc13-1 5460
pif1-m2 exo1Δ cdc13-1 5461
pif1-hd exo1Δ cdc13-1 5780
pif1-hd exo1Δ cdc13-1 5781
pif1Δ exo1Δ cdc13-1 5323
pif1Δ exo1Δ cdc13-1 5324
23°C
30°C
36°C

Figure 21: Nuclear, helicase activity of Pif1 inhibits the growth of *cdc13-1 exo1*Δ mutants

Saturated cultures of the genotypes indicated, lacking either mitochondrial Pif1 (*pif1-m1*) or nuclear Pif1 (*pif1-m2*), carrying a helicase-dead allele of Pif1 (*pif1-hd*) or deleted for Pif1 (*pif1*Δ) were serially-diluted across YEPD plates and grown at the temperatures indicated for 3 days.

5.2 Results

5.2.1 Nuclear, helicase activity of Pif1 inhibits the growth of cdc13-1 mutants

Pif1 exists as nuclear and mitochondrial isoforms (Schulz and Zakian, 1994) and Pif1 is responsible for the residual resection that inhibits the growth of *cdc13-1 exo1*Δ mutants with uncapped telomeres (Figure 6, Figure 16). To test the hypothesis that the nuclear, but not mitochondrial form of Pif1 inhibits the growth of *cdc13-1 exo1*Δ mutants, point mutations were inserted into the genome of *cdc13-1 exo1*Δ mutants to eliminate either nuclear Pif1 (*pif1-m2*) or mitochondrial Pif1 (*pif1-m1*) (Schulz and Zakian, 1994). *cdc13-1 exo1*Δ *pif1-m2* mutants and *cdc13-1 exo1*Δ *pif1*Δ mutants were able to grow at 30°C and 36°C, while *cdc13-1 exo1*Δ and *cdc13-1 pif1*Δ*-m1* mutants were not (Figure 21). It was noted that *cdc13-1 exo1*Δ *pif1-m2* mutants grew slightly worse at 36°C than *cdc13-1 exo1*Δ *pif1*Δ mutants. However, this is consistent with other reports that *pif1-m2* mutants retain a very low level of nuclear Pif1 activity (Schulz and Zakian, 1994, Ribeyre et al., 2009). It was concluded that nuclear, not mitochondrial Pif1 activity inhibits the growth of *cdc13-1 exo1*Δ mutants.

The ability of Pif1 to unwind telomerase RNA from telomeric DNA and to unwind G quadruplex structures *in vitro* is dependent upon its helicase activity (Boule et al., 2005, Ribeyre et al., 2009). Although *S. cerevisiae* Pif1 has no reported cellular functions independent of its helicase activity, *H. sapiens* Pif1 has been reported to possess strand annealing activity (George et al., 2009). Thus it was possible that Pif1 might have an unidentified, helicase-independent catalytic activity at uncapped telomeres that inhibits the growth of *cdc13-1 exo1*Δ mutants. To test the hypothesis that Pif1 inhibits the growth of *cdc13-1 exo1*Δ mutants independently of its helicase activity, a point mutation was introduced into the genome of *cdc13-1 exo1*Δ mutants to eliminate the helicase activity of Pif1 (*pif1-hd*), thus causing a catalytically dead Pif1 to be expressed (Ribeyre et al., 2009). At 30°C and 36°C, *cdc13-1 exo1*Δ mutants were unable to grow, while *cdc13-1 exo1*Δ *pif1*Δ and *cdc13-1 exo1*Δ *pif1-hd* mutants were able to grow (Figure 21). It was concluded that the helicase activity of Pif1, rather than some other unidentified catalytic activity, inhibits the growth of *cdc13-1 exo1*Δ mutants.

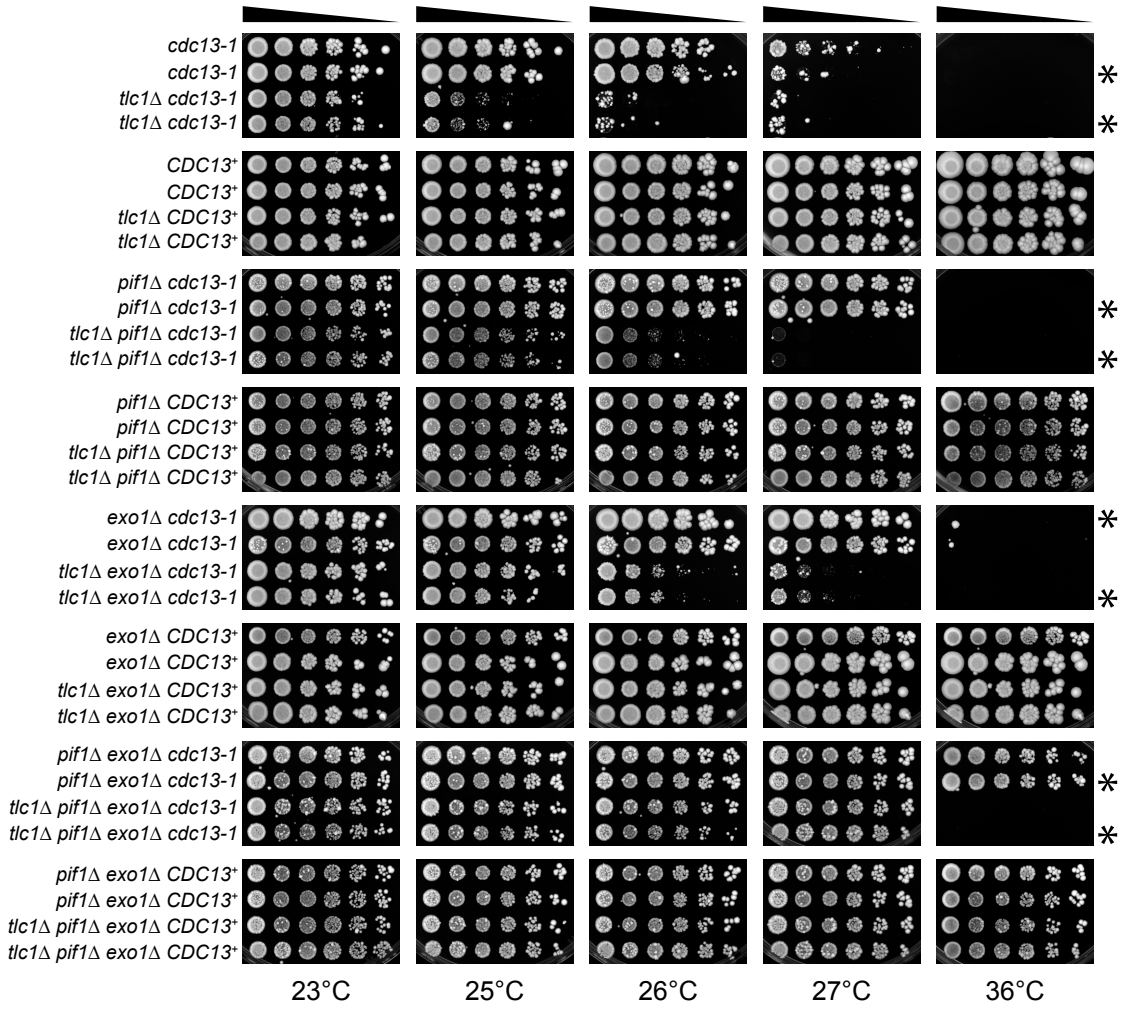
cdc13-1
cdc13-1
tlc1Δ cdc13-1
tlc1Δ cdc13-1
CDC13+
CDC13+
tlc1Δ CDC13+
tlc1Δ CDC13+
pif1Δ cdc13-1
pif1Δ cdc13-1
tlc1Δ pif1Δ cdc13-1
tlc1Δ pif1Δ cdc13-1
pif1Δ CDC13+
pif1Δ CDC13+
tlc1Δ pif1Δ CDC13+
tlc1Δ pif1Δ CDC13+
exo1Δ cdc13-1
exo1Δ cdc13-1
tlc1Δ exo1Δ cdc13-1
tlc1Δ exo1Δ cdc13-1
exo1Δ CDC13+
exo1Δ CDC13+
tlc1Δ exo1Δ CDC13+
tlc1Δ exo1Δ CDC13+
pif1Δ exo1Δ cdc13-1
pif1Δ exo1Δ cdc13-1
tlc1Δ pif1Δ exo1Δ cdc13-1
tlc1Δ pif1Δ exo1Δ cdc13-1
pif1Δ exo1Δ CDC13+
pif1Δ exo1Δ CDC13+
tlc1Δ pif1Δ exo1Δ CDC13+
tlc1Δ pif1Δ exo1Δ CDC13+
23°C
25°C
26°C
27°C
36°C

Figure 22: Pif1 inhibits the growth of *cdc13-1 tlc1*Δ mutants

Saturated cultures of the genotypes indicated were serially diluted across YEPD plates and grown at the temperatures indicated for 4 days. All strains and controls were germinated simultaneously from the same diploid at 23°C for 3 days.

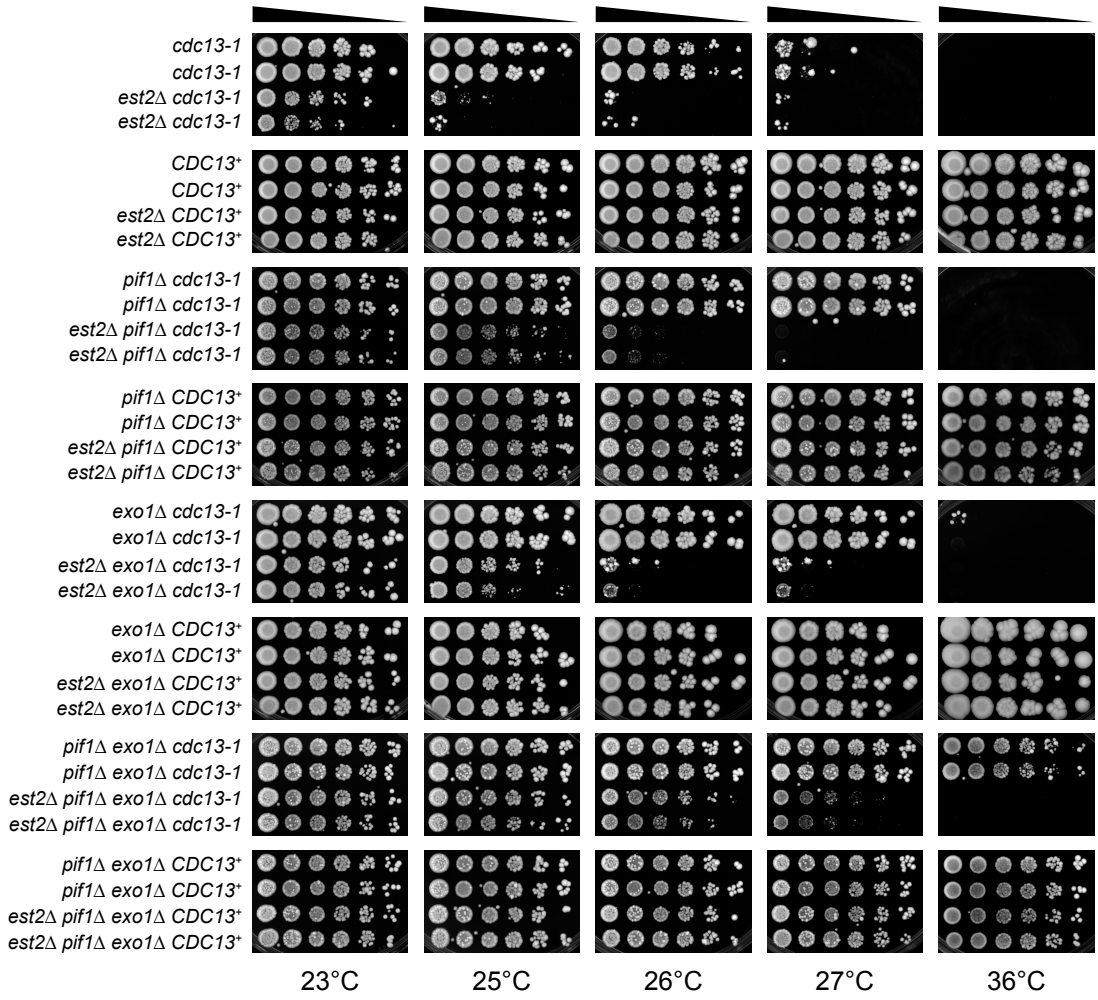
cdc13-1
cdc13-1
est2Δ cdc13-1
est2Δ cdc13-1
CDC13+
CDC13+
est2Δ CDC13+
est2Δ CDC13+
pif1Δ cdc13-1
pif1Δ cdc13-1
est2Δ pif1Δ cdc13-1
est2Δ pif1Δ cdc13-1
pif1Δ CDC13+
pif1Δ CDC13+
est2Δ pif1Δ CDC13+
est2Δ pif1Δ CDC13+
exo1Δ cdc13-1
exo1Δ cdc13-1
est2Δ exo1Δ cdc13-1
est2Δ exo1Δ cdc13-1
exo1Δ CDC13+
exo1Δ CDC13+
est2Δ exo1Δ CDC13+
est2Δ exo1Δ CDC13+
pif1Δ exo1Δ cdc13-1
pif1Δ exo1Δ cdc13-1
est2Δ pif1Δ exo1Δ cdc13-1
est2Δ pif1Δ exo1Δ cdc13-1
pif1Δ exo1Δ CDC13+
pif1Δ exo1Δ CDC13+
est2Δ pif1Δ exo1Δ CDC13+
est2Δ pif1Δ exo1Δ CDC13+
23°C
25°C
26°C
27°C
36°C

Figure 23: Pif1 inhibits the growth of *cdc13-1 est2*Δ mutants

Saturated cultures of the genotypes indicated were serially diluted across YEPD plates and grown at the temperatures indicated for 4 days. All strains and controls were germinated simultaneously from the same diploid at 23°C for 3 days.

5.2.2 Pif1 functions independently of telomerase at uncapped telomeres in cdc13-1 mutants

Pif1 has been suggested to contribute to nuclease activity at uncapped telomeres by removing telomerase from telomeres and facilitating access by nucleases (Vega et al., 2007), but this model is inconsistent with data presented here showing that Pif1 functions primarily away from the very ends of the telomeres (Figure 18). Thus, it was important to test whether the roles of Pif1 in the DDR at uncapped telomeres were dependent upon telomerase or not.

Pif1 acts upon the TLC1 subunit of telomerase to remove telomerase from telomeric DNA (Boule et al., 2005). It was hypothesized that Pif1 might function independently of this activity at uncapped telomeres and thus would inhibit the growth of *cdc13-1* and *cdc13-1 exo1*Δ mutants even in the absence of TLC1. To test this hypothesis, the effect of Pif1 on the growth of *tlc1*Δ *cdc13-1* and *tlc1*Δ *cdc13-1 exo1*Δ mutants was examined. Cells lacking telomerase undergo a gradual decrease in proliferative capacity over time due to telomere shortening, so in order to examine the growth of *cdc13-1* mutants lacking the TLC1 subunit of telomerase, *tlc1*Δ*/TLC1*$^{+}$ *cdc13-1/CDC13*$^{+}$ *exo1*Δ*/EXO1*$^{+}$ *pif1*Δ */PIF1*$^{+}$ diploids were generated, sporulated and spores germinated to generate all experimental strains and controls simultaneously. At 25°C, *tlc1*Δ *cdc13-1* mutants grew poorly, while *tlc1*Δ *cdc13-1 pif1*Δ mutants grew well (Figure 22). Similarly, at 26°C and 27°C, *tlc1*Δ *cdc13-1 exo1*Δ mutants grew poorly, while *tlc1*Δ *cdc13-1 pif1*Δ *exo1*Δ mutants grew well (Figure 22). It was concluded that Pif1 inhibits the growth of *cdc13-1* and *cdc13-1 exo1*Δ mutants independently of TLC1.

It was noted that *tlc1*Δ *cdc13-1* mutants showed a severe growth defect at 25°C while *cdc13-1* mutants did not (Figure 22). Similarly, *tlc1*Δ *cdc13-1 exo1*Δ and *tlc1*Δ *cdc13-1 pif1*Δ mutants showed a severe growth defect at 26°C, while *cdc13-1 exo1*Δ and *cdc13-1 pif1*Δ mutants did not (Figure 22) and *tlc1*Δ *cdc13-1 exo1*Δ *pif1*Δ mutants were unable to grow at 36°C while *cdc13-1 exo1*Δ *pif1*Δ mutants were not (Figure 22). In conclusion, TLC1 plays a protective role in all *cdc13-1* mutants and is required for the growth of *cdc13-1 exo1*Δ *pif1*Δ mutants at 36°C, suggesting that *cdc13-1 exo1*Δ *pif1*Δ mutants are unable to survive at 36°C without telomerase.

Pif1 clearly inhibited the growth of *cdc13-1* mutants independently of TLC1 (Figure 22). However, it was conceivable that Pif1 also removed telomerase from telomeres by

a hereto-unprecedented TLC1-independent mechanism. To test this hypothesis, it was necessary to examine the effect of Pif1 in *cdc13-1* mutants lacking Est2, the catalytic subunit of telomerase, which believed to be responsible for inhibiting nucleases at the telomeres of *cdc13-1 pif1*Δ mutants (Vega et al., 2007). Similarly to before, *est2*Δ*/EST2*$^{+}$ *cdc13-1/CDC13*$^{+}$ *exo1*Δ*/EXO1*$^{+}$ *pif1*Δ */PIF1*$^{+}$ diploids were generated, sporulated and spores germinated to generate all experimental strains and controls simultaneously. At 25°C *est2*Δ *cdc13-1* mutants grew poorly while *est2*Δ *cdc13-1 pif1*Δ mutants grew better (Figure 23). Similarly, at 26°C, *est2*Δ *cdc13-1 exo1*Δ mutants grew poorly but *est2*Δ *cdc13-1 exo1*Δ *pif1*Δ mutants grew better (Figure 23). It was concluded that Pif1 inhibits the growth of *cdc13-1* and *cdc13-1 exo1*Δ mutants independently of Est2.

It was also noted that the absence of Est2 (Figure 23) conferred a similar defect to the absence of TLC1 (Figure 22). At 25°C, *est2*Δ *cdc13-1* mutants had a severe growth defect while *cdc13-1* mutants did not (Figure 23). *est2*Δ *cdc13-1 exo1*Δ and *est2*Δ *cdc13-1 pif1*Δ mutants showed a severe growth defect at 26°C while *cdc13-1 exo1*Δ and *cdc13-1 pif1*Δ mutants did not (Figure 23) and *est2*Δ *cdc13-1 exo1*Δ *pif1*Δ mutants were unable to grow at 36°C while *cdc13-1 exo1*Δ *pif1*Δ mutants were (Figure 23). It was concluded that Est2, like TLC1, plays a protective role at uncapped telomeres in all *cdc13-1* mutants.

*pif1*Δ mutants have long telomeres and telomerase is required for this (Zhou et al., 2000). Furthermore *cdc13-1 exo1*Δ *pif1*Δ mutants are able to grow at 36°C, while *cdc13-1 exo1*Δ *pif1*Δ mutants lacking telomerase (TLC1, Est2, Figures 22-23) are not. Thus, it is possible that the long telomeres play an important causal role in permitting the growth of *cdc13-1 exo1*Δ *pif1*Δ mutants at 36°C. Alternatively, it is possible that the long telomeres seen in *pif1*Δ mutants are consequential of an increased requirement for telomerase and this requirement is heightened in *cdc13-1 exo1*Δ *pif1*Δ mutants. However, without investigating the consequences of telomere uncapping in *cdc13-1 exo1*Δ *pif1*Δ mutants with short telomeres and in telomerase-deficient *cdc13-1 exo1*Δ *pif1*Δ mutants with long telomeres, no definitive conclusion can be made.

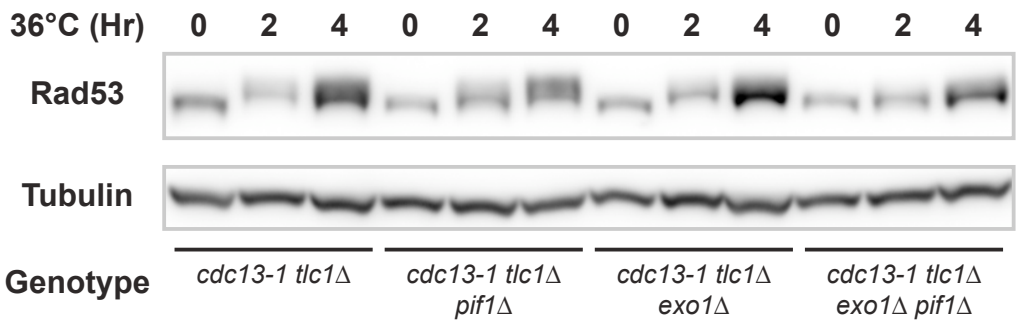
36°C (Hr)
0 2 4 0 2 4 0 2 4 0 2 4
Rad53
Tubulin
Genotype
cdc13-1 tlc1Δ
cdc13-1 tlc1Δ pif1Δ
cdc13-1 tlc1Δ exo1Δ
cdc13-1 tlc1Δ exo1Δ pif1Δ

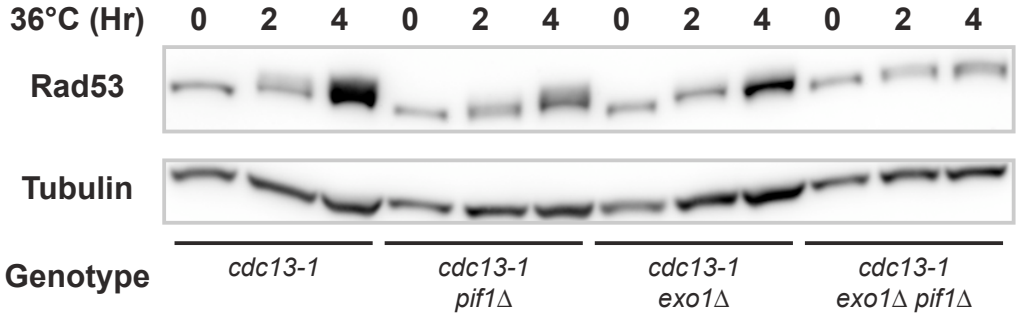
36°C (Hr)
0 2 4 0 2 4 0 2 4 0 2 4
Rad53
Tubulin
Genotype
cdc13-1
cdc13-1 pif1Δ
cdc13-1 exo1Δ
cdc13-1 exo1Δ pif1Δ

Figure 24: Pif1 contributes to Rad53 activation following telomere uncapping in *cdc13-1* mutants lacking telomerase

Exponentially-dividing cultures of *cdc13-1* and *cdc13-1 tlc1*Δ mutants (those indicated with an asterisk in Figure 22) were shifted to 36°C to induce telomere uncapping. Samples were taken for Western blots, which were performed to detect Rad53 and tubulin as a loading control. Upper and lower panels were run on separate gels but transferred and detected simultaneously.

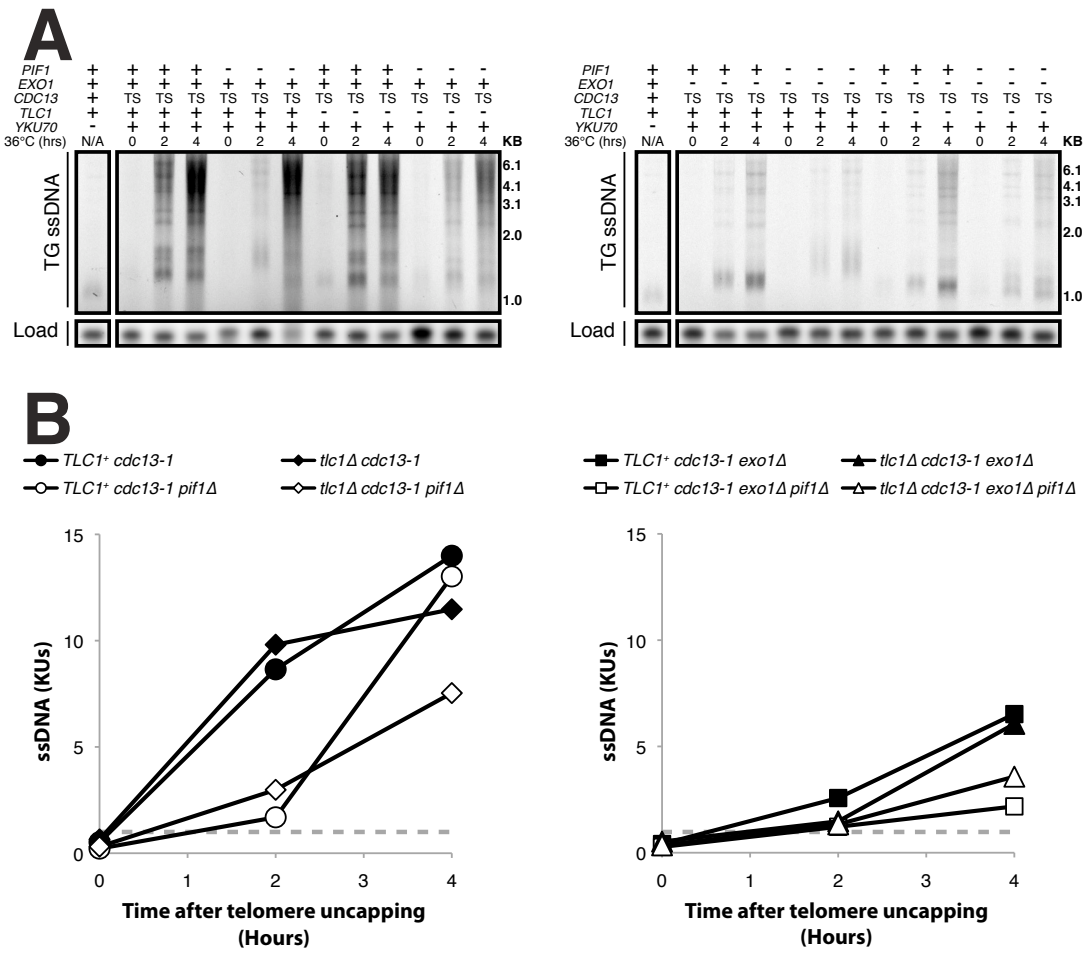
A
PIF1
EXO1
CDC13
TLC1
YKU70
36°C (hrs)
N/A
0 2 4 0 2 4 0 2 4 0 2 4
KB
6.1
4.1
3.1
2.0
1.0
TG ssDNA
Load
B
TLC1+ cdc13-1
tlc1Δ cdc13-1
TLC1+ cdc13-1 pif1Δ
tlc1Δ cdc13-1 pif1Δ
TLC1+ cdc13-1 exo1Δ
tlc1Δ cdc13-1 exo1Δ
TLC1+ cdc13-1 exo1Δ pif1Δ
tlc1Δ cdc13-1 exo1Δ pif1Δ
ssDNA (KUs)
Time after telomere uncapping
(Hours)

Figure 25: Pif1 contributes to ssDNA generation in the TG repeats of *cdc13-1* mutants lacking telomerase

A. Exponentially-dividing cultures of *cdc13-1* and *cdc13-1 tlc1*Δ mutants (those indicated with an asterix in Figure 22) were shifted to 36°C to induce telomere uncapping. Samples were taken every two hours to measure ssDNA in the TG repeats by in-gel assay, then Southern Blots were performed to probe for *CDC15* as a loading control. **B.** Quantification of the data shown in **A.**, as in Figure 18B. Dashed line represents the level of ssDNA detected in an asynchronously dividing *yku70*Δ mutant at 23°C.

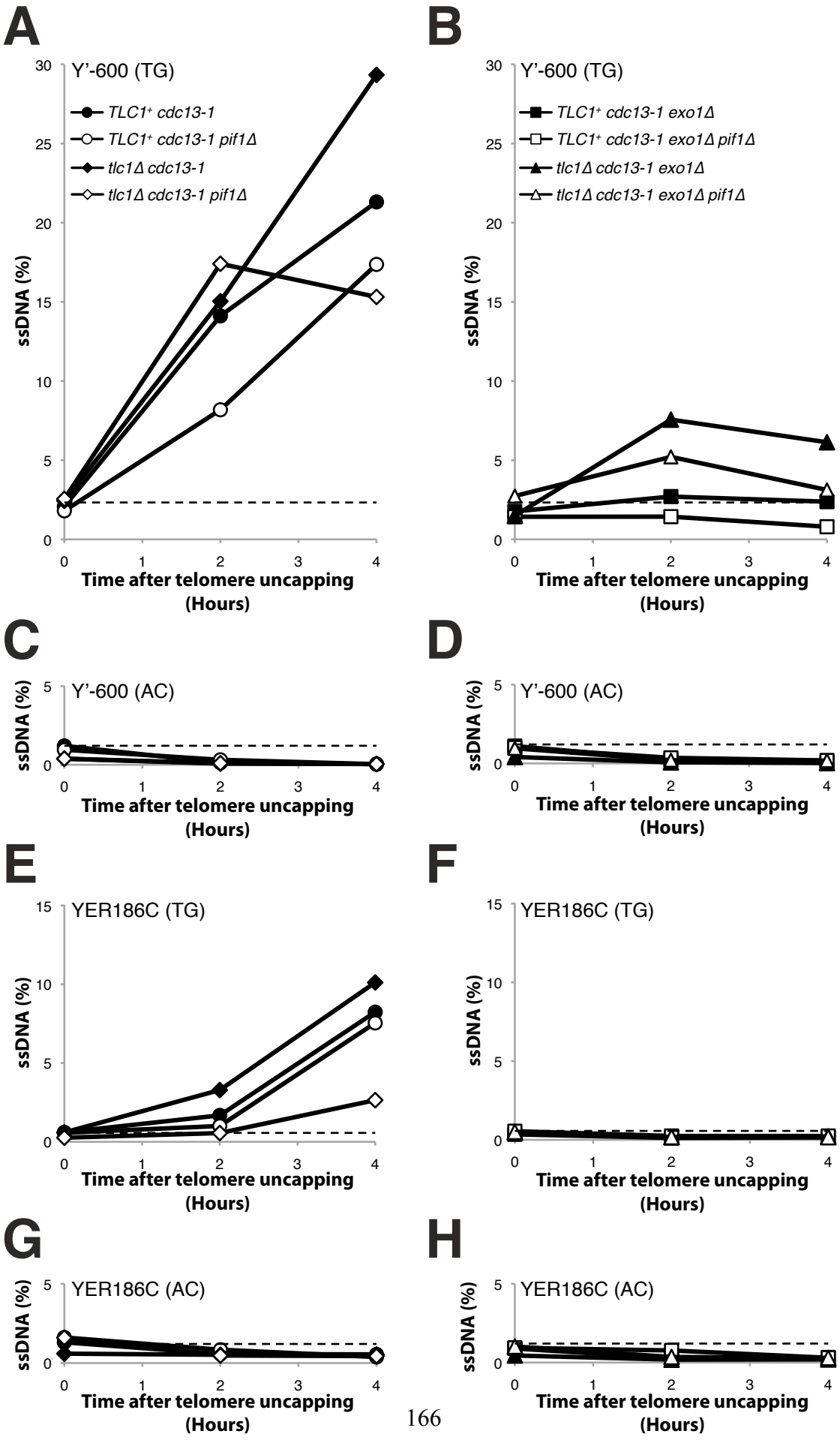
A
Y'-600 (TG)
TLC1+ cdc13-1
TLC1+ cdc13-1 pif1Δ
tlc1Δ cdc13-1
tlc1Δ cdc13-1 pif1Δ
ssDNA (%)
Time after telomere uncapping (Hours)
B
Y'-600 (TG)
TLC1+ cdc13-1 exo1Δ
TLC1+ cdc13-1 exo1Δ pif1Δ
tlc1Δ cdc13-1 exo1Δ
tlc1Δ cdc13-1 exo1Δ pif1Δ
ssDNA (%)
Time after telomere uncapping (Hours)
C
Y'-600 (AC)
ssDNA (%)
Time after telomere uncapping (Hours)
D
Y'-600 (AC)
ssDNA (%)
Time after telomere uncapping (Hours)
E
YER186C (TG)
ssDNA (%)
Time after telomere uncapping (Hours)
F
YER186C (TG)
ssDNA (%)
Time after telomere uncapping (Hours)
G
YER186C (AC)
ssDNA (%)
Time after telomere uncapping (Hours)
H
YER186C (AC)
ssDNA (%)
Time after telomere uncapping (Hours)

Figure 26: Pif1 inhibits ssDNA generation up to 14,500bp from the chromosome end in *cdc13-1* mutants lacking telomerase

Exponentially dividing cultures of *cdc13-1* and *cdc13-1 tlc1*Δ mutants (those indicated with an asterisk in Figure 22) were shifted to 36°C to induce telomere uncapping. Samples were taken every two hours to measure ssDNA in the TG repeats by in-gel assay (Figure 25). Samples were then used to measure ssDNA by QAOS at selected loci shown in Figure 16A.

ssDNA was measured at the Y'600 locus (approximately 600bp from the chromosome end) on the TG strand (**A.** and **B.**) or the AC strand (**C.** and **D.**) and at the *YER186C* locus (approximately 14,500bp from the chromosome end) on the TG strand (**E.** and **F.**) or the AC strand (**G.** and **H.**). In all cases, the horizontal dashed line represents ssDNA detected in an asynchronously-dividing *yku70*Δ mutant at the permissive temperature.

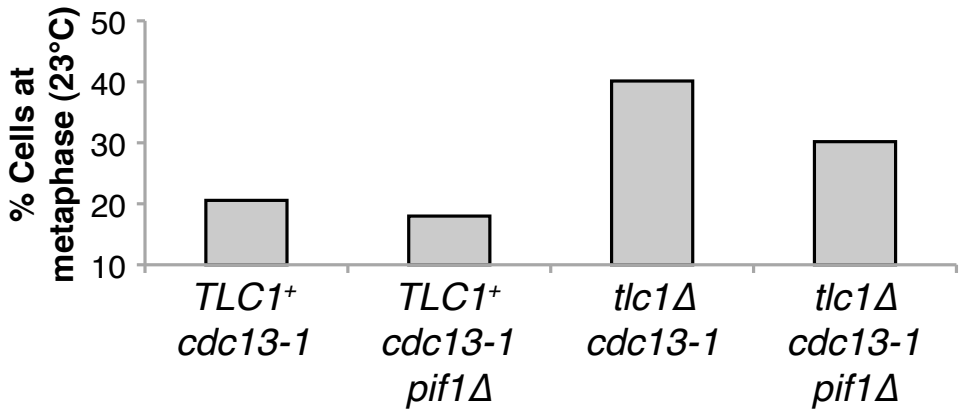
% Cells at metaphase (23°C)
50
40
30
20
10
TLC1+ cdc13-1
TLC1+ cdc13-1 pif1Δ
tlc1Δ cdc13-1
tlc1Δ cdc13-1 pif1Δ

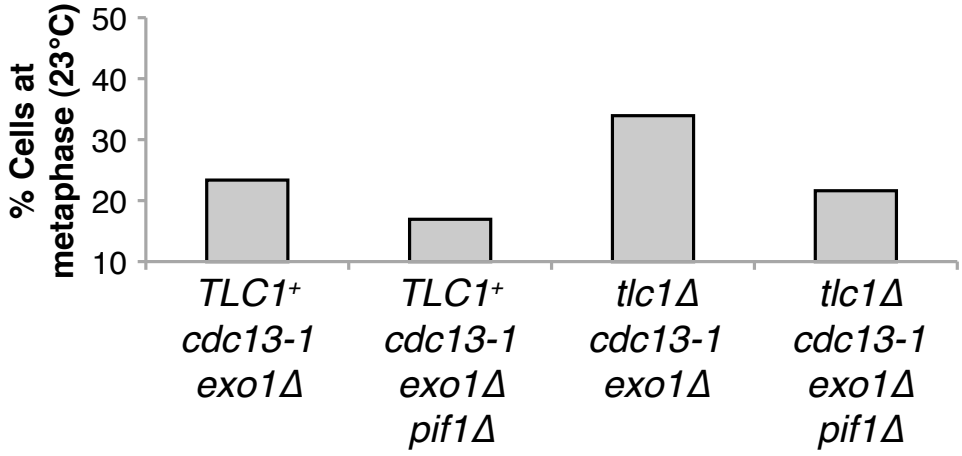
% Cells at metaphase (23°C)
50
40
30
20
10
TLC1+ cdc13-1 exo1Δ
TLC1+ cdc13-1 exo1Δ pif1Δ
tlc1Δ cdc13-1 exo1Δ
tlc1Δ cdc13-1 exo1Δ pif1Δ

Figure 27: *cdc13-1* mutants lacking telomerase accumulate at metaphase at the permissive temperature

Samples were taken from exponentially dividing cultures of *cdc13-1* and *cdc13-1 tlc1*Δ mutants (those indicated with an asterisk in Figure 22) at 23°C, then fixed and scored for the percentage of cells at metaphase.

5.2.3 Pif1 is a component of the DDR at uncapped telomeres in cdc13-1 mutants lacking telomerase

Pif1 inhibits the growth of *cdc13-1 exo1*Δ mutants and Pif1 promotes checkpoint activation in *cdc13-1 exo1*Δ mutants in synchronous cultures (Figure 14D). Pif1 also inhibits the growth of *tlc1*Δ *cdc13-1 exo1*Δ mutants (Figure 22) so it was hypothesized that Pif1 might also contribute to checkpoint activation in *tlc1*Δ *cdc13-1 exo1*Δ mutants in synchronous cultures. However, due to the difficulty in working with telomerase-deficient strains and the requirement to generate all strains and controls simultaneously, it was not feasible to carry out such an experiment in a synchronous culture system. Instead, the contribution of Pif1 to checkpoint activation in *tlc1*Δ *cdc13-1 exo1*Δ mutants was determined in asynchronous cultures, using the strains indicated in Figure 22, and the contribution to checkpoint activation in *cdc13-1 exo1*Δ strains was determined as a control.

Asynchronously dividing *cdc13-1* and tlc1Δ *cdc13-1* mutants were shifted to 36°C to induce telomere uncapping and samples were taken at 0, 2 and 4 hours to assess Rad53 phosphorylation. *cdc13-1 exo1*Δ mutants displayed a slight decrease in Rad53 mobility 2 and 4 hours after telomere uncapping, while no discernable mobility shift could be seen in *cdc13-1 exo1*Δ *pif1*Δ mutants (Figure 24) consistent with previous results in synchronous cultures (Figure 14D). *tlc1*Δ *cdc13-1 exo1*Δ mutants also displayed a decrease in Rad53 mobility 2 and 4 hours after telomere uncapping and *tlc1*Δ *cdc13-1 exo1*Δ *pif1*Δ mutants also displayed a decrease in Rad53 mobility, but to a lesser extent than *tlc1*Δ *cdc13-1 exo1*Δ mutants (Figure 24). It was concluded that Pif1 contributes to checkpoint activation in *tlc1*Δ *cdc13-1 exo1*Δ mutants, but while *cdc13-1 exo1*Δ *pif1*Δ mutants displayed no detectable Rad53 activation, this was partially restored in *tlc1*Δ *cdc13-1 exo1*Δ *pif1*Δ mutants. Thus, telomerase was required to prevent checkpoint activation in *cdc13-1 exo1*Δ *pif1*Δ mutants, providing an explanation for the inability of *tlc1*Δ *cdc13-1 exo1*Δ *pif1*Δ mutants to grow at 36°C (Figure 22).

Pif1 has an important role in cell cycle arrest in asynchronously dividing *cdc13-1* mutants (Figure 13). It was hypothesized that Pif1 might also contribute to checkpoint activation in asynchronously-dividing *tlc1*Δ *cdc13-1* mutants. To test this hypothesis, the contribution of Pif1 to Rad53 activation in *cdc13-1* and *tlc1*Δ *cdc13-1* mutants was

assessed. *cdc13-1* mutants showed a decrease in Rad53 mobility following telomere uncapping and this was diminished in *cdc13-1 pif1*Δ mutants (Figure 24). *tlc1*Δ *cdc13-1 pif1*Δ mutants also showed a decrease in Rad53 mobility following telomere uncapping and this was also diminished in *tlc1*Δ *cdc13-1 pif1*Δ mutants (Figure 24). It was concluded that in asynchronous cultures, Pif1 contributes to checkpoint activation in *cdc13-1* mutants, consistent with its contribution to cell cycle arrest in asynchronous cultures (Figure 13) and that Pif1 contributes to checkpoint activation even in cells lacking telomerase.

As Pif1 contributes to checkpoint activation in *cdc13-1 exo1*Δ mutants lacking telomerase (Figure 25), it was hypothesized that it might also contribute to ssDNA generation in *cdc13-1* mutants lacking telomerase, which is the stimulus for checkpoint activation (Figure 25). To test this hypothesis, asynchronous cultures of the *cdc13-1* and *tlc1*Δ *cdc13-1* mutants shown in Figure 22 were subjected to telomere uncapping and then ssDNA in the telomeric TG repeats was measured by in-gel assay (as in Figure 18). *tlc1*Δ *cdc13-1* strains underwent an approximately 10 fold increase in ssDNA in the TG repeats compared to a *yku70*Δ mutant and this was severely diminished in a *tlc1*Δ *cdc13-1* mutant both 2 and 4 hours after telomere uncapping (Figure 25A-B). *tlc1*Δ *cdc13-1 exo1*Δ mutants generated a similar level of ssDNA to a *yku70*Δ mutant 2 hours after telomere uncapping and this was not altered in a *tlc1*Δ *cdc13-1 exo1*Δ *pif1*Δ mutants (Figure 25A-B). However, 4 hours after telomere uncapping, *tlc1*Δ *cdc13-1 exo1*Δ mutants displayed an approximately 5-fold more increase telomeric ssDNA than a *yku70*Δ mutant and this was reduced in a *tlc1*Δ *cdc13-1 exo1*Δ *pif1*Δ mutant (Figure 25A-B). It was concluded that Pif1 contributes to ssDNA generation in the telomeric TG repeats even in cells lacking telomerase.

Following telomere uncapping in asynchronous cultures, *cdc13-1 pif1*Δ mutants generated much less ssDNA than *cdc13-1* mutants in the telomeric TG repeats 2 hours after telomere uncapping, but by 4 hours there was no distinguishable difference between *cdc13-1* and *cdc13-1 pif1*Δ mutants (Figure 25). This was in contrast to in synchronous cultures where there was a consistent, but slight, reduction in ssDNA in the TG repeats of *cdc13-1 pif1*Δ mutants compared to *cdc13-1* mutants 2 and 4 hours after telomere uncapping (Figure 18). To clarify the role of Pif1 in the resection of uncapped telomeres in asynchronous cultures of *cdc13-1* and *tlc1*Δ *cdc13-1* mutants,

QAOS was performed to measure ssDNA in the telomeric Y'600 and *YER186C* loci, approximately 600bp and 14,500bp from the chromosome end, respectively.

Asynchronously grown *cdc13-1* mutants generated large quantities of ssDNA at the Y'600 locus following telomere uncapping and this was markedly reduced in *cdc13-1 pif1*Δ mutants (Figure 26A), as observed in synchronous cultures (Figure 16B). ssDNA generation was specific to the TG strand and none was detected on the AC strand (Figure 26C). At the *YER186C* locus, *cdc13-1* mutants generated a slight increase in ssDNA 2 hours after telomere uncapping and a large increase 4 hours after telomere uncapping (Figure 26E) and this was slightly reduced in *cdc13-1 pif1*Δ mutants (Figure 26E). This was different to synchronous cultures, where *cdc13-1* mutants had generated a large increase in ssDNA by 2 hours, which increased slightly by 4 hours and was drastically reduced in *cdc13-1 pif1*Δ mutants (Figure 17D). ssDNA generation in asynchronously dividing *cdc13-1* mutants at the *YER186C* locus was specific to the TG strand a none was detected on the AC strand (Figure 26G). It was concluded that in asynchronous cultures, just like in synchronous cultures, Pif1 was most important for ssDNA generation in the Y' elements, but unlike synchronous cultures, Pif1 was relatively unimportant for ssDNA generation further from the chromosome end in asynchronous cultures. These differences in ssDNA generation following telomere uncapping between synchronous and asynchronous cultures of *cdc13-1 pif1*Δ and *tlc1*Δ *cdc13-1 pif1*Δ mutants made it difficult to use these strains to draw conclusions about the effect of Pif1 on resection of uncapped telomeres in telomerase-deficient *cdc13-1* mutants.

It was hypothesized that ssDNA generation in Y' elements and beyond at uncapped telomeres in *cdc13-1 exo1*Δ and *cdc13-1 exo1*Δ *pif1*Δ mutants might be more comparable between asynchronous and synchronous cultures than was seen for *cdc13-1* and *cdc13-1 pif1*Δ mutants (Figure 26). To test this hypothesis, ssDNA was measured following telomere uncapping in asynchronously-dividing cultures of *cdc13-1 exo1*Δ and *cdc13-1 exo1*Δ *pif1*Δ mutants (Figure 26). *cdc13-1 exo1*Δ mutants showed a very slight increase in ssDNA generation in the Y' elements following telomere uncapping (Figure 26B) and no increase was seen in asynchronously grown *cdc13-1 exo1*Δ *pif1*Δ mutants, as observed in synchronous cultures (Figure 16B). ssDNA generation by *cdc13-1 exo1*Δ mutants at the *Y'600* locus was specific to the TG strand as no ssDNA accumulated on the AC strand (Figure 16D). Additionally, no ssDNA accumulated on

the AC or TG strands in *cdc13-1 exo1*Δ or *cdc13-1 exo1*Δ *pif1*Δ mutants, consistent with previous results that synchronous cultures of *cdc13-1 exo1*Δ and *cdc13-1 exo1*Δ *pif1*Δ mutants did not generate any ssDNA beyond the Y' elements (Figure 16E). It was concluded that in asynchronous cultures, *cdc13-1 exo1*Δ mutants behave similarly to in synchronous cultures and that Exo1 is important for ssDNA in the Y' elements and essential for ssDNA generation beyond the Y' elements.

Following telomere uncapping, *cdc13-1 exo1*Δ mutants generated comparable levels of ssDNA when grown synchronously or asynchronously, so were therefore used to examine the effect of Pif1 and telomerase (TLC1) on the resection of uncapped telomeres. At the Y'600 locus, *tlc1*Δ *cdc13-1 exo1*Δ and *tlc1*Δ *cdc13-1 exo1*Δ *pif1*Δ mutants generated elevated levels of ssDNA compared to *cdc13-1 exo1*Δ and *cdc13-1 exo1*Δ *pif1*Δ mutants, respectively, and also in comparison to an asynchronously dividing *yku70*Δ mutant (Figure 26B). However, asynchronously dividing *tlc1*Δ *cdc13-1 exo1*Δ *pif1*Δ mutants generated less ssDNA than a *tlc1*Δ *cdc13-1 exo1*Δ mutant (Figure 26B). At the *YER186C* locus, no ssDNA was detectable in *tlc1*Δ *cdc13-1 exo1*Δ, *tlc1*Δ *cdc13-1 exo1*Δ *pif1*Δ, *cdc13-1 exo1*Δ or *cdc13-1 exo1*Δ *pif1*Δ mutants (Figure 26F). It was concluded that Pif1 contributes to ssDNA generation at uncapped telomeres even in *cdc13-1* mutants lacking telomerase (TLC1) and that telomerase inhibits ssDNA generation independently of both Pif1 and Exo1 in the Y' elements but not at internal loci (such as *YER186C*).

It had been concluded that telomerase inhibits ssDNA generation in *cdc13-1* mutants (Figure 26B). However, 4 hours after telomere uncapping, *tlc1*Δ *cdc13-1 pif1*Δ mutants generated less ssDNA than *cdc13-1 pif1*Δ mutants in both the Y'600 and YER186C loci (Figure 26A,E). Furthermore, at *YER186C*, 4 hours after telomere uncapping, asynchronously grown *tlc1*Δ *cdc13-1 pif1*Δ mutants showed a huge decrease in ssDNA at YER186C compared to *tlc1*Δ *cdc13-1* mutants, while *cdc13-1 pif1*Δ mutants showed only a very slight decrease in ssDNA compared to *cdc13-1* mutants (Figure 26E). As slightly different amounts of ssDNA were generated following telomere uncapping in synchronous cultures and asynchronous cultures (Figure 16B, Figure 26A) and ssDNA generation at uncapped telomeres is a cell cycle regulated process, occurring primarily at metaphase (Vodenicharov and Wellinger, 2006), it was hypothesized that these differences in ssDNA generation might be due to altered cell cycle progression and altered kinetics of arrest following telomere uncapping in *cdc13-1* mutants.

To test this hypothesis, exponentially dividing cultures of *cdc13-1* and *tlc1*Δ *cdc13-1* mutants were fixed and the fraction of cells at metaphase was scored (Figure 27). In *TLC1*$^{+}$ *cdc13-1*, *TLC1*$^{+}$ *cdc13-1 pif1*Δ, *TLC1*$^{+}$ *cdc13-1 exo1*Δ and *TLC1*$^{+}$ *cdc13-1 exo1*Δ *pif1*Δ mutants approximately 15-20% of cells were at metaphase in asynchronously dividing cultures grown at 23°C (Figure 27). However, in *tlc1*Δ *cdc13-1*, *tlc1*Δ *cdc13-1 pif1*Δ and *tlc1*Δ *cdc13-1 exo1*Δ mutants 30-40% of cells were at metaphase (Figure 27). Notably this was not the case for *tlc1*Δ *cdc13-1 exo1*Δ *pif1*Δ mutants of which only 20% were at metaphase (Figure 27). In conclusion elimination of telomerase (TLC1) causes accumulation of *cdc13-1* mutants at metaphase, even at the permissive temperature, and this cell cycle defect is likely to account for the increased ssDNA generation in *cdc13-1 pif1*Δ mutants compared to *tlc1*Δ *cdc13-1 pif1*Δ mutants (Figure 26E). Interestingly, the this cycle defect was not seen in *cdc13-1 exo1*Δ *pif1*Δ mutants lacking telomerase, suggesting that elimination of Pif1 and Exo1 might synergistically suppress defects caused by lack of telomerase.

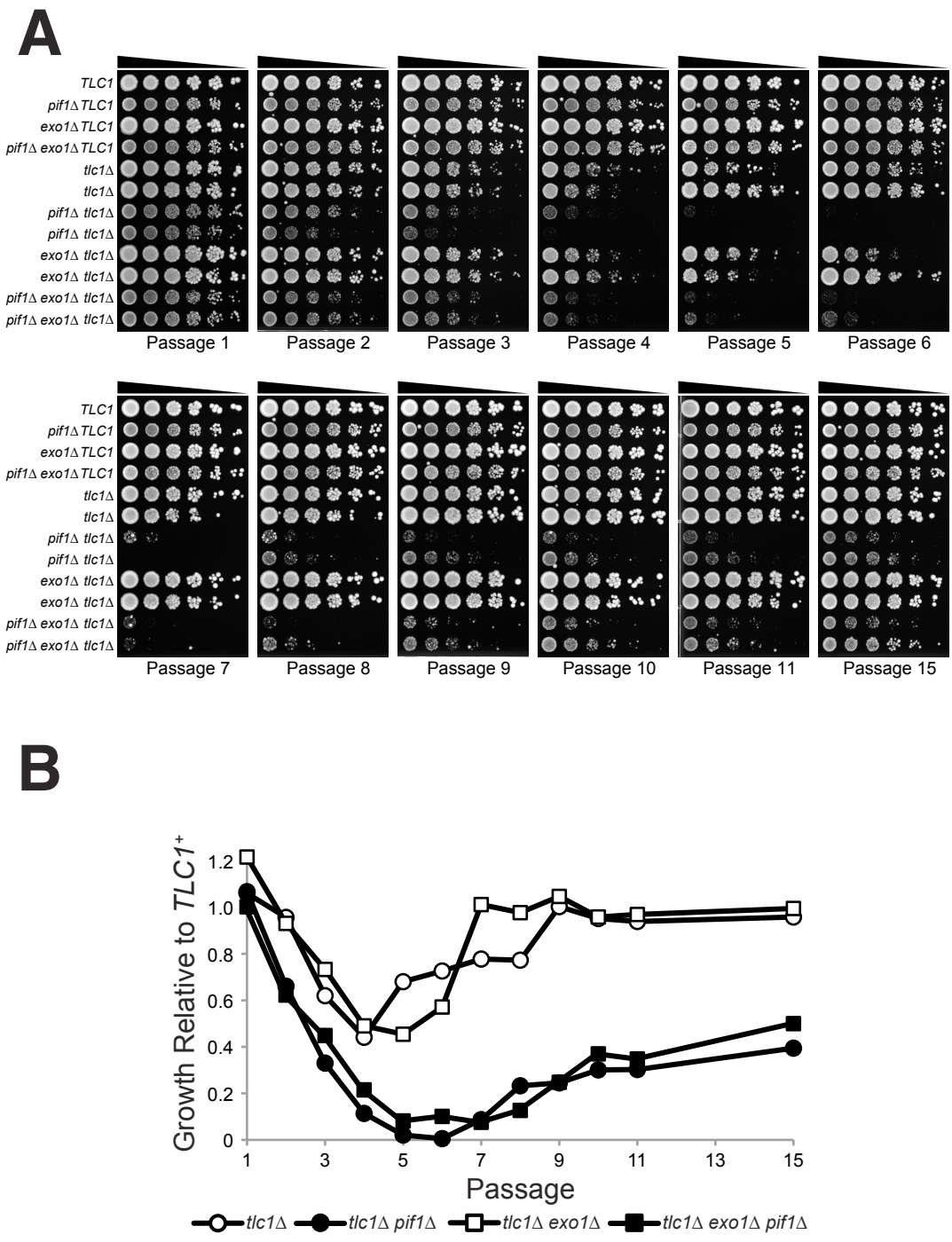
A
TLC1
pif1Δ TLC1
exo1Δ TLC1
pif1Δ exo1Δ TLC1
tlc1Δ
tlc1Δ
pif1Δ tlc1Δ
pif1Δ tlc1Δ
exo1Δ tlc1Δ
exo1Δ tlc1Δ
pif1Δ exo1Δ tlc1Δ
pif1Δ exo1Δ tlc1Δ
Passage 1
Passage 2
Passage 3
Passage 4
Passage 5
Passage 6
Passage 7
Passage 8
Passage 9
Passage 10
Passage 11
Passage 15
B
Growth Relative to TLC1+
1.2
1.0
0.8
0.6
0.4
0.2
0
1
3
5
7
9
11
13
15
Passage
tlc1Δ
tlc1Δ pif1Δ
tlc1Δ exo1Δ
tlc1Δ exo1Δ pif1Δ

Figure 28: Pif1 inhibits entry into, and promotes exit from, senescence

A. Multiple colonies from strains of the genotypes indicated from the passages indicated were inoculated into YEPD and grown up to give saturated cultures which were serially-diluted across YEPD plates and grown at 30°C for 2 days. **B.** Quantification of the growth shown in A., each curve is the mean of two independent *tlc1*Δ strains relative to the appropriate *TLC1*$^{+}$ strain.

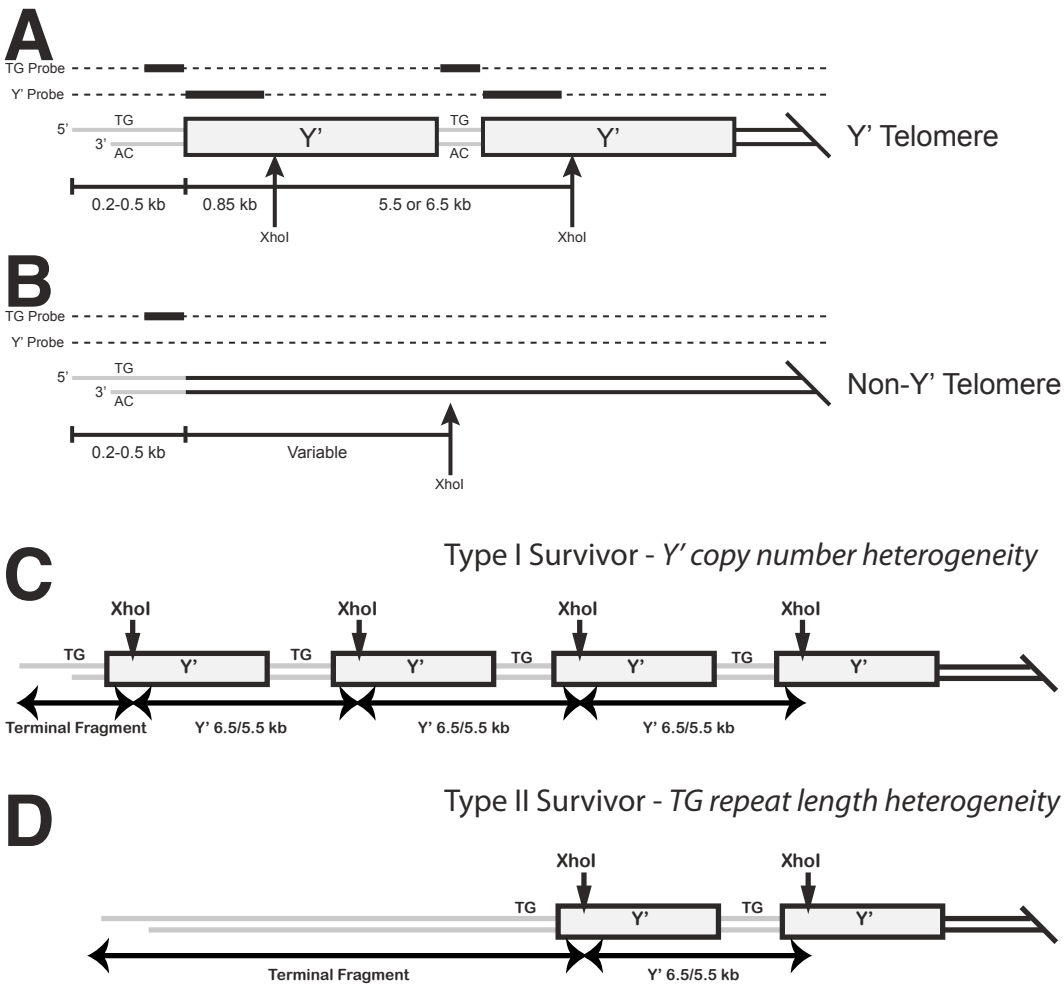
A
TG Probe
Y' Probe
5'
3'
TG
AC
Y'
Y' Telomere
0.2-0.5 kb
0.85 kb
5.5 or 6.5 kb
XhoI
B
Non-Y' Telomere
Variable
C
Type I Survivor - Y' copy number heterogeneity
XhoI
Terminal Fragment
Y' 6.5/5.5 kb
D
Type II Survivor - TG repeat length heterogeneity

Figure 29: Schematic of yeast telomeres as detected by Southern Blot

A. XhoI digestion of a telomere containing Y' elements will yield a 5.5 or 6.5kb Y' fragment and a terminal fragment of approximately 850bp Y' sequence in addition to the telomeric repeats. Both fragments will be detected by a Y' or TG probe. **B.** XhoI digestion of a telomere lacking Y' elements will yield a single fragment, varying in size from telomere-to-telomere depending upon the length of the TG repeats and the distance of the terminal XhoI fragment from the TG repeats. This fragment should only be detectable by a TG probe. **C.** Type I survivors undergo massive amplification of the Y' elements but maintain short only short terminal TG repeats, to the terminal fragments are homogenous. **D.** Type II survivors undergo a modest amplification of the Y' elements but a massive amplification of the TG repeats, leading to long, heterogeneous terminal fragments.

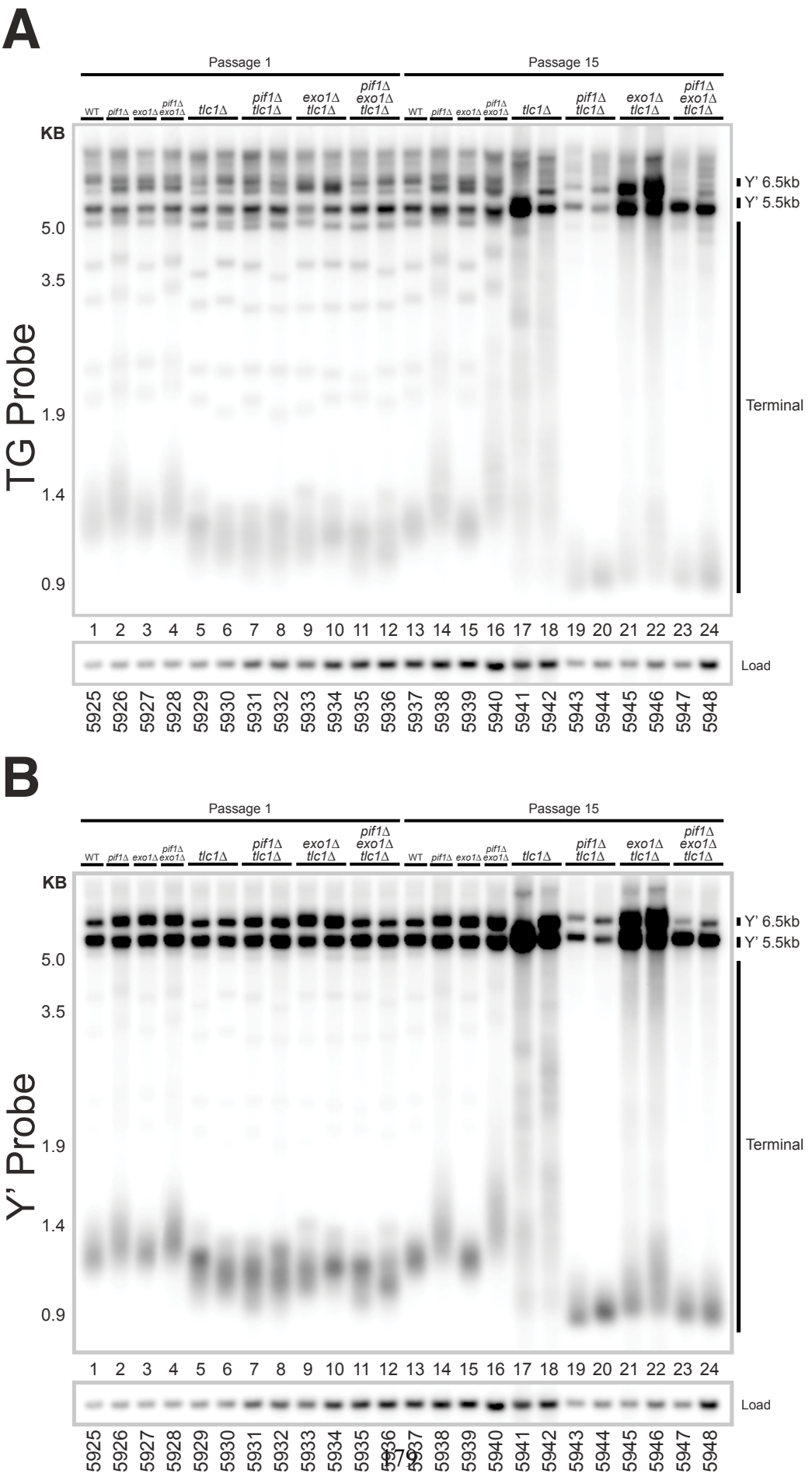
A
Passage 1
Passage 15
WT
pif1Δ
exo1Δ
pif1Δ exo1Δ
tlc1Δ
pif1Δ tlc1Δ
exo1Δ tlc1Δ
pif1Δ exo1Δ tlc1Δ
KB
5.0
3.5
1.9
1.4
0.9
TG Probe
Y' 6.5kb
Y' 5.5kb
Terminal
1 2 3 4 5 6 7 8 9 10 11 12 13 14 15 16 17 18 19 20 21 22 23 24
Load
5925 5926 5927 5928 5929 5930 5931 5932 5933 5934 5935 5936 5937 5938 5939 5940 5941 5942 5943 5944 5945 5946 5947 5948
B
Passage 1
Passage 15
WT
pif1Δ
exo1Δ
pif1Δ exo1Δ
tlc1Δ
pif1Δ tlc1Δ
exo1Δ tlc1Δ
pif1Δ exo1Δ tlc1Δ
KB
5.0
3.5
1.9
1.4
0.9
Y' Probe
Y' 6.5kb
Y' 5.5kb
Terminal
1 2 3 4 5 6 7 8 9 10 11 12 13 14 15 16 17 18 19 20 21 22 23 24
Load
5925 5926 5927 5928 5929 5930 5931 5932 5933 5934 5935 5936 5937 5938 5939 5940 5941 5942 5943 5944 5945 5946 5947 5948

Figure 30: Pif1 facilitates the generation of Type I and Type II survivors

Strains of the genotypes indicated from the passages indicated were grown to saturation and then telomere Southern Blots were performed to detect **A.** TG repeats then stripped and reprobed for **B.** Y' elements. Blots were stripped and reprobed for *CDC15* as a loading control.

5.2.4 Pif1 inhibits entry into, and promotes recovery from, senescence in cells lacking telomerase

Elimination of Pif1 and Exo1 eliminates telomere dysfunction caused by inactivation of Cdc13-1 (Figure 16) and eliminates the accumulation at metaphase seen in telomerase-deficient *cdc13-1* mutants at the permissive temperature (Figure 27). Elimination of Exo1 also inhibits telomere-dysfunction driven senescence caused by telomerase-deficiency (Maringele and Lydall, 2004a). Thus it was hypothesized that elimination of Pif1 might also inhibit senescence and that elimination of both Pif1 and Exo1 might show synergy in inhibiting senescence.

Telomerase-deficient yeast cultures undergo a gradual loss in proliferative capacity due to telomere shortening (senescence), before adopting telomerase-independent mechanisms of telomere maintenance corresponding to a subsequent increase in proliferative capacity (recovery) (Lundblad and Blackburn, 1993, Teng and Zakian, 1999). To test the hypothesis that elimination of Pif1 might inhibit senescence, like elimination of Exo1, and that elimination of both Pif1 and Exo1 might show synergy in inhibiting senescence, *tlc1*Δ, *tlc1*Δ *exo1*Δ*, tlc1*Δ *pif1*Δ and *tlc1*Δ *exo1*Δ *pif1*Δ mutants and corresponding $TLC1^{+}$ controls were germinated simultaneously and passaged over time by restreaking on agar plates. At various passage numbers, strains were inoculated into liquid medium, grown to saturation and then spotted onto agar plates to assess growth (Figure 28A), which was then quantified for each *tlc1*Δ strain relative to the growth of the appropriate $TLC1^{+}$ strain (Figure 28B).

*tlc1*Δ mutants grew well at passage 1, decreased in growth from passages 2-4 (senescence) and improved in growth from passages 5-8 (recovery), before growing well again from passage 9 onwards (Figure 28B). *tlc1*Δ *exo1*Δ mutants also grew well at passage 1, decreasing in growth from passages 2-5 and improved in growth from passages 6-8, before growing well from passage 9 onwards (Figure 28B). At passages 3-4 *tlc1*Δ *exo1*Δ mutants grew slightly better than *tlc1*Δ mutants, corresponding to inhibited entry into senescence, as expected (Figure 28B) (Maringele and Lydall, 2004a). Both *tlc1*Δ *pif1*Δ mutants and *tlc1*Δ *exo1*Δ *pif1*Δ mutants grew well at passage 1, decreased in growth from passages 2-6 (senescence) and then slowly improved in growth from passages 6-15. Strikingly, *tlc1*Δ *pif1*Δ and *tlc1*Δ *pif1*Δ *exo1*Δ mutants

underwent a much more rapid and more protracted decline in growth (senescence) than *tlc1*Δ and *tlc1*Δ *exo1*Δ mutants, and by the end of the senescence period (passage 6, Figure 28A-B) had almost completely lost proliferative capacity compared to *tlc1*Δ and *tlc1*Δ *exo1*Δ mutants, which had retained significant proliferative capacity at the end of their senescence periods (passages 4-5 Figure 28A-B). Furthermore, although *tlc1*Δ *pif1*Δ and *tlc1*Δ *pif1*Δ *exo1*Δ mutants had improved in growth from passage 6 onwards, by passage 15 they still grew extremely poorly compared to *tlc1*Δ and *tlc1*Δ *exo1*Δ mutants, which grew well (Figure 28B). In conclusion, elimination of Pif1 does not inhibit entry into senescence, but enhances it. Instead, it appears that elimination of Pif1 (in the presence or absence of Exo1) causes a very rapid senescence, resulting in a near-total loss in proliferative capacity. Furthermore, following senescence, *tlc1*Δ mutants lacking Pif1 continue to grow poorly, suggesting that they might not recover from senescence.

When yeast cultures recover from senescence, 'survivors' are generated, which usually utilize recombination-dependent mechanisms to maintain telomeres even in the absence of telomerase, but in rare cases can also utilize recombination-independent mechanisms (Maringele and Lydall, 2005). However, in all cases, recovery from senescence leads to clear alterations in telomere structure. Most budding yeast telomeres containing repetitive Y' elements, with a terminal TG repeats (Figure 29A), while some telomeres contain no Y' elements and terminate in only a TG repeats (Figure 29B). Two types of survivors are generated by recombination-dependent mechanisms, leading to two different types of alteration in telomere structure (Teng and Zakian, 1999, Lundblad and Blackburn, 1993). In Type I survivors, very short TG repeats are maintained but a massive amplification of Y' elements is seen as Y' elements spread to all telomeres and undergo amplification to produce many tandem copies at the end of each telomere (Figure 29C). In Type II survivors there is only a slight amplification of Y' elements and dramatic amplification of the terminal TG repeats is believed to occur by rolling-circle-like mechanisms of DNA replication, producing extremely long telomeres which have a great variance in length (Figure 29D).

To test whether *tlc1*Δ *pif1*Δ and *tlc1*Δ *pif1*Δ *exo1*Δ mutants recovered from senescence and generated 'survivors', Southern blots were performed to examine telomere structure, by probing to detect telomeric TG repeats (Figure 30A) and Y' sequences (Figure 30B). Deletion of Pif1 has been reported to lead to telomere lengthening, so as

expected, at passage 1 WT and *exo1*Δ mutants had shorter telomeres than *pif1*Δ and *pif1*Δ *exo1*Δ mutants (Compare terminal fragments in 1 and 3 to lanes 2 and 4, Figure 30A-B) and no distinguishable differences in Y' copy number could be seen (compare Y' 6.5kb and Y' 5.5kb bands in lanes 1-4, Figure 30A-B). At passage 1, *tlc1*Δ, *tlc1*Δ *pif1*Δ, *tlc1*Δ *exo1*Δ and *tlc1*Δ *exo1*Δ *pif1*Δ all had short telomeres but had undergone no alterations in Y' copy number (lanes 5-12, Figure30A-B). By passage 15, *pif1*Δ and *pif1*Δ *exo1*Δ mutants had increased in telomere length, but WT, *pif1*Δ, *exo1*Δ and *pif1*Δ *exo1*Δ mutants had not altered in telomere structure (lanes 13-16, Figure 30A-B). In contrast, *tlc1*Δ mutants had undergone amplification of both the Y' elements and TG repeats to generate Type II survivors (lanes 17-18, Figure 30A-B), while *tlc1*Δ *exo1*Δ mutants had undergone amplification of the Y' elements to generate Type I survivors (lanes 21-22, Figure 30A-B). In contrast, neither *tlc1*Δ *pif1*Δ nor *tlc1*Δ *exo1*Δ mutants had generated typical Type I or Type II survivors, but instead had undergone a slight reduction in Y' elements and maintained short terminal fragments (lanes 19-20, 23-24, Figure 30A-B). However, *tlc1*Δ *pif1*Δ and *tlc1*Δ *exo1*Δ mutants did share one characteristic with Type I survivors – no telomeres lacking Y' elements (i.e. individual bands 1.4kb<5.0kb bands) were visible, indicating that all telomeres had acquired a terminal Y' element (Figure 30A). It was notable, though, that the terminal fragments of *tlc1*Δ *pif1*Δ and *tlc1*Δ *pif1*Δ *exo1*Δ mutants were even shorter than the terminal fragments of Type I survivors, which themselves possess very few TG repeats (Figure 30A-B). In conclusion, although *tlc1*Δ *pif1*Δ and *tlc1*Δ *pif1*Δ *exo1*Δ mutants undergo only subtle alterations in telomere structure and clearly do not adopt typical Type I or Type II survivor structures and by passage 15 (Figure 28B), *tlc1*Δ *pif1*Δ and *tlc1*Δ *exo1*Δ mutants cannot be conclusively said to have recovered from senescence. Thus, Pif1 is required for full recovery from senescence.

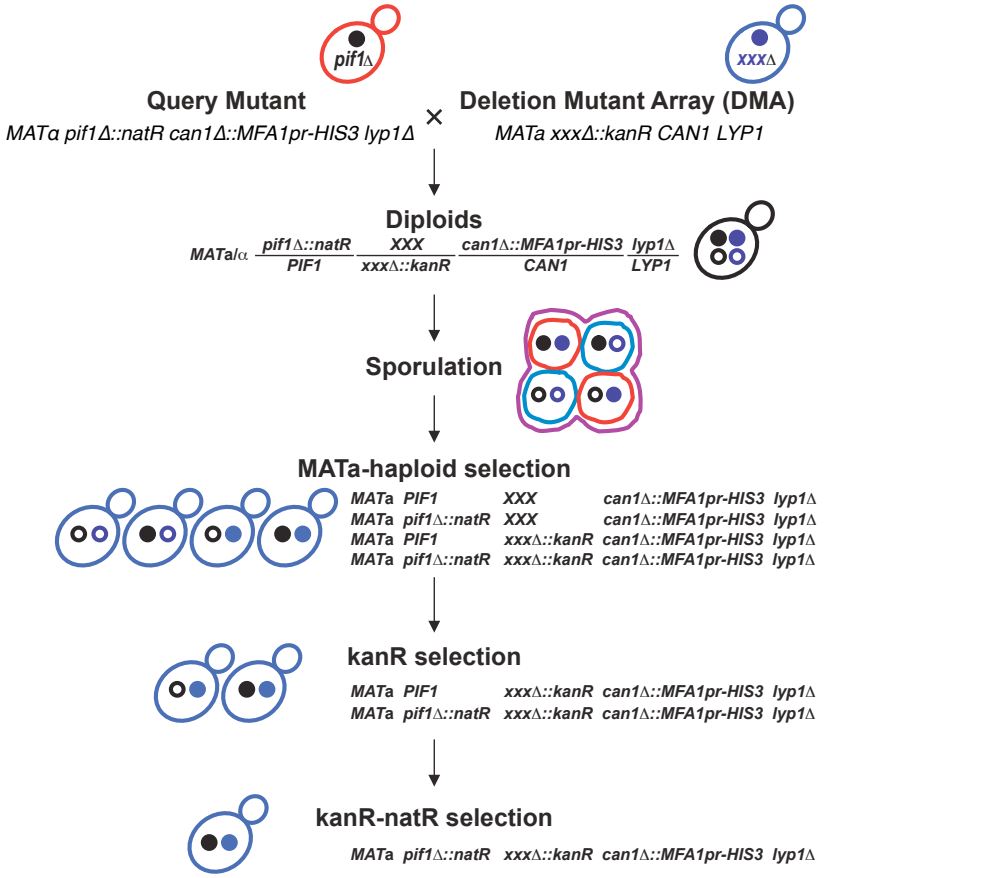

Adapted from Tong & Boone (2006) *Methods Mol Biol*

Figure 31: Overview of the Pif1 Synthetic Genetic Array (SGA)

A query mutant containing the *pif1*Δ mutation (marked with *natR*) was crossed to a deletion library of approximately 4,500 non-essential yeast genes (each deletion marked with *kanR*). Diploids were selected, sporulated and *MATa* haploids were selected for. *MATa* progeny carrying the library mutations were selected for (kanR selection) then *MATa* progeny carrying both the library mutation and *pif1*Δ were selected for (kanR-natR selection) to obtain double mutants, where viable.

ORF	Gene	kanR-natR:kanR Variance	kanR-natR:kanR Lethality	Confirmed Phenotype	Function
YOR297C	*TIM18*	4/4	1	-	Membrane Trafficking.
YIL098C	*FMC1*	4/4	1	Synthetic Lethal	Mitochondria.
YNL315C	*ATP11*	4/4	1	Synthetic Lethal	Mitochondria.
YJR120W		4/4	1	Synthetic Lethal	Respiration/Fermentation.
YDR388W	*RVS167*	4/4	0.5	-	Cytoskeleton.
YLR234W	*TOP3*	4/4	0.5	-	DNA Damage Response.
YBR036C	*CSG2*	4/4	0.5	-	Endoplastmic Reticulum.
YIR023W	*DAL81*	4/4	0.5	-	Nitrogen Utilization.
YML006C	*GIS4*	4/4	0.5	-	RAS/cAMP
YGL045W	*RIM8*	4/4	0.5	-	RIM101-Related.
YOR275C	*RIM20*	4/4	0.5	-	RIM101-Related.
YOL004W	*SIN3*	4/4	0.5	Low Germination Efficiency	Chromatin Remodelling.
YDL035C	*GPR1*	3/4	1	-	RAS/cAMP
YNL021W	*HDA1*	3/4	0.5	No Sporulation	Chromatin Remodelling.
YMR063W	*RIM9*	3/4	0.5	-	RIM101-Related.
YNL294C	*RIM21*	3/4	0.5	-	RIM101-Related.
YML034W	*SRC1*	3/4	0.5	-	Transcription.
YNL253W	*TEX1*	3/4	0.5	-	Transcription.
YBR200W	*BEM1*	2/4	1	-	Cell Polarity.
YBR231C	*SWC5*	2/4	1	-	Chromatin Remodelling.
YNL246W	*VPS75*	2/4	1	-	Chromatin Remodelling.
YJR117W	*STE24*	2/4	1	-	Mating.
YNL106C	*INP52*	2/4	1	-	Membrane Trafficking.
YNL259C	*ATX1*	2/4	1	-	Mitochondria.
YBL011W	*SCT1*	2/4	1	-	Respiration/Fermentation.
YGL029W	*CGR1*	2/4	1	Not Tested	Ribosome.
YNL302C	*RPS19B*	2/4	1	-	Ribosome.
YDL074C	*BRE1*	2/4	1	No sporulation	Chromatin Remodelling.
YML032C	*RAD52*	2/4	0.5	-	DNA Damage Response.

Table 4: Results of a SGA for genes that showed synthetic lethal or synthetic sick interactions with *PIF1*

A *PIF1* SGA was performed as in Figure 31. Genes were scored by comparing the growth of the double mutant *MATa* progeny (i.e. on the kanR-natR selection plate) to the growth of the single mutant *MATa* progeny (i.e. on the kanR selection plate). Lethality was scored as 0.5 for a growth defect of the double mutants compared to the single mutants (i.e. synthetic sickness) and 1.0 for a very strong growth defect of the double mutants compared to the single mutants (i.e. synthetic lethality). Variance was scored as the number of biological repeats in which the growth defect was seen. The genes listed had a growth defect of 0.5 or 1.0 in 2/4 or more biological repeats. Synthetic lethality was confirmed by tetrad dissection, where possible (Alain Nicolas, personal communication) and function was manually annotated using Saccharomyces Genome Database (Costanzo et al., 2009).

5.2.5 PIF1 displays essential, functional redundancy with few genes

Pif1 contributes to resection of uncapped telomere in *cdc13-1* mutants lacking telomerase (Figures 25-26) and also has important roles in telomere maintenance in cells lacking telomerase (Figure 30A-B). Together these data suggest that negative regulation of telomerase, the role most commonly ascribed to Pif1, may not be the main role of Pif1 within the cell. To attempt to identify potentially novel roles for Pif1, a Synthetic Genetic Array was performed to identify genes with which Pif1 shared an essential but redundant role (Tong and Boone, 2006).

A 'query' mutant was constructed in which the *pif1*Δ mutation was marked with the *NATMX* resistance cassette (conferring resistance to the antibiotic ClonNAT), in which *LYP1* was deleted (conferring recessive resistance to thialysine) and in which the *CAN1* gene was deleted (conferring recessive resistance to canavanine) and replaced with *HIS3* driven by the *MFA1* promoter, which is only expressed in *MATa* yeast. The 'query' mutant was mated to a Deletion Mutant Array library of approximately 4,500 strains in which non-essential genes had been deleted (library mutations) and replaced with the KANMX resistance cassette (conferring resistance to G418) (Figure 31). Diploids were selected by selecting for $G418^R$ and $ClonNAT^R$ cells, and were then sporulated and allowed to germinate (Figure 31). Following germination of spores, haploids were selected for by growing cells on media containing canavanine (lethal to $CAN1^+$ haploids or $can1\Delta^+/CAN1^+$ diploids) and thialysine (lethal to $LYP1^+$ haploids or $lyp1\Delta/LYP1^+$ diploids) and only *MATa* haploids were allowed to grow by excluding Histidine from the medium (as *HIS3* would only be expressed in *MATa* yeast, Figure 31). Finally, strains containing either the query mutation alone or the query mutation and *pif1*Δ were selected for by selecting for $G418^R$ cells and then strains containing both the query mutation and *pif1*Δ were selected for by selecting for $G418^R$ $ClonNAT^R$ cells (Figure 31).

In order to rule out artifacts caused by the SGA process, a control SGA should usually be carried out using a query mutant that has been deleted for a gene that should not affect growth (for example, an auxotrophy gene corresponding to a nutrient that the growth medium is fully-supplemented for) (Tong and Boone, 2006). This also allows for alleviating genetic interactions to be determined, where the final double mutant

grows better than the library mutant (Costanzo et al., 2010). However, for the purposes of this experiment only synthetic lethal interactions were of interest, so this SGA could be controlled simply by comparing the kanR-natR selection plates to the kanR selection plates (Figure 31). Growth on the kanR selection plates indicated that viable haploid strains containing the library mutation (*xxx*Δ*::KANMX*) had been produced, while decreased growth on the kanR-natR plates indicated that cells containing both the library and query mutations were either inviable, indicating a synthetic lethality between the mutations, or that cells containing both mutations grew very poorly, indicating a synthetic sick relationship.

For each library mutation, four biological replicates were performed and scored manually for whether there was no growth defect (0.0), a growth defect (0.5) or a severe growth defect (1.0) along with the frequency at which the defect occurred. A list of 29 hits was compiled in which at least half of the biological replicates displayed some growth defect (Table 4). Of these 29 hits, 28 were manually checked by mating a *pif1*Δ mutant to the appropriate library strains and performing tetrad dissection to see whether double mutants were obtained (A. Nicolas, personal communication). Null mutations in only 3 of the 29 hits gave a confirmed synthetic lethal interaction with *PIF1 – FMC1*, *ATP11* and *YJR120W* (Table 4). However, this constituted 75% of the genes that were identified as having a severe growth defect in 4/4 biological replicates (Table 4). Fmc1 and Atp11 are both required for assembly of the F1 subunit of the F_1-F_0 mitochondrial ATPase, while the gene product of *YJR120W* is of unknown function but appears to be required for respiration (Ackerman and Tzagoloff, 1990, Dunn et al., 2006, Lefebvre-Legendre et al., 2001). Thus, it was concluded that the only genes in this screen with which Pif1 has a synthetic lethal relationship are mitochondrial genes, which probably reflects the role of Pif1 in maintenance of mtDNA (Lahaye et al., 1991). As the role of Pif1 at uncapped telomeres has been shown to be due to the nuclear, not mitochondrial role of Pif1 (Figure 21) the study of *FMC1*, *ATP11* and *YJR120W* was unlikely to be informative about the role of Pif1 at uncapped telomeres.

However, in addition to the 3 synthetic lethal interactions that were verified, a further 3 out of the 29 hits were verified to display some sort of genetic interaction that was not synthetic lethality. Interestingly, these 3 hits (*SIN3, HDA1*, *BRE1*) all have roles in chromatin remodeling (Sussel et al., 1995, Wu et al., 2001, Yamashita et al., 2004). *sin3*Δ *pif1*Δ mutants were viable, but had a reduced germination efficiency (Table 4).

*hda1*Δ*/HDA1*$^{+}$ *pif1*Δ*/PIF1*$^{+}$ and *bre1*Δ*/BRE1*$^{+}$ *pif1*Δ*/PIF1*$^{+}$ diploids did not sporulate, suggesting that diploids heterozygous for these mutations were unable to pass through meiosis. It is not realistic to draw generalized conclusions about the interplay between Pif1 and processes involving chromatin remodeling, given the ambiguity of these genetic interactions. Indeed, given that only 3 chromatin remodeling genes are hits, this suggests a very specific interaction between *SIN3*, *HDA1* and *BRE1*. It is concluded that Pif1 might have roles that interact with specific components of the chromatin remodeling machinery, but further work is required to elucidate those roles.

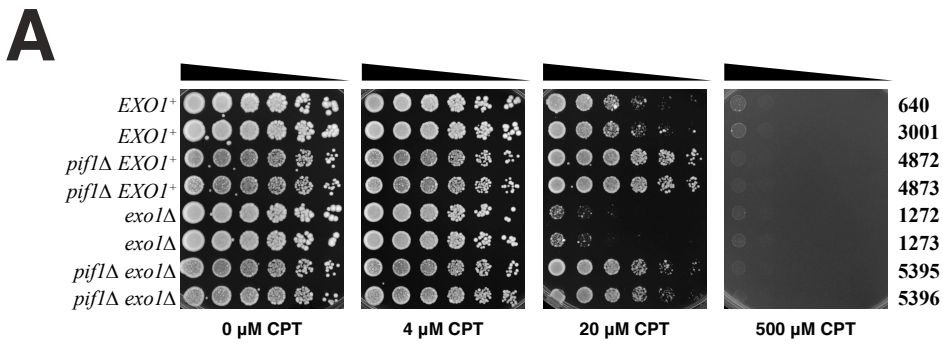
A
EXO1+
EXO1+
pif1Δ EXO1+
pif1Δ EXO1+
exo1Δ
exo1Δ
pif1Δ exo1Δ
pif1Δ exo1Δ
640
3001
4872
4873
1272
1273
5395
5396
0 μM CPT
4 μM CPT
20 μM CPT
500 μM CPT

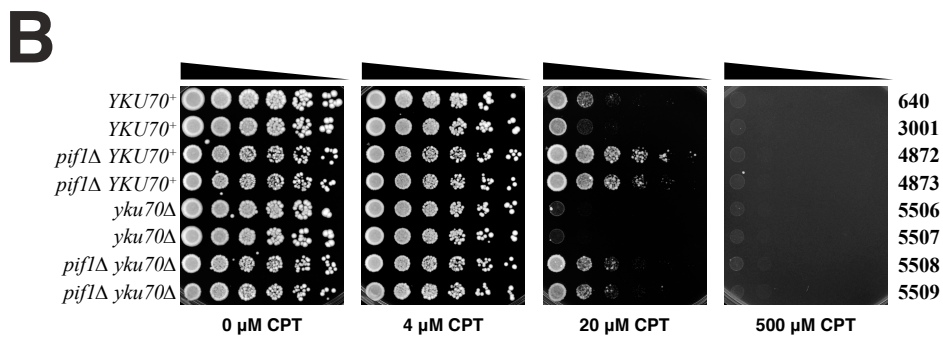
B
YKU70+
YKU70+
pif1Δ YKU70+
pif1Δ YKU70+
yku70Δ
yku70Δ
pif1Δ yku70Δ
pif1Δ yku70Δ
640
3001
4872
4873
5506
5507
5508
5509
0 μM CPT
4 μM CPT
20 μM CPT
500 μM CPT

Figure 32: Pif1 contributes to the vitality of cells following camptothecin treatment, independently of Ku and Exo1

A. and **B.** strains of the genotypes indicated were serially-diluted across YEPD plates containing camptothecin at the concentrations indicated and grown at 30°C for 2 days.

5.2.6 Pif1 functions in different pathways to Exo1 and Yku70 to confer sensitivity to camptothecin

Pif1 and Exo1 appear to constitute parallel pathways that inhibit the growth of *cdc13-1* mutants and elimination of both Pif1 and Exo1 eliminates the growth defect seen in *cdc13-1* mutants (Figure 5). The DDR at uncapped telomeres is believed to be a consequence of the DDR inappropriately recognizing uncapped telomeres as DNA damage (Lydall, 2009). Thus, it was hypothesized that Pif1 and Exo1 might constitute parallel pathways in a DNA repair process that aberrantly recognizes uncapped telomeres. If this was the case, then treatment with a chemical agent that induces the type of damage that Pif1 and Exo1 are involved in responding to should inhibit the growth of cells lacking Pif1 or Exo1 (due to an impaired ability to repair the damage) and should cause a severe growth defect in cells lacking both Pif1 and Exo1 (due to a severely impaired ability to repair the damage).

Uncapped telomeres are believed to trigger a DDR because they resemble DSBs, but *exo1*Δ mutants in themselves are not sensitive to DSB-inducing agents such as Bleomycin. However *exo1*Δ mutants are sensitive to camptothecin, which induces replication-associated DSBs (Morin et al., 2008). Thus it was hypothesized that, Pif1 and Exo1 might function in parallel pathways involved in the repair of replication-associated DSBs. To test this hypothesis, the effect of Pif1 and Exo1 on the growth camptothecin-treated cells was measured. *exo1*Δ mutants grew slightly worse than $EXO1^{+}$ mutants when treated with 4μM camptothecin and *exo1*Δ mutants were almost completely inviable when treated with 20μM camptothecin, while $EXO1^{+}$ mutants grew poorly (Figure 32A). Surprisingly, *pif1*Δ mutants showed almost no growth defect when treated with 20μM and grew better than $EXO1^{+}$ mutants (Figure 32A). Additionally, *exo1*Δ *pif1*Δ mutants showed only a slight growth defect when treated with 20μM camptothecin and clearly grew better than *exo1*Δ mutants (Figure 32A). It was concluded that Pif1 and Exo1 do not constitute parallel pathways involved in the repair of replication associated DSBs. Instead Pif1 contributes to the lethality of replication-associated DSBs while Exo1 promotes vitality in response to replication-associated DSBs.

The resistance of *pif1*Δ mutants to camptothecin treatment was surprising. It was hypothesized that Pif1 might be involved in the processing of structures arising from replication associated DSBs and that elimination of Pif1 might direct these DSBs towards a more efficient repair pathway. As elimination of Pif1 was able to increase the resistance of *exo1*Δ mutants to camptothecin, this pathway was unlikely to be HR (Figure 32A). Therefore, it was hypothesized that elimination of Pif1 might direct replication-associated DSBs towards NHEJ for more efficient repair. To test this hypothesis, the effect of Pif1 and Yku70 (required for NHEJ) on the growth of camptothecin-treated cells was measured. *yku70*Δ mutants grew worse than *YKU70*$^{+}$ mutants when treated with 20μM camptothecin (Figure 32B). As before, *pif1*Δ mutants grew better than *YKU70*$^{+}$ mutants treated with 20μM camptothecin (Figure 32B) but *yku70*Δ *pif1*Δ mutants still grew better than *yku70*Δ mutants when treated with 20μM camptothecin (Figure 32B). In conclusion, NHEJ contributes to the vitality of cells in response to replication-associated DSBs, and elimination of Pif1 does not reduce the lethality associated with replication-associated DSBs by directing them towards NHEJ.

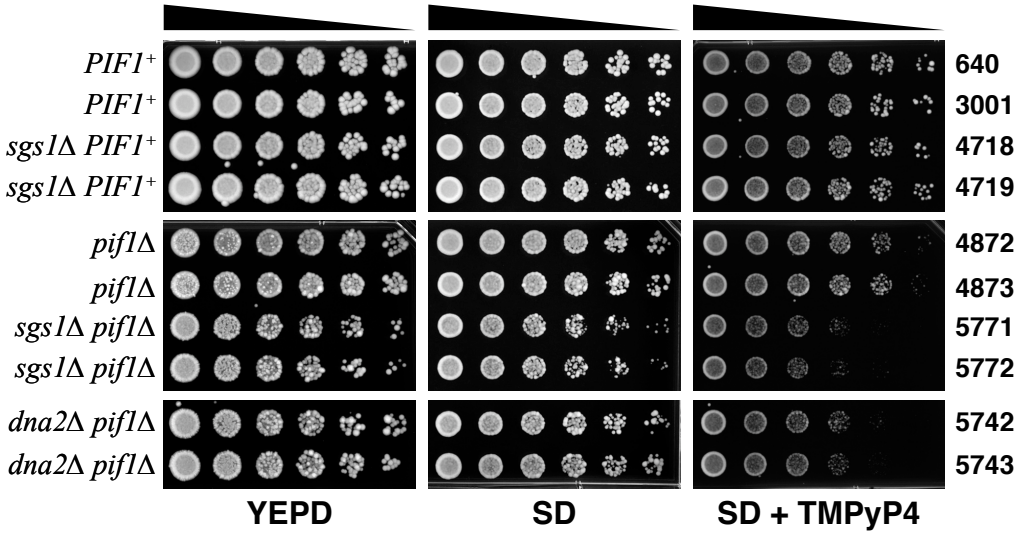
PIF1+
PIF1+
sgs1Δ PIF1+
sgs1Δ PIF1+
pif1Δ
pif1Δ
sgs1Δ pif1Δ
sgs1Δ pif1Δ
dna2Δ pif1Δ
dna2Δ pif1Δ
640
3001
4718
4719
4872
4873
5771
5772
5742
5743
YEPD
SD
SD + TMPyP4

Figure 33: Pif1, Sgs1 and Dna2 promote tolerance to G-quadruplex structures
Saturated cultures of the genotypes indicated were serially diluted across agar plates and grown at 23°C for 3 days on YEPD or 4 days on Synthetic (SD) or TMPyP4-containing media. Strains grown on each medium were split into separate panels for presentation purposes but were grown on the same plate.

5.2.7 The helicases Pif1, Sgs1 and Dna2 cooperate in unwinding G-quadruplex structures

The Pif1 helicase has been shown *in vitro* to unwind dsDNA containing G-quadruplex structures and has been shown *in vivo* to be important for the genomic stability of G-quadruplex containing sequences (Ribeyre et al., 2009). It was hypothesized that the role of Pif1 in ssDNA generation at uncapped telomeres might be due to Pif1 unwinding G-quadruplex structures to facilitate nuclease access. To test this hypothesis, the effect of Pif1 on the growth of cells treated with the G-quadruplex stabilizing ligand TMPyP4 was assessed, in comparison to the helicases Sgs1 and Dna2, which also have roles following telomere uncapping and in the unwinding of G-quadruplex structures (Huber et al., 2002, Lopes et al., 2002).

As expected, *pif1*Δ mutants treated with TMPyP4 grew worse than *PIF1*$^{+}$ strains (Figure 33). However, *sgs1*Δ strains showed no growth defect compared to *PIF1*$^{+}$strains (Figure 33). Surprisingly, *pif1*Δ *sgs1*Δ and *pif1*Δ *dna2*Δ mutants showed a severe growth defect in comparison to *pif1*Δ mutants when treated with TMPyP4 (Figure 33). It was concluded that Pif1 is important for the processing of G-quadruplex structures that arise following TMPyP4 treatment, while Dna2 and Sgs1 are important for processing G-quadruplex structures in *pif1*Δ mutants. This contrasts to the roles of these proteins in maintaining the stability of a G-quadruplex containing microsatellite, where Pif1, Sgs1 and Dna2 all contribute to maintenance of G-quadruplex containing sequences but Sgs1 and Dna2 have no role in *pif1*Δ mutants (Ribeyre et al., 2009). Furthermore, Pif1 inhibits the growth of *cdc13-1* mutants and promotes growth on TMPyP4 (Figure 5), while Dna2 and Sgs1 promote the vitality of *cdc13-1 pif1*Δ mutants and promote growth on TMPyP4 (Figures 8-9). As there appears to be no correlation between the effect of these 3 helicases on the growth of cells following telomere uncapping and treatment with a G-quadruplex stabilizing drug, it suggests there is little correlation between these two biological processes and thus that Pif1 is unlikely to generate ssDNA at uncapped telomeres by unwinding G quadruplex structures.

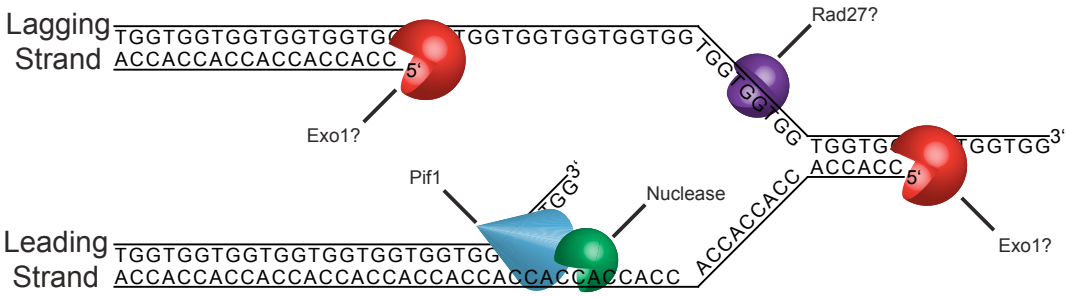
Lagging
Strand
TGGTGGTGGTGGTGGTG
ACCACCACCACCACCACC
5'
Exo1?
Rad27?
TGGTGGTGGTGGTGG
TGGTGG
3'
ACCACC
5'
Exo1?
Pif1
Nuclease
Leading
Strand
TGGTGGTGGTGGTGGTGGTGG
ACCACCACCACCACCACCACCACCACCACCACC
ACCACCACC

Figure 34: A model for how Pif1, Exo1 and Rad27 might function at stalled replication forks following telomere uncapping

If stalled replication forks occurred following telomere uncapping, Pif1 could recognize exposed 5' ssDNA on the leading strand and generate ssDNA to be cleaved by an unidentified nuclease. Exo1 could, in principle, act upon either the native telomeric overhang or the lagging strand of a stalled replication fork. Rad27 appears to function in the same pathway as Exo1 (Figure 12) and the gap endonuclease activity reported for Rad27 could, in principle, liberate a lagging strand to be resected by Exo1.

5.3 Discussion

Pif1 contributes to ssDNA generation at uncapped telomeres, checkpoint activation and poor growth of cells with uncapped telomeres (Figure 5, Figures 16-18) even in cells lacking telomerase (Figures 22-26). Interestingly, elimination of Pif1 does not affect telomere length in cells lacking telomerase (Figure 30), which provides a clear demonstration that Pif1 has a direct effect on the resection of uncapped telomeres independent of any effects it might have on telomere length (Figure 25). Furthermore, it is the nuclear, helicase activity of Pif1 responsible for its effect at uncapped telomeres, which is the same previously proposed to be responsible for removing telomerase from the telomeres (Boule et al., 2005, Zhou et al., 2000). Finally, it has been shown that Pif1 has crucial roles in senescence and recovery of telomerase-deficient cells. These data conclusively demonstrate that Pif1 does not inhibit the growth of *cdc13-1* mutants by removing telomerase from the telomere facilitate access to telomeres by nucleases, and call into question the very notion that Pif1 removes telomerase from telomeres (Vega et al., 2007, Schulz and Zakian, 1994).

Three supportive lines of evidence have been used to argue that Pif1 functions to remove telomerase from yeast telomeres; *pif1*Δ mutants have long telomeres (Schulz and Zakian, 1994); telomere lengthening in *pif1*Δ mutants does not occur in the absence of telomerase (Zhou et al., 2000); Pif1 can be biochemically demonstrated to remove telomerase from telomeric substrates *in vitro* (Boule et al., 2005). For each line of evidence, a severe caveat exists; null or hypomorphic mutations in many genes are now known to increase telomere length (Askree et al., 2004, Ungar et al., 2009, Gatbonton et al., 2006); almost no genes have been identified that increase telomere length in the absence of telomerase (Zhou et al., 2000, Maringele and Lydall, 2004); Pif1 has been shown *in vitro* to be capable of at least 4 distinct biochemical activities (Boule et al., 2005, George et al., 2009, Pike et al., 2009, Ribeyre et al., 2009, Rossi et al., 2008). Biochemical evidence for Pif1 function becomes particularly questionable when considering that it has all been carried out with unphosphorylated forms of Pif1, yet Pif1 is subject to a basal phosphorylation and removing Pif1 phosphorylation sites can lead to a null mutant phenotype (Makovets and Blackburn, 2009).

The main, conclusive line of evidence that Pif1 negatively regulates telomerase has been that induction of a DSB in *pif1*Δ cells leads to a dramatic increase in the number of breaks healed by *de novo* telomere addition compared to Wild Type cells (Schulz and Zakian, 1994). However, elimination of the nucleases Rad27 or Mre1 or elimination of Sgs1 and Exo1 also increases the rate at which DSBs are healed by *de novo* telomere addition (Chen and Kolodner, 1999, Marrero and Symington, 2010). Finally, *pif1*Δ mutants have been shown to have a severe BIR defect at DSBs, suggesting that the increased rate of healing by *de novo* telomere addition could be an indirect consequence of an impaired ability of *pif1*Δ mutants to repair DSBs (Chung et al., 2010). Thus, as proposed here, Pif1 is likely to function at DSBs, telomeres and uncapped telomeres by unwinding DNA substrates to be processed by nucleases.

The reported BIR defect caused by elimination of Pif1 provides a possible explanation for the behavior of *tlc1*Δ *pif1*Δ cells (Figures 28-30). BIR is required for the generation of Type I and Type II survivor structures and elimination of Pol32, which is essential for BIR, causes *tlc1*Δ mutants to senesce rapidly and prevents their recovery (Lydeard et al., 2007). The rapid senescence of *tlc1*Δ cells lacking Pif1, their protracted poor growth period after senescence and relatively unaltered telomere structure are consistent with being defective enough in BIR to cause rapid senescence and inhibit recovery, but proficient enough to undergo slight alterations in telomere structure and maintain viability.

The search for synthetic lethal interactions between *PIF1* and other genes yielded only mitochondrial genes involved in respiration, so was not informative as to the nuclear function of Pif1 (Table 4). Furthermore, attempts to correlate the sensitivity caused by elimination of the helicases Pif1, Sgs1 and Dna2 to G-quadruplex structures with their effect on the growth of *cdc13-1* mutants with uncapped telomeres were unsuccessful, so it does not seem likely that Pif1 functions at uncapped telomeres to unwind G-quadruplex structures (Figure 32). However, elimination of Pif1 did confer a strong resistance to camptothecin treatment, in *exo1*Δ, *yku70*Δ and even $EXO1^{+}$ $PIF1^{+}$ mutants (Figure 32). This was surprising, as cells lacking Exo1 were highly sensitive to Camptothecin and it was expected that Pif1 might function, like Exo1 at DDRs other than the one at uncapped telomeres (Morin et al., 2008).

Camptothecin treatment leads to the formation replication-associated DSBs, causing replication fork collapse. One possible explanation for the resistance to Camptothecin conferred by the elimination of Pif1 is that Pif1 is involved in the destabilization of stalled replication forks. Such a function for Pif1 has previously been proposed and human Pif1 has been shown to be capable of unwinding DNA structures that resemble the leading strand of a stalled replication fork (George et al., 2009, Chang et al., 2009). Thus, it is hypothesized that at uncapped telomeres, replication fork stalling occurs and Pif1 generates ssDNA at the lagging strand of stalled replication forks to be cleaved by an unidentified ssDNA endocnuclease (Figure 34). This is consistent with work in human cells demonstrating that telomeres are sites of replication stress and other work showing that the CST complex in plants and mammals is recruited to sites of replication difficulty (Sfeir et al., 2009, Surovtseva et al., 2009, Miyake et al., 2009).

If Pif1 acts upon the leading strand of stalled replication forks, it is possible that Exo1 acts upon the lagging strand of stalled replication forks (Figure 34). Alternatively Exo1 might act upon the region ahead of the chromosome, at the native telomeric overhang, as previously proposed. Interestingly, Rad27 appears to act in the same pathway as Exo1 in *cdc13-1* mutants (Figure 12) and gap endonuclease activity of Rad27 would be capable of liberating the lagging strand of stalled replication fork for further processing by Exo1 (Figure 34). Such a model seems very possible, given that FEN1, the mammalian orthologue of Rad27, ensures telomere stability by facilitating replication fork restart (Saharia et al., 2010).

Finally, it has been definitively shown that Pif1, like Exo1, directly contributes to the resection and degradation of uncapped telomeres in budding yeast. EXO1 also contributes to the premature mortality seen in third generation telomerase knock-out mice, which age prematurely due to short, dysfunctional telomeres and elimination of EXO1 extends their lifespan (Schaetzlein et al., 2007). The implication of this is that in mammalian cells, EXO1 acts upon dysfunctional telomeres to facilitate cellular ageing. If the DDRs in mammalian cells resemble those at uncapped telomeres in budding yeast, then mammalian PIF1 should also act upon dysfunctional telomeres to facilitate cellular ageing and elimination of murine PIF1 should also extend the lifespan of telomerase knock-out mice (Snow et al., 2007). However, Pif1 plays an important protective role at telomeres in senescing yeast cells and is important to prevent rapid senescence (Figure 28). Therefore, it is possible that elimination of murine PIF1 might

accelerate senescence in telomerase knock-out mice. Thus, understanding the roles of mammalian PIF1 and EXO1 at dysfunctional telomeres caused by telomerase-deficiency will provide a valuable opportunity to understand whether the DDRs at uncapped telomeres in budding yeast (such as those in *cdc13-1* and *yku70*Δ mutants) or at short telomeres in senescing cells (such as those in *tlc1*Δ) mutants are a better model for the DDRs that occur during the mammalian ageing process.

5.4 Further Work

It will be important to elucidate a generalized role for Pif1 within cells, one that is independent of telomerase. First, it will be important to establish whether *tlc1*Δ *pol32*Δ *pif1*Δ mutants senesce more rapidly than *tlc1*Δ *pol32*Δ mutants and thus whether Pif1 functions to inhibit senescence and promote recovery from senescence by promoting BIR or by some other mechanism (Figure 28) (Chung et al., 2010, Lydeard et al., 2007). If Pif1 does function in the same pathway as Pol32 during senescence, it will be important to understand the more general role of Pif1 in BIR, though this work has been reported to already be underway (Chung et al., 2010).

It will also be interesting to know whether Pif1 fulfills the same role in resection of uncapped telomeres in *cdc13-1* mutants as at DSBs. Phosphomimetic (*pif1-s4d*) and phosphodeficient (*pif1-s4a)* alleles of Pif1 have been described that affect the function of Pif1 at DSBs (assayed by rate of telomerase-mediated healing of DSBs) but not at telomeres (assayed by alterations in telomere length) and these will be useful tools to probe Pif1 function (Makovets and Blackburn, 2009). Furthermore, Pif1 is a 5'-3' helicase. If Pif1 does directly participate in the resection of uncapped telomeres, then it must recognize 5' (AC) ssDNA at uncapped telomeres, which might be expected to accumulate in *cdc13-1 pif1*Δ mutants following telomere uncapping. As the in-gel assay can detect short (<20bp) stretches of ssDNA, it will be interesting to see whether it can be used to detect 5' (AC) ssDNA at uncapped telomeres. If 5' ssDNA can be detected at uncapped telomeres, it will also be interesting to use an inducible DSB system to see whether Pif1 also processes 5' ssDNA at DSBs.

It has previously been proposed that Pif1 functions to destabilize stalled replication forks and human Pif1 has been shown to be capable of participating in reactions which would be equivalent to unwinding the leading strand of a stalled replication fork (Chang et al., 2009, George et al., 2009). Here, it has been shown that Pif1 is a major cause of

the toxicity associated with camptothecin treatment, which is suggestive of a role for Pif1 at stalled replication forks (Figure 32). Thus, it will be interesting to see if stalled replication forks accumulate at uncapped telomeres in *cdc13-1* mutants and whether Pif1 affects their processing. If stalled replication forks do accumulate at uncapped telomeres, it will be interesting to take a biochemical approach with nucleases and helicases known to function at uncapped telomeres (Pif1, Sgs1 and Exo1, and possibly Rad27, Figure 34) and apply them to structures resembling stalled replication forks *in vitro* to investigate how they might function individually and how they might cooperate.

Finally, Exo1 activity is restrained at both uncapped telomeres and stalled replication forks by the checkpoint kinase Rad53 (Jia et al., 2004, Segurado and Diffley, 2008). Correspondingly, *cdc13-1 rad53*Δ mutants generate elevated levels of Exo1-dependent ssDNA and *rad53*Δ mutants are hypersensitive to MMS in an Exo1-dependent manner. Interestingly, *mec1*Δ mutants are hypersensitive to MMS in an Exo1-independent manner, suggesting that Mec1 inhibits a separate activity to promote the stability of stalled replication forks and it would be interesting to see if this activity is Pif1 (Segurado and Diffley, 2008).

6 Can cells live without telomere capping?

"Because all of biology is connected, one can often make a breakthrough with an organism that exaggerates a particular phenomenon, and later explore the generality."

- Thomas R. Cech

6.1 Introduction

Elimination of Pif1 and Exo1 permitted *cdc13-1* mutants to grow at 36°C, at which temperature *cdc13-1* is believed to be completely inactive (Figure 5B) suggesting that Cdc13 might be dispensable for survival in these cells. Survival in the absence of Cdc13 can be achieved through several mechanisms. First, attenuation of nuclease activities and checkpoint components at uncapped telomeres by elimination of Exo1 and Rad9 or Rad24 permits the generation of cells that are viable without Cdc13 at a rate of approximately 4-6x10^{-5} (Zubko and Lydall, 2006). More recently it has been shown that elimination of Exo1, Rad9 and Sgs1 permits the viability of essentially all cells lacking Cdc13 but elimination of Cdc13 confers a severe growth defect and ultimately leads to senescence (Ngo and Lydall, 2010). Second, the alterations in telomere structure seen in Type I and Type II post-senescence survivors are sufficient to maintain viability in the absence of Cdc13 at a rate of approximately 8.5x10^{-4}-1.3x10^{-3} (Larrivee and Wellinger, 2006). However, it should be noted that the generation of Type I and Type II post-senescence survivors is itself a very rare event. Finally, the essential requirement for Cdc13 can be overcome by over-expression of the C terminus of Stn1 with concurrent over-expression of Ten1 to permit viability in the absence of Cdc13 in aproximately 1.6x10^{-1} of cells (Petreaca et al., 2006). Interestingly, this last mechanism does not eliminate the requirement for Cdc13-dependent telomere capping, but uses selective overexpression to fulfill the usual function of Cdc13 (to tether Stn1 and Ten1 to the telomere) by alternate means and is reminiscent of earlier work showing that Cdc13 function can by bypassed by fusing the DNA binding domain of Cdc13 to Stn1 (Pennock et al., 2001).

This work focused on determining whether cells lacking Pif1 and Exo1 eliminated the requirement for Cdc13. If so, it would be important to determine the alterations in telomere structure that occurred in the absence of Cdc13 along in addition to determining the mechanisms through which these cells maintained their telomeres.

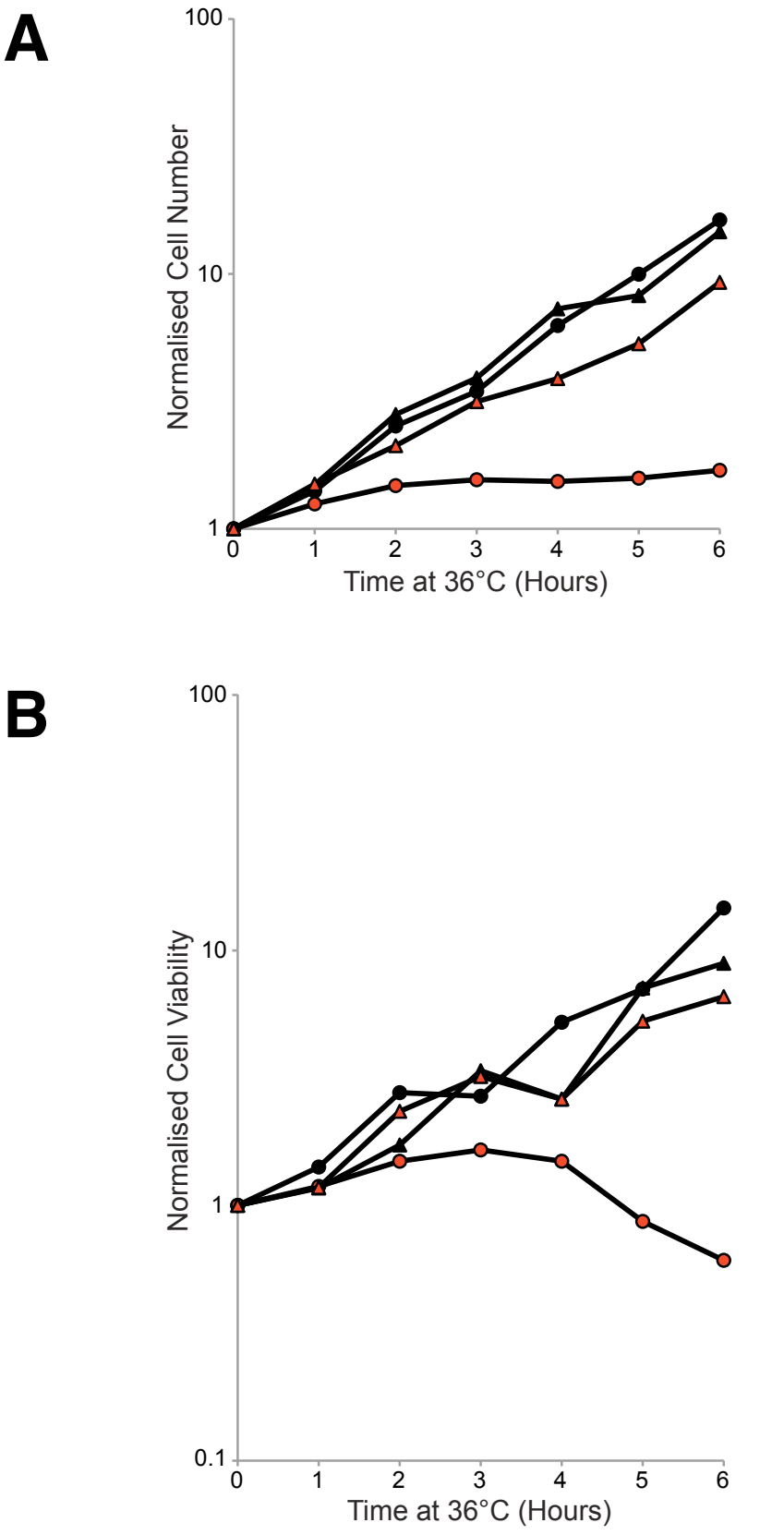
A
100
10
1
Normalised Cell Number
0
1
2
3
4
5
6
Time at 36°C (Hours)
B
100
10
1
0.1
Normalised Cell Viability
0
1
2
3
4
5
6
Time at 36°C (Hours)
640 CDC13
1108 cdc13-1
5395 CDC13 pif1Δ exo1Δ
5323 cdc13-1 pif1Δ exo1Δ

Figure 35: *cdc13-1 exo1*Δ *pif1*Δ mutants have a detectable growth defect at 36°C
Exponentially-dividing cultures of the genotypes indicated were grown at 23°C then shifted to 36°C for 6 hours. Every hour samples were taken to measure **A.** total cell number and **B.** viable cell number.

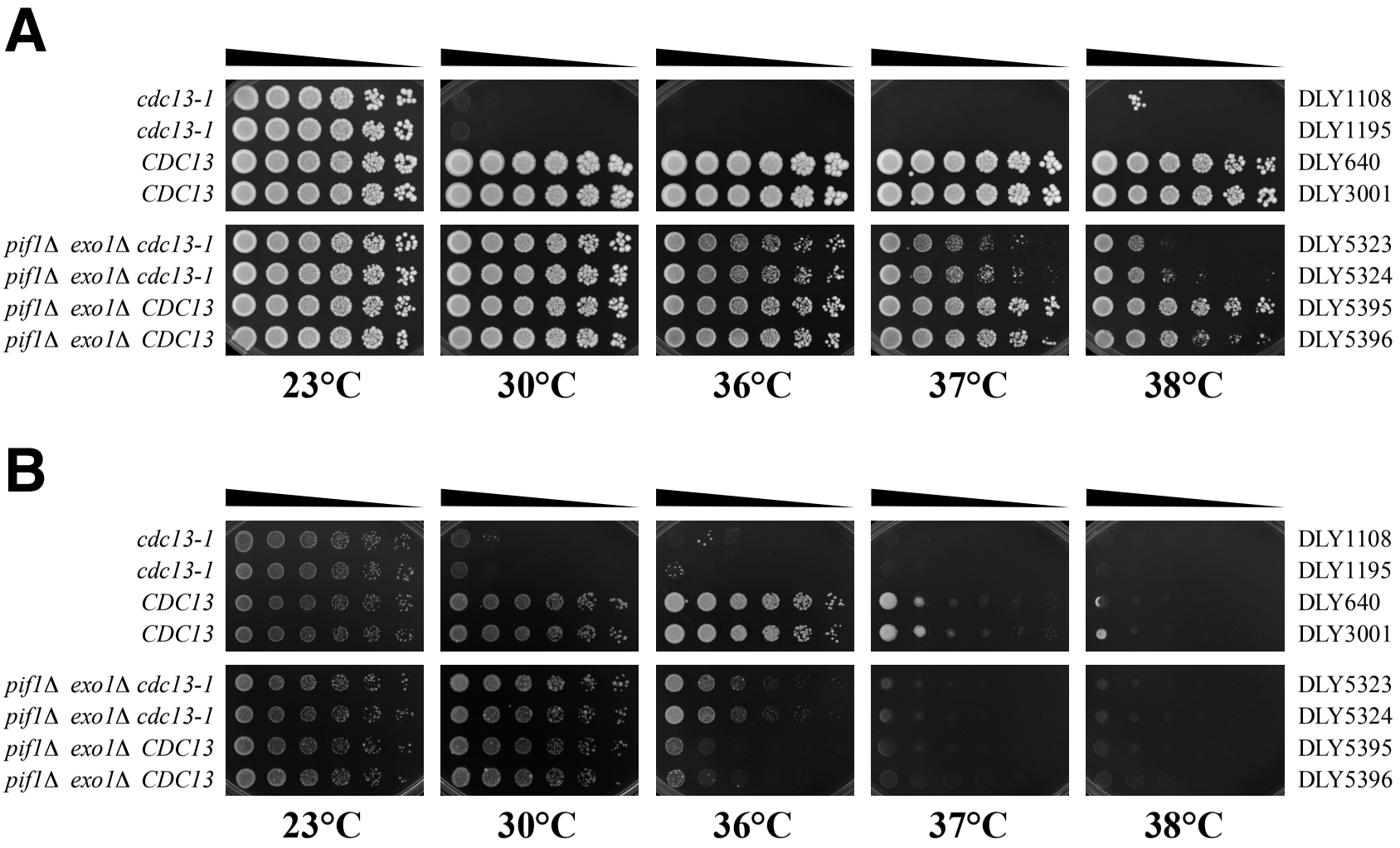
A
cdc13-1
cdc13-1
CDC13
CDC13
pif1Δ exo1Δ cdc13-1
pif1Δ exo1Δ cdc13-1
pif1Δ exo1Δ CDC13
pif1Δ exo1Δ CDC13
DLY1108
DLY1195
DLY640
DLY3001
DLY5323
DLY5324
DLY5395
DLY5396
23°C
30°C
36°C
37°C
38°C
B
cdc13-1
cdc13-1
CDC13
CDC13
pif1Δ exo1Δ cdc13-1
pif1Δ exo1Δ cdc13-1
pif1Δ exo1Δ CDC13
pif1Δ exo1Δ CDC13
DLY1108
DLY1195
DLY640
DLY3001
DLY5323
DLY5324
DLY5395
DLY5396
23°C
30°C
36°C
37°C
38°C

Figure 36: *cdc13-1 exo1*Δ *pif1*Δ mutants have a growth defect above 36°C

Saturated cultures of the genotypes indicated were serially-diluted across **A.** YEPD or **B.** YEPG plates and grown at the temperatures indicated for 3 days.

6.2 Results

6.2.1 Cells lacking Pif1 and Exo1 have a detectable growth defect following telomere uncapping

*cdc13-1 exo1*Δ *pif1*Δ mutants were able to grow at 36°C (Figure 5) and did not accumulate telomeric ssDNA (Figure 16) or undergo metaphase arrest (Figure 14), suggesting the possibility that there was no growth defect or loss in viability caused by telomere uncapping in these strains. To test this hypothesis, asynchronously dividing cultures of *cdc13-1* and *CDC13*$^{+}$ mutants grown at 23°C were shifted to 36°C to induce telomere uncapping and cell number and viability were measured over time. As expected, *CDC13*$^{+}$ mutants increased in both cell number (Figure 35A) and viable cell number (Figure 35B) over time. *cdc13-1* mutants increased in both cell number (Figure 35A) and viable cell number (Figure 35B) for the first two hours, but subsequently underwent no further increase in cell number (Figure 35A) and showed a decrease in viable cell number at 5 and 6 hours (Figure 35B) corresponding to a loss in viability caused by persistent telomere uncapping. In contrast, both *CDC13*$^{+}$ *exo1*Δ *pif1*Δ and *cdc13-1 exo1*Δ *pif1*Δ mutants continued to increase in both cell number and viable cell number over time (Figure 35A-B). However, *cdc13-1 exo1*Δ *pif1*Δ mutants clearly showed a decrease in growth rate compared to *CDC13*$^{+}$ *exo1*Δ *pif1*Δ mutants (Figure 35A). It was concluded that there was a slight growth defect in *cdc13-1 exo1*Δ *pif1*Δ mutants following telomere uncapping.

Although *cdc13-1 exo1*Δ *pif1*Δ mutants were able to grow at 36°C, it was possible that extremely low levels of Cdc13-1 activity persisted at this temperature and contributed to their growth (Figure 5). To test this hypothesis, the growth of *cdc13-1 exo1*Δ *pif1*Δ mutants was compared to that of *CDC13*$^{+}$ *exo1*Δ *pif1*Δ mutants at temperatures of 36°C and higher. At 23°C and 30°C, there was no discernable difference in growth between *cdc13-1 exo1*Δ *pif1*Δ and *CDC13*$^{+}$*exo1*Δ *pif1*Δ mutants (Figure 36A). However at 36°C *cdc13-1 exo1*Δ *pif1*Δ mutants grew slightly worse than *CDC13*$^{+}$ *exo1*Δ *pif1*Δ mutants, while at 37°C-38°C *cdc13-1 exo1*Δ *pif1*Δ mutants clearly grew worse than *CDC13*$^{+}$ *exo1*Δ *pif1*Δ mutants (Figure 36A). However, it should be noted that at 37°C *CDC13*$^{+}$ *exo1*Δ *pif1*Δ mutants grew slightly worse than *CDC13*$^{+}$ mutants (Figure 36A) and *CDC13*$^{+}$ and *CDC13*$^{+}$ *exo1*Δ *pif1*Δ mutants both grew worse at 38°C than at lower

temperatures. It was concluded that low levels of Cdc13-1 activity persisted at 36-38°C and contributed to the growth of *cdc13-1 exo1*Δ *pif1*Δ mutants (Figure 36A).

Mitochondrial activity inhibits the growth of *cdc13-1* mutants (Addinall et al., 2008) and at high temperatures cells lacking Pif1 gradually lose mitochondrial function (Van Dyck et al., 1992). Thus, it was hypothesized that mitochondrial defects in *cdc13-1 pif1*Δ *exo1*Δ mutants might contribute to their growth at 36°C. To test this hypothesis, the growth of *cdc13-1 pif1*Δ *exo1*Δ mutants was compared to the growth of $CDC13^{+}$ *exo1*Δ *pif1*Δ mutants at high temperatures on YEPG plates. On YEPG plates, the only carbon source provided is Glycerol, which is non-fermentable, so only cells with functional mitochondria will be able to grow and form colonies. It was expected that if mitochondrial dysfunction contributed to the growth of *cdc13-1 exo1*Δ *pif1*Δ mutants at 36°C, then growing them under conditions where only cells with functional mitochondria could grow and form colonies (YEPG) should lead to a growth defect. Surprisingly, *cdc13-1 exo1*Δ *pif1*Δ mutants actually grew better than $CDC13^{+}$ *exo1*Δ *pif1*Δ mutants at 36°C (Figure 36B). It was concluded that mitochondrial defects in *cdc13-1 exo1*Δ *pif1*Δ mutants did not contribute to their growth at 36°C. Instead, the improved growth of *cdc13-1 exo1*Δ *pif1*Δ mutants at 36°C suggested that inactivation of Cdc13-1 actually improved the retention of mitochondrial function in *cdc13-1 exo1*Δ *pif1*Δ mutants.

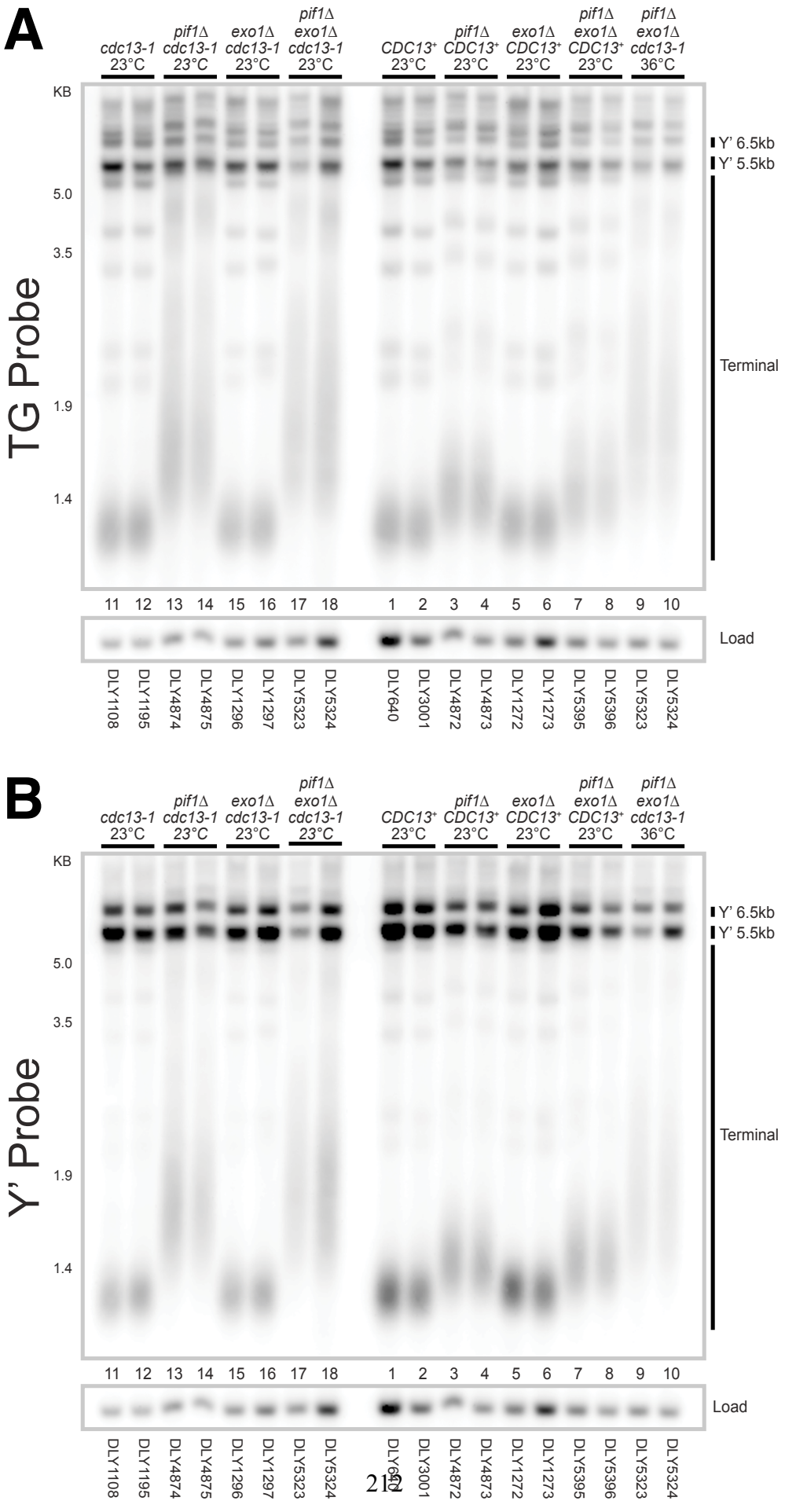
A
cdc13-1 23°C
pif1Δ cdc13-1 23°C
exo1Δ cdc13-1 23°C
pif1Δ exo1Δ cdc13-1 23°C
CDC13+ 23°C
pif1Δ CDC13+ 23°C
exo1Δ CDC13+ 23°C
pif1Δ exo1Δ CDC13+ 23°C
pif1Δ exo1Δ cdc13-1 36°C
KB
5.0
3.5
1.9
1.4
TG Probe
Y' 6.5kb
Y' 5.5kb
Terminal
11 12 13 14 15 16 17 18 1 2 3 4 5 6 7 8 9 10
Load
DLY1108 DLY1195 DLY4874 DLY4875 DLY1296 DLY1297 DLY5323 DLY5324 DLY640 DLY3001 DLY4872 DLY4873 DLY1272 DLY1273 DLY5395 DLY5396 DLY5323 DLY5324
B
cdc13-1 23°C
pif1Δ cdc13-1 23°C
exo1Δ cdc13-1 23°C
pif1Δ exo1Δ cdc13-1 23°C
CDC13+ 23°C
pif1Δ CDC13+ 23°C
exo1Δ CDC13+ 23°C
pif1Δ exo1Δ CDC13+ 23°C
pif1Δ exo1Δ cdc13-1 36°C
KB
5.0
3.5
1.9
1.4
Y' Probe
Y' 6.5kb
Y' 5.5kb
Terminal
11 12 13 14 15 16 17 18 1 2 3 4 5 6 7 8 9 10
Load
DLY1108 DLY1195 DLY4874 DLY4875 DLY1296 DLY1297 DLY5323 DLY5324 DLY640 DLY3001 DLY4872 DLY4873 DLY1272 DLY1273 DLY5395 DLY5396 DLY5323 DLY5324

Figure 37: *cdc13-1 exo1*Δ *pif1*Δ mutants do not undergo alterations in telomere structure that could account for their ability to grow at 36°C

Saturated cultures of the genotypes indicated were grown to stationary phase at 23°C then diluted 1:500 and grown to stationary phase once more at either 23°C or 36°C (as indicated). DNA prepared from stationary phase cultures was then used for Southern blots that were performed to detect **A.** TG repeats or **B.** Y' elements, as in Figure 30.

6.2.2 cdc13-1 mutants lacking Pif1 and Exo1 do not generate alterations in telomere structure that permit telomere maintenance following telomere uncapping

The alterations in telomere structure seen in Type I and Type II post-senescent survivors facilitate telomere maintenance in the absence of Cdc13, albeit at a low rate (Larrivee and Wellinger, 2006). It was hypothesized that at 23°C, *cdc13-1 exo1*Δ *pif1*Δ mutants might also undergo alterations in telomere structure, efficiently permitted their survival at 36°C, following inactivation of Cdc13-1. To test this hypothesis, Southern Blots were performed to examine the telomeres of *cdc13-1 exo1*Δ *pif1*Δ mutants at 23°C and 36°C using probes to detect TG (Figure 37A) and Y' (Figure 37B) sequences.

The telomeres of *CDC13*$^{+}$*pif1*Δ and *CDC13*$^{+}$ *exo1*Δ *pif1*Δ mutants were longer and more varied in length than those of *CDC13*$^{+}$ and *CDC13*$^{+}$ *exo1*Δ mutants (Figure 37A-B), as expected (Figure 30A-B) (Schulz and Zakian, 1994). Surprisingly, the telomeres of *cdc13-1 pif1*Δ and *cdc13-1 exo1*Δ *pif1*Δ mutants were even longer and more varied in length than *CDC13*$^{+}$ *pif1*Δ and *CDC13*$^{+}$ *exo1*Δ *pif1*Δ mutants (Figure 37-B). This was consistent with data showing that Cdc13-1 at 23°C is still slightly defective compared to Cdc13 (Addinall et al., 2008, Foster et al., 2006) and that Cdc13 negatively regulates telomere length (Chandra et al., 2001, Ungar et al., 2009). It was concluded that Cdc13 plays an important role in negative regulation of telomere length in cells lacking Pif1 and that Cdc13-1, even at 23°C, has a defect in telomere length regulation that becomes apparent in cells lacking Pif1.

At 36°C, the telomeres of *cdc13-1 exo1*Δ *pif1*Δ mutants were longer than those of *CDC13*$^{+}$ *exo1*Δ *pif1*Δ mutants but had undergone no other noticeable rearrangements in either the terminal fragments or Y' elements (Figure 37A-B). However, the telomeres of *cdc13-1 exo1*Δ *pif1*Δ mutants grown at 36°C were identical to those of *cdc13-1 exo1*Δ *pif1*Δ mutants grown at 23°C (Figure 37A-B), indicating that no alterations in telomere structure occur when *cdc13-1 exo1*Δ *pif1*Δ mutants are grown for short periods of time with uncapped telomeres. Furthermore, the telomere structure of *cdc13-1 exo1*Δ *pif1*Δ mutants at 36°C was identical to that of *cdc13-1 pif1*Δ mutants at 23°C (Figure 37A-B). As *cdc13-1 pif1*Δ mutants are unable to grow at 36°C (Figure 5), this indicates that the telomere structure shared by *cdc13-1 exo1*Δ *pif1*Δ and *cdc13-1 pif1*Δ mutants cannot

account for the growth of *cdc13-1 exo1*Δ *pif1*Δ mutants at 36°C. It was concluded that *cdc13-1 exo1*Δ *pif1*Δ mutants do not undergo alterations in telomere structure that efficiently permit their survival at 36°C.

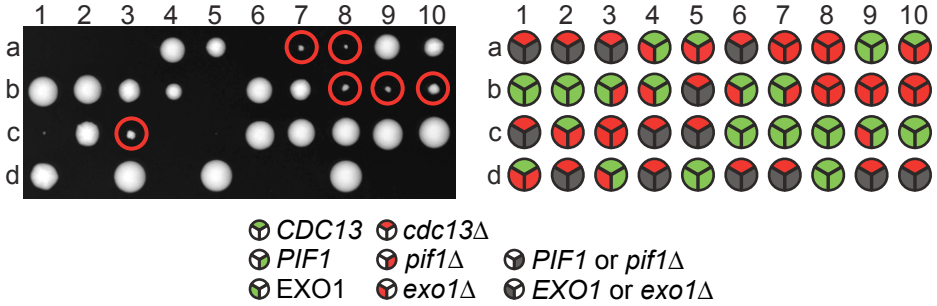
1 2 3 4 5 6 7 8 9 10
a
b
c
d
1 2 3 4 5 6 7 8 9 10
a
b
c
d
CDC13
cdc13Δ
PIF1
pif1Δ
PIF1 or pif1Δ
EXO1
exo1Δ
EXO1 or exo1Δ

Figure 38: *cdc13*Δ *exo1*Δ *pif1*Δ mutants are viable

*cdc13*Δ/*CDC13*$^{+}$ *exo1*Δ/*EXO1*$^{+}$ *pif1*Δ/*PIF1*$^{+}$ diploids were generated, sporulated and spores micromanipulated apart on a YEPD plate and allowed to form colonies at 23°C for 5 days. Tetrad dissection plate is shown on the left, a key showing (where possible) the inferred genotypes of the spore manipulated to each position is shown on the right. *cdc13*Δ *exo1*Δ *pif1*Δ mutants are circled.

Diploid	Spores Dissected	*PIF1*$^+$ *EXO1*$^+$ *CDC13*$^+$ colonies (expected)	*PIF1*$^+$ *EXO1*$^+$ *CDC13*$^+$ colonies (observed)	*pif1*Δ *exo1*Δ *CDC13*$^+$ colonies (observed)	*pif1*Δ *exo1*Δ *cdc13*Δ colonies (observed)	*cdc13*Δ/ *CDC13*$^+$ viability (%)
DDY340	176	22	17	13	12	92
DDY341	176	22	23	19	16	84

Table 5: *cdc13*Δ *exo1*Δ *pif1*Δ mutants have a high rate of viability

176 spores each from two independently generated diploids were dissected as in Figure 38. The genotypes of viable spores were determined by replica plating to selective media. Table shows the number of strains obtained for each relevant genotype to determine the viability of *cdc13*Δ *exo1*Δ *pif1*Δ mutants.

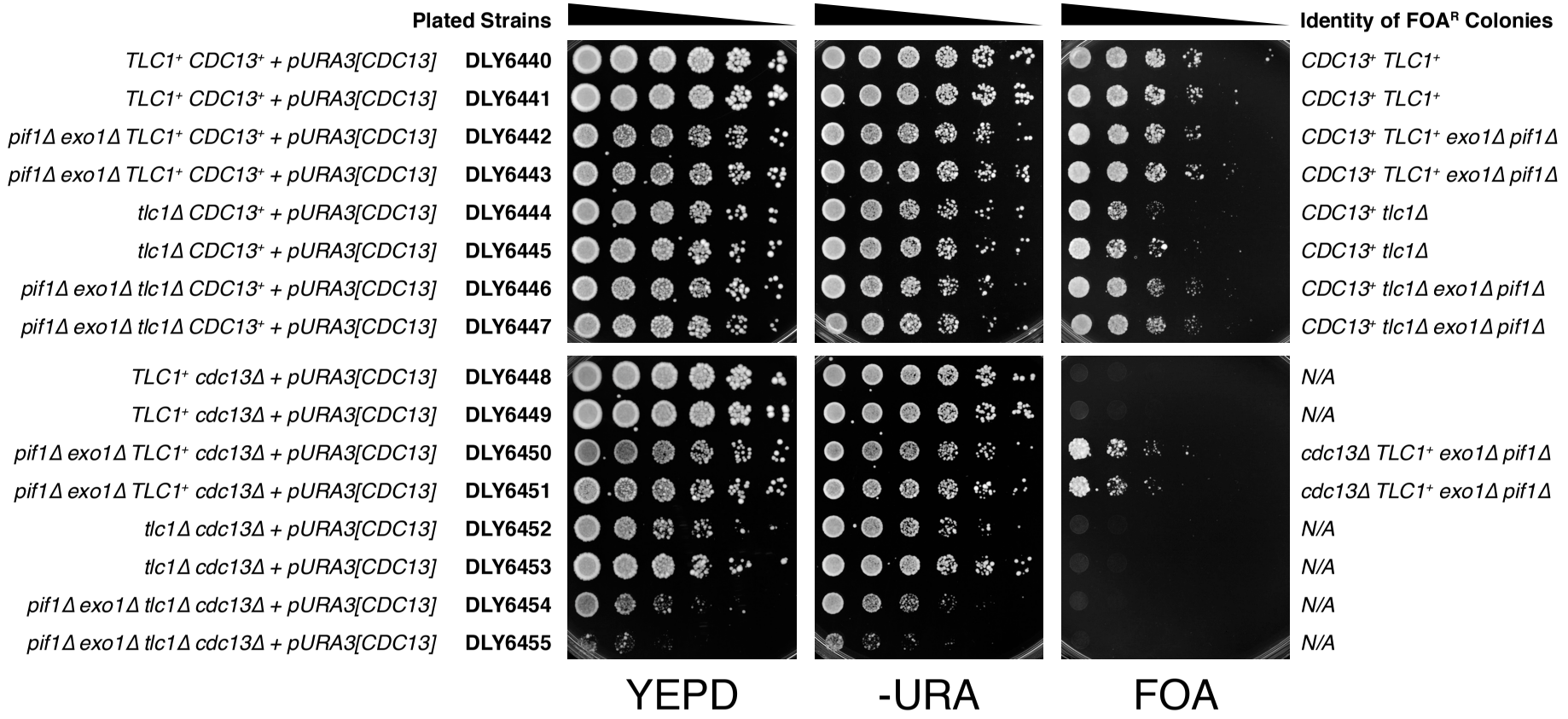
Plated Strains
Identity of FOA^R Colonies
TLC1+ CDC13+ + pURA3[CDC13] DLY6440 CDC13+ TLC1+
TLC1+ CDC13+ + pURA3[CDC13] DLY6441 CDC13+ TLC1+
pif1Δ exo1Δ TLC1+ CDC13+ + pURA3[CDC13] DLY6442 CDC13+ TLC1+ exo1Δ pif1Δ
pif1Δ exo1Δ TLC1+ CDC13+ + pURA3[CDC13] DLY6443 CDC13+ TLC1+ exo1Δ pif1Δ
tlc1Δ CDC13+ + pURA3[CDC13] DLY6444 CDC13+ tlc1Δ
tlc1Δ CDC13+ + pURA3[CDC13] DLY6445 CDC13+ tlc1Δ
pif1Δ exo1Δ tlc1Δ CDC13+ + pURA3[CDC13] DLY6446 CDC13+ tlc1Δ exo1Δ pif1Δ
pif1Δ exo1Δ tlc1Δ CDC13+ + pURA3[CDC13] DLY6447 CDC13+ tlc1Δ exo1Δ pif1Δ
TLC1+ cdc13Δ + pURA3[CDC13] DLY6448 N/A
TLC1+ cdc13Δ + pURA3[CDC13] DLY6449 N/A
pif1Δ exo1Δ TLC1+ cdc13Δ + pURA3[CDC13] DLY6450 cdc13Δ TLC1+ exo1Δ pif1Δ
pif1Δ exo1Δ TLC1+ cdc13Δ + pURA3[CDC13] DLY6451 cdc13Δ TLC1+ exo1Δ pif1Δ
tlc1Δ cdc13Δ + pURA3[CDC13] DLY6452 N/A
tlc1Δ cdc13Δ + pURA3[CDC13] DLY6453 N/A
pif1Δ exo1Δ tlc1Δ cdc13Δ + pURA3[CDC13] DLY6454 N/A
pif1Δ exo1Δ tlc1Δ cdc13Δ + pURA3[CDC13] DLY6455 N/A
YEPD
-URA
FOA

Figure 39: Telomerase is essential for the viability of *cdc13*Δ *exo1*Δ *pif1*Δ mutants
Strains of the genotypes indicated were all germinated from the same diploid for 3 days at 30°C, then struck onto –URA for 3 days at 30°C to ensure retention of the plasmid. Saturated cultures were then grown in YEPD, serially diluted across agar plates and grown for 2 days on YEPD or –URA or 5 days on FOA media. Growth from the lowest-dilution spot for each strain was struck onto YEPD, then single colonies replicated to selective media to determine the genotype of any FOA-resistant colonies.

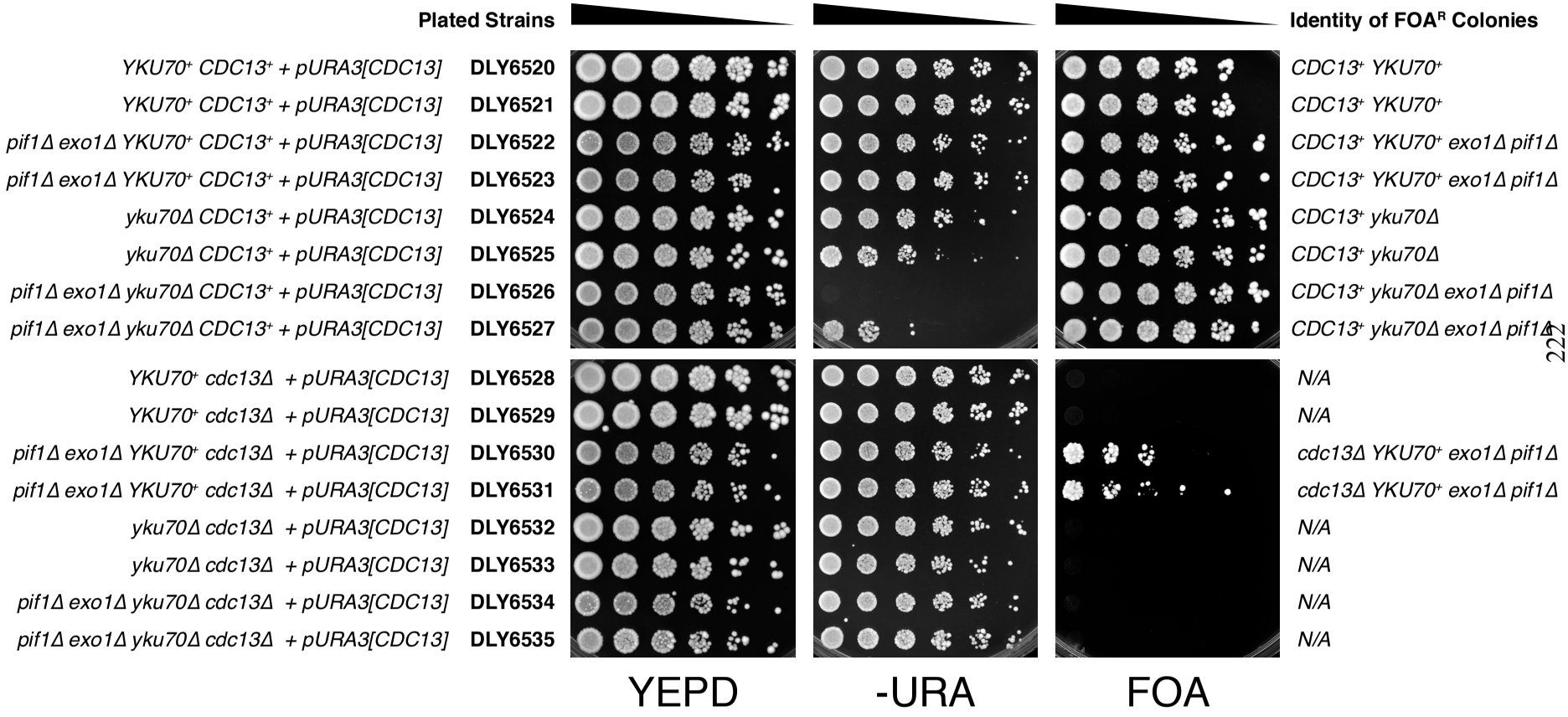
Plated Strains
Identity of FOA^R Colonies
YKU70+ CDC13+ + pURA3[CDC13] DLY6520 CDC13+ YKU70+
YKU70+ CDC13+ + pURA3[CDC13] DLY6521 CDC13+ YKU70+
pif1Δ exo1Δ YKU70+ CDC13+ + pURA3[CDC13] DLY6522 CDC13+ YKU70+ exo1Δ pif1Δ
pif1Δ exo1Δ YKU70+ CDC13+ + pURA3[CDC13] DLY6523 CDC13+ YKU70+ exo1Δ pif1Δ
yku70Δ CDC13+ + pURA3[CDC13] DLY6524 CDC13+ yku70Δ
yku70Δ CDC13+ + pURA3[CDC13] DLY6525 CDC13+ yku70Δ
pif1Δ exo1Δ yku70Δ CDC13+ + pURA3[CDC13] DLY6526 CDC13+ yku70Δ exo1Δ pif1Δ
pif1Δ exo1Δ yku70Δ CDC13+ + pURA3[CDC13] DLY6527 CDC13+ yku70Δ exo1Δ pif1Δ
YKU70+ cdc13Δ + pURA3[CDC13] DLY6528 N/A
YKU70+ cdc13Δ + pURA3[CDC13] DLY6529 N/A
pif1Δ exo1Δ YKU70+ cdc13Δ + pURA3[CDC13] DLY6530 cdc13Δ YKU70+ exo1Δ pif1Δ
pif1Δ exo1Δ YKU70+ cdc13Δ + pURA3[CDC13] DLY6531 cdc13Δ YKU70+ exo1Δ pif1Δ
yku70Δ cdc13Δ + pURA3[CDC13] DLY6532 N/A
yku70Δ cdc13Δ + pURA3[CDC13] DLY6533 N/A
pif1Δ exo1Δ yku70Δ cdc13Δ + pURA3[CDC13] DLY6534 N/A
pif1Δ exo1Δ yku70Δ cdc13Δ + pURA3[CDC13] DLY6535 N/A
YEPD
-URA
FOA

Figure 40: Ku is essential for the viability of *cdc13*Δ *exo1*Δ *pif1*Δ mutants
Strains of the genotypes indicated were all germinated from the same diploid for 3 days at 30°C, then struck onto –URA for 3 days at 30°C to ensure retention of the plasmid. Saturated cultures were then grown in YEPD, serially diluted across agar plates and grown for 2 days on YEPD or –URA or 5 days on FOA media. Growth from the lowest-dilution spot for each strain was struck onto YEPD, then single colonies replicated to selective media to determine the genotype of any FOA-resistant colonies.

Note: *yku70*Δ *exo1*Δ *pif1*Δ mutants grew very poorly on –URA so had to be grown up on YEPD.

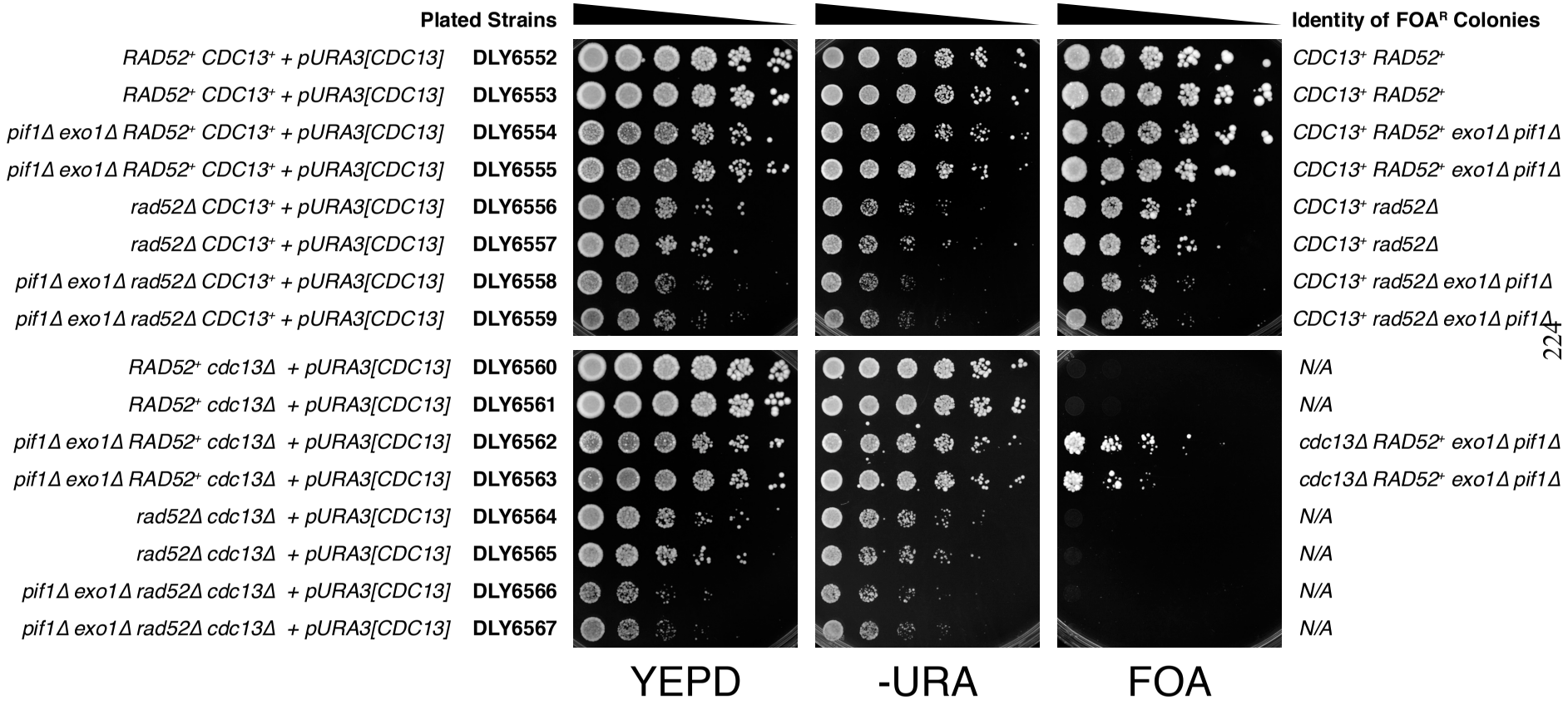
Plated Strains
Identity of FOA^R Colonies
RAD52+ CDC13+ + pURA3[CDC13] DLY6552 CDC13+ RAD52+
RAD52+ CDC13+ + pURA3[CDC13] DLY6553 CDC13+ RAD52+
pif1Δ exo1Δ RAD52+ CDC13+ + pURA3[CDC13] DLY6554 CDC13+ RAD52+ exo1Δ pif1Δ
pif1Δ exo1Δ RAD52+ CDC13+ + pURA3[CDC13] DLY6555 CDC13+ RAD52+ exo1Δ pif1Δ
rad52Δ CDC13+ + pURA3[CDC13] DLY6556 CDC13+ rad52Δ
rad52Δ CDC13+ + pURA3[CDC13] DLY6557 CDC13+ rad52Δ
pif1Δ exo1Δ rad52Δ CDC13+ + pURA3[CDC13] DLY6558 CDC13+ rad52Δ exo1Δ pif1Δ
pif1Δ exo1Δ rad52Δ CDC13+ + pURA3[CDC13] DLY6559 CDC13+ rad52Δ exo1Δ pif1Δ
RAD52+ cdc13Δ + pURA3[CDC13] DLY6560 N/A
RAD52+ cdc13Δ + pURA3[CDC13] DLY6561 N/A
pif1Δ exo1Δ RAD52+ cdc13Δ + pURA3[CDC13] DLY6562 cdc13Δ RAD52+ exo1Δ pif1Δ
pif1Δ exo1Δ RAD52+ cdc13Δ + pURA3[CDC13] DLY6563 cdc13Δ RAD52+ exo1Δ pif1Δ
rad52Δ cdc13Δ + pURA3[CDC13] DLY6564 N/A
rad52Δ cdc13Δ + pURA3[CDC13] DLY6565 N/A
pif1Δ exo1Δ rad52Δ cdc13Δ + pURA3[CDC13] DLY6566 N/A
pif1Δ exo1Δ rad52Δ cdc13Δ + pURA3[CDC13] DLY6567 N/A
YEPD
-URA
FOA

Figure 41: Rad52 is essential for the viability of *cdc13*Δ *exo1*Δ *pif1*Δ mutants
Strains of the genotypes indicated were all germinated from the same diploid for 3 days at 30°C, then struck onto –URA for 3 days at 30°C to ensure retention of the plasmid. Saturated cultures were then grown in YEPD, serially diluted across agar plates and grown for 2 days on YEPD or –URA or 5 days on FOA media. Growth from the lowest-dilution spot for each strain was struck onto YEPD, then single colonies replicated to selective media to determine the genotype of any FOA-resistant colonies.

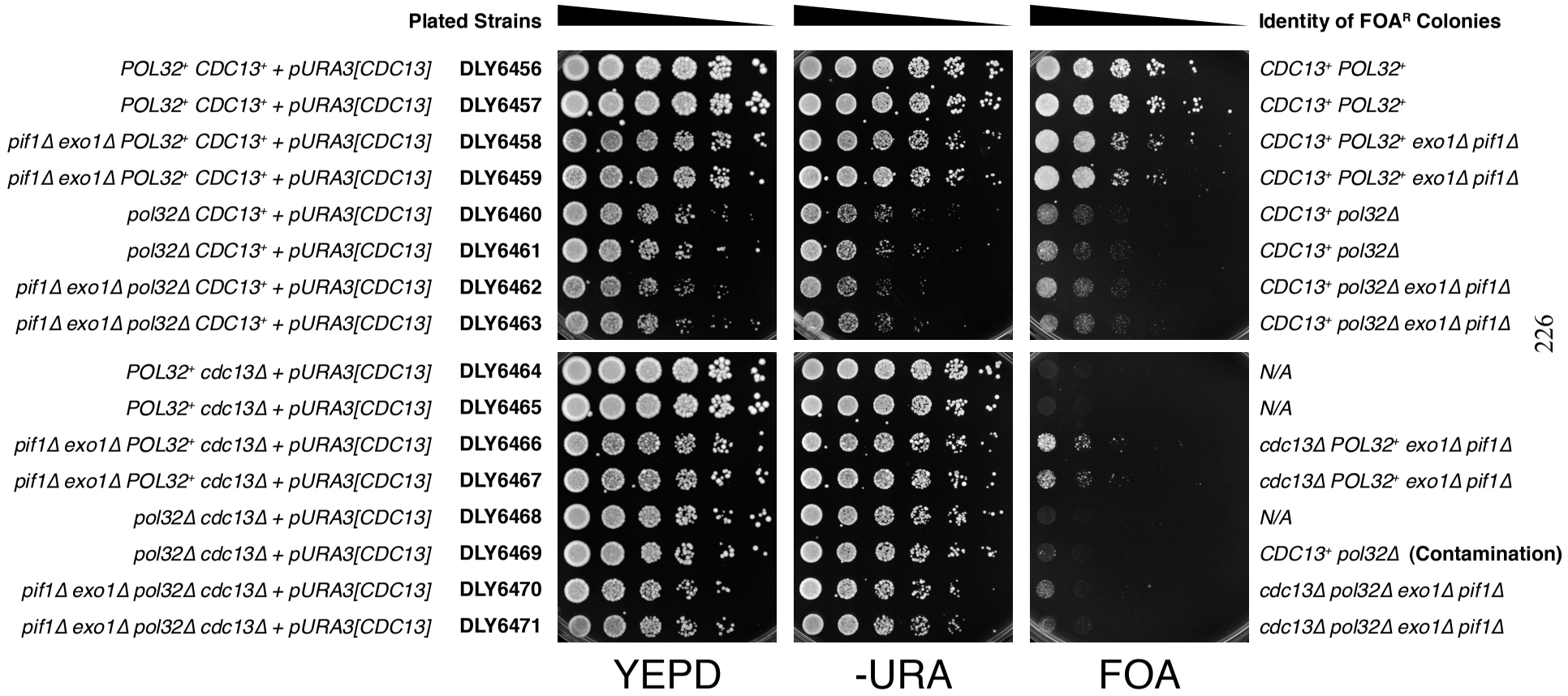
Plated Strains
Identity of FOA^R Colonies
POL32+ CDC13+ + pURA3[CDC13] DLY6456 CDC13+ POL32+
POL32+ CDC13+ + pURA3[CDC13] DLY6457 CDC13+ POL32+
pif1Δ exo1Δ POL32+ CDC13+ + pURA3[CDC13] DLY6458 CDC13+ POL32+ exo1Δ pif1Δ
pif1Δ exo1Δ POL32+ CDC13+ + pURA3[CDC13] DLY6459 CDC13+ POL32+ exo1Δ pif1Δ
pol32Δ CDC13+ + pURA3[CDC13] DLY6460 CDC13+ pol32Δ
pol32Δ CDC13+ + pURA3[CDC13] DLY6461 CDC13+ pol32Δ
pif1Δ exo1Δ pol32Δ CDC13+ + pURA3[CDC13] DLY6462 CDC13+ pol32Δ exo1Δ pif1Δ
pif1Δ exo1Δ pol32Δ CDC13+ + pURA3[CDC13] DLY6463 CDC13+ pol32Δ exo1Δ pif1Δ
POL32+ cdc13Δ + pURA3[CDC13] DLY6464 N/A
POL32+ cdc13Δ + pURA3[CDC13] DLY6465 N/A
pif1Δ exo1Δ POL32+ cdc13Δ + pURA3[CDC13] DLY6466 cdc13Δ POL32+ exo1Δ pif1Δ
pif1Δ exo1Δ POL32+ cdc13Δ + pURA3[CDC13] DLY6467 cdc13Δ POL32+ exo1Δ pif1Δ
pol32Δ cdc13Δ + pURA3[CDC13] DLY6468 N/A
pol32Δ cdc13Δ + pURA3[CDC13] DLY6469 CDC13+ pol32Δ (Contamination)
pif1Δ exo1Δ pol32Δ cdc13Δ + pURA3[CDC13] DLY6470 cdc13Δ pol32Δ exo1Δ pif1Δ
pif1Δ exo1Δ pol32Δ cdc13Δ + pURA3[CDC13] DLY6471 cdc13Δ pol32Δ exo1Δ pif1Δ
YEPD
-URA
FOA

Figure 42: Pol32 is not required for the viability of *cdc13*Δ *exo1*Δ *pif1*Δ mutants
Strains of the genotypes indicated were all germinated from the same diploid for 3 days at 30°C, then struck onto –URA for 3 days at 30°C to ensure retention of the plasmid. Saturated cultures were then grown in YEPD, serially diluted across agar plates and grown for 2 days on YEPD or –URA or 5 days on FOA media. Growth from the lowest-dilution spot for each strain was struck onto YEPD, then single colonies replicated to selective media to determine the genotype of any FOA-resistant colonies.

6.2.3 Cells lacking Pif1 and Exo1 do not require Cdc13 for survival, provided that telomerase, Ku and Rad52 are present

*cdc13-1 exo1*Δ *pif1*Δ mutants were able to grow at 36°C, suggesting that *exo1*Δ *pif1*Δ mutants might not need Cdc13 for viability (Figure 5). However, at 37°C -38°C, inactivation of Cdc13-1 caused a noticeable growth defect (Figure 36), suggesting that *cdc13*Δ *exo1*Δ *pif1*Δ mutants might grow poorly or be inviable. To test this hypothesis, it was decided to investigate whether *cdc13*Δ *exo1*Δ *pif1*Δ mutants were viable.

*cdc13*Δ*/CDC13*$^{+}$ *exo1*Δ*/EXO1*$^{+}$ *pif1*Δ*/PIF1*$^{+}$ diploids were generated, sporulated, tetrads dissected and then spores micromanipulated apart on agar plates to allow viable meiotic progeny to form colonies (Figure 38). Surprisingly, *cdc13*Δ *exo1*Δ *pif1*Δ mutants were viable (Spores 3c, 7a, 8a, 8b, 9b, 10b, Figure 38) but clearly grew poorly compared to *CDC13*$^{+}$ *exo1*Δ *pif1*Δ mutants (spores 1d, 2c, 5a, 10a, Figure 38). Two independently-derived diploids were dissected, and the fraction of *cdc13*Δ *exo1*Δ *pif1*Δ mutants compared to *CDC13*$^{+}$ *exo1*Δ *pif1*Δ mutants was determined (Table 5). These data indicated that the germination efficiency of *cdc13*Δ *exo1*Δ *pif1*Δ mutants was 88% ±5.7%. It was concluded that essentially all *exo1*Δ *pif1*Δ mutants did not require Cdc13 for viability, but elimination of Cdc13 conferred a severe growth defect.

*cdc13*Δ *exo1*Δ *pif1*Δ mutants were viable (Figure 38), just like *cdc13-1 exo1*Δ *pif1*Δ mutants grown at 36°C (Figure 5). However, telomerase was essential for the growth of *cdc13-1 exo1*Δ *pif1*Δ mutants at 36°C (Figures 22-23). Thus it was hypothesized that telomerase might be required for the viability of *cdc13*Δ *exo1*Δ *pif1*Δ mutants. To test this hypothesis a *cdc13*Δ*/CDC13*$^{+}$ *exo1*Δ*/EXO1*$^{+}$ *pif1*Δ*/PIF1*$^{+}$ *tlc1*Δ*/TLC1*$^{+}$ diploid was generated containing a plasmid expressing *URA3* and over-expressing *CDC13* (*pURA3[CDC13]*). Sporulation of the diploid and tetrad dissection was then used to yield *CDC13*$^{+}$ and *cdc13*Δ strains containing *pURA3[CDC13]*. Strains were passaged on –URA media to ensure retention of *pURA3[CDC13]*, then grown up in liquid culture and serially-diluted across YEPD, -URA and FOA plates. Expression of *URA3* permits growth on media lacking uracil (-URA) but is toxic to cells grown on media containing FOA. Thus, on –URA only cells able to tolerate overexpression of *CDC13* would be able to grow while on FOA only cells able to tolerate the loss of plasmid-borne *CDC13* would be able to grow.

CDC13^{+} *TLC1*$^{+}$, *CDC13*$^{+}$ *TLC1*$^{+}$ *exo1*Δ *pif1*Δ, *CDC13*$^{+}$ *tlc1*Δ and *CDC13*$^{+}$ *tlc1*Δ *exo1*Δ *pif1*Δ were all able to grow on YEPD, -URA and FOA plates, indicating that overexpression of *CDC13* was not toxic and that the additional copy of *CDC13* was not essential (Figure 39). As expected, *cdc13*Δ *TLC1*$^{+}$ strains could grow on YEPD and –URA, but not FOA, indicating that the additional copy of *CDC13* was essential. In contrast, *cdc13*Δ *TLC1*$^{+}$ *exo1*Δ *pif1*Δ mutants were able to grow on YEPD, –URA, and FOA indicating that the additional copy of *CDC13* was not essential in this genetic background. However, *cdc13*Δ *TLC1*$^{+}$ *exo1*Δ *pif1*Δ mutants grew much worse than *CDC13*$^{+}$ *TLC1*$^{+}$ *exo1*Δ *pif1*Δ mutants on FOA, indicating a growth defect in these strains, consistent with previous results (Figure 38). Both *cdc13*Δ *tlc1*Δ and *cdc13*Δ *tlc1*Δ *exo1*Δ *pif1*Δ mutants could grow on YEPD and –URA, but not on FOA, indicating that the additional copy of *CDC13* was essential.

*cdc13*Δ *tlc1*Δ *exo1*Δ *pif1*Δ mutants grew very poorly on both YEPD and –URA, while *CDC13*$^{+}$ *tlc1*Δ *exo1*Δ *pif1*Δ mutants did not (Figure 39). This suggested that the *cdc13*Δ mutation conferred a growth defect in *tlc1*Δ *exo1*Δ *pif1*Δ mutants that over-expression of *CDC13* could not compensate for. It also raised the possibility that *tlc1*Δ *cdc13*Δ *exo1*Δ *pif1*Δ mutants might be viable without the plasmid, but grow so poorly (due to the combined growth defects seen in *tlc1*Δ *cdc13*Δ *exo1*Δ *pif1*Δ mutants carrying *pURA3[CDC13]* and in *cdc13*Δ *exo1*Δ *pif1*Δ mutants) that they could not be detected. However, the growth of *cdc13*Δ *tlc1*Δ *exo1*Δ *pif1*Δ mutants on –URA plates was judged to not be sufficiently worse than that of *cdc13*Δ *TLC1*$^{+}$*exo1*Δ *pif1*Δ to prevent the detection of *cdc13*Δ *tlc1*Δ *exo1*Δ *pif1*Δ mutants on FOA plates, if they were viable. Thus, it was concluded that telomerase is essential for the viability of *cdc13*Δ *exo1*Δ *pif1*Δ mutants.

In addition to its role in inhibition of nuclease activities at telomeres, Cdc13 is essential to recruit telomerase to the telomere. This is highlighted by the *cdc13-2* mutation, which ablates the telomerase recruitment function of Cdc13 and confers the same phenotype as *tlc1*Δ, leading to telomere shortening and senescence (Nugent et al., 1996). Therefore it was surprising that telomerase was essential for the growth of *cdc13-1 exo1*Δ *pif1*Δ mutants at 36°C (Figure 22) and for the viability of *cdc13*Δ *exo1*Δ *pif1*Δ mutants (Figure 39), given that Cdc13 should be either inactive or absent, respectively, and thus it should not be possible to recruit telomerase to the telomeres. However, the requirement of telomerase for the viability of *cdc13-1 exo1*Δ *pif1*Δ mutants at 36°C and

for the viability of *cdc13*Δ *exo1*Δ *pif1*Δ mutants suggested that telomerase had an essential function at the telomeres of these mutants and was being recruited independently of Cdc13. The DDR protein Ku (Yku70-Yku80) binds to telomeres and DSBs, and aids in telomerase recruitment by interaction with the TLC1 subunit of telomerase (Peterson et al., 2001). Thus, it was hypothesized that Ku might recruit telomerase to the telomeres of *cdc13*Δ *exo1*Δ *pif1*Δ mutants and thus be essential.

To test this hypothesis, strains containing mutations in all combinations of *CDC13*, *YKU70*, *EXO1* and *PIF1* and carrying a *CDC13* overexpression plasmid (*pURA3[CDC13]*) were generated as above (Figure 39) then tested for growth on YEPD, -URA and FOA plates. *CDC13*$^+$ *YKU70*$^+$, *CDC13*$^+$ *YKU70*$^+$ *exo1*Δ *pif1*Δ and *CDC13*$^+$ *yku70*Δ and *CDC13*$^+$ *yku70*Δ *exo1*Δ *pif1*Δ mutants were all able to grow on YEPD and FOA plates, indicating that the additional copy of *CDC13* was not essential (Figure 40). As expected, *cdc13*Δ *YKU70*$^+$ strains could grow on YEPD and –URA, but not FOA, indicating that the additional copy of *CDC13* was essential, while *cdc13*Δ *YKU70*$^+$ *exo1*Δ *pif1*Δ mutants could grow on YEPD, -URA and FOA, indicating that the additional copy of *CDC13* was not essential (Figure 40). Furthermore, *cdc13*Δ *yku70*Δ and *cdc13*Δ *yku70*Δ *exo1*Δ *pif1*Δ mutants were able to grow on YEPD and –URA but not on FOA, indicating that *pURA3[CDC13]* was essential (Figure 40). It was noted that it was not possible to passage *CDC13*$^+$ *yku70*Δ *exo1*Δ *pif1*Δ mutants on –URA, indicating that overexpression of *CDC13* in this background was highly toxic, resulting in poor-to-no growth on –URA plates (Figure 40). However, *cdc13*Δ *yku70*Δ *exo1*Δ *pif1*Δ mutants were able to grow on both YEPD and –URA so it was judged that this toxicity was not an issue in the *cdc13*Δ *yku70*Δ *exo1*Δ *pif1*Δ mutants and did not affect the conclusions of the assay. In conclusion, Ku (Yku70) is essential for the survival of *cdc13*Δ *exo1*Δ *pif1*Δ mutants, suggesting that Ku functions to recruit telomerase to the telomeres in *cdc13*Δ *exo1*Δ *pif1*Δ mutants.

As Ku and telomerase were essential for the survival of *cdc13*Δ *exo1*Δ *pif1*Δ mutants, even in the absence of Cdc13, it suggested Cdc13-independent telomerase-dependent mechanisms of telomere maintenance were being utilized. HR also contributes to telomere maintenance, and HR-based mechanisms are solely responsible for telomere maintenance in Type I and Type II post-senescent survivors (Lundblad and Blackburn, 1993, Teng and Zakian, 1999). It was hypothesized that Cdc13-independent telomerase-dependent mechanisms might be sufficient for telomere maintenance even in the

absence of HR. To test this hypothesis, strains containing mutations in all combinations of *CDC13*, *RAD52* (essential for HR), *EXO1* and *PIF1* and carrying a *CDC13* overexpression plasmid (*pURA3[CDC13]*) were generated as above (Figures 39-40) then tested for growth on YEPD, -URA and FOA plates.

CDC13$^+$ *RAD52*$^+$, *CDC13*$^+$ *RAD52*$^+$ *exo1*Δ *pif1*Δ, *CDC13*$^+$ *rad52*Δ and *CDC13*$^+$ *rad52*Δ *exo1*Δ *pif1*Δ mutants were all able to grow on YEPD, -URA and FOA, indicating that *pURA3[CDC13]* was not essential for the viability of these strains. As expected, *cdc13*Δ *RAD52*$^+$ *exo1*Δ *pif1*Δ mutants were also able to grow on FOA, indicating that *pURA3[CDC13]* was not essential for viability of these strains. However, *cdc13*Δ *rad52*Δ *exo1*Δ *pif1*Δ, *cdc13*Δ *RAD52*$^+$ and *cdc13*Δ *rad52*Δ mutants were able to grow on YEPD and –URA, but not on FOA, indicating *pURA3[CDC13]* was essential for the viability of these strains. It was concluded that Rad52 is essential for the viability of *cdc13*Δ *exo1*Δ *pif1*Δ mutants and thus HR is likely to be required for telomere maintenance in *cdc13*Δ *exo1*Δ *pif1*Δ mutants.

*cdc13*Δ *exo1*Δ *pif1*Δ mutants require telomerase for survival (and presumably telomere maintenance) but also show characteristics of telomerase-independent post-senescent survivors (the requirement for HR for viability). Thus, it was possible that *cdc13*Δ *exo1*Δ *pif1*Δ mutants might utilized both telomerase-dependent mechanisms of telomere maintenance and survivor-like mechanisms. To test this hypothesis, it was decided to test whether the Pol32 subunit of DNA Polymerase δ, required for BIR (a subcategory of HR) and for the generation of Type I and Type II survivors was required for the viability of *cdc13*Δ *exo1*Δ *pif1*Δ mutants (Lydeard et al., 2007). To do so, strains containing mutations in all combinations of *CDC13*, *POL32*, *EXO1* and *PIF1* and carrying a *CDC13* overexpression plasmid (*pURA3[CDC13]*) were generated as above (Figures 39-41) then tested for growth on YEPD, -URA and FOA plates.

CDC13$^+$ *POL32*$^+$, *CDC13*$^+$ *POL32*$^+$ *exo1*Δ *pif1*Δ, *CDC13*$^+$ *pol32*Δ and *CDC13*$^+$ *pol32*Δ *exo1*Δ *pif1*Δ mutants were all able to grow on YEPD, -URA and FOA, indicating that *pURA3[CDC13]* was not essential for the viability of these strains. As expected, *cdc13*Δ *POL32*$^+$ and *cdc13*Δ *pol32*Δ strains were able to grow on YEPD and –URA, but not on FOA, indicating that *pURA3[CDC13]* was essential for the viability of these strains. (Note: several colonies of *cdc13*Δ *pol32*Δ strain 6469 did grow on the FOA plate, but upon passage and genotyping they were determined to be contaminating

CDC13^{+} *pol32*Δ strains). Surprisingly, both *cdc13*Δ *POL32*$^{+}$ *exo1*Δ *pif1*Δ and *cdc13*Δ *pol32*Δ *exo1*Δ *pif1*Δ mutants were also able to grow on FOA, indicating that *pURA3[CDC13]* was not essential for viability of these strains. It was noted that the growth on FOA of the *cdc13*Δ *pol32*Δ *exo1*Δ *pif1*Δ mutants was extremely poor, but this was also true of *CDC13*$^{+}$ *pol32*Δ and *CDC13*$^{+}$ *pol32*Δ *exo1*Δ *pif1*Δ strains, suggesting this was in large part due to FOA sensitivity of *pol32*Δ strains rather than an indication that *cdc13*Δ *pol32*Δ *exo1*Δ *pif1*Δ mutants were extremely sick without *pURA3[CDC13]*. It was concluded that Pol32 was not essential for the viability of *cdc13*Δ *exo1*Δ *pif1*Δ mutants and thus they presumably relied on mechanisms that were clearly distinct from those of Type I and Type II survivors.

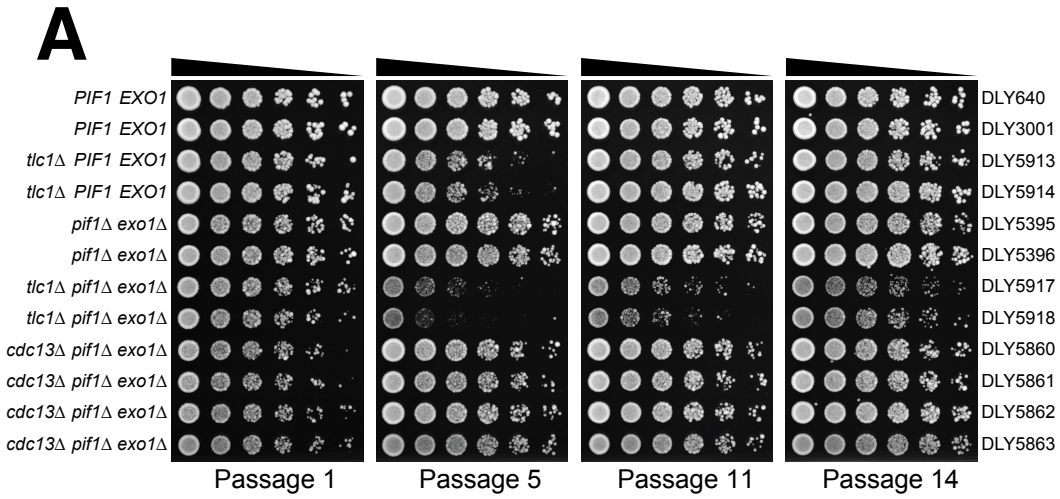
A
PIF1 EXO1
PIF1 EXO1
tlc1Δ PIF1 EXO1
tlc1Δ PIF1 EXO1
pif1Δ exo1Δ
pif1Δ exo1Δ
tlc1Δ pif1Δ exo1Δ
tlc1Δ pif1Δ exo1Δ
cdc13Δ pif1Δ exo1Δ
cdc13Δ pif1Δ exo1Δ
cdc13Δ pif1Δ exo1Δ
cdc13Δ pif1Δ exo1Δ
DLY640
DLY3001
DLY5913
DLY5914
DLY5395
DLY5396
DLY5917
DLY5918
DLY5860
DLY5861
DLY5862
DLY5863
Passage 1
Passage 5
Passage 11
Passage 14

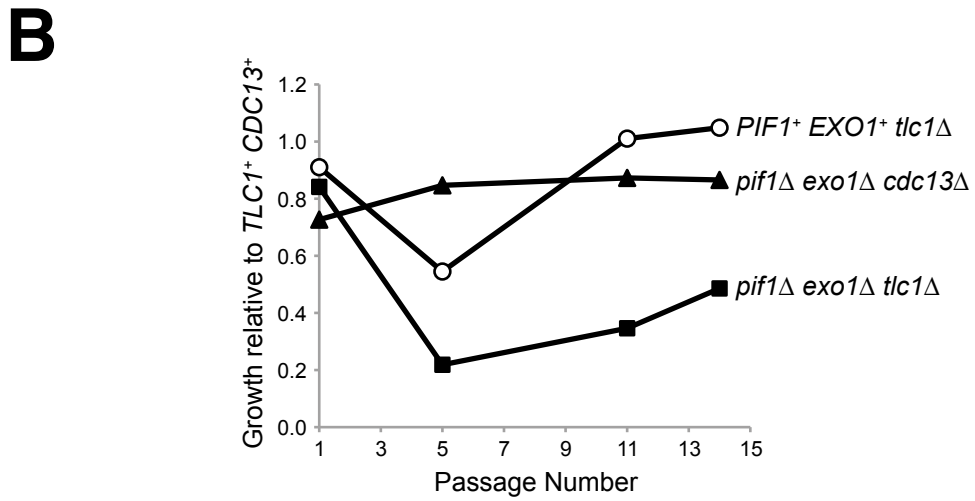
B
Growth relative to TLC1+ CDC13+
1.2
1.0
0.8
0.6
0.4
0.2
0.0
1
3
5
7
9
11
13
15
Passage Number
PIF1+ EXO1+ tlc1Δ
pif1Δ exo1Δ cdc13Δ
pif1Δ exo1Δ tlc1Δ

Figure 43: *cdc13*Δ *exo1*Δ *pif1*Δ mutants do not senesce

A. Multiple colonies from strains of the genotypes indicated at the passage indicated were inoculated into YEPD and grown to saturation, then serially-diluted across YEPD plates and allowed to grow at 30°C for 2 days. **B.** Quantification of the plates shown in A. with the growth given relative to the appropriate *CDC13+ TLC1+* strain.

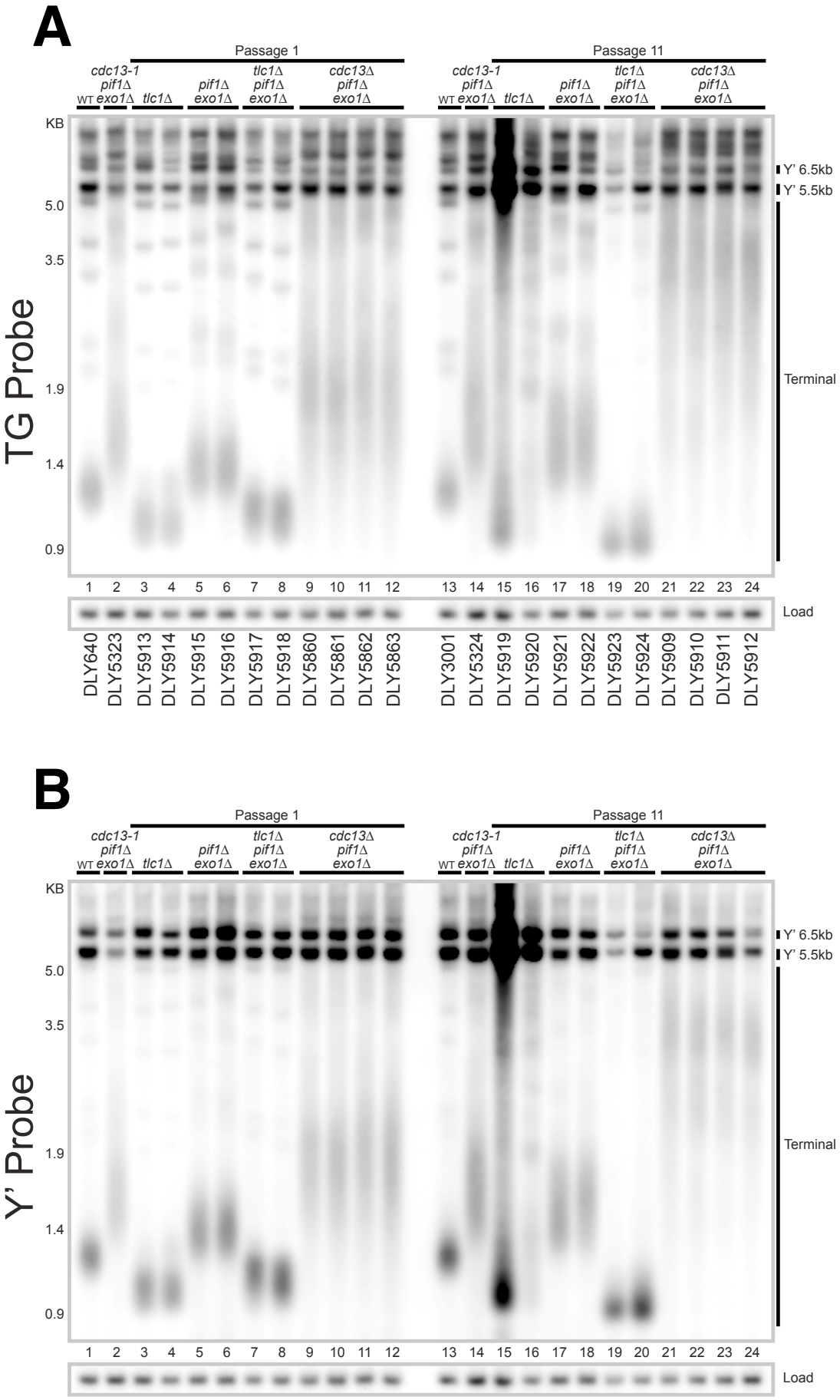
A
Passage 1
Passage 11
cdc13-1 pif1Δ exo1Δ
WT
tlc1Δ
pif1Δ exo1Δ
tlc1Δ pif1Δ exo1Δ
cdc13Δ pif1Δ exo1Δ
KB
5.0
3.5
1.9
1.4
0.9
TG Probe
Y' 6.5kb
Y' 5.5kb
Terminal
Load
1 2 3 4 5 6 7 8 9 10 11 12 13 14 15 16 17 18 19 20 21 22 23 24
DLY640 DLY5323 DLY5913 DLY5914 DLY5915 DLY5916 DLY5917 DLY5918 DLY5860 DLY5861 DLY5862 DLY5863 DLY3001 DLY5324 DLY5919 DLY5920 DLY5921 DLY5922 DLY5923 DLY5924 DLY5909 DLY5910 DLY5911 DLY5912
B
Passage 1
Passage 11
cdc13-1 pif1Δ exo1Δ
WT
tlc1Δ
pif1Δ exo1Δ
tlc1Δ pif1Δ exo1Δ
cdc13Δ pif1Δ exo1Δ
KB
5.0
3.5
1.9
1.4
0.9
Y' Probe
Y' 6.5kb
Y' 5.5kb
Terminal
Load
1 2 3 4 5 6 7 8 9 10 11 12 13 14 15 16 17 18 19 20 21 22 23 24

Figure 44: *cdc13*Δ *exo1*Δ *pif1*Δ mutants maintain their telomeres for up to 11 passages

Multiple colonies of strains of the genotypes indicated, at the passages indicated, were grown to saturation, then DNA was prepared and Southern Blots were performed to detect **A.** TG repeats and **B.** Y' fragments as in Figure 30.

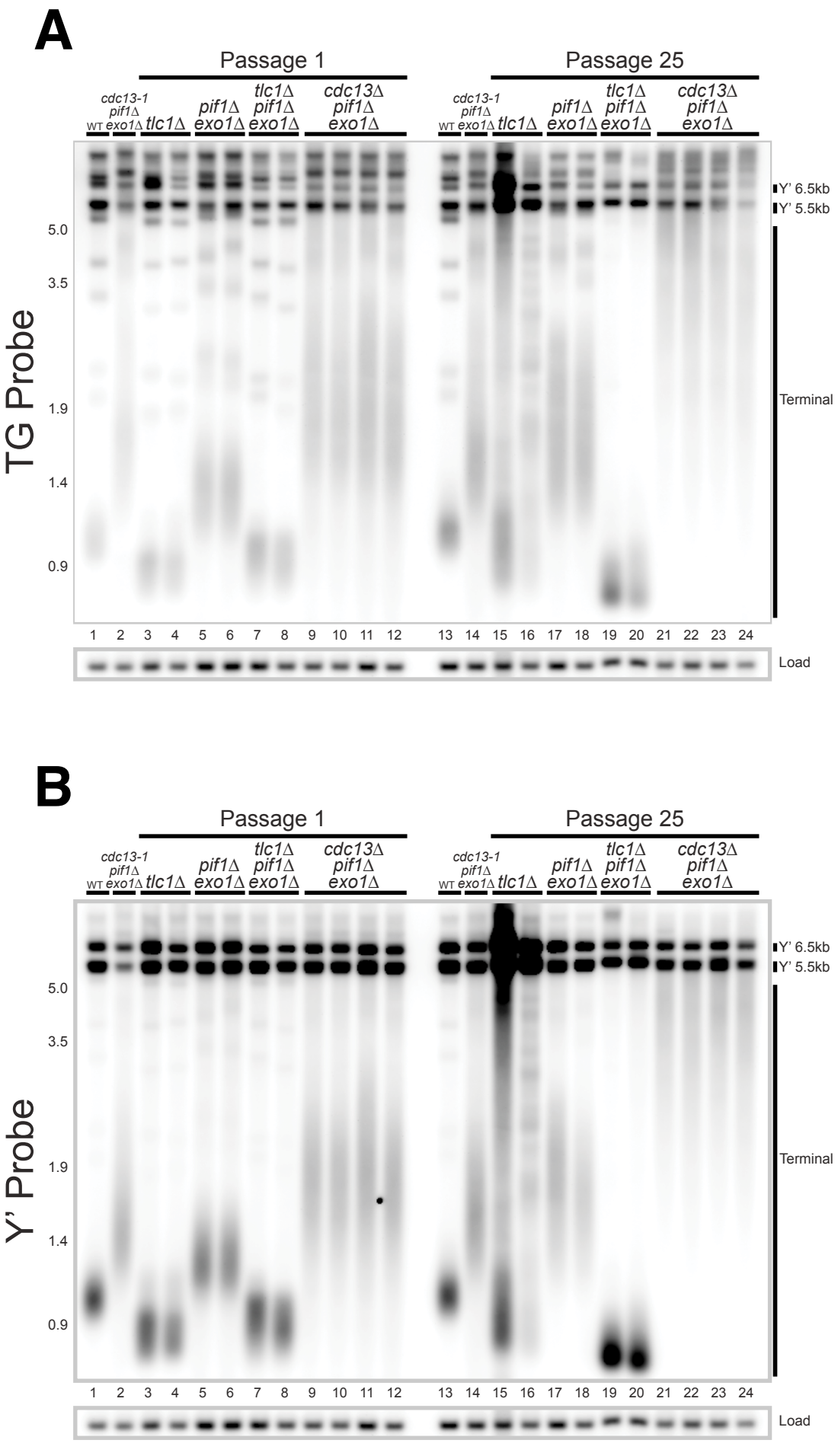
A
Passage 1
Passage 25
cdc13-1 pif1Δ WT exo1Δ
tlc1Δ
pif1Δ exo1Δ
tlc1Δ pif1Δ exo1Δ
cdc13Δ pif1Δ exo1Δ
TG Probe
5.0
3.5
1.9
1.4
0.9
Y' 6.5kb
Y' 5.5kb
Terminal
1 2 3 4 5 6 7 8 9 10 11 12 13 14 15 16 17 18 19 20 21 22 23 24
Load
B
Passage 1
Passage 25
cdc13-1 pif1Δ WT exo1Δ
tlc1Δ
pif1Δ exo1Δ
tlc1Δ pif1Δ exo1Δ
cdc13Δ pif1Δ exo1Δ
Y' Probe
5.0
3.5
1.9
1.4
0.9
Y' 6.5kb
Y' 5.5kb
Terminal
1 2 3 4 5 6 7 8 9 10 11 12 13 14 15 16 17 18 19 20 21 22 23 24
Load

Figure 45: *cdc13*Δ *exo1*Δ *pif1*Δ mutants maintain their telomeres for up to 25 passages

Multiple colonies of strains of the genotypes indicated, at the passages indicated, were grown to saturation, then DNA was prepared and Southern Blots were performed to detect **A.** TG repeats and **B.** Y' fragments as in Figure 30.

6.2.4 *cdc13*Δ *exo1*Δ *pif1*Δ mutants do not senesce and maintain their telomeres over time

Cells lacking Cdc13, Exo1 and Pif1 required telomerase and HR for viability and (presumably) for telomere maintenance (Figures 39-40). Though *cdc13*Δ *exo1*Δ *pif1*Δ mutants were clearly viable for long enough to form colonies (assuming ~10^6 cells/Wild Type colony, <20 generations) but were clearly very sick on the germination plate (Figure 38). Thus, it was possible that the *cdc13*Δ *exo1*Δ *pif1*Δ strains were entering into a rapid senescence and HR and Ku-mediated telomerase recruitment were sufficient only to allow the cell to divide enough to form colonies, not for sustained growth.

To test this hypothesis, *exo1*Δ *pif1*Δ *cdc13*Δ mutants were germinated simultaneously (as in Figure 28 and Figure 38) and passaged over time, alongside *exo1*Δ *pif1*Δ *tlc1*Δ mutants and *tlc1*Δ mutants (Figure 43A). Growth of the strains at different passage number was then measured relative to the appropriate *TLC1*$^+$ *CDC13*$^+$ strain and quantified (Figure 43B). At early passage, *cdc13*Δ *exo1*Δ *pif1*Δ mutants displayed a slight growth defect (Figure 43A-B) consistent with the growth defect seen on the germination plates (Figure 38). However, by passage 5, *cdc13*Δ *exo1*Δ *pif1*Δ mutants had improved in growth and continued to grow well for all subsequent passages (Figure 43B). This was in contrast to *tlc1*Δ mutants, which underwent a clear senescence period (passage 5, Figure 43A-B), followed by a dramatic recovery (passage 11, Figure 43A-B). In contrast, *tlc1*Δ *pif1*Δ *exo1*Δ mutants underwent a rapid senescence (passage 5, Figure 43A-B) and slowly improved in growth afterwards but did not recover (passage 11-14, Figure 43A-B), consistent with previous results (Figure 28). It was concluded that *cdc13*Δ *exo1*Δ *pif1*Δ mutants did not undergo typical patterns of senescence and recovery or follow the same rapid senescence and protracted period of poor growth as *tlc1*Δ *exo1*Δ *pif1*Δ mutants (Figure 43A-B). Thus it was unlikely that *cdc13*Δ *exo1*Δ *pif1*Δ mutants were entering into senescence on the germination plate (Figure 38).

Type I and Type II survivors undergo alterations in telomere structure that can permit telomere maintenance in the absence of Cdc13 (Larrivee and Wellinger, 2006). Additionally, cells that bypass the need for telomere capping, either through attenuation of the DDR at uncapped telomeres (Zubko and Lydall, 2006) or by co-overexpression of Stn1 and Ten1 (Petreaca et al., 2006) frequently undergo rearrangements in telomere

structure. *cdc13-1 exo1*Δ *pif1*Δ mutants can grow for approximately 9 generations without undergoing alterations in telomere structure (a 1:500 dilution is approximately $1:2^9$, see Figure 37) and *cdc13*Δ *exo1*Δ *pif1*Δ mutants grow poorly after approximately <20 generations of growth (Figure 38) but subsequently grow well upon passage (Figure 43). Thus it was hypothesized that *cdc13*Δ *exo1*Δ *pif1*Δ mutants might maintain a relatively normal telomere structure at early passage (like *cdc13-1 exo1*Δ *pif1*Δ mutants) but undergo rearrangements in telomere structure that permitted them to improve in growth at later passage.

To test this hypothesis, Southern Blots were performed to analyze telomere structure of *cdc13*Δ *exo1*Δ *pif1*Δ mutants at passages 1 and 11 compared to *tlc1*Δ and *tlc1*Δ *exo1*Δ *pif1*Δ mutants (Figures 44A-B). As expected, *tlc1*Δ and *tlc1*Δ *exo1*Δ *pif1*Δ mutants had short telomeres at passage 1 (lanes 3-4, 7-8 Figure 44A-B). Consistent with previous results (Figure 28), by passage 11 *tlc1*Δ mutants had generated survivors (Type I - lane 15, Type II - lane 16, Figure 44A-B) while *tlc1*Δ *exo1*Δ *pif1*Δ mutants had undergone a reduction in Y' elements, acquired terminal Y' elements at all telomeres and maintained extremely short terminal fragments (lanes 19-20, Figure 44A-B). In contrast, *cdc13*Δ *exo1*Δ *pif1*Δ mutants had extremely long telomeres at passage 1, with great variance in length (lanes 9-12, Figure 44A-B) and by passage 11 their telomeres had increased in length and variance but had otherwise undergone no alterations in telomere structure (lanes 21-24, Figure 44A-B). It was concluded that *cdc13*Δ *exo1*Δ *pif1*Δ mutants did not undergo gross rearrangements in telomere structure that permitted them to improve their growth in the absence of Cdc13.

Interestingly, the telomeres of *cdc13*Δ *exo1*Δ *pif1*Δ mutants most closely resembled those of *cdc13-1 exo1*Δ *pif1*Δ mutants (which were not passaged) grown at 23°C (compare lanes 2 and 14 to lanes 9-12 and 21-24, Figure 44A-B). Furthermore, the telomeres of *exo1*Δ *pif1*Δ mutants, like those of *cdc13*Δ *exo1*Δ *pif1*Δ mutants also increased in length and variance with passage (compare lanes 5-6 to lanes 17-18, Figure 44A-B). It was possible that telomere lengthening in *cdc13-1 exo1*Δ *pif1*Δ mutants and *cdc13*Δ *exo1*Δ *pif1*Δ mutants was an acceleration of the telomere lengthening that occurred with passage in *exo1*Δ *pif1*Δ mutants with passage number. If this was the case, then *cdc13*Δ *exo1*Δ *pif1*Δ and *exo1*Δ *pif1*Δ mutants should continue to increase in length over time and *exo1*Δ *pif1*Δ mutants should ultimately become as long a *cdc13-1 exo1*Δ *pif1*Δ mutants. To test this hypothesis, all strains (except Wild Type and *cdc13-1*

*exo1*Δ *pif1*Δ controls) were passaged a further 14 times, (up to passage 25, amounting to a total of 100 days growth at 23°C) and Southern Blots were performed to analyze telomere length (Figure 45A-B).

By passage 25, *cdc13*Δ *exo1*Δ *pif1*Δ mutants had increased in telomere length (compare lanes 21-24, Figure 44A-B to lanes 21-24, Figure 45A-B). This was also true for *exo1*Δ *pif1*Δ mutants (compares lanes 17-18, Figure 44A-B to lanes 17-18, Figure 45A-B), which by passage 25 had longer telomeres than an unpassaged *cdc13-1 exo1*Δ *pif1*Δ mutant (compares lanes 17-18 to lane 14, Figure 45A-B). Indeed, by passage 25 the telomeres of *pif1*Δ *exo1*Δ mutants were almost identical to those of *cdc13*Δ *exo1*Δ *pif1*Δ mutants at passage 1 (compare lanes 17-18 to lanes 9-12, Figure 45A-B). Thus, it was concluded that the telomere lengthening in *cdc13*Δ *exo1*Δ *pif1*Δ mutants was not specifically caused by impaired (*cdc13-1*) or absent Cdc13 (*cdc13*Δ), but was an acceleration of the telomere lengthening phenotype seen in *exo1*Δ *pif1*Δ mutants. As the *pif1*Δ mutation is responsible for the telomere lengthening seen in *exo1*Δ *pif1*Δ and *cdc13-1 exo1*Δ *pif1*Δ mutants (Figure 37A-B) this telomere lengthening is probably due to the absence of Pif1.

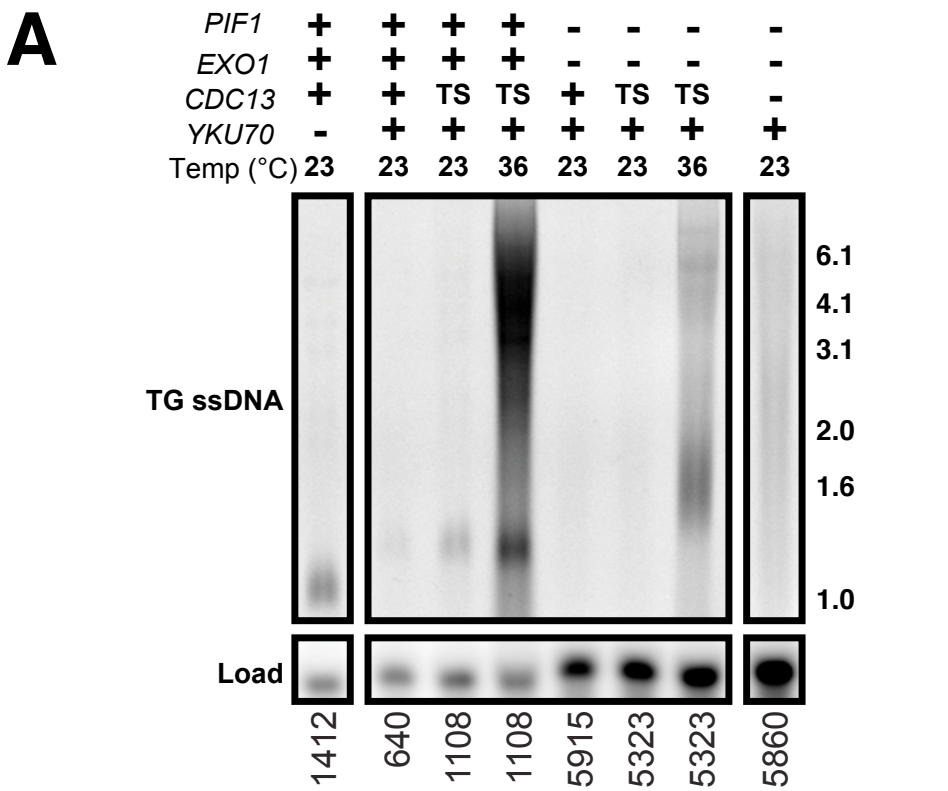
A
PIF1 + + + + - - - -
EXO1 + + + + - - - -
CDC13 + + TS TS + TS TS -
YKU70 - + + + + + + +
Temp (°C) 23 23 23 36 23 23 36 23
TG ssDNA
6.1
4.1
3.1
2.0
1.6
1.0
Load
1412
640
1108
1108
5915
5323
5323
5860

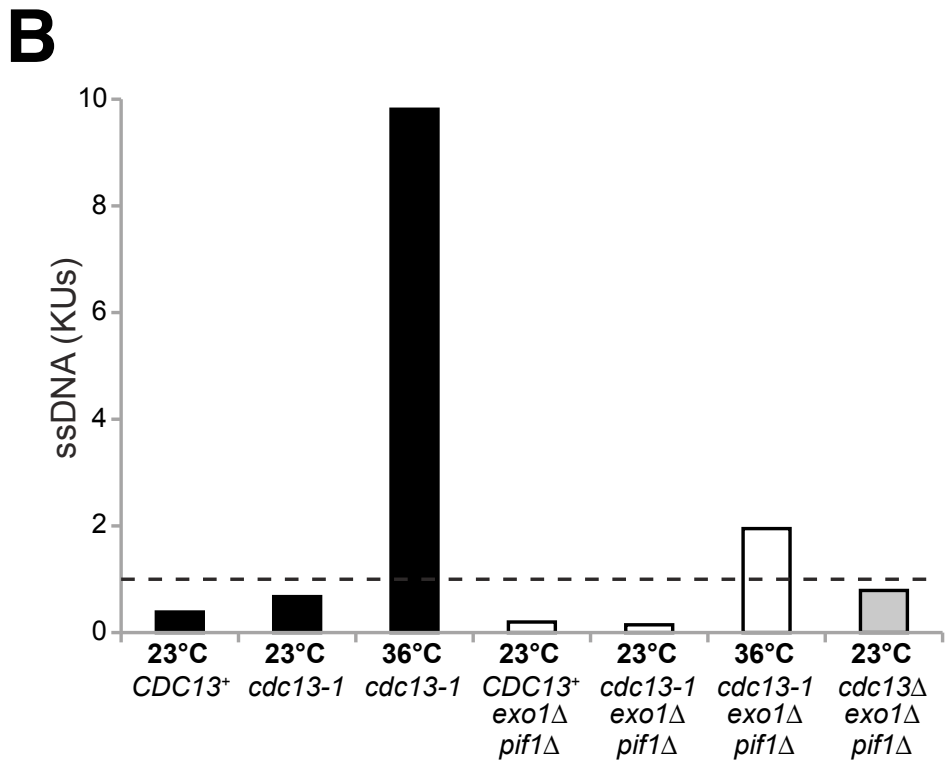
B
ssDNA (KUs)
10
8
6
4
2
0
23°C CDC13+
23°C cdc13-1
36°C cdc13-1
23°C CDC13+ exo1Δ pif1Δ
23°C cdc13-1 exo1Δ pif1Δ
36°C cdc13-1 exo1Δ pif1Δ
23°C cdc13Δ exo1Δ pif1Δ

Figure 46: growth in the absence of Cdc13 does not cause accumulation of ssDNA
A. Exponentially-dividing cultures of strains of the indicated genotypes were either grown at 23°C for a further 4 hours or split and half the culture grown at 23°C for a further 4 hours while the other half was grown at 36°C. Samples were taken and DNA was prepared by for in-gel assays which were performed as in Figure 18. Gel is split into panels for presentation purposes, but all samples were run on the same gel. **B.** Quantification of the data given in A, as in Figure 18. Horizontal dashed line represents one KU.

6.2.5 Long term survival in the absence of Cdc13 does not lead to the accumulation of telomeric ssDNA

Over a single cell cycle, *cdc13-1 exo1*Δ *pif1*Δ mutants accumulated only transient ssDNA in the telomeric TG repeats following telomere uncapping (Figure 18A-B) and none in the Y' elements (Figure 16B). However, when asynchronously dividing *cdc13-1 exo1*Δ *pif1*Δ mutants were subjected to telomere uncapping, a slight accumulation of ssDNA in the TG repeats could be seen (Figure 25B) but none in the Y' elements (Figure 26B) and telomerase appeared to inhibit ssDNA generation in TG repeats of *cdc13-1* independently of both Pif1 and Exo1 (Figure 25A-B). This suggested the possibility that a third nuclease activity was functioning at a low level in the absence of Pif1 and Exo1, causing *exo1*Δ *pif1*Δ mutants to gradually accumulate ssDNA with continued cell division in the absence of Cdc13.

It was assumed that if a residual nuclease activity functioned in the absence of Pif1 and Exo1, following telomere uncapping, that the low level of telomeric TG repeat ssDNA seen in *cdc13-1 exo1*Δ *pif1*Δ mutants would be increased in *cdc13*Δ *exo1*Δ *pif1*Δ mutants which had gone through many more cell cycles in the absence of Cdc13. To test this hypothesis, asynchronously dividing cultures of *cdc13-1* mutants and *cdc13-1 exo1*Δ *pif1*Δ mutants were shifted to 36°C for 4 hours to induce telomere uncapping and ssDNA in the telomeric TG repeats was measured by in-gel assay in comparison to an asynchronously dividing *cdc13*Δ *exo1*Δ *pif1*Δ mutant and an asynchronously-dividing *yku70*Δ control (Figure 46A-B). *cdc13-1* mutants at 36°C for 4 hours (approximately 1 generation with uncapped telomeres) generated an approximately 10-fold increase in ssDNA in the TG repeats over a *yku70*Δ mutant (Figure 46A-B) consistent with previous results (Figure 25A-B). *cdc13-1 exo1*Δ *pif1*Δ mutants at 36°C for 4 hours (approximately 2 generations with uncapped telomeres) generated an approximately 2-fold increase in ssDNA in the TG repeats (Figure 46A-B) consistent with previous results (Figure 25A-B). *cdc13*Δ *exo1*Δ *pif1*Δ mutants passaged once (approximately 50 generations with uncapped telomeres, Figures 43-44) generated less ssDNA than a *yku70*Δ mutant. It was concluded that *exo1*Δ *pif1*Δ mutants grown continuously in the absence of Cdc13 (50 generations with uncapped telomeres) did not accumulate more ssDNA than a *cdc13-1 exo1*Δ *pif1*Δ mutant grown at 36°C (2 generations with

uncapped telomeres) and thus there were unlikely to be residual nuclease activities functioning at uncapped telomeres in *exo1*Δ *pif1*Δ mutants.

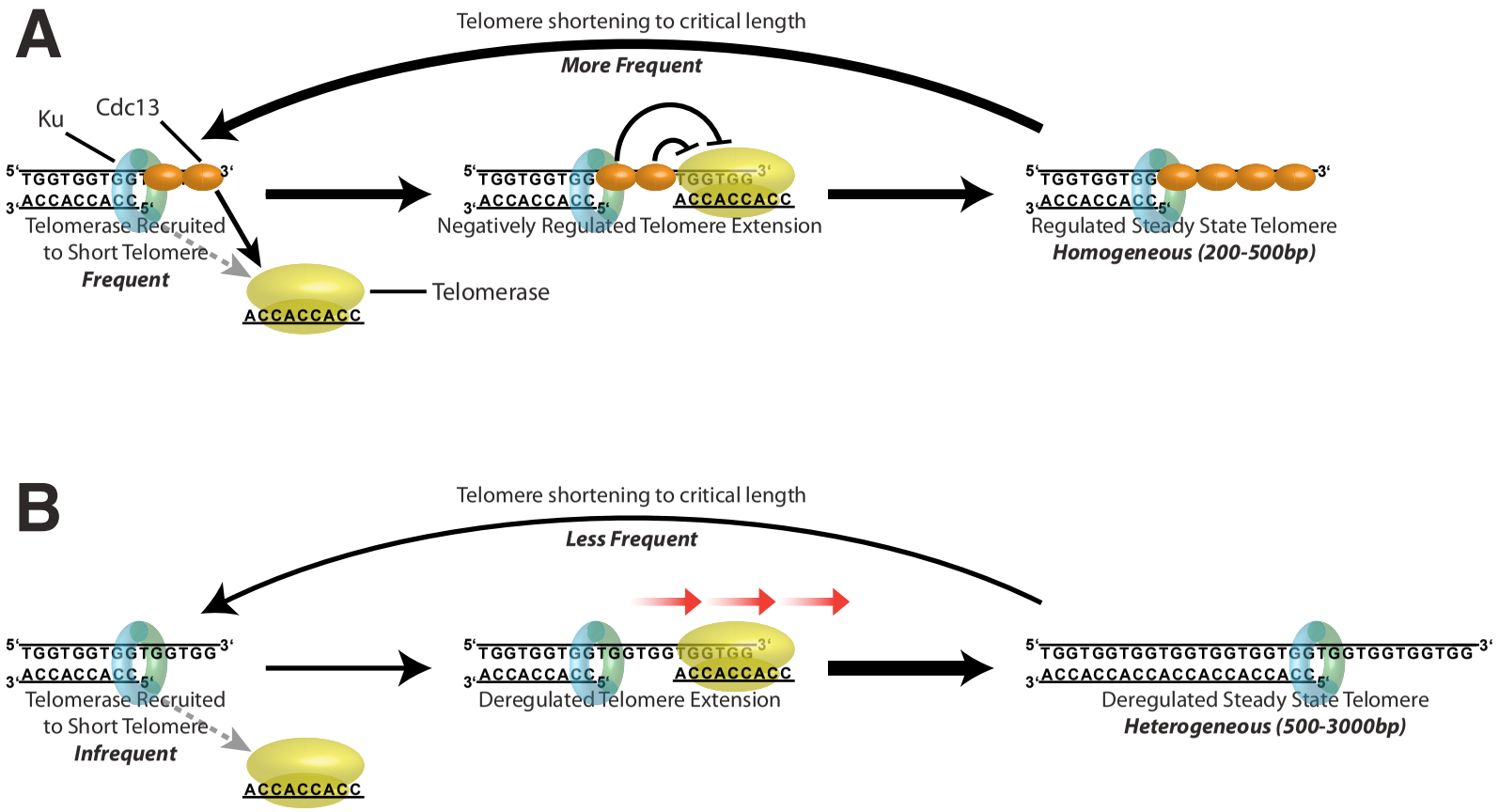
A
Telomere shortening to critical length
More Frequent
Ku
Cdc13
5‘ TGGTGGTGG 3‘
3‘ ACCACCACC 5‘
Telomerase Recruited
to Short Telomere
Frequent
ACCACCACC
Telomerase
5‘ TGGTGGTGG TGGTGG 3‘
3‘ ACCACCACC 5‘ ACCACCACC
Negatively Regulated Telomere Extension
5‘ TGGTGGTGG 3‘
3‘ ACCACCACC 5‘
Regulated Steady State Telomere
Homogeneous (200-500bp)
B
Telomere shortening to critical length
Less Frequent
5‘ TGGTGGTGGTGGTGG 3‘
3‘ ACCACCACC 5‘
Telomerase Recruited
to Short Telomere
Infrequent
ACCACCACC
5‘ TGGTGGTGGTGGTGG TGGTGG 3‘
3‘ ACCACCACC 5‘ ACCACCACC
Deregulated Telomere Extension
5‘ TGGTGGTGGTGGTGGTGGTGGTGGTGGTGG 3‘
3‘ ACCACCACCACCACCACCACC 5‘
Deregulated Steady State Telomere
Heterogeneous (500-3000bp)

Figure 47: A model for the regulation of telomerase at the telomeres of *cdc13*Δ *exo1*Δ *pif1*Δ mutants

A. At wild type telomeres, telomerase is primarily recruited by Cdc13 but aided by Ku. Cdc13 also negatively regulates telomere length at each telomere extension event by negatively regulating telomerase, ensuring that telomeres will become critically short within a relatively small number of divisions and thus telomere length is tightly regulated. **B.** At the telomeres of *cdc13*Δ *exo1*Δ *pif1*Δ mutants, telomerase is recruited at a very low rate by Ku alone. However, as Cdc13 is not present, each telomere extension event by telomerase produces a very long telomere, which will take many cell divisions to become critically short.

6.3 Discussion

Previous work showed that elimination of checkpoint genes and nuclease activities (Exo1, Rad9 and Rad24) at uncapped telomeres permitted the generation of cells that were viable without Cdc13 at a rate of approximately 4-6x10^{-5}. Here, it is shown that elimination of Exo1 and Pif1 is sufficient to permit the viability of approximately 90% (9x10^{-1}) of cells in the absence of Cdc13 (Figure 38, Table 5). Furthermore, cells lacking Pif1 and Exo1 do not undergo alterations in telomeres structure that could account for their growth in the absence of Cdc13 (Figure 37) and selective expression of telomere cap components was not required, confirming that *cdc13*Δ *exo1*Δ *pif1*Δ mutants are viable due to attenuation of the DDR at uncapped telomeres (Larrivee and Wellinger, 2006, Peterson et al., 2001).

Recently, it has been shown that elimination of Rad9, Exo1 and Sgs1 permits the viability of approximately 70% of cells lacking Cdc13 (Ngo and Lydall, 2010). Like *cdc13*Δ *exo1*Δ *pif1*Δ mutants, *cdc13*Δ *rad9*Δ *exo1*Δ *sgs1*Δ mutants grow poorly at germination. However, unlike *cdc13*Δ *exo1*Δ *pif1*Δ mutants, *cdc13*Δ *rad9*Δ *exo1*Δ *sgs1*Δ mutants undergo senescence and recovery, with corresponding rearrangements in telomere structure (though not alterations typical of Type I and Type II survivors). Though elimination of Sgs1 and Exo1 almost completely eliminates resection at uncapped telomeres in *cdc13-1* mutants, accumulation of ssDNA is still detectable in the Y' elements (presumably due to Pif1 activity) (Ngo and Lydall, 2010). It is likely that resection in the Y' elements by Pif1 causes *cdc13*Δ *rad9*Δ *exo1*Δ *sgs1*Δ mutants to senesce, perhaps with recovery corresponding to alterations in telomere structure that attenuate Pif1 activity.

In contrast to *cdc13*Δ *rad9*Δ *exo1*Δ *sgs1*Δ mutants, *cdc13*Δ *exo1*Δ *pif1*Δ mutants do not senesce and instead show a growth defect upon germination, but improve in growth with passage number and grow robustly for ≥100 days, undergoing no alterations in telomere structure other than lengthening of their telomeres (Figures 43-45). Furthermore, the survival of these mutants is dependent upon Ku, telomerase and homologous recombination (Figures 39-41). These data lend themselves easily to a model of telomerase regulation at the telomeres of *CDC13*$^{+}$ and *cdc13*Δ (*exo1*Δ *pif1*Δ) cells (Figure 47A-B).

In *CDC13*$^{+}$ cells, Cdc13 is essential to recruit telomerase to the telomeres and Ku aids in the recruitment of telomerase (Figure 47A). Cdc13 also negatively regulates extension by telomerase, preventing the addition of more than 200-500 bases to telomeres (Figure 47A). This leads to regular shortening of individual telomeres to critical length, followed by telomerase recruitment and re-extension of the telomere by telomerase, causing telomere length to be tightly regulated within the cell.

In *cdc13*Δ cells, Ku alone recruits telomerase at a very low level (Figure 47B). This low level of telomerase recruitment means that cells will be defective at responding to short telomeres, possibly explaining the poor growth of *cdc13*Δ *exo1*Δ *pif1*Δ mutants on the tetrad dissection plate (Figure 38) and at early passage (Figure 43). As Cdc13 is not present to negatively regulate telomeres, each telomerase recruitment event will lead to deregulated extension of the telomere by telomerase, producing a telomere of up to several kilobases (Figure 47B). Consistent with this, the telomeres of *cdc13*Δ *exo1*Δ *pif1*Δ mutants strongly resemble those of *cdc13-5* mutants, which have a defect in negative regulation of telomerase (Chandra et al., 2001). The very long telomeres created by each telomerase extension event will become critically short only after many cell divisions. This means that recruitment of telomerase to the telomeres will only be required very infrequently as telomeres lengthen overall and thus the defect in telomerase recruitment will not pose a significant barrier to population growth. This may explain the improvement in growth and corresponding lengthening of *cdc13*Δ *exo1*Δ *pif1*Δ mutants over time (Figures 43-45). Interestingly, as Rad52 is required for the viability of *cdc13*Δ *exo1*Δ *pif1*Δ mutants, it suggests that homologous recombination can be used to distribute telomeric repeats from longer telomeres to shorter telomeres to aid in telomere maintenance.

Although it is appealing to consider a model in which Ku alone recruits telomerase to the telomeres of *cdc13*Δ *exo1*Δ *pif1*Δ mutants and thus is essential for survival, Ku might also be essential for the survival of *cdc13*Δ *exo1*Δ *pif1*Δ mutants to inhibit nuclease activity at telomeres, as reported in *CDC13*$^{+}$ mutants (Maringele and Lydall, 2002, Teo and Jackson, 2001). However, *yku70*Δ *exo1*Δ *pif1*Δ (Figure 19) mutants with uncapped telomeres do not appear to show a growth defect, suggesting that there is no Pif1- and Exo1-independent nuclease activity at uncapped telomeres lacking Ku,making it unlikely that the essential role of Ku in *cdc13*Δ *exo1*Δ *pif1*Δ mutants is to inhibit a nuclease activity. However, at DSBs, independently-functioning nuclease activities

dependent upon Sgs1 and Exo1 are inhibited by Ku (Mimitou and Symington, 2010). Furthermore, at least some situations exist in which Sgs1 functions independently of Exo1 to resect uncapped telomeres lacking Cdc13 (i.e. in *cdc13-1 rad9*Δ mutants) (Ngo and Lydall, 2010). Thus it is possible, though unlikely, that the essential role of Ku in *cdc13*Δ *exo1*Δ *pif1*Δ mutants is to inhibit Sgs1 or some other nuclease activity at the telomeres.

One question remains about *cdc13*Δ *exo1*Δ *pif1*Δ mutants – why is telomerase so important? The above model (Figure 47) proposes that in *cdc13*Δ *exo1*Δ *pif1*Δ mutants, telomerase is necessary to counteract shortened telomeres. However telomere shortening alone should not trigger such a pronounced lethality as seen in *cdc13*Δ *exo1*Δ *pif1*Δ mutants (Figure 39). This is highlighted by cultures of yeast lacking telomerase, which are usually viable for several generations before the growth of the culture goes through a gradual decline in growth (senescence) due to telomere shortening (Lundblad and Blackburn, 1993, Teng and Zakian, 1999). Instead, it is likely that *cdc13*Δ *exo1*Δ *pif1*Δ mutants have such a pronounced requirement for telomerase because they lack Pif1. Consistent with this, the telomere lengthening over passage in *cdc13*Δ *exo1*Δ *pif1*Δ mutants resembles an exaggeration of the telomere lengthening over passage seen in $CDC13^{+}$ *pif1*Δ and $CDC13^{+}$ *exo1*Δ *pif1*Δ mutants (Figure 30, Figure 44). Indeed, telomerase-deficient cells lacking Pif1 undergo rapid senescence, suggestive of a severe defect in telomerase-independent telomere maintenance (Figure 28). Furthermore, it has been hypothesized that increased utilization of telomerase at the telomeres of *pif1*Δ mutants is a consequence of a severe defect in telomere maintenance that requires telomerase to heal unresolvable DNA substrates (Chang et al., 2009). Thus, it will be important to determine which DNA substrates Pif1 processes at DNA ends. In addition, it will be interesting to try and identify other genes that inhibit the growth of *cdc13-1* mutants in the same pathway as *PIF1*, but are less important for telomerase-independent telomere maintenance, to see if it is possible to eliminate the requirement for telomerase for survival in the absence of Cdc13.

Finally, it is important to consider the implications that the viability of *cdc13*Δ *exo1*Δ *pif1*Δ mutants have for human cancers. *cdc13*Δ *exo1*Δ *pif1*Δ mutants utilize telomerase for survival, but the levels of telomerase at the telomeres must be incredibly low due to the absence of Cdc13 (Figure 47). Similarly, in human somatic cells, telomerase recruitment to telomeres must also be extraordinarily low (due to low total cellular

levels of telomerase) (Kim et al., 1994). *cdc13*Δ *exo1*Δ *pif1*Δ mutants are able to survive without overexpression of telomerase because attenuation of the DDR (elimination of Pif1 and Exo1) has facilitated loss of a key negative regulators of telomerase (Cdc13) thus permitting low levels of telomeric telomerase to maintain telomeres. Perhaps a similar situation exists in a subset of the approximately 15% of human cancers that maintain telomeres without up-regulation of telomerase components (Bryan et al., 1997) that has been thought to occur by ALT mechanisms (Cesare and Reddel, 2010). Thus it is possible that in human cancers, elimination of DDR components also permits the loss of negative regulators of telomerase and allows for telomerase-dependent telomere maintenance without up-regulation of telomerase. It will be interesting to see whether Pif1 and Exo1 are both components of the telomeric DDR in mammalian cells.

6.4 Further Work

Here it has been shown that elimination of Pif1 and Exo1 permits the viability of cells in the absence of Cdc13 and the viability of these cells depends upon telomerase, Ku and homologous recombination. Four main lines of enquiry stem from this work.

First, a model has been proposed for how telomerase is recruited to telomeres in the absence of Cdc13 (Figure 47), however this remains to be formally proven. This could be performed genetically by mutagenesis of TLC1, the telomerase template RNA, in *cdc13*Δ *pif1*Δ *exo1*Δ mutants to introduce a restriction site and passaging cells to look for incorporation of the restriction site into the telomeres over time (Singer and Gottschling, 1994). Alternatively, ChIP could be performed to show that telomerase is still recruited to telomeres in *cdc13*Δ *pif1*Δ *exo1*Δ mutants.

Second, *cdc13*Δ *exo1*Δ *pif1*Δ mutants are viable but grow poorly at early passage and it will be important to test why (Figures 38, 43). It is proposed (Figure 47) that the poor growth of *cdc13*Δ *pif1*Δ *exo1*Δ mutants at early passage (Figures 38, 43) is due to an impaired ability to deal with short telomeres. This could be tested by introducing an inducible short telomere cassette into *cdc13*Δ *exo1*Δ *pif1*Δ mutants to follow growth after the induction of a single short telomere (Bianchi et al., 2004). Alternatively, it is possible that low levels of Sgs1-dependent resection occur at early passage in *cdc13*Δ *exo1*Δ *pif1*Δ mutants (though unlikely, as very limited ssDNA occurs, Figure 46) and it would be useful to test this (Ngo and Lydall, 2010) Additionally, the checkpoint kinase Tel1 is required for responding to short telomeres while Mec1 is involved in the

response to DSBs and uncapped telomeres (Bianchi and Shore, 2008). Therefore, it would be interesting to know whether either Mec1 or Tel1 restrains the growth of *cdc13*Δ *exo1*Δ *pif1*Δ mutants at early passage to determine whether the telomeres of *cdc13*Δ *exo1*Δ *pif1*Δ mutants are recognized as DSBs or short telomeres. Furthermore, it would be interesting to see whether the elimination of Mec1 or Tel1 affects the long-term viability of *cdc13*Δ *exo1*Δ *pif1*Δ mutants.

Third, an important role of the telomere cap is believed to be to promote genome stability (Longhese, 2008). *cdc13*Δ *exo1*Δ *pif1*Δ mutants provide a valuable tool to study the role of Cdc13 in genome stability. In particular, it will be interesting to examine the number of gross chromosomal rearrangements and telomere-telomere fusion events in these cells, using established methods (Chen and Kolodner, 1999, Pobiega and Marcand, 2010). Additionally, though Cdc13 is also non-essential in *rad9*Δ *exo1*Δ *sgs1*Δ mutants, the *rad9*Δ mutation also eliminates the Mec1-dependent checkpoint (Ngo and Lydall, 2010). As *cdc13*Δ *exo1*Δ *pif1*Δ mutants do not require the elimination of any checkpoint components for viability, they provide a model system for studying the interplay between checkpoint components and telomere capping proteins in the maintenance of genome stability.

Fourth and finally, orthologues of Cdc13-Stn1-Ten1 (the CST complex) have recently been discovered in mammalian and plant cells (Miyake et al., 2009, Surovtseva et al., 2009). These orthologous complexes appear to have roles at sites of replicational difficulty, including telomeres. It may prove informative to study the roles of Pif1 and Exo1 orthologues following knock-down of the Cdc13 orthologue in the cells of higher organisms.

7 Conclusions

"Nothing in biology makes sense except in the light of evolution"

- Theodosius Dobzhansky

7.1 The yeast CST complex has telomere-specific roles, but the mammalian CST complex does not

Cdc13 is the founding member of the CST (Cdc13-Stn1-Ten1) complex in budding yeast (Gao et al., 2007). In *S. cerevisiae* inactivation of Cdc13 leads to the accumulation of ssDNA specifically at telomeres (Garvik et al., 1995). In mammalian, plant and human cells, knocking down the CST components also leads to increased telomeric ssDNA (Miyake et al., 2009, Surovtseva et al., 2009). However, in contrast to yeast CST (yCST), mammalian CST (mCST) binds to DNA in a sequence-independent manner and only partially localizes to telomeres, suggesting that CST functions in some aspect of DNA metabolism frequently required at telomeres but also utilized elsewhere (Miyake et al., 2009). Yet, a more generalized function for the yCST complex is at odds with its highly specific telomeric role in yeast. The best illustration of the specific telomeric role of the CST complex in budding yeast is the requirement for Cdc13 to recruit telomerase to telomeres (Nugent et al., 1996). Thus, any model for the conserved roles of the CST complex must account for a highly specialized telomeric role in yCST and a more generalized role in mCST.

Cdc13 has been assumed to function as a telomere 'capping' protein, protecting the telomere from recognition as a DSB by the cell's DNA damage response (Lydall, 2009). However, Pif1 and Exo1 function in parallel pathways to coordinate the DDR at uncapped telomeres, but not at DSBs, calling this into question (Figures 14-18) (Zhu et al., 2008). Indeed, following inactivation of Cdc13, the nuclease components Sgs1 and Exo1, which function in different pathways in DSBR seem to function in a single pathway at uncapped telomeres, while Pif1 functions in a parallel pathway (Figure 20) (Ngo and Lydall, 2010, Mimitou and Symington, 2008). Elimination of Pif1 and Exo1 displays remarkable synergy in eliminating the DDR at uncapped telomeres (Figure 5). However, the finding that Pif1 and Exo1 have opposite effects following camptothecin treatment (one of the few forms of DNA damage that Exo1 alone is absolutely crucial for the response to) suggests that Pif1 and Exo1 have remarkably different responses in most DDRs (Figure 32) (Morin et al., 2008). In fact, there is not a single published

example of Pif1 and Exo1 functioning in the same process except, as described here, at uncapped telomeres. Even at uncapped telomeres Pif1 and Exo1 appear to recognize different substrates – Pif1 is more important for resection away from the end of the chromosome, while the importance of Exo1 in resection increases closer to the chromosome end (Figure 16, Figure 18). Thus, any model for yCST function must explain how the nuclease activities that resect uncapped telomeres have such different properties at other sites in the genome.

To resolve these issues, it is proposed that yCST fulfills two roles – a telomere-nonspecific role, analogous to that of mCST, in dealing with a specific kind of DNA substrate and a telomere-specific role, including 'end protection' and telomerase recruitment, perhaps analogous to that of POT1 in mammalian cells. mCST is predicted to be structurally similar to RPA (Gao et al., 2007) and telomeric repeat sequences (either at the telomeres or when placed elsewhere in the genome) are sites of replicational difficulty (Sfeir et al., 2009). Thus, the proposed model of mCST functioning in a specialized aspect of DNA replication is favored for the telomere-nonspecific role of yCST (Miyake et al., 2009). The Pif1 helicase enhances the toxicity of replicative lesions caused by camptothecin (Figure 32) or hydroxyurea (Chang et al., 2009), has roles in Okazaki fragment processing (Pike et al., 2009) and must recognize 5' ssDNA occurring at uncapped telomeres away from the chromosome end (Figure 16, Figure 18). Thus, a role for Pif1 in responding to some form of replicative lesion caused by inactivation of yCST is favorable. These observations lead to the proposition Pif1 functions to initiate the DDR at replicative lesions that occur following inactivation of the telomere-nonspecific role of yCST, while Exo1 functions to initiate the DDR that occurs following inactivation of the telomere-specific role of yCST.

7.2 In the light of evolution

The *S. cerevisiae* genome is relatively free of simple repetitive sequences and in general possesses less non-coding DNA than higher organisms (Lander et al., 2001, Cherry et al., 1997). Thus, it is possible that telomeric DNA in budding yeast could be the only site that poses a specific replicational difficulty of the sort that the mCST complex might be required to deal with. This would mean that in an ancestor of *S. cerevisiae*, an evolutionary ancestor of the current yCST or 'pre-CST' would naturally be deposited at telomeres due to its role in DNA replication. It is not unreasonable to assume that such a pre-CST might be co-opted to also fulfill telomere-specific roles, while in mammalian

cells multiple sites of replicational difficulty might have necessitated the telomere-specific roles of yCST to be taken up by a separate protein, such as POT1 (Wu et al., 2006).

A caveat with such a model is that the budding yeast genome certainly does have at least one other site of repetitive sequence in the yeast genome – the ribosomal DNA (rDNA) (Cherry et al., 1997). Curiously, Rrm3, the budding yeast paralogue of Pif1, is required for proper replication fork progression through rDNA (Torres et al., 2004). Furthermore, Pif1 is important for the stability of G-rich repetitive sequences in budding yeast and although this has been attributed to the ability of Pif1 to unwind G quadruplexes *in vitro* it could be due to a more generalized role of Pif1 at sites of replicational difficulty (Ribeyre et al., 2009). Additionally, overexpression of Pif1 renders cells hypersensitive to hydroxyurea and MMS, suggesting that it causes replication fork disassembly (Chang et al., 2009). Consistent with such a model, Pif1 appears to generate ssDNA away from the end of the chromosome, perhaps recognizing and disassembling stalled replication forks (Figure 16, Figure 18). It will be important to investigate the role of mammalian Pif1 in response to dysfunction of the mCST orthologues.

Here, the telomeric role of the yCST is assumed to be the same as the current working model for yCST in 'end protection' – to prevent recognition of the telomeric DNA as a DSB (de Lange, 2009, Lydall, 2009). The notion of Exo1 'chewing away at DNA ends' is consistent with the increasing importance of Exo1 in resection of uncapped telomeres closer to the chromosome end (Figure 16, Figure 18). The lack of a requirement for MRX in this process is presumably that telomeres are unique, in that they already possess ssDNA that can be readily extended by a rampant nuclease activity (Foster et al., 2006). At uncapped telomeres in *yku70*Δ mutants, Exo1 is almost entirely responsible for resection, but Pif1 clearly plays a role in inhibiting the growth of *yku70*Δ mutants at higher temperatures. This raises the possibility that although the primary defect caused by inactivation of Ku at the telomeres is one of resection by Exo1, a replication defect might also occur (Figure 19) (Maringele and Lydall, 2002). It is tempting to consider that telomere 'capping' may be a universal phenomenon, consisting of a combination of the 'end protection' and 'end replication' problems. Indeed, the Ku complex functions as a 'last resort' at stalled replication forks in higher organisms (Adamo et al., 2010).

It is tempting to speculate on exactly which aspect of DNA replication telomeres are defective in (Sfeir et al., 2009) and thus what process mCST and Pif1 might be involved in. Given the unidirectionality of DNA replication at telomeres, the resolution of replisomes at telomeres must require some specialized mechanism compared to sites of bidirectional replication within the genome. Though telomeric repeats cause replicational difficulty when placed within the genome, it is noteworthy that telomeric repeat sequences are *de facto* regions of DNA sequence that lack origins of replication. If the converging replisomes were not sufficiently stable to synthesize across the entire sequence, such regions would also require unidirection replisome resolution, much like the terminal replisome. Perhaps the CST complex plays a role in the resolution of the terminal replisome and perhaps Pif1 is a helicase that has roles in replisome resolution. Intriguingly, the Pif1 paralogue Rrm3 has recently been show to have roles in replisome resolution (Fachinetti et al., 2010).

8 References

ABDALLAH, P., LUCIANO, P., RUNGE, K. W., LISBY, M., GELI, V., GILSON, E. & TEIXEIRA, M. T. (2009) A two-step model for senescence triggered by a single critically short telomere. *Nat Cell Biol,* 11**,** 988-93.

ABRAMOFF, M. D., MAGELHAES, P. J. & RAM, S. J. (2004) Image Processing with ImageJ. *Biophotonics International,* 11**,** 36-42.

ACKERMAN, S. H. & TZAGOLOFF, A. (1990) Identification of two nuclear genes (ATP11, ATP12) required for assembly of the yeast F1-ATPase. *Proc Natl Acad Sci U S A,* 87**,** 4986-90.

ADAMO, A., COLLIS, S. J., ADELMAN, C. A., SILVA, N., HOREJSI, Z., WARD, J. D., MARTINEZ-PEREZ, E., BOULTON, S. J. & LA VOLPE, A. (2010) Preventing nonhomologous end joining suppresses DNA repair defects of Fanconi anemia. *Mol Cell,* 39**,** 25-35.

ADDINALL, S. G., DOWNEY, M., YU, M., ZUBKO, M. K., DEWAR, J., LEAKE, A., HALLINAN, J., SHAW, O., JAMES, K., WILKINSON, D. J., WIPAT, A., DUROCHER, D. & LYDALL, D. (2008) A genomewide suppressor and enhancer analysis of cdc13-1 reveals varied cellular processes influencing telomere capping in Saccharomyces cerevisiae. *Genetics,* 180**,** 2251-66.

AGARWAL, R., TANG, Z., YU, H. & COHEN-FIX, O. (2003) Two distinct pathways for inhibiting pds1 ubiquitination in response to DNA damage. *J Biol Chem,* 278**,** 45027-33.

ALLSHIRE, R. C., DEMPSTER, M. & HASTIE, N. D. (1989) Human telomeres contain at least three types of G-rich repeat distributed non-randomly. *Nucleic Acids Res,* 17**,** 4611-27.

ASKREE, S. H., YEHUDA, T., SMOLIKOV, S., GUREVICH, R., HAWK, J., COKER, C., KRAUSKOPF, A., KUPIEC, M. & MCEACHERN, M. J. (2004) A genome-wide screen for Saccharomyces cerevisiae deletion mutants that affect telomere length. *Proc Natl Acad Sci U S A,* 101**,** 8658-63.

AYLON, Y. & KUPIEC, M. (2003) The checkpoint protein Rad24 of Saccharomyces cerevisiae is involved in processing double-strand break ends and in recombination partner choice. *Mol Cell Biol,* 23**,** 6585-96.

BAE, N. S. & BAUMANN, P. (2007) A RAP1/TRF2 complex inhibits nonhomologous end-joining at human telomeric DNA ends. *Mol Cell,* 26**,** 323-34.

BAUMANN, P. & CECH, T. R. (2001) Pot1, the putative telomere end-binding protein in fission yeast and humans. *Science,* 292**,** 1171-5.

BESSLER, M., WILSON, D. B. & MASON, P. J. (2010) Dyskeratosis congenita. *FEBS Lett,* 584**,** 3831-8.

BIANCHI, A. & DE LANGE, T. (1999) Ku binds telomeric DNA in vitro. *J Biol Chem,* 274**,** 21223-7.

BIANCHI, A., NEGRINI, S. & SHORE, D. (2004) Delivery of yeast telomerase to a DNA break depends on the recruitment functions of Cdc13 and Est1. *Mol Cell,* 16**,** 139-46.

BIANCHI, A. & SHORE, D. (2007) Increased association of telomerase with short telomeres in yeast. *Genes Dev,* 21**,** 1726-30.

BIANCHI, A. & SHORE, D. (2008) How telomerase reaches its end: mechanism of telomerase regulation by the telomeric complex. *Mol Cell,* 31**,** 153-65.

BILAUD, T., BRUN, C., ANCELIN, K., KOERING, C. E., LAROCHE, T. & GILSON, E. (1997) Telomeric localization of TRF2, a novel human telobox protein. *Nat Genet,* 17**,** 236-9.

BLACKBURN, E., GREIDER, C., YONATH, A. & OSTROM, E. (2009) 2009 Nobels: break or breakthrough for women? Interview by Jeffrey Mervis and Kate Travis. *Science,* 326**,** 656-8.

BLACKBURN, E. H., GREIDER, C. W. & SZOSTAK, J. W. (2006) Telomeres and telomerase: the path from maize, Tetrahymena and yeast to human cancer and aging. *Nat Med,* 12**,** 1133-8.

BLANKLEY, R. T. & LYDALL, D. (2004) A domain of Rad9 specifically required for activation of Chk1 in budding yeast. *J Cell Sci,* 117**,** 601-8.

BLASCO, M. A. (2007) Telomere length, stem cells and aging. *Nat Chem Biol,* 3**,** 640-9.

BLASCO, M. A., LEE, H. W., HANDE, M. P., SAMPER, E., LANSDORP, P. M., DEPINHO, R. A. & GREIDER, C. W. (1997) Telomere shortening and tumor formation by mouse cells lacking telomerase RNA. *Cell,* 91**,** 25-34.

BODNAR, A. G., OUELLETTE, M., FROLKIS, M., HOLT, S. E., CHIU, C. P., MORIN, G. B., HARLEY, C. B., SHAY, J. W., LICHTSTEINER, S. & WRIGHT, W. E. (1998) Extension of life-span by introduction of telomerase into normal human cells. *Science,* 279**,** 349-52.

BOITEUX, S. & GUILLET, M. (2004) Abasic sites in DNA: repair and biological consequences in Saccharomyces cerevisiae. *DNA Repair (Amst),* 3**,** 1-12.

BOMBARDE, O., BOBY, C., GOMEZ, D., FRIT, P., GIRAUD-PANIS, M. J., GILSON, E., SALLES, B. & CALSOU, P. (2010) TRF2/RAP1 and DNA-PK mediate a double protection against joining at telomeric ends. *EMBO J,* 29**,** 1573-84.

BONETTI, D., CLERICI, M., ANBALAGAN, S., MARTINA, M., LUCCHINI, G. & LONGHESE, M. P. (2010) Shelterin-like proteins and Yku inhibit nucleolytic processing of Saccharomyces cerevisiae telomeres. *PLoS Genet,* 6**,** e1000966.

BONETTI, D., MARTINA, M., CLERICI, M., LUCCHINI, G. & LONGHESE, M. P. (2009) Multiple pathways regulate 3' overhang generation at S. cerevisiae telomeres. *Mol Cell,* 35**,** 70-81.

BOOTH, C., GRIFFITH, E., BRADY, G. & LYDALL, D. (2001) Quantitative amplification of single-stranded DNA (QAOS) demonstrates that cdc13-1 mutants generate ssDNA in a telomere to centromere direction. *Nucleic Acids Res,* 29**,** 4414-22.

BOULE, J. B., VEGA, L. R. & ZAKIAN, V. A. (2005) The yeast Pif1p helicase removes telomerase from telomeric DNA. *Nature,* 438**,** 57-61.

BROCCOLI, D., SMOGORZEWSKA, A., CHONG, L. & DE LANGE, T. (1997) Human telomeres contain two distinct Myb-related proteins, TRF1 and TRF2. *Nat Genet,* 17**,** 231-5.

BRYAN, T. M., ENGLEZOU, A., DALLA-POZZA, L., DUNHAM, M. A. & REDDEL, R. R. (1997) Evidence for an alternative mechanism for maintaining telomere length in human tumors and tumor-derived cell lines. *Nat Med,* 3**,** 1271-4.

BUDD, M. E., REIS, C. C., SMITH, S., MYUNG, K. & CAMPBELL, J. L. (2006) Evidence suggesting that Pif1 helicase functions in DNA replication with the Dna2 helicase/nuclease and DNA polymerase delta. *Mol Cell Biol,* 26**,** 2490-500.

BUNTING, S. F., CALLEN, E., WONG, N., CHEN, H. T., POLATO, F., GUNN, A., BOTHMER, A., FELDHAHN, N., FERNANDEZ-CAPETILLO, O., CAO, L., XU, X., DENG, C. X., FINKEL, T., NUSSENZWEIG, M., STARK, J. M. & NUSSENZWEIG, A. (2010) 53BP1 inhibits homologous recombination in Brca1-deficient cells by blocking resection of DNA breaks. *Cell,* 141**,** 243-54.

CEJKA, P., CANNAVO, E., POLACZEK, P., MASUDA-SASA, T., POKHAREL, S., CAMPBELL, J. L. & KOWALCZYKOWSKI, S. C. (2010) DNA end resection by Dna2-Sgs1-RPA and its stimulation by Top3-Rmi1 and Mre11-Rad50-Xrs2. *Nature,* 467**,** 112-6.

CELLI, G. B. & DE LANGE, T. (2005) DNA processing is not required for ATM-mediated telomere damage response after TRF2 deletion. *Nat Cell Biol,* 7**,** 712-8.

CESARE, A. J. & REDDEL, R. R. (2010) Alternative lengthening of telomeres: models, mechanisms and implications. *Nat Rev Genet,* 11**,** 319-30.

CHAN, A., BOULE, J. B. & ZAKIAN, V. A. (2008) Two pathways recruit telomerase to Saccharomyces cerevisiae telomeres. *PLoS Genet,* 4**,** e1000236.

CHANDRA, A., HUGHES, T. R., NUGENT, C. I. & LUNDBLAD, V. (2001) Cdc13 both positively and negatively regulates telomere replication. *Genes Dev,* 15**,** 404-14.

CHANG, M., LUKE, B., KRAFT, C., LI, Z., PETER, M., LINGNER, J. & ROTHSTEIN, R. (2009) Telomerase is essential to alleviate pif1-induced replication stress at telomeres. *Genetics,* 183**,** 779-91.

CHEN, C. & KOLODNER, R. D. (1999) Gross chromosomal rearrangements in Saccharomyces cerevisiae replication and recombination defective mutants. *Nat Genet,* 23**,** 81-5.

CHEN, S. H., SMOLKA, M. B. & ZHOU, H. (2007) Mechanism of Dun1 activation by Rad53 phosphorylation in Saccharomyces cerevisiae. *J Biol Chem,* 282**,** 986-95.

CHERRY, J. M., BALL, C., WENG, S., JUVIK, G., SCHMIDT, R., ADLER, C., DUNN, B., DWIGHT, S., RILES, L., MORTIMER, R. K. & BOTSTEIN, D. (1997) Genetic and physical maps of Saccharomyces cerevisiae. *Nature,* 387**,** 67-73.

CHIKASHIGE, Y. & HIRAOKA, Y. (2001) Telomere binding of the Rap1 protein is required for meiosis in fission yeast. *Curr Biol,* 11**,** 1618-23.

CHUNG, W. H., ZHU, Z., PAPUSHA, A., MALKOVA, A. & IRA, G. (2010) Defective resection at DNA double-strand breaks leads to de novo telomere formation and enhances gene targeting. *PLoS Genet,* 6**,** e1000948.

CHURIKOV, D. & PRICE, C. M. (2008) Pot1 and cell cycle progression cooperate in telomere length regulation. *Nat Struct Mol Biol,* 15**,** 79-84.

CICCIA, A. & ELLEDGE, S. J. (2010) The DNA damage response: making it safe to play with knives. *Mol Cell,* 40**,** 179-204.

CIMINO-REALE, G., PASCALE, E., ALVINO, E., STARACE, G. & D'AMBROSIO, E. (2003) Long telomeric C-rich 5'-tails in human replicating cells. *J Biol Chem,* 278**,** 2136-40.

CIOSK, R., ZACHARIAE, W., MICHAELIS, C., SHEVCHENKO, A., MANN, M. & NASMYTH, K. (1998) An ESP1/PDS1 complex regulates loss of sister chromatid cohesion at the metaphase to anaphase transition in yeast. *Cell,* 93**,** 1067-76.

CLINE, M. S., SMOOT, M., CERAMI, E., KUCHINSKY, A., LANDYS, N., WORKMAN, C., CHRISTMAS, R., AVILA-CAMPILO, I., CREECH, M., GROSS, B., HANSPERS, K., ISSERLIN, R., KELLEY, R., KILLCOYNE, S., LOTIA, S., MAERE, S., MORRIS, J., ONO, K., PAVLOVIC, V., PICO, A. R., VAILAYA, A., WANG, P. L., ADLER, A., CONKLIN, B. R., HOOD, L., KUIPER, M., SANDER, C., SCHMULEVICH, I., SCHWIKOWSKI, B., WARNER, G. J., IDEKER, T. & BADER, G. D. (2007) Integration of biological networks and gene expression data using Cytoscape. *Nat Protoc,* 2**,** 2366-82.

COHEN, H. & SINCLAIR, D. A. (2001) Recombination-mediated lengthening of terminal telomeric repeats requires the Sgs1 DNA helicase. *Proc Natl Acad Sci U S A,* 98**,** 3174-9.

COHN, M. & BLACKBURN, E. H. (1995) Telomerase in yeast. *Science,* 269**,** 396-400.

COOPER, J. P., NIMMO, E. R., ALLSHIRE, R. C. & CECH, T. R. (1997) Regulation of telomere length and function by a Myb-domain protein in fission yeast. *Nature,* 385**,** 744-7.

COOPER, J. P., WATANABE, Y. & NURSE, P. (1998) Fission yeast Taz1 protein is required for meiotic telomere clustering and recombination. *Nature,* 392**,** 828-31.

COSTANZO, M. C., SKRZYPEK, M. S., NASH, R., WONG, E., BINKLEY, G., ENGEL, S. R., HITZ, B., HONG, E. L. & CHERRY, J. M. (2009) New mutant phenotype data curation system in the Saccharomyces Genome Database. *Database (Oxford),* 2009**,** bap001.

D'ADDA DI FAGAGNA, F., REAPER, P. M., CLAY-FARRACE, L., FIEGLER, H., CARR, P., VON ZGLINICKI, T., SARETZKI, G., CARTER, N. P. &

JACKSON, S. P. (2003) A DNA damage checkpoint response in telomere-initiated senescence. *Nature,* 426**,** 194-8.

DE LANGE, T. (2005) Shelterin: the protein complex that shapes and safeguards human telomeres. *Genes Dev,* 19**,** 2100-10.

DE LANGE, T. (2009) How telomeres solve the end-protection problem. *Science,* 326**,** 948-52.

DE LANGE, T., SHIUE, L., MYERS, R. M., COX, D. R., NAYLOR, S. L., KILLERY, A. M. & VARMUS, H. E. (1990) Structure and variability of human chromosome ends. *Mol Cell Biol,* 10**,** 518-27.

DIONNE, I. & WELLINGER, R. J. (1996) Cell cycle-regulated generation of single-stranded G-rich DNA in the absence of telomerase. *Proc Natl Acad Sci U S A,* 93**,** 13902-7.

DOWNEY, M., HOULSWORTH, R., MARINGELE, L., ROLLIE, A., BREHME, M., GALICIA, S., GUILLARD, S., PARTINGTON, M., ZUBKO, M. K., KROGAN, N. J., EMILI, A., GREENBLATT, J. F., HARRINGTON, L., LYDALL, D. & DUROCHER, D. (2006) A genome-wide screen identifies the evolutionarily conserved KEOPS complex as a telomere regulator. *Cell,* 124**,** 1155-68.

DOWNS, J. A., ALLARD, S., JOBIN-ROBITAILLE, O., JAVAHERI, A., AUGER, A., BOUCHARD, N., KRON, S. J., JACKSON, S. P. & COTE, J. (2004) Binding of chromatin-modifying activities to phosphorylated histone H2A at DNA damage sites. *Mol Cell,* 16**,** 979-90.

DUNHAM, M. A., NEUMANN, A. A., FASCHING, C. L. & REDDEL, R. R. (2000) Telomere maintenance by recombination in human cells. *Nat Genet,* 26**,** 447-50.

DUNN, C. D., LEE, M. S., SPENCER, F. A. & JENSEN, R. E. (2006) A genomewide screen for petite-negative yeast strains yields a new subunit of the i-AAA protease complex. *Mol Biol Cell,* 17**,** 213-26.

ELLISON, V. & STILLMAN, B. (2003) Biochemical characterization of DNA damage checkpoint complexes: clamp loader and clamp complexes with specificity for 5' recessed DNA. *PLoS Biol,* 1**,** E33.

FACHINETTI, D., BERMEJO, R., COCITO, A., MINARDI, S., KATOU, Y., KANOH, Y., SHIRAHIGE, K., AZVOLINSKY, A., ZAKIAN, V. A. & FOIANI, M. (2010) Replication termination at eukaryotic chromosomes is

mediated by Top2 and occurs at genomic loci containing pausing elements. *Mol Cell,* 39**,** 595-605.

FALCK, J., COATES, J. & JACKSON, S. P. (2005) Conserved modes of recruitment of ATM, ATR and DNA-PKcs to sites of DNA damage. *Nature,* 434**,** 605-11.

FAURE, V., COULON, S., HARDY, J. & GELI, V. (2010) Cdc13 and telomerase bind through different mechanisms at the lagging- and leading-strand telomeres. *Mol Cell,* 38**,** 842-52.

FELDMANN, H. & WINNACKER, E. L. (1993) A putative homologue of the human autoantigen Ku from Saccharomyces cerevisiae. *J Biol Chem,* 268**,** 12895-900.

FISHER, T. S., TAGGART, A. K. & ZAKIAN, V. A. (2004) Cell cycle-dependent regulation of yeast telomerase by Ku. *Nat Struct Mol Biol,* 11**,** 1198-205.

FOIANI, M., MARINI, F., GAMBA, D., LUCCHINI, G. & PLEVANI, P. (1994) The B subunit of the DNA polymerase alpha-primase complex in Saccharomyces cerevisiae executes an essential function at the initial stage of DNA replication. *Mol Cell Biol,* 14**,** 923-33.

FOSTER, S. S., ZUBKO, M. K., GUILLARD, S. & LYDALL, D. (2006) MRX protects telomeric DNA at uncapped telomeres of budding yeast cdc13-1 mutants. *DNA Repair (Amst),* 5**,** 840-51.

FRIEDMAN, K. L., HEIT, J. J., LONG, D. M. & CECH, T. R. (2003) N-terminal domain of yeast telomerase reverse transcriptase: recruitment of Est3p to the telomerase complex. *Mol Biol Cell,* 14**,** 1-13.

FUSTER, J. J. & ANDRES, V. (2006) Telomere biology and cardiovascular disease. *Circ Res,* 99**,** 1167-80.

GANGLOFF, S., MCDONALD, J. P., BENDIXEN, C., ARTHUR, L. & ROTHSTEIN, R. (1994) The yeast type I topoisomerase Top3 interacts with Sgs1, a DNA helicase homolog: a potential eukaryotic reverse gyrase. *Mol Cell Biol,* 14**,** 8391-8.

GAO, H., CERVANTES, R. B., MANDELL, E. K., OTERO, J. H. & LUNDBLAD, V. (2007) RPA-like proteins mediate yeast telomere function. *Nat Struct Mol Biol,* 14**,** 208-14.

GARVIK, B., CARSON, M. & HARTWELL, L. (1995) Single-stranded DNA arising at telomeres in cdc13 mutants may constitute a specific signal for the RAD9 checkpoint. *Mol Cell Biol,* 15**,** 6128-38.

GATBONTON, T., IMBESI, M., NELSON, M., AKEY, J. M., RUDERFER, D. M., KRUGLYAK, L., SIMON, J. A. & BEDALOV, A. (2006) Telomere length as a quantitative trait: genome-wide survey and genetic mapping of telomere length-control genes in yeast. *PLoS Genet,* 2**,** e35.

GEORGE, J. A., DEBARYSHE, P. G., TRAVERSE, K. L., CELNIKER, S. E. & PARDUE, M. L. (2006) Genomic organization of the Drosophila telomere retrotransposable elements. *Genome Res,* 16**,** 1231-40.

GEORGE, T., WEN, Q., GRIFFITHS, R., GANESH, A., MEUTH, M. & SANDERS, C. M. (2009) Human Pif1 helicase unwinds synthetic DNA structures resembling stalled DNA replication forks. *Nucleic Acids Res,* 37**,** 6491-502.

GOLDSTEIN, A. L. & MCCUSKER, J. H. (1999) Three new dominant drug resistance cassettes for gene disruption in Saccharomyces cerevisiae. *Yeast,* 15**,** 1541-53.

GRAVEL, S., CHAPMAN, J. R., MAGILL, C. & JACKSON, S. P. (2008) DNA helicases Sgs1 and BLM promote DNA double-strand break resection. *Genes Dev,* 22**,** 2767-72.

GRAVEL, S., LARRIVEE, M., LABRECQUE, P. & WELLINGER, R. J. (1998) Yeast Ku as a regulator of chromosomal DNA end structure. *Science,* 280**,** 741-4.

GRIFFITH, J. D., COMEAU, L., ROSENFIELD, S., STANSEL, R. M., BIANCHI, A., MOSS, H. & DE LANGE, T. (1999) Mammalian telomeres end in a large duplex loop. *Cell,* 97**,** 503-14.

HAMMET, A., MAGILL, C., HEIERHORST, J. & JACKSON, S. P. (2007) Rad9 BRCT domain interaction with phosphorylated H2AX regulates the G1 checkpoint in budding yeast. *EMBO Rep,* 8**,** 851-7.

HARLEY, C. B., FUTCHER, A. B. & GREIDER, C. W. (1990) Telomeres shorten during ageing of human fibroblasts. *Nature,* 345**,** 458-60.

HARRISON, J. C. & HABER, J. E. (2006) Surviving the breakup: the DNA damage checkpoint. *Annu Rev Genet,* 40**,** 209-35.

HAYFLICK, L. (1965) The Limited in Vitro Lifetime of Human Diploid Cell Strains. *Exp Cell Res,* 37**,** 614-36.

HEISS, N. S., KNIGHT, S. W., VULLIAMY, T. J., KLAUCK, S. M., WIEMANN, S., MASON, P. J., POUSTKA, A. & DOKAL, I. (1998) X-linked dyskeratosis congenita is caused by mutations in a highly conserved gene with putative nucleolar functions. *Nat Genet,* 19**,** 32-8.

HIRANO, Y., FUKUNAGA, K. & SUGIMOTO, K. (2009) Rif1 and rif2 inhibit localization of tel1 to DNA ends. *Mol Cell,* 33**,** 312-22.

HOCKEMEYER, D., PALM, W., ELSE, T., DANIELS, J. P., TAKAI, K. K., YE, J. Z., KEEGAN, C. E., DE LANGE, T. & HAMMER, G. D. (2007) Telomere protection by mammalian Pot1 requires interaction with Tpp1. *Nat Struct Mol Biol,* 14**,** 754-61.

HOUGHTALING, B. R., CUTTONARO, L., CHANG, W. & SMITH, S. (2004) A dynamic molecular link between the telomere length regulator TRF1 and the chromosome end protector TRF2. *Curr Biol,* 14**,** 1621-31.

HSU, H. L., GILLEY, D., BLACKBURN, E. H. & CHEN, D. J. (1999) Ku is associated with the telomere in mammals. *Proc Natl Acad Sci U S A,* 96**,** 12454-8.

HSU, H. L., GILLEY, D., GALANDE, S. A., HANDE, M. P., ALLEN, B., KIM, S. H., LI, G. C., CAMPISI, J., KOHWI-SHIGEMATSU, T. & CHEN, D. J. (2000) Ku acts in a unique way at the mammalian telomere to prevent end joining. *Genes Dev,* 14**,** 2807-12.

HU, F., WANG, Y., LIU, D., LI, Y., QIN, J. & ELLEDGE, S. J. (2001) Regulation of the Bub2/Bfa1 GAP complex by Cdc5 and cell cycle checkpoints. *Cell,* 107**,** 655-65.

HUBER, M. D., LEE, D. C. & MAIZELS, N. (2002) G4 DNA unwinding by BLM and Sgs1p: substrate specificity and substrate-specific inhibition. *Nucleic Acids Res,* 30**,** 3954-61.

HUGHES, T. R., EVANS, S. K., WEILBAECHER, R. G. & LUNDBLAD, V. (2000) The Est3 protein is a subunit of yeast telomerase. *Curr Biol,* 10**,** 809-12.

IVANOV, E. L., SUGAWARA, N., WHITE, C. I., FABRE, F. & HABER, J. E. (1994) Mutations in XRS2 and RAD50 delay but do not prevent mating-type switching in Saccharomyces cerevisiae. *Mol Cell Biol,* 14**,** 3414-25.

JAIN, D., HEBDEN, A. K., NAKAMURA, T. M., MILLER, K. M. & COOPER, J. P. (2010) HAATI survivors replace canonical telomeres with blocks of generic heterochromatin. *Nature,* 467**,** 223-7.

JASKELIOFF, M., MULLER, F. L., PAIK, J. H., THOMAS, E., JIANG, S., ADAMS, A. C., SAHIN, E., KOST-ALIMOVA, M., PROTOPOPOV, A., CADINANOS, J., HORNER, J. W., MARATOS-FLIER, E. & DEPINHO, R. A. (2010)

Telomerase reactivation reverses tissue degeneration in aged telomerase-deficient mice. *Nature,* 469**,** 102-6.

JAZAYERI, A., FALCK, J., LUKAS, C., BARTEK, J., SMITH, G. C., LUKAS, J. & JACKSON, S. P. (2006) ATM- and cell cycle-dependent regulation of ATR in response to DNA double-strand breaks. *Nat Cell Biol,* 8**,** 37-45.

JIA, X., WEINERT, T. & LYDALL, D. (2004) Mec1 and Rad53 inhibit formation of single-stranded DNA at telomeres of Saccharomyces cerevisiae cdc13-1 mutants. *Genetics,* 166**,** 753-64.

JIN, Y. H., OBERT, R., BURGERS, P. M., KUNKEL, T. A., RESNICK, M. A. & GORDENIN, D. A. (2001) The 3'-->5' exonuclease of DNA polymerase delta can substitute for the 5' flap endonuclease Rad27/Fen1 in processing Okazaki fragments and preventing genome instability. *Proc Natl Acad Sci U S A,* 98**,** 5122-7.

KANOH, J. & ISHIKAWA, F. (2001) spRap1 and spRif1, recruited to telomeres by Taz1, are essential for telomere function in fission yeast. *Curr Biol,* 11**,** 1624-30.

KARLSEDER, J., BROCCOLI, D., DAI, Y., HARDY, S. & DE LANGE, T. (1999) p53- and ATM-dependent apoptosis induced by telomeres lacking TRF2. *Science,* 283**,** 1321-5.

KELLEHER, C., KURTH, I. & LINGNER, J. (2005) Human protection of telomeres 1 (POT1) is a negative regulator of telomerase activity in vitro. *Mol Cell Biol,* 25**,** 808-18.

KHADAROO, B., TEIXEIRA, M. T., LUCIANO, P., ECKERT-BOULET, N., GERMANN, S. M., SIMON, M. N., GALLINA, I., ABDALLAH, P., GILSON, E., GELI, V. & LISBY, M. (2009) The DNA damage response at eroded telomeres and tethering to the nuclear pore complex. *Nat Cell Biol,* 11**,** 980-7.

KIM, E. M. & BURKE, D. J. (2008) DNA damage activates the SAC in an ATM/ATR-dependent manner, independently of the kinetochore. *PLoS Genet,* 4**,** e1000015.

KIM, N. W., PIATYSZEK, M. A., PROWSE, K. R., HARLEY, C. B., WEST, M. D., HO, P. L., COVIELLO, G. M., WRIGHT, W. E., WEINRICH, S. L. & SHAY, J. W. (1994) Specific association of human telomerase activity with immortal cells and cancer. *Science,* 266**,** 2011-5.

KIM, S. H., KAMINKER, P. & CAMPISI, J. (1999) TIN2, a new regulator of telomere length in human cells. *Nat Genet,* 23**,** 405-12.

LAHAYE, A., STAHL, H., THINES-SEMPOUX, D. & FOURY, F. (1991) PIF1: a DNA helicase in yeast mitochondria. *EMBO J,* 10**,** 997-1007.

LANDER, E. S., LINTON, L. M., BIRREN, B., NUSBAUM, C., ZODY, M. C., BALDWIN, J., DEVON, K., DEWAR, K., DOYLE, M., FITZHUGH, W., FUNKE, R., GAGE, D., HARRIS, K., HEAFORD, A., HOWLAND, J., KANN, L., LEHOCZKY, J., LEVINE, R., MCEWAN, P., MCKERNAN, K., MELDRIM, J., MESIROV, J. P., MIRANDA, C., MORRIS, W., NAYLOR, J., RAYMOND, C., ROSETTI, M., SANTOS, R., SHERIDAN, A., SOUGNEZ, C., STANGE-THOMANN, N., STOJANOVIC, N., SUBRAMANIAN, A., WYMAN, D., ROGERS, J., SULSTON, J., AINSCOUGH, R., BECK, S., BENTLEY, D., BURTON, J., CLEE, C., CARTER, N., COULSON, A., DEADMAN, R., DELOUKAS, P., DUNHAM, A., DUNHAM, I., DURBIN, R., FRENCH, L., GRAFHAM, D., GREGORY, S., HUBBARD, T., HUMPHRAY, S., HUNT, A., JONES, M., LLOYD, C., MCMURRAY, A., MATTHEWS, L., MERCER, S., MILNE, S., MULLIKIN, J. C., MUNGALL, A., PLUMB, R., ROSS, M., SHOWNKEEN, R., SIMS, S., WATERSTON, R. H., WILSON, R. K., HILLIER, L. W., MCPHERSON, J. D., MARRA, M. A., MARDIS, E. R., FULTON, L. A., CHINWALLA, A. T., PEPIN, K. H., GISH, W. R., CHISSOE, S. L., WENDL, M. C., DELEHAUNTY, K. D., MINER, T. L., DELEHAUNTY, A., KRAMER, J. B., COOK, L. L., FULTON, R. S., JOHNSON, D. L., MINX, P. J., CLIFTON, S. W., HAWKINS, T., BRANSCOMB, E., PREDKI, P., RICHARDSON, P., WENNING, S., SLEZAK, T., DOGGETT, N., CHENG, J. F., OLSEN, A., LUCAS, S., ELKIN, C., UBERBACHER, E., FRAZIER, M., et al. (2001) Initial sequencing and analysis of the human genome. *Nature,* 409**,** 860-921.

LANSDORP, P. M. (2009) Telomeres and disease. *EMBO J,* 28**,** 2532-40.

LARRIVEE, M. & WELLINGER, R. J. (2006) Telomerase- and capping-independent yeast survivors with alternate telomere states. *Nat Cell Biol,* 8**,** 741-7.

LAWLESS, C., WILKINSON, D. J., YOUNG, A., ADDINALL, S. G. & LYDALL, D. A. (2010) Colonyzer: automated quantification of micro-organism growth characteristics on solid agar. *BMC Bioinformatics,* 11**,** 287.

LAZZARO, F., SAPOUNTZI, V., GRANATA, M., PELLICIOLI, A., VAZE, M., HABER, J. E., PLEVANI, P., LYDALL, D. & MUZI-FALCONI, M. (2008)

Histone methyltransferase Dot1 and Rad9 inhibit single-stranded DNA accumulation at DSBs and uncapped telomeres. *EMBO J,* 27**,** 1502-12.

LEE, H. W., BLASCO, M. A., GOTTLIEB, G. J., HORNER, J. W., 2ND, GREIDER, C. W. & DEPINHO, R. A. (1998a) Essential role of mouse telomerase in highly proliferative organs. *Nature,* 392**,** 569-74.

LEE, S. E., MOORE, J. K., HOLMES, A., UMEZU, K., KOLODNER, R. D. & HABER, J. E. (1998b) Saccharomyces Ku70, mre11/rad50 and RPA proteins regulate adaptation to G2/M arrest after DNA damage. *Cell,* 94**,** 399-409.

LEE, S. J., SCHWARTZ, M. F., DUONG, J. K. & STERN, D. F. (2003) Rad53 phosphorylation site clusters are important for Rad53 regulation and signaling. *Mol Cell Biol,* 23**,** 6300-14.

LEFEBVRE-LEGENDRE, L., VAILLIER, J., BENABDELHAK, H., VELOURS, J., SLONIMSKI, P. P. & DI RAGO, J. P. (2001) Identification of a nuclear gene (FMC1) required for the assembly/stability of yeast mitochondrial F(1)-ATPase in heat stress conditions. *J Biol Chem,* 276**,** 6789-96.

LENDVAY, T. S., MORRIS, D. K., SAH, J., BALASUBRAMANIAN, B. & LUNDBLAD, V. (1996) Senescence mutants of Saccharomyces cerevisiae with a defect in telomere replication identify three additional EST genes. *Genetics,* 144**,** 1399-412.

LI, B., OESTREICH, S. & DE LANGE, T. (2000) Identification of human Rap1: implications for telomere evolution. *Cell,* 101**,** 471-83.

LI, S., MAKOVETS, S., MATSUGUCHI, T., BLETHROW, J. D., SHOKAT, K. M. & BLACKBURN, E. H. (2009) Cdk1-dependent phosphorylation of Cdc13 coordinates telomere elongation during cell-cycle progression. *Cell,* 136**,** 50-61.

LIN, T. T., LETSOLO, B. T., JONES, R. E., ROWSON, J., PRATT, G., HEWAMANA, S., FEGAN, C., PEPPER, C. & BAIRD, D. M. (2010) Telomere dysfunction and fusion during the progression of chronic lymphocytic leukemia: evidence for a telomere crisis. *Blood,* 116**,** 1899-907.

LINGNER, J., CECH, T. R., HUGHES, T. R. & LUNDBLAD, V. (1997) Three Ever Shorter Telomere (EST) genes are dispensable for in vitro yeast telomerase activity. *Proc Natl Acad Sci U S A,* 94**,** 11190-5.

LISBY, M., BARLOW, J. H., BURGESS, R. C. & ROTHSTEIN, R. (2004) Choreography of the DNA damage response: spatiotemporal relationships among checkpoint and repair proteins. *Cell,* 118**,** 699-713.

LIU, D., SAFARI, A., O'CONNOR, M. S., CHAN, D. W., LAEGELER, A., QIN, J. & SONGYANG, Z. (2004) PTOP interacts with POT1 and regulates its localization to telomeres. *Nat Cell Biol,* 6**,** 673-80.

LOAYZA, D. & DE LANGE, T. (2003) POT1 as a terminal transducer of TRF1 telomere length control. *Nature,* 423**,** 1013-8.

LONGHESE, M. P. (2008) DNA damage response at functional and dysfunctional telomeres. *Genes Dev,* 22**,** 125-40.

LONGTINE, M. S., MCKENZIE, A., 3RD, DEMARINI, D. J., SHAH, N. G., WACH, A., BRACHAT, A., PHILIPPSEN, P. & PRINGLE, J. R. (1998) Additional modules for versatile and economical PCR-based gene deletion and modification in Saccharomyces cerevisiae. *Yeast,* 14**,** 953-61.

LOPES, J., DEBRAUWERE, H., BUARD, J. & NICOLAS, A. (2002) Instability of the human minisatellite CEB1 in rad27Delta and dna2-1 replication-deficient yeast cells. *EMBO J,* 21**,** 3201-11.

LU, J. & LIU, Y. (2009) Deletion of Ogg1 DNA glycosylase results in telomere base damage and length alteration in yeast. *EMBO J,* 29**,** 398-409.

LUNDBLAD, V. & BLACKBURN, E. H. (1993) An alternative pathway for yeast telomere maintenance rescues est1- senescence. *Cell,* 73**,** 347-60.

LYDALL, D. (2009) Taming the tiger by the tail: modulation of DNA damage responses by telomeres. *EMBO J,* 28**,** 2174-2187.

LYDALL, D. & WEINERT, T. (1995) Yeast checkpoint genes in DNA damage processing: implications for repair and arrest. *Science,* 270**,** 1488-91.

LYDEARD, J. R., JAIN, S., YAMAGUCHI, M. & HABER, J. E. (2007) Break-induced replication and telomerase-independent telomere maintenance require Pol32. *Nature,* 448**,** 820-3.

MAJKA, J. & BURGERS, P. M. (2003) Yeast Rad17/Mec3/Ddc1: a sliding clamp for the DNA damage checkpoint. *Proc Natl Acad Sci U S A,* 100**,** 2249-54.

MAKOVETS, S. & BLACKBURN, E. H. (2009) DNA damage signalling prevents deleterious telomere addition at DNA breaks. *Nat Cell Biol,* 11**,** 1383-6.

MANTIERO, D., CLERICI, M., LUCCHINI, G. & LONGHESE, M. P. (2007) Dual role for Saccharomyces cerevisiae Tel1 in the checkpoint response to double-strand breaks. *EMBO Rep,* 8**,** 380-7.

MARCAND, S., PARDO, B., GRATIAS, A., CAHUN, S. & CALLEBAUT, I. (2008) Multiple pathways inhibit NHEJ at telomeres. *Genes Dev,* 22**,** 1153-8.

MARINGELE, L. & LYDALL, D. (2002) EXO1-dependent single-stranded DNA at telomeres activates subsets of DNA damage and spindle checkpoint pathways in budding yeast yku70Delta mutants. *Genes Dev,* 16**,** 1919-33.

MARINGELE, L. & LYDALL, D. (2004a) EXO1 plays a role in generating type I and type II survivors in budding yeast. *Genetics,* 166**,** 1641-9.

MARINGELE, L. & LYDALL, D. (2004b) Telomerase- and recombination-independent immortalization of budding yeast. *Genes Dev,* 18**,** 2663-75.

MARINGELE, L. & LYDALL, D. (2005) The PAL-mechanism of chromosome maintenance: causes and consequences. *Cell Cycle,* 4**,** 747-51.

MARRERO, V. A. & SYMINGTON, L. S. (2010) Extensive DNA end processing by exo1 and sgs1 inhibits break-induced replication. *PLoS Genet,* 6**,** e1001007.

MIMITOU, E. P. & SYMINGTON, L. S. (2008) Sae2, Exo1 and Sgs1 collaborate in DNA double-strand break processing. *Nature,* 455**,** 770-4.

MIMITOU, E. P. & SYMINGTON, L. S. (2009) DNA end resection: many nucleases make light work. *DNA Repair (Amst),* 8**,** 983-95.

MIMITOU, E. P. & SYMINGTON, L. S. (2010) Ku prevents Exo1 and Sgs1-dependent resection of DNA ends in the absence of a functional MRX complex or Sae2. *EMBO J,* 29**,** 3358-69.

MINAMINO, T., ORIMO, M., SHIMIZU, I., KUNIEDA, T., YOKOYAMA, M., ITO, T., NOJIMA, A., NABETANI, A., OIKE, Y., MATSUBARA, H., ISHIKAWA, F. & KOMURO, I. (2009) A crucial role for adipose tissue p53 in the regulation of insulin resistance. *Nat Med,* 15**,** 1082-7.

MISHRA, K. & SHORE, D. (1999) Yeast Ku protein plays a direct role in telomeric silencing and counteracts inhibition by rif proteins. *Curr Biol,* 9**,** 1123-6.

MITCHELL, J. R., WOOD, E. & COLLINS, K. (1999) A telomerase component is defective in the human disease dyskeratosis congenita. *Nature,* 402**,** 551-5.

MIYAKE, Y., NAKAMURA, M., NABETANI, A., SHIMAMURA, S., TAMURA, M., YONEHARA, S., SAITO, M. & ISHIKAWA, F. (2009) RPA-like mammalian Ctc1-Stn1-Ten1 complex binds to single-stranded DNA and protects telomeres independently of the Pot1 pathway. *Mol Cell,* 36**,** 193-206.

MIYOSHI, T., KANOH, J., SAITO, M. & ISHIKAWA, F. (2008) Fission yeast Pot1-Tpp1 protects telomeres and regulates telomere length. *Science,* 320**,** 1341-4.

MORIN, I., NGO, H. P., GREENALL, A., ZUBKO, M. K., MORRICE, N. & LYDALL, D. (2008) Checkpoint-dependent phosphorylation of Exo1 modulates the DNA damage response. *EMBO J,* 27**,** 2400-10.

MURGIA, C., PRITCHARD, J. K., KIM, S. Y., FASSATI, A. & WEISS, R. A. (2006) Clonal origin and evolution of a transmissible cancer. *Cell,* 126**,** 477-87.

NAKADA, D., HIRANO, Y. & SUGIMOTO, K. (2004) Requirement of the Mre11 complex and exonuclease 1 for activation of the Mec1 signaling pathway. *Mol Cell Biol,* 24**,** 10016-25.

NAKADA, D., MATSUMOTO, K. & SUGIMOTO, K. (2003) ATM-related Tel1 associates with double-strand breaks through an Xrs2-dependent mechanism. *Genes Dev,* 17**,** 1957-62.

NEGRINI, S., RIBAUD, V., BIANCHI, A. & SHORE, D. (2007) DNA breaks are masked by multiple Rap1 binding in yeast: implications for telomere capping and telomerase regulation. *Genes Dev,* 21**,** 292-302.

NGO, H. P. & LYDALL, D. (2010) Survival and Growth of Yeast without Telomere Capping by Cdc13 in the absence of Sgs1, Exo1, and Rad9. *PLoS Genet,* 6**,** e1001072.

NICOLETTE, M. L., LEE, K., GUO, Z., RANI, M., CHOW, J. M., LEE, S. E. & PAULL, T. T. (2010) Mre11-Rad50-Xrs2 and Sae2 promote 5' strand resection of DNA double-strand breaks. *Nat Struct Mol Biol,* 17**,** 1478-85.

NIU, H., CHUNG, W. H., ZHU, Z., KWON, Y., ZHAO, W., CHI, P., PRAKASH, R., SEONG, C., LIU, D., LU, L., IRA, G. & SUNG, P. (2010) Mechanism of the ATP-dependent DNA end-resection machinery from Saccharomyces cerevisiae. *Nature,* 467**,** 108-11.

NUGENT, C. I., HUGHES, T. R., LUE, N. F. & LUNDBLAD, V. (1996) Cdc13p: a single-strand telomeric DNA-binding protein with a dual role in yeast telomere maintenance. *Science,* 274**,** 249-52.

OHKI, R. & ISHIKAWA, F. (2004) Telomere-bound TRF1 and TRF2 stall the replication fork at telomeric repeats. *Nucleic Acids Res,* 32**,** 1627-37.

OLOVNIKOV, A. M. (1971) [Principle of marginotomy in template synthesis of polynucleotides]. *Dokl Akad Nauk SSSR,* 201**,** 1496-9.

OSTERHAGE, J. L., TALLEY, J. M. & FRIEDMAN, K. L. (2006) Proteasome-dependent degradation of Est1p regulates the cell cycle-restricted assembly of telomerase in Saccharomyces cerevisiae. *Nat Struct Mol Biol,* 13**,** 720-8.

PALM, W., HOCKEMEYER, D., KIBE, T. & DE LANGE, T. (2009) Functional dissection of human and mouse POT1 proteins. *Mol Cell Biol,* 29**,** 471-82.

PARDO, B. & MARCAND, S. (2005) Rap1 prevents telomere fusions by nonhomologous end joining. *EMBO J,* 24**,** 3117-27.

PENNOCK, E., BUCKLEY, K. & LUNDBLAD, V. (2001) Cdc13 delivers separate complexes to the telomere for end protection and replication. *Cell,* 104**,** 387-96.

PETERSON, S. E., STELLWAGEN, A. E., DIEDE, S. J., SINGER, M. S., HAIMBERGER, Z. W., JOHNSON, C. O., TZONEVA, M. & GOTTSCHLING, D. E. (2001) The function of a stem-loop in telomerase RNA is linked to the DNA repair protein Ku. *Nat Genet,* 27**,** 64-7.

PETREACA, R. C., CHIU, H. C., ECKELHOEFER, H. A., CHUANG, C., XU, L. & NUGENT, C. I. (2006) Chromosome end protection plasticity revealed by Stn1p and Ten1p bypass of Cdc13p. *Nat Cell Biol,* 8**,** 748-55.

PIKE, J. E., BURGERS, P. M., CAMPBELL, J. L. & BAMBARA, R. A. (2009) Pif1 helicase lengthens some Okazaki fragment flaps necessitating Dna2 nuclease/helicase action in the two-nuclease processing pathway. *J Biol Chem,* 284**,** 25170-80.

PITT, C. W. & COOPER, J. P. (2010) Pot1 inactivation leads to rampant telomere resection and loss in one cell cycle. *Nucleic Acids Res*.

POBIEGA, S. & MARCAND, S. (2010) Dicentric breakage at telomere fusions. *Genes Dev,* 24**,** 720-33.

POLOTNIANKA, R. M., LI, J. & LUSTIG, A. J. (1998) The yeast Ku heterodimer is essential for protection of the telomere against nucleolytic and recombinational activities. *Curr Biol,* 8**,** 831-4.

PORTER, S. E., GREENWELL, P. W., RITCHIE, K. B. & PETES, T. D. (1996) The DNA-binding protein Hdf1p (a putative Ku homologue) is required for maintaining normal telomere length in Saccharomyces cerevisiae. *Nucleic Acids Res,* 24**,** 582-5.

RAICES, M., VERDUN, R. E., COMPTON, S. A., HAGGBLOM, C. I., GRIFFITH, J. D., DILLIN, A. & KARLSEDER, J. (2008) C. elegans telomeres contain G-strand and C-strand overhangs that are bound by distinct proteins. *Cell,* 132**,** 745-57.

RASCHLE, M., KNIPSCHEER, P., ENOIU, M., ANGELOV, T., SUN, J., GRIFFITH, J. D., ELLENBERGER, T. E., SCHARER, O. D. & WALTER, J. C. (2008)

Mechanism of replication-coupled DNA interstrand crosslink repair. *Cell,* 134**,** 969-80.

REAGAN, M. S., PITTENGER, C., SIEDE, W. & FRIEDBERG, E. C. (1995) Characterization of a mutant strain of Saccharomyces cerevisiae with a deletion of the RAD27 gene, a structural homolog of the RAD2 nucleotide excision repair gene. *J Bacteriol,* 177**,** 364-71.

RIBEYRE, C., LOPES, J., BOULE, J. B., PIAZZA, A., GUEDIN, A., ZAKIAN, V. A., MERGNY, J. L. & NICOLAS, A. (2009) The yeast Pif1 helicase prevents genomic instability caused by G-quadruplex-forming CEB1 sequences in vivo. *PLoS Genet,* 5**,** e1000475.

RITCHIE, K. B., MALLORY, J. C. & PETES, T. D. (1999) Interactions of TLC1 (which encodes the RNA subunit of telomerase), TEL1, and MEC1 in regulating telomere length in the yeast Saccharomyces cerevisiae. *Mol Cell Biol,* 19**,** 6065-75.

RONG, Y. S. (2008) Telomere capping in Drosophila: dealing with chromosome ends that most resemble DNA breaks. *Chromosoma,* 117**,** 235-42.

ROSSI, M. L., PIKE, J. E., WANG, W., BURGERS, P. M., CAMPBELL, J. L. & BAMBARA, R. A. (2008) Pif1 helicase directs eukaryotic Okazaki fragments toward the two-nuclease cleavage pathway for primer removal. *J Biol Chem,* 283**,** 27483-93.

ROZEN, S. & SKALETSKY, H. (2000) Primer3 on the WWW for general users and for biologist programmers. *Methods Mol Biol,* 132**,** 365-86.

SAHARIA, A., TEASLEY, D. C., DUXIN, J. P., DAO, B., CHIAPPINELLI, K. B. & STEWART, S. A. (2010) FEN1 ensures telomere stability by facilitating replication fork re-initiation. *J Biol Chem,* 285**,** 27057-66.

SAMPER, E., GOYTISOLO, F. A., SLIJEPCEVIC, P., VAN BUUL, P. P. & BLASCO, M. A. (2000) Mammalian Ku86 protein prevents telomeric fusions independently of the length of TTAGGG repeats and the G-strand overhang. *EMBO Rep,* 1**,** 244-52.

SANCHEZ, Y., BACHANT, J., WANG, H., HU, F., LIU, D., TETZLAFF, M. & ELLEDGE, S. J. (1999) Control of the DNA damage checkpoint by chk1 and rad53 protein kinases through distinct mechanisms. *Science,* 286**,** 1166-71.

SANDELL, L. L. & ZAKIAN, V. A. (1993) Loss of a yeast telomere: arrest, recovery, and chromosome loss. *Cell,* 75**,** 729-39.

SARTORI, A. A., LUKAS, C., COATES, J., MISTRIK, M., FU, S., BARTEK, J., BAER, R., LUKAS, J. & JACKSON, S. P. (2007) Human CtIP promotes DNA end resection. *Nature,* 450**,** 509-14.

SCHAETZLEIN, S., KODANDARAMIREDDY, N. R., JU, Z., LECHEL, A., STEPCZYNSKA, A., LILLI, D. R., CLARK, A. B., RUDOLPH, C., KUHNEL, F., WEI, K., SCHLEGELBERGER, B., SCHIRMACHER, P., KUNKEL, T. A., GREENBERG, R. A., EDELMANN, W. & RUDOLPH, K. L. (2007) Exonuclease-1 deletion impairs DNA damage signaling and prolongs lifespan of telomere-dysfunctional mice. *Cell,* 130**,** 863-77.

SCHULZ, V. P. & ZAKIAN, V. A. (1994) The saccharomyces PIF1 DNA helicase inhibits telomere elongation and de novo telomere formation. *Cell,* 76**,** 145-55.

SCHWARTZ, M. F., DUONG, J. K., SUN, Z., MORROW, J. S., PRADHAN, D. & STERN, D. F. (2002) Rad9 phosphorylation sites couple Rad53 to the Saccharomyces cerevisiae DNA damage checkpoint. *Mol Cell,* 9**,** 1055-65.

SEGURADO, M. & DIFFLEY, J. F. (2008) Separate roles for the DNA damage checkpoint protein kinases in stabilizing DNA replication forks. *Genes Dev,* 22**,** 1816-27.

SFEIR, A., KABIR, S., VAN OVERBEEK, M., CELLI, G. B. & DE LANGE, T. (2010) Loss of Rap1 induces telomere recombination in the absence of NHEJ or a DNA damage signal. *Science,* 327**,** 1657-61.

SFEIR, A., KOSIYATRAKUL, S. T., HOCKEMEYER, D., MACRAE, S. L., KARLSEDER, J., SCHILDKRAUT, C. L. & DE LANGE, T. (2009) Mammalian telomeres resemble fragile sites and require TRF1 for efficient replication. *Cell,* 138**,** 90-103.

SHACHAR, R., UNGAR, L., KUPIEC, M., RUPPIN, E. & SHARAN, R. (2008) A systems-level approach to mapping the telomere length maintenance gene circuitry. *Mol Syst Biol,* 4**,** 172.

SHAMPAY, J. & BLACKBURN, E. H. (1988) Generation of telomere-length heterogeneity in Saccharomyces cerevisiae. *Proc Natl Acad Sci U S A,* 85**,** 534-8.

SHORE, D. & NASMYTH, K. (1987) Purification and cloning of a DNA binding protein from yeast that binds to both silencer and activator elements. *Cell,* 51**,** 721-32.

SINGER, M. S. & GOTTSCHLING, D. E. (1994) TLC1: template RNA component of Saccharomyces cerevisiae telomerase. *Science,* 266**,** 404-9.

SINGER, M. S., KAHANA, A., WOLF, A. J., MEISINGER, L. L., PETERSON, S. E., GOGGIN, C., MAHOWALD, M. & GOTTSCHLING, D. E. (1998) Identification of high-copy disruptors of telomeric silencing in Saccharomyces cerevisiae. *Genetics,* 150**,** 613-32.

SMITH, S., BANERJEE, S., RILO, R. & MYUNG, K. (2008) Dynamic regulation of single-stranded telomeres in Saccharomyces cerevisiae. *Genetics,* 178**,** 693-701.

STANSEL, R. M., DE LANGE, T. & GRIFFITH, J. D. (2001) T-loop assembly in vitro involves binding of TRF2 near the 3' telomeric overhang. *EMBO J,* 20**,** 5532-40.

STARK, C., BREITKREUTZ, B. J., REGULY, T., BOUCHER, L., BREITKREUTZ, A. & TYERS, M. (2006) BioGRID: a general repository for interaction datasets. *Nucleic Acids Res,* 34**,** D535-9.

STITH, C. M., STERLING, J., RESNICK, M. A., GORDENIN, D. A. & BURGERS, P. M. (2008) Flexibility of eukaryotic Okazaki fragment maturation through regulated strand displacement synthesis. *J Biol Chem,* 283**,** 34129-40.

SUN, Z., HSIAO, J., FAY, D. S. & STERN, D. F. (1998) Rad53 FHA domain associated with phosphorylated Rad9 in the DNA damage checkpoint. *Science,* 281**,** 272-4.

SUROVTSEVA, Y. V., CHURIKOV, D., BOLTZ, K. A., SONG, X., LAMB, J. C., WARRINGTON, R., LEEHY, K., HEACOCK, M., PRICE, C. M. & SHIPPEN, D. E. (2009) Conserved telomere maintenance component 1 interacts with STN1 and maintains chromosome ends in higher eukaryotes. *Mol Cell,* 36**,** 207-18.

SUSSEL, L., VANNIER, D. & SHORE, D. (1995) Suppressors of defective silencing in yeast: effects on transcriptional repression at the HMR locus, cell growth and telomere structure. *Genetics,* 141**,** 873-88.

SWEENEY, F. D., YANG, F., CHI, A., SHABANOWITZ, J., HUNT, D. F. & DUROCHER, D. (2005) Saccharomyces cerevisiae Rad9 acts as a Mec1 adaptor to allow Rad53 activation. *Curr Biol,* 15**,** 1364-75.

TAKAI, H., SMOGORZEWSKA, A. & DE LANGE, T. (2003) DNA damage foci at dysfunctional telomeres. *Curr Biol,* 13**,** 1549-56.

TENG, S. C. & ZAKIAN, V. A. (1999) Telomere-telomere recombination is an efficient bypass pathway for telomere maintenance in Saccharomyces cerevisiae. *Mol Cell Biol,* 19**,** 8083-93.

TEO, S. H. & JACKSON, S. P. (2001) Telomerase subunit overexpression suppresses telomere-specific checkpoint activation in the yeast yku80 mutant. *EMBO Rep,* 2**,** 197-202.

TING, N. S., YU, Y., POHORELIC, B., LEES-MILLER, S. P. & BEATTIE, T. L. (2005) Human Ku70/80 interacts directly with hTR, the RNA component of human telomerase. *Nucleic Acids Res,* 33**,** 2090-8.

TOMKINSON, A. E., BARDWELL, A. J., BARDWELL, L., TAPPE, N. J. & FRIEDBERG, E. C. (1993) Yeast DNA repair and recombination proteins Rad1 and Rad10 constitute a single-stranded-DNA endonuclease. *Nature,* 362**,** 860-2.

TONG, A. H. & BOONE, C. (2006) Synthetic genetic array analysis in Saccharomyces cerevisiae. *Methods Mol Biol,* 313**,** 171-92.

TORRES, J. Z., SCHNAKENBERG, S. L. & ZAKIAN, V. A. (2004) Saccharomyces cerevisiae Rrm3p DNA helicase promotes genome integrity by preventing replication fork stalling: viability of rrm3 cells requires the intra-S-phase checkpoint and fork restart activities. *Mol Cell Biol,* 24**,** 3198-212.

TRAN, P. T., ERDENIZ, N., DUDLEY, S. & LISKAY, R. M. (2002) Characterization of nuclease-dependent functions of Exo1p in Saccharomyces cerevisiae. *DNA Repair (Amst),* 1**,** 895-912.

TSOLOU, A. & LYDALL, D. (2007) Mrc1 protects uncapped budding yeast telomeres from exonuclease EXO1. *DNA Repair (Amst),* 6**,** 1607-17.

TSUBOUCHI, H. & OGAWA, H. (2000) Exo1 roles for repair of DNA double-strand breaks and meiotic crossing over in Saccharomyces cerevisiae. *Mol Biol Cell,* 11**,** 2221-33.

UNGAR, L., YOSEF, N., SELA, Y., SHARAN, R., RUPPIN, E. & KUPIEC, M. (2009) A genome-wide screen for essential yeast genes that affect telomere length maintenance. *Nucleic Acids Res,* 37**,** 3840-9.

USUI, T., FOSTER, S. S. & PETRINI, J. H. (2009) Maintenance of the DNA-damage checkpoint requires DNA-damage-induced mediator protein oligomerization. *Mol Cell,* 33**,** 147-59.

USUI, T., OGAWA, H. & PETRINI, J. H. (2001) A DNA damage response pathway controlled by Tel1 and the Mre11 complex. *Mol Cell,* 7**,** 1255-66.

VAN DYCK, E., FOURY, F., STILLMAN, B. & BRILL, S. J. (1992) A single-stranded DNA binding protein required for mitochondrial DNA replication in S. cerevisiae is homologous to E. coli SSB. *EMBO J,* 11**,** 3421-30.

VAN STEENSEL, B. & DE LANGE, T. (1997) Control of telomere length by the human telomeric protein TRF1. *Nature,* 385**,** 740-3.

VEGA, L. R., PHILLIPS, J. A., THORNTON, B. R., BENANTI, J. A., ONIGBANJO, M. T., TOCZYSKI, D. P. & ZAKIAN, V. A. (2007) Sensitivity of yeast strains with long G-tails to levels of telomere-bound telomerase. *PLoS Genet,* 3**,** e105.

VENCLOVAS, C. & THELEN, M. P. (2000) Structure-based predictions of Rad1, Rad9, Hus1 and Rad17 participation in sliding clamp and clamp-loading complexes. *Nucleic Acids Res,* 28**,** 2481-93.

VODENICHAROV, M. D., LATERREUR, N. & WELLINGER, R. J. (2010) Telomere capping in non-dividing yeast cells requires Yku and Rap1. *EMBO J***,** In Press.

VODENICHAROV, M. D. & WELLINGER, R. J. (2006) DNA degradation at unprotected telomeres in yeast is regulated by the CDK1 (Cdc28/Clb) cell-cycle kinase. *Mol Cell,* 24**,** 127-37.

VULLIAMY, T., MARRONE, A., GOLDMAN, F., DEARLOVE, A., BESSLER, M., MASON, P. J. & DOKAL, I. (2001) The RNA component of telomerase is mutated in autosomal dominant dyskeratosis congenita. *Nature,* 413**,** 432-5.

VULLIAMY, T., MARRONE, A., SZYDLO, R., WALNE, A., MASON, P. J. & DOKAL, I. (2004) Disease anticipation is associated with progressive telomere shortening in families with dyskeratosis congenita due to mutations in TERC. *Nat Genet,* 36**,** 447-9.

WAGA, S. & STILLMAN, B. (1998) The DNA replication fork in eukaryotic cells. *Annu Rev Biochem,* 67**,** 721-51.

WANG, Y., GHOSH, G. & HENDRICKSON, E. A. (2009) Ku86 represses lethal telomere deletion events in human somatic cells. *Proc Natl Acad Sci U S A,* 106**,** 12430-5.

WATSON, J. D. (1972) Origin of concatemeric T7 DNA. *Nat New Biol,* 239**,** 197-201.

WEI, K., CLARK, A. B., WONG, E., KANE, M. F., MAZUR, D. J., PARRIS, T., KOLAS, N. K., RUSSELL, R., HOU, H., JR., KNEITZ, B., YANG, G., KUNKEL, T. A., KOLODNER, R. D., COHEN, P. E. & EDELMANN, W. (2003) Inactivation of Exonuclease 1 in mice results in DNA mismatch repair defects, increased cancer susceptibility, and male and female sterility. *Genes Dev,* 17**,** 603-14.

WILSON, T. E., GRAWUNDER, U. & LIEBER, M. R. (1997) Yeast DNA ligase IV mediates non-homologous DNA end joining. *Nature,* 388**,** 495-8.

WOTTON, D. & SHORE, D. (1997) A novel Rap1p-interacting factor, Rif2p, cooperates with Rif1p to regulate telomere length in Saccharomyces cerevisiae. *Genes Dev,* 11**,** 748-60.

WU, J., CARMEN, A. A., KOBAYASHI, R., SUKA, N. & GRUNSTEIN, M. (2001) HDA2 and HDA3 are related proteins that interact with and are essential for the activity of the yeast histone deacetylase HDA1. *Proc Natl Acad Sci U S A,* 98**,** 4391-6.

WU, L., MULTANI, A. S., HE, H., COSME-BLANCO, W., DENG, Y., DENG, J. M., BACHILO, O., PATHAK, S., TAHARA, H., BAILEY, S. M., BEHRINGER, R. R. & CHANG, S. (2006) Pot1 deficiency initiates DNA damage checkpoint activation and aberrant homologous recombination at telomeres. *Cell,* 126**,** 49-62.

WYSOCKI, R., JAVAHERI, A., ALLARD, S., SHA, F., COTE, J. & KRON, S. J. (2005) Role of Dot1-dependent histone H3 methylation in G1 and S phase DNA damage checkpoint functions of Rad9. *Mol Cell Biol,* 25**,** 8430-43.

XU, L., PETREACA, R. C., GASPARYAN, H. J., VU, S. & NUGENT, C. I. (2009) TEN1 is essential for CDC13-mediated telomere capping. *Genetics,* 183**,** 793-810.

YAMAGUCHI, H., CALADO, R. T., LY, H., KAJIGAYA, S., BAERLOCHER, G. M., CHANOCK, S. J., LANSDORP, P. M. & YOUNG, N. S. (2005) Mutations in TERT, the gene for telomerase reverse transcriptase, in aplastic anemia. *N Engl J Med,* 352**,** 1413-24.

YAMASHITA, K., SHINOHARA, M. & SHINOHARA, A. (2004) Rad6-Bre1-mediated histone H2B ubiquitylation modulates the formation of double-strand breaks during meiosis. *Proc Natl Acad Sci U S A,* 101**,** 11380-5.

YE, J., LENAIN, C., BAUWENS, S., RIZZO, A., SAINT-LEGER, A., POULET, A., BENARROCH, D., MAGDINIER, F., MORERE, J., AMIARD, S., VERHOEYEN, E., BRITTON, S., CALSOU, P., SALLES, B., BIZARD, A., NADAL, M., SALVATI, E., SABATIER, L., WU, Y., BIROCCIO, A., LONDONO-VALLEJO, A., GIRAUD-PANIS, M. J. & GILSON, E. (2010) TRF2 and apollo cooperate with topoisomerase 2alpha to protect human telomeres from replicative damage. *Cell,* 142**,** 230-42.

YE, J. Z., HOCKEMEYER, D., KRUTCHINSKY, A. N., LOAYZA, D., HOOPER, S. M., CHAIT, B. T. & DE LANGE, T. (2004) POT1-interacting protein PIP1: a

telomere length regulator that recruits POT1 to the TIN2/TRF1 complex. *Genes Dev,* 18**,** 1649-54.

ZHAO, X. & ROTHSTEIN, R. (2002) The Dun1 checkpoint kinase phosphorylates and regulates the ribonucleotide reductase inhibitor Sml1. *Proc Natl Acad Sci U S A,* 99**,** 3746-51.

ZHONG, Z., SHIUE, L., KAPLAN, S. & DE LANGE, T. (1992) A mammalian factor that binds telomeric TTAGGG repeats in vitro. *Mol Cell Biol,* 12**,** 4834-43.

ZHOU, J., MONSON, E. K., TENG, S. C., SCHULZ, V. P. & ZAKIAN, V. A. (2000) Pif1p helicase, a catalytic inhibitor of telomerase in yeast. *Science,* 289**,** 771-4.

ZHU, Z., CHUNG, W. H., SHIM, E. Y., LEE, S. E. & IRA, G. (2008) Sgs1 helicase and two nucleases Dna2 and Exo1 resect DNA double-strand break ends. *Cell,* 134**,** 981-94.

ZOU, L. & ELLEDGE, S. J. (2003) Sensing DNA damage through ATRIP recognition of RPA-ssDNA complexes. *Science,* 300**,** 1542-8.

ZOU, L., LIU, D. & ELLEDGE, S. J. (2003) Replication protein A-mediated recruitment and activation of Rad17 complexes. *Proc Natl Acad Sci U S A,* 100**,** 13827-32.

ZUBKO, M. K., GUILLARD, S. & LYDALL, D. (2004) Exo1 and Rad24 differentially regulate generation of ssDNA at telomeres of Saccharomyces cerevisiae cdc13-1 mutants. *Genetics,* 168**,** 103-15.

ZUBKO, M. K. & LYDALL, D. (2006) Linear chromosome maintenance in the absence of essential telomere-capping proteins. *Nat Cell Biol,* 8**,** 734-40.

ZUBKO, M. K., MARINGELE, L., FOSTER, S. S. & LYDALL, D. (2006) Detecting repair intermediates in vivo: effects of DNA damage response genes on single-stranded DNA accumulation at uncapped telomeres in budding yeast. *Methods Enzymol,* 409**,** 285-300.

9 Publications

1. Addinall SG, Downey M, Yu M, Zubko MK, Dewar J, Leake A, Hallinan J, Shaw O, James K, Wilkinson DJ, Wipat A, Durocher D, Lydall D (2008) A genomewide suppressor and enhancer analysis of cdc13-1 reveals varied cellular processes influencing telomere capping in *Saccharomyces cerevisiae*. ***Genetics***, 180(4):2251-66.

2. Dewar JM, Lydall D (2010) Telomere replication: Mre11 leads the way. ***Mol Cell***, 38(6):777-9.

3. Dewar JM, Lydall D (2010) Pif1- and Exo1-dependent nucleases coordinate checkpoint activation following telomere uncapping. ***EMBO J***, 29(23):4020-34.

DOI: 10.1534/genetics.108.092577

A Genomewide Suppressor and Enhancer Analysis of *cdc13-1* Reveals Varied Cellular Processes Influencing Telomere Capping in *Saccharomyces cerevisiae*

S. G. Addinall,* M. Downey,†,‡ M. Yu,* M. K. Zubko,*,[1] J. Dewar,* A. Leake,* J. Hallinan,*,§ O. Shaw,*,§ K. James,*,§ D. J. Wilkinson,*, A. Wipat,*,§ D. Durocher†,‡ and D. Lydall*,[2]**

*Centre for Integrated Systems Biology of Ageing and Nutrition, Ageing Research Laboratories, Institute for Ageing and Health, Newcastle University, Campus for Ageing and Vitality, Newcastle upon Tyne NE4 5PL, United Kingdom, †Samuel Lunenfeld Research Institute, Toronto, Ontario M5G 1X5, Canada, ‡Department of Molecular Genetics, University of Toronto, Ontario M5S 1A8, Canada, **School of Mathematics and Statistics, Newcastle University, Newcastle upon Tyne NE1 7RU, United Kingdom and §School of Computing Science, Newcastle University, Newcastle upon Tyne NE1 7RU, United Kingdom

Manuscript received June 11, 2008
Accepted for publication September 25, 2008

ABSTRACT

In *Saccharomyces cerevisiae*, Cdc13 binds telomeric DNA to recruit telomerase and to "cap" chromosome ends. In temperature-sensitive *cdc13-1* mutants telomeric DNA is degraded and cell-cycle progression is inhibited. To identify novel proteins and pathways that cap telomeres, or that respond to uncapped telomeres, we combined *cdc13-1* with the yeast gene deletion collection and used high-throughput spot-test assays to measure growth. We identified 369 gene deletions, in eight different phenotypic classes, that reproducibly demonstrated subtle genetic interactions with the *cdc13-1* mutation. As expected, we identified DNA damage checkpoint, nonsense-mediated decay and telomerase components in our screen. However, we also identified genes affecting casein kinase II activity, cell polarity, mRNA degradation, mitochondrial function, phosphate transport, iron transport, protein degradation, and other functions. We also identified a number of genes of previously unknown function that we term *RTC*, for *r*estriction of *t*elomere *c*apping, or *MTC*, for *m*aintenance of *t*elomere *c*apping. It seems likely that many of the newly identified pathways/processes that affect growth of budding yeast *cdc13-1* mutants will play evolutionarily conserved roles at telomeres. The high-throughput spot-testing approach that we describe is generally applicable and could aid in understanding other aspects of eukaryotic cell biology.

LINEAR chromosomes are a feature of all eukaryotes. The single-celled model eukaryote *Saccharomyces cerevisiae*, for example, has 16 linear chromosomes with ends that are, in principle, no different from double-stranded breaks elsewhere in the genome. However, whereas *S. cerevisiae* cells can tolerate 32 or more chromosome ends throughout its cell cycle, a single double-stranded DNA break (DSB) elsewhere in the genome elicits a swift and precise response (Sandell and Zakian 1993). This response includes checkpoint activation, which leads to cell-cycle arrest prior to repair of the break. The difference between DSBs and chromsosome ends, then, comes down to specific nucleoprotein complexes that occupy the ends of chromosomes to form a structure referred to as a telomere (Longhese 2008).

A further issue at the ends of chromosomes is the inability of semi-conservative DNA replication to reach the very ends of linear double-stranded DNA molecules—the "end replication problem" (Olovnikov 1973). Telomerase (Greider and Blackburn 1985), a telomere-specific reverse-transcriptase complex, solves this problem by adding G-rich repeat sequences to the 3′-end of chromosomes, using a bound RNA molecule as a template. As a result, eukaryotic chromosomes have long stretches of TG repeats at their ends. These sequences serve as a binding platform for proteins involved in end protection and telomerase recruitment.

The length of telomere repeat sequences in growing and dividing cells depends on a balance between shortening, due to the end replication problem, and lengthening, due to the actions of telomerase. Should the length of telomere repeat sequences fall below a critical level, budding yeast and mammalian cells stop dividing in a checkpoint-dependent process referred to as senescence (Reaper *et al.* 2004). In rare instances, cells can evade this fate by employing telomerase-independent, recombination-based pathways for maintaining a functional number of TG repeats at the ends of chromosomes. In cells that lack telomerase—as is the case for the majority of human somatic cells—telomere length reduces with each cellular division until senescence is

[1]*Present address:* School of Biology, Chemistry and Health Science, Manchester Metropolitan University, John Dalton Bldg., Manchester M1 5GD, United Kingdom.

[2]*Corresponding author:* Centre for Integrated Systems Biology of Ageing and Nutrition, Ageing Research Laboratories, Institute for Ageing and Health, Newcastle University, Campus for Ageing and Vitality, Newcastle upon Tyne NE4 5PL, United Kingdom. E-mail: d.a.lydall@ncl.ac.uk

induced at a critical length. This is considered to serve as a mechanism for determining a finite cellular life span, and thus the link between telomeres, cancer, and aging has been of wide interest (Blasco 2007; Cheung and Deng 2008). A fuller understanding of telomere homeostasis is therefore an important goal, critical for understanding cellular senescence and the mechanisms by which the response to DNA damage is appropriately regulated and/or limited in eukaryotic cells. *S. cerevisiae* provides an excellent model in which to carry out such studies.

In *S. cerevisiae*, Cdc13 is a single-stranded DNA (ssDNA)-binding protein that binds to short ssDNA overhangs at telomeres and plays at least two important roles at telomeres: (1) recruitment of telomerase (Nugent *et al.* 1996) and (2) telomere capping (Garvik *et al.* 1995). The *cdc13-1* point mutation confers temperature sensitivity such that Cdc13-1 is proficient in telomere capping at the permissive temperature (23°) but deficient at the nonpermissive temperature (>26°). Thus, in *cdc13-1* mutant cells grown at ≥26°, telomeres become "uncapped" and recognized as sites of DNA damage, eliciting a checkpoint response (Garvik *et al.* 1995). Once uncapped, the telomeres are vulnerable to 5′–3′ exonuclease activity, which can generate extensive regions of ssDNA, thus amplifying the DNA damage signal.

Applying a temperature shift to *S. cerevisiae* cells harboring the *cdc13-1* mutation is a simple method by which telomere capping can be compromised and the response to DNA damage at chromosome ends can be induced and studied. For this reason *cdc13-1* has proven to be an informative tool for identifying genes whose products function at uncapped telomeres and in the DNA damage response. For example, *cdc13-1* was the primary tool used to show that Mec1, Mec3, Rad53 (Mec2), Rad17, and Rad24 are involved in DNA damage checkpoint control (Weinert *et al.* 1994). Similarly, deletion of the *EXO1* gene, which encodes a 5′–3′ exonuclease, allows *cdc13-1* mutant cells to grow and divide at 27°, thus efficiently suppressing the temperature-sensitive telomere-capping defect (Maringele and Lydall 2002; Zubko *et al.* 2004). This led to the discovery that Exo1 resects the ends of unprotected telomeres in at least two different situations (*cdc13-1* mutants and *yku70*Δ cells), resulting in long stretches of ssDNA, which, in turn, act as a potent DNA damage signal (Maringele and Lydall 2002; Zubko *et al.* 2004). Importantly, the role of *EXO1* and checkpoint genes in responding to uncapped telomeres appears to be conserved in mammals because it has been shown that deletion of exonuclease-1 or the CDK inhibitor p21 leads to an extension of life span in a mouse telomerase knockout model (Choudhury *et al.* 2007; Schaetzlein *et al.* 2007). Therefore the identification of new genetic interactions similar to those between *RAD9* or *EXO1* and *cdc13-1* in yeast has the potential to identify novel conserved molecular pathways involved in the response to telomere uncapping, for example (Maringele and Lydall 2002; Zubko *et al.* 2004).

Here we describe a genomewide screen for gene deletion mutations that demonstrate synthetic genetic, suppressor, or enhancer interactions with the *cdc13-1* mutation. Previously, we described the identification and characterization of a novel, evolutionarily conserved, telomere regulator complex (Downey *et al.* 2006). The results of the complete screen reveals that multiple cellular processes influence telomere capping and/or the response to telomere uncapping.

MATERIALS AND METHODS

Genomewide screens: During the progression of this study, approaches to performing genomewide genetic screens evolved considerably; for example, yeast growth tests progressed from manual to robotic spotting and from scoring by eye to scoring by photography and automated image analysis. The evolution of the screening process is described in supplemental material and supplemental Table S1.

Strains: Strains used in this study are described in supplemental Table S2.

Synthetic genetic array: The synthetic genetic array (SGA) technique (Tong *et al.* 2001; Tong and Boone 2006) was used to combine a genomewide collection of gene deletions with the recessive *cdc13-1* temperature-sensitive mutation, flanked by the selectable *LEU2* and *URA3* markers (Tong *et al.* 2001; Downey *et al.* 2006; Tong and Boone 2006). This technique was first performed on a Virtek Versarray Robot (BioRad) in 768-spot format, using a 768- × 1-mm pin tool and, subsequently, in 1536-spot format on a Biomatrix BM3-09 robot (S&P Robotics, Toronto) using a 384- × 1-mm pin tool (supplemental Table S1).

Temperature oscillation: The UP–DOWN assay was performed in a programmable Sanyo 153 incubator. Plates were incubated at 20° for 5 hr followed by 36° for 5 hr, and this cycle was repeated a total of three times. Incubation was then continued at 20° for the remainder of the experiment and plates were photographed as described above.

Gene ontology analysis: Version 2.4.0 of GOStats (Falcon and Gentleman 2007) was used with the cutoff set to $P = 0.00001$ (empirically determined as returning no overrepresented terms from random lists of genes) and the test-type set as conditional. Genes identified in this study were compared to a list of 4292 screened genes, not including slow growers, strains that consistently perform poorly in SGA analysis (Tong *et al.* 2001), or genes encoding markers used in strain construction (*e.g.*, *CAN1*). Gene ontology (GO) term annotations were current as of December 18, 2007.

Gene list analysis: For systematic analysis of ontology annotations and convenient access to gene functional information, OSPREY (Breitkreutz *et al.* 2003) was used to access the Biogrid database (Stark *et al.* 2006; Breitkreutz *et al.* 2008).

Hierarchical clustering: Data from multiple high-throughput studies were collated and converted to a simplified scoring system as described in the supplemental Methods. These were then analyzed alongside our own data by hierarchical clustering using Cluster 3.0 for Mac OS X (Michiel de Hoon, Seiya Imoto, and Satoru Miyano, Human Genome Center, University of Tokyo). Genes were clustered by centroid linkage using the "absolute correlation (uncentered)" similarity metric (Eisen *et al.* 1998) based on properties defined in 10 cate-

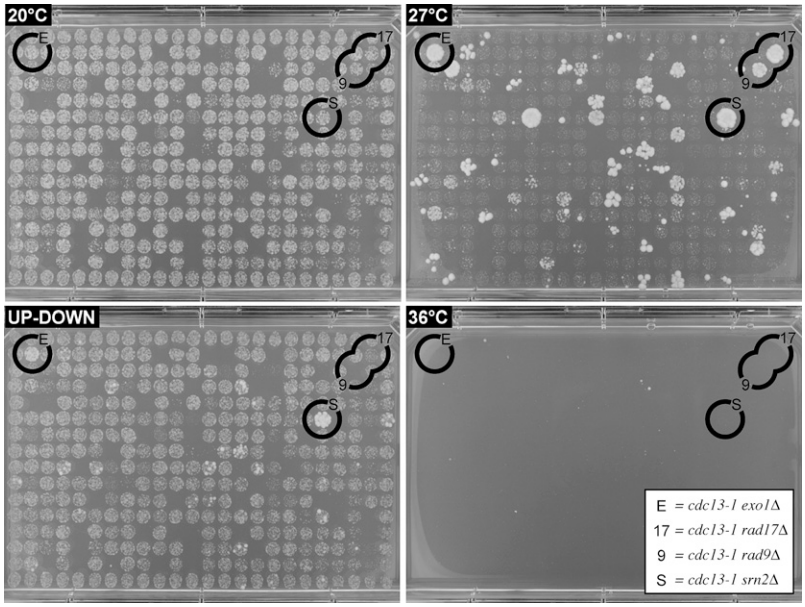

FIGURE 1.—High-throughput robotic yeast growth assay in 384-spot format. A total of 384 yeast strains were spotted onto four solid agar plates, each of which was incubated under different conditions, indicated in the top left corner of each panel (20°, 27°, 36°, and the UP–DOWN assay). Circles are drawn around examples of UD^S (9, *rad9*Δ; 17, *rad17*Δ) and UD^R (E, *exo1*Δ; S, *srn2*Δ) strains, all four of which are also *cdc13-1* suppressors.

gories: suppressors, enhancers, UP–DOWN assay, telomere length (ASKREE *et al.* 2004; GATBONTON *et al.* 2006; SHACHAR *et al.* 2008), nonsense-mediated decay upregulation (HE *et al.* 2003), regulation in response to MMS (JELINSKY and SAMSON 1999), sensitivity to MMS (CHANG *et al.* 2002), sensitivity to UV (BIRRELL *et al.* 2001), sensitivity to ionizing radiation (BENNETT *et al.* 2001), and requirement for replication of Brome mosaic virus (KUSHNER *et al.* 2003); see supplemental Methods. Clustering was displayed using Treeview (SALDANHA 2004).

RESULTS

A screen for gene deletions that suppress or enhance *cdc13-1* temperature sensitivity was undertaken using the SGA technique (TONG *et al.* 2001; TONG and BOONE 2006) as described in MATERIALS AND METHODS and supplemental Methods. High-throughput yeast spot tests (MATERIALS AND METHODS; supplemental Methods; Figure 1) were used to identify gene deletions, which allowed growth of strains carrying the *cdc13-1* mutation at the otherwise nonpermissive temperature of 27°. Five of these (identified during initial screens 1 and 2; supplemental Table S1) were described previously (DOWNEY *et al.* 2006). At the end of a comprehensive screening process during which a minimum of 4 and a maximum of 15 biological replicates for each viable gene deletion had been tested (supplemental Table S1), a high confidence list of 238 gene deletion suppressors of *cdc13-1* temperature sensitivity was obtained (Table 1). Of these 238, 37 strains that grew at the higher nonpermissive temperature of 28° (screens 3 and 4, supplemental Table S1) were classed as strong suppressors (Table 1). A number of gene deletions that have previously been described as *cdc13-1* suppressors were identified in our screen (Table 2). These included deletions of *RAD9*, *RAD17*, *RAD24*, *EXO1*, and *CHK1* among the group of strong suppressors (Table 1), consistent with previous studies (*e.g.*, MARINGELE and LYDALL 2002; ZUBKO *et al.* 2004).

Our approach also allowed us to identify gene deletions that were lethal or sick in combination with *cdc13-1* because double mutants were either missing or poor growers after SGA (MATERIALS AND METHODS; supplemental Methods; supplemental Figure S2). Twenty genes demonstrated synthetic lethal and 32 showed synthetic-sick interactions with *cdc13-1* at 20° (Table 3).

In the DISCUSSION, we speculate on the roles of these *cdc13-1* suppressor and enhancer genes in telomere biology.

Conservation of suppression in an alternative genetic background: It is possible that second-site mutations in gene deletion strains were responsible for suppression of the *cdc13-1* temperature-sensitive phenotype. Therefore, to confirm that the relevant gene deletions suppressed *cdc13-1*, 10 suppressor genes were deleted by transformation in the different W303 *cdc13-1* genetic background and tested for growth at 26°, 26.5°, and/or 27°. In all 10 cases, growth was observed at a higher temperature than the control *cdc13-1* strains (Table 2). In addition, as a result of identification of *OCA1*, *OCA2*, *SIW14* (*OCA3*), *OCA4*, and *OCA6* as suppressors of *cdc13-1*, we also tested deletion of the *OCA5* gene in the W303 genetic background and found it to suppress (Table 2); *OCA5* was dropped from the list of suppressors in this study at the screen 5 stage (see supplemental Methods). Since 10/10 gene deletions that we identified through high-throughput screening also suppress *cdc13-1* in the W303 genetic background, we conclude that the majority of the *cdc13-1* suppressors that we have identified are likely to be true suppressors.

The UP–DOWN screen: Given the large number of *cdc13-1* suppressors, we wanted to differentiate between different types of *cdc13-1* suppressors. Therefore, we

TABLE 1

Genes whose deletion rescues temperature sensitivity of *cdc13-1*

Strong suppressors		Suppressors									
ORF	Gene	ORF	Gene	ORF	Gene	ORF	Gene	ORF	Gene	ORF	Gene
YOL138C	RTC1[a]	YBR147W	RTC2	YKL087C	CYT2	YKL008C	LAC1	YAL023C	PMT2	YNL224C	SQS1
YER177W	BMH1	YHR087W	RTC3	YGL078C	DBP3	YJL134W	LCB3	YPL144W	POC4	YLR119W	SRN2
[YFL023W	BUD27]	YNL254C	RTC4	YFL001W	DEG1	YNL323W	LEM3	YIL160C	POT1	YHR066W	SSF1
YBR274W	CHK1	YOR118W	RTC5	YKR035W-A	DID2	YLR451W	LEU3	YBL068W	PRS4	YBR283C	SSH1
[YJR109C	CPA2]	YPL183W-A	RTC6	YGR227W	DIE2	YDL051W	LHP1	[YDL006W	PTC1]	YLR150W	STM1
YIL036W	CST6	YDL119C	YDL119C	YKL213C	DOA1	YJR070C	LIA1	YDR496C	PUF6	YDR320C	SWA2
YPL194W	DDC1	YGR201C	YGR201C	YDR206W	EBS1	YNL307C	MCK1	YPR191W	QCR2	YNL081C	SWS2
[YNL080C	EOS1]	YIL055C	YIL055C	YBL047C	EDE1	YPL098C	MGR2	YKR055W	RHO4	YLR354C	TAL1
YOR033C	EXO1	YIL057C	YIL057C	YKL048C	ELM1	YLR035C	MLH2	YNL180C	RHO5	YIL011W	TIR3
YCR034W	FEN1	YIL161W	YIL161W	YDR512C	EMI1	YIL110W	MNI1	YIL053W	RHR2	YPR074C	TKL1
YMR058W	FET3	YLR404W	YLR404W	YMR015C	ERG5	YPR045C	MNI2	YLR453C	RIF2	YER007C-A	TMA20
[YLR192C	HCR1]	YIL079C	AIR1	[YML008C	ERG6]	YIR002C	MPH1	YIL066C	RNR3	YJR014W	TMA22
YOL095C	HMI1	YER073W	ALD5	YER145C	FTR1	YKL062W	MSN4	YDL082W	RPL13A	YGR260W	TNA1
YMR080C	NAM7	YPL061W	ALD6	YPL262W	FUM1	YPR134W	MSS18	[YKL006W	RPL14A]	YNL070W	TOM7
YHR077C	NMD2	YGL148W	ARO2	YBL016W	FUS3	YBR057C	MUM2	YBR084C-A	RPL19A	YNL121C	TOM70
YOR209C	NPT1	YDR101C	ARX1	YIL097W	FYV10	YHR004C	NEM1	YPL079W	RPL21B	YIL138C	TPM2
YPL052W	OAZ1	[YMR116C	ASC1]	YOR183W	FYV12	YLR363C	NMD4	YFR031C-A	RPL2A	YPL030W	TRM44
YDL232W	OST4	YKL185W	ASH1	YMR307W	GAS1	YER002W	NOP16	YLR406C	RPL31B	YLR425W	TUS1
YOR368W	RAD17	YBL089W	AVT5	YJR040W	GEF1	YNL183C	NPR1	YOR234C	RPL33B	YER151C	UBP3
YER173W	RAD24	YIL124W	AYR1	YGL020C	GET1	YNL099C	OCA1	YER056C-A	RPL34A	YFR010W	UBP6
YDR217C	RAD9	YKR099W	BAS1	YHL031C	GOS1	YNL056W	OCA2	YDL191W	RPL35A	YMR067C	UBX4
YLR039C	RIC1	YPL115C	BEM3	YOL059W	GPD2	YCR095C	OCA4	[YLR185W	RPL37A]	YBR273C	UBX7
YCR028C-A	RIM1	YDR099W	BMH2	YDL035C	GPR1	YDR067C	OCA6	YDR500C	RPL37B	YDL190C	UFD2
YNL069C	RPL16B	YIL159W	BNR1	YML121W	GTR1	YML060W	OGG1	[YPR043W	RPL43A]	YNL229C	URE2
YDR389W	SAC7	YFL025C	BST1	YGL084C	GUP1	YGR202C	PCT1	YBR031W	RPL4A	YKR042W	UTH1
YDR143C	SAN1	YAR014C	BUD14	YGL237C	HAP2	[YER178W	PDA1]	YLR448W	RPL6B	YDL077C	VAM6
YER120W	SCS2	[YGR262C	BUD32[b]]	YBL021C	HAP3	YER153C	PET122	YGL147C	RPL9A	YGL212W	VAM7
[YOR035C	SHE4]	YIL034C	CAP2	YOR358W	HAP5	YOR017W	PET127	YER139C	RTR1	YIL135C	VHS2
YDL033C	SLM3	YGR174C	CBP4	YCR065W	HCM1	YLR191W	PEX13	YLR180W	SAM1	YIL017C	VID28
YOR327C	SNC2	YKL208W	CBT1	YHL002W	HSE1	YOL044W	PEX15	YDR181C	SAS4	YKR001C	VPS1
YLR313C	SPH1	YML036W	CGI121[c]	YGL253W	HXK2	YAL055W	PEX22	YKL051W	SFK1	YPL120W	VPS30
YLR372W	SUR4	YIL035C	CKA1	[YJR118C	ILM1]	YDR329C	PEX3	YNL032W	SIW14	YJL154C	VPS35
YBR126C	TPS1	YOR061W	CKA2	YDR315C	IPK1	YGR133W	PEX4	YLR398C	SKI2	YKR020W	VPS51
YBR082C	UBC4	YOR039W	CKB2	YFR055W	IRC7	YGR231C	PHB2	YPR189W	SKI3	YDR486C	VPS60
YGR072W	UPF3	YOL008W	COQ10	YGL016W	KAP122	YJL117W	PHO86	YOR076C	SKI7	YIL101C	XBP1
YOR089C	VPS21	YPL172C	COX10	YHR158C	KEL1	YCR037C	PHO87	YGL213C	SKI8	YIL023C	YKE4
YAL002W	VPS8	YLL009C	COX17	YNL238W	KEX2	YGL023C	PIB2	YNL311C	SKP2	YBR104W	YMC2
		YHR116W	COX23	YJL094C	KHA1	[YML061C	PIF1[b]]	YBL007C	SLA1	YDR349C	YPS7
		[YMR256C	COX7]	YAR018C	KIN3	YDR466W	PKH3	YGR229C	SMI1	[YLR262C	YPT6]
		YDL117W	CYK3	YNL322C	KRE1	YDL095W	PMT1	YER161C	SPT2	YML001W	YPT7
		YOR065W	CYT1								

Underlined genes lie adjacent to other genes whose deletion rescues *cdc13-1*. In such cases, an effect on transcription of the neighboring gene cannot be discounted. Brackets indicate genes previously identified as synthetic with wild-type during SGA (Tong *et al.* 2001).

[a] The *RTC* gene name is reserved for previously unnamed ORFs.

[b] Deletion of *PIF1* and *BUD32* rescues *cdc13-1* (Downey *et al.* 2006) but these genes were not tested further in robotic assays due to slow growth.

[c] Deletion of *CGI121* rescues *cdc13-1* (Downey *et al.* 2006) but this was not detected in robotic assays subsequent to initial scoring.

also screened for gene deletions that, when combined with the *cdc13-1* mutation, significantly enhanced or reduced cell viability in a temperature oscillation (or "UP–DOWN") experiment (materials and methods). The *cdc13-1* mutation has a reversible temperature-sensitive phenotype; that is, cells with the *cdc13-1* mutation maintain high viability and efficiently form colonies when returned to permissive temperature after short periods at nonpermissive temperature. DNA damage checkpoint pathways, which inhibit cell division in response to uncapped telomeres in *cdc13-1* mutants, are important for maintaining *cdc13-1* cell viability (Weinert *et al.* 1994; Zubko *et al.* 2004). In addition, nucleases and nuclease inhibitors, which affect single-stranded DNA produc-

TABLE 2

Comparison of expected *cdc13-1* suppressors with actual results and testing of novel suppressors in an alternative genetic background

Gene deletion	Suppressor of *cdc13-1* in BY4741 (this work)	Suppressor of *cdc13-1* in W303 (this work)	Previously documented suppressor of *cdc13-1*
*rad9*Δ	++	NA	+
*chk1*Δ	++	NA	+
*ddc1*Δ	++	NA	+
*rad24*Δ	++	NA	+
*rad17*Δ	++	NA	+
*upf3*Δ	++	NA	+
*nmd2*Δ	++	NA	+
*nam7*Δ	++	NA	+
*exo1*Δ	++	NA	+
*bub2*Δ	−	NA	+
*mec3*Δ	−[a]	NA	+
*bmh1*Δ	+	NA	+ (Downey *et al.* 2006)
*san1*Δ	++	NA	+ (Downey *et al.* 2006)
*pif1*Δ	+[b]	NA	+ (Downey *et al.* 2006)
*cgi121*Δ	+[c]	NA	+ (Downey *et al.* 2006)
*ebs1*Δ	+	NA	+ (Downey *et al.* 2006)
*scs2*Δ	++	+	−
*poc4*Δ	+	+	−
*snc2*Δ	++	+	−
*pkh3*Δ	+	+	−
*pda1*Δ	+	+	−
*oca1*Δ	+	+	−
*oca2*Δ	+	+	−
*siw14*Δ *(oca3*Δ*)*	+	+	−
*oca4*Δ	+	+	−
*oca6*Δ	+	+	−
*oca5*Δ	−	+	−

++, yes, a strong suppressor; +, yes; −, no.

[a] Deletion of *MEC3* rescues *cdc13-1* but was not tested in robotic assays due to slow growth.

[b] Deletion of *PIF1* rescues *cdc13-1* (Downey *et al.* 2006) but was not tested further in robotic assays due to slow growth.

[c] Deletion of *CGI121* rescues *cdc13-1* (Downey *et al.* 2006) but was not detected in robotic assays subsequent to initial scoring.

tion at uncapped telomeres of *cdc13-1* mutants, affect the ability of *cdc13-1* to grow for periods at nonpermissive temperature.

In an UP–DOWN assay, *cdc13-1* mutants are cycled between permissive and nonpermissive conditions and then allowed to form colonies at permissive temperature. In an UP–DOWN assay, *rad9*Δ *cdc13-1* strains do not form colonies efficiently because they do not arrest cell division in response to telomere uncapping and accumulate very high levels of single-stranded DNA. Conversely, *exo1*Δ *cdc13-1* cells grow demonstrably faster than *EXO*$^+$ *RAD*$^+$ *cdc13-1* strains in this assay (Zubko *et al.* 2004; Figure 1), presumably because high levels of Exo1-dependent ssDNA at telomeres of *cdc13-1* cells inhibit cell division for long periods even after cells are returned to permissive temperature. Therefore, we hypothesized that an UP–DOWN screen would allow us to identify genes that interact with *cdc13-1* in a *RAD9*-like or *EXO1*-like manner.

The UP–DOWN assay was performed on between 2 and 10 biological replicates of *cdc13-1* SGA strains. Those gene deletions that, in conjunction with *cdc13-1*, showed consistently poor growth (Figure 1) were scored as UP–DOWN sensitive (UD^S) while those that grew consistently better than *cdc13-1 his3*::KANMX controls (Figure 1) were scored as UP–DOWN resistant (UD^R) (Table 4).

A total of 96 UD^S and five UD^R genes were identified. Interestingly, both classes included both genes that suppress *cdc13-1* when deleted and genes that do not. The 15 UD^S genes that are *cdc13-1* suppressors included *RAD9*, *RAD17*, *RAD24*, and *CHK1*, which have well-characterized roles in coordinating the DNA damage response to uncapped telomeres, indicating that other novel genes with this "*RAD9*-like" phenotype are likely to be of interest. The 81 UD^S genes that are not *cdc13-1* suppressors included *YKU70*, *YKU80*, *EST1*, *EST2*, and *EST3*. These, too, have well-defined roles in telomere biology, indicating that this class is also likely to contain novel genes of interest. Deletion of *YKU70*, *YKU80*, and others in this category has previously been reported to be synthetically sick with *cdc13-1* (Polotnianka *et al.* 1998). However, since we germinated spores at 20°, rather than the 23° or 25° that is more usually used to grow *cdc* mutants, we probably masked the *YKU70/80 cdc13-1* synthetic-sick interactions previously reported. Presumably, other synthetic-sick interactions were also missed. There was only one gene (*YME1*) that reproducibly fell into both categories. Three of the five UD^R genes were also *cdc13-1* suppressors and hence *EXO1*-like; however, the only gene in this category that has previously been connected to telomere biology is *EXO1* itself.

Thus, through a systematic and iterative process, we arrived at a reliable classification of genes as one or more of the following: *cdc13-1* suppressor, UD^S, *RAD9*-like, UD^R, *EXO1*-like, *cdc13-1* synthetic lethal, and *cdc13-1* synthetic sick (Tables 1, 3, and 4; Figure 2).

Neighboring genes that interact with *cdc13-1*: In our lists of *cdc13-1* interactors, we identified a number of pairs or sets of genes that are adjacent to each other in the genome. For example, *YIL034C* (*CAP2*), *YIL035C* (*CKA1*), and *YIL036W* (*CST5*) are all classed as *cdc13-1* suppressors (Table 1). A likely explanation for such a group is that one gene has a true genetic interaction with *cdc13-1* and disruption of the neighboring gene(s) affects the expression of the gene of interest. Indeed, a previous study (Alvaro *et al.* 2007) has demonstrated that deletion of either overlapping or adjacent open reading frames can occasionally result in false positives in genomewide screens such as these. An inference can be made as to whether a gene is a true interactor or is having an effect

TABLE 3

Genes whose deletion exacerbates the growth defects of *cdc13-1* cells

Synthetic lethal		Synthetic sick			
ORF	Gene	ORF	Gene	ORF	Gene
YJL123C	*MTC1*[a]	*YKL098W*	*MTC2*	*YMR035W*	*IMP2*
YNL196C	*YNL196C*	*YGL226W*	*MTC3*	*YGR238C*	*KEL2*
YOR058C	*ASE1*	*YBR255W*	*MTC4*	*YOL064C*	*MET22*
YGL029W	*CGR1*	*YDR128W*	*MTC5*	*YKL167C*	*MRP49*
YBR036C	*CSG2*	*YHR151C*	*MTC6*	*YOL041C*	*NOP12*
YHR059W	*FYV4*	*YDL218W*	*YDL218W*	*YML103C*	*NUP188*
YEL003W	*GIM4*	*YIL040W*	*APQ12*	*YBR093C*	*PHO5*
YNL014W	*HEF3*	*YBR131W*	*CCZ1*	*YIL153W*	*RRD1*
YOL108C	*INO4*	*YGR157W*	*CHO2*	*YHR178W*	*STB5*
YNL106C	*INP52*	*YGL078C*	*DBP3*[b]	*YBR231C*	*SWC5*
YKL176C	*LST4*	*YCL016C*	*DCC1*	*YNL081C*	*SWS2*[b]
YGR078C	*PAC10*	*YDL219W*	*DTD1*	*YJL138C*	*TIF2*
YNL015W	*PBI2*	*YLR342W*	*FKS1*	*YPR173C*	*VPS4*
YNL003C	*PET8*	*YDL222C*	*FMP45*	*YPR024W*	*YME1*[c]
YBL027W	*RPL19B*	*YHR108W*	*GGA2*	*YGL255W*	*ZRT1*
YGR118W	*RPS23A*	*YML121W*	*GTR1*[b]	*YOL012C*	*HTZ1*
YNL206C	*RTT10*				
YOR297C	*TIM18*				
YNL197C	*WHI3*				
YMR302C	*YME2*				

Underlined genes lie adjacent to other genes whose deletion has synthetic interactions with *cdc13-1*. In such cases, an effect on transcription of the neighboring gene cannot be discounted.

[a] The *MTC* gene name is reserved for previously unnamed ORFs.

[b] Also a suppressor of *cdc13-1* (see Table 1).

[c] Also classed as UD^S.

on transcription of neighboring genes. In the case of *CKA1* (above), for example, the identification of two other subunits of casein kinase, *CKA2* and *CKB2*, as suppressors (neither of which lie adjacent to other suppressors in the yeast genome) supports classification of *CKA1* as a suppressor. Also, genes with previously well-characterized roles in telomere/checkpoint biology such as *CHK1* (adjacent to *UBX7*) may safely be assumed to be classified correctly. However, in most cases, inferring a role is potentially misleading. We have therefore highlighted (by underlining or boldface text in Tables 1, 3, 4, and 5; Figure 3) genes that, within a particular classification, lie near each other on the chromosome and have omitted them from statistical analyses of GO.

Gene ontology analysis of interactors: To better understand the types of processes that interact with uncapped telomeres, the different classes of *cdc13-1*-interacting genes were subjected to statistical analysis using the GOstats Bioconductor package (Falcon and Gentleman 2007). GOstats analysis (supplemental Table S3) allowed us to identify GO terms that were overrepresented. Genes previously identified as having roles in telomere maintenance (GO:0000723) are overrepresented in the results from both the *cdc13-1* suppressor screen (23 genes annotated as GO:0000723) and the UP–DOWN assay (18 more genes annotated as GO:0000723); 3 genes annotated as both "telomerase activity" (GO:0003720) and "telomerase holoenzyme complex" (GO:0005697): *EST1*, *EST2*, and *EST3* (supplemental Table S3). The list of strong suppressors (Table 1) is enriched for genes involved in DNA damage checkpoint control—namely *DDC1*, *RAD17*, *RAD24*, and *RAD9*—and in nonsense-mediated decay—namely *NAM7*, *NMD2*, and *UPF3*. *RAD9*-like genes (see Table 4) included the same four genes involved in DNA damage checkpoint control (*DDC1*, *RAD17*, *RAD24*, and *RAD9*) together with the "cell-cycle checkpoint" (GO:0000075) annotated *ELM1*. Finally, the UD^S genes that do not suppress *cdc13-1* temperature sensitivity when deleted had multiple overrepresented GO terms describing aspects of chromosome architecture (supplemental Table S3).

All of the processes highlighted by statistical analysis of *cdc13-1* interactors have well-characterized links to telomere biology. This analysis clearly shows that our screens were successful in identifying known *CDC13* interactors and suggests therefore that genes identified in this study that were not previously linked to telomeres are likely to have telomere-related roles.

Systematic analysis of gene lists: One caveat with statistical analysis of GO terms is that annotations may be biased toward processes that have been extensively studied. Also, we used a relatively high *P*-value cutoff (materials and methods) to mitigate the likelihood of false positives. We therefore performed a different sys-

TABLE 4

Genes whose deletion imparts a phenotype in the *cdc13-1* UP–DOWN assay

UD sensitive		UD sensitive		UD sensitive		UD resistant	
ORF	Gene	ORF	Gene	ORF	Gene	ORF	Gene
YEL033W	*MTC7*[a]	*YJR075W*	*HOC1*	*YML032C*	*RAD52*	*[YMR116C*	*ASC1*[b]*]*
[YNL171C	*YNL171C]*	*YDR158W*	*HOM2*	*YDR217C*	*RAD9*[b]	*YOR033C*	*EXO1*[b]
[YLR370C	*ARC18]*	*YER052C*	*HOM3*	*YHL027W*	*RIM101*	*YKL029C*	*MAE1*
YLR242C	*ARV1*	*YJR139C*	*HOM6*	*YOR275C*	*RIM20*	*YCR009C*	*RVS161*
YJR053W	*BFA1*	*YJL092W*	*HPR5*	*YPR018W*	*RLF2*	*YLR119W*	*SRN2*[b]
YER016W	*BIM1*	*[YHR067W*	*HTD2]*	*YJL136C*	*RPS21B*		
YLR015W	*BRE2*	*YIL154C*	*IMP2′*	*[YBL072C*	*RPS8A]*		
[YGR188C	*BUB1]*	*YDR123C*	*INO2*	*YDR289C*	*RTT103*		
YMR055C	*BUB2*	*YMR294W*	*JNM1*	*YLL002W*	*RTT109*		
[YOR026W	*BUB3]*	*YOR123C*	*LEO1*	*YFR040W*	*SAP155*		
YMR038C	*CCS1*	*YPL055C*	*LGE1*	*YMR127C*	*SAS2*		
YLR418C	*CDC73*	*YAL024C*	*LTE1*	*YDR181C*	*SAS4*[b]		
YBR274W	*CHK1*[b]	*YPR164W*	*MMS1*	*YBR171W*	*SEC66*		
YMR198W	*CIK1*	*YJL183W*	*MNN11*	*YBL031W*	*SHE1*		
YPR119W	*CLB2*	*YCL061C*	*MRC1*	*[YOR035C*	*SHE4*[b]*]*		
YCR086W	*CSM1*	*YPL184C*	*MRN1*	*YER118C*	*SHO1*		
YPR135W	*CTF4*	*[YKL009W*	*MRT4]*	*YKR101W*	*SIR1*		
YKR024C	*DBP7*	*YBR057C*	*MUM2*[b]	*YPR189W*	*SKI3*[b]		
YPL194W	*DDC1*[b]	*YNL119W*	*NCS2*	*YMR016C*	*SOK2*		
YKL213C	*DOA1*[b]	*YKL040C*	*NFU1*	*YPR032W*	*SRO7*		
[YDR440W	*DOT1]*	*[YKR082W*	*NUP133]*	*YOR027W*	*STI1*		
YKL204W	*EAP1*	*YKL120W*	*OAC1*	*YMR039C*	*SUB1*		
YBL047C	*EDE1*[b]	*YCR077C*	*PAT1*	*YAR003W*	*SWD1*		
YOR144C	*ELG1*	*YGR193C*	*PDX1*	*YBR175W*	*SWD3*		
YKL048C	*ELM1*[b]	*YDR276C*	*PMP3*	*[YLR182W*	*SWI6]*		
YMR202W	*ERG2*	*YPL179W*	*PPQ1*	*YDR260C*	*SWM1*		
YGL054C	*ERV14*	*YGR135W*	*PRE9*	*YOL018C*	*TLG2*		
YLR233C	*EST1*	*YMR201C*	*RAD14*	*YKR042W*	*UTH1*[b]		
YLR318W	*EST2*	*YOR368W*	*RAD17*[b]	*YOR089C*	*VPS21*[b]		
YIL009C-A	*EST3*	*YER173W*	*RAD24*[b]	*YMR284W*	*YKU70*		
YLL043W	*FPS1*	*YKL113C*	*RAD27*	*YMR106C*	*YKU80*		
YMR307W	*GAS1*[b]	*YER162C*	*RAD4*	*YPR024W*	*YME1*[c]		
YDR108W	*GSG1*						

Underlined genes lie adjacent to other genes whose deletion imparts a phenotype in the UP–DOWN assay distinct from *cdc13-1* alone. In such cases, an effect on transcription of the neighboring gene cannot be discounted. Brackets indicate genes previously identified as synthetic with wild type during SGA (Tong *et al.* 2001).

[a] The *MTC* gene name is reserved for previously un-named ORFs.

[b] Also a suppressor of *cdc13-1* and so "*RAD9*-like" (see Table 1).

[c] Also classed as synthetic sick.

tematic analysis of *cdc13-1* interactors, which this time included all genes identified in our study (see above; Tables 1, 3, and 4). We grouped genes with clearly related functions together, irrespective of GO term frequency and chromosomal position, using the functional descriptions in BioGrid (Stark *et al.* 2006; Breitkreutz *et al.* 2008).

Suppressors of *cdc13-1* temperature sensitivity (Table 1) included clusters of genes involved in bud-site selection; mitochondrial function (including multiple genes for electron transport, mitochondrial genome integrity, mitochondrial ribosomes, and mitochondrial integrity); nonsense-mediated decay; chromatin architecture; phosphate transport; signal transduction; ribosome function; protein degradation; mRNA degradation; vesicular transport; response to DNA damage; iron ion transport; the actin cytoskeleton, cell polarity and mRNA localization; and HO function (Table 5). Also of note in this category were five putative tyrosine phosphatases of largely unknown function [*OCA1*, *OCA2*, *SIW14* (*OCA3*), *OCA4*, and *OCA6*)], four killer-toxin-related genes, two aldehyde dehydrogenase genes, three genes from the CCAAT-binding complex, and three of four subunits of casein kinase 2 (Table 5).

A similar analysis of UD[s] genes (Table 4) identified groups of genes with roles in the telomerase holoenzyme: the spindle checkpoint; the mitotic exit network; the DNA damage checkpoint; regulation of transcription termination and transposition; ribosome function; chromosome architecture (including multiple SAS complex, COMPASS complex, and Paf1 complex genes); the

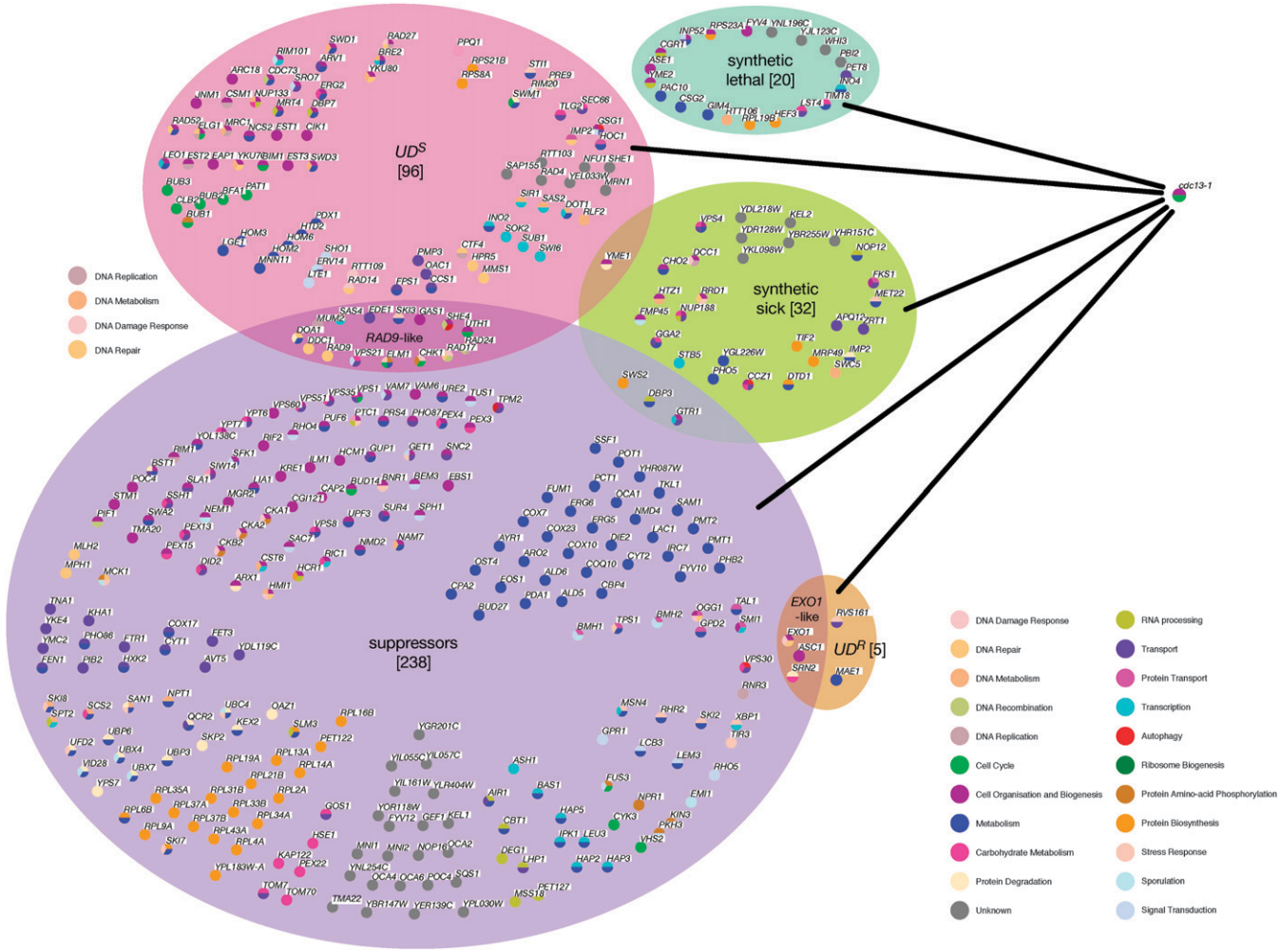

FIGURE 2.—Summary of *cdc13-1* interactors. Genes designated as *cdc13-1* suppressors (purple shaded area), UD^S (red), UD^R (orange), synthetic sick (green), and synthetic lethal with *cdc13-1* (blue) were arranged using OSPREY. Genes belonging to more than one category (including *RAD9*-like and *EXO1*-like genes) are indicated in the overlap regions of shaded areas. Individual genes are represented as solid circles, color coded by OSPREY with each color representing a gene ontology term, up to a maximum of four. Relevant gene ontology terms are indicated in the color key.

actin cytoskeleton, cell polarity and mRNA localization; glycerol osmosensing; methionine and threonine synthesis; and vesicular transport (Table 5).

Finally, analysis of genes whose deletion exacerbates the *cdc13-1* phenotype (Table 3) provided multiple "hits" affecting ribosome function, mitochondrial integrity, and histone H2AZ exchange (chromatin remodeling) (Table 5).

Uncharacterized genes identified in the *cdc13-1* screen: A number of genes identified as *cdc13-1* interactors in this study were of previously unknown function. Suppressor genes, when present, have a negative effect on telomere capping in *cdc13-1* mutant cells at the nonpermissive temperature; therefore we have named such genes *RTC* (*r*estriction of *t*elomere *c*apping; Table 1). Genes of previously unknown function whose deletion exacerbates the *cdc13-1* phenotype have been named *MTC* (*m*aintenance of *t*elomere *c*apping) since their presence increases the fitness of *cdc13-1* mutant cells at permissive temperature or during the UP–DOWN assay (Tables 3 and 4). We did not apply new acronyms to otherwise uncharacterized *cdc13-1* interactors if (1) they lay next to other *cdc13-1* interactors in the genome (see above) or (2) they were classified as dubious open reading frames in the SACCHAROMYCES GENOME DATABASE (2008) and were adjacent to other genes that could reasonably account for their deletion phenotype (see supplemental Table S4); however, this could be updated in the future.

DISCUSSION

The objective of our study was to identify proteins and pathways that cap telomeres or regulate the cellular response to uncapped telomeres. We combined the *S. cerevisiae* gene deletion collection with the well-defined, temperature-sensitive, and reversible *cdc13-1* mutation using the SGA strain construction technique and we

TABLE 5

Groups of functionally related genes among *cdc13-1* interactors

Group	Function of related genes	Suppressors	UP–DOWN	Synthetic
1	DNA repair/DNA damage checkpoint/telomeres	*MLH2*, *MPH1*, ***CHK1***, *DDC1*, *EXO1*, *RAD17*, *RAD24*, *RAD9*, ***DOA1***	***CHK1***,[a] *DDC1*,[a] *RAD17*,[a] *RAD24*,[a] *RAD9*,[a] *MRC1*, ***RAD14***, *RAD4*, *RAD27*, *RAD52*, *YKU70*, *YKU80*, *ELG1*, *DOA1*,[a] *HPR5*, *MMS1*, *IMP2*	
2	Protein degradation	***UBP3***, *UBP6*, *UBX4*, ***UBX7***, ***UFD2***, ***DOA1***, ***UBC4***, *SAN1*, *VID28*, *POC4*	*PRE9*	
3	Nonsense-mediated decay	*NMD4*, *NAM7*, *UPF3*, *EBS1*, *NMD2*		
4	Chromatin architecture/ silencing/histone modification	*SCS2*, *SPT2*, *NPT1*, *SAS4*, ***RIF2***	[*SAS2*, *SAS4*;[a] SAS complex], [*SWD1*, *SWD3*, *BRE2*; COMPASS complex], [*CDC73*, *LEO1*; *Paf1* complex], *DOT1*, *SIR1*, *RLF2*, *LGE1*	*[SWC5, HTZ1; SWR1 complex]*
5	Vesicular transport	***PEX13***, *PEX15*, *PEX22*, *PEX3*, *PEX4*, *VAM6*, ***VAM7***, *YPT6*, *YPT7*, *VPS1*, *VPS30*, *VPS35*, *VPS51*, *VPS60*, *DID2*, *SRN2*, *HSE1*, *PIB2*, *RIC1*, *VPS21*, *VPS8*, *SWA2*, *SSH1*, *SNC2*, *GOS1*	*[MNN11, HOC1; golgi mannosyl transferase complex]*, *ERV14*, *SEC66*, *TLG2*, *RUD3*, *GSG1*, *SRO7*, *SRN2*[a]	*CCZ1*, ***PBI2***,[b] *VPS4*
6	Casein kinase 2	***CKA1***, *CKA2*, *CKB2*		
7	Ribosome function	*RPL13A*, ***RPL14A***, ***RPL19A***, *RPL21B*, *RPL2A*, ***RPL31B***, *RPL33B*, *RPL34A*, ***RPL35A***, *RPL37A*, *RPL37B*, ***RPL43A***, *RPL4A*, *RPL6B*, ***RPL9A***, ***RPL16B***, *NOP16*, ***ARX1***, *ASC1*, *DBP3*, ***HCR1***, *TMA20*, *TMA22*	*RPS21B*, *RPS8A*, *ASC1*,[a] *DBP7*, *MRT4*	*RPL19B*,[b] *DBP3*,[a] *RPS23A*,[b] *NOP12*, *CGR1*[b]
8	Mitochondrial electron transport/genome/ ribosomes and integrity	*MSS18*, *COX7*, *COX10*, *COX17*, *COX23*, *CYT1*, *CYT2*, ***QCR2***, *CBP4*, *COQ10*, ***PET122***, *PET127*, *ILM1*, ***PIF1***, *MGR2*, *HMI1*, *RIM1*, ***TOM7***, *TOM70*, *YMC2*, ***YDL119C***, ***SWS2***, *[HAP2, HAP3, HAP5; CCAAT-binding complex]*	*UTH1*[a]	*SWS2*,[a] *MRP49*, *TIM18*,[b] *YME1*, *YME2*[b]
9	Tyrosine phosphatase	*OCA1*, *OCA2*, *OCA4*, *OCA6*, *SIW14*		
10	Signal transduction	***BMH1***, ***BMH2***		
11	Bud site selection	*BEM3*, *BUD14*, ***BUD27***		
12	Actin cytoskeleton/ cell polarity/mRNA localization	*EDE1*, *RHO4*, ***BNR1***, *SLA1*	*EDE1**, *ARC18*, *RVS161*	
13	Ergosterol biosynthesis	*ERG5*, *ERG6*	***ERG2***	
14	Iron ion transport	*FTR1*, *FET3*		
15	Aldehyde dehydrogenases	*ALD5*, *ALD6*		
16	HO function	*ASH1*, *PUF6*, *SHE4*	*SHE4*[a]	
17	mRNA degradation	*SKI2*, ***SKI3***, *SKI7*, ***SKI8***	***SKI3***[a]	
18	Phosphate transport	*PHO86*, *PHO87*		
19	Killer toxin related	*FYV10*, *FYV12*, ***KRE1***		*FYV4*[b]
20	Protein O mannosylation	*PMT1*, *PMT2*		
21	Telomerase holoenzyme		*EST1*, *EST2*, *EST3*	
22	Spindle checkpoint		*BUB1*, ***BUB3***, *BIM1*	
23	Mitotic exit network	*KEL1*	*BFA1*, *BUB2*, *LTE1*, *SWM1*	*KEL2*
24	Transposition		*RTT103*, *RTT109*	*RTT106*[b]
25	Glycerol osmosensing		*SHO1*, *FPS1*	
26	Methionine/threonine biosynthesis		*HOM2*, *HOM3*, *HOM6*	

Genes in boldface lie adjacent to other *cdc13-1* interactors of the same category (*e.g.*, synthetic); strong suppressors are underlined. A number for each group of genes is indicated on the left.

[a] Also a suppressor of *cdc13-1*.

[b] Deletion of gene is synthetically lethal with *cdc13-1*.

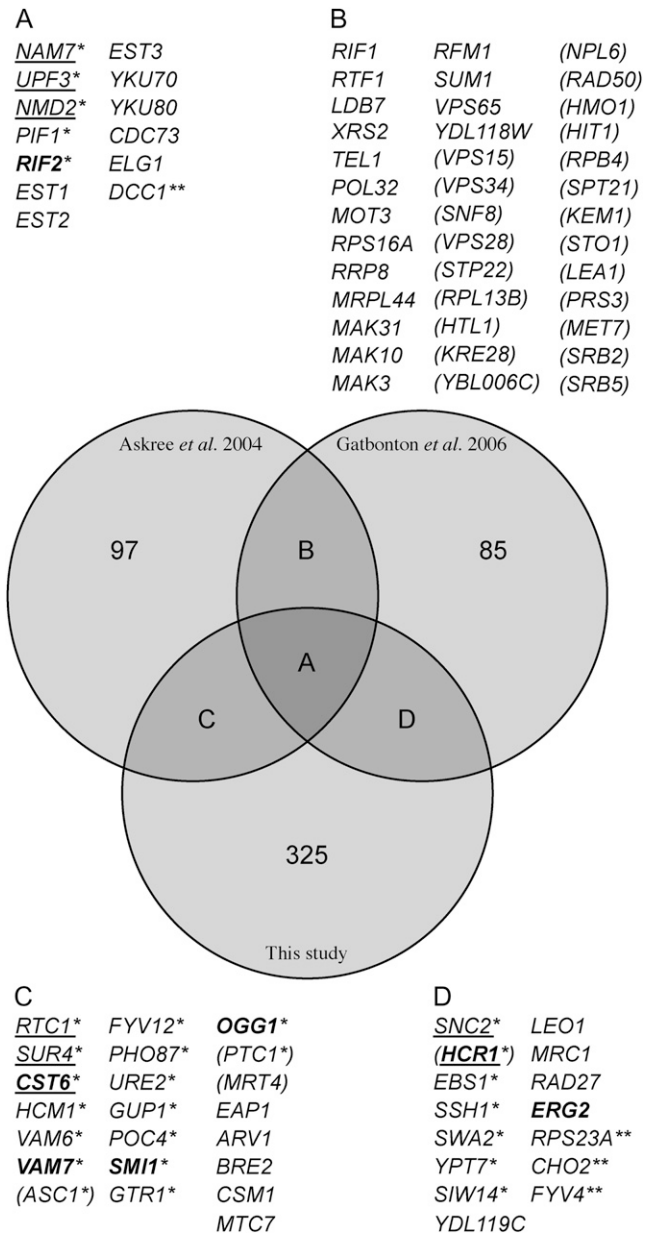

Figure 3.—Comparison of *CDC13*-interacting genes with telomere length genes. A Venn diagram shows hits from two separate genomewide screens for telomere length regulating genes compared to a list of *cdc13-1* interactors. Lists of genes that make up the cross sections between studies are displayed and indicated by letters. The numbers of genes in each segment are indicated. Boldface text highlights genes that have neighboring genes in the genome whose deletion results in a similar phenotype. **cdc13-1* suppressor (strong suppressors are underlined); **synthetic (sick or lethal) with *cdc13-1*; genes in parentheses either were not tested in this study due to slow growth or were identified previously as giving consistently poor performance in SGA studies.

developed and optimized high-throughput yeast growth assays. Although others have looked systematically for synthetic lethality with temperature-sensitive mutations (*e.g.*, Measday *et al.* 2005; Baetz *et al.* 2006), to the best of our knowledge, a genomewide screen for gene deletions that confer subtle suppressor/enhancer phenotypes on a temperature-sensitive mutation has not previously been reported. Our approach therefore complements other high-throughput genetic techniques such as SGA (Tong *et al.* 2001; Roguev *et al.* 2007) and synthetic dosage lethal analysis (Measday *et al.* 2005).

We screened for gene deletions that suppress the lethality of *cdc13-1* at the nonpermissive temperature and genes that compromise or contribute to the "reversibility" of *cdc13-1* mutants. Combined with synthetic-lethal and synthetic-sick data from the SGA procedure, this resulted in five overlapping categories of *CDC13* interactors: suppressors of *cdc13-1*, synthetic lethal with *cdc13-1*, synthetic sick with *cdc13-1*, UD^S, and UD^R—the latter two categories, respectively, having *RAD9*-like and *EXO1*-like subclasses, giving eight classes in all. Many of the genes identified as interacting with *CDC13* fit into pathways with previously recognized roles in telomere biology (Table 5). However, a significant number of genes identified in this study have previously uncharacterized relationships to telomere function. A more detailed analysis of their roles is likely to provide novel information about eukaryotic telomere biology; for example, in the same way as Exo1, discovered to have telomere-related function in yeast (Maringele and Lydall 2002), plays a role in life-span determination of telomerase knockout mice (Schaetzlein *et al.* 2007).

***cdc13-1* suppressors:** *cdc13-1* suppressors encode proteins that inhibit growth of *cdc13-1* mutant cells at the nonpermissive temperature. Previous work has shown that suppression of the temperature sensitivity of *cdc13-1* can occur through different pathways and to different extents. For example, deletion of *EXO1* (which encodes a 5′–3′ exonuclease required for resection at telomere ends in the event of telomere uncapping) suppresses *cdc13-1* temperature sensitivity through a different mechanism from suppression by deletion of *RAD9*, which is required for signaling cell-cycle arrest. There is therefore no single, simple explanation for the actions of the many novel gene deletions that we have identified as suppressing *cdc13-1* (Table 1).

Some of the biological functions common to genes identified as *cdc13-1* suppressors (Table 5) have well-understood relationships with telomere function. DNA damage checkpoint and related genes, for example, act at telomeres to detect uncapping and transduce signals to the DNA repair and cell-cycle machinery (group 1, Table 5; supplemental Figure S3) (Lydall 2003; Longhese 2008).

For other "clusters" of genes, there are plausible hypotheses to explain how they might affect telomeres. Genes involved in protein degradation (group 2, Table 5; supplemental Figure S3) could potentially affect the levels of many telomere-associated proteins. An example is *SAN1*, the product of which functions in ubiquitin-dependent degradation of aberrant proteins in the cell nucleus. San1 degrades the defective Cdc13-1 protein and therefore deletion of *SAN1* stabilizes Cdc13-1 levels

(Gardner *et al.* 2005). What little function Cdc13-1 has at elevated temperature might therefore be increased in the absence of *SAN1*. Deletion of nonsense-mediated decay genes (group 3, Table 5; supplemental Figure S3) alters the stoichiometry of telomere cap components and in particular elevates transcript levels for the essential Cdc13-interacting Stn1 protein (Dahlseid *et al.* 2003; Enomoto *et al.* 2004).

Genes that affect chromatin architecture, silencing, and/or histone modification influence telomere biology, presumably by modifying the accessibility of chromatin to telomere proteins, for example (Yu *et al.* 2007). Chromatin modifiers are represented both as *cdc13-1* suppressors and as UD^{s} genes in this category (group 4, Table 5) and at least one silencing gene (*SAS4*) is *RAD9*-like in that it is both a suppressor and UD^{s}. Therefore, the relationship between chromatin and the telomere cap is complex. Recent experiments show how the histone H3K79 methyl transferase Dot1 (identifed as UD^{s} in our study) is required for checkpoint activation and inhibition of resection in *cdc13-1* mutants (Lazzaro *et al.* 2008).

A large number of suppressor genes have vesicular trafficking functions (group 5, Table 5). This is consistent with the observation that many vesicular traffic genes affect telomere length (Askree *et al.* 2004). At least some of those were shown to act upon telomere length in a *YKU70*-dependent manner (Rog *et al.* 2005); however, it seems likely from our studies that others may influence Cdc13 function. There are extensive interactions, described in BioGrid, between vesicular traffic genes and other types of *cdc13-1* suppressors (supplemental Figure S3); hence mutations that alter vesicular trafficking may affect telomeres through multiple different pathways. It is interesting to note that transport of telomerase proteins and *TLC1* RNA across the nuclear membrane is important for telomerase function (Teixeira *et al.* 2002; Gallardo *et al.* 2008) and that deletion of *KAP122*, required for import of *TLC1* from the cytoplasm to the nucleus (Gallardo *et al.* 2008), suppresses *cdc13-1*.

Phosphorylation by human casein kinase 2 (CK2) has been shown to regulate binding of human Trf1 to telomeres (Kim *et al.* 2008). Human Trf1 negatively regulates telomere length by inhibiting access of telomerase to telomeres. Possible Trf1 functional homologs in *S. cerevisiae* are Tbf1 and Rap1, both of which are essential TTAGGG-binding proteins with roles in gene silencing at telomeres (Fourel *et al.* 1999; Koering *et al.* 2000; Bhattacharya and Warner 2008; Hogues *et al.* 2008). It is possible therefore that yeast CK2 (group 6, Table 5; supplemental Figure S3) acts directly upon either Tbf1 or Rap1. Alternatively, multiple interactions between CK2 subunits and genes involved in modulating chromatin architecture are known, including multiple genes identified in this study (supplemental Figure S4) and so *S. cerevisiae* CK2 may exert an influence on telomere function through a general effect on chromatin. A third alternative route through which CK2 might influence the *cdc13-1* phenotype is its influence on checkpoint control, which was reported previously (Toczyski *et al.* 1997). Further studies will be required to distinguish among these possibilities.

A large group of ribosomal protein genes (group 7, Table 5; supplemental Figure S3) and a smaller number of other genes with ribosome-related function were identified as suppressors of *cdc13-1*. We have no clear explanation for this; however, a clue may come from the observation that chromosomal regions containing ribosomal protein genes and telomeres have similar mechanisms for regulating their chromatin architecture (Bhattacharya and Warner 2008; Hogues *et al.* 2008). Remarkably, this group includes 16 large ribosomal protein subunit genes but only one component of the small ribososmal subunit.

Numerous groups of genes identified in this study have not previously been linked to telomere function. Genes affecting mitochrondrial function (group 8, Table 5) (particularly those involved in electron transport and import into mitochondria), for example, are *cdc13-1* suppressors when deleted. Interestingly, Nautiyal *et al.* (2002) showed that many mitochondrial genes are transcriptionally upregulated in telomerase-deficient mutants and we have recently found similar results in *cdc13-1* mutants (A. Greenall and D. Lydall, personal communication). Furthermore, there appear to be evolutionarily conserved interactions between mitochondria and telomeres (Passos *et al.* 2007). Therefore, one possible explanation of why so many genes involved in mitochondrial function suppress *cdc13-1* when deleted is that loss of mitochondrial function, and the ability to respire, suppresses the poor growth of *cdc13-1* mutants. Indeed, we find that many petite mutants suppress the *cdc13-1* defect (Table 1).

The suppression of *cdc13-1* temperature sensitivity by petite mutations as a whole is interesting and warrants further investigation. We sought to test whether many other gene deletions might be suppressing *cdc13-1* indirectly by causing loss of mitochondrial function. Mitochondrial function (respiration) is essential for growth on glycerol; therefore we spotted single-gene deletion strains [corresponding to all *cdc13-1* suppressors (Table 1)] using glycerol as the sole carbon source. We found that only those previously described as "petite" were unable to grow on glycerol (data not shown). We also found that suppression by petite mutations is not due simply to slower growth because growth on synthetic medium does not suppress *cdc13-1* temperature sensitivity and there are multiple nonpetite mutations that confer slow growth but fail to suppress *cdc13-1* temperature sensitivity (data not shown). We conclude that the vast majority of *cdc13-1* suppressors that we have identified are not suppressing because they disrupt mitochondrial function.

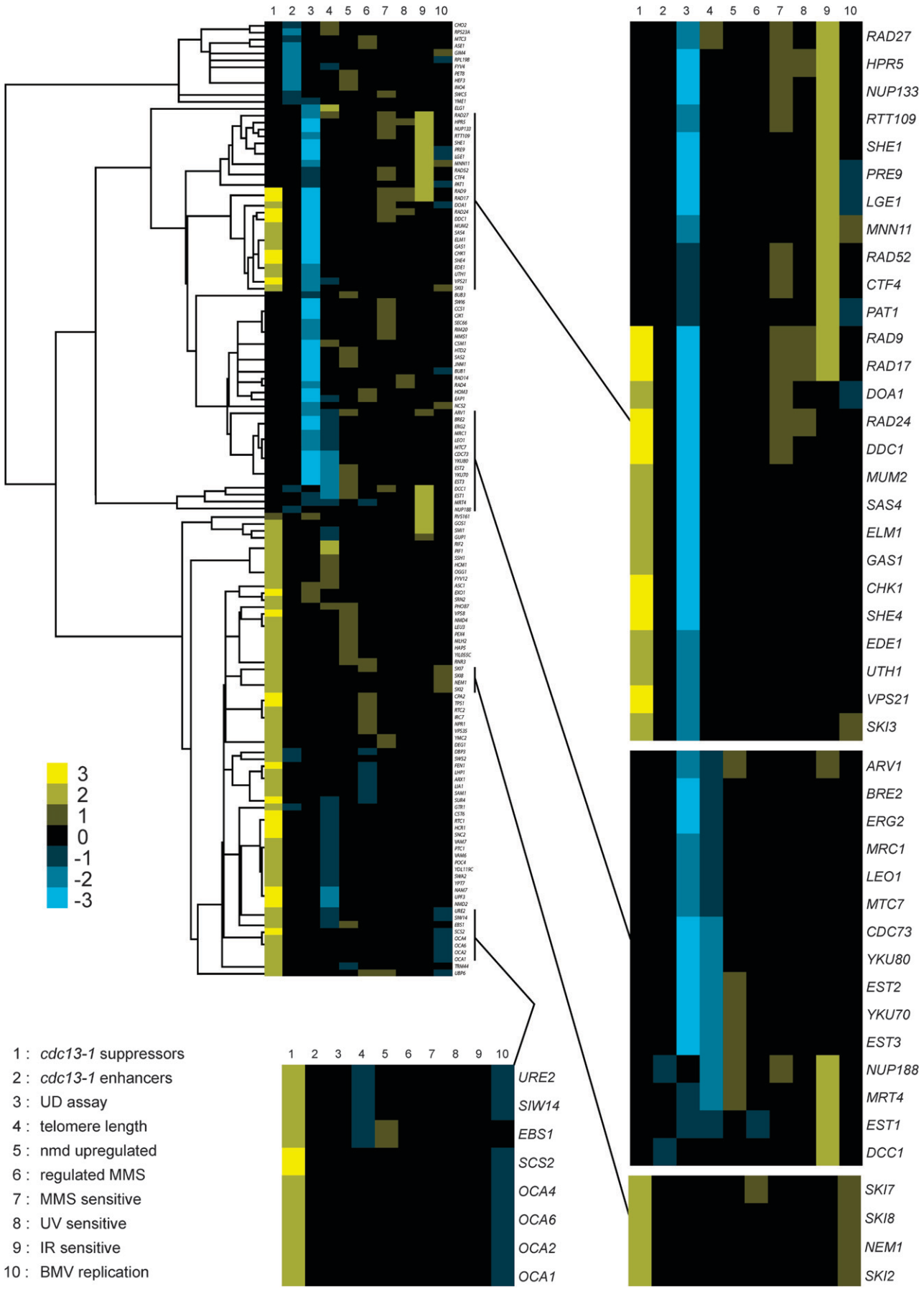
1 2 3 4 5 6 7 8 9 10
3
2
1
0
-1
-2
-3
RAD27
HPR5
NUP133
RTT109
SHE1
PRE9
LGE1
MNN11
RAD52
CTF4
PAT1
RAD9
RAD17
DOA1
RAD24
DDC1
MUM2
SAS4
ELM1
GAS1
CHK1
SHE4
EDE1
UTH1
VPS21
SKI3
ARV1
BRE2
ERG2
MRC1
LEO1
MTC7
CDC73
YKU80
EST2
YKU70
EST3
NUP188
MRT4
EST1
DCC1
SKI7
SKI8
NEM1
SKI2
URE2
SIW14
EBS1
SCS2
OCA4
OCA6
OCA2
OCA1
1 : cdc13-1 suppressors
2 : cdc13-1 enhancers
3 : UD assay
4 : telomere length
5 : nmd upregulated
6 : regulated MMS
7 : MMS sensitive
8 : UV sensitive
9 : IR sensitive
10 : BMV replication

Five genes (*OCA1*, *OCA2*, *OCA4*, *OCA6*, *SIW14*; group 9, Tables 2 and 5; supplemental Figure S3) containing a highly conserved tyrosine phosphatase motif were identified as suppressors of *cdc13-1*. Little is known about their function except that *OCA1* and *SIW14* have roles in checkpoint response to oxidative stress and actin filament organization, respectively (Alic *et al.* 2001; Care *et al.* 2004). Suppression of *cdc13-1* has been confirmed in a separate genetic background (W303) for *OCA2*, *OCA4*, *OCA6*, and *SIW14*. It was also found that *OCA5*, which lacks the tyrosine phosphatase motif and was not detected as a suppressor in this screen, does suppress *cdc13-1* temperature sensitivity in the W303 background (Table 2). It will be interesting to determine how the OCA gene family interacts with uncapped telomeres, possibly by interacting with the checkpoint kinase cascade or perhaps by affecting telomere capping.

The partially redundant *BMH1* and *BMH2* genes (group 10, Table 5; supplemental Figure S3) encode 14-3-3 proteins, which bind phosphopeptides (van Heusden and Steensma 2006). It has been shown that Bmh1 and Bmh2 affect checkpoint signal transduction (Lottersberger *et al.* 2003, 2006, 2007) and therefore, like Rad9 and Rad24, their absence is expected to improve the growth of *cdc13-1* mutants. Further experiments will be necessary to explain the roles of other groups of genes (groups 11–20, Table 5; supplemental Figure S3) in exacerbating the *cdc13-1* telomere-capping defect.

UP–DOWN sensitive genes: We classify UD^{S} genes as those that contribute to the viability of *cdc13-1* mutant cells during brief incubation periods at high temperature. Their deletion causes *cdc13-1* cells to grow poorly in the UP–DOWN assay. Deletion of *RAD9* suppresses the temperature sensitivity of *cdc13-1*, as well as rendering *cdc13-1* cells sensitive to temperature oscillation (Figure 1) and we predicted that other UD^{S} genes that similarly suppressed *cdc13-1* would be identified in this screen and classed as truly "*RAD9*-like." Indeed, *RAD9*, *CHK1*, *DDC1*, *RAD17*, *RAD24*, and other genes with DNA-repair-related roles (*DOA1*) were identified. However, also included were genes for cell polarity and cellular morphogenesis (*ELM1*, *SHE4*), membrane traffic (*EDE1*, *VPS21*), response to oxidative stress (*UTH1*), mRNA degradation (*SKI3*), DNA replication in meiosis (*MUM2*), chromatin architecture (*SAS4*), and cell-wall biogenesis (*GAS1*). *SHE4* in particular is interesting since its deletion causes strong suppression (Table 1) and a strong UD^{S} phenotype (Table 4 and data not shown). She4 is an UNC domain protein that interacts with type I and type V myosins and has roles in mating-type switching (by helping to localize the mRNA for Ash1) and endocytosis. Since other genes involved in both vesicular traffic and Ash1 function have been identified in this study, it remains to be determined through which of these pathways *SHE4* exerts an influence on telomere biology.

Rather less predictable was a large number of UD^{S} genes (81), which do not suppress *cdc13-1* temperature sensitivity when deleted (Table 4, Figure 2). Deletion of some of these genes caused reduced growth during spot tests (not detected in SGA analysis; supplemental Figure S2), even at the permissive temperature of 20° (data not shown). They were classed as UD^{S} because growth was still poor in the UP–DOWN assay relative to growth at the permissive temperature. There is a subtle distinction, therefore, between this class of genes and those that exhibit a synthetic sick interaction with *cdc13-1* at temperatures >23°.

Only deletion of *YME1* appeared to demonstrate both UD^{S} (in screens 3 and 4; supplemental Table S1) and synthetic sick (in screen 7; supplemental Table S1) interactions with *cdc13-1*; null mutations in this mitochondrial protease have previously been shown to be pleiotropic, including exhibiting cold sensitivity on rich glucose medium (Thorsness *et al.* 1993). Genes such as this with apparently "variable" phenotypes were rare. However, another example is *ASC1*. Deletion of *ASC1* has previously resulted in synthetic interactions with wild-type query strains in the SGA procedure (Tong *et al.* 2001; see supplemental Methods); however, we obtained viable progeny from SGA in 5 of 10 biological replicates with this gene deletion. Four of five of these demonstrated suppression of *cdc13-1* and UD^{R} so *ASC1* is, tentatively, classified as a suppressor and UD^{R}, that is, *EXO1*-like.

EST1, *EST2*, and *EST3* genes encoding telomerase holoenzyme components fell into the UD^{S} category (group 21, Table 5; supplemental Figure S4). This is almost certainly because telomerase, and its product telomeric DNA, contribute to forming the telomere cap. The absence of telomerase therefore sensitizes *cdc13-1* mutants to high temperature. Conversely, deleting *PIF1*, which encodes a helicase that removes telomerase, suppresses the temperature sensitivity of *cdc13-1* mutants.

The UD^{S} genes included genes for both subunits of the Ku complex (*YKU70* and *YKU80*), *BRE2*, and *DOT1*. The latter encodes the H3K79 methylase and appears to

Figure 4.—Hierarchical clustering of *cdc13-1* genetic interactions with data from multiple genomewide studies. *cdc13-1* suppressor and enhancer data are combined with data from genomewide studies of telomere length, nonsense-mediated decay (nmd upregulated), the effect of MMS on gene transcriptions (regulated MMS), MMS sensitivity, UV sensitivity, ionizing radiation sensitivity (IR sensitive), and Brome mosaic virus (BMV) replication. *cdc13-1* synthetic sick and synthetic lethal interactions are grouped under the heading "*cdc13-1* enhancers," separately from interactors identified in the UP–DOWN (UD) assay. Yellow and blue shading on the heat map indicate positive and negative values, respectively (as defined in the supplemental Methods). Four interesting clusters are highlighted with magnified heat maps. One of these clusters (center, right) contains the previously uncharacterized *MTC7* gene, identified in this study (see discussion).

help recruit Rad9 to chromatin and, like Rad9, inhibits resection at uncapped telomeres (Lazzaro *et al.* 2008).

Spindle checkpoint and mitotic exit genes (groups 22 and 23, Table 5; supplemental Figure S4) also helped *cdc13-1* cells to recover from shifts to high temperature, presumably because, after a period of arrest prior to entry into mitosis, the mitotic exit network is important for efficient completion of the cell cycle.

The telomere-related roles of genes involved in transposition, glycerol osmosensing, or methionine and threonine synthesis (groups 24–26, Table 5; supplemental Figure S4) remain unclear, although the former group has been implicated in chromatin remodeling.

UP–DOWN-resistant genes: *EXO1* encodes a nuclease that contributes to the vulnerability of *cdc13-1* mutant cells to brief incubation periods at high temperature. A likely explanation for this is that deletion of *EXO1* results in less resection and thus less DNA damage at the nonpermissive temperature, thus hastening the cells' recovery when returned to the permissive temperature (Zubko *et al.* 2004). We have hypothesized that other nucleases, such as a putative *RAD24*-dependent nuclease ExoX, also regulate resection at uncapped telomeres (Jia *et al.* 2004; Zubko *et al.* 2004). Therefore, we searched for other *EXO1*-like genes. Deletion of *EXO1* suppresses the temperature sensitivity of *cdc13-1*, as well as rendering *cdc13-1* cells less sensitive to temperature oscillation (Figure 1). In fact, only two genes—*ASC1* and *SRN2*—fall into this category. *ASC1* encodes a core component of the 40S ribosomal subunit, which acts as a guanine nucleotide dissociation inhibitor for Gpa2 (Zeller *et al.* 2007), and its deletion results in longer telomeres (Askree *et al.* 2004). Srn2 is a member of the ESCRT-1 endosomal sorting complex (Kostelansky *et al.* 2007), which targets proteins to endosomes in a ubiquitin-dependent manner. The other two subunits of this complex (Stp22 and Vps28) were in the group of slow-growing deletion strains that were not tested in this study but have been shown previously to have shorter telomeres, whereas deletion of *SRN2* is not reported to affect telomere length (Askree *et al.* 2004; Gatbonton *et al.* 2006). Two other genes were UD^R without being *cdc13-1* suppressors: *MAE1* and *RVS161*. *RVS161* encodes an amphiphysin-like raft protein, which acts (with Rvs167) to regulate polarization of the actin cytoskeleton; thus its deletion has pleiotropic effects, which include disruption of endocytosis (Breton *et al.* 2001; Lombardi and Riezman 2001). *MAE1* encodes a mitochondrial malic enzyme that catalyzes the oxidative decarboxylation of malate to pyruvate (Boles *et al.* 1998). None of the *EXO1*-like genes identified here are likely candidates for ExoX. Therefore, ExoX does not exist, was missing from our library, is encoded by an essential gene, or its activity is encoded by multiple, redundant genes.

Comparisons with telomere length screens: Two previous genomewide studies of telomere biology have measured the length of telomere repeat regions in gene deletion strains (Askree *et al.* 2004; Gatbonton *et al.* 2006). Interestingly, there was less overlap than might have been expected between the two studies in terms of the specific genes identified; however, the processes that affected telomere length in each study were similar (Gatbonton *et al.* 2006). Comparison of our results with these two previous studies reveals moderate overlap (Figure 3) but, again, some similar cellular processes were identified.

Thirteen genes were identified in all three studies and this clearly represents an important set of telomere-related genes. Seven of these were found to support telomere capping in our study—*EST1*, *EST2*, and *EST3* (encoding subunits of telomerase); *YKU70* and *YKU80* (encoding the Ku heterodimer); and *CDC73* and *DCC1*—and show reduced telomere length when deleted. Deletion of *ELG1* (UD^S) results in longer telomeres. Deletion of *PIF1* (Downey *et al.* 2006), which encodes a helicase that removes telomerase from telomeres, and of *RIF2* (Wotton and Shore 1997), which inhibits telomerase activity, results in long telomeres and suppression of *cdc13-1*. Deletion of *NAM7*, *UPF3*, and *NMD2*, which regulate nonsense-mediated RNA decay, affecting levels of the Cdc13-interacting protein Stn1, results in strong suppression of *cdc13-1* and short telomeres. Clearly, the implications of altered telomere length or genetic interaction with *cdc13-1* arising from a gene deletion study are complex.

Many of the genes identified by Askree *et al.* (2004) or Gatbonton *et al.* (2006), which were not identified by our screens, are particularly poor growing strains or those previously demonstrated as working poorly in the SGA techniques (in parentheses in Figure 3; Tong *et al.* 2001). Conversely, there are 326 genes identified in our study as interacting with *cdc13-1*, which do not significantly alter telomere length. These include genes that are known to affect the response to telomere uncapping without affecting telomere length (*e.g.*, the checkpoint genes *RAD9* and *CHK1*). However, it also seems likely that *cdc13-1* mutants are sensitive to deletion of some genes where the resulting changes in telomere length are too small to be detected using high-throughput Southern blot analysis.

Comparisons with multiple high-throughput studies: In addition to telomere length, multiple genomewide studies have examined processes that are relevant to telomere biology including, for example, UV irradiation (Birrell *et al.* 2001), ionizing radiation (Bennett *et al.* 2001), alkylating agents (Jelinsky and Samson 1999; Chang *et al.* 2002), and nonsense-mediated decay (He *et al.* 2003). We combined these data sets, a study of genes affecting replication of a positive-strand DNA virus (Kushner *et al.* 2003), and the telomere length studies (Askree *et al.* 2004; Gatbonton *et al.* 2006; Shachar *et al.* 2008) with our own data to produce a hierarchical clustering map (Figure 4). For two previously uncharacterized genes identified in this study, such clustering

may provide clues to their putative function. For example, *MTC7* lies in a cluster of genes that, when deleted, confer UP–DOWN sensitivity and short telomeres. This cluster includes telomere maintenance, histone methylation, and silencing genes (Figure 4), indicating that Mtc7 might influence telomere biology through one of these processes. *RTC1* lies in a cluster of genes that, when deleted, confer suppression of *cdc13-1* temperature sensitivity and short telomeres (Figure 4). This cluster includes genes involved in nonsense-mediated decay and membrane transport, indicating that Rtc1 might influence telomere biology through one of these processes.

In conclusion, the budding yeast telomere cap and the response to telomere uncapping induced in *cdc13-1* mutants appear to be affected by numerous and diverse cellular pathways and processes. Further analyses will be necessary to understand how these pathways and processes interact at yeast telomeres. It seems likely that a significant fraction of the pathways and processes identified in yeast will play roles at human telomeres and thereby affect cancer and/or aging.

The authors thank Charlie Boone and Renee Brost for providing strains and advice on the SGA technique; Centre for Integrated Systems Biology of Ageing and Nutrition colleagues past and present (in particular, Allyson Lister for help with the Robot Object Database, Dan Swan for computer support, and Suzanne Advani for excellent technical help); Tim Humphrey for helpful suggestions regarding the manuscript; Cammie Lesser and Roger Kramer for productive discussions about spot scoring; and Sasan Raghibizadeh, Pedram Raghibizadeh, and Ewan Grant for help with robotics. This work was supported by the Wellcome Trust (075294) and the Biotechnology and Biological Sciences Research Council (BB/C008200/1).

LITERATURE CITED

Alic, N., V. J. Higgins and I. W. Dawes, 2001 Identification of a *Saccharomyces cerevisiae* gene that is required for G1 arrest in response to the lipid oxidation product linoleic acid hydroperoxide. Mol. Biol. Cell **12:** 1801–1810.

Alvaro, D., M. Lisby and R. Rothstein, 2007 Genomewide analysis of Rad52 foci reveals diverse mechanisms impacting recombination. PLoS Genet. **3:** e228.

Askree, S. H., T. Yehuda, S. Smolikov, R. Gurevich, J. Hawk *et al.*, 2004 A genome-wide screen for *Saccharomyces cerevisiae* deletion mutants that affect telomere length. Proc. Natl. Acad. Sci. USA **101:** 8658–8663.

Baetz, K., V. Measday and B. Andrews, 2006 Revealing hidden relationships among yeast genes involved in chromosome segregation using systematic synthetic lethal and synthetic dosage lethal screens. Cell Cycle **5:** 592–595.

Bennett, C. B., L. K. Lewis, G. Karthikeyan, K. S. Lobachev, Y. H. Jin *et al.*, 2001 Genes required for ionizing radiation resistance in yeast. Nat. Genet. **29:** 426–434.

Bhattacharya, A., and J. R. Warner, 2008 Tbf1 or not Tbf1? Mol. Cell **29:** 537–538.

Birrell, G. W., G. Giaever, A. M. Chu, R. W. Davis and J. M. Brown, 2001 A genome-wide screen in Saccharomyces cerevisiae for genes affecting UV radiation sensitivity. Proc. Natl. Acad. Sci. USA **98:** 12608–12613.

Blasco, M. A., 2007 Telomere length, stem cells and aging. Nat. Chem. Biol. **3:** 640–649.

Boles, E., P. de Jong-Gubbels and J. T. Pronk, 1998 Identification and characterization of *MAE1*, the *Saccharomyces cerevisiae* structural gene encoding mitochondrial malic enzyme. J. Bacteriol. **180:** 2875–2882.

Breitkreutz, B. J., C. Stark and M. Tyers, 2003 Osprey: a network visualization system. Genome Biol. **4:** R22.

Breitkreutz, B. J., C. Stark, T. Reguly, L. Boucher, A. Breitkreutz *et al.*, 2008 The BioGRID Interaction Database: 2008 update. Nucleic Acids Res. **36:** D637–D640.

Breton, A. M., J. Schaeffer and M. Aigle, 2001 The yeast Rvs161 and Rvs167 proteins are involved in secretory vesicles targeting the plasma membrane and in cell integrity. Yeast **18:** 1053–1068.

Care, A., K. A. Vousden, K. M. Binley, P. Radcliffe, J. Trevethick *et al.*, 2004 A synthetic lethal screen identifies a role for the cortical actin patch/endocytosis complex in the response to nutrient deprivation in *Saccharomyces cerevisiae*. Genetics **166:** 707–719.

Chang, M., M. Bellaoui, C. Boone and G. W. Brown, 2002 A genome-wide screen for methyl methanesulfonate-sensitive mutants reveals genes required for S phase progression in the presence of DNA damage. Proc. Natl. Acad. Sci. USA **99:** 16934–16939.

Cheung, A. L., and W. Deng, 2008 Telomere dysfunction, genome instability and cancer. Front. Biosci. **13:** 2075–2090.

Choudhury, A. R., Z. Ju, M. W. Djojosubroto, A. Schienke, A. Lechel *et al.*, 2007 Cdkn1a deletion improves stem cell function and lifespan of mice with dysfunctional telomeres without accelerating cancer formation. Nat. Genet. **39:** 99–105.

Dahlseid, J. N., J. Lew-Smith, M. J. Lelivelt, S. Enomoto, A. Ford *et al.*, 2003 mRNAs encoding telomerase components and regulators are controlled by UPF genes in *Saccharomyces cerevisiae*. Eukaryot. Cell **2:** 134–142.

Downey, M., R. Houlsworth, L. Maringele, A. Rollie, M. Brehme *et al.*, 2006 A genome-wide screen identifies the evolutionarily conserved KEOPS complex as a telomere regulator. Cell **124:** 1155–1168.

Eisen, M. B., P. T. Spellman, P. O. Brown and D. Botstein, 1998 Cluster analysis and display of genome-wide expression patterns. Proc. Natl. Acad. Sci. USA **95:** 14863–14868.

Enomoto, S., L. Glowczewski, J. Lew-Smith and J. G. Berman, 2004 Telomere cap components influence the rate of senescence in telomerase-deficient yeast cells. Mol. Cell. Biol. **24:** 837–845.

Falcon, S., and R. Gentleman, 2007 Using GOstats to test gene lists for GO term association. Bioinformatics **23:** 257–258.

Fourel, G., E. Revardel, C. E. Koering and E. Gilson, 1999 Cohabitation of insulators and silencing elements in yeast subtelomeric regions. EMBO J. **18:** 2522–2537.

Gallardo, F., C. Olivier, A. T. Dandjinou, R. J. Wellinger and P. Chartrand, 2008 *TLC1* RNA nucleo-cytoplasmic trafficking links telomerase biogenesis to its recruitment to telomeres. EMBO J. **27:** 748–757.

Gardner, R. G., Z. W. Nelson and D. E. Gottschling, 2005 Degradation-mediated protein quality control in the nucleus. Cell **120:** 803–815.

Garvik, B., M. Carson and L. Hartwell, 1995 Single-stranded DNA arising at telomeres in *cdc13* mutants may constitute a specific signal for the *RAD9* checkpoint. Mol. Cell. Biol. **15:** 6128–6138.

Gatbonton, T., M. Imbesi, M. Nelson, J. M. Akey, D. M. Ruderfer *et al.*, 2006 Telomere length as a quantitative trait: genome-wide survey and genetic mapping of telomere length-control genes in yeast. PLoS Genet. **2:** e35.

Greider, C. W., and E. H. Blackburn, 1985 Identification of a specific telomere terminal transferase activity in *Tetrahymena* extracts. Cell **43:** 405–413.

He, F., X. Li, P. Spatrick, R. Casillo, S. Dong *et al.*, 2003 Genome-wide analysis of mRNAs regulated by the nonsense-mediated and 5′ to 3′ mRNA decay pathways in yeast. Mol. Cell **12:** 1439–1452.

Hogues, H., H. Lavoie, A. Sellam, M. Mangos, T. Roemer *et al.*, 2008 Transcription factor substitution during the evolution of fungal ribosome regulation. Mol. Cell **29:** 552–562.

Jelinsky, S. A., and L. D. Samson, 1999 Global response of Saccharomyces cerevisiae to an alkylating agent. Proc. Natl. Acad. Sci. USA **96:** 1486–1491.

Jia, X., T. Weinert and D. Lydall, 2004 Mec1 and Rad53 inhibit formation of single-stranded DNA at telomeres of *Saccharomyces cerevisiae cdc13-1* mutants. Genetics **166:** 753–764.

Kim, M. K., M. R. Kang, H. W. Nam, Y. S. Bae, Y. S. Kim *et al.*, 2008 Regulation of telomeric-repeat binding factor 1 binding to telomeres by casein kinase 2-mediated phosphorylation. J. Biol. Chem. **283:** 14144–14152.

Koering, C. E., G. Fourel, E. Binet-Brasselet, T. Laroche, F. Klein *et al.*, 2000 Identification of high affinity Tbf1p-binding sites within the budding yeast genome. Nucleic Acids Res. **28:** 2519–2526.

Kostelansky, M. S., C. Schluter, Y. Y. Tam, S. Lee, R. Ghirlando *et al.*, 2007 Molecular architecture and functional model of the complete yeast ESCRT-I heterotetramer. Cell **129:** 485–498.

Kushner, D. B., B. D. Lindenbach, V. Z. Grdzelishvili, A. O. Noueiry, S. M. Paul *et al.*, 2003 Systematic, genome-wide identification of host genes affecting replication of a positive-strand RNA virus. Proc. Natl. Acad. Sci. USA **100:** 15764–15769.

Lazzaro, F., V. Sapountzi, M. Granata, A. Pellicioli, M. Vaze *et al.*, 2008 Histone methyltransferase Dot1 and Rad9 inhibit single-stranded DNA accumulation at DSBs and uncapped telomeres. EMBO J. **27:** 1502–1512.

Lombardi, R., and H. Riezman, 2001 Rvs161p and Rvs167p, the two yeast amphiphysin homologs, function together in vivo. J. Biol. Chem. **276:** 6016–6022.

Longhese, M. P., 2008 DNA damage response at functional and dysfunctional telomeres. Genes Dev. **22:** 125–140.

Lottersberger, F., F. Rubert, V. Baldo, G. Lucchini and M. P. Longhese, 2003 Functions of *Saccharomyces cerevisiae* 14-3-3 proteins in response to DNA damage and to DNA replication stress. Genetics **165:** 1717–1732.

Lottersberger, F., A. Panza, G. Lucchini, S. Piatti and M. P. Longhese, 2006 The *Saccharomyces cerevisiae* 14-3-3 proteins are required for the G1/S transition, actin cytoskeleton organization and cell wall integrity. Genetics **173:** 661–675.

Lottersberger, F., A. Panza, G. Lucchini and M. P. Longhese, 2007 Functional and physical interactions between yeast 14-3-3 proteins, acetyltransferases, and deacetylases in response to DNA replication perturbations. Mol. Cell. Biol. **27:** 3266–3281.

Lydall, D., 2003 Hiding at the ends of yeast chromosomes: telomeres, nucleases and checkpoint pathways. J. Cell Sci. **116:** 4057–4065.

Maringele, L., and D. Lydall, 2002 *EXO1*-dependent single-stranded DNA at telomeres activates subsets of DNA damage and spindle checkpoint pathways in budding yeast *yku70*Delta mutants. Genes Dev. **16:** 1919–1933.

Measday, V., K. Baetz, J. Guzzo, K. Yuen, T. Kwok *et al.*, 2005 Systematic yeast synthetic lethal and synthetic dosage lethal screens identify genes required for chromosome segregation. Proc. Natl. Acad. Sci. USA **102:** 13956–13961.

Nautiyal, S., J. L. DeRisi and E. H. Blackburn, 2002 The genome-wide expression response to telomerase deletion in *Saccharomyces cerevisiae*. Proc. Natl. Acad. Sci. USA **99:** 9316–9321.

Nugent, C. I., T. R. Hughes, N. F. Lue and V. Lundblad, 1996 Cdc13p: a single-strand telomeric DNA-binding protein with a dual role in yeast telomere maintenance. Science **274:** 249–252.

Olovnikov, A. M., 1973 A theory of marginotomy. The incomplete copying of template margin in enzymic synthesis of polynucleotides and biological significance of the phenomenon. J. Theor. Biol. **41:** 181–190.

Passos, J. F., G. Saretzki, S. Ahmed, G. Nelson, T. Richter *et al.*, 2007 Mitochondrial dysfunction accounts for the stochastic heterogeneity in telomere-dependent senescence. PLoS Biol. **5:** e110.

Polotnianka, R. M., J. Li and A. J. Lustig, 1998 The yeast Ku heterodimer is essential for protection of the telomere against nucleolytic and recombinational activities. Curr. Biol. **8:** 831–834.

Reaper, P. M., F. di Fagagna and S. P. Jackson, 2004 Activation of the DNA damage response by telomere attrition: a passage to cellular senescence. Cell Cycle **3:** 543–546.

Rog, O., S. Smolikov, A. Krauskopf and M. Kupiec, 2005 The yeast VPS genes affect telomere length regulation. Curr. Genet. **47:** 18–28.

Roguev, A., M. Wiren, J. S. Weissman and N. J. Krogan, 2007 High-throughput genetic interaction mapping in the fission yeast *Schizosaccharomyces pombe*. Nat. Methods **4:** 861–866.

Saldanha, A. J., 2004 Java Treeview: extensible visualization of microarray data. Bioinformatics **20:** 3246–3248.

Sandell, L. L., and V. A. Zakian, 1993 Loss of a yeast telomere: arrest, recovery, and chromosome loss. Cell **75:** 729–739.

Schaetzlein, S., N. R. Kodandaramireddy, Z. Ju, A. Lechel, A. Stepczynska *et al.*, 2007 Exonuclease-1 deletion impairs DNA damage signaling and prolongs lifespan of telomere-dysfunctional mice. Cell **130:** 863–877.

Saccharomyces Genome Database, 2008 Saccharomyces Genome Database. http://www.yeastgenome.org.

Shachar, R., L. Ungar, M. Kupiec, E. Ruppin and R. Sharan, 2008 A systems-level approach to mapping the telomere length maintenance gene circuitry. Mol. Syst. Biol. **4:** 172.

Stark, C., B. J. Breitkreutz, T. Reguly, L. Boucher, A. Breitkreutz *et al.*, 2006 BioGRID: a general repository for interaction datasets. Nucleic Acids Res. **34:** D535–D539.

Teixeira, M. T., K. Forstemann, S. M. Gasser and J. Lingner, 2002 Intracellular trafficking of yeast telomerase components. EMBO Rep. **3:** 652–659.

Thorsness, P. E., K. H. White and T. D. Fox, 1993 Inactivation of *YME1*, a member of the *ftsH-SEC18-PAS1-CDC48* family of putative ATPase-encoding genes, causes increased escape of DNA from mitochondria in *Saccharomyces cerevisiae*. Mol. Cell. Biol. **13:** 5418–5426.

Toczyski, D. P., D. J. Galgoczy and L. H. Hartwell, 1997 CDC5 and CKII control adaptation to the yeast DNA damage checkpoint. Cell **90:** 1097–1106.

Tong, A. H., and C. Boone, 2006 Synthetic genetic array analysis in *Saccharomyces cerevisiae*. Methods Mol. Biol. **313:** 171–192.

Tong, A. H., M. Evangelista, A. B. Parsons, H. Xu, G. D. Bader *et al.*, 2001 Systematic genetic analysis with ordered arrays of yeast deletion mutants. Science **294:** 2364–2368.

van Heusden, G. P., and H. Y. Steensma, 2006 Yeast 14-3-3 proteins. Yeast **23:** 159–171.

Weinert, T. A., G. L. Kiser and L. H. Hartwell, 1994 Mitotic checkpoint genes in budding yeast and the dependence of mitosis on DNA replication and repair. Genes Dev. **8:** 652–665.

Wotton, D., and D. Shore, 1997 A novel Rap1p-interacting factor, Rif2p, cooperates with Rif1p to regulate telomere length in *Saccharomyces cerevisiae*. Genes Dev. **11:** 748–760.

Yu, E. Y., O. Steinberg-Neifach, A. T. Dandjinou, F. Kang, A. J. Morrison *et al.*, 2007 Regulation of telomere structure and functions by subunits of the *INO80* chromatin remodeling complex. Mol. Cell. Biol. **27:** 5639–5649.

Zeller, C. E., S. C. Parnell and H. G. Dohlman, 2007 The RACK1 ortholog Asc1 functions as a G-protein beta subunit coupled to glucose responsiveness in yeast. J. Biol. Chem. **282:** 25168–25176.

Zubko, M. K., S. Guillard and D. Lydall, 2004 Exo1 and Rad24 differentially regulate generation of ssDNA at telomeres of *Saccharomyces cerevisiae cdc13-1* mutants. Genetics **168:** 103–115.

Communicating editor: B. J. Andrews

small RNAs, such as piRNAs from mammals and *Drosophila*, 22G-RNAs from *C. elegans*, and primal RNAs from fission yeast (Ghildiyal and Zamore, 2009). Dicer-independent small RNAs have not been reported in plants, although they are likely also present in plants. All of the described small RNAs are ultimately loaded onto an effector protein for carrying out their regulatory functions (Figure 1). Most of the small RNAs reported to date appear to associate with AGOs. It should be noted that some AGO proteins have the ability to bind longer RNAs, such as 30- to 40-nt small RNAs in the fission yeast AGO1 complex (Halic and Moazed, 2010) and the milRNA precursors in the QDE-2 complex (Lee et al., 2010), suggesting that more complex functions of these AGO proteins remain to be discovered. In addition, some small RNAs may associate with other types of RNA-binding proteins, which may confer different functions (Zheng et al., 2008).

The work of Lee et al. in this issue of *Molecular Cell* provides an excellent example of how new small RNAs can be discovered by examining AGO-interacting small RNAs. Importantly, this study revealed previously unsuspected diversity and complexity in small RNA biogenesis in fungal systems. It begs the question, how many more small RNA biogenesis pathways are there?

REFERENCES

Bartel, D.P. (2004). Cell *116*, 281–297.

Borsani, O., Zhu, J.H., Verslues, P.E., Sunkar, R., and Zhu, J.K. (2005). Cell *123*, 1279–1291.

Ghildiyal, M., and Zamore, P.D. (2009). Nat. Rev. Genet. *10*, 94–108.

Halic, M., and Moazed, D. (2010). Cell *140*, 504–516.

Katiyar-Agarwal, S., Morgan, R., Dahlbeck, D., Borsani, O., Villegas, A., Zhu, J.K., Staskawicz, B.J., and Jin, H.L. (2006). Proc. Natl. Acad. Sci. USA *103*, 18002–18007.

Lee, H.C., Chang, S.S., Choudhary, S., Aalto, A.P., Maiti, M., Bamford, D.H., and Liu, Y. (2009). Nature *459*, 274–277.

Lee, H.C., Li, L., Gu, W., Xue, Z., Crosthwaite, S.K., Pertsemlidis, A., Lewis, Z.A., Freitag, M., Selker, E.U., Mello, C.C., and Liu, Y. (2010). Mol. Cell *38*, this issue, 803–814.

Okamura, K., and Lai, E.C. (2008). Nat. Rev. Mol. Cell Biol. *9*, 673–678.

Zheng, X.W., Pontes, O., Zhu, J.H., Miki, D., Zhang, F., Li, W.X., Iida, K., Kapoor, A., Pikaard, C.S., and Zhu, J.K. (2008). Nature *455*, 1259–1270.

Telomere Replication: Mre11 Leads the Way

James M. Dewar[1] and David Lydall[1,2,*]
[1]Centre for Integrated Systems Biology of Ageing and Nutrition, Institute for Ageing and Health
[2]Institute for Cell and Molecular Biosciences
Newcastle University, Newcastle upon Tyne, Tyne-and-Wear NE4 5PL, UK
*Correspondence: d.a.lydall@ncl.ac.uk
DOI 10.1016/j.molcel.2010.06.003

In this issue of *Molecular Cell*, Faure et al. (2010) establish a critical role for the Mre11 complex in the recruitment of telomerase to leading- but not lagging-strand telomeres of budding yeast.

Chromosomes of most eukaryotic organisms terminate in specialized nucleoprotein structures called telomeres, which contain double-stranded DNA (dsDNA) with 3′ single-stranded DNA (ssDNA) overhangs. Most chromosomal regions can be replicated by replication forks moving in either direction, but a telomere can only be replicated by a fork moving in a single direction, toward the chromosome end. The inherent directionality of telomere replication means that there is a clear distinction between those telomeric DNA strands that are replicated by leading- or lagging-strand replication machinery (Figure 1A). The G-rich 3′ strands, are replicated by lagging-stand machinery, while the C-rich 5′ strands are replicated by leading-strand machinery. Lagging-strand replication leaves 3′ ssDNA overhangs at the telomere, as the replication machinery is unable to replicate the region of the template strand that is occupied by the RNA primer of the terminal Okazaki fragment, and this constitutes the well-recognized ''end replication problem.'' Leading-strand polymerases are presumed to be able to replicate to the end of the chromosome, producing blunt ends. Thus, while lagging-strand synthesis has the inherent ability to produce telomeric DNA structures with 3′ overhangs, the leading strand most likely requires further processing to convert blunt ends into 3′ overhang structures. In this issue, Faure et al. (2010) provide important insights into the processing of leading and lagging strands after telomere replication.

Telomeric DNA in eukaryotes is bound by a number of specialized telomere-capping proteins and more general DNA damage response (DDR) proteins, which cooperate to maintain telomere function (de Lange, 2009; Lydall, 2009). Faure et al. (2010) asked whether specific proteins bind to telomeres replicated by the leading-strand machinery, the lagging-strand machinery, or both. To do this, the authors incorporated BrdU into DNA during a single S phase and

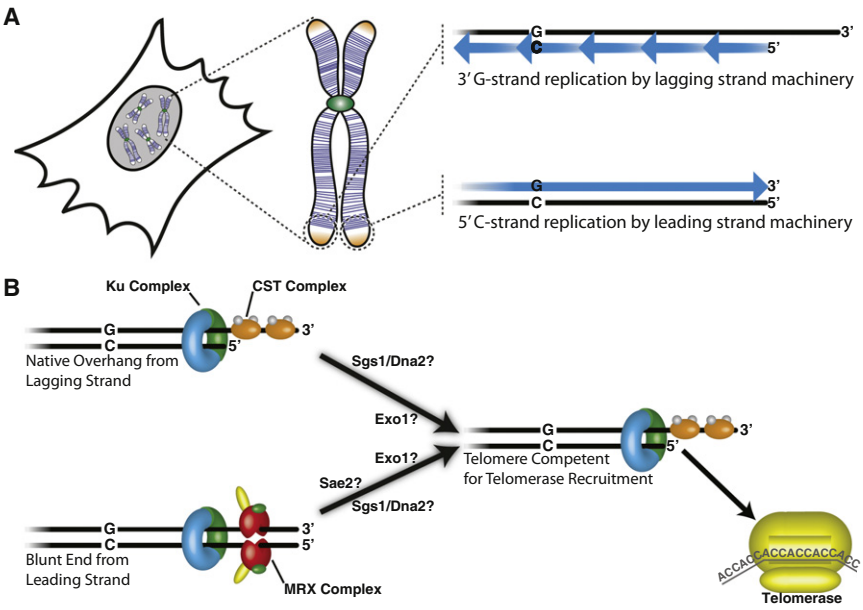

Figure 1. Telomere Replication

(A) Telomeres are nucleoprotein caps at the end of eukaryotic chromosomes. Replication of telomeric DNA occurs from sub-telomeric origins. This dictates that the G strand is replicated by the lagging strand machinery, resulting in a 3′ ssDNA overhang, while the C strand is replicated by the leading strand machinery, resulting in a blunt end.

(B) In budding yeast, telomeres are bound by the Ku complex (Yku70-Yku80) and the CST complex (Cdc13-Stn1-Ten1), which cooperate to recruit telomerase to the telomere. The CST complex only binds 3′ ssDNA overhangs, while the Ku complex can bind to both blunt-ended telomeres and those with a 3′ ssDNA overhang. The work of Faure et al. (presented in this issue) and others in the field, supports a model where the MRX/MRN (Mre11-Rad50-Xrs2/Nbs1) complex converts blunt-ended products of leading strand synthesis into 3′ overhangs to which the CST complex can bind, in a process essential for telomerase recruitment.

performed ChIP after either an initial or a successive round of DNA replication to measure binding of specific proteins at the leading- and lagging-strand telomeres.

Budding yeast telomeres are capped in part by binding of the CST complex (Cdc13-Stn1-Ten1) to telomeric 3′ ssDNA (Gao et al., 2007). Interestingly, Faure et al. (2010) found that the CST complex and telomerase bound both leading- and lagging-strand telomeres. This suggested that blunt ends generated by leading-strand synthesis of telomeric DNA (Figure 1A) are modified to generate ssDNA, the substrate for CST binding. Consistent with this hypothesis, Faure et al. (2010) showed that Mre11, a component of the MRX complex (Mre11-Rad50-Xrs2/Nbs1), bound only to the leading-strand telomeres and was critical for CST complex and telomerase binding to leading-strand telomeres (Figure 1B). Importantly, Mre11 was not required for binding of all proteins to leading-strand telomeres because the Ku complex (Yku70-Yku80), a DDR component that binds nonspecifically to dsDNA ends, could bind telomeres in the absence of Mre11.

One outstanding question arising from the work of Faure et al. (2010) is how MRX functions at leading-strand telomeres. MRX has multiple functions at DNA ends; one is to recruit the checkpoint kinase Tel1 (ATM) via the Xrs2 subunit, and this aids in telomerase recruitment to telomeres; another MRX activity is to help generate 3′ ssDNA overhangs via the endonuclease Sae2 (CtIP) (Mimitou and Symington, 2009). Therefore at least two plausible mechanisms could explain the role of Mre11 at leading-strand telomeres—one activating the Tel1 checkpoint kinase, the other regulating nuclease activity. It will be interesting to see if Sae2 or Tel1 also preferentially binds leading-strand telomeres.

Interestingly, it seems that blunt-ended telomeres induced by making DNA double-strand breaks (DSBs) near telomeric DNA in metaphase-arrested cells are converted to 3′ ssDNA overhangs using similar mechanisms to the resection of internal DSBs (Bonetti et al., 2009; Mimitou and Symington, 2009). In both cases, Mre11 cooperates with Sae2 to create an initial overhang, which is then extended by Sgs1/Dna2 in cooperation with Exo1. It is therefore possible that during normal telomere replication Mre11/Sae2-generated overhangs on the leading strand and the overhangs on the lagging strand are processed by nuclease activities dependent upon Sgs1/Dna2 and Exo1 (Figure 1B). Alternatively, Mre11/Sae2, Sgs1, and Exo1 might be confined to the leading-strand telomere, with 3′ ssDNA on the lagging strand being generated entirely by the removal of the RNA primer. The latter hypothesis would likely require a specific mechanism for exclusion of nuclease activities from the lagging strand and would be consistent with the role of Cdc13 in inhibiting nuclease activities at telomeres. Using the approaches developed by Faure et al. (2010) it should now be possible to ask if Sae2, Sgs1, Exo1, or Dna2 shows any preference for binding to leading- or lagging-strand telomeres.

Intriguingly, in fission yeast it has recently been demonstrated that leading-strand replication of telomeres precedes lagging-strand replication (Moser et al., 2009), suggesting perhaps that earlier replication of the leading strand provides more time for postreplicative processing of this strand. Furthermore, Mre11 is important for telomere function in *Drosophila*, an organism that does not use telomerase to maintain chromosome ends (Ciapponi et al., 2004), and therefore Mre11-dependent postreplicative processing of leading strands might be a fundamental property of replication to the end of all linear DNA molecules in eukaryotes. It is clear that leading- and lagging-strand telomeres of mammalian cells also behave differently. For example, in one study of human cells, inactivation of the telomere-binding protein TRF2 caused telomere-telomere fusions specifically between leading-strand telomeres (Bailey et al., 2001). In another study of mouse cells, inactivation of TRF2 combined with deletion of Mre11 biased fusions to leading- rather than lagging-strand telomeres (Deng et al., 2009). Finally, very recent experiments have shown that other telomere-binding proteins inhibit nuclease activities at yeast telomeres (Bonetti et al., 2010). Future

studies should help clarify the important roles of telomere-binding proteins, nucleases, and other DDR proteins at leading- and lagging-strand telomeres.

REFERENCES

Bailey, S.M., Cornforth, M.N., Kurimasa, A., Chen, D.J., and Goodwin, E.H. (2001). Science *293*, 2462–2465.

Bonetti, D., Martina, M., Clerici, M., Lucchini, G., and Longhese, M.P. (2009). Mol. Cell *35*, 70–81.

Bonetti, D., Clerici, M., Anbalagan, S., Martina, M., Lucchini, G., and Longhese, M.P. (2010). PLoS Genet. *6*, e1000966. 10.1371/journal.pgen.1000966.

Ciapponi, L., Cenci, G., Ducau, J., Flores, C., Johnson-Schlitz, D., Gorski, M.M., Engels, W.R., and Gatti, M. (2004). Curr. Biol. *14*, 1360–1366.

de Lange, T. (2009). Science *326*, 948–952.

Deng, Y., Guo, X., Ferguson, D.O., and Chang, S. (2009). Nature *460*, 914–918.

Faure, V., Coulon, C., Hardy, J., and Géli, V. (2010). Mol. Cell *38*, this issue, 842–852.

Gao, H., Cervantes, R.B., Mandell, E.K., Otero, J.H., and Lundblad, V. (2007). Nat. Struct. Mol. Biol. *14*, 208–214.

Lydall, D. (2009). EMBO J. *28*, 2174–2187.

Mimitou, E.P., and Symington, L.S. (2009). Nature *8*, 983–995.

Moser, B.A., Subramanian, L., Chang, Y.T., Noguchi, C., Noguchi, E., and Nakamura, T.M. (2009). EMBO J. *28*, 810–820.

A Role for SIRT1 in the Hypoxic Response

Scott F. Leiser[1] and Matt Kaeberlein[1,2,*]
[1]Department of Pathology, University of Washington, Seattle, WA 98195, USA
[2]Institute of Aging Research, Guangdong Medical College, Dongguan 523808, China
*Correspondence: kaeber@u.washington.edu
DOI 10.1016/j.molcel.2010.06.015

In this issue of *Molecular Cell*, Lim et al. (2010) show that SIRT1 deacetylates HIF-1α and regulates its ability to respond to hypoxia, revealing yet another important function of SIRT1 and suggesting a connection between HIF function in aging and sirtuin enzymes.

Appropriately responding to changes in oxygen availability is essential for life. At the cellular level, this response is largely mediated by the hypoxia-inducible factor, HIF (Semenza, 2007). HIF acts as a transcriptional regulator of genes involved in survival during periods of low oxygen (the hypoxic response) and is regulated primarily via oxygen-dependent proteasomal degradation. Degradation of the regulated HIF subunits (HIF-1α and HIF-2α) is mediated by the von Hippel-Lindau tumor suppressor pVHL, a ubiquitin E3 ligase (Figure 1). Mutations in pVHL stabilize HIF and cause the genetic von Hippel-Lindau disease, which is characterized by a high frequency of renal carcinoma. HIF-1α and HIF-2α are frequently overexpressed in tumors and are a negative predictor for survival. Recently, a role for HIF in the biology of aging has been revealed in a series of studies in the nematode *Caenorhabditis elegans*. Hypoxic growth or normoxic overexpression of the nematode HIF protein, HIF-1, dramatically increases life span and delays disease progression in transgenic models of Huntington's and Alzheimer's diseases (Mehta et al., 2009; Zhang et al., 2009). Interestingly, loss of HIF-1 can also increase life span in *C. elegans* under some conditions (Chen et al., 2009; Zhang et al., 2009), defining HIF-1 as a context-dependent modifier of longevity (Kaeberlein and Kapahi, 2009).

Three reports have recently suggested an important connection between HIF and another aging-related family of enzymes, the sirtuins. Sirtuins are NAD-dependent protein deacetylases, named for their founding member, the yeast histone deacetylase Sir2 (Finkel et al., 2009). Overexpression of sirtuins has been shown to slow aging in yeast, nematodes, and flies, and the mammalian sirtuin, SIRT1, has been implicated in a variety of age-related disease processes. Dioum and colleagues (Dioum et al., 2009) first uncovered the link between HIF and sirtuins by showing that SIRT1 deacetylates and activates HIF-2α in cultured cells subjected to hypoxia. In a second study, Zhong et al. (2010) found that another sirtuin, SIRT6, regulates HIF-1α-responsive genes by deacetylating histones and impairing transcription at HIF-1-responsive promoters.

In this issue, Lim et al. (2010) report that SIRT1 also interacts with HIF-1α in multiple cell lines and mouse tissues. They show that SIRT1 deacetylates HIF-1α at a conserved residue, Lys674, which is acetylated by the PCAF acetyltransferase. Unlike the previously reported activation of HIF-2α by SIRT1 (Dioum et al., 2009), the current study indicates that deacetylation of HIF-1α by SIRT1 *inhibits* HIF activity (Lim et al., 2010). The data of Lim et al. (Lim et al., 2010) also confirmed the prior interaction between SIRT1 and HIF-2α and indicated that that HIF-1α and HIF-2α may compete for SIRT1 binding. HIF-1α and HIF-2α activate separate but overlapping gene subsets and are differentially expressed in various tissues and times after onset of hypoxia (Wang et al., 2005), suggesting a complex interplay between the two hypoxia-responsive factors and SIRT1.

In addition to describing yet another function for SIRT1, this study also provides a potentially important new mechanism

The EMBO Journal (2010) 29, 4020–4034 | © 2010 European Molecular Biology Organization | Some Rights Reserved 0261-4189/10
www.embojournal.org

THE EMBO JOURNAL

EMBO open

Pif1- and Exo1-dependent nucleases coordinate checkpoint activation following telomere uncapping

James M Dewar[1] and David Lydall[1,2,*]

[1]Centre for Integrated Systems Biology of Ageing and Nutrition, Institute for Ageing and Health, Newcastle upon Tyne, Tyne-and-Wear, UK and [2]Institute for Cell and Molecular Biosciences, Newcastle University, Newcastle upon Tyne, Tyne-and-Wear, UK

Essential telomere 'capping' proteins act as a safeguard against ageing and cancer by inhibiting the DNA damage response (DDR) and regulating telomerase recruitment, thus distinguishing telomeres from double-strand breaks (DSBs). Uncapped telomeres and unrepaired DSBs can both stimulate a potent DDR, leading to cell cycle arrest and cell death. Using the *cdc13-1* mutation to conditionally 'uncap' telomeres in budding yeast, we show that the telomere capping protein Cdc13 protects telomeres from the activity of the helicase Pif1 and the exonuclease Exo1. Our data support a two-stage model for the DDR at uncapped telomeres; Pif1 and Exo1 resect telomeric DNA <5 kb from the chromosome end, stimulating weak checkpoint activation; resection is extended >5 kb by Exo1 and full checkpoint activation occurs. Cdc13 is also crucial for telomerase recruitment. However, cells lacking Cdc13, Pif1 and Exo1, do not senesce and maintain their telomeres in a manner dependent upon telomerase, Ku and homologous recombination. Thus, attenuation of the DDR at uncapped telomeres can circumvent the need for otherwise-essential telomere capping proteins.

The EMBO Journal (2010) **29,** 4020–4034. doi:10.1038/emboj.2010.267; Published online 2 November 2010
Subject Categories: genome stability & dynamics
Keywords: Cdc13; DNA damage response; Exo1; Pif1; uncapped telomeres

Introduction

Telomeres consist of double-stranded DNA (dsDNA) and single-stranded DNA (ssDNA), bound by dsDNA- and ssDNA-binding proteins (Blackburn *et al*, 2006; Lydall, 2009). This nucleoprotein 'cap' has at least two functions: to shield the telomeric DNA from stimulating the DNA damage response (DDR) and to regulate elongation of the telomere by telomerase. In human senescent cells, dysfunctional telomeres induce a sustained DDR (d'Adda di Fagagna *et al*, 2003). In both budding yeast and mice, nuclease activities that attack dysfunctional telomeres contribute to telomere-driven senescence (Maringele and Lydall, 2004; Schaetzlein *et al*, 2007). Therefore, understanding the regulation of nuclease activities at dysfunctional telomeres in yeast is likely to be informative about similar processes occurring at mammalian telomeres and the human ageing process.

dsDNA-binding proteins and accessory factors are required at both human telomeres (TRF1, TRF2, TIN2, TPP1, RAP1) and budding yeast telomeres (Rap1, Rif1, Rif2) to prevent DDRs (Wotton and Shore, 1997; de Lange, 2005; Celli and de Lange, 2005; Marcand *et al*, 2008; Bonetti *et al*, 2010; Vodenicharov *et al*, 2010). In budding yeast, telomeric ssDNA is bound by Cdc13 with accessory proteins Stn1 and Ten1, whereas in human cells, it is bound by POT1 (de Lange, 2005; Gao *et al*, 2007). Cdc13–Stn1–Ten1 forms an evolutionarily conserved complex (the CST complex) that has telomeric roles in most organisms studied so far (Miyake *et al*, 2009; Surovtseva *et al*, 2009). POT1 binds telomeric ssDNA and is connected to the dsDNA-binding proteins of the telomere cap by TPP1 and TIN2 (de Lange, 2009). Inactivation of POT1 or Cdc13 induces 'telomere uncapping' and has similar consequences—initiation of a DDR and resection of the telomeric DNA by nuclease activities (Garvik *et al*, 1995; Baumann and Cech, 2001; Pitt and Cooper, 2010).

The response to telomere uncapping is readily studied in budding yeast by inactivation of Cdc13 using the thermosensitive allele *cdc13-1* (Garvik *et al*, 1995). Following Cdc13 inactivation, a potent DDR is initiated; telomeric DNA is resected by nucleases, which degrade the AC (5′) strand to generate extensive TG (3′) ssDNA that stimulates activation of the DNA damage checkpoint, in a manner analogous to that at DNA double-strand breaks (DSBs) (Figure 1A) (Garvik *et al*, 1995; Lydall and Weinert, 1995; Vodenicharov and Wellinger, 2006). There is relatively little understanding of the nuclease activities responsible for generating ssDNA at uncapped telomeres (Zubko *et al*, 2004). In contrast, there has been much recent progress identifying nuclease activities that function at DSBs (Gravel *et al*, 2008; Mimitou and Symington, 2008; Zhu *et al*, 2008).

Exo1 is the only nuclease known to generate ssDNA at uncapped telomeres in budding yeast (Maringele and Lydall, 2002). Exo1 is a 5′ to 3′ dsDNA exonuclease involved in DSB resection and in mismatch repair (Tsubouchi and Ogawa, 2000; Gravel *et al*, 2008; Mimitou and Symington, 2008; Zhu *et al*, 2008). In the absence of Exo1, ssDNA is still generated following Cdc13 inactivation, demonstrating that

*Corresponding author. Institute for Cell and Molecular Biosciences, Newcastle University, Newcastle upon Tyne, Tyne and Wear NE2 4HH, UK. Tel.: +44 191 222 5318; Fax: +44 191 222 7424;
E-mail: d.a.lydall@ncl.ac.uk

Received: 27 April 2010; accepted: 29 September 2010; published online: 2 November 2010

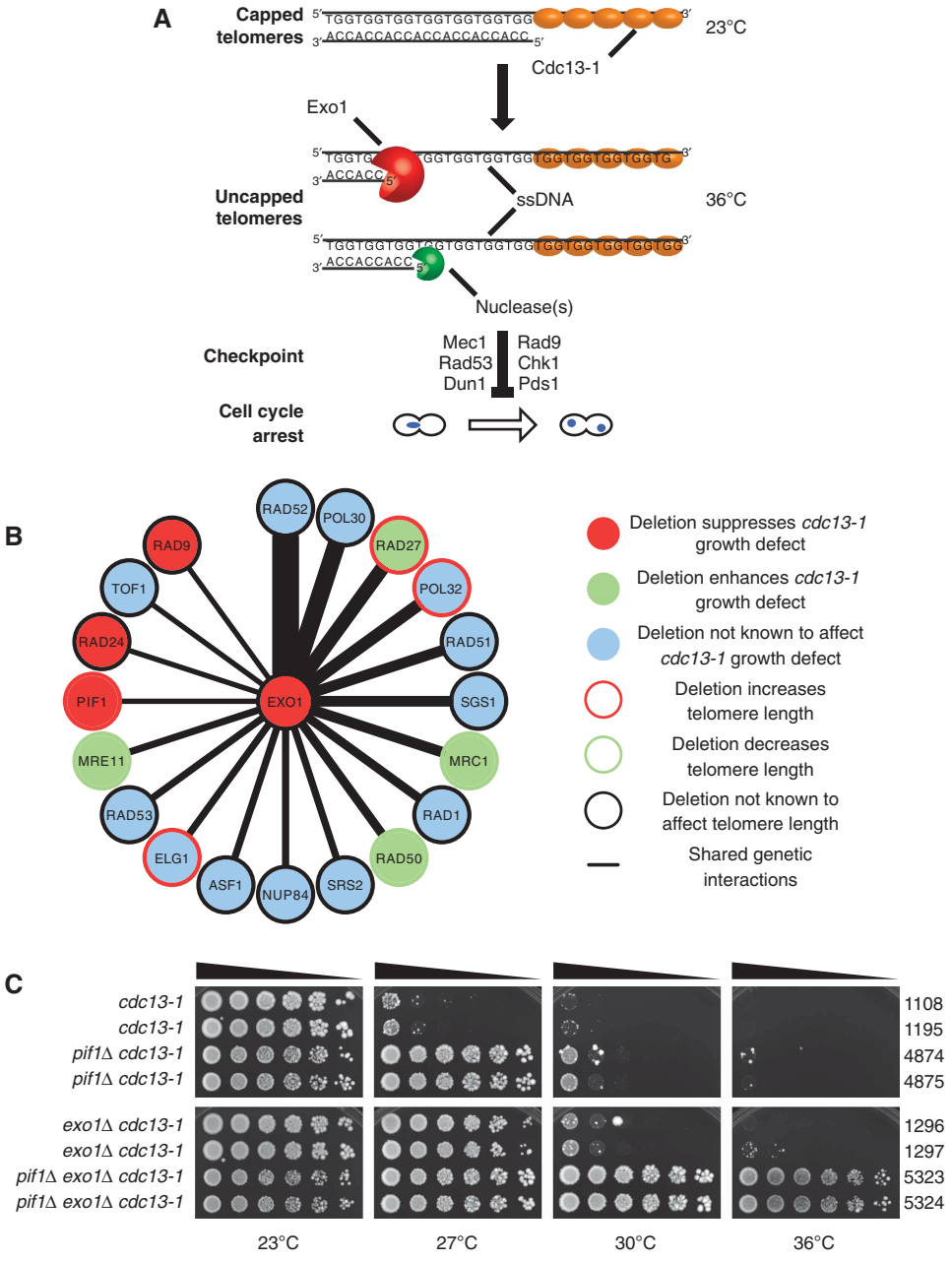

Figure 1 Pif1 and Exo1 inhibit growth of *cdc13-1* mutants. (**A**) Inactivation of Cdc13 by use of the temperature-sensitive allele *cdc13-1* leads to telomere uncapping. Exo1 and additional nuclease(s) generate ssDNA at uncapped telomeres, which is the stimulus for Mec1-dependent checkpoint activation and cell cycle arrest. (**B**) Ranked diagram of genes that share genetic interactions with *EXO1* and are important in the context of telomeres. (Thicker lines mean more shared genetic interactions). (**C**) Strains of the genotypes shown were serially diluted across agar plates and grown at the temperatures indicated for 3 days. In this and other figures, strain numbers (DLYs) are shown adjacent.

other nuclease activities must also function at uncapped telomeres. The determinant(s) of this Exo1-independent ssDNA generation have not so far been identified, but at least two hypothetical nuclease activities have been proposed (ExoX and ExoY) (Zubko *et al*, 2004).

We sought to identify additional nuclease activities functioning at uncapped telomeres following inactivation of Cdc13. Bioinformatic analysis of genetic interactions found the helicase Pif1 to be a candidate for contributing to nuclease activity. Consistent with this hypothesis, we found that Pif1 and Exo1 are required for different nuclease activities that generate ssDNA and activate the DNA damage checkpoint following Cdc13 inactivation. Furthermore, deletion of both *PIF1* and *EXO1* permits yeast cells to tolerate complete loss of the essential telomere capping protein Cdc13.

Results

PIF1 and EXO1 define parallel pathways that inhibit growth of cdc13-1 mutants

To identify potential nuclease(s) active in *cdc13-1* mutants, we reasoned that genes responsible for such activities would interact with similar genes to those that *EXO1* interacts with. We used the BioGRID database to create a ranked list of genes

that had similar genetic interactions to *EXO1* (Figure 1B) (Stark *et al*, 2006). Of these, 9/19 affected *cdc13-1* growth or telomere length. Deletion of *EXO1* suppresses *cdc13-1* growth defects, so we focussed on those genes that also suppressed *cdc13-1* growth defects. By these criteria, two previously characterized checkpoint genes (*RAD9* and *RAD24*) and the helicase-encoding *PIF1* behaved similarly to *EXO1* (Figure 1B). Rad9 and Rad24 do indeed regulate nuclease activities at uncapped telomeres and are required for checkpoint activation (Garvik *et al*, 1995; Lydall and Weinert, 1995; Zubko *et al*, 2004). Pif1 has been shown to inhibit growth of *cdc13-1* mutants (Downey *et al*, 2006), whereas overexpression of Pif1 has been shown to enhance growth defects seen in *cdc13-1* mutants, but the contribution of Pif1 to the nuclease activity and checkpoint activation in *cdc13-1* mutants had not been assessed (Vega *et al*, 2007; Chang *et al*, 2009).

Pif1 is a helicase with both mitochondrial and nuclear functions (Van Dyck *et al*, 1992; Schulz and Zakian, 1994). In the nucleus, Pif1 has been implicated in negative regulation of telomerase, generation of long flaps during Okazaki fragment processing, unwinding of G-quadruplexes and disassembly of stalled replication forks (Zhou *et al*, 2000; Boule *et al*, 2005; Budd *et al*, 2006; Chang *et al*, 2009; George *et al*, 2009; Makovets and Blackburn, 2009; Pike *et al*, 2009; Ribeyre *et al*, 2009; Zhang and Durocher, 2010). To test the hypothesis that Pif1 contributes to a nuclease activity at uncapped telomeres in *cdc13-1* mutants, we compared the effects of Pif1 and Exo1 on cell growth after Cdc13-1 inactivation. At the permissive temperature (23°C), Cdc13-1 is functional and efficiently caps the telomeres, permitting growth of *cdc13-1* mutants. At the non-permissive temperature (36°C), Cdc13-1 is completely defective and *cdc13-1* mutants are unable to grow (Figure 1A and C). At semi-permissive temperatures (25–29°C), moderate Cdc13-1 inactivation occurs and growth of *cdc13-1* mutants is inhibited (Figure 1C). As previously reported, *cdc13-1 pif1*Δ and *cdc13-1 exo1*Δ mutants are able to grow at 27°C, whereas *cdc13-1* mutants are not (Figure 1C) (Zubko *et al*, 2004; Downey *et al*, 2006). These effects on growth are consistent with the hypothesis that Pif1, like Exo1, contributes to nuclease activity at uncapped telomeres.

Pif1 and Exo1 inhibit growth of *cdc13-1* mutants, possibly by contributing to nuclease activity at uncapped telomeres. To test whether the two proteins worked in the same pathway/complex or in different pathways, we examined the effect Pif1 on growth of *cdc13-1 exo1*Δ mutants. *cdc13-1 exo1*Δ mutants were unable to grow at 30°C, whereas *cdc13-1 exo1*Δ *pif1*Δ mutants were able to grow at 30 and 36°C (Figure 1C). Remarkably, at 36°C, the growth of *cdc13-1 exo1*Δ *pif1*Δ mutants was barely distinguishable from that of *CDC13*$^+$ *exo1*Δ *pif1*Δ mutants (Supplementary Figure S1A). We confirmed that this effect was due to the *pif1*Δ and *exo1*Δ mutations and not due to second site suppressors arising in our strains by crossing a *cdc13-1* mutant able to grow at 36°C, with a *cdc13-1* strain and confirming that all *cdc13-1 exo1*Δ *pif1*Δ progeny could all grow at 36°C (Supplementary Figure S1B). We conclude that Pif1 and Exo1 inhibit growth of *cdc13-1* mutants through different pathways, and inactivation of these pathways may eliminate the requirement for telomere capping by Cdc13.

At DSBs, parallel nuclease activities dependent upon Exo1, the helicase Sgs1 and nuclease Dna2 generate extensive ssDNA (Gravel *et al*, 2008; Mimitou and Symington, 2008; Zhu *et al*, 2008). We hypothesized that, as with Exo1, elimination of Sgs1 or Dna2 in cells lacking Pif1 might improve the growth of *cdc13-1* mutants and perhaps even permit growth at 36°C. However, we found that *cdc13-1 pif1*Δ *dna2*Δ mutants grew less well than *cdc13-1 pif1*Δ mutants (Supplementary Figure S2A). We were unable to examine the effect of *dna2*Δ on the growth of *cdc13-1 PIF1*$^+$ mutants, as *DNA2* is an essential gene unless *PIF1* is deleted (Budd *et al*, 2006). We also found that *cdc13-1 pif1*Δ *sgs1*Δ mutants grew slightly less well than *cdc13-1 pif1*Δ mutants and that *cdc13-1 sgs1*Δ mutants grew slightly less well than *cdc13-1* mutants (Supplementary Figure S2B), consistent with other work from our laboratory (Ngo and Lydall, 2010). We conclude that Exo1 inhibits the growth of *cdc13-1* mutants with uncapped telomeres, whereas Sgs1 and Dna2 contribute to the vitality of such cells. Therefore, we chose to focus on the roles of Pif1 and Exo1 at uncapped telomeres.

Elimination of Pif1 and Exo1 permits telomere maintenance following inactivation of Cdc13

Yeast cells can overcome the requirement for Cdc13 by altering telomere structure, as observed in rare variants, which can be selected for after inactivation of telomerase or after attenuation of nuclease/checkpoint activities at uncapped telomeres (Larrivee and Wellinger, 2006; Zubko and Lydall, 2006). To test whether elimination of Pif1 and Exo1 caused alterations in telomere structure that could explain the growth of *cdc13-1* cells at 36°C, we performed Southern blots to examine telomere structure, probing for Y′ sequences (Figure 2B), which are components of the majority of yeast telomeres (Supplementary Figure S3A and B). The Y′ probe contained G-rich sequences and weakly cross-hybridized to telomeres that did not contain Y′ sequences, so we also probed for TG repeat sequences to detect telomeres that lacked Y′ elements (Supplementary Figure S4).

*pif1*Δ mutants have long telomeres (Schulz and Zakian, 1994) and consistent with this, *CDC13*$^+$ *exo1*Δ *pif1*Δ mutants have longer telomeres than *CDC13*$^+$ *EXO1*$^+$ *PIF1*$^+$ strains (compare lanes 1–2, 3–4 and 7–8; Figure 2B). The telomeres of *cdc13-1 exo1*Δ *pif1*Δ mutants grown at 36°C were longer than those of *CDC13*$^+$ *exo1*Δ *pif1*Δ mutants grown at 23°C (compare lanes 9–10 with lanes 7–8, Figure 2B) but indistinguishable from those of *cdc13-1 exo1*Δ *pif1*Δ mutants grown at 23°C (compare lanes 9–10 with lanes 17–18, Figure 2B). This demonstrates that no gross alterations in telomere structure occur when *cdc13-1 exo1*Δ *pif1*Δ mutants are grown at 36°C. Furthermore, *cdc13-1 exo1*Δ *pif1*Δ mutants are able to grow at 36°C, whereas *cdc13-1 pif1*Δ mutants are not, but are indistinguishable in telomere structure (compare lanes 13–14 with lanes 17–18, Figure 2B). We conclude that alterations in telomere structure most likely do not account for the growth of *cdc13-1 exo1*Δ *pif1*Δ mutants at 36°C.

Pif1 exists as both nuclear and mitochondrial isoforms (Schulz and Zakian, 1994). Therefore, we wanted to know whether the nuclear or mitochondrial function of Pif1 inhibited growth of *cdc13-1 exo1*Δ mutants at 36°C. The *pif1-m2* allele, lacking nuclear Pif1, permitted growth of *cdc13-1 exo1*Δ mutants at 36°C, whereas the *pif1-m1* allele, lacking mitochondrial Pif1, did not (Figure 2C). We note that the growth of *cdc13-1 exo1*Δ *pif1-m2* mutants at 36°C is less than *cdc13-1 exo1*Δ *pif1*Δ mutants (Figure 2C). This is consistent with other

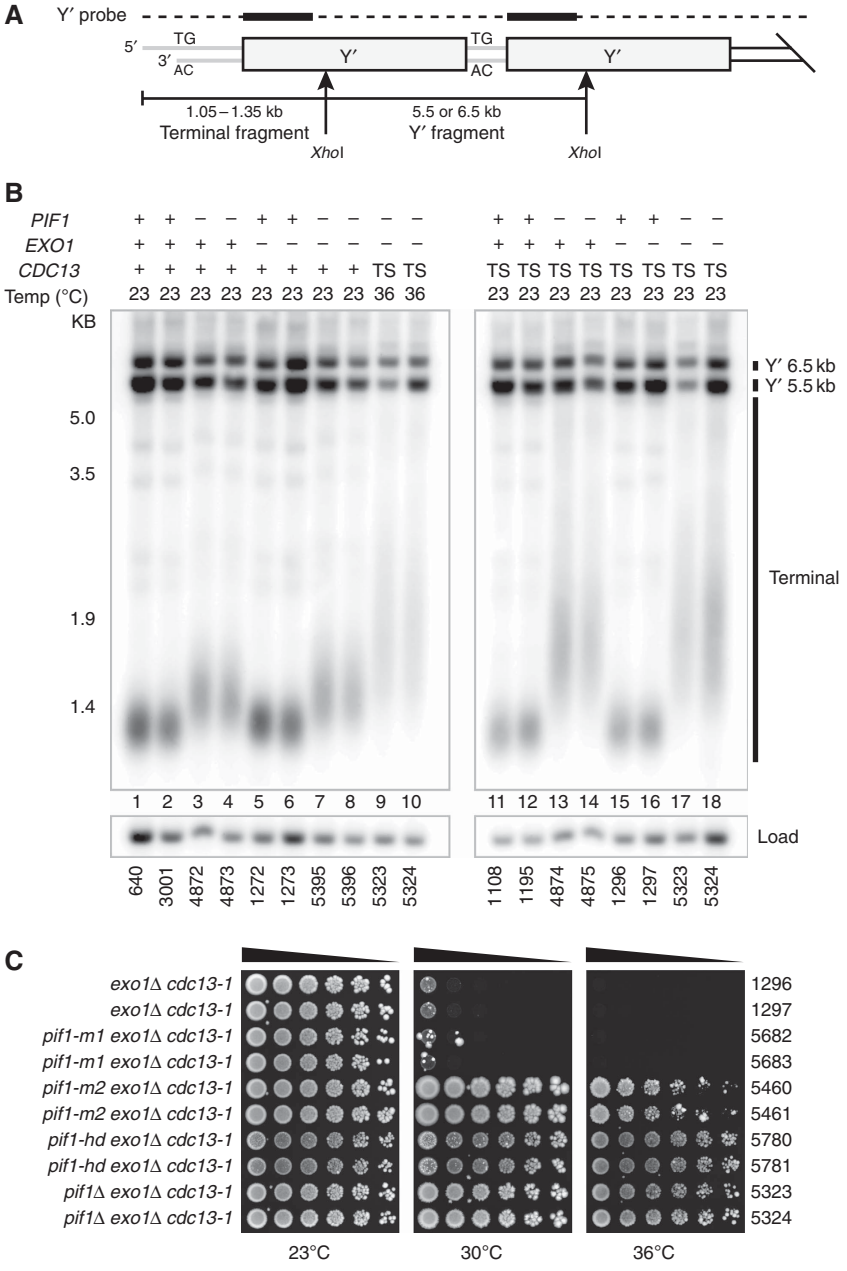

Figure 2 Exo1 and nuclear, helicase activity of Pif1 prevent telomere maintenance following inactivation of Cdc13. (**A**) Cartoon of yeast telomeres, indicating the fragments detected by telomere Southern blots using Y′ probe. Arrows represent *Xho*I cut sites. (**B**) Genomic DNA was prepared from two independent *CDC13*$^{+}$ (+) or *cdc13-1* (TS) strains, grown at 23 or 36°C, digested with *Xho*I and Southern blotted to detect telomeric Y′ and terminal fragments. Blots were reprobed to detect *CDC15* as a loading control. Also see Supplementary Figure S4. (**C**) *cdc13-1 exo1*Δ mutants defective in nuclear Pif1 (*pif1-m2*), mitochondrial Pif1 (*pif1-m1*) or carrying the helicase-deficient allele of Pif1 (*pif1-hd)* were serially diluted across agar plates and grown at the temperatures indicated for 3 days.

reports that low levels of nuclear Pif1 activity persist in *pif1-m2* mutants (Schulz and Zakian, 1994; Ribeyre *et al*, 2009). We also confirmed that helicase activity of Pif1 inhibited growth of *cdc13-1 exo1*Δ mutants because the *pif1-hd* allele, deficient in helicase activity, also permitted growth at 36°C (Figure 2C) (Zhou *et al*, 2000; Ribeyre *et al*, 2009). We conclude that nuclear, helicase-dependent activity of Pif1 inhibits growth of telomere capping-defective *cdc13-1* mutants.

Pif1- and Exo1-dependent nucleases initiate the DDR following Cdc13 inactivation

Upon Cdc13 inactivation, nuclease activities generate ssDNA, which stimulates checkpoint kinase cascades and induces metaphase arrest (Figure 1A) (Garvik *et al*, 1995). To test the role of Pif1 in cell cycle arrest, *cdc13-1* mutants were synchronized in G1 using α factor at 23°C, then released to 36°C to assess metaphase arrest (Figure 3A). All strains also harboured the *cdc15-2* mutation so that any cells that overcame *cdc13-1*-induced metaphase arrest would arrest in late anaphase due to *cdc15-2* and be unable to enter another cell cycle (Figure 3A) (Lydall and Weinert, 1995; Zubko *et al*, 2004). As expected, *cdc13-1* mutants accumulated at metaphase and did not pass through to anaphase (Figure 3B and C). *cdc13-1 exo1*Δ mutants accumulated at metaphase with similar kinetics to *cdc13-1* mutants but, as previously reported, a subpopulation of *cdc13-1 exo1*Δ cells escaped metaphase

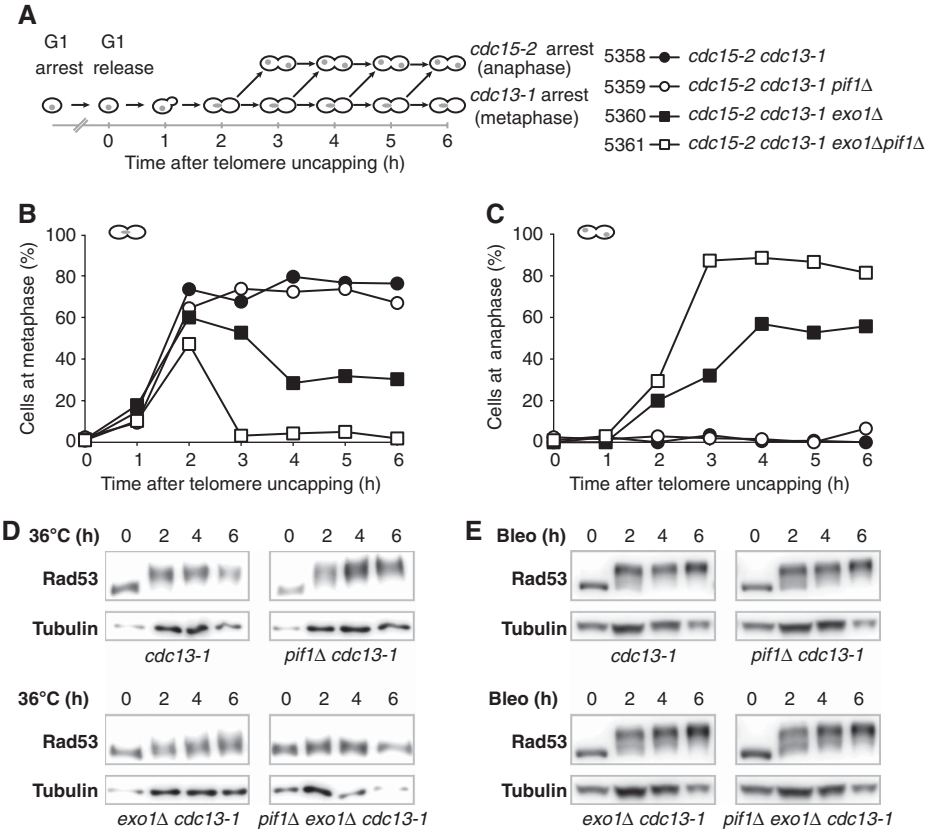

Figure 3 Pif1 and Exo1 stimulate cell cycle arrest following inactivation of Cdc13. (**A**) Synchronous culture experiments to examine the effect of Pif1 and Exo1 on cell cycle arrest following telomere uncapping. *cdc15-2 cdc13-1* cells were synchronized in G1 using α-factor then released at 36°C. Cells arrest at metaphase from telomere uncapping (*cdc13-1*) or at anaphase from Cdc15 inactivation (*cdc15-2*). Samples taken at the time points indicated were stained with DAPI and >100 cells of each genotype scored for cell cycle position (Zubko *et al*, 2006). (**B**) Percentage of cells at metaphase. (**C**) Percentage of cells at late anaphase. (**D**) Western blots of Rad53 following shift to 36°C. Upper and lower panels were run in parallel on separate gels, but transferred, detected and imaged simultaneously. (**E**) Western blots of Rad53 following treatment with bleomycin. Corresponding scoring of cells at metaphase and anaphase given as Supplementary Figure S5.

arrest and accumulated in late anaphase due to the *cdc15-2* mutation (Figure 3B and C) (Zubko *et al*, 2004). *cdc13-1 pif1*Δ mutants behaved like *cdc13-1* mutants and did not pass through to anaphase (Figure 3B and C). Interestingly, *cdc13-1 exo1*Δ *pif1*Δ mutants did not accumulate in metaphase at all and passed readily through to anaphase (Figure 3B and C). Taken together, these results show that Pif1 has no effect on metaphase arrest of *cdc13-1* mutants at 36°C when Exo1 is present, but it is responsible for the arrest of a subpopulation of cells when Exo1 is absent.

Following inactivation of Cdc13, Mec1-dependent checkpoint activation occurs, leading to activation and hyperphosphorylaiton of the kinase Rad53 (Figure 1A) (Sweeney *et al*, 2005; Morin *et al*, 2008). We used the synchronous cultures to examine Rad53 phosphorylation by western blot (Figure 3A). *cdc13-1* and *cdc13-1 pif1*Δ mutants exhibited strong Rad53 phosphorylation, indicated by a marked upward mobility shift of Rad53 (upper panels, Figure 3D). A reduction in Rad53 phosphorylation was seen in *cdc13-1 exo1*Δ mutants, correlating with the recovery from metaphase arrest displayed by *cdc13-1 exo1*Δ mutants following telomere uncapping (Figure 3C and D). Interestingly, no discernable change in the mobility of Rad53 could be seen in *cdc13-1 exo1*Δ *pif1*Δ mutants, consistent with their complete failure to arrest cell division at 36°C (Figure 3C and D). We conclude that in the absence of Pif1 and Exo1, the checkpoint kinase Rad53 is not activated after telomere uncapping in *cdc13-1* mutants.

To see whether *cdc13-1 exo1*Δ *pif1*Δ strains were defective in the DDR after other types of DNA damage as well as after telomere uncapping, we treated cells with bleomycin to induce DSBs. At both DSBs and uncapped telomeres, ssDNA is an important stimulus for the Mec1-dependent checkpoint. We treated the same set of strains examined in Figure 3B–D, with bleomycin at 23°C after release from G1 arrest. *cdc13-1*, *cdc13-1 pif1*Δ, *cdc13-1 exo1*Δ and *cdc13-1 exo1*Δ *pif1*Δ mutants all behaved similarly, phosphorylating Rad53 and arresting at methaphase (Figure 3E; Supplementary Figure S4). We conclude that a functional DDR pathway operates in (*cdc13-1*) *exo1*Δ *pif1*Δ cells but that these cells are specifically defective in responding to telomere uncapping.

Telomeric ssDNA stimulates metaphase arrest following telomere uncapping (Garvik *et al*, 1995). We used synchronous cultures (Figure 3A) and quantitative amplification of ssDNA (QAOS) to measure subtelomeric ssDNA in repetitive Y′ elements (present on Chromosome V and most other chromosome ends) following Cdc13 inactivation (Figure 4A) (Booth *et al*, 2001). c*dc13-1* mutants with uncapped telomeres generated ssDNA at both the Y′600 and Y′5000 loci (Figure 4B and C). *cdc13-1 exo1*Δ mutants generated less ssDNA following telomere uncapping at the Y′ loci, as

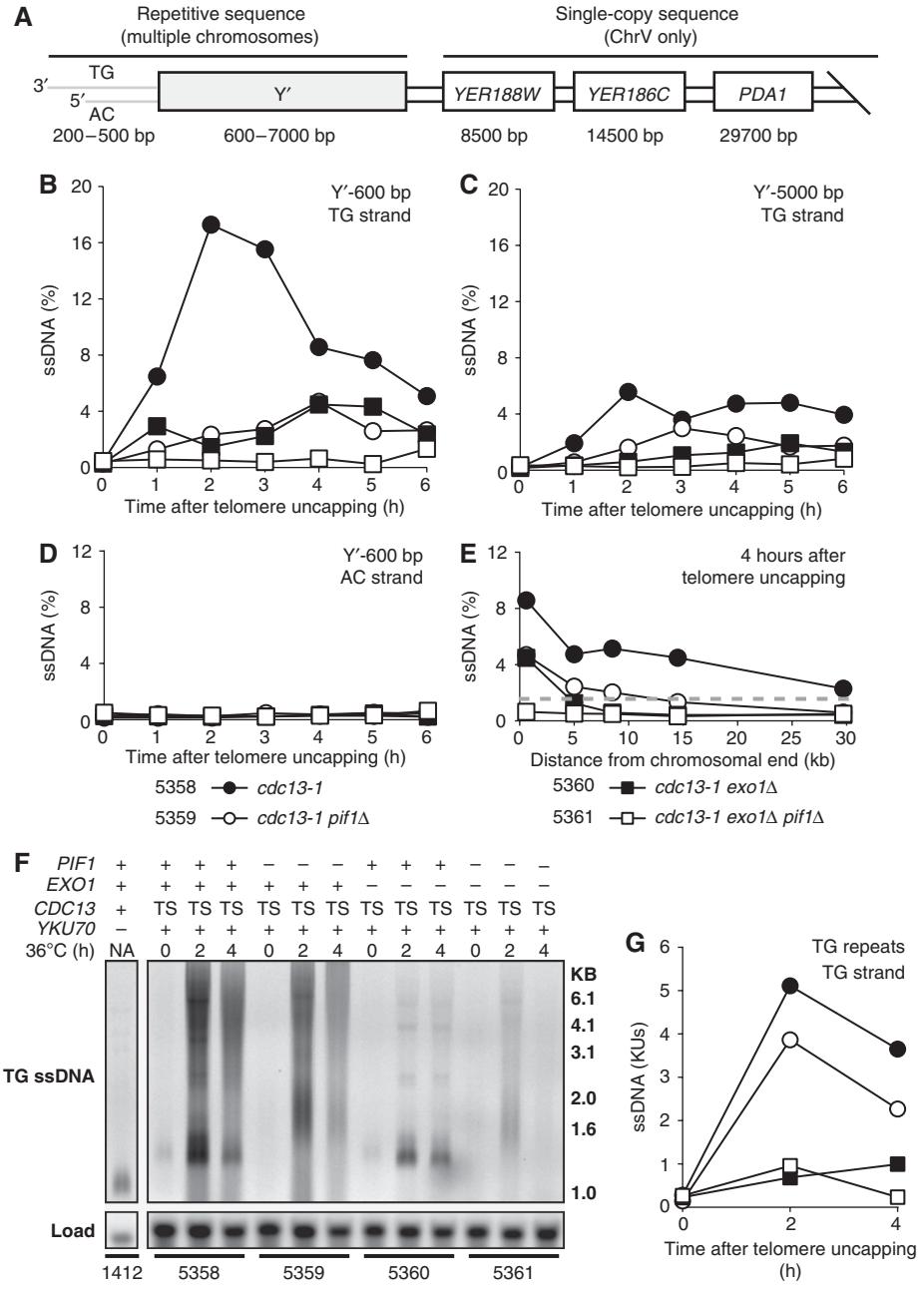

Figure 4 Pif1 and Exo1 generate ssDNA at uncapped telomeres. (**A**) Physical map of the right telomere of Chromosome V. Synchronous cultures were subjected to telomere uncapping as in Figure 3A, and samples were taken to measure ssDNA. (**B**) TG-strand ssDNA 600 bp from the end of the telomere (Y′600) measured by QAOS. (**C**) TG-strand ssDNA 5000 bp away from the end of the telomere (Y′5000). (**D**) AC-strand ssDNA 600 bp away from the end of the telomere. (**E**) TG-strand ssDNA generated at loci indicated in (**A**), 4 h after telomere uncapping. Dashed line represents 1.56% (1/64), corresponding to the value expected for 1 single-stranded locus per yeast cell in G2. (**F**) TG-strand ssDNA in the telomeric TG repeats detected by in-gel assay, comparing *cdc13-1* mutants (TS) to a *yku70*Δ control. Loading determined by Southern hybridization with a *CDC15* probe. Lanes were run and detected on the same gel and cropped for presentation purposes. (**G**) Quantification of the ssDNA signal in each lane in (**F**). ssDNA is measured in KUs (Ku units). In all, 1 Ku Unit is the ssDNA signal in an asynchronously dividing *yku70*Δ control at 23°C.

previously reported (Maringele and Lydall, 2002; Zubko *et al*, 2004). Interestingly, *cdc13-1 pif1*Δ mutants, like *cdc13-1 exo1*Δ mutants showed reduced ssDNA generation in the Y′600 and Y′5000 loci following telomere uncapping. Furthermore, *cdc13-1 exo1*Δ *pif1*Δ mutants generated no detectable ssDNA at Y′600 or Y′5000 loci following telomere uncapping (Figure 4B and C). We confirmed that ssDNA generation occurred on the TG (3′) strand due to degradation of the AC (5′) strand, as we were unable to detect ssDNA on the AC strand (Figure 4D). We conclude that Pif1, like Exo1, is important for ssDNA generation after telomere uncapping in *cdc13-1* mutants and appears to regulate a nuclease activity, which functions in parallel to Exo1 at chromosome ends.

To examine how Pif1 and Exo1 affect ssDNA accumulation further from chromosome ends, we measured ssDNA at single-copy loci on Chromosome V after Cdc13 inactivation. At 4 h, *cdc13-1* mutants generated ssDNA at all loci examined, with

the amount of ssDNA decreasing at loci further from the chromosome end, as previously reported (Zubko *et al*, 2004). *cdc13-1 exo1*Δ mutants generated less ssDNA in the Y′ repeats and no ssDNA in single-copy loci on Chromosome V, also as previously reported (Figure 4E) (Zubko *et al*, 2004). *cdc13-1 pif1*Δ mutants generated similar amounts of ssDNA to *cdc13-1 exo1*Δ mutants in the Y′ repeats. However, at more distal, single-copy loci, *cdc13-1 pif1*Δ mutants generated less ssDNA than *cdc13-1* mutants but more than *exo1*Δ *cdc13-1* mutants. The higher levels of ssDNA generated further from the chromosome end in *cdc13-1 pif1*Δ mutants, in comparison with *cdc13-1 exo1*Δ mutants, most likely accounts for their sustained metaphase arrest following telomere uncapping (Figure 3B and C). Furthermore, the ssDNA generated by *cdc13-1* and *cdc13-1 pif1*Δ mutants <10 kb from the chromosome end is $>1.6\%$ (1/64) (Figure 4E). Assuming 1 single-stranded telomere per cell is sufficient to stimulate arrest, this suggests that ssDNA extending <10 kb on one of the 64 G2 telomeres in *Saccharomyces cerevisiae* is sufficient to stimulate metaphase arrest (Figure 4E) (Sandell and Zakian, 1993; Vaze *et al*, 2002; Zubko *et al*, 2004).

No checkpoint activation was detected in *cdc13-1 exo1*Δ *pif1*Δ mutants following telomere uncapping, and no ssDNA was detected in the Y′ elements (Figures 3D and 4B). However, *yku70*Δ mutants at 23°C have detectable ssDNA in the telomeric TG repeats but do not undergo checkpoint activation (Gravel *et al*, 1998; Polotnianka *et al*, 1998; Maringele and Lydall, 2002). Thus, we hypothesized that *cdc13-1 exo1*Δ *pif1*Δ mutants might still generate detectable ssDNA in the TG repeats. We used synchronous cultures (Figure 3A) and measured ssDNA by in-gel assay to measure ssDNA in the TG repeats in *cdc13-1* mutants (Figure 4F and G). *cdc13-1* mutants generated large amounts of TG ssDNA at 2 and 4 h following telomere uncapping (Figure 4F), corresponding to an approximately five-fold increase in signal compared with *yku70*Δ mutants (Figure 4G). *cdc13-1 exo1*Δ *pif1*Δ mutants also generated detectable ssDNA 2 h following telomere uncapping, but at a level approximately equal to that of a *yku70*Δ mutant (Figure 4F and G). However, the ssDNA generated in *cdc13-1 exo1*Δ *pif1*Δ mutants was transient and was no longer detectable 4 h after telomere uncapping (Figure 4F and G). Surprisingly, *cdc13-1 pif1*Δ mutants displayed only a modest decrease in ssDNA generation in the TG repeats following telomere uncapping, whereas *cdc13-1 exo1*Δ mutants generated very little ssDNA (Figure 4F and G). We conclude that *cdc13-1 exo1*Δ *pif1*Δ mutants generate limited, transient ssDNA that is insufficient to stimulate checkpoint activation and that Exo1 is much more important than Pif1 for ssDNA generation in the TG repeats following telomere uncapping.

Pif1 has important functions in cells lacking telomerase

It has been suggested that increased levels of telomerase at the telomeres of *cdc13-1 pif1*Δ cells shields uncapped telomeres from nuclease activities (Vega *et al*, 2007). However, this is somewhat inconsistent with our observation that Pif1 has relatively little effect on ssDNA generation in the telomeric TG repeats, where telomerase presumably binds (Figure 4G). Therefore, we wanted to know whether the ability of the *pif1*Δ mutation to improve the growth of *cdc13-1* mutants was dependent upon the telomerase template component (TLC1) or catalytic subunit (Est2). Interestingly, we found that *cdc13-1 tlc1*Δ *pif1*Δ and *cdc13-1 tlc1*Δ *exo1*Δ mutants grew better at 25°C than *cdc13-1 tlc1*Δ mutants (compare rows 7–8 and 11–12 with 3–4, Figure 5A; Supplementary Figure S6). We also found that *cdc13-1 est2*Δ *pif1*Δ and *cdc13-1 est2*Δ *exo1*Δ mutants were able to grow at 25°C, whereas *cdc13-1 est2*Δ mutants were not (Supplementary Figure S7). We conclude that Pif1 has a telomerase (TLC1, Est2) independent effect at uncapped telomeres. However, we note that *est2*Δ *cdc13-1* and *tlc1*Δ *cdc13-1* mutants grow worse than *cdc13-1* mutants, demonstrating that telomerase contributes to telomere capping following inactivation of Cdc13.

Pif1 is responsible for the residual checkpoint activation in *cdc13-1 exo1*Δ mutants (Figure 3D) and inhibits growth of *cdc13-1* mutants lacking telomerase (Figure 5A). We hypothesized that Pif1 would contribute to ssDNA generation at uncapped telomeres and subsequent checkpoint activation, even in *cdc13-1* mutants lacking telomerase. To test this, we measured Rad53 phosphorylation (Supplementary Figure S8A) and telomeric TG repeat ssDNA (Supplementary Figure S8B and C) in *cdc13-1* and *cdc13-1 tlc1*Δ mutants, before and after telomere uncapping. In *cdc13-1 tlc1*Δ *exo1*Δ *pif1*Δ mutants, there was a decrease in Rad53 phosphorylation compared with *cdc13-1 tlc1*Δ *exo1*Δ mutants (Supplementary Figure S8A). We also found that *cdc13-1 tlc1*Δ *pif1*Δ and *cdc13-1 tlc1*Δ *exo1*Δ *pif1*Δ mutants generated less ssDNA than *cdc13-1 tlc1*Δ and *cdc13-1 tlc1*Δ *exo1*Δ mutants, respectively, following telomere uncapping (Supplementary Figure S8B and C). We conclude that Pif1 has a contribution to ssDNA generation and checkpoint activation following telomere uncapping that is independent of telomerase. However, we note that 40% of *cdc13-1 tlc1*Δ cells were at metaphase at 23°C compared with 30% of *cdc13-1 tlc1*Δ *pif1*Δ cells (Supplementary Figure S8D). Thus, we cannot exclude the possibility that reduced ssDNA generation in *cdc13-1 tlc1*Δ *pif1*Δ mutants is due to altered kinetics of accumulation at metaphase.

Although Pif1 clearly demonstrates a telomerase-independent effect in *cdc13-1* mutants, we note that *cdc13-1 tlc1*Δ *exo1*Δ mutants could grow at 27°C, whereas *cdc13-1 tlc1*Δ *pif1*Δ mutants could not (compare rows 11–12 with 7–8, Figure 5A). In contrast, *cdc13-1 TLC1*$^+$ *exo1*Δ mutants and *cdc13-1 TLC1*$^+$ *pif1*Δ mutants could both grow similarly at 27°C (compare rows 9–10 with 5–6, Figure 5A). This shows that Pif1 is less potent than Exo1 at inhibiting growth of *cdc13-1 tlc1*Δ mutants than *cdc13-1 TLC1*$^+$ mutants.

To help clarify the role of Pif1 in *cdc13-1 tlc1*Δ and *cdc13-1 TLC1*$^+$ mutants, we examined the effect of Pif1 in *CDC13*$^+$ *tlc1*Δ mutants. Yeast strains that cannot recruit telomerase (e.g. *tlc1*Δ) lose telomeric DNA with each cell division until the cultures senesce and lose proliferative capacity, much like mammalian fibroblasts. Senescent, telomerase-deficient yeast cultures usually recover, using telomerase-independent, recombination-dependent mechanisms of telomere maintenance, leading to clear changes in telomere structure (Lundblad and Blackburn, 1993; Teng and Zakian, 1999). Therefore, we germinated spores containing combinations of null mutations in telomerase (*TLC1*), *PIF1* and *EXO1*, and assessed growth at various passages (Figure 5B). As expected, *tlc1*Δ mutants grew well at passage 1, poorly from passages 2–5 (senescence) and grew well again from passage 7 (recovery) (Figure 5B). *tlc1*Δ *exo1*Δ mutants showed a similar pattern of growth to *tlc1*Δ mutants but grew slightly

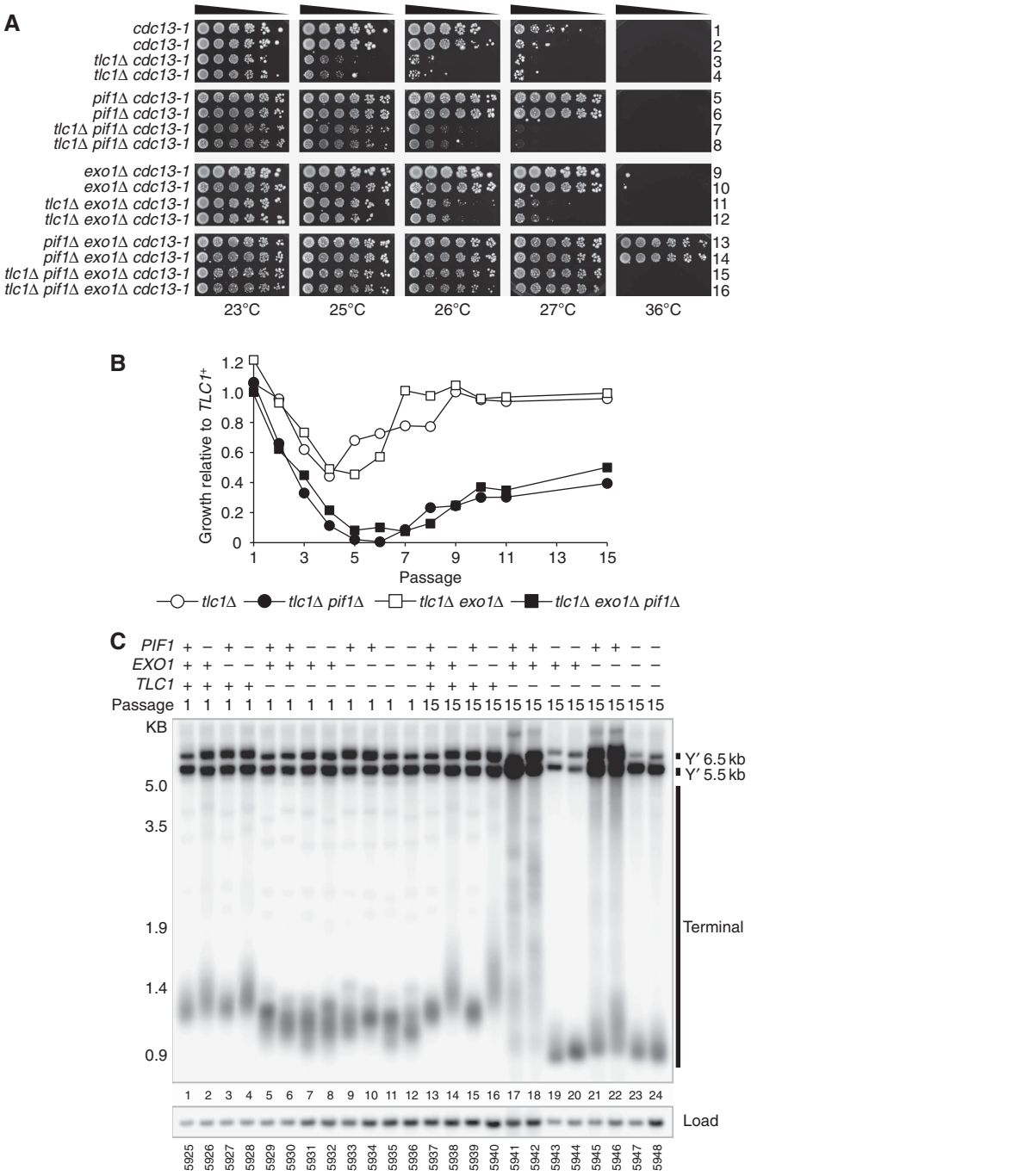

Figure 5 Pif1 has telomerase-independent effects at telomeres. (**A**) A *cdc13-1/CDC13*$^+$ *tlc1*Δ*/TLC1*$^+$ *exo1*Δ*/EXO1*$^+$ *pif1*Δ*/PIF1*$^+$ diploid (DLY1628 x DLY5324) was sporulated, dissected and germinated at 23°C to generate strains of the indicated genotype at 23°C. These were taken from the germination plate, grown to saturation, then serially diluted across agar plates and grown at the temperatures indicated for 3 days. (**B**) Strains of the genotypes indicated were passaged repeatedly by restreaking at 30°C for 3 days along with *TLC1*$^+$ controls. At the passages indicated, strains were assayed for growth, which was then quantified (Supplementary Figure S9). Growth at each passage is given as a fraction of the growth of the relevant *TLC1*$^+$ strain and the mean of two independent strains is shown. (**C**) At passages 1 and 15, strains assayed for growth in (**B**) had genomic DNA isolated and were Southern blotted with Y′ probe, as in Figure 2B. See Supplementary Figure S10 for detection with TG probe.

better prior to senescence, as previously reported (passages 3 and 4, Figure 5B) (Maringele and Lydall, 2004). In contrast, *tlc1*Δ *pif1*Δ and *tlc1*Δ *pif1*Δ *exo1*Δ strains showed a rapid decline in growth from passages 2–6 (senescence) and exhibited a protracted senescence period but slowly recovered by passage 15 (Figure 5B). We conclude that Pif1 inhibits entry into senescence and promotes recovery. Taken with the data discussed earlier, Pif1 contributes to good growth of *tlc1*Δ mutants from passage 2 onwards, yet inhibits growth of *cdc13-1* mutants (Figures 1C and 5A). In contrast, Exo1 has only a small effect on the growth of *tlc1*Δ mutants, yet inhibits growth of *cdc13-1* mutants (Figures 1C and 5A). Thus, it is likely that the relatively poor growth of *cdc13-1 tlc1*Δ *pif1*Δ compared with *cdc13-1 tlc1*Δ *exo1*Δ mutants is due to the poor growth of *tlc1*Δ *pif1*Δ mutants compared with *tlc1*Δ *exo1*Δ mutants.

After long cultivation (passage 15, 45 days growth) *tlc1*Δ *pif1*Δ and *tlc1*Δ *pif1*Δ *exo1*Δ mutants could be distinguished from those of *tlc1*Δ and *tlc1*Δ *exo1*Δ mutants by their poor growth (Figure 5B). Telomerase-deficient survivors typically show clear alterations in telomere structure—type I survivors undergo dramatic amplification of Y′ elements and retain short TG overhangs, whereas type II survivors show modest amplification of Y′ elements but amplify their TG overhangs (Teng and Zakian, 1999). Therefore, we examined the telomeres of *tlc1*Δ *pif1*Δ and *tlc1*Δ *pif1*Δ *exo1*Δ mutants. At passage 1, before entry into senescence, *tlc1*Δ, *tlc1*Δ *exo1*Δ, *tlc1*Δ *pif1*Δ and *tlc1*Δ *pif1*Δ *exo1*Δ mutants all had short telomeres (compare lanes 1–4 with lanes 5–12, Figure 5C). At passage 15, *tlc1*Δ mutants and *tlc1*Δ *exo1*Δ mutants had amplified Y′ elements and terminal fragments to generate type II (lanes 17–18, Figure 5D) or type I (lanes 21–22, Figure 5D) survivors. In contrast, *tlc1*Δ *pif1*Δ and *tlc1*Δ *pif1*Δ *exo1*Δ mutants at passage 15 had shorter telomeres than at passage 1 and had undergone a reduction in Y′ elements, but did not appear to have generated type I or type II survivor telomere structures (compare lanes 7–8 with 19–20 and lanes 11–12 with 23–24, Figure 5D). We noted that *tlc1*Δ *pif1*Δ and *tlc1*Δ *pif1*Δ *exo1*Δ mutants resembled type I survivors in that our TG probe did not detect any individual telomeres further up the gel (marked with arrows, compare lanes 7–8 with 19–20 and lanes 11–12 with 23–24, Supplementary Figure S10), indicating that all telomeres in these strains had acquired a terminal Y′ fragment. However, the terminal fragments of *tlc1*Δ *pif1*Δ and *tlc1*Δ *pif1*Δ *exo1*Δ were even shorter than those of type I survivors and they had undergone a reduction, not an amplification in Y′ elements, clearly distinguishing them from typical type I survivors (compares lanes 19–20, 23–24 with lanes 21–22, Figure 5D). We conclude that Pif1 is required for the generation of type I and type II survivors and that in the absence of Pif1, cells lacking telomerase can improve growth following senescence without adopting typical type I or type II survivor structures.

Telomerase is crucial for survival in the absence of Cdc13

Cdc13 has two crucial functions at telomeres—one, to shield telomeres from nuclease activities and the second to recruit telomerase to the telomere (Nugent *et al*, 1996). Although elimination of Pif1 and Exo1 permits *cdc13-1* mutants to grow at 36°C (presumably when *cdc13-1* is completely inactivated), this does not permit *cdc13-1 tlc1*Δ mutants to grow at 36°C (compare rows 13–14 with 15–16, Figure 5A), demonstrating that telomerase has a function in *cdc13-1* mutants at 36°C. Therefore, we hypothesized that at 36°C, Cdc13-1 might retain the ability to recruit telomerase, and Cdc13-dependent telomerase activity might be essential for growth. Alternatively, telomerase might be recruited to telomeres in a Cdc13-independent manner.

To test whether Cdc13-1 retained the ability to recruit telomerase in *cdc13-1 exo1*Δ *pif1*Δ cells at 36°C, we decided to delete *CDC13*. We generated diploid strains heterozygous for *pif1*Δ, *exo1*Δ and *cdc13*Δ mutations. Diploids were sporulated, tetrads dissected and vegetative cells containing combinations of the three deletion mutations were allowed to form colonies. Figure 6A shows a representative image of one

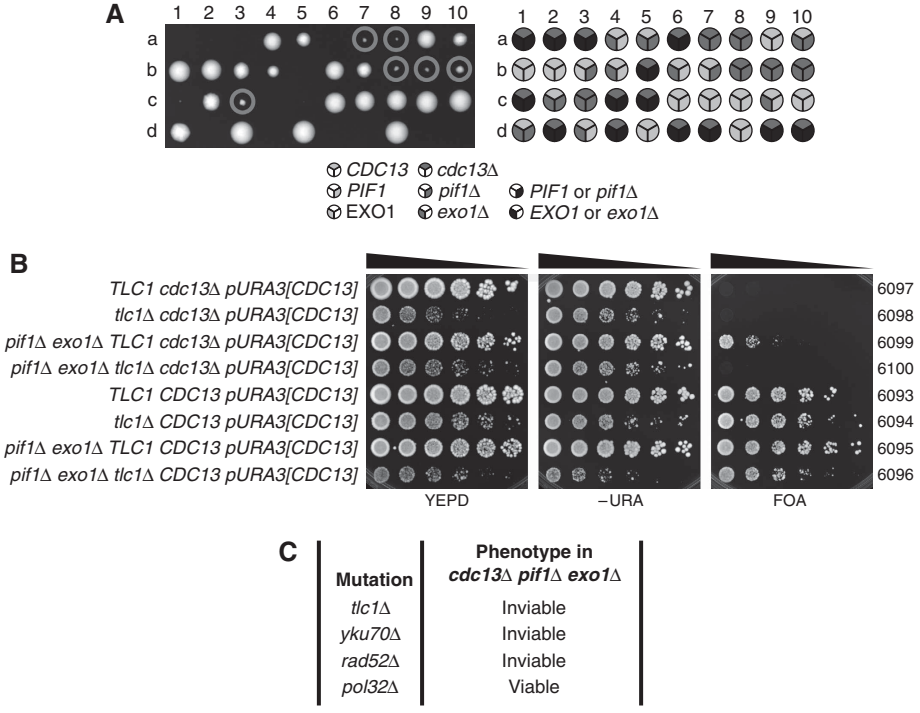

C

Mutation	Phenotype in *cdc13*Δ *pif1*Δ *exo1*Δ
*tlc1*Δ	Inviable
*yku70*Δ	Inviable
*rad52*Δ	Inviable
*pol32*Δ	Viable

Figure 6 *cdc13*Δ *exo1*Δ *pif1*Δ cells are viable but depend upon telomerase and homologous recombination for survival. (**A**) *cdc13*Δ*/CDC13 exo1*Δ*/EXO1 pif1*Δ*/PIF1* diploids (DDY341) were dissected. Viable *cdc13*Δ *exo1*Δ *pif1*Δ meiotic progeny are circled. Spores were incubated for 5 days at 23°C before genotypes were determined by replica plating to selective medium. (**B**) Strains of the genotypes indicated, all carrying a p*URA3[CDC13]* plasmid (pDL1012) were germinated, grown to saturation, then serially diluted across YEPD, −URA and FOA agar plates. Plates were incubated at 30°C for 4 days, YEPD plate shown after 2 days, −URA plate shown after 3 days and FOA plate shown after 4 days. (**C**) Summary of the roles of various telomere-related genes and their role in the survival of *cdc13*Δ *pif1*Δ *exo1*Δ mutants as assessed in Supplementary Figures S11 and S12.

tetrad dissection plate. Importantly, we found that *cdc13*Δ *exo1*Δ *pif1*Δ strains were viable and had a germination efficiency of ~90% compared with *CDC13 exo1*Δ *pif1*Δ strains (Figure 6A; Supplementary Table SI). However, it was clear that *cdc13*Δ *exo1*Δ *pif1*Δ mutants grew less well than *CDC13*$^+$ *exo1*Δ *pif1*Δ mutants on the tetrad dissection plates (Figure 6A). No viable colonies were formed from *cdc13*Δ cells that were either *PIF1*$^+$ or *EXO1*$^+$. We conclude that neither Cdc13-dependent telomerase activity nor Cdc13-dependent capping activities are required for growth following elimination of Pif1 and Exo1.

The viability of *cdc13*Δ *exo1*Δ *pif1*Δ strains was surprising in the light of the requirement for telomerase in *cdc13-1 exo1*Δ *pif1*Δ strains. We hypothesized that Cdc13-independent telomerase activity was essential for the viability of *cdc13*Δ *exo1*Δ *pif1*Δ strains. To test this, we generated diploid strains heterozygous for *pif1*Δ, *exo1*Δ, *cdc13*Δ and *tlc1*Δ mutations, containing a plasmid that carried a wild-type copy of *CDC13*. Diploids were sporulated and tetrad dissection was performed to generate strains containing combinations of the four deletion mutations, in addition to the wild-type copy of *CDC13*. These strains were diluted across agar plates either fully supplemented (YEPD), lacking uracil (−URA) or containing FOA (FOA). FOA is toxic to cells with an active uracil biosynthetic pathway so only cells able to survive in the absence of the *URA3*- and *CDC13*-containing plasmid would be able to grow. As expected, *cdc13*Δ *TLC1*$^+$ and *cdc13*Δ *tlc1*Δ mutants were able to grow on YEPD and –URA, but not on FOA medium, demonstrating that *CDC13* was essential for survival of these cell types (Figure 6B). *cdc13*Δ *TLC1*$^+$ *exo1*Δ *pif1*Δ strains were able to grow on FOA, YEPD and –URA, demonstrating that *CDC13* was not essential in this background (Figure 6B). However, *cdc13*Δ *TLC1*$^+$ *exo1*Δ *pif1*Δ cells grew much more poorly on FOA than on –URA and YEPD consistent the poor growth of *cdc13*Δ *exo1*Δ *pif1*Δ cells on the tetrad dissection plate(s) (Figure 6A). Importantly, *cdc13*Δ *tlc1*Δ *exo1*Δ *pif1*Δ cells were able to grow on YEPD and –URA but not on FOA, demonstrating that they could not survive in the absence of Cdc13. We conclude that telomerase is essential for the survival of *cdc13*Δ *exo1*Δ *pif1*Δ mutants, suggesting that Cdc13-independent recruitment of telomerase is essential for their survival.

We used the same plasmid-based method to assess the requirement for various proteins involved in telomere maintenance to the growth of *cdc13*Δ *exo1*Δ *pif1*Δ mutants. We confirmed that TLC1 was required for the viability of *cdc13*Δ *pif1*Δ *exo1*Δ as *cdc13*Δ *pif1*Δ *exo1*Δ *tlc1*Δ mutants could not lose a plasmid carrying *CDC13* (*p[URA3]CDC13*) (Figure 6C). We also found that Yku70 (a component of the Ku complex, which binds TLC1 to aid in recruitment of telomerase to the telomere) and Rad52 (required for homologous recombination and the generation of type I and type II survivor telomere structures) were required for the viability of *cdc13*Δ *pif1*Δ *exo1*Δ mutants (Figure 6C). However, we found that Pol32 (subunit of Polymerase δ, required for the generation of type I and type II survivor telomere structures) was dispensable for the viability of *cdc13*Δ *pif1*Δ *exo1*Δ mutants (Figure 6C), although elimination of Pol32 did reduce the frequency at which *cdc13*Δ *pif1*Δ *exo1*Δ mutants were able to lose the *pURA3[CDC13]* (Supplementary Figure S12). We conclude that *cdc13*Δ *pif1*Δ *exo1*Δ mutants are distinct from type I and type II survivors, as they do not require Pol32, and their telomeres are maintained through a combination of homologous recombination, Ku and telomerase activity.

If *cdc13*Δ *exo1*Δ *pif1*Δ mutants are able to recruit telomerase then they may not senesce or undergo the rearrangements in telomere structure characteristic of telomerase-deficient strains. To test this hypothesis, we compared the growth and telomere structure of *cdc13*Δ *exo1*Δ *pif1*Δ strains with *tlc1*Δ and *tlc1*Δ *exo1*Δ *pif1*Δ strains. As expected, telomerase-deficient *tlc1*Δ mutants senesced and recovered (Figure 7A) and by passage 11 they had generated type I (lane 15, Figure 7B) and type II (lane 16, Figure 7B) survivors. Interestingly, *cdc13*Δ *exo1*Δ *pif1*Δ strains showed a slight growth defect at passage 1 (Figure 7A), consistent with the small colonies formed by *cdc13*Δ *exo1*Δ *pif1*Δ mutants on the tetrad dissection plate (Figure 6A) and the growth defect of *cdc13*Δ *TLC1*$^+$ *exo1*Δ *pif1*Δ *pURA3[CDC13]* mutants grown on FOA (Figure 6B). However, by passage 5 and in all subsequent passages *cdc13*Δ *exo1*Δ *pif1*Δ mutants had improved in growth (Figure 7A). The telomeres of *cdc13*Δ *exo1*Δ *pif1*Δ mutants were long with more variation in length, and by passage 11, the median telomere length and variance in length increased (lanes 9–12, 21–24, Figure 7B). This is consistent with previous work showing that hypomorphic alleles of Cdc13 can cause increased telomere length and variance in telomere length (Chandra *et al*, 2001). No clear alterations in the telomere structure of *cdc13*Δ *exo1*Δ *pif1*Δ mutants were observed, and at passage 1, their telomeres most closely resembled those of *cdc13-1 exo1*Δ *pif1*Δ mutants with capped telomeres, which notably do not senesce (compare lanes 2, 14 with lanes 9–12, Figure 7B). The growth and telomere structure of *cdc13*Δ *exo1*Δ *pif1*Δ mutants was clearly distinct from that of telomerase-deficient *tlc1*Δ *exo1*Δ *pif1*Δ mutants, which rapidly senesced and slowly recovered (Figure 7A), while maintaining a relatively normal telomere structure (compare lanes 7–8 with lanes 19–20, Figure 7B). We conclude that *cdc13*Δ *exo1*Δ *pif1*Δ mutants do not undergo senescence and maintain their telomeres for at least 11 passages (44 days). This is consistent with our notion that *cdc13*Δ *exo1*Δ *pif1*Δ mutants are able to maintain telomeres in a telomerase-dependent manner, even in the absence of Cdc13.

Finally, although we observed that *cdc13-1 exo1*Δ *pif1*Δ mutants generated ssDNA only in the TG repeats, transiently over the course of a single cell cycle, we wished to know whether repeated cell division in the absence of telomere capping would lead to accumulation of ssDNA. By in-gel assay, we found that *cdc13-1 exo1*Δ *pif1*Δ mutants grown at 36°C for 4 h (~2 population doublings with uncapped telomeres) and *cdc13*Δ *exo1*Δ *pif1*Δ mutants from Passage 1 (~50 population doublings with uncapped telomeres) generated comparable levels of ssDNA in the TG repeats to a *yku70*Δ mutant (Figure 7C and D). This was comparable to the transient level of ssDNA seen in *cdc13-1 exo1*Δ *pif1*Δ mutants 2 h after telomere uncapping, within a single cell cycle (Figure 4G). We conclude that continued growth following telomere uncapping in *exo1*Δ *pif1*Δ mutants does not lead to ssDNA accumulation. This suggests that no residual nuclease activities continue to resect uncapped telomeres in the absence of Pif1 and Exo1.

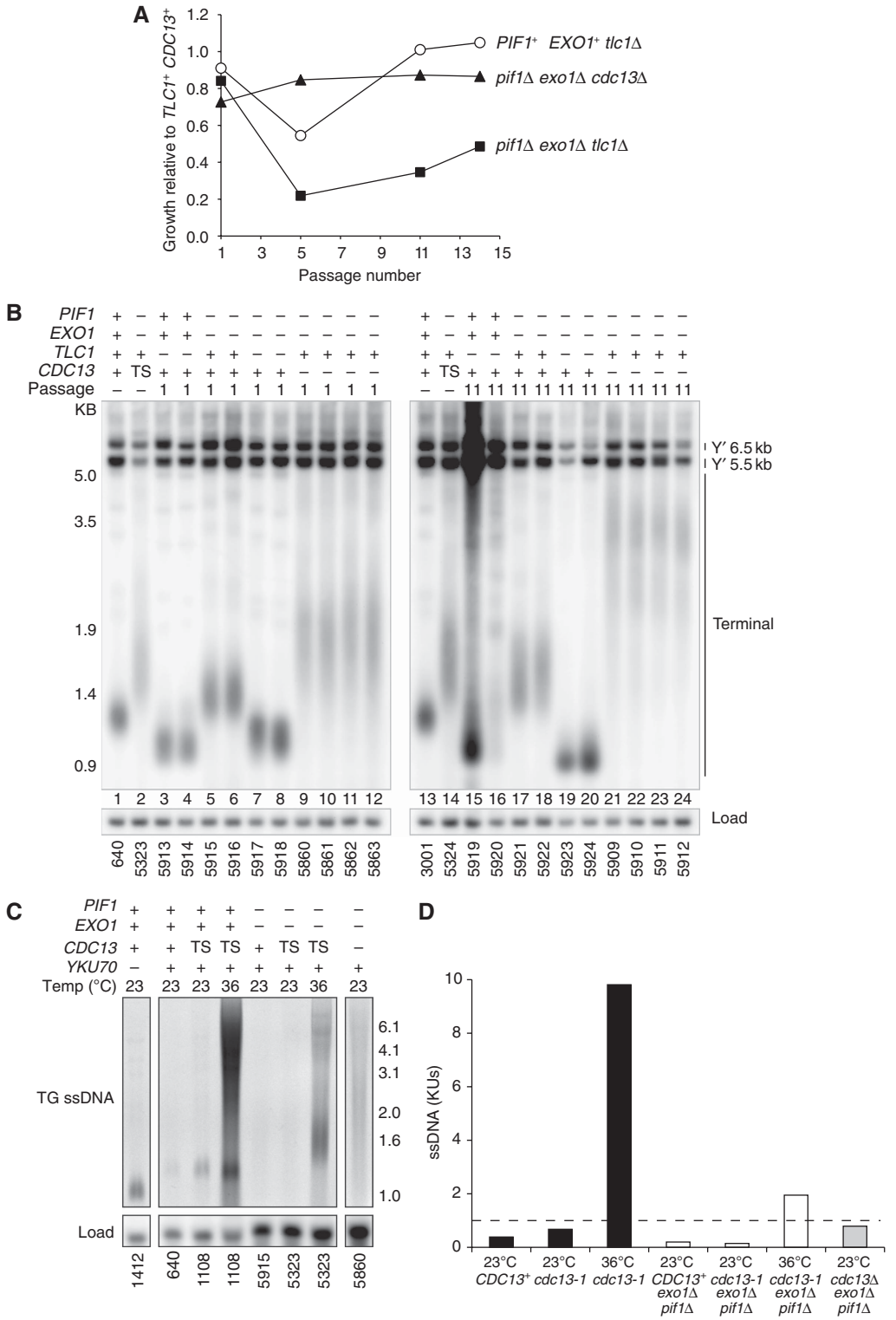

Figure 7 Cells lacking Cdc13 maintain telomeres and do not senesce. (**A**) Strains of the genotypes indicated were passaged repeatedly at 23°C for 4 days along with *TLC1*$^+$*CDC13*$^+$ controls. At the passages indicated, strains were assayed for growth (Supplementary Figure S13). Growth at each passage is given as a fraction of the growth of the relevant *TLC1*$^+$ *CDC13*$^+$ strain. The mean of two *tlc1*Δ strains or four *cdc13*Δ strains is shown. (**B**) At passages 1 and 11, strains that were assayed for growth in (**A**) had genomic DNA isolated and were Southern blotted, as in Figure 2B. *PIF1*$^+$*EXO1*$^+$*CDC13*$^+$ and *exo1*Δ *pif1*Δ *cdc13-1* (TS) strains were grown independently. See Supplementary Figure S14 for original blot probed with Y′ and TG probe. (**C**) *CDC13*$^+$ (+), *cdc13*Δ (−) and *cdc13-1* (TS) strains of the genotypes indicated were either grown exponentially at 23 or 36°C for 4 h before their DNA was isolated and telomeric TG ssDNA was detected by in-gel assay as in Figure 4F. (**D**) Quantification of ssDNA from the in-gel assay shown in (**C**), as in Figure 4F.

Discussion

We have shown that Pif1 and Exo1 are responsible for extensive ssDNA generation at uncapped telomeres in *cdc13-1* mutants and also that Pif1 has telomerase-independent functions at telomeres. This leads us to propose a model where Pif1 can initiate the DDR at uncapped telomeres by controlling nuclease activity. Furthermore, and remarkably, cells lacking Pif1 and Exo1 are viable and grow well in the absence of the usually essential telomere capping protein Cdc13.

In our model (Figure 8), Pif1 unwinds telomeric duplex DNA, generating ssDNA that is cleaved by an unidentified ssDNA endonuclease in a manner analogous to the function of Pif1 in Okazaki fragment processing and at stalled replication forks (Budd *et al*, 2006; Chang *et al*, 2009; George *et al*, 2009; Pike *et al*, 2009). We propose that close to the chromosome end (<5 kb) both Pif1- and Exo1-dependent activities generate ssDNA, causing weak initial checkpoint activation. We propose that Exo1 subsequently generates ssDNA >5 kb from the chromosome end, leading to stronger checkpoint activation that is sufficient to arrest all cells with uncapped telomeres. Our model is consistent with Pif1 being ExoY, a hypothetical nuclease proposed to function in parallel to Exo1 at uncapped telomeres (Zubko *et al*, 2004). Pif1, like ExoY, is more important for ssDNA generation at the end of the chromosome than further away (Figure 4E).

In our model, Exo1 recognizes the junction between 3′ (TG) ssDNA and duplex DNA, at native telomeric overhangs as previously suggested (Maringele and Lydall, 2002) or at stalled replication forks (Segurado and Diffley, 2008). We propose that Pif1 binds and unwinds 5′ (AC) overhangs because Pif1 is a 5′–3′ helicase (Lahaye *et al*, 1991; Zhou *et al*, 2000; Pike *et al*, 2009). If Pif1 does engage telomeric dsDNA and convert it to ssDNA, 5′ (AC) ssDNA presumably exists (Supplementary Figure S15A). Interestingly, 5′ telomeric ssDNA has been observed both in mammalian cells and in *Caenorhabditis elegans* (Cimino-Reale *et al*, 2003; Raices *et al*, 2008) and but not so far in *S. cerevisiae*. However, 5′ ssDNA overhangs could in principle occur at stalled replication fork structures (Supplementary Figure S15B) or Okazaki fragments.

DSBs that can be repaired by homologous recombination and DSB-induced shortened telomeres are processed by nucleases dependent upon Sgs1/Dna2, Exo1 and MRX/Sae2 (Gravel *et al*, 2008; Zhu *et al*, 2008; Mimitou and Symington, 2009). Other work recently published from our laboratory demonstrates that Sgs1 also contributes to resection of uncapped telomeres, but elimination of Sgs1 and Exo1 is insufficient to prevent the resection of uncapped telomeres in *cdc13-1* mutants (Ngo and Lydall, 2010). The work presented here demonstrates that elimination of Pif1 and Exo1 prevents resection of uncapped telomeres in *cdc13-1* mutants. However, at DSBs that can be repaired by homologous recombination or at DSB-induced shortened telomeres, Pif1 has little effect on resection (Zhu *et al*, 2008; Bonetti *et al*, 2009). Interestingly, Pif1 has been shown to have a critical role repair of DSBs where break-induced replication (BIR) is the main repair pathway (Chung *et al*, 2010). A major challenge will be to determine which substrates are exposed at DSBs, shortened telomeres and uncapped telomeres and how nuclease activities are coordinated to process them.

Pif1 contributes to the vitality of cells lacking telomerase, both before and after recovery from senescence (Figure 5B). Interestingly, *pif1*Δ cells improve their growth following senescence without adopting typical survivor-like telomeric DNA structures (Figure 5C). Usually following senescence, survivors are generated by homologous-recombination- and BIR-dependent alterations in telomere structure (Teng and Zakian, 1999; Lydeard *et al*, 2007). If BIR is eliminated, cells lacking telomerase senesce and undergo a complete loss in viability (Lydeard *et al*, 2007). The relatively unaltered telomere structure and poor growth following senescence in cells lacking Pif1 and telomerase is consistent with the impaired BIR seen in cells lacking Pif1 (Chung *et al*, 2010). Therefore, reduced BIR in *pif1*Δ cells may be sufficient to

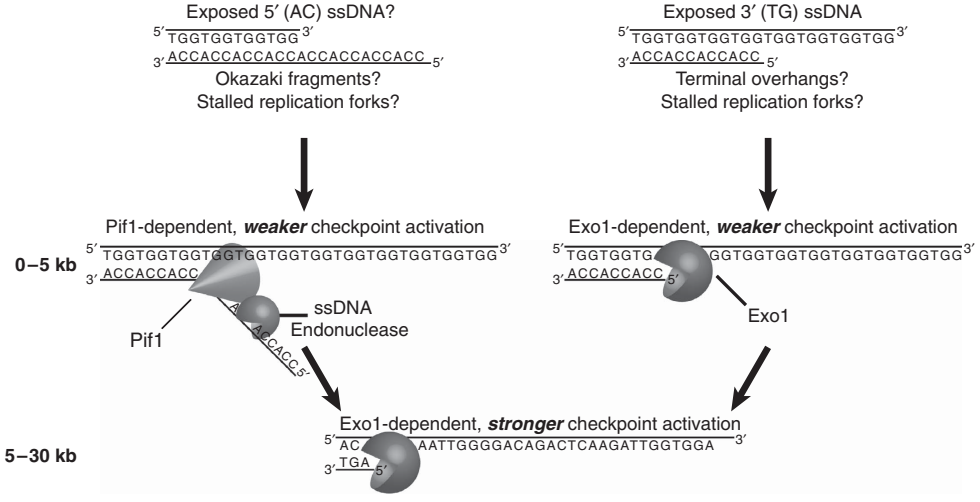

Figure 8 A model for the roles of Pif1 and Exo1 in the DDR at uncapped telomeres. Following telomere uncapping, 5′ and 3′ ssDNA is exposed within 5 kb of the chromosome end, serving as a substrate for resection. 5′ ssDNA is unwound by Pif1 and presumably cleaved by an unidentified ssDNA endonuclease, whereas the junction between 3′ ssDNA and dsDNA is recognized and resected by the exonuclease Exo1. This low-level processing leads to weak checkpoint activation. Resection of 3′ ssDNA overhangs beyond 5 kb requires Exo1. This further processing causes robust checkpoint activation.

maintain comparatively normal telomere structure in telomerase-deficient cells but insufficient to permit the typical amplification of Y′ elements or terminal TG repeats seen in survivors. The absence of telomeric repeat amplification could prevent these cells from achieving the high levels of post-senescence growth seen in other telomerase-deficient mutants.

We have demonstrated that attenuation of the DDR at uncapped telomeres, by elimination of Pif1 and Exo1 permits telomere maintenance in a Cdc13-indpendent but telomerase and Ku-dependent manner. This is surprising because Cdc13 is considered crucial for efficient recruitment of telomerase and thus to prevent senescence (Nugent *et al*, 1996). We propose that in the absence of Cdc13, Yku80 binds TLC1, the telomerase RNA, to help recruit telomerase to the telomere (Peterson *et al*, 2001). The requirement for Rad52 for the survival of *cdc13*Δ *exo1*Δ *pif1*Δ mutants is surprising. It will be interesting to investigate whether telomeric repeats from extremely long telomeres in *cdc13*Δ *exo1*Δ *pif1*Δ mutants (Figure 7B) can be distributed to shorter telomeres by homologous recombination, thus preventing short telomeres from becoming critically short. Finally, it will also be paramount to determine whether the requirement for telomerase in *cdc13*Δ *exo1*Δ *pif1*Δ mutants is a consequence of the increased utilization of telomerase that has been reported at the telomeres of cells lacking Pif1 (Boule *et al*, 2005).

We show that following inactivation of Cdc13 or telomerase, telomeric DNA can be stabilized by elimination of Pif1, eliminating resection of uncapped telomeres in cells lacking Cdc13 or permitting telomere maintenance without the generation of typical type I or type II survivor structures in cells lacking telomerase. As Pif1 and Exo1 are conserved from yeast, to mice, to humans, Pif1 might also contribute to the premature mortality caused by telomere dysfunction in telomerase knockout mice (Lahaye *et al*, 1991; Huang and Symington, 1993; Wei *et al*, 2003; Mateyak and Zakian, 2006; Snow *et al*, 2007). *pif1*$^{-/-}$ and *exo1*$^{-/-}$ mice have previously been examined (Wei *et al*, 2003; Snow *et al*, 2007), and it might be interesting to combine these mutations in a telomerase knockout background to investigate the consequences of telomere dysfunction in *pif1*$^{-/-}$ *exo1*$^{-/-}$ mice, as EXO1 contributes to the telomere dysfunction and premature mortality seen in telomerase knockout mice (Schaetzlein *et al*, 2007).

Materials and methods

Bioinformatics/analysis

A genetic interaction network was created in Cytoscape using *S. cerevisiae* genetic interactions from BioGRID (v2.0.53) (Stark *et al*, 2006; Cline *et al*, 2007). Genes that had genetic interactions with *EXO1* were identified (first neighbours of *EXO1*). A ranked list of all known genes was created, according to how many of the first neighbours of *EXO1* they had a genetic interaction with. The top 10% of this ranked list were then shown. Nodes for each gene were coloured according to whether the genes affected *cdc13-1* growth defects or telomere length (Askree *et al*, 2004; Zubko *et al*, 2004; Downey *et al*, 2006; Gatbonton *et al*, 2006; Tsolou and Lydall, 2007; Addinall *et al*, 2008; Ungar *et al*, 2009).

Yeast strains

All strains used in this study are *RAD5*$^{+}$ and in the W303 genetic background (Strain Table, Supplementary data). Standard genetic procedures of transformation and tetrad analysis were used. New gene deletions were constructed by transforming a diploid with PCR-based deletion modules (Goldstein and McCusker, 1999). Point mutations were generated integrated into the genome as described (Schulz and Zakian, 1994; Ribeyre *et al*, 2009).

Yeast growth assays

Growth assays were performed as previously described (Zubko *et al*, 2004). Pooled colonies were inoculated into 2 ml of YEPD and grown to saturation at 23°C. Five-fold serial dilutions were replicated onto agar plates and grown at a range of temperatures. Plates were photographed using an SPimager (S&P Robotics). Levels were adjusted with Photoshop CS4.

Passage experiments and quantification of growth

To passage cultures, multiple individual colonies were pooled and restruck. Where growth was quantified, unmodified images were analysed with Colonyzer (Lawless *et al*, 2010) and the sum of the trimmed greyscale pixel values for all pixels corresponding to spots and colonies of each strain were used as a measure of growth. Growth was then expressed relative to a *TLC1*$^{+}$ or *TLC1*$^{+}$ *CDC13*$^{+}$ strain included on the same plate.

Telomere length detection

Southern hybridization to examine telomere length and structure was performed similarly to previously described (Maringele and Lydall, 2004). Genomic DNA was extracted, digested with *Xho*I then run overnight on a 1% agarose gel at 1 V/cm. Southern transfer and detection was then performed using DIG-High Prime Labelling and Detection Kit (Roche) as per the manufacturer's instructions and visualized on a FUJI LAS4000. Telomeric probes were synthesized using PCR DIG Probe Synthesis Kit (Roche). TG probe was ~180 bp of TG repeats, whereas Y′ probe was ~820 bp of Y′ sequence, both amplified from pDL987 (pHT128) (Tsubouchi and Ogawa, 2000) using oligos m933 and m934 or m935 and m936, respectively. *CDC15* probe was synthesized using oligos m1045 and m1046 as previously described (Foster *et al*, 2006).

Synchronous cultures, cell cycle scoring and QAOS

Experiments to measure cell cycle progression and ssDNA following telomere uncapping were carried out in *bar1*Δ *cdc15-2 cdc13-1* cells and performed as described (Zubko *et al*, 2006). Where indicated, cells were treated with Bleomycin at a final concentration of 50 μg/ml (Morin *et al*, 2008).

Rad53 phosphorylation

Western blotting to detect Rad53 phosphorylation was performed essentially as described (Morin *et al*, 2008). Antibodies against Rad53 were from Dan Durocher, Toronto. Anti-tubulin antibodies were from Keith Gull, Oxford. Multiple gels were run to process all samples from a single experiment, but were transferred and detected in parallel and imaged simultaneously.

In-gel assay

In-gel assays were performed essentially as previously described (Zubko and Lydall, 2006) using a Cy5-labelled oligonucleotide (m2188) detected on a GE Healthcare Typhoon Trio imager. Following detection of ssDNA, the gel was subjected to Southern transfer and hybridization to detect *CDC15*. To quantify ssDNA, the fluorescent signal from the 0.7 to 12 kb range on the gel was measured, relative to the intensity of an exponentially dividing *yku70*Δ mutant on the same gel. All values were then normalized relative to the *CDC15* signal as determined by Southern blot.

Supplementary data

Supplementary data are available at *The EMBO Journal* Online (http://www.embojournal.org).

Acknowledgements

We gratefully acknowledge the members of our laboratory for input, particularly H Ngo and A Greenall and especially for A Leake's invaluable assistance. We thank our colleagues in the ONDEX project, particularly J Weile. We thank V Zakian, A Nicolas, H Tsubouchi, V Geli, D Durocher, A Bianchi and K Gull for providing strains, plasmids or antibodies. B Connolly, T Richardson and J Brown provided invaluable advice on fluorescent labelling of oligonucleotide probes and detection by phosphorimager.

We especially thank L Harrington and S Makovets for critically reading the paper. This study was supported by BBSRC ONDEX (BB/F006039/1), MRC and Wellcome Trust (075294).

Conflict of interest

The authors declare that they have no conflict of interest.

References

Addinall SG, Downey M, Yu M, Zubko MK, Dewar J, Leake A, Hallinan J, Shaw O, James K, Wilkinson DJ, Wipat A, Durocher D, Lydall D (2008) A genomewide suppressor and enhancer analysis of cdc13-1 reveals varied cellular processes influencing telomere capping in Saccharomyces cerevisiae. *Genetics* **180:** 2251–2266

Askree SH, Yehuda T, Smolikov S, Gurevich R, Hawk J, Coker C, Krauskopf A, Kupiec M, McEachern MJ (2004) A genome-wide screen for Saccharomyces cerevisiae deletion mutants that affect telomere length. *Proc Natl Acad Sci USA* **101:** 8658–8663

Baumann P, Cech TR (2001) Pot1, the putative telomere end-binding protein in fission yeast and humans. *Science* **292:** 1171–1175

Blackburn EH, Greider CW, Szostak JW (2006) Telomeres and telomerase: the path from maize, Tetrahymena and yeast to human cancer and aging. *Nat Med* **12:** 1133–1138

Bonetti D, Clerici M, Anbalagan S, Martina M, Lucchini G, Longhese MP (2010) Shelterin-like proteins and Yku inhibit nucleolytic processing of Saccharomyces cerevisiae telomeres. *PLoS Genet* **6:** e1000966

Bonetti D, Martina M, Clerici M, Lucchini G, Longhese MP (2009) Multiple pathways regulate 3′ overhang generation at S. cerevisiae telomeres. *Mol Cell* **35:** 70–81

Booth C, Griffith E, Brady G, Lydall D (2001) Quantitative amplification of single-stranded DNA (QAOS) demonstrates that cdc13-1 mutants generate ssDNA in a telomere to centromere direction. *Nucleic Acids Res* **29:** 4414–4422

Boule JB, Vega LR, Zakian VA (2005) The yeast Pif1p helicase removes telomerase from telomeric DNA. *Nature* **438:** 57–61

Budd ME, Reis CC, Smith S, Myung K, Campbell JL (2006) Evidence suggesting that Pif1 helicase functions in DNA replication with the Dna2 helicase/nuclease and DNA polymerase delta. *Mol Cell Biol* **26:** 2490–2500

Celli GB, de Lange T (2005) DNA processing is not required for ATM-mediated telomere damage response after TRF2 deletion. *Nat Cell Biol* **7:** 712–718

Chandra A, Hughes TR, Nugent CI, Lundblad V (2001) Cdc13 both positively and negatively regulates telomere replication. *Genes Dev* **15:** 404–414

Chang M, Luke B, Kraft C, Li Z, Peter M, Lingner J, Rothstein R (2009) Telomerase is essential to alleviate pif1-induced replication stress at telomeres. *Genetics* **183:** 779–791

Chung WH, Zhu Z, Papusha A, Malkova A, Ira G (2010) Defective resection at DNA double-strand breaks leads to *de novo* telomere formation and enhances gene targeting. *PLoS Genet* **6:** e1000948

Cimino-Reale G, Pascale E, Alvino E, Starace G, D′Ambrosio E (2003) Long telomeric C-rich 5′-tails in human replicating cells. *J Biol Chem* **278:** 2136–2140

Cline MS, Smoot M, Cerami E, Kuchinsky A, Landys N, Workman C, Christmas R, Avila-Campilo I, Creech M, Gross B, Hanspers K, Isserlin R, Kelley R, Killcoyne S, Lotia S, Maere S, Morris J, Ono K, Pavlovic V, Pico AR *et al* (2007) Integration of biological networks and gene expression data using Cytoscape. *Nat Protoc* **2:** 2366–2382

d'Adda di Fagagna F, Reaper PM, Clay-Farrace L, Fiegler H, Carr P, Von Zglinicki T, Saretzki G, Carter NP, Jackson SP (2003) A DNA damage checkpoint response in telomere-initiated senescence. *Nature* **426:** 194–198

de Lange T (2005) Shelterin: the protein complex that shapes and safeguards human telomeres. *Genes Dev* **19:** 2100–2110

de Lange T (2009) How telomeres solve the end-protection problem. *Science* **326:** 948–952

Downey M, Houlsworth R, Maringele L, Rollie A, Brehme M, Galicia S, Guillard S, Partington M, Zubko MK, Krogan NJ, Emili A, Greenblatt JF, Harrington L, Lydall D, Durocher D (2006) A genome-wide screen identifies the evolutionarily conserved KEOPS complex as a telomere regulator. *Cell* **124:** 1155–1168

Foster SS, Zubko MK, Guillard S, Lydall D (2006) MRX protects telomeric DNA at uncapped telomeres of budding yeast cdc13-1 mutants. *DNA Repair (Amst)* **5:** 840–851

Gao H, Cervantes RB, Mandell EK, Otero JH, Lundblad V (2007) RPA-like proteins mediate yeast telomere function. *Nat Struct Mol Biol* **14:** 208–214

Garvik B, Carson M, Hartwell L (1995) Single-stranded DNA arising at telomeres in cdc13 mutants may constitute a specific signal for the RAD9 checkpoint. *Mol Cell Biol* **15:** 6128–6138

Gatbonton T, Imbesi M, Nelson M, Akey JM, Ruderfer DM, Kruglyak L, Simon JA, Bedalov A (2006) Telomere length as a quantitative trait: genome-wide survey and genetic mapping of telomere length-control genes in yeast. *PLoS Genet* **2:** e35

George T, Wen Q, Griffiths R, Ganesh A, Meuth M, Sanders CM (2009) Human Pif1 helicase unwinds synthetic DNA structures resembling stalled DNA replication forks. *Nucleic Acids Res* **37:** 6491–6502

Goldstein AL, McCusker JH (1999) Three new dominant drug resistance cassettes for gene disruption in Saccharomyces cerevisiae. *Yeast* **15:** 1541–1553

Gravel S, Chapman JR, Magill C, Jackson SP (2008) DNA helicases Sgs1 and BLM promote DNA double-strand break resection. *Genes Dev* **22:** 2767–2772

Gravel S, Larrivee M, Labrecque P, Wellinger RJ (1998) Yeast Ku as a regulator of chromosomal DNA end structure. *Science* **280:** 741–744

Huang KN, Symington LS (1993) A 5′-3′ exonuclease from Saccharomyces cerevisiae is required for *in vitro* recombination between linear DNA molecules with overlapping homology. *Mol Cell Biol* **13:** 3125–3134

Lahaye A, Stahl H, Thines-Sempoux D, Foury F (1991) PIF1: a DNA helicase in yeast mitochondria. *EMBO J* **10:** 997–1007

Larrivee M, Wellinger RJ (2006) Telomerase- and capping-independent yeast survivors with alternate telomere states. *Nat Cell Biol* **8:** 741–747

Lawless C, Wilkinson DJ, Young A, Addinall SG, Lydall DA (2010) Colonyzer: automated quantification of micro-organism growth characteristics on solid agar. *BMC Bioinformatics* **11:** 287

Lundblad V, Blackburn EH (1993) An alternative pathway for yeast telomere maintenance rescues est1- senescence. *Cell* **73:** 347–360

Lydall D (2009) Taming the tiger by the tail: modulation of DNA damage responses by telomeres. *EMBO J* **28:** 2174–2187

Lydall D, Weinert T (1995) Yeast checkpoint genes in DNA damage processing: implications for repair and arrest. *Science* **270:** 1488–1491

Lydeard JR, Jain S, Yamaguchi M, Haber JE (2007) Break-induced replication and telomerase-independent telomere maintenance require Pol32. *Nature* **448:** 820–823

Makovets S, Blackburn EH (2009) DNA damage signalling prevents deleterious telomere addition at DNA breaks. *Nat Cell Biol* **11:** 1383–1386

Marcand S, Pardo B, Gratias A, Cahun S, Callebaut I (2008) Multiple pathways inhibit NHEJ at telomeres. *Genes Dev* **22:** 1153–1158

Maringele L, Lydall D (2002) EXO1-dependent single-stranded DNA at telomeres activates subsets of DNA damage and spindle checkpoint pathways in budding yeast yku70Delta mutants. *Genes Dev* **16:** 1919–1933

Maringele L, Lydall D (2004) EXO1 plays a role in generating type I and type II survivors in budding yeast. *Genetics* **166:** 1641–1649

Mateyak MK, Zakian VA (2006) Human PIF helicase is cell cycle regulated and associates with telomerase. *Cell Cycle* **5:** 2796–2804

Mimitou EP, Symington LS (2008) Sae2, Exo1 and Sgs1 collaborate in DNA double-strand break processing. *Nature* **455:** 770–774

Mimitou EP, Symington LS (2009) DNA end resection: many nucleases make light work. *DNA Repair (Amst)* **8:** 983–995

Miyake Y, Nakamura M, Nabetani A, Shimamura S, Tamura M, Yonehara S, Saito M, Ishikawa F (2009) RPA-like mammalian Ctc1-Stn1-Ten1 complex binds to single-stranded DNA and protects telomeres independently of the Pot1 pathway. *Mol Cell* **36:** 193–206

Morin I, Ngo HP, Greenall A, Zubko MK, Morrice N, Lydall D (2008) Checkpoint-dependent phosphorylation of Exo1 modulates the DNA damage response. *EMBO J* **27:** 2400–2410

Ngo HP, Lydall D (2010) Survival and growth of yeast without telomere capping by Cdc13 in the absence of Sgs1, Exo1, and Rad9. *PLoS Genet* **6:** e1001072

Nugent CI, Hughes TR, Lue NF, Lundblad V (1996) Cdc13p: a single-strand telomeric DNA-binding protein with a dual role in yeast telomere maintenance. *Science* **274:** 249–252

Peterson SE, Stellwagen AE, Diede SJ, Singer MS, Haimberger ZW, Johnson CO, Tzoneva M, Gottschling DE (2001) The function of a stem-loop in telomerase RNA is linked to the DNA repair protein Ku. *Nat Genet* **27:** 64–67

Pike JE, Burgers PM, Campbell JL, Bambara RA (2009) Pif1 helicase lengthens some Okazaki fragment flaps necessitating Dna2 nuclease/helicase action in the two-nuclease processing pathway. *J Biol Chem* **284:** 25170–25180

Pitt CW, Cooper JP, Pot1 inactivation leads to rampant telomere resection and loss in one cell cycle. *Nucleic Acids Res* (advance online publication 3 July 2010; doi:10.1093/nar/gkq580)

Polotnianka RM, Li J, Lustig AJ (1998) The yeast Ku heterodimer is essential for protection of the telomere against nucleolytic and recombinational activities. *Curr Biol* **8:** 831–834

Raices M, Verdun RE, Compton SA, Haggblom CI, Griffith JD, Dillin A, Karlseder J (2008) C. elegans telomeres contain G-strand and C-strand overhangs that are bound by distinct proteins. *Cell* **132:** 745–757

Ribeyre C, Lopes J, Boule JB, Piazza A, Guedin A, Zakian VA, Mergny JL, Nicolas A (2009) The yeast Pif1 helicase prevents genomic instability caused by G-quadruplex-forming CEB1 sequences *in vivo*. *PLoS Genet* **5:** e1000475

Sandell LL, Zakian VA (1993) Loss of a yeast telomere: arrest, recovery, and chromosome loss. *Cell* **75:** 729–739

Schaetzlein S, Kodandaramireddy NR, Ju Z, Lechel A, Stepczynska A, Lilli DR, Clark AB, Rudolph C, Kuhnel F, Wei K, Schlegelberger B, Schirmacher P, Kunkel TA, Greenberg RA, Edelmann W, Rudolph KL (2007) Exonuclease-1 deletion impairs DNA damage signaling and prolongs lifespan of telomere-dysfunctional mice. *Cell* **130:** 863–877

Schulz VP, Zakian VA (1994) The saccharomyces PIF1 DNA helicase inhibits telomere elongation and *de novo* telomere formation. *Cell* **76:** 145–155

Segurado M, Diffley JF (2008) Separate roles for the DNA damage checkpoint protein kinases in stabilizing DNA replication forks. *Genes Dev* **22:** 1816–1827

Snow BE, Mateyak M, Paderova J, Wakeham A, Iorio C, Zakian V, Squire J, Harrington L (2007) Murine Pif1 interacts with telomerase and is dispensable for telomere function *in vivo*. *Mol Cell Biol* **27:** 1017–1026

Stark C, Breitkreutz BJ, Reguly T, Boucher L, Breitkreutz A, Tyers M (2006) BioGRID: a general repository for interaction datasets. *Nucleic Acids Res* **34** (Database issue)**:** D535–D539

Surovtseva YV, Churikov D, Boltz KA, Song X, Lamb JC, Warrington R, Leehy K, Heacock M, Price CM, Shippen DE (2009) Conserved telomere maintenance component 1 interacts with STN1 and maintains chromosome ends in higher eukaryotes. *Mol Cell* **36:** 207–218

Sweeney FD, Yang F, Chi A, Shabanowitz J, Hunt DF, Durocher D (2005) Saccharomyces cerevisiae Rad9 acts as a Mec1 adaptor to allow Rad53 activation. *Curr Biol* **15:** 1364–1375

Teng SC, Zakian VA (1999) Telomere-telomere recombination is an efficient bypass pathway for telomere maintenance in Saccharomyces cerevisiae. *Mol Cell Biol* **19:** 8083–8093

Tsolou A, Lydall D (2007) Mrc1 protects uncapped budding yeast telomeres from exonuclease EXO1. *DNA Repair (Amst)* **6:** 1607–1617

Tsubouchi H, Ogawa H (2000) Exo1 roles for repair of DNA double-strand breaks and meiotic crossing over in Saccharomyces cerevisiae. *Mol Biol Cell* **11:** 2221–2233

Ungar L, Yosef N, Sela Y, Sharan R, Ruppin E, Kupiec M (2009) A genome-wide screen for essential yeast genes that affect telomere length maintenance. *Nucleic Acids Res* **37:** 3840–3849

Van Dyck E, Foury F, Stillman B, Brill SJ (1992) A single-stranded DNA binding protein required for mitochondrial DNA replication in S cerevisiae is homologous to E. coli SSB. *EMBO J* **11:** 3421–3430

Vaze MB, Pellicioli A, Lee SE, Ira G, Liberi G, Arbel-Eden A, Foiani M, Haber JE (2002) Recovery from checkpoint-mediated arrest after repair of a double-strand break requires Srs2 helicase. *Mol Cell* **10:** 373–385

Vega LR, Phillips JA, Thornton BR, Benanti JA, Onigbanjo MT, Toczyski DP, Zakian VA (2007) Sensitivity of yeast strains with long G-tails to levels of telomere-bound telomerase. *PLoS Genet* **3:** e105

Vodenicharov MD, Laterreur N, Wellinger RJ (2010) Telomere capping in non-dividing yeast cells requires Yku and Rap1. *EMBO J* **29:** 3007–3019

Vodenicharov MD, Wellinger RJ (2006) DNA degradation at unprotected telomeres in yeast is regulated by the CDK1 (Cdc28/Clb) cell-cycle kinase. *Mol Cell* **24:** 127–137

Wei K, Clark AB, Wong E, Kane MF, Mazur DJ, Parris T, Kolas NK, Russell R, Hou Jr H, Kneitz B, Yang G, Kunkel TA, Kolodner RD, Cohen PE, Edelmann W (2003) Inactivation of Exonuclease 1 in mice results in DNA mismatch repair defects, increased cancer susceptibility, and male and female sterility. *Genes Dev* **17:** 603–614

Wotton D, Shore D (1997) A novel Rap1p-interacting factor, Rif2p, cooperates with Rif1p to regulate telomere length in Saccharomyces cerevisiae. *Genes Dev* **11:** 748–760

Zhang W, Durocher D (2010) *De novo* telomere formation is suppressed by the Mec1-dependent inhibition of Cdc13 accumulation at DNA breaks. *Genes Dev* **24:** 502–515

Zhou J, Monson EK, Teng SC, Schulz VP, Zakian VA (2000) Pif1p helicase, a catalytic inhibitor of telomerase in yeast. *Science* **289:** 771–774

Zhu Z, Chung WH, Shim EY, Lee SE, Ira G (2008) Sgs1 helicase and two nucleases Dna2 and Exo1 resect DNA double-strand break ends. *Cell* **134:** 981–994

Zubko MK, Guillard S, Lydall D (2004) Exo1 and Rad24 differentially regulate generation of ssDNA at telomeres of Saccharomyces cerevisiae cdc13-1 mutants. *Genetics* **168:** 103–115

Zubko MK, Lydall D (2006) Linear chromosome maintenance in the absence of essential telomere-capping proteins. *Nat Cell Biol* **8:** 734–740

Zubko MK, Maringele L, Foster SS, Lydall D (2006) Detecting repair intermediates *in vivo*: effects of DNA damage response genes on single-stranded DNA accumulation at uncapped telomeres in budding yeast. *Methods Enzymol* **409:** 285–300

